

FINAL REPORT

Phase II: Identification and Characterization of Natural Sources of Perchlorate

SERDP Project ER-1435

JANUARY 2017

Dr. Paul B. Hatzinger
CB&I Federal Services

Mr. Greg Harvey
United States Air Force

Dr. W. Andrew Jackson
Texas Tech University

Dr. J.K. Böhlke
U.S. Geological Survey

Dr. Neil C. Sturchio
University of Delaware

Dr. Baohua Gu
Oak Ridge National Laboratory

Dr. David Grantz
University of California, Riverside

Dr. Kent Burkey
U.S. Department of Agriculture

Dr. Margaret McGrath
Cornell University

Distribution Statement A

This document has been cleared for public release



Page Intentionally Left Blank

This report was prepared under contract to the Department of Defense Strategic Environmental Research and Development Program (SERDP). The publication of this report does not indicate endorsement by the Department of Defense, nor should the contents be construed as reflecting the official policy or position of the Department of Defense. Reference herein to any specific commercial product, process, or service by trade name, trademark, manufacturer, or otherwise, does not necessarily constitute or imply its endorsement, recommendation, or favoring by the Department of Defense.

Page Intentionally Left Blank

REPORT DOCUMENTATION PAGE				<i>Form Approved</i> OMB No. 0704-0188	
<small>The public reporting burden for this collection of information is estimated to average 1 hour per response, including the time for reviewing instructions, searching existing data sources, gathering and maintaining the data needed, and completing and reviewing the collection of information. Send comments regarding this burden estimate or any other aspect of this collection of information, including suggestions for reducing the burden, to the Department of Defense, Executive Services and Communications Directorate (0704-0188). Respondents should be aware that notwithstanding any other provision of law, no person shall be subject to any penalty for failing to comply with a collection of information if it does not display a currently valid OMB control number.</small> PLEASE DO NOT RETURN YOUR FORM TO THE ABOVE ORGANIZATION.					
1. REPORT DATE (DD-MM-YYYY) 12-31-2016		2. REPORT TYPE Final		3. DATES COVERED (From - To) September 2008 - December 2016	
4. TITLE AND SUBTITLE Identification and Characterization of Natural Sources of Perchlorate				5a. CONTRACT NUMBER W912-HQ-08-C-0061	
				5b. GRANT NUMBER NA	
				5c. PROGRAM ELEMENT NUMBER NA	
6. AUTHOR(S) Hatzinger, Paul B. (CB&I) Harvey, Greg (USAF) Böhlke, J.K. (USGS) Sturchio, Neil C. (Univ. of Delaware) Jackson, Andrew W. (Texas Tech Univ) Gu, Baohua (Oak Ridge National Lab) Grantz, David (UC, Riverside) Burkey, Kent (USDA) McGrath, Margaret (Cornell Univ)				5d. PROJECT NUMBER ER-1435	
				5e. TASK NUMBER NA	
				5f. WORK UNIT NUMBER NA	
7. PERFORMING ORGANIZATION NAME(S) AND ADDRESS(ES) CB&I Federal Services, LLC. 17 Princess Road Lawrenceville, NJ 08648				8. PERFORMING ORGANIZATION REPORT NUMBER NA	
9. SPONSORING/MONITORING AGENCY NAME(S) AND ADDRESS(ES) Strategic Environmental Research and Development Program 4800 Mark Center Drive, Suite 17D08 Alexandria, VA 22350-3605				10. SPONSOR/MONITOR'S ACRONYM(S) SERDP	
				11. SPONSOR/MONITOR'S REPORT NUMBER(S) NA	
12. DISTRIBUTION/AVAILABILITY STATEMENT Distribution Statement A: Approved for Public Release, Distribution is Unlimited					
13. SUPPLEMENTARY NOTES None					
14. ABSTRACT The objective of this research effort was to develop an improved understanding of (1) the distribution and isotopic characteristics of natural perchlorate worldwide, (2) the mechanisms of natural perchlorate production and (3) the contributing processes resulting in the ubiquitous distribution of this anion and its stable isotope characteristics in soils, groundwater, and vegetation. Data from the project reveal that natural perchlorate is widely distributed in soils and groundwater in arid and semi-arid environments worldwide. Natural perchlorate was also found to be the dominant source on this anion in the U.S. Great Lakes, at concentrations ranging from 0.05 to 0.13 µg/L. Both UV-photolysis and ozone mediated mechanisms may contribute to the formation of natural perchlorate and to its isotopic characteristics. Biological synthesis of perchlorate in bacteria or plants was not observed. However, many plant species were observed to bioaccumulate perchlorate, particularly in leaf tissue. The isotopic signature of this plant-accumulated perchlorate represented that of the dominant environmental source, potentially providing a means to identify sources in produce.					
15. SUBJECT TERMS perchlorate, nitrate, chlorate, UV-photolysis, ozone, stable isotope, oxygen-18, oxygen-17, chlorine-37, chlorine-36, plants, arid, Great Lakes, groundwater, synthesis, Atacama, Antarctica, southwest, bioaccumulation, CSIA, produce					
16. SECURITY CLASSIFICATION OF:			17. LIMITATION OF ABSTRACT UU	18. NUMBER OF PAGES	19a. NAME OF RESPONSIBLE PERSON Dr. Paul B. Hatzinger
a. REPORT U	b. ABSTRACT U	c. THIS PAGE U			19b. TELEPHONE NUMBER (Include area code) 609-895-5356

Page Intentionally Left Blank

Table of Contents

LIST OF TABLES	i
LIST OF FIGURES	iii
Acronyms and Abbreviations	ix
1.0 PROJECT BACKGROUND AND OBJECTIVES	5
1.1 Background	5
1.2 Research Objectives and Associated Major Tasks	11
2.0 PROJECT TASKS	14
2.1 Occurrence and Isotopic Signature of Natural ClO_4^- in Soils and Groundwater in the U.S... 14	14
2.1.1 Background: Natural Perchlorate and Nitrate	14
2.1.2 Materials and Methods.....	15
2.1.3 Results and Discussion	20
2.1.4 Isotopic Constraints on Origins of Natural Perchlorate	32
2.1.5 Implications for Perchlorate Isotope Forensics.....	35
2.2 Occurrence and Stable Isotope Analysis of Perchlorate in the U.S. Great Lakes	36
2.2.1 Background	36
2.2.2 Materials and Methods.....	36
2.2.3 Results and Discussion	40
2.3 Occurrence of Natural Perchlorate and Relationship with Nitrate in Arid and Semi-Arid Environments Worldwide	53
2.3.1 Background	53
2.3.2 Site and Sample Descriptions	53
2.3.3 Materials and Methods.....	60
2.3.4 Data Analysis	61
2.3.5 Results and Discussion	61
2.3.6 Conclusions.....	83
2.4 Perchlorate and Chlorate in the Ice-Covered Lakes of McMurdo Dry Valleys, Antarctica....	85
2.4.1 Background	85
2.4.2 Materials and Methods.....	85

2.4.3 Analysis.....	86
2.4.4 Modeling	86
2.4.5 Results and Discussion	87
2.4.6 Summary and Conclusions	103
2.5 Evaluate Cl and O Stable Isotope Signatures of UV and O ₃ Generated Perchlorate.....	104
2.5.1 Background	104
2.5.2 Methods.....	104
2.5.3 Results.....	113
2.5.4 Discussion	129
2.5.5 Conclusions.....	177
2.6 Evaluation of Bacterial Production of Perchlorate	179
2.6.1 Background	179
2.6.2 Initial Studies using Haloperoxidase Enzymes and Natural Sunlight	179
2.6.3 Controlled Studies using Haloperoxidase Enzymes, Produced UV and Sunlight	183
2.6.4 Perchlorate Formation under Nitrifying Conditions	188
2.6.5 Perchlorate Formation Tests Using <i>Starkeya novella</i> and West Texas Soil Enrichments	190
2.7 Evaluate the Accumulation of ClO ₄ ⁻ in Plants and their Role in Ozone-Mediated Production of ClO ₄ ⁻	193
2.7.1 ClO ₄ ⁻ Accumulation at Environmentally-Relevant O ₃ Concentrations.	193
2.7.2 ClO ₄ ⁻ Accumulation at Elevated O ₃ Concentrations.....	213
2.8 Effect of Plant Uptake on Stable Isotope Composition of ClO ₄ ⁻	227
2.8.1 Background	227
2.8.2 Materials and Methods.....	228
2.8.3 Results.....	233
2.8.4 Discussion	250
2.9 Publications.....	253
3.0 CONCLUSIONS and IMPLICATIONS FOR FUTURE RESEARCH	254
4.0 REFERENCES CITED.....	257
Appendix A: Proposed Mechanisms of Perchlorate Formation	280

LIST OF TABLES

Table 2.1.1. Information about soil and caliche samples.

Table 2.1.2. Well information with chemical and isotopic data for groundwater samples.

Table 2.1.3. Selected chemical and isotopic data for caliche-type salts in unconsolidated surficial material from the Atacama Desert in Chile and the Death Valley clay hills region of the Mojave Desert in California, USA.

Table 2.1.4 Selected chemical and isotopic data for groundwater samples from the southwestern United States and Chile.

Table 2.2.1. Concentrations and isotopic compositions of perchlorate from the Great Lakes.

Table 2.2.2. Perchlorate concentrations in the water samples from the Great Lakes.

Table 2.2.3. Physical parameters of the Great Lakes.

Table 2.2.4. Perchlorate mass-balance model results.

Table 2.3.1. Locations, sample types, summary statistics for ClO_4^- , NO_3^- , and Cl^- in groundwater and deposition sample sets.

Table 2.3.2. Locations, sample types, summary statistics for ClO_4^- , NO_3^- , and Cl^- in soil/caliche sample sets.

Table 2.4.1. ClO_3^- , ClO_4^- , Cl^- and SO_4^{2-} concentrations in surface waters of the Dry Valleys.

Table 2.5.1. Experimental conditions for O_3 oxidation of various Cl/ClO_x species

Table 2.5.2. Experimental conditions for UV oxidation of various ClO_x species

Table 2.5.3. Cl amounts in ClO_x species of initial and final solutions, Cl mass balance, and product yields for UV and O_3 experiments

Table 2.5.4. Proposed reactions possibly leading to the formation of ClO_4^- via O_3 oxidation of ClO_x species

Table 2.5.5. Calculated $\Delta^{17}\text{O}$ values of ClO_4^- produced in the UV experiments using the coefficient (λ) range of 0.50 – 0.53 in the various definitions of $\Delta^{17}\text{O}$.

Table 2.6.1. Evaluation of perchlorate production from H_2O_2 and Cl^- with vanadium chloroperoxidase (VCP).

Table 2.6.2. Evaluation of the influence of UV on perchlorate production by fungal iron chloroperoxidase.

Table 2.6.3. Evaluation of the influence of H₂O₂ concentration on perchlorate production by fungal iron chloroperoxidase.

Table 2.6.4. Perchlorate levels (µg/L) in UV light experiments.

Table 2.6.5. Perchlorate levels (µg/L) in natural sunlight experiments.

Table 2.6.6. Variations of DSMZ Medium 69 used in the perchlorate formation studies.

Table 2.6.7. Perchlorate concentrations (µg/L) in studies with *Starkeya novella* and TSP69.

Table 2.7.1. ClO₄⁻ content of unused irrigation water, potting medium, and fertilizer.

Table 2.7.2. Perchlorate content (µg kg⁻¹) of young leaves of a range of crop species as a function of O₃ exposure (ppb, 12 hr mean) sampled at the time of final harvest.

Table 2.7.3. Perchlorate content of older, senescing leaves of a range of crop species as a function of O₃ exposure (ppb, 12 hr mean) sampled at the time of final harvest.

Table 2.7.4. Perchlorate content (µg (kg dry wt)⁻¹) of potting medium after use for plant growth by a range of crop species, sampled at the time of final harvest (mean ± S.E.), as a function of O₃ exposure (ppb, 12 hr mean).

Table 2.7.5. Perchlorate content (µg (kg dry wt)⁻¹) of potting medium before and after use for plant growth, sampled directly from the commercial container or from pots of all species at the time of final harvest (mean ± S.E.), as a function of O₃ exposure (ppb, 12 hr mean).

Table 2.7.6. Perchlorate concentration (µg (kg dry wt)⁻¹) of young leaves of contrasting crop species exposed to filtered air.

Table 2.7.7. Perchlorate concentration (µg (kg dry wt)⁻¹) of potting medium used for plant growth by contrasting crop species exposed to high O₃.

Table. 2.7.8. Effect of exposure to ozone on stomatal conductance in contrasting species.

Table 2.8.1. Summary of initial experimental conditions for ClO₄⁻ treatments in experiment 1 and 2.

Table 2.8.2. Average ClO₄⁻, NO₃⁻, Cl⁻ and total-N fractional mass distribution in growth solution and snap bean plant tissue

Table 2.8.3 Irrigation, rainfall, and foliage ClO₄⁻ data for the Raleigh, NC and Long Island, NY snap bean field studies.

LIST OF FIGURES

Figure 1.1.1. Comparison of $\delta^{37}\text{Cl}$ versus $\delta^{18}\text{O}$ (Plot A) and $\Delta^{17}\text{O}$ versus $\delta^{18}\text{O}$ (Plot B) in natural indigenous ClO_4^- in the U.S., natural Chilean ClO_4^- , and synthetic ClO_4^- .

Figure 1.1.2. Values of $^{36}\text{Cl}/\text{Cl}$ (mole fraction) versus $\delta^{37}\text{Cl}$ in representative samples of synthetic ClO_4^- reagents and products, natural ClO_4^- and Cl^- extracted from soil and groundwater from the Atacama Desert, Chile, and natural ClO_4^- extracted from groundwater and soil from the southwestern U.S.

Figure 2.1.1. Sample locations for natural perchlorate.

Figure 2.1.2. Summary of new isotope data for ClO_4^- from SHP and MRGB groundwater, SHP unsaturated sub-soil, Death Valley and Atacama caliches displayed with previously published ClO_4^- isotope data (Böhlke et al., 2005; Sturchio et al., 2006; Bao and Gu, 2004).

Figure 2.1.3. Comparison of $\text{NO}_3^-/\text{ClO}_4^-$ and $\text{Cl}^-/\text{ClO}_4^-$ molar ratios in new samples with previously published values for wet deposition across the contiguous United States (excluding coastal sites) (Rajagopalan et al., 2009) and vadose-zone salt accumulations in the southwestern United States (Rao et al., 2007).

Figure 2.1.4. Relations between $\Delta^{17}\text{O}$ and $\delta^{18}\text{O}$ in ClO_4^- and NO_3^- (data from this study and Böhlke et al., 2005; Sturchio et al., 2006; Bao and Gu, 2004; USGA, 2010; Rao et al., 2010).

Figure 2.1.5. Distribution of ClO_4^- and other anions with depth below land surface at a rangeland site in the southern High Plains, western Texas.

Figure 2.1.6. Relation between $\delta^{15}\text{N}$ and $\delta^{18}\text{O}$ of NO_3^- in groundwater and leachate samples.

Figure 2.2.1. Perchlorate concentration vs. depth in the Great Lakes.

Figure 2.2.2. Diagrams showing $\delta^{37}\text{Cl}$ vs. $\delta^{18}\text{O}$ values (upper diagram) and $\Delta^{17}\text{O}$ vs. $\delta^{18}\text{O}$ values (lower diagram) for Great Lakes perchlorate samples.

Figure 2.2.3. Diagram comparing $^{36}\text{Cl}/\text{Cl}$ vs. $\delta^{37}\text{Cl}$ values for perchlorate from the Great Lakes, in comparison with synthetic perchlorate, and natural perchlorate from Atacama (Chile) and the western USA.

Figure 2.2.4. Estimated perchlorate fluxes in the Great Lakes.

Figure 2.3.1. Map of Sample Locations

Figure 2.3.2. Relations among ClO_4^- , NO_3^- , and Cl^- concentrations in groundwater. Ratios for all groundwater samples are shown by solid black lines.

Figure 2.3.3. Relations between concentrations of ClO_4^- and NO_3^- and Cl^- for all soils and caliches.

Figure 2.3.4. Relations among ClO_4^- , NO_3^- , and Cl^- in groundwater from arid and semi-arid locations.

Figure 2.3.5. Relations among ClO_4^- , NO_3^- , and Cl^- concentrations in soils and caliches from arid and semi-arid locations.

Figure 2.3.6. Relation between $\delta^{15}\text{N}$ and $\delta^{18}\text{O}$ of NO_3^- in groundwater and leachate from soil and caliche samples.

Figure 2.3.7. Variation of (A) $\text{NO}_3^-/\text{ClO}_4^-$ or (B) $\text{Cl}^-/\text{ClO}_4^-$ ratios with respect to $\text{Cl}^-/\text{NO}_3^-$ ratios in soils and groundwaters from arid and semi-arid locations as well as wet and dry deposition in North America.

Figure 2.3.8. Relation between $\delta^{18}\text{O}$ of NO_3^- and bulk $\text{NO}_3^-/\text{ClO}_4^-$ ratios in soils and groundwaters from arid and semi-arid locations as well as wet and dry deposition in North America.

Figure 2.4.1. Map of Taylor Valley, Antarctica showing the locations of Lake Fryxell, Lake Bonney, and Lake Hoare.

Figure 2.4.2. Concentration profiles of ClO_4^- and ClO_3^- , Cl^- and SO_4^{2-} in Lake Hoare, December 2009.

Figure 2.4.3. Molar ratios of $\text{ClO}_4^-/\text{Cl}^-$ and $\text{ClO}_3^-/\text{Cl}^-$ with depth in MCM lakes and feed waters for lake basins in Taylor Valley and the Onyx River in Wright Valley.

Figure 2.4.4. Concentration profiles of ClO_4^- and ClO_3^- , Cl^- and SO_4^{2-} in the EL of Lake Bonney, December 2009.

Figure 2.4.5. Relationship of ClO_3^- and ClO_4^- concentration in Dry Valley Lakes.

Figure 2.4.6. Concentration profiles of ClO_4^- and ClO_3^- , Cl^- and SO_4^{2-} in the WL of Lake Bonney, December 2009.

Figure 2.4.7. Concentration profiles of ClO_4^- and ClO_3^- , Cl^- and SO_4^{2-} in Lake Fryxell, December 2008.

Figure 2.4.8. Concentration profiles of ClO_4^- and ClO_3^- , Cl^- and SO_4^{2-} in Lake Miers, December 2008.

Figure 2.5.1. Chlorine dioxide gas-generating absorption system.

Figure 2.5.2. Experimental set-up for aqueous O₃ oxidation experiments.

Figure 2.5.3. Experimental set-up for O₃ oxidation of dry Cl⁻.

Figure 2.5.4. Experimental set-up for UV oxidation experiments using the Rayonet photochemical chamber.

Figure 2.5.5. Stable isotopic composition of initial and final species for O₃ oxidized dry Cl⁻.

Figure 2.5.6. Stable isotopic composition of initial and final species for O₃ oxidized solutions of Cl⁻ (aq).

Figure 2.5.7. Stable isotopic composition of initial and final species for O₃ oxidized solutions of OCl⁻ (aq).

Figure 2.5.8. Stable isotopic composition of initial and final species for O₃ oxidized solutions of ClO₂⁻ (aq).

Figure 2.5.9. Stable isotopic composition of initial and final species for O₃ oxidized solutions of ClO₂ (aq).

Figure 2.5.10. Stable isotopic composition of initial and final species for solutions of OCl⁻ (aq) exposed to 350 nm irradiation.

Figure 2.5.11. Stable isotopic composition of initial and final species for solutions of ClO₂⁻ (aq) exposed to 350 nm irradiation.

Figure 2.5.12. Stable isotopic composition of initial and final species for solutions of ClO₂ (aq) exposed to 350 nm irradiation.

Figure 2.5.13. Stable isotopic compositions ($\delta^{37}\text{Cl}$, $\delta^{18}\text{O}$, $\Delta^{17}\text{O}$) of reactant species and final ClO₄⁻ for O₃ oxidized solutions.

Figure 2.5.14. Stable isotopic composition ($\delta^{37}\text{Cl}$, $\delta^{18}\text{O}$, $\Delta^{17}\text{O}$) of reactant species and final ClO₄⁻ for UV oxidized solutions.

Figure 2.5.15. Relationship between $\delta^{37}\text{Cl}$ of final ClO₄⁻ produced by UV and O₃ mediated oxidation of Cl⁻ (s), Cl⁻ (aq), OCl⁻ (aq), ClO₂⁻ (aq), ClO₂ (aq) and the oxidation state of Cl in precursor ClO_x species.

Figure 2.5.16. Combined final pathways determined responsible for ClO_4^- formation by O_3 oxidation of Cl^- (dry and aq).

Figure 2.5.17. Combined final pathways determined responsible for ClO_4^- formation by O_3 oxidation of Cl^- including possible pathways for ClO_3^- formation (aq).

Figure 2.5.18. Combined final pathways determined responsible for ClO_4^- formation by O_3 oxidation of Cl^- (aq) including possible pathways for ClO_3^- formation.

Figure 2.5.19. Combined final pathways determined responsible for ClO_4^- formation by O_3 oxidation of OCl^- (aq).

Figure 2.5.20. Combined final pathways determined responsible for ClO_4^- formation by O_3 oxidation of OCl^- including possible pathways for ClO_3^- formation (aq).

Figure 2.5.21. Combined final pathways determined responsible for ClO_4^- formation by O_3 oxidation of ClO_2^- (aq).

Figure 2.5.22. Combined final pathways determined responsible for ClO_4^- formation by O_3 oxidation of ClO_2^- including possible pathways for ClO_3^- formation (aq).

Figure 2.5.23. O_3 oxidation of ClO_2 (aq). Note the thick maroon lines indicate the pathway leading to the formation of the ClO_4^- and black solid circles represent reaction number from Table 3.4. This pathway leads to the formation one ClO_4^- molecule containing two O from O_3 .

Figure 2.5.24. UV oxidation of OCl^- (aq).

Figure 2.5.25. UV oxidation of ClO_2^- (aq).

Figure 2.5.26. UV oxidation of ClO_2 (aq).

Figure 2.5.27. Stable O isotopic compositions ($\delta^{18}\text{O}$ and $\Delta^{17}\text{O}$) of reactant species and final ClO_4^- for O_3 oxidized ClO_x solutions including expected $\delta^{18}\text{O}$ and $\Delta^{17}\text{O}$ of ClO_4^- formed from the mixture of H_2O and O_3 (with complete site preference of the heavy O isotope in the terminal O atoms of O_3) (black circles) and expected $\delta^{18}\text{O}$ and $\Delta^{17}\text{O}$ of ClO_4^- formed from the mixture of H_2O and O_3 (with no site preference of the heavy O isotope in the terminal O atoms of O_3) (green circles).

Figure 2.5.28. Summary of isotope data for ClO_4^- produced in the O_3 (square symbols) and UV (circle symbols) generation experiments.

Figure 2.6.1. Results of MCD assays.

Figure 2.7.1. Inter-specific differences in perchlorate content ($\mu\text{g (kg dry wt)}^{-1}$) of youngest fully expanded leaves of a range of crop species (mean over all O_3 exposures \pm SE). Bars with different letters differ at $P < 0.05$.

Figure 2.7.2. There was no significant relationship between basal perchlorate content (at 4 ppb O_3) and the change in ClO_4^- content (unitless) between 4 and 59 ppb O_3 (circles) and between 4 and 114 ppb (squares) of youngest fully expanded leaves of a range of crop species.

Figure 2.7.3. There was no significant relationship between O_3 exposure (A; $r^2 = 0.0034$) or O_3 dose (cumulative flux; B; $r^2 = 0.0018$) and ClO_4^- content of young leaves normalized by the median ClO_4^- content of each species shown in Figure 2.7.1 for which O_3 flux data were available.

Figure 2.7.4. Significant relationship between perchlorate concentration ($\mu\text{g (kg dry wt)}^{-1}$) of potting medium exposed in the CSTRs and O_3 exposure (nL L^{-1} ; 12 hr mean; $r^2 = 0.99$; $P = 0.0714$).

Figure 2.7.5. Relationship between perchlorate concentration ($\mu\text{g (kg dry wt)}^{-1}$) of young leaves and O_3 exposure.

Figure 2.7.6. Effect of O_3 exposure on stomatal conductance (g_s).

Figure 2.7.7. Relationship between (A) perchlorate concentration of young leaves ($\mu\text{g (kg dry wt)}^{-1}$) and O_3 dose; or (B) perchlorate concentration (unitless) normalized by the median concentration over all O_3 within each species, and O_3 dose.

Figure 2.8.1. Cumulative volume of growth solution uptaken by pooled replicate treatments in both experiments.

Figure 2.8.2. Fraction of ClO_4^- , Cl^- , and NO_3^- mass remaining in nutrient solutions at the time of harvest.

Figure 2.8.3. Relationship between fraction of total (a) ClO_4^- , (b) Cl^- , and (c) NO_3^- mass lost from solution and cumulative volume of solution transpired over the course of experiment 2.

Figure 2.8.4. Stable ClO_4^- isotopic composition of nutrient solutions and leaf extracts of replicate treatments in experiment 1 and 2.

Figure 2.8.5. Stable isotopic composition of NO_3^- in nutrient solutions as a function of time for experiment 1 (a, b) and experiment 2 (d, e).

Figure 2.8.6. Rayleigh plots of the change in the $\delta^{15}\text{N}$ and $\delta^{18}\text{O}$ of NO_3^- in nutrient solutions of experiment 1 (a, b, c) and experiment 2 (d, e, f). =F

Figure 2.8.7. Stable isotopic composition of NO_3^- in final growth solutions (solid symbols) and leaf extracts (open symbols) of pooled replicate treatments in experiments 1 and 2.

Figure 2.8.8. Summary of isotope data for ClO_4^- from Raleigh, NC and Long Island, NY field studies and commercial spinach displayed with previously published ClO_4^- isotope data from synthetic and natural sources from the Atacama Desert in Chile, Death Valley (DV), California, and the Southern High Plains (SHP) and Middle Rio Grande Basin (MRGB) of Texas and New Mexico (Jackson et al., 2010; Böhlke et al., 2005; Bao and Gu, 2004; Hatzinger et al., 2011).

ACRONYM LIST

Acronyms and Abbreviations

‰	per mil
δ, Δ	delta, relative difference of isotope ratios
ACS	American Chemical Society
ANOVA	Analysis of Variance
Ag	silver
AgCl	silver chloride
AgNO ₃	silver nitrate
Al	aluminum
Al ₂ O ₃	activated alumina
AMS	accelerator mass spectrometry
Aq	aqueous
Ar	argon
Br ⁻	bromide
BV	bed volumes
°C	degrees Celsius
Ca	calcium
ccSTP	cubic centimeters at Standard Temperature and Pressure
CCL	Contaminant Candidate List of USEPA
CFC	chlorofluorocarbon
CF-IRMS	continuous-flow isotope ratio mass spectrometry
CH ₄	methane
CH ₃ Cl	methyl chloride
CH ₃ I	methyl iodide
Cl ⁻	chloride
Cl	chlorine
³⁵ Cl	chlorine-35
³⁶ Cl	chlorine-36
³⁷ Cl	chlorine-37
ClO ₂	chlorine dioxide
ClO ₂ ⁻	chlorite
ClO ₃ ⁻	chlorate
ClO ₄ ⁻	perchlorate
ClO _x	oxychlorine species
cm	centimeters
CO	carbon monoxide
CO ₂	carbon dioxide
COC	chain of custody
CsCl	cesium chloride
CsClO ₄	cesium perchlorate
CsOH	cesium hydroxide

CSTR	continuously stirred tank reactor
DDI	distilled deionized water
DI	deionized water
DI-IRMS	dual-inlet isotope ratio mass spectrometry
DO	dissolved oxygen
DOC	dissolved organic carbon
DoD	Department of Defense
EL	East Lobe Lake Bonney, Antarctica
EPA	Environmental Protection Agency
ESTCP	Environmental Security Technology Certification Program
Fe³⁺	Iron (III)
FeCl₃	iron (III) chloride
FeCl₄⁻	tetrachloroferrate
Fe(OH)₃	iron (III) hydroxide
ft	feet
FW	fresh weight
g	gram
gal	gallon
GC	gas chromatograph
g_s	stomatal conductance
³H	tritium
ha	hectare
HCl	hydrochloric acid
HClO₄	perchloric acid
HCO₃	bicarbonate
He	helium
HNO₃	nitric acid
H₂O	water
H₂O₂	hydrogen peroxide
HPLC-UV	high performance liquid chromatography with ultraviolet detection
hr	hours
H₂SO₄	sulfuric acid
IAEA	International Atomic Energy Agency
IC	ion chromatography
IO₃⁻	iodate
IRMS	isotope-ratio mass-spectrometry
ITRC	Interstate Technology & Regulatory Council
IX	ion exchange
k	one thousand
K	potassium
KCl	potassium chloride
KClO₄	potassium perchlorate
kg	kilogram
km²	square kilometer

KNO₃	potassium nitrate
KOH	potassium hydroxide
L	liter
LUB	Lower Umatilla Basin
LC-MS/MS	liquid chromatography-tandem mass spectrometry
µg	microgram
µg/L	microgram per liter
µm	micron
µmol	micromole
M	molar
m	meter
MDL	method detection limit
MDV	McMurdo Dry Valleys, Antarctica
Mg	magnesium
mg	milligram
MRGB	Middle Rio Grande Basin
min	minute
mL	milliliter
mm	millimeter
mM	millimolar
MS	mass spectrometry
Msl	mean sea level
<i>n</i>	amount of substance
N	nitrogen or normal or number of entities
N₂	nitrogen gas
Na	sodium
NaCl	sodium chloride
NaClO₄	sodium perchlorate
NaOCl	sodium hypochlorite (bleach)
NaOH	sodium hydroxide
NASA	National Aeronautics and Space Administration
Na₂S₂O₃	sodium thiosulfate
Ne	neon
ng	nanogram
NH₄ClO₄	ammonium perchlorate
NH₄	ammonia
Ni	nickel
nL	nanoliter
N₂O	nitrous oxide
NO₂⁻	nitrite
NO₃⁻	nitrate
NO₃-N	nitrate as nitrogen
NRC	National Research Council of the National Academies of Science
O	oxygen

¹⁶O	oxygen-16
¹⁷O	oxygen-17
¹⁸O	oxygen-18
O₂	oxygen gas
O₃	ozone
OCl⁻	hypochlorite
ORNL	Oak Ridge National Laboratory
ORP	oxidation-reduction potential
per mil (‰)	part per thousand ($\times 10^{-3}$)
ppb	part per billion ($\times 10^{-9}$)
pmc	percent modern carbon
ppm	part per million ($\times 10^{-6}$)
PO₄³⁻	phosphate
PRIME	Purdue Rare Isotope Measurement Laboratory
QA/QC	Quality Assurance/Quality Control
RfD	reference dose
S	sulfur
SERDP	Strategic Environmental Research and Development Program
SHP	Southern High Plains
SMOC	Standard Mean Ocean Chloride
SO₂	sulfur dioxide
SO₄²⁻	sulfate
TDS	total dissolved solids
TOC	total organic carbon
TU	tritium unit
μg	micrograms
UIC	University of Illinois at Chicago
U.S.	United States
UV	ultraviolet
USEPA	United States Environmental Protection Agency
USGS	U.S. Geological Survey
VOCs	volatile organic compounds
VSMOW	Vienna Standard Mean Ocean Water
WL	West Lobe Lake Bonney, Antarctica
x	mole fraction
yr	year

ACKNOWLEDGEMENTS

The project team includes Dr. Paul B. Hatzinger (CB&I Federal Services, LLC; CB&I; formerly Shaw Environmental, Inc), Mr. Greg Harvey (U.S. Air Force), Dr. W. Andrew Jackson (Texas Tech University), Dr. Neil C Sturchio (University of Delaware; formerly at University of Illinois at Chicago), Dr. J.K. Böhlke, (USGS), Dr. Baohua Gu (Oak Ridge National Laboratory), Dr. David Grantz (University of California, Riverside), Dr. Kent Burkey (USDA-ARS Plant Science Research Unit), and Dr. Margaret McGrath (Cornell University). Our research team gratefully acknowledges the financial and technical support provided for this project by the Strategic Environmental Research and Development Program (SERDP). We also acknowledge support provided by the USGS National Research Program. Oak Ridge National Laboratory is managed by UT-Battelle LLC for U.S. Department of Energy under contract DE-AC05-00OR22725. We thank Dr. Andrea Leeson from SERDP for her guidance and the support staff at Hydrogeologic for their administrative assistance. Major contributors to this work included Stanley Mroczkowski (USGS), Linnea Heraty, Abe Beloso Jr., and Armen Poghosyan (University of Illinois at Chicago), Sheryl Streger and Charles Condee (CB&I), Dr. Balaji Rao and Dr. Nubia Estrada (Texas Tech University: TTU). Any use of trade, product, or firm names is for descriptive purposes only and does not imply endorsement by the U.S. Government. Views, opinions, and/or findings contained in this report are those of the authors and should not be construed as an official Department of Defense position or decision unless designated by other official documentation.

EXECUTIVE SUMMARY

Objectives

Perchlorate (ClO_4^-) has both synthetic and natural sources. Stable isotope analysis of O ($\delta^{18}\text{O}$, $\delta^{17}\text{O}$) and stable ($\delta^{37}\text{Cl}$) and radioactive (^{36}Cl) isotope analysis of Cl in ClO_4^- allows natural and synthetic ClO_4^- to be distinguished from each other and provides information on the potential origin(s) of natural ClO_4^- . The goal of this research effort was to develop an improved understanding of (1) the distribution and isotopic characteristics of natural ClO_4^- worldwide, (2) the mechanisms of natural ClO_4^- production and (3) the contributing processes resulting in the ubiquitous distribution of this anion and its stable isotope characteristics in soils, groundwater, and vegetation.

Technical Approach

In order to achieve these goals, several different laboratory and field research tasks were undertaken. These objectives and tasks were designed to fill existing data gaps on the production, distribution and isotopic characteristics of natural ClO_4^- . The first tasks were designed to improve our understanding of ClO_4^- distribution, significant environmental ClO_4^- production mechanisms and the stable isotopic signature of the produced ClO_4^- . These tasks included the following: (1) determination of the isotopic signature of ClO_4^- produced by O_3 and UV oxidation of Cl^- and relevant ClO_x species; (2) development of an improved understanding of the occurrence and isotopic signature of natural ClO_4^- and its relationship with NO_3^- and other anions in arid and semi-arid environments worldwide; and (3) evaluation of the potential for microbial production of ClO_4^- . A second set of tasks were designed to better understand plant accumulation of environmental ClO_4^- , whether its isotopic signature is altered during uptake and accumulation, and/or whether plants can actually generate ClO_4^- via an O_3 -mediated mechanism.

Results

The results from a range of different laboratory studies evaluating ClO_4^- formation mechanisms confirm that there are multiple potential pathways of ClO_4^- generation from both UV-photolysis and O_3 -mediated oxidation of Cl^- and other ClO_x precursors. Laboratory studies were successful in producing Cl and O isotopic variations in ClO_4^- that incorporate much of the reported stable isotope variation in natural ClO_4^- . Only the characteristic low $\delta^{37}\text{Cl}$ values of Atacama ClO_4^- (Chile) were not reproduced and these remain enigmatic. Data indicate that final ClO_4^- isotopic composition is dependent on the precursor species oxidized. The reaction rates and intermediate species proposed to be involved in ClO_4^- formation require further study and additional experiments are required to resolve the reason for the low $\delta^{37}\text{Cl}$ values of Atacama ClO_4^- , but significant progress was made in constraining pathways of ClO_4^- production in nature by application of stable isotope analysis.

Soil and groundwater sampling was conducted worldwide (including the continental US, South Africa, South America, China, Antarctica, and the Middle East) to evaluate concentrations of

ClO_4^- and its relationship with common co-occurring anions such as Cl^- and NO_3^- among others. The data indicate that ClO_4^- is globally distributed in soil and groundwater in arid and semi-arid regions on Earth at concentrations ranging from 10^{-1} to 10^6 $\mu\text{g/kg}$. Generally, the ClO_4^- concentration in these regions increases with aridity index, but this also depends on the duration of arid conditions. In many arid and semi-arid areas, NO_3^- and ClO_4^- co-occur at consistent ratios ($\text{NO}_3^-/\text{ClO}_4^-$) that vary between $\sim 10^4$ and $\sim 10^5$. This is not the case for $\text{Cl}^-/\text{ClO}_4^-$ ratios, which vary widely among locations. The $\text{NO}_3^-/\text{ClO}_4^-$ ratios are largely preserved in hyper-arid areas that support little or no biological activity (e.g. plants or bacteria), but can be altered in areas with more active biological processes. In general, the co-occurrence of ClO_4^- and NO_3^- in arid and semi-arid locations, and associated variations in the isotopic composition of the NO_3^- , are consistent with a conceptual model of atmospheric origin, global co-deposition, and variable alteration of the NO_3^- pool by biogenic addition, assimilation, and/or recycling on the surface. The Atacama Desert appears to be unique compared to other arid and semi-arid locations. There, exceptional enrichment in ClO_4^- compared to Cl^- or NO_3^- , accompanied by unique ClO_4^- isotopic characteristics, may reflect an unusually efficient, but yet unknown, *in situ* production mechanism, regionally elevated atmospheric ClO_4^- production rates, or higher ClO_4^- production rates in pre-Pleistocene times.

Stable isotope analysis of Cl and O and radioactive isotope analysis of ^{36}Cl in natural ClO_4^- confirmed and extended initial data suggesting that indigenous ClO_4^- sources in the southwestern U.S. show some isotopic variation by location and environment but remain isotopically distinct from synthetic and Atacama ClO_4^- when all relevant isotope ratios are considered. ClO_4^- concentration and isotope analysis was conducted in all five of the North American Great Lakes. The data showed average ClO_4^- concentrations ranging from 0.05 to 0.13 $\mu\text{g/L}$ (varying by lake) with concentrations being nearly constant with depth. Interestingly, the overall ranges of stable isotopic compositions of Great Lakes ClO_4^- resemble those of indigenous natural ClO_4^- measured in groundwaters of the western USA indicating a predominantly natural atmospheric source of ClO_4^- in all of the lakes. Bomb-pulse ^{36}Cl is largely retained in Lake Superior because of the 191-yr water residence time in the lake.

Several potential biological mechanisms of ClO_4^- generation were evaluated to determine if any could be a secondary source of this anion in the environment and to help explain the isotopic characteristics and variation in some natural ClO_4^- samples. Bacterial production of ClO_4^- was assessed using (1) various nitrifying cultures and enrichments that oxidize NH_4 to NO_3^- ; (2) natural haloperoxidase enzymes that are known to oxidize Cl^- to hypochlorous acid (HClO) and potentially to ClO_4^- (possibly via additional photochemical or biological reactions); and (3) organisms capable of oxidizing sulfite or phosphite. A variety of experiments were conducted with Cl^- or ClO_x precursors in the presence of different enzymes, organisms, and conditions as summarized above. While some ClO_4^- generation was initially indicated via haloperoxidase enzymes in the presence of UV light, this result was not consistent and is unlikely to account for

significant ClO_4^- production. The other organisms and processes evaluated did not result in ClO_4^- formation.

A variety of plant species were also evaluated for their potential to accumulate and even generate ClO_4^- via O_3 -mediated processes. Plants, particularly in arid environments, may contain abundant Cl^- in their tissues; display a vast array of hydrated internal and external reaction surfaces; and catalyze a multitude of redox reactions that could be involved in biosynthesis of ClO_4^- . These factors, the ubiquitous distribution of plants, and the post-industrial increase in O_3 exposure are consistent with the possibility that tropospheric O_3 may induce biosynthesis of ClO_4^- from Cl^- in plants. This was evaluated as a potentially novel source of ClO_4^- in the environment.

A broad range of crop species was observed to accumulate ClO_4^- from growth media, and these species differed widely in their bioconcentration of the anion. Foliar ClO_4^- concentration was greatest in older leaves, which ultimately contribute to the litter layer, suggesting that scavenging of ClO_4^- from deeper soil horizons could lead to redistribution on the soil surface. However, there was no evidence that exposure of leaves to ambient O_3 or at significantly elevated O_3 induced any increase in tissue contents of ClO_4^- . The results indicate that O_3 does not lead to increased phyto-accumulation or plant biosynthesis of ClO_4^- .

The impact of plant accumulation of ClO_4^- on Cl and O stable isotope values was also evaluated in both hydroponic laboratory studies and field crops grown in different parts of the U.S. In hydroponic studies with snap beans, no substantial differences were observed in the $\delta^{37}\text{Cl}$, $\delta^{18}\text{O}$, or $\Delta^{17}\text{O}$ values of ClO_4^- between the growth solutions and leaf extracts. In contrast to ClO_4^- , $\delta^{15}\text{N}$ of NO_3^- in plant tissue was fractionated substantially (~10-20‰). The $\epsilon^{15}\text{N}/\epsilon^{18}\text{O}$ ratios of 1.04 – 1.07 support previous experimental studies showing similar ratios via assimilatory nitrate reductase. The data indicate that plants do not metabolize and assimilate ClO_4^- similarly to NO_3^- .

Similar to hydroponically grown plants, field grown plants exposed to environmentally relevant ClO_4^- concentrations also did not appear to affect foliar ClO_4^- isotopic composition. ClO_4^- extracted from snap beans grown in Raleigh, NC varied somewhat in isotopic composition between two growing seasons based presumably on the source of irrigation water, but the stable isotope data clearly showed a significant component of Atacama-type ClO_4^- from past fertilizer use which was also the predominant source in local groundwater based on isotopic analysis. Commercial spinach was also extracted and analyzed for ClO_4^- stable isotopes. The spinach had an isotopic composition similar to that of indigenous natural ClO_4^- from the Southern High Plains of West Texas and New Mexico as well as the North American Great Lakes. This result could indicate the spinach was exposed to natural ClO_4^- with a similar isotopic composition in soil or irrigation water in one or both of the potential source areas of the spinach (Arizona and southwestern California). Although this spinach that was extracted represents only one composite sample, these results combined with those of field bean and hydroponic studies suggest that it should be possible to evaluate the dominant source of ClO_4^- (i.e., synthetic, Atacama, indigenous) in commercial produce and in other plant-based food products through

stable isotope analysis of plant accumulated ClO_4^- . This finding is important because most of the exposure to ClO_4^- in the U.S. population and likely the populations of many other countries is through ingestion of produce.

Benefits:

Overall, the results of this project have provided important new information on natural ClO_4^- in the environment. Significant progress was made concerning potential mechanisms of its formation, isotopic characterization of natural ClO_4^- sources in groundwater, lakes, soils and plants, and its worldwide occurrence and accumulation in arid and semi-arid environments. The data support previous studies showing that natural and synthetic ClO_4^- can be differentiated by stable isotope methods, and suggest for the first time that the source(s) of ClO_4^- in food crops may be determined by isotopic analysis of ClO_4^- in plant tissue.

1.0 PROJECT BACKGROUND AND OBJECTIVES

1.1 Background

In the United States (U.S.), perchlorate (ClO_4^-) is mainly used as an oxidant in the production of rocket propellants and missile fuel by the U.S. Department of Defense (DOD), the National Aeronautics and Space Administration (NASA), and other munitions facilities. These facilities, along with road safety flares, fireworks, blasting explosives, and electrolytic chlorine products, like hypochlorite (OCl^-) and chlorate (ClO_3^-), are major contributors to the ClO_4^- contamination of water supplies in North America (ITRC, 2005; Geosyntec, 2005; Dasgupta et al., 2006). California and Nevada are two states heavily impacted by the anthropogenic use of ClO_4^- . A former chemical manufacturing factory outside of Las Vegas, Nevada is considered to be the source of surface water contamination in Lake Mead and the Colorado River, along with groundwater in the area (Hogue, 2003). These waters are used as a drinking water resource for communities in California, Nevada, and Arizona and are also used for irrigation of crops grown in those regions (Hogue, 2003). Because of the use of ClO_4^- contaminated waters like these for irrigation purposes, vegetation has also been found to contain the ClO_4^- anion and could thus be transferred to humans or animals that ingest these crops (Hogue, 2003; Jackson et al., 2005). Along with edible vegetation, ClO_4^- has also been detected in milk, wine, beer, and vitamins (Jackson et al., 2005; Kirk et al., 2003; El Aribi et al., 2006; Snyder et al., 2006).

Studies conducted over the past few decades reveal that ClO_4^- occurrence is not limited to anthropogenic production or use. The oldest, most widely known natural source of ClO_4^- in the environment is the Atacama Desert in northern Chile. The Atacama Desert is one of the most arid places on Earth and contains caliche ores rich in nitrate (NO_3^-) salts, which also contain ClO_4^- (Ericksen, 1983). Since the 1830s, the nitrate deposits have been used extensively as a nitrate source in fertilizers in many parts of the world (Ericksen, 1983). In more recent years, ClO_4^- of atmospheric origin has also been found in the groundwater of New Mexico and northwest Texas, rainwater across the U.S., and various unsaturated zones of the southwest U.S. (Plummer et al., 2006; Rajagopalan et al., 2006, 2009; Rao et al., 2007; Jackson et al., 2010, 2016). The extent of naturally occurring ClO_4^- is not exclusive to North America, but has also been reported in high concentrations in the dry valleys of Antarctica and most interestingly in the soil of the planet Mars (Kounaves et al., 2010; Hecht et al., 2009).

The presence of ClO_4^- in produce and drinking water has created a public health concern and has further sparked debate on the importance of its removal from contaminated sites. Ingestion of the contaminant inhibits the uptake of iodide by the sodium-iodide symporter of the human thyroid, ultimately depressing the production of key thyroid hormones in humans (Greer et al., 2002). Because the thyroid gland is responsible for the neurological development and growth of youth, particularly infants and fetuses, proper thyroid hormone function is an important factor for proper maturity (Porterfield et al., 1994). Pregnant mothers and people who have iodine

deficiencies are more prone to be affected by ClO_4^- ingestion, with the deficiency in the mothers being more likely to affect the fetuses (Porterfield et al., 1994).

In 2005, the National Research Council (NRC) of the National Academies of Science presented a review outlining the health implications of ClO_4^- exposure to sensitive populations, such as those described above (National Academies, 2005). The Environmental Protection Agency (EPA) subsequently established a reference dose (RfD) for ClO_4^- of $0.7\mu\text{g}$ per kg body weight per day (USEPA, 2005). Although EPA has not officially set a national drinking water regulation for ClO_4^- , the Agency has included the contaminant in the Contaminant Candidate List (CCL) for: 1998, 2005, and 2009. In February 2011 the EPA announced its intention to develop a drinking water standard for ClO_4^- (USEPA, 2011), but as of the publication of this document, this standard has not been set. Due to the lack of federal regulation, Massachusetts and California have established their own drinking water standard for ClO_4^- of 2 parts per billion (ppb; $\mu\text{g/L}$) and 6 $\mu\text{g/L}$, respectively. Other states have followed suit by setting guidance levels for ClO_4^- of their own in both drinking water and groundwater ranging from 1 to 18 $\mu\text{g/L}$ (GAO, 2010). Federal regulatory guidelines for ClO_4^- are also important in establishing proper disposal techniques as well as lowering the cost of the cleanup of the contaminant by the facilities responsible for the discharge of the contaminant into the environment (GAO, 2010).

The chemical properties of ClO_4^- provide insight into its ubiquity and its potential for remediation. The ClO_4^- anion has a tetrahedral shape, with a central chlorine atom surrounded by four oxygen atoms. The chlorine atom in the ClO_4^- species has a charge of +7, an extremely high oxidation state, which makes it a desirable oxidizing agent (Brown et al., 2006). Perchlorate is meta-stable in aqueous systems and is especially resistant to reduction (Urbansky, 2002). High activation energy is required to break the kinetic barrier for ClO_4^- reduction, and thus reduction has been observed only under highly acidic conditions or by bacteria with specific enzymes (Brown et al., 2006; Urbansky, 2002; Coates and Achenbach, 2004). At ambient conditions, the ClO_4^- anion is unreactive and its low charge density inhibits formation of insoluble complexes with metals, hence its persistence in natural waters (Urbansky, 2002).

At the initiation of this research in 2008, few published data existed concerning the overall stable isotope signatures of natural ClO_4^- in the United States and abroad (Bao and Gu, 2004; Böhlke et al., 2005; Sturchio et al., 2006). However, these limited data indicated that natural ClO_4^- present in the southwest US was isotopically distinct from that found in the Atacama Desert, and that natural ClO_4^- from both areas was distinct from synthetic ClO_4^- . These data were obtained mainly via ESTCP Project ER-200509, whose primary objective was the development and validation of stable isotope methods for chlorine (^{37}Cl and ^{35}Cl) and oxygen (^{18}O , ^{17}O , and ^{16}O) in ClO_4^- (Böhlke et al., 2005, 2009; Sturchio et al., 2006, 2011, 2014; Hatzinger et al., 2011, 2013). Characterization of radioactive ^{36}Cl in ClO_4^- was also accomplished during that project (Sturchio et al., 2009). In conjunction with additional sampling and analysis conducted during the present project (see details in Section 2.1), the isotopic characteristics of natural ClO_4^-

(Atacama and U.S. indigenous) were more clearly defined and compared to synthetic sources. The isotopic characteristics of these different types of ClO_4^- are illustrated in Figure 1.1.1 and 1.1.2 and summarized as follows (from Hatzinger et al., 2013):

- Synthetic ClO_4^- produced by electrochemical reaction is characterized by (1) a mean $\delta^{37}\text{Cl}$ value (with respect to Standard Mean Ocean Chloride; SMOC) of 0.6 ‰ and relatively narrow range of variation (-3.1 to +1.6 ‰), (2) more variable $\delta^{18}\text{O}$ values (with respect to Vienna Standard Mean Ocean Water; VSMOW) ranging from -24.8 to -12.5 ‰, and (3) $\Delta^{17}\text{O}$ values near 0 ‰, consistent with mass-dependent isotopic fractionation of O during ClO_4^- synthesis. This material also is characterized by low $^{36}\text{Cl}/\text{Cl}$ ratios (^{36}Cl mole fractions) of 1×10^{-15} to 40×10^{-15} .
- Natural ClO_4^- from caliche deposits in the Atacama Desert of Chile, and in nitrate fertilizers derived from this material, has reported $\delta^{37}\text{Cl}$ values ranging from -14.5 ‰ to -11.8 ‰, with a mean value more than 10 ‰ lower than that of synthetic ClO_4^- . Reported $\delta^{18}\text{O}$ values of Atacama ClO_4^- (-24.8 ‰ to -4.2 ‰) exhibit substantial overlap with the $\delta^{18}\text{O}$ values of synthetic ClO_4^- , but the Atacama ClO_4^- is characterized by substantially elevated values of $\Delta^{17}\text{O}$ (+4.2 to +9.6 ‰), indicating that non-mass-dependent isotope effects or precursors contributed to its formation, most likely during atmospheric generation. This natural ClO_4^- has higher $^{36}\text{Cl}/\text{Cl}$ ratios (22×10^{-15} to 590×10^{-15}) compared to synthetic ClO_4^- .
- Natural ClO_4^- from the southwestern U.S. varies somewhat by location and environment. Samples collected from a large area of the Southern High Plains (SHP) and the Middle Rio Grande Basin (MRGB) of Texas and New Mexico are similar isotopically, with $\delta^{37}\text{Cl}$ values ranging from +3.1 to +5.0 ‰, $\delta^{18}\text{O}$ values ranging from +0.6 to +3.8 ‰, and $\Delta^{17}\text{O}$ values ranging from +0.3 to +1.3 ‰. Samples collected from the arid Lower Umatilla Basin (LUB) of northeastern OR were similar isotopically to the SHP and MRGB samples, except that their $\Delta^{17}\text{O}$ values were somewhat higher (+1.7 to +2.9 ‰). The data indicate that indigenous natural ClO_4^- in the western US (represented by samples from the SHP, MRGB, and LUB) is distinguishable from both Chilean ClO_4^- and synthetic ClO_4^- when all relevant stable isotope ratios are considered.
- Natural ClO_4^- samples from caliche deposits in and around Death Valley, California have lower $\delta^{37}\text{Cl}$ values (-0.8 to -3.7 ‰) and much higher $\Delta^{17}\text{O}$ values (+8.6 to +18.4 ‰) compared to the SHP, MRGB, and LUB samples. Interestingly, however, all of the SHP, MRGB, LUB, and Death Valley samples analyzed to date are characterized by substantially elevated $^{36}\text{Cl}/\text{Cl}$ values (3130×10^{-15} to $28,800 \times 10^{-15}$) compared to those of synthetic or Chilean ClO_4^- . Overall, the SHP, LUB, MRGB, and Death Valley samples can be considered together as U.S. indigenous sources and, even though there are substantial ranges in the individual isotope ratios, this indigenous grouping is isotopically distinct from synthetic and Chilean ClO_4^- when all relevant isotope ratios are considered.

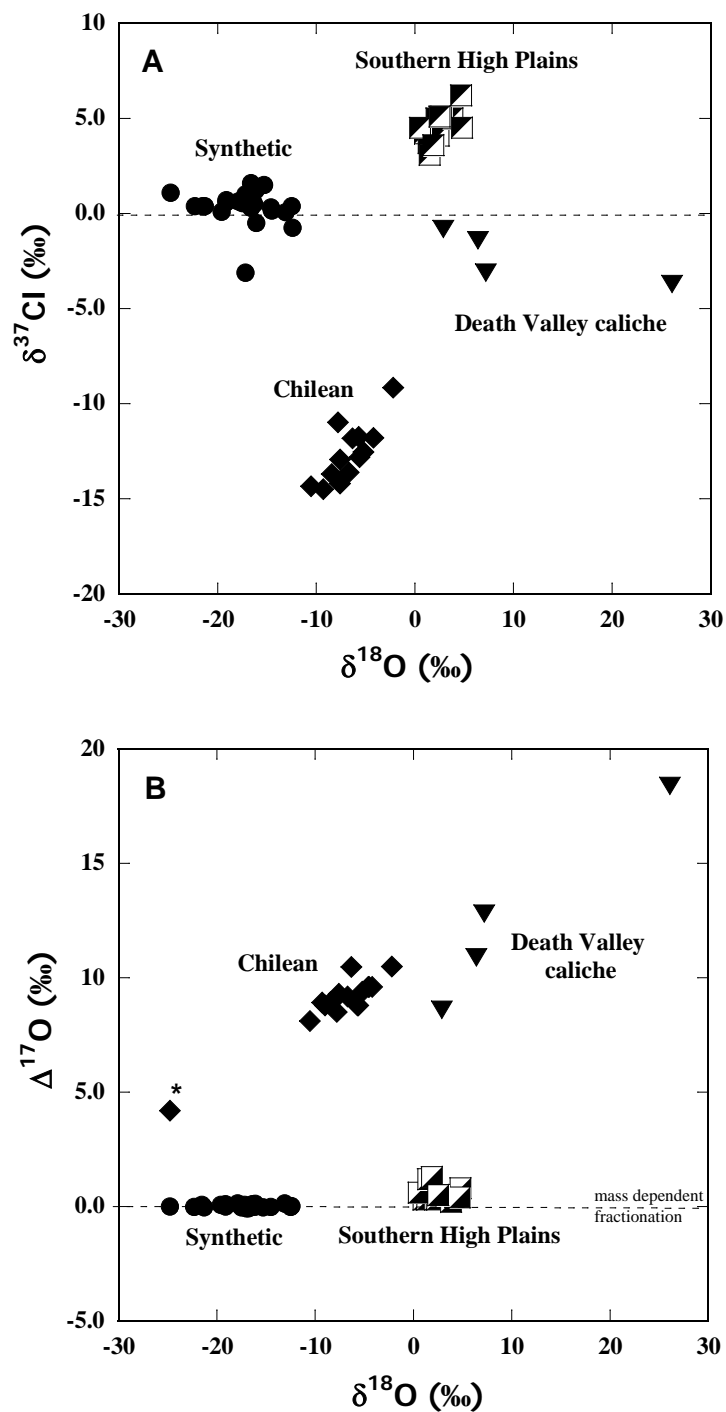


Figure 1.1.1. Comparison of $\delta^{37}\text{Cl}$ versus $\delta^{18}\text{O}$ (Plot A) and $\Delta^{17}\text{O}$ versus $\delta^{18}\text{O}$ (Plot B) in natural indigenous ClO_4^- in the U.S., natural Chilean ClO_4^- , and synthetic ClO_4^- . The single value on Plot B labeled with an asterisk is from Bao and Gu (2004). The graphs are from Hatzinger et al. (2013).

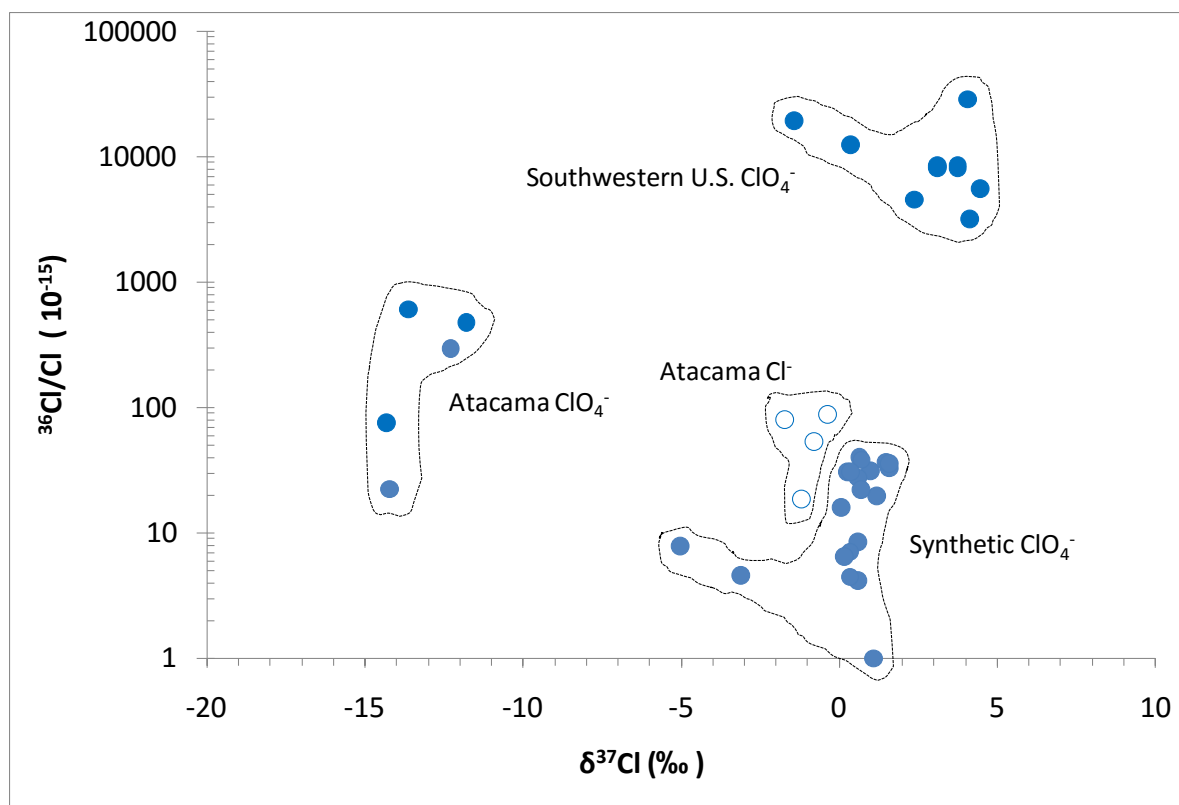


Figure 1.1.2. Values of $^{36}\text{Cl}/\text{Cl}$ (mole fraction) versus $\delta^{37}\text{Cl}$ in representative samples of synthetic ClO_4^- reagents and products, natural ClO_4^- and Cl^- extracted from soil and groundwater from the Atacama Desert, Chile, and natural ClO_4^- extracted from groundwater and soil from the southwestern U.S. Figure from Hatzinger et al., 2013.

The apparent widespread occurrence of natural ClO_4^- in the western U.S., and the differing isotopic characteristics between natural ClO_4^- derived from the Atacama Desert and that derived from the U.S., as well as the differences among samples from different regions of the southwest U.S. have generated new questions regarding the overall distribution of natural ClO_4^- worldwide, mechanisms involved in the natural generation of ClO_4^- and how isotopic compositions of the anion may be altered by various biotic and abiotic processes (Böhlke et al., 2005; Sturchio et al., 2009; Bao and Gu, 2004; Hatzinger et al., 2013). The isotopic data suggest that different ClO_4^- production pathways exist and/or that post-depositional exchanges occur in nature.

Although ClO_4^- production pathways for O_3 and UV reacting with a number of Cl starting materials have been demonstrated (e.g., Rao et al., 2010; Wang et al., 2011; Kang et al., 2008, 2009), it is still unclear which mechanism(s) or reactants are most significant in the environment. One way to approach this issue is to evaluate the stable isotopic composition of ClO_4^- produced by these mechanisms and their associated starting materials in order to compare with the known natural isotopic compositions. Secondly, there are several common enzymatic oxidation reactions in nature (e.g., nitrification, hypochlorous acid generation from chloride, sulfur oxidation) that suggest the possibility of a biological mechanism for ClO_4^- generation, which could help explain the isotopic variation in some of the natural ClO_4^- samples. Furthermore, because there is a high potential for plants to uptake, accumulate, and possibly produce ClO_4^- , there is a need to examine ClO_4^- interactions in plants and isotopic changes that may occur. No extensive research has been conducted to determine if real world plant samples grown under similar conditions all exhibit similar ClO_4^- isotopic compositions or if ClO_4^- isotopic compositions vary significantly between species. In addition, little research has examined the ability for plant uptake and transformation processes to fractionate ClO_4^- .

The core objectives and associated major tasks associated with this project address the significant questions posed above. These objectives are described in detail in Section 1.2.

1.2 Research Objectives and Associated Major Tasks

Objective 1. Evaluate ClO_4^- distribution, significant environmental ClO_4^- production mechanisms and the stable isotopic signature of the produced ClO_4^- .

Task 1. Occurrence and isotopic signature of natural ClO_4^- .

At the initiation of this project, there were relatively few data concerning the stable isotope signatures of natural ClO_4^- , most of which were gained through ESTCP Project ER-200509 (Hatzinger et al., 2013). During the current project, additional samples were collected and analyzed from various locations, including the Atacama Desert of Chile, the southwest US, and the US Great Lakes, among others. These data are reported herein.

Task 2. Occurrence of natural ClO_4^- and relationship with NO_3^- and other anions in arid and semi-arid environments worldwide.

Samples of soil and groundwater were collected from various arid and semi-arid locations around the world. Correlations between concentrations of ClO_4^- and other co-occurring anions, including NO_3^- , Cl^- , SO_4^{2-} and ClO_3^- were evaluated. These data are important for understanding the origins, relationships, and environmental fate of these different species.

Task 3. Determine the isotopic signature of ClO_4^- produced by O_3 and UV-driven oxidation of relevant Cl species.

A variety of chemical reactions and precursors could theoretically account for natural ClO_4^- in the environment. Currently available isotopic data for natural ClO_4^- indicate that multiple mechanisms may be producing natural ClO_4^- and contributing to its broad distribution. However, the actual formation mechanism(s) of ClO_4^- from various precursors are largely uncharacterized. The oxidation of chlorine and/or oxychlorine species to ClO_4^- most likely results from reaction(s) with O_3 and/or another UV-driven photochemical process. One key objective of this research was to evaluate each potential reaction with respect to O_3 or UV-produced radicals to better understand likely mechanisms of formation of natural ClO_4^- in the environment.

The isotopic composition of each product and initial reactant (e.g. O_3 , H_2O , Cl , OCl^- , ClO_2^- , ClO_3^- , and ClO_4^-) in studies of UV and O_3 generation of ClO_4^- was characterized to the extent possible. This entailed a series of purification steps followed by isotopic analysis. This information allowed evaluation of mechanistically correct formation pathway(s) of ClO_4^- consistent with isotopic signatures of reactants and products as well as new constraints on the likely formation mechanisms of natural ClO_4^- .

Task 4. Evaluate the potential for microbial production of ClO_4^- .

One potential production mechanism for natural ClO_4^- that has not been previously evaluated is microbiological generation. Nitrifying bacteria generate NO_3^- through the oxidation of NH_4 (e.g., *Nitrosomonas* spp.) and NO_2^- (e.g., *Nitrobacter* spp.) (Paerl, 1997). During this well-studied process, NH_4 serves as a microbial electron donor and oxygen as an electron acceptor (Capone, 1997). There are also anaerobic oxidation processes by which NO_3^- is biologically generated from reduced nitrogen species. Moreover, a class of widely occurring haloperoxidase enzymes produced by specific fungi, algae, and bacteria are known to oxidize Cl^- to hypochlorous acid (HClO) (Griffin, 1991; Vilter, 1995). This could represent an initial biological step in the production of natural ClO_4^- in some environments (possibly followed by additional photochemical or biological reactions). During this task, we evaluated whether microbial generation of ClO_4^- (as well as HClO , ClO_2^- , and ClO_3^-) is possible in aerobic environments using pure cultures, pure enzymes and microbial enrichments.

Objective 2. Evaluate the role of plants in production of ClO_4^- and their impact on the isotopic signature of natural ClO_4^- .

Task 5. Evaluate the role of ozone in ClO_4^- accumulation in plants.

Recent reports indicate that a substantial percentage of total exposure may be linked to ingestion of food, mainly leafy vegetables, containing ClO_4^- (e.g., USFDA, 2008; Blount et al., 2007). The ClO_4^- concentrations in plant leaves and other tissues may reflect a variety of factors, including climatic conditions and species-specific physiological parameters. Sensitivity to ozone (O_3) may be particularly important in determining ClO_4^- levels in plants. Tropospheric O_3 is a common air pollutant that has adverse effects on the growth of natural vegetation and agricultural crops worldwide (Burkey et al., 2002). Ambient ozone concentrations in the eastern United States range from 30-50 $\mu\text{g/L}$ with episodes that may exceed 100 $\mu\text{g/L}$ (Patterson et al., 2000). Ozone and associated reactive oxygen species react with all plant surfaces, but most of the O_3 damage is caused after these species enter the stomata (Heber et al., 1995). Upon passing the stomata, O_3 enters the apoplastic space of internal leaf tissues. It is within this apoplastic space that plant oxidative defense typically occurs. Some plants are more sensitive to O_3 than others. When plant oxidative defense capabilities are overwhelmed, visible foliar damage such as bronzing, flecking, and chlorosis can occur.

As natural ClO_4^- could be produced from surface oxidation reactions of Cl^- or oxychlorine species with O_3 (Kang et al., 2008), it is possible that ClO_4^- may be directly produced in plant material from interaction of ambient O_3 with Cl^- , especially in certain O_3 sensitive plants that do not have active defense systems. In addition, plants have the capacity to process (uptake and re-release) a significant portion of natural ClO_4^- even in arid climates. The isotopic composition of ClO_4^- present within plants, and changes thereof due to processing have not yet been evaluated.

Therefore, it is important to understand:

1. If plants contribute to the natural ClO_4^- pool by acting as platforms for oxidation of Cl^- by O_3 ;
2. If plants can alter the isotopic signature of ClO_4^- during uptake or internal processing;

During this task, studies were conducted with a variety of different plants at atmospheric and elevated O_3 concentrations to determine species variability and to assess whether plant production of ClO_4^- with O_3 as a reactant could be substantiated. Task 6 addresses the question concerning alteration of the isotopic signature of O and Cl in plant ClO_4^- after uptake.

Task 6. Ion selectivity and isotope effects during plant uptake and accumulation of ClO_4^- and NO_3^- .

A primary objective of this task was to investigate the potential for plants to alter the stable isotopic composition of ClO_4^- either during uptake or due to transformation or exchange within the plant. This was accomplished by comparing the stable isotopic compositions of ClO_4^- accumulated in hydroponically grown snap bean plants (*Phaseolus vulgaris* L.) with those of the starting reference materials and growth solutions. Results for NO_3^- uptake, assimilation, accumulation, and isotope effects were evaluated in the same experiments. Studies were also conducted with field-grown snap bean crops in Long Island, NY and Raleigh, NC to determine the isotopic signature of Cl and O in ClO_4^- in these crops and whether sources (e.g., synthetic vs Atacama) could be distinguished from plant-derived ClO_4^- . Finally, a commercially obtained spinach sample that was conventionally grown was extracted and the ClO_4^- obtained was analyzed for Cl and O isotopes. These isotope data were compared to those from potential ClO_4^- perchlorate sources.

2.0 PROJECT TASKS

2.1 Occurrence and Isotopic Signature of Natural ClO_4^- in Soils and Groundwater in the U.S.

2.1.1 Background: Natural Perchlorate and Nitrate

During the past decade, it has become apparent that ClO_4^- is much more widely distributed in the environment than previously thought, and that a variety of natural and anthropogenic sources may contribute to its ubiquity. Major documented sources of ClO_4^- distributed in the environment by human activities include: 1) electrochemically produced salts used as oxidants in solid rockets, air-bags, fireworks, flares, munitions and other industrial products; 2) hypochlorite and chlorate salts, which contain ClO_4^- as a minor constituent; and 3) natural NO_3^- -rich caliche salt deposits containing ClO_4^- from the Atacama Desert in Chile, which have been imported to the U.S. and elsewhere, primarily for use as fertilizer (Dasgupta et al., 2006; Aziz et al., 2006).

Natural ClO_4^- that is unrelated to the Atacama source has now been detected widely in groundwater and soils in the southwestern United States (U.S.). This “indigenous” ClO_4^- has been described in groundwater beneath a large area (53,000 km²) of the southern High Plains (SHP) of Texas and New Mexico (Rajagopalan et al., 2006), in groundwater of Holocene and Pleistocene age in the Middle Rio Grande Basin (MRGB) in New Mexico (Plummer et al., 2005), and in pre-modern (mainly Holocene) atmospherically deposited salt accumulations in the vadose zone throughout the arid southwestern U.S. (Rao et al., 2007). Perchlorate is also ubiquitous in precipitation (Rajagopalan et al., 2009) and was detected ($>40 \text{ ng L}^{-1}$) in more than 55 % of groundwater samples in a national survey of wells presumed to be minimally impacted by human activities (Parker et al., 2008). Given the widespread occurrence and potential regulatory importance of natural ClO_4^- , its origins and distinguishing characteristics (e.g., isotopic composition) are receiving increased attention, but remain poorly understood. Additional data are required to establish the isotopic characteristics and origin (or origins) of natural ClO_4^- in the diverse environments in which it has been identified.

Stable isotope ratio analysis of Cl and O in ClO_4^- has been used to distinguish anthropogenic ClO_4^- from Atacama-derived natural ClO_4^- in source materials and groundwaters (Bao and Gu, 2004; Böhlke et al., 2005, 2009; Sturchio et al., 2006). Electrochemically produced ClO_4^- has relatively well-constrained $\delta^{37}\text{Cl}$ values (-3 to $+2 \text{ ‰}$), but more variable $\delta^{18}\text{O}$ values (-25 to -13 ‰) likely reflecting variations in the source water and fraction of O lost during production, and $\Delta^{17}\text{O}$ values that are consistent with mass-dependent fractionation of O isotopes ($\Delta^{17}\text{O} = 0.0 \pm 0.1 \text{ ‰}$) (Bao and Gu, 2004; Böhlke et al., 2005, 2009; Sturchio et al., 2006). In contrast, Atacama ClO_4^- from saline caliche deposits and imported Chilean nitrate fertilizers has isotopic compositions ($\delta^{37}\text{Cl} = -15$ to -12 ‰ ; $\delta^{18}\text{O} = -25$ to -3 ‰ and $\Delta^{17}\text{O} = +4$ to $+11 \text{ ‰}$) that are distinct from those of synthetic perchlorate. Elevated $\Delta^{17}\text{O}$ values in ClO_4^- from the Atacama Desert have been interpreted as evidence that ClO_4^- were formed in part by reactions involving

ozone (O_3) in the atmosphere, as atmospheric O_3 is known to be ^{17}O -enriched with measured and modeled $\Delta^{17}\text{O}$ values of $\sim +30$ to 40‰ (Bao and Gu, 2004; Johnson et al., 2000). Moreover, concentrations of cosmogenic ^{36}Cl are consistent with an upper atmospheric origin for natural ClO_4^- (Sturchio et al., 2009). Reported kinetic isotope effects accompanying biological reduction of ClO_4^- alter its isotopic composition in a predictable manner (Sturchio et al., 2003, 2007; Hatzinger et al., 2009) that does not obscure distinctions between synthetic and Atacama ClO_4^- when all relevant isotope ratios are considered (i.e., $\delta^{37}\text{Cl}$, $\delta^{18}\text{O}$, and $\Delta^{17}\text{O}$).

At the initiation of this project, almost no information was available regarding the stable isotopic composition of natural ClO_4^- indigenous to the U.S. Two samples from groundwater wells in the SHP had reported isotopic compositions ($\delta^{37}\text{Cl} = +6.2, +5.1\text{‰}$; $\delta^{18}\text{O} = +4.7, +2.5\text{‰}$; $\Delta^{17}\text{O} = +0.4, +0.5\text{‰}$) that were different from those of both anthropogenic and Atacama ClO_4^- (Sturchio et al., 2006). These data indicated that the SHP groundwater ClO_4^- was either a mixture of biologically fractionated, electrochemically produced ClO_4^- and a much smaller amount of Atacama-like ClO_4^- , or that it represented an isotopically distinct type of natural ClO_4^- . As a result of recent studies on the distribution and potential sources of ClO_4^- in the SHP (Rajagopalan et al., 2006), and rapidly increasing detection of trace ClO_4^- in soils (Rao et al., 2007), groundwater (Plummer et al., 2005; Parker et al., 2008), and precipitation (Rajagopalan et al., 2009) throughout the U.S., the latter explanation now appears more likely, but additional ClO_4^- isotope data are required to confirm this hypothesis and expand the database to other indigenous ClO_4^- occurrences. In addition, because ClO_4^- and NO_3^- typically coexist in terrestrial environments, relations between NO_3^- and ClO_4^- isotopes can provide important constraints on their sources and transport.

The purpose of this task was to develop data showing the variation in the isotopic composition of natural ClO_4^- indigenous to the southwestern U.S. Samples were collected from natural occurrences in soils and groundwater from the SHP of Texas and New Mexico and the MRGB in New Mexico; unsaturated sub-soil from the SHP of Texas; and surficial NO_3^- -rich caliche deposits from the Mojave Desert near Death Valley, CA. These data were combined with other chemical and isotopic data to evaluate environmental factors responsible for ClO_4^- distribution and isotopic characteristics, including the origin and isotopic composition of co-occurring NO_3^- . These studies were conducted in conjunction with ESTCP Project ER-200509.

2.1.2 Materials and Methods

2.1.2.1 Sampling Locations

Samples for ClO_4^- stable isotope ratio analysis were obtained from groundwater, unsaturated sub-soils, and caliche-type saline mineral deposits within the southwestern U.S. (Figure 2.1.1). These sites were selected because previous studies indicate that they represent natural occurrences. Additional samples were obtained from the Atacama Desert including one groundwater sample and 5 soil/caliche samples (Table 2.1.1 and 2.1.2).

Groundwater ClO_4^- samples were obtained from the SHP (including one sample from the adjacent rolling plains) of western Texas and eastern New Mexico (n=8) and from the MRGB of central New Mexico (n=2) (Table 2.1.2). The SHP wells were at 5 distinct sites, with two wells (MW2 and MW3) installed at the same location but screened at different intervals. These wells were sampled in duplicate (MW2A,B and MW3A,B) (Figure 2.1.1). A single sample (SHP-V) was obtained from a natural subsurface accumulation of salts within unsaturated sub-soils at the Range Ecology Research Site at Texas Tech University. This site is a 142 ha section of land that has been used to study numerous aspects of range ecology but has not been irrigated or subjected to other surface activity that would impact the presence of ClO_4^- . Lastly, ClO_4^- was obtained from near-surface caliche-type salt deposits on clay hills at four locations in the Death Valley region of the Mojave Desert, CA (Figure 2.1.1). Clay-hills caliche salts in this area were studied previously because of their unusually high NO_3^- concentrations, which resemble those in the Atacama Desert (Böhlke et al., 1997; Ericksen et al., 1988; Noble, L.F. 1931; Michalski et al., 2004).

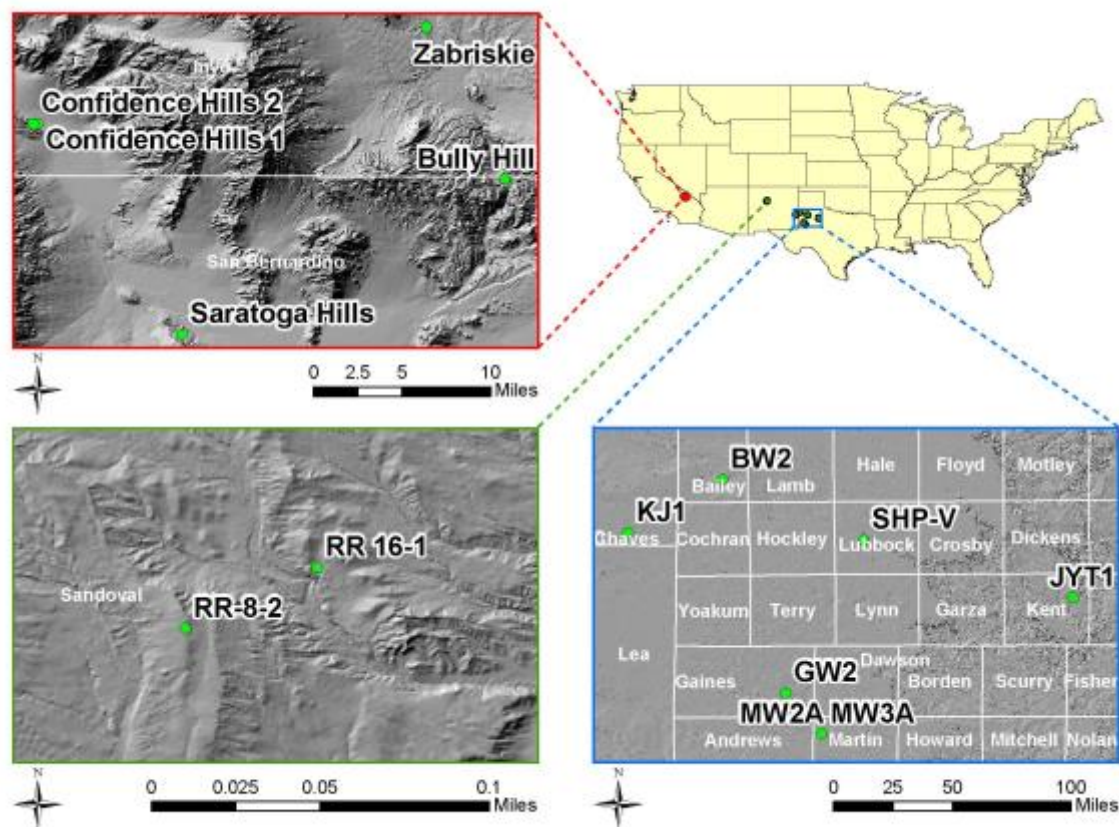


Figure 2.1.1. Sample locations for natural perchlorate. Surface deposits were collected from Death Valley, CA (red box), groundwater from the Rio Grande Basin of NM (green box) and vadose soils and groundwater from the SHP of Texas (blue box).

2.1.2.1 Sample Collection

ClO_4^- in groundwater was collected by pumping water from each well through columns containing ClO_4^- -selective anion-exchange resin (Purolite A-530E, Purolite Co., Bala Cynwyd, PA). Groundwater from wells MW3, MW2, BW2, RR8, and RR16 was pumped through resin columns in the field at flow rates ranging from ~ 0.1 to 2 L min^{-1} . For the remaining wells, water was pumped into clean polyethylene drums (208-L capacity), which were then transported to Texas Tech University where the water was passed through ion-exchange columns, as described above. The total volume of water pumped through each column varied with ClO_4^- concentration, with the final objective being to extract at least 5 mg of ClO_4^- for purification and isotopic analysis. Groundwater was also collected for major anions, other isotopic analyses (NO_3^- , SO_4^{2-} , H_2O), major dissolved gases, and environmental tracers including ^3H , ^3He , SF_6 , and chlorofluorocarbons (CFCs) (Table 2.1.2).

Perchlorate dispersed in the unsaturated zone (SHP-V) was collected by leaching soluble salts from the sub-soil and then passing the leachate through a resin column as described above for groundwater. Initially, depth-dependent samples were obtained by hand auger to evaluate the vertical distribution of salts in the unsaturated zone. Based on these data, sub-soil from approximately 2 to 4 m (depth range of maximum ClO_4^- concentration) was collected using a back hoe and placed on a tarp. Salts were extracted by mixing batches of sub-soil (40 to 60 L) and water (80 L) in a pre-cleaned cement mixer for ~ 10 minutes to form a slurry. Tap water from Lubbock, Texas was used for the extraction. Prior to use, this tap water was passed through a large column ($\sim 1,000 \text{ cm}^3$) packed with Purolite A-530E resin to reduce ClO_4^- to $< 0.05 \mu\text{g L}^{-1}$. After mixing, the slurry was allowed to settle for several hours, and then the water was decanted into polyethylene drums. The slurry in the drums was allowed to settle further overnight, after which the supernatant was pumped through a sediment pre-filter (50- μm pore-size; General Electric Co., Trevose, PA) and then through a resin column. Influent and effluent samples were taken routinely to determine the concentration of ClO_4^- applied to the column and the efficiency of perchlorate removal by the column. A total of $\sim 5,600 \text{ kg}$ of soil and $\sim 3,000 \text{ L}$ of water were processed for the extraction.

The specific location and depth of the caliche-type salt accumulations collected from Death Valley were based on the NO_3^- content of the deposits, which were determined by field testing. NO_3^- was used as an indicator of ClO_4^- based on previous data. Bulk samples (20 to 50 kg) from each location were shipped to Texas Tech University and portions of these samples were leached using ClO_4^- -free ($< 0.05 \mu\text{g L}^{-1}$) distilled de-ionized water. The samples were sequentially extracted three times with a $\sim 1:5$ solid to water mass ratio each time. The ClO_4^- dissolved in the supernatant of these extracts was combined and collected on resin columns as described above. The concentrations of soluble salts in the bulk solids were estimated after drying and weighing the leached material after extraction. Aliquots of the leachate solutions were filtered and stored for chemical and isotopic analysis of solutes including ClO_4^- , NO_3^- , SO_4^{2-} , and Cl^- .

2.1.2.3 Methods for Separating and Purifying Perchlorate for Isotopic Analysis

The perchlorate samples were purified according to the methods described in Hatzinger et al., (2011). In summary, the resin from each IX column (from soils or groundwater) was dispersed in deionized water or 4M HCl in the laboratory, ultrasonically cleaned, and then repacked into a column for elution. Prior to elution, the resin was flushed with three to five bed volumes (BV) of 4M HCl to remove anions (NO_3^- , SO_4^{2-} , HCO_3^- , organic anions, etc.) and other impurities. Then ClO_4^- was eluted with 3-5 BV of a mixed solution of 1M FeCl_3 and 4M HCl, and is usually concentrated in <0.5 BV of the eluent solution. To remove Fe^{+3} from the eluent solution, neutralization with NaOH solution to pH 9-10, followed by settling and centrifugation was used to remove Fe precipitates. The resulting clear solution was then reduced by evaporation to a smaller volume (0.5-10 mL) for analysis of ClO_4^- concentration and other anionic impurities by Raman spectroscopy and/or ion chromatography. Hydrogen peroxide may be added during evaporation to oxidize organics. If necessary, a second stage of purification using a smaller A-530E column or solid-phase extractant was used to remove residual ions and impurities to achieve the desired purity of ClO_4^- as described by Hatzinger et al. (2011). Finally, the purified and concentrated ClO_4^- in solution was crystallized by the addition of CsCl or CsOH to cause supersaturation and precipitation of CsClO_4 . The CsClO_4 precipitate was then washed with 90% MeOH and air dried prior to isotopic analysis by isotope-ratio mass spectrometry. Purity of final CsClO_4 crystals was verified by micro-Raman spectroscopy. Additional details pertaining to the use of A-530E resin for ClO_4^- extraction and purification are provided elsewhere (Hatzinger et al., 2011; Gu et al., 2011).

2.1.2.4 Sample Analysis

Purified ClO_4^- in the form of CsClO_4 was shipped to the USGS laboratory in Reston Virginia for analysis of $\delta^{18}\text{O}$ and $\Delta^{17}\text{O}$ on O_2 produced by decomposition. Chloride residue from the decomposed ClO_4^- was analyzed for $\delta^{37}\text{Cl}$ at the University of Illinois at Chicago as described below. ClO_4^- concentrations were measured by sequential IC-MS/MS with a method detection limit of $0.05 \mu\text{g L}^{-1}$ (Rao et al., 2007). Major anions (Cl^- , NO_3^- , SO_4^{2-} , and Br^-) were analyzed by ion chromatography following EPA Method 300.0. Major dissolved gases, and stable isotope ratios in NO_3^- and SO_4^{2-} ($\delta^{18}\text{O}$, $\delta^{15}\text{N}$, and $\delta^{34}\text{S}$) were analyzed at the USGS in Reston (USGS, 2010). $\Delta^{17}\text{O}$ analyses of NO_3^- were also performed at the USGS in Reston on O_2 produced by thermal decomposition of purified NO_3^- [see next section]. Tritium was analyzed by electrolytic enrichment and scintillation counting at the USGS in Menlo Park, CA. ^{14}C was analyzed by accelerator mass spectrometry under contract to the USGS National Water-Quality Laboratory (Table 2.1.2).

2.1.2.5 Methods for Perchlorate Stable Isotope Analysis and Reporting

Tabulated and plotted values of $\delta^{18}\text{O}$, $\Delta^{17}\text{O}$, and $\delta^{37}\text{Cl}$ for ClO_4^- were determined by off-line sealed-tube decomposition and dual-inlet isotope-ratio mass spectrometry on O_2 (designated O2-DIIRMS) and CH_3Cl , and the data were calibrated by analyzing ClO_4^- reference materials with

the samples as described elsewhere (Hatzinger et al., 2011; Böhlke et al., 2016). Reference values adopted provisionally for USGS37: $\delta^{37}\text{Cl} = +0.6\text{‰}$, $\delta^{18}\text{O} = -17.0\text{‰}$, and $\Delta^{17}\text{O} = 0.0\text{‰}$; and for USGS38: $\delta^{37}\text{Cl} = -87.2\text{‰}$, $\delta^{18}\text{O} = +52.4\text{‰}$, and $\Delta^{17}\text{O} = +73.3\text{‰}$. A subset of the samples were also analyzed for $\delta^{18}\text{O}$ by an alternative method involving high-temperature reaction with C to produce CO, with continuous-flow isotope-ratio mass spectrometry on the CO (designated CO-CFIRMS), calibrated using the same reference materials as above. For reagents and samples with relatively high original ClO_4^- concentrations, $\delta^{18}\text{O}$ values determined by O2-DIIRMS and CO-CFIRMS methods generally were indistinguishable. For some samples purified from low ClO_4^- soils and groundwaters, however, the O2-DIIRMS values tend to be slightly lower (commonly of the order of 0.5 to 1.0 ‰). These differences are not completely understood and may be due to trace contaminants in the samples that are most difficult to purify. Nevertheless, the analytical differences are small compared to the range of isotopic compositions reported for the different ClO_4^- sources. Detailed descriptions of analytical interferences and calibrations are given by Böhlke et al. (2016).

2.1.2.6 Methods for Nitrate Stable Isotope Analysis

$\delta^{15}\text{N}$ and $\delta^{18}\text{O}$ in NO_3^- were measured by continuous-flow isotope-ratio mass spectrometry on N_2O produced from NO_3^- by bacterial reduction (Sigman et al., 2001; Casciotti et al., 2002; Coplen et al., 2004). The data were calibrated by analyzing NO_3^- isotope reference materials using calibration data in Böhlke et al. (2003). For USGS34, $\delta^{15}\text{N} = -1.8\text{‰}$ and $\delta^{18}\text{O} = -27.9\text{‰}$; for USGS32, $\delta^{15}\text{N} = 180.0\text{‰}$; for USGS35, $\delta^{18}\text{O} = +57.5\text{‰}$. For samples with elevated $\Delta^{17}\text{O}$ of NO_3^- , $\delta^{15}\text{N}$ values measured by the bacterial method using conventional normalization equations were adjusted downward to account for non-mass-dependent $\Delta^{17}\text{O}$ effects on the N_2O ion ratios, based on the measured $\Delta^{17}\text{O}$ values of the NO_3^- (Sigman et al., 2001; Böhlke et al., 2003; Coplen et al., 2004). This adjustment to $\delta^{15}\text{N}$ was equal to 0 when $\Delta^{17}\text{O} = 0$ and -1.1 ‰ when $\Delta^{17}\text{O} = +21\text{‰}$.

$\Delta^{17}\text{O}$ in NO_3^- was measured by dual-inlet isotope-ratio analysis of O_2 produced by off-line partial decomposition of AgNO_3 (Michalski et al., 2002). NO_3^- was isolated from mixed salt solutions by trapping on large-volume AG1X8 ion-exchange resin columns, followed by gradual elution with 0.5 M KCl to separate anions (Hannon et al., 2008). The KCl- KNO_3 eluent was passed through AG-MP50 cation-exchange resin columns in the Ag form to remove Cl and exchange K for Ag, then freeze dried to produce AgNO_3 salt. The AgNO_3 was heated under vacuum at 520°C while connected to a 5Å mol-sieve trap cooled with liquid N_2 to collect O_2 , which was then isolated and transferred to the mass spectrometer and analyzed against tank O_2 . No adjustments were made to the $\Delta^{17}\text{O}$ data, as the measured $\Delta^{17}\text{O}$ values of NO_3^- isotopic reference materials RSIL-N11 and USGS35 were indistinguishable from reported values of -0.2 and +21.1 ‰, respectively (Böhlke et al., 2003; Coplen et al., 2004).

2.1.3 Results and Discussion

2.1.3.1 Death Valley Caliche Salts

In the U.S., surficial NO_3^- -rich caliche deposits exist in the clay hills around the southern end of Death Valley within the Mojave Desert. These NO_3^- deposits were first described in the early 1920s and are much smaller in both aerial extent and total mass than the Atacama deposits, although the NO_3^- concentrations and $\text{NO}_3^-/\text{Cl}^-$ ratios locally are similar to those of the Atacama NO_3^- ores (Böhlke et al., 1997; Ericksen et al., 1988; Noble, 1931; Noble et al., 1922). Isotopic analyses of the Death Valley NO_3^- deposits indicate a large fraction of the NO_3^- may be atmospheric in origin, whereas the remainder is presumed to have formed via microbial nitrification (Böhlke et al., 1997; Michalski et al., 2004). Similar processes were hypothesized to account for NO_3^- in the Atacama NO_3^- deposits based on isotopic analyses with a larger fraction due to atmospheric origin (Böhlke et al., 1997; Michalski et al., 2004). As part of the current study, new samples of NO_3^- and ClO_4^- from caliche salts and groundwater in the Atacama Desert were analyzed isotopically, confirming previous results (Figure 2.1.2; Table 2.1.3). Unlike the Atacama deposits, where the presence of ClO_4^- is well established, ClO_4^- has not previously been documented as a common constituent of the Death Valley deposits (Noble, 1931; Ericksen, 1981).

In the collected Death Valley caliche samples, ClO_4^- concentrations ranged from 0.25 to 1.7 mg kg^{-1} , which are the highest reported ClO_4^- concentrations in any natural material in North America, but still approximately 1-3 orders of magnitude lower than in the Atacama NO_3^- -rich caliches (Ericksen et al., 1981). Interestingly, the NO_3^- content of the Death Valley caliche is similar to that of the Atacama caliche, or at most an order of magnitude lower (Figure 2.1.3; Table 2.1.3). Nitrate stable isotope ratios ($\delta^{18}\text{O}$, $\Delta^{17}\text{O}$, and $\delta^{15}\text{N}$) of the Death Valley caliche samples collected for this study overlap previously reported values for these deposits (Böhlke et al., 1997; Michalski et al., 2004) confirming a substantial atmospheric component of the NO_3^- (Table 2.1.3, Figure 2.1.4).

Perchlorate stable isotopic compositions of the Death Valley caliches are distinct from those of previously reported sources (Figure 2.1.2; Table 2.1.3). The $\delta^{37}\text{Cl}$ values are higher than those of Atacama ClO_4^- (including new data reported here) and generally lower than those of synthetic ClO_4^- . The $\delta^{18}\text{O}$ values are higher than those of both Atacama and synthetic ClO_4^- . However, the $\Delta^{17}\text{O}$ values of Death Valley caliche ClO_4^- generally are similar to those of Atacama ClO_4^- with the exception of the Zabriskie sample ($\Delta^{17}\text{O} = +18.4\text{‰}$), which has the highest $\Delta^{17}\text{O}$ value reported to date for ClO_4^- (Figure 2.1.2). Combined data from Death Valley and Atacama indicate a positive correlation between $\Delta^{17}\text{O}$ and $\delta^{18}\text{O}$ in caliche ClO_4^- , with one end of the correlation line pointing toward the isotopic composition of atmospheric O_3 and the other end approaching the terrestrial mass-dependent fractionation line at a negative $\delta^{18}\text{O}$ value (Figure 2.1.3) (see also Bao and Gu, 2004). This pattern is similar to the one defined by NO_3^- isotopic data, for which atmospheric and biogenic end-members have been proposed (Figure 2.1.4).

2.1.3.2 Middle Rio Grande Basin Groundwater

ClO_4^- is present in Pleistocene and Holocene groundwater (0 to 28,000 years old) with minimal anthropogenic influence in the MRGB, New Mexico, at concentrations ranging from 0.12 to 1.8 $\mu\text{g L}^{-1}$ and with no systematic relation between groundwater age and ClO_4^- concentration (Plummer et al., 2005). Wells sampled for the current study (RR8 and RR16; Table 2.1.2) are within the area of Pleistocene groundwater mapped previously as “northwestern recharge zone” and attributed to mountain-front recharge from low elevations around the southern part of the Jemez Mountains (Plummer et al., 2004). This water is relatively dilute, with high dissolved O_2 , and major anion concentrations (Cl^- , Br^- , SO_4^{2-}) that may largely represent atmospheric fluxes with varying amounts of evapotranspiration (Plummer et al., 2004). The $\delta^{18}\text{O}$ values of the NO_3^- in these wells are much lower than those of atmospheric NO_3^- and are consistent with values produced by nitrification in soils. The $\delta^{15}\text{N}$ values of the NO_3^- are higher than those of atmospheric N species, possibly indicating partial loss and isotope fractionation of N in soils prior to nitrification (McMahon et al., 2006; see Figure 2.1.4). Dissolved gas concentrations and NO_3^- isotopes do not indicate denitrification in the saturated zone, hence it is also unlikely that ClO_4^- was reduced in the saturated zone given the residual NO_3^- in solution.

The sampled wells in this previously documented aquifer location had similar ClO_4^- concentrations and ClO_4^- isotopic compositions (Figure 2.1.2; Table 2.1.4). Estimated groundwater ages for both samples are greater than 10,000 yrs ($^3\text{H} \leq 0.3$ TU and DIC $^{14}\text{C} < 12$ pmc) (Table 2.1.4). Multiple lines of chemical, isotopic, and chronologic evidence indicate that this groundwater ClO_4^- is natural in origin (Plummer et al., 2004, 2005; Table 2.1.2 and 2.1.4), yet the ClO_4^- isotopic composition is distinct from those of the natural caliche-type occurrences, particularly with respect to the much lower MRGB $\Delta^{17}\text{O}$ values (Figure 2.1.2). Instead; the MRGB ClO_4^- is similar isotopically to ClO_4^- from SHP groundwater (see next section and Böhlke et al., 2005).

2.1.3.3 Southern High Plains Groundwater

ClO_4^- is present in groundwater (~ 0.1 to 200 $\mu\text{g L}^{-1}$) in at least 54 counties covering 155,000 km^2 in the SHP of Texas and New Mexico (Rajagopalan et al., 2004). The distribution and total mass of ClO_4^- in SHP groundwater appear to preclude anthropogenic sources (e.g. Atacama nitrate fertilizer, chlorate defoliants, fireworks, explosives, or flares) (Rajagopalan et al., 2004). Rather, the SHP ClO_4^- was interpreted to be natural and may represent wet and/or dry atmospheric deposition that accumulated in the unsaturated zone over millennial time scales and then was flushed to groundwater as widespread irrigation became common starting in the 1930s (Rajagopalan et al., 2004). Groundwater from wells evaluated in this study have apparent groundwater ages that range from modern (e.g., JYT-1 with 100 percent modern C and post-bomb ^3H) to more than 10,000 years (e.g., MW3 with 34 percent modern C and ^3H near the detection limit); however, there is evidence for mixing of old and young water in some cases (MW2 with low ^{14}C and post-bomb ^3H) (Table 2.1.4).

Samples for ClO_4^- isotopic analysis were collected from groundwater at five sites in the SHP, including two previously sampled sites, spread across an area of $\sim 40,000 \text{ km}^2$ (Figure 2.1.1). ClO_4^- concentrations in these samples ranged from 1.8 to $200 \mu\text{g L}^{-1}$ (Table 2.1.4). The new SHP ClO_4^- samples all have similar isotopic compositions that are indistinguishable from those of the two SHP ClO_4^- samples analyzed previously (Böhlke et al., 2005) (Figure 2.1.2; Table 2.1.4). Two hypotheses were advanced previously as possible explanations of ClO_4^- isotope data in SHP groundwater: (1) it is a mixture of biologically degraded synthetic ClO_4^- plus a small ($\sim 5\%$) amount of Atacama ClO_4^- ; or (2) it is an isotopically distinct form of natural ClO_4^- (Böhlke et al., 2005). Given the reported ubiquity of ClO_4^- in the SHP groundwater and soils, its relatively homogeneous isotopic composition in samples with a wide range of concentrations, and its similarity to ClO_4^- in old groundwater in the MRGB, it appears likely these data represent a major natural ClO_4^- province that is isotopically different from the Atacama and Death Valley caliche ClO_4^- occurrences (Figure 2.1.2). The alternative hypothesis (mixing of biodegraded synthetic perchlorate plus Atacama ClO_4^-) would require the unlikely circumstance of a consistent mixing proportion of synthetic and Atacama ClO_4^- , along with a constant isotopic shift due to biodegradation, over a wide geographical region.

NO_3^- in the SHP groundwater generally had $\delta^{18}\text{O}$ values consistent with biogenic sources. Two SHP NO_3^- samples had low $\Delta^{17}\text{O}$ values ($+0.3$ and $+0.1$ ‰ for MW2 and KJ1, respectively), also consistent with a predominantly biogenic source of the NO_3^- . Sample GW2 had relatively low O_2 concentration, high $\delta^{15}\text{N}$, and high $\delta^{18}\text{O}$, possibly indicating partial denitrification.

2.1.3.4 Southern High Plains Unsaturated Zone

To further test the hypothesis that ClO_4^- in SHP groundwater was remobilized after having accumulated naturally in the unsaturated (vadose) zone, a sample of ClO_4^- for isotopic analysis (SHP-V) was extracted from unsaturated sub-soil (2-4m) beneath undisturbed rangeland. High concentrations of disseminated salts peaking at depth in the unsaturated zone are common in the southwestern U.S. and have been interpreted as atmospheric salts accumulated largely during Holocene time since the last major wet climate period in this region (Rao et al., 2006; Phillips, 1994; Walvoord et al., 2002). The ClO_4^- and Cl^- concentrations in these accumulations are correlated ($r=0.59-0.99$) and the estimated mass of ClO_4^- in the unsaturated zone ($408 \pm 88 \text{ g ha}^{-1}$) is more than sufficient to account for the estimated mass of ClO_4^- in SHP groundwater (Rao et al., 2006). The depth profiles of ClO_4^- and Cl^- at our sample site are similar to previously reported profiles in the SHP and elsewhere in the southwestern U.S., with an apparent concentration maximum at $\sim 3-4 \text{ m}$ depth and maximum Cl^- and ClO_4^- concentrations of 370 mg kg^{-1} and $3.3 \mu\text{g kg}^{-1}$, respectively (Figure 2.1.5). Our profile data are incomplete, as we did not sample below 4 m, yet the mass of Cl^- above 4 m represents $>5,000$ years of accumulation based on a Cl^- deposition rate of 157 mg/ha-year (Rao et al., 2004). The ClO_4^- isotopic composition of this sample ($\delta^{37}\text{Cl} = +3.7$ ‰; $\delta^{18}\text{O} = +2.1$ ‰; and $\Delta^{17}\text{O} = +0.8$ ‰) falls within the range of the SHP and MRGB groundwater samples (Figure 2.1.2). This sample therefore supports the

interpretation that widespread ClO_4^- in groundwater throughout the SHP is of natural origin and has a characteristic isotopic composition distinct from those of Atacama and Death Valley caliches.

Table 2.1.1. Information about soil and caliche samples.

Sample ID	Location	Land Use	Latitude	Longitude	Date Sampled	Sample Depth	Sample Description	Elevation (m)
Confidence Hills 1	Death Valley, California, USA (Clay Hills)	National Park	N 35 50.350	W 116 35.256	2/16/2006	<1 m	Salt-cemented salt and clay	4
Confidence Hills 2			N 35 50.372	W 116 35.47	1/25/2008	~10-30cm	Salt-cemented green and red clay with chunks of mixed salts	40
Saratoga Hills			N 35 40.050	W 116 28.197		~5-30cm	Salt-cemented red clay streaked with white veins	130
Bully Hill			N 35 47.647	W 116 12.346		~5-30cm	Salt-cemented green and red clay with chunks of mixed salts	390
Zabriskie		Bureau of Land Management	N 35 55.103	W 116 16.234		~5-30cm	Salt-cemented green and red clay with chunks of mixed salts	420
P1	Baquedano District, Chile	Surface NO ₃ ⁻ mines	S23 11.863	W69 40.635	10/12/2007	>6m	Salts in fractured andesite	1279
P2			S23 11.863	W69 40.635		>6m	Salts in fractured andesite	1279
P3			S23 12.059	W69 40.205		25cm	Unconsolidated sediments	1304
P4			S23 12.059	W69 40.205		50cm	NaNO ₃ caliche	1304
GJ01	Chile	Unknown	Unknown		Unknown	Unknown	caliche	Unknown
UIC 24	Chile	Railway Cut	S23.16.53	W 69.46.14	11/03/2007	5m	NO ₃ ⁻ vertical vein in regolith	1137

Table 2.1.2. Well information with chemical and isotopic data for groundwater samples.

	Middle Rio Grande Basin		Southern High Plains					
Well Name	RR8	RR16	MW2	MW3	BW2	JYT1	GW2	KJ1
Well Type	PSW ¹	PSW	Monitor	Monitor	Monitor	Irrigation	Monitor	PSW
County, State	Sandoval, NM	Sandoval, NM	Martin, TX	Martin, TX	Bailey, TX	Kent, TX	Gaines, TX	Roosevelt NM
Latitude (N)	35.274	35.292	32.417	32.416	33.966	33.246	32.667	33.643
Longitude (W)	-106.732	-106.693	-102.155	-102.155	-102.765	-100.622	-102.376	-103.34
Land Surface Elevation (m)	1776	1686	881	881	1170	612	954	1285
Mid-Screen Elevation (m)	1383	1257	843	830	1147	594	943	
Screen Elevation ± (m)	94	178	1.2	3	3	1.2	3	
Water-Table Elevation (m)	1468	1488	846	846	1150	604	945	1250
Unsaturated-Zone Thickness (m)	308	198	35	35	21	8	9.0	35
Sample Date	9/12/2007	9/13/2007	11/8/2005	11/7/2005	11/9/2005	1/10/2006	6/1/2006	3/1/2007
Field parameters								
T (°C)			22.6	21.5	20.4	25.9	20.1	16.1
Specific Conductivity (µs/cm)			4709	4508	731	1818	6935	2411
Field O ₂ (µmol/L)			213	174	236	190	91	230
Field pH			6.95	8.25	7.47		6.45	6.64
Water Chemistry								
TDS (g/l)			3.06	2.97	0.52	1.8	4.96	1.89
F (µmol/L)	38	58	215	192	128		190	66
Cl (µmol/L)	255	598	25000	37000	1600	5300	29000	12000
Br (µmol/L)	2	2	68	111	5	8	98	27
NO ₃ (µmol/L)	187	137	577	209	120	437	129	370
SO ₄ (µmol/L)	669	1039	13000	9500	1100	8100	26000	7400
ClO ₄ (µmol/L)	0.0067	0.0085	0.20	0.11	0.02	0.04	2.05	0.15
Alkalinity (µmol/L as HCO ₃)			4200	4000	4500	3200	6600	2800
Isotopes								
H ₂ O δ ² H (‰)	-85.4	-96.8	-42.6	-46.6	-39.0	-32.1	-39.0	-42.8
H ₂ O δ ¹⁸ O (‰)	-11.66	-12.90	-5.75	-6.54	-5.71	-5.22	-5.43	-5.96
H ₂ O δ ³ H (TU) (±)	-0.22 (0.27)	0.32(0.22)	2.54(0.2)	0.34(0.17)	0.14(0.16)	3.68(0.22)	1.15(0.19)	0.15(0.23)
DIC δ ¹³ C (‰)	-7.7	-6.4	-6.4	-6.4	-3.9	-11.2	-9.9	-7.7
DIC δ ¹³ C (pmc ²)(±)	11.6(0.2)	5.9(0.1)	38.4(0.3)	33.6(0.3)	83.5(0.5)	99.7(0.4)	98.1(0.4)	91.5(0.4)
DIC pmc Age (years) ³	17300	22700	7700	8700	1450	25	151	710
SO ₄ ²⁻ δ ³⁴ S (‰)	1.1(0.2)	4.8(0.2)	7.3(0.2)	7.7(0.2)	7.4(0.2)	10.2(0.2)	8.7(0.2)	10.1(0.2)
SO ₄ ²⁻ δ ¹⁸ O (‰)	3.0(0.2)	4.5(0.1)	7.7(0.1)	8.4(0.1)	4.6(0.2)	8.8(0.2)	3.7(0.1)	2.9(0.1)
Dissolved Gases								
CH ₄ (µmol/L) (±)	0.000	0.000	0.000	0.000	0.000	0.055 (0.007)	0.000	0.000
Ar (µmol/L) (±)	12.35 (0.02)	13. (0.03)	13.91 (0.03)	13.9 (0.08)	13.91 (0.09)	13.52 (0.08)	15.22	13.21 (0.01)
N ₂ (µmol/L) (±)	497(2)	534(1)	606(2)	581(4)	557(2)	589(8)	615	547(2)
Ar-N ₂ equilibration T (°C)	19.2	16.3	20.5	18.6	15.2	23.2	12.8	18.3
Ar-N ₂ excess air (ccSTP/L)	1.4	1.7	2.5	2.5	1.4	3.4	2.0	2.2

Table 2.1.3. Selected chemical and isotopic data for caliche-type salts in unconsolidated surficial material from the Atacama Desert in Chile and the Death Valley clay hills region of the Mojave Desert in California, USA.

Site	Non-soluble fraction	Concentration				ClO ₄ ⁻ isotopes			NO ₃ ⁻ isotopes		
		ClO ₄ ⁻	Cl ⁻	NO ₃ ⁻ -N	SO ₄ ⁻²	δ ³⁷ Cl ^d	δ ¹⁸ O ^b	Δ ¹⁷ O ^e	δ ¹⁵ N ^c	δ ¹⁸ O ^b	Δ ¹⁷ O ^e
Death Valley	%	mg kg ⁻¹	g kg ⁻¹			‰			‰		
Confidence Hills 1	NA	0.25	320	1.8	72	-0.81	+2.9	+8.6	+3.4	+25.0	+7.9
Confidence Hills 2	49	0.85	180	5.5	100	-3.1	+7.2	+12.8	-1.0	+34.5	+12.7
Saratoga Hills	78	0.95	63	5.9	23	-1.4	+6.4	+10.9	-0.1	+43.6	+15.5
Bully Hill	62	0.82	80	28	6.5	NA	NA	NA	+5.1	+20.9	+7.2
Zabriskie	64	1.7	140	4.4	39	-3.7	+26.1	+18.4	+3.4	+32.8	+10.8
Atacama											
P1	42	243	80	12	57	-14.3	-10.5	+8.1	+0.2	+55.5	18.4
P2	50	328	456	44	84	-13.6	-6.7	+9.2	+0.6	+52.8	+17.3
P3	13	113	50	15	51	-11.8	-5.7	+8.8	-2.5	+55.9	+20.7
P4	51	132	61	22	51	NA	-7.8	+8.5	-2.1	+56.5	+20.7
GJ01	NA	5.4	6	1.2	13	-12.5	-5.2	+9.4	-0.2	+55.3	+20.7
UIC 24 (J-470)	NA	220	127	66	20	-12.8	-5.6	+8.8	+0.4	+49.6	+16.2

^aNA= Not Analyzed; ^bδ¹⁸O = R_{sample}/R_{standard}-1, where R= ¹⁸O/¹⁶O; ^cδ¹⁵N = R_{sample}/R_{standard}-1, where R= ¹⁵N/¹⁴N; ^dδ³⁷Cl = R_{sample}/R_{standard}-1, where R= ³⁷Cl/³⁵Cl; ^eΔ¹⁷O= [(1+δ¹⁷O)/(1+ δ¹⁸O)^{0.525}]-1; ‰ = parts per thousand; δ³⁷Cl, δ¹⁸O, and Δ¹⁷O values are referenced to 0 for SMOC, VSMOW, and VSMOW, respectively.

Table 2.1.4 Selected chemical and isotopic data for groundwater samples from the southwestern United States and Chile.

Well	Location	ClO ₄ ⁻	NO ₃ ⁻ -N	Cl ⁻	O ₂	³ H	Dissolved Inorganic Carbon ¹⁴ C	ClO ₄ ⁻ δ ³⁷ Cl ^d	ClO ₄ ⁻ δ ¹⁸ O ^b	ClO ₄ ⁻ Δ ¹⁷ O ^g	NO ₃ ⁻ δ ¹⁵ N ^c	NO ₃ ⁻ δ ¹⁸ O ^b	NO ₃ ⁻ Δ ¹⁷ O ^g
		μg L ⁻¹	mg L ⁻¹			TU ^e (±)	pmc ^f (±)	‰			‰		
MW2A	SHP, Texas and New Mexico, USA	24	2.9	1,300	6.8	2.5 (0.2)	38.4 (0.3)	+4.2	+1.0	+0.3	+5.5	+2.0	+0.3
MW2B								+3.7	+1.4	+0.3	NA	NA	NA
MW3A		19	8.1	930	5.6	0.3 (0.2)	33.6 (0.3)	+5.0	+2.2	+0.3	+6.6	+2.0	NA
MW3B								+4.1	+2.4	+0.3	NA	NA	NA
GW2		200	1.8	1,000	2.9	1.2 (0.2)	98.1 (0.4)	+5.0	+3.8	+0.2	+19.5	+16.0	NA
BW2		1.8	1.7	61	7.6	0.1 (0.2)	83.5 (0.5)	+4.5	+0.55	+0.6	+9.1	+3.7	NA
JYT1		3.8	6.1	190	6.1	3.7 (0.2)	99.7 (0.4)	+5.1	+2.7	+0.5	+9.9	+5.2	NA
KJ1		15	5.2	430	7.4	0.2 (0.2)	91.5 (0.4)	+4.5	+4.8	+0.8	+6.3	+0.3	+0.1
RR-8	MRGB, New Mexico,U SA	0.67	2.6	9.0	NA	-0.2 (0.3)	11.6 (0.2)	+3.1	+1.5	+1.2	+4.8	-1.2	NA
RR 16		0.85	1.9	21	NA	0.3 (0.2)	5.9 (0.1)	+3.6	+1.9	+1.3	+4.9	-1.0	NA
UIC-25	Chile	21,600	2,900	7,840	NA	NA ^a	NA	-12.9	-7.6	+9.3	+0.4	+49.9	+16.5

^aNA= Not Analyzed; ^bδ¹⁸O = R_{sample}/R_{standard}-1, where R= ¹⁸O/¹⁶O; ^cδ¹⁵N = R_{sample}/R_{standard}-1, where R= ¹⁵N/¹⁴N; ^dδ³⁷Cl = R_{sample}/R_{standard}-1, where R= ³⁷Cl/³⁵Cl;

^eTU = Tritium Units = 10¹⁸ x ³H atoms/H atoms. ^fpmc= percent modern carbon (not normalized for δ¹³C); ^gΔ¹⁷O= [(1+δ¹⁷O)/(1+ δ¹⁸O)^{0.525}]-1; ^h‰ = parts per thousand; δ³⁷Cl, δ¹⁸O, and Δ¹⁷O values are referenced to 0 for SMOC, VSMOW, and VSMOW, respectively

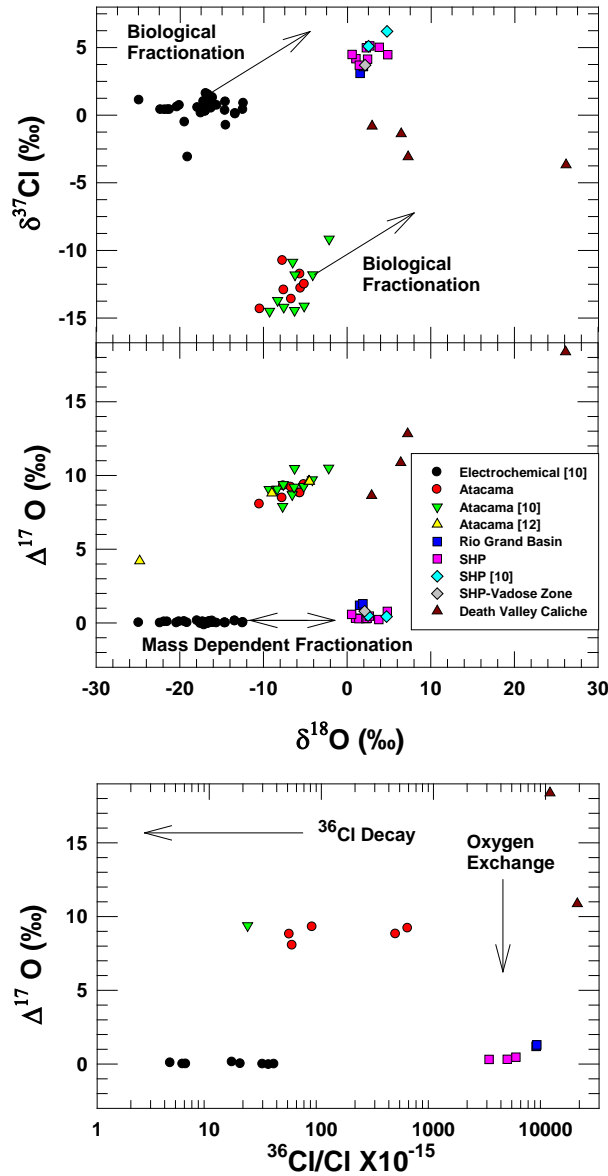


Figure 2.1.2. Summary of new isotope data for ClO_4^- from Southern High Plains (SHP) and Middle Rio Grande Basin (MRGB) groundwater, SHP unsaturated sub-soil, Death Valley and Atacama caliches displayed with previously published ClO_4^- isotope data (Böhlke et al., 2005; Sturchio et al., 2006; Bao and Gu, 2004). Arrows represent microbial fractionation slopes (Sturchio et al., 2007; Hatzinger et al., 2009), direction of mass dependent fractionation, direction of ^{36}Cl decay, and direction due to oxygen exchange. $\delta^{37}\text{Cl}$, $\delta^{18}\text{O}$, and $\Delta^{17}\text{O}$ values are referenced to 0 for SMOC, VSMOW, and VSMOW, respectively. ^{36}Cl values are from Sturchio et al., (2009) with the exception of the Zabriskie sample (Death Valley caliche with the highest $\Delta^{17}\text{O}$) (Table 2.1.3). $\delta^{18}\text{O} = R_{\text{sample}}/R_{\text{standard}} - 1$, where $R = ^{18}\text{O}/^{16}\text{O}$; $\delta^{37}\text{Cl} = R_{\text{sample}}/R_{\text{standard}} - 1$, where $R = ^{37}\text{Cl}/^{35}\text{Cl}$ and $\Delta^{17}\text{O} = [(1 + \delta^{17}\text{O})/(1 + \delta^{18}\text{O})^{0.525}] - 1$.

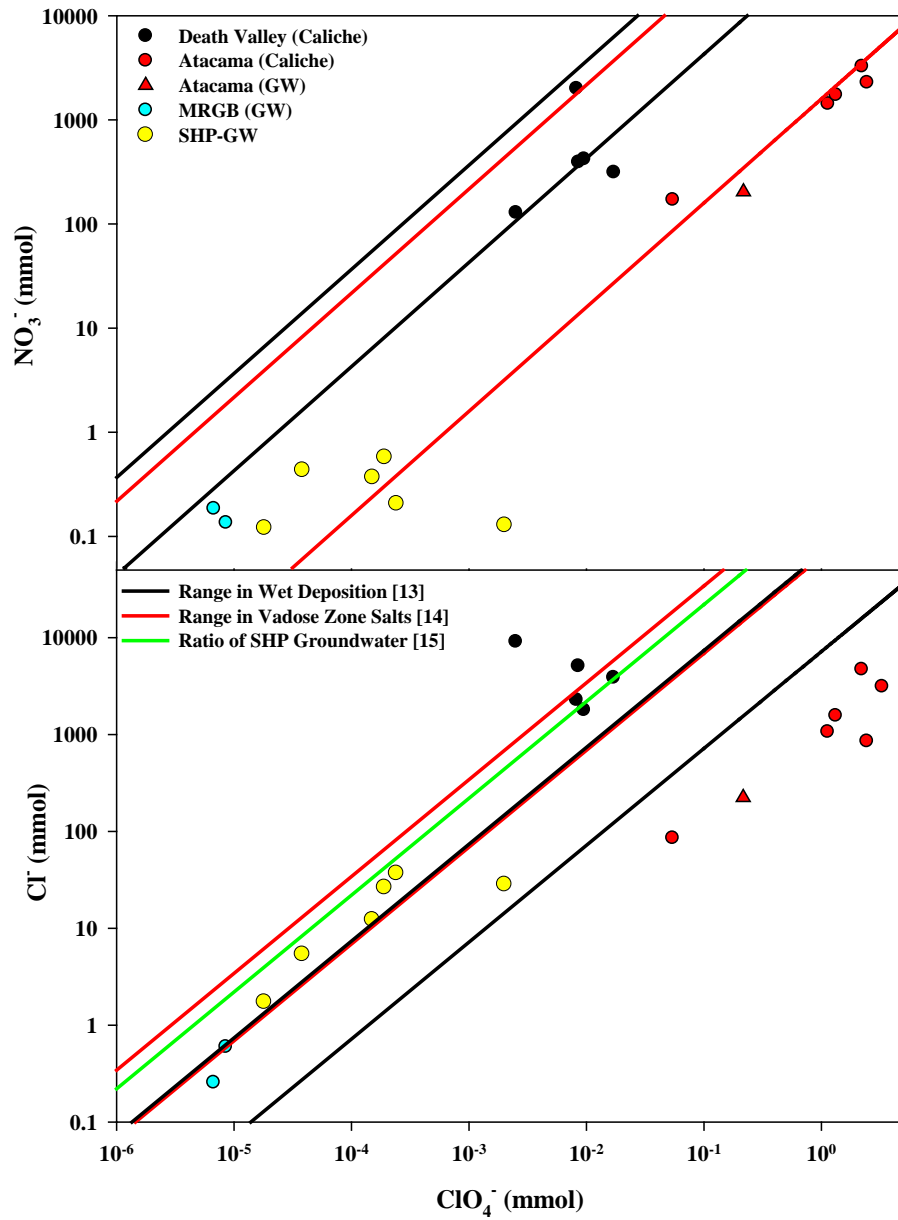


Figure 2.1.3. Comparison of $\text{NO}_3^-/\text{ClO}_4^-$ and $\text{Cl}^-/\text{ClO}_4^-$ molar ratios in new samples with previously published values for wet deposition across the contiguous United States (excluding coastal sites) (Rajagopalan et al., 2009) and vadose-zone salt accumulations in the southwestern United States (Rao et al., 2007). The reported average $\text{Cl}^-/\text{ClO}_4^-$ ratio is shown for groundwater (GW) in the SHP (Rajagopalan et al., 2006).

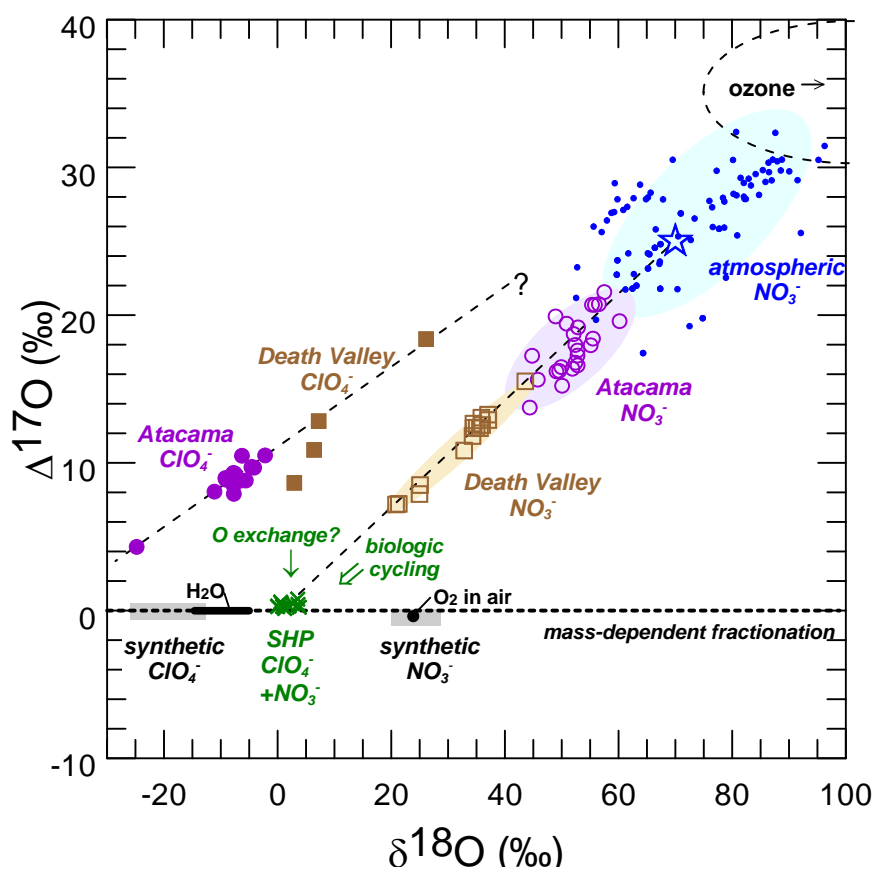


Figure 2.1.4. Relations between $\Delta^{17}\text{O}$ and $\delta^{18}\text{O}$ in ClO_4^- and NO_3^- (data from this study and Böhlke et al., 2005; Sturchio et al., 2006; Bao and Gu, 2004; USGA, 2010; Rao et al., 2010). $\delta^{18}\text{O}$ and $\Delta^{17}\text{O}$ values are referenced to 0 for VSMOW (Böhlke et al., 2005). A hypothetical trend line is shown for NO_3^- mixtures consisting of biogenic and atmospheric (O_3 -generated) endmembers. A hypothetical trend line through Atacama and Death Valley ClO_4^- could indicate varying expression of O_3 -generated components.

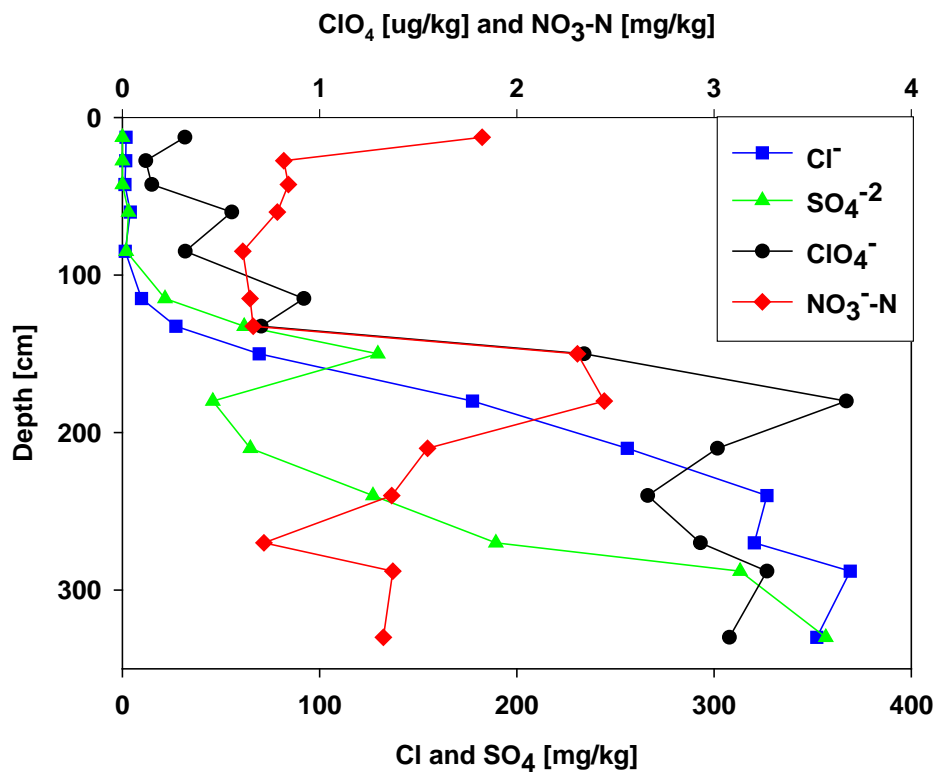


Figure 2.1.5. Distribution of ClO₄⁻ and other anions with depth below land surface at a rangeland site in the SHP, western Texas. The water table was more than 15 m below land surface. Concentrations are given as mass of leachable anions per mass of solid material that was leached. Sample SHP-V was taken from 200-400 cm below land surface at this site.

2.1.4 Isotopic Constraints on Origins of Natural Perchlorate

The data obtained in this task expand the range of known isotopic variation in natural ClO_4^- , based on a combination of $\delta^{37}\text{Cl}$, $\delta^{18}\text{O}$, and $\Delta^{17}\text{O}$ data. Three major sample groups compared in this study have distinctive isotopic characteristics: Atacama caliche-type ClO_4^- , Death Valley caliche-type ClO_4^- , and SHP unsaturated-zone and groundwater ClO_4^- (Figure 2.1.2). The most variable of these individual groups is the Death Valley samples, which exhibit a wide range and positive correlation of $\delta^{18}\text{O}$ and $\Delta^{17}\text{O}$ values, including the highest values reported to date for ClO_4^- (Figure 2.1.4). Isotopic differences within and among these groups could be variably related to: (1) isotopic compositions of precursor compounds prior to ClO_4^- formation, (2) isotopic fractionations accompanying ClO_4^- formation, (3) isotopic exchange between ClO_4^- and associated chemical species such as H_2O in the environment, and (4) kinetic isotopic fractionation caused by ClO_4^- -consuming reactions such as microbial reduction. The importance of these different effects and their relation to regional variation in terrestrial ClO_4^- isotopic composition are not completely resolved. Additional constraints are provided by laboratory experiments, ^{36}Cl concentrations in ClO_4^- , and O isotopes in NO_3^- .

One possible explanation for isotopic differences between different natural ClO_4^- occurrences is different mechanisms and (or) locations of ClO_4^- formation. High $\Delta^{17}\text{O}$ values presumably indicate O transfer from O_3 during photochemical Cl oxidation in the atmosphere, whereas low $\Delta^{17}\text{O}$ values could indicate photochemical processes involving oxidants other than O_3 , possibly occurring in the atmosphere or at the Earth's surface (see Section 2.1). Experiments indicate that ClO_4^- can be produced from reactions of oxy-chlorine intermediates (HOCl , ClO_2^-) by irradiation with UV or sunlight (Section 2.1; Kang et al., 2006; Rao et al., 2010). Chlorine dioxide (ClO_2) exists in the stratosphere and may be a precursor compound for a non- O_3 -mediated process of ClO_4^- generation (Solomon et al., 1989). The apparent correlation between $\Delta^{17}\text{O}$ and $\delta^{18}\text{O}$ values in both Atacama and Death Valley ClO_4^- could be interpreted as a mixing line between O_3 mediated and non- O_3 -mediated production mechanisms similar to atmospheric NO_3^- (Figure 2.1.4). However, this hypothesis may be difficult to reconcile with the geographic distributions of $^{36}\text{Cl}/\text{Cl}$ ratios and $\Delta^{17}\text{O}$ values in ClO_4^- . Data for a subset of our samples indicate relatively high concentrations of cosmogenic ^{36}Cl in natural ClO_4^- from both the Death Valley and SHP occurrences, and lower concentrations in Atacama ClO_4^- (Figure 2.1.2; Sturchio et al., 2009). High $^{36}\text{Cl}/\text{Cl}$ ratios in the U.S. samples ($8,000\text{--}28,000 \times 10^{-15}$) seem to preclude formation of ClO_4^- from common Cl precursors in the troposphere or near the land surface. The ^{36}Cl data could be consistent with ClO_4^- having formed in the upper atmosphere and deposited onto the land surface, followed by varying amounts of radioactive decay depending on the accumulation times of the different deposits (of the order of $10^6\text{--}10^7$ years in the Atacama and 10^4 years in Death Valley and the SHP) (Sturchio et al., 2009). If the bulk of the ClO_4^- in all of these occurrences formed in the stratosphere and was unreactive after deposition, then differences in the measured stable Cl and O isotopes would seem to require spatial variations in either the formation mechanisms or the isotopic compositions of precursor compounds in the atmosphere.

However, the large range of $\Delta^{17}\text{O}$ values locally among the Death Valley samples, and the near absence of elevated $\Delta^{17}\text{O}$ values in the other southwestern U.S. ClO_4^- samples compared to the Death Valley samples, would be difficult to rationalize on the basis of high-altitude source variations.

Alternatively, post-deposition alteration of ClO_4^- isotopic composition could account for local variations in the stable isotopic composition of atmospherically produced ClO_4^- , and it could be related to similar processes affecting the isotopic composition of atmospheric NO_3^- . Microbial reduction of ClO_4^- is known to occur in soils and groundwaters under suboxic conditions, and it is known to cause large fractionation effects in Cl and O isotopes (Sturchio et al., 2007; Hatzinger et al., 2009). However, available data indicate these isotope fractionation effects would not be consistent with many of the differences observed among the natural ClO_4^- sample groups in Figure 2.1.2 (e.g., microbial reduction follows a specific trajectory in $\delta^{37}\text{Cl}$ and $\delta^{18}\text{O}$ and would not alter $\Delta^{17}\text{O}$ substantially because it is mass-dependent), so biodegradation is not considered to be the major cause of the observed differences.

Our data indicate strong positive correlations between $\Delta^{17}\text{O}$ and $\delta^{18}\text{O}$ values in ClO_4^- and NO_3^- from Death Valley and the Atacama Desert (Figure 2.1.4). Both compounds had relatively high $\Delta^{17}\text{O}$ in hyper-arid and barren settings (Atacama and Death Valley clay hills), although the relative positions of Atacama and Death Valley samples were reversed for the two compounds. Both compounds had relatively low $\Delta^{17}\text{O}$ values in less arid settings. For NO_3^- , although atmospheric production mechanisms have been proposed to vary both spatially and temporally, published analyses indicate consistently high mean annual $\Delta^{17}\text{O}$ values in atmospheric NO_3^- from many regions of the world, and it is considered likely that the full range of $\Delta^{17}\text{O}$ in terrestrial NO_3^- is largely a reflection of varying proportions of atmospheric NO_3^- (with high $\Delta^{17}\text{O}$) and biogenic NO_3^- (with $\Delta^{17}\text{O}$ at or near 0) (Michalski et al., 2003, 2004; Ewing et al., 2007). In the current study, the highest $\Delta^{17}\text{O}$ values in NO_3^- (+17 to +21 ‰) were from the Atacama Desert and could indicate 60-80 % of the NO_3^- was unaltered atmospheric NO_3^- , assuming a long-term average atmospheric NO_3^- $\Delta^{17}\text{O}$ value of +25 ‰ (McMahon et al., 2006). Somewhat lower $\Delta^{17}\text{O}$ values in NO_3^- from the Death Valley region (+7 to +15 ‰) could indicate somewhat lower fractions of atmospheric NO_3^- (30-60 %), based on the same assumption. Much lower NO_3^- $\Delta^{17}\text{O}$ values were obtained from two of the SHP samples (+0.1 and +0.3 ‰), indicating almost no unaltered atmospheric NO_3^- . From the strong correlation between values of $\Delta^{17}\text{O}$ and $\delta^{18}\text{O}$ for NO_3^- (Figure 2.1.4), we infer that the generally low $\delta^{18}\text{O}$ values of the other groundwater samples from SHP and MRGB also indicate little or no unaltered atmospheric NO_3^- in those samples. The presence or absence of atmospheric isotopic characteristics in NO_3^- in these environments is qualitatively consistent with the potential for biological N cycling in local soils (assimilation, N_2 fixation, mineralization, and nitrification) (Figure 2.1.6). These processes are expected to be more active in the SHP than in the Atacama Desert or the clay hills of Death Valley because of the low precipitation and general absence of plant life and organic soils in the latter environments. However, whereas nitrification of reduced

N (including atmospheric NO_3^- formerly assimilated into biota and re-mineralized) is a well-documented mechanism for diluting or replacing the atmospheric $\Delta^{17}\text{O}$ signature of deposited NO_3^- , a comparable mechanism for similarly altering the isotopic composition of ClO_4^- has not been shown. Therefore, although terrestrial biologic processes can account for O isotopic variations in NO_3^- , and although the distribution of $\Delta^{17}\text{O}$ variations in both NO_3^- and ClO_4^- appear to be related spatially to local biologic activity, it is not yet possible to attribute ClO_4^- isotopic variation to the same processes that generally are thought to affect NO_3^- isotopes in these environments.

Another possible explanation for local variations in natural terrestrial ClO_4^- derived from the atmosphere is post-deposition isotope exchange (partial equilibration). Isotope exchange between ClO_4^- and H_2O would be expected to cause a decrease in $\Delta^{17}\text{O}$ and could be consistent with the ClO_4^- isotope data if exchange was more advanced in wetter or more biologically active environments. Equilibrium O isotope fractionation factors between ClO_4^- and H_2O are not known, but we expect $\delta^{18}\text{O}$ of ClO_4^- could be higher than $\delta^{18}\text{O}$ of coexisting H_2O by analogy with reported fractionation effects ranging from about +14 to +30 ‰ for SO_4^{2-} , HSO_4^- , NO_3^- , and NO_2^- at room temperature (Mizutani et al., 1969; Zeebe et al., 2010; Böhlke et al., 2003; Casciotti et al., 2007). Therefore, both the $\Delta^{17}\text{O}$ and $\delta^{18}\text{O}$ values of SHP and MRGB ClO_4^- could be qualitatively consistent with partial O isotopic exchange of Death Valley-type ClO_4^- with local H_2O ($\delta^{18}\text{O} = -13$ to -5 ‰) (Figure 2.1.4). Theoretical calculations indicate that $\delta^{37}\text{Cl}$ of ClO_4^- could be 73 ‰ higher than that of coexisting Cl^- at equilibrium (Schauble et al., 2003). Thus, the relatively high $\delta^{37}\text{Cl}$ values of SHP and MRGB ClO_4^- might indicate partial exchange of Cl isotopes between ClO_4^- and Cl^- (or another Cl species) with increasing moisture and(or) biologic activity if the ClO_4^- source(s) had relatively low $\delta^{37}\text{Cl}$, as in Atacama or Death Valley ClO_4^- . However, it is difficult to envision a mechanism that could accomplish Cl isotope exchange, especially in the absence of O isotope exchange (e.g., to explain differences between Atacama and Death Valley $\delta^{37}\text{Cl}$ and $\Delta^{17}\text{O}$). Limited data indicate abiotic exchange of O isotopes between ClO_4^- and H_2O is slow, if it occurs at all, in simple laboratory experiments [time constant > 100 years, Hoering et al. (1958); > 4500 years, Hatzinger et al. (2011)], but exchange might be catalyzed by other solid or aqueous species in soils and groundwaters, perhaps including organic compounds, as demonstrated for NO_3^- and PO_4^{3-} (Böhlke et al., 2003; Blake et al., 1997; Bunton et al., 1953). Field data indicate that Atacama ClO_4^- introduced into humid soils and groundwaters in the eastern U.S., and synthetic ClO_4^- contamination in groundwater in southern Nevada, did not exchange Cl or O isotopes substantially, despite groundwater residence times of the order of 30-40 years (Böhlke et al., 2005, 2009), although potential catalyzed exchange in unsaturated soils may have been precluded in those particular settings by rapid infiltration and recharge. Thus, although post-depositional isotope exchange could provide an explanation for some of the local natural ClO_4^- isotopic variations, it is not possible to predict rates of exchange with certainty, and it is not clear if any simple exchange model would produce the range of natural ClO_4^- isotopic compositions observed.

2.1.5 Implications for Perchlorate Isotope Forensics

Given present information, it is not yet possible to fully explain the observed variations in the isotopic composition of natural ClO_4^- sources, other than to say that some of the Atacama and Death Valley ClO_4^- probably formed as a result of reactions with O_3 . The data permit the interpretation that natural ClO_4^- may have more than one formation mechanism, there may be global variations in the isotopic compositions of precursor compounds, and it may be subject to isotopic modification in the terrestrial environment. Resolving these issues would contribute to understanding atmospheric Cl chemistry, as well as supporting the basis of the isotopic approach for quantifying ClO_4^- sources in the environment. Nevertheless, despite uncertainty about processes responsible for some of the isotopic variations, this study indicates that natural ClO_4^- indigenous to the southwestern U.S. is distinguishable from synthetic ClO_4^- and from imported Atacama ClO_4^- on the basis of isotopic composition. These differences in isotopic composition may find important applications in resolving questions of ClO_4^- source apportionment for contaminated water supplies.

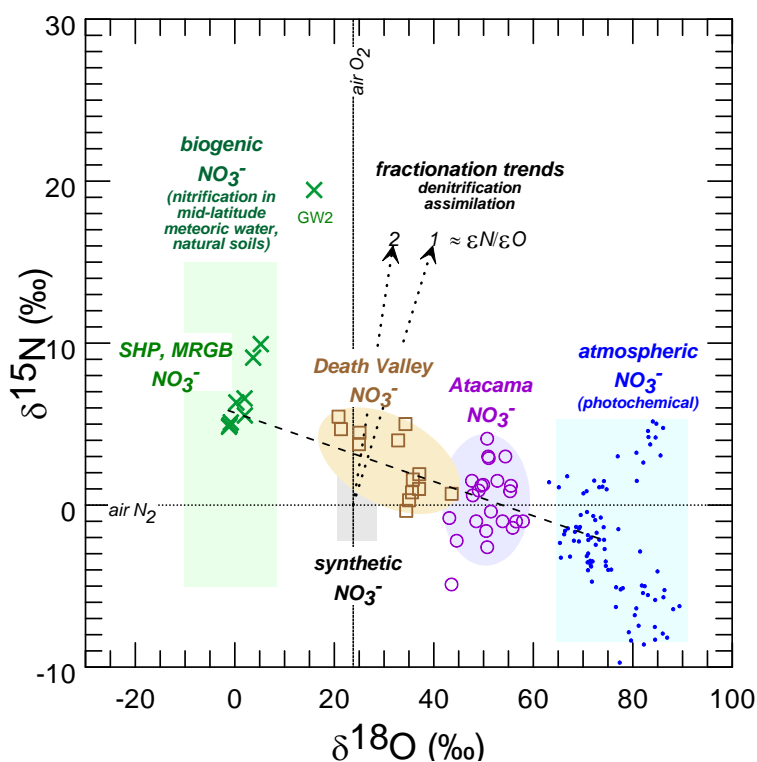


Figure 2.1.6. Relation between $\delta^{15}\text{N}$ and $\delta^{18}\text{O}$ of NO_3^- in groundwater and leachate samples. A rough inverse correlation between $\delta^{15}\text{N}$ and $\delta^{18}\text{O}$ shown here is consistent with varying mixtures of natural biogenic NO_3^- and atmospheric NO_3^- indicated by a positive correlation between $\delta^{17}\text{O}$ and $\delta^{18}\text{O}$ (Figure 2.1.4).

2.2 Occurrence and Stable Isotope Analysis of Perchlorate in the U.S. Great Lakes

2.2.1 Background

Initial measurements conducted during this research project demonstrated that ClO_4^- is present at low concentration throughout the water of the Great Lakes. The only previously published report of ClO_4^- concentrations in the Great Lakes was for surface water samples from Lakes Huron and Erie, and Hamilton Harbour of Lake Ontario, by Backus et al. (2005). However, only a few samples from Hamilton Harbour and some Canadian river water samples had detectable ClO_4^- in the range of 0.16 to 0.33 $\mu\text{g/L}$, and concentrations in all samples from the open waters of the Great Lakes were below that study's method detection limit of 0.19 $\mu\text{g/liter}$ (Backus et al., 2005).

The Great Lakes formed about 10,000 to 15,000 years ago in basins excavated by kilometers-thick glaciers (Hough, 1963; Larson and Schaetzl, 2001). The five-lake system contains about 20 percent of the world's surface freshwater and 95 percent of the surface freshwater of the US, thus making this lake system one of the world's most important and valuable natural resources. The Great Lakes have vital importance for drinking water, and other industrial and agricultural water needs in the region. Over thirty million people in the US and in Canada depend on the Great Lakes for their drinking water supply (Rheaume et al., 1995; Pearson et al., 2010; EPA, 2000).

We hypothesize that most of the ClO_4^- present in the Great Lakes is from direct atmospheric deposition, and thus its isotopic composition may be representative of the indigenous atmospheric ClO_4^- in the region with possible modification by processes occurring in the water column and/or the watershed (Poghosyan et al., 2014). The objective of this task was to quantify ClO_4^- inventories in the Great Lakes, characterize isotopic compositions of ClO_4^- ($\Delta^{17}\text{O}$, $\delta^{18}\text{O}$, $\delta^{37}\text{Cl}$, $^{36}\text{Cl}/\text{Cl}$), and to use these measurements to identify the source(s) of ClO_4^- , elucidate its general geochemical behavior, and evaluate the potential extent of its biodegradation in the Great Lakes.

2.2.2 Materials and Methods

2.2.2.1 Sample Collection

Great Lakes water samples were collected aboard the US Environmental Protection Agency's *R.V. Peter Wise Lake Guardian* during two routine monitoring cruises in August 2007 and August 2008. Samples for concentration analysis were collected from Lakes Michigan and Huron in August 2007, and we tested a method using multiple 100-mL ion-exchange resin columns to concentrate perchlorate from lake water for isotopic analysis. A more complete set of samples from all five lakes was collected for concentration analysis, and isotopic samples were collected on 1-liter resin columns in August 2008. The ship departed Milwaukee, WI on August 1, 2008, and sampled the lakes in the following sequence: Michigan, Huron, Erie, Ontario, and Superior, reaching Duluth, MN on August 24, 2008. A total of 74 unfiltered water

samples (~100 mL each) for ClO_4^- concentration analysis were collected from a rosette sampler at EPA monitoring stations, including at least one depth profile for each lake (Morrison, 2009)

Perchlorate samples for isotopic analysis were extracted from large amounts of lake water by using one-liter clear PVC columns filled with Purolite A530E bifunctional anion exchange resin. Similar columns with a 100-mL volume have been used extensively to collect perchlorate from groundwater (e.g., Section 2.2; Böhlke et al., 2009). Water was pumped up from a port at one-meter depth to an on-board laboratory and through two sediment filters in series (1st coarse + 2nd fine) to remove particles down to about 5 μm nominal size. A second pump was placed after the filters to push water through the 1 L ion exchange resin column. Water was passed continuously through a single resin column at a rate of ~10 L/min for the duration of the traverse on each lake. A new column was used for each lake. The total water volumes passed through the resin columns were: Lake Superior (20,430 L), Lake Michigan (31,780 L), Lake Huron (23,780 L), Lake Erie (15,260 L), and Lake Ontario (19,700 L). The sediment filters were changed two or three times per lake. Residence time in the two filter housings was not more than about three seconds each, and the water being passed through the filters was oxic, therefore the likelihood of any ClO_4^- biodegradation as water passed through the filter housings was minimal. Concentration samples were also collected before and after the resin columns to determine the efficiency of ClO_4^- extraction from water. All samples were stored in a walk-in freezer aboard the ship, and transferred from the ship to the Environmental Isotope Geochemistry Laboratory of the University of Illinois at Chicago in coolers with ice, where they were refrigerated until analysis.

The amount of ClO_4^- recovered from the Lake Superior sample from August 2008 was not sufficient for the planned isotopic analyses, so a second sampling trip was conducted to Lake Superior during September 24 - 28, 2010 to collect additional samples at the water filtration plant of Marquette, MI. Marquette was chosen because no major rivers discharge to Lake Superior in the region. The plant produces about 3 million gallons of Lake Superior water per day from an intake located 400 m off shore at about 18.3 m depth. Two one-liter sample columns were collected at Marquette, one from the raw intake water and another from the pre-filtered (500 μm) water supply. Fiberglass filters and glass wool fillings inside the perchlorate columns became clogged with sediments during sample collection, and these were changed daily to maintain flow through the columns. Total volumes of 86,000 L (Superior R) and 73,000 L (Superior P) were passed through raw and pre-filtered water-sample resin columns, respectively.

2.2.2.2 Concentration Analysis

Perchlorate concentrations in all of our water samples were measured by liquid chromatography coupled with tandem mass spectrometry (LC-MS-MS) at the Environmental Analysis Laboratory of Texas Tech University as previously described in Section 2.1, 2.2 and elsewhere (Rajagopalan et al., 2006, Rao et al., 2007). All samples were spiked with an oxygen isotope (^{18}O) labeled ClO_4^- internal standard. Sample concentrations were determined from the ratio of the sample

ClO_4^- peak to the internal standard peak, with a reporting limit of 0.05 $\mu\text{g/L}$ based on the lowest calibration point. The method detection limit and limit of quantification have previously been defined as 7 ng/L and 18 ng/L, respectively (Rajagopalan et al., 2009, Rao et al., 2012, Rao, 2010). The samples were analyzed in batches of eight followed by an analytical duplicate, spike, blank and a continuing calibration check (CCC). The tolerance for deviation in the duplicate samples and CCC was 20%, and for recovery of sample spike was 80 to 120%. If any one of the above conditions was not met, or if ClO_4^- in the laboratory reagent blank was greater than 0.3 times the quantification limit, then the results of that batch were discarded and the samples were reanalyzed.

2.2.2.3 Perchlorate Elution for Isotopic Analysis.

The 1L resin columns containing adsorbed ClO_4^- were first flushed with 4 bed volumes of 4 mol/L HCl in order to elute anions other than perchlorate and 2 bed volumes of ethanol to remove organic material coating the resin. The columns were then flushed with 1 bed volume of deionized water and the resin was removed for ultrasonic cleaning in deionized water. After these steps, ClO_4^- was eluted by tetrachloroferrate (FeCl_4^-) in a solution containing 1 mol/L FeCl_3 and 4 mol/L HCl (Section 2.2; Bao and Gu., 2004; Gu et al., 2001; 2007). The ClO_4^- -bearing eluent was diluted with deionized water (to convert tetrachloroferrate to cationic Fe species) and Fe was removed by passing the solution through a column of Bio-Rad AG50W-X12 cation exchange resin. The solution was then evaporated to a volume of about 25 mL following addition of a few milliliters of 30 % H_2O_2 . An aliquot of this solution was used for ion chromatographic analysis of the amount of ClO_4^- recovered from the sample column. The solution was then neutralized to a pH of just above 1 using 10 mol/L NaOH, and reloaded onto 2 mL of resin for a repeat of the elution and Fe-removal steps described above. The eluent solution was then evaporated down to ~0.5 mL to remove HCl. The solution was then diluted with 3 mL deionized water and pushed through Ag-treated On-Guard columns for Cl^- removal and Ba-treated cation-exchange columns for SO_4^{2-} removal. The solution was then passed through solid-phase extraction (SPE) columns for removal of organics, and finally mixed with excess CsOH to precipitate CsClO_4 . Final purification of perchlorate samples were conducted by precipitation and recrystallization of tetra-n-pentylammonium perchlorate (TPAClO_4) salts (Dosch, 1968). The sample processing blank for perchlorate was about 50 μg (from reagents), comprising <5 % of the perchlorate recovered for isotopic analysis.

2.2.2.4 Isotopic Analysis of Perchlorate by SIMS

Stable isotope ratios of O and Cl in perchlorate are normally analyzed by isotope-ratio mass spectrometry (IRMS) as detailed in Section 2.2. However, we used an alternative method to maximize the amount of data we could obtain from the small amounts of perchlorate recovered from the Great Lakes. Secondary ion mass spectrometry (SIMS) measurements of O and Cl isotope ratios were performed on TPAClO_4 . Samples were mounted by pressing into indium metal in a 2.5-cm diameter sample holder and coating the surface with 50 nm of gold. The samples were analyzed at the Center for Microanalysis of California Institute of Technology by

using the CAMECA IMS 7f-GEO SIMS instrument. Analyses were performed with a 10 keV Cs⁺ primary ion beam. The ion beam was focused to a diameter of ~20 µm with 5-6 nA of beam current. All isotope ratio analyses were performed by pre-sputtering of a 100 × 100 µm raster area for 120 sec, and then scanning a 75 × 75 µm raster during data collection. ³⁴S contribution to ³⁵Cl results was negligible at a mass resolving power (MRP) of 1200; this was also confirmed under MRP of 5000. A higher MRP of 6500 was used for oxygen isotope ratio measurements, but it was sometimes difficult to eliminate the effect of large ¹⁶OH interference on ¹⁷O. This ¹⁶OH interference caused relatively large errors for the ¹⁷O results, therefore SIMS results for ¹⁷O/¹⁶O ratios are not reported. An energy bandwidth of 45 eV was set for all SIMS measurements of both chlorine and oxygen isotopes. Secondary ion accelerating voltage was -9 keV for all isotopic analyses. For oxygen isotopes, a Faraday cup was used for ¹⁶O, and an electron multiplier for ¹⁷O and ¹⁸O, with data collection times of 1 sec, 10 sec, and 2 sec per cycle, respectively, for a total of 100 cycles. Chlorine isotopes ³⁵Cl and ³⁷Cl were measured by Faraday cups with data collection times of 1 sec and 2 sec per cycle, respectively, for a total of 20 cycles. Data are normalized to measurements of KClO₄ isotopic reference materials USGS37 and USGS38, which were converted to TPAClO₄. Stable isotope ratios are reported in the conventional delta (δ) notation, as follows:

$$\delta^{18}\text{O} (\text{‰}) = [({}^{18}\text{O}/{}^{16}\text{O})_{\text{sample}}/({}^{18}\text{O}/{}^{16}\text{O})_{\text{VSMOW}} - 1] \times 1000$$

$$\delta^{37}\text{Cl} (\text{‰}) = [({}^{37}\text{Cl}/{}^{35}\text{Cl})_{\text{sample}}/({}^{37}\text{Cl}/{}^{35}\text{Cl})_{\text{SMOC}} - 1] \times 1000$$

where VSMOW and SMOC are the isotopic references Vienna Standard Mean Ocean Water (Coplen, 1996) and Standard Mean Ocean Chloride (Godon et al., 2004), respectively. Analytical precisions (1σ) based on replicate measurements of reference materials are ±1.8 ‰ for δ¹⁸O and ±1.0 ‰ for δ³⁷Cl. SIMS produced acceptable results for δ¹⁸O and δ³⁷Cl analysis but ¹⁷O/¹⁶O measurements encountered difficulties in eliminating the effect of large ¹⁶OH interference on ¹⁷O (which may have been related to the use of TPAClO₄ as a target).

2.2.2.5. Isotopic Analysis of Perchlorate by Dual-inlet IRMS

Because of the difficulty encountered in precise determination of ¹⁷O/¹⁶O ratios by SIMS, samples were converted from TPAClO₄ to KClO₄ by using 0.5 mol/L KOH in absolute ethanol solution, for measurement of oxygen isotope ratios by dual-inlet IRMS of O₂ produced by sealed-tube decomposition of KClO₄ at 600°C. Reported ¹⁷O/¹⁶O ratios are given in units of Δ¹⁷O, where:

$$\Delta^{17}\text{O} (\text{‰}) = [(1 + \delta^{17}\text{O}/1000) / (1 + \delta^{18}\text{O}/1000)^{0.525}] - 1] \times 1000$$

Analytical precision of Δ¹⁷O based on replicate measurements of USGS-37 KClO₄ isotopic reference material is ±0.2 ‰.

2.2.2.6 ^{36}Cl Abundance Analysis by AMS

Accelerator mass spectrometry (AMS) measurements of ^{36}Cl isotopic abundances in AgCl (prepared from the KCl produced by decomposition of KClO_4 for IRMS $\Delta^{17}\text{O}$ analyses) were conducted at the Purdue Rare Isotope Measurement (PRIME) Laboratory at Purdue University. Prior to precipitation of AgCl, the chloride was purified by the standard ion chromatography developed by the PRIME Lab for ^{36}Cl analyses. The ^{36}Cl results were corrected for the instrumental background and are reported in units of $^{36}\text{Cl}/\text{Cl} \times 10^{-15}$ along with errors based on counting statistics.

2.2.3 Results and Discussion

2.2.3.1 Perchlorate Concentrations

A group of 74 samples were analyzed for ClO_4^- concentrations in the Great Lakes, and the concentrations ranged from 0.05 to 0.13 $\mu\text{g}/\text{L}$ (averages per lake are provided in Table 2.2.1 and all data are provided in Table 2.2.2). The profiles of ClO_4^- concentrations with depth in each lake are graphed in Figure 2.2.1. Although the perchlorate concentrations in some of the samples are just above the reporting limit, they all exceed the method detection limit by a factor of seven or more. Depth profiles of ClO_4^- concentration were determined for two locations on Lake Superior and one location on each of the other lakes (Figure 2.2.1). Concentrations were nearly constant with depth. The lack of stratification reflects vertical mixing caused by seasonal overturns of the water column (Fuller et al., 1995). Therefore, we consider our data to be fairly representative of the concentrations and isotopic compositions of perchlorate in each of the lakes. All water samples collected after the ion-exchange resin columns had perchlorate concentrations below the reporting limit of 0.05 $\mu\text{g}/\text{L}$, consistent with perchlorate removal by the resin columns.

Table 2.2.1. Concentrations and isotopic compositions of perchlorate from the Great Lakes.

<i>Lakes</i>	Sample^a volume (L)	Mean ClO₄⁻ (µg/L)^c	δ³⁷Cl (‰)	δ¹⁸O (‰)	Δ¹⁷O (‰)	³⁶Cl/Cl (10⁻¹⁵)
Superior R^b	86000	0.06	+3.9	-4.8	+2.7	71200 ± 1700
Superior P^b	73000	0.06	+4.0	-3.4	+2.6	61900 ± 1100
Michigan	31780	0.10	+3.3	-1.3	+1.7	26600 ± 800
Huron	23780	0.11	+3.2	-2.7	+1.6	15800 ± 600
Erie	15260	0.08	+3.2	+4.0	+1.8	9300 ± 300
Ontario	19700	0.09	+3.0	+1.9	+1.7	7400 ± 300

^a sample volume used for isotopic analysis. ^b Superior R and Superior P are samples collected from raw and pre-filtered water supplies, respectively. ^c perchlorate concentrations have standard deviation of ± 0.01 µg/L.

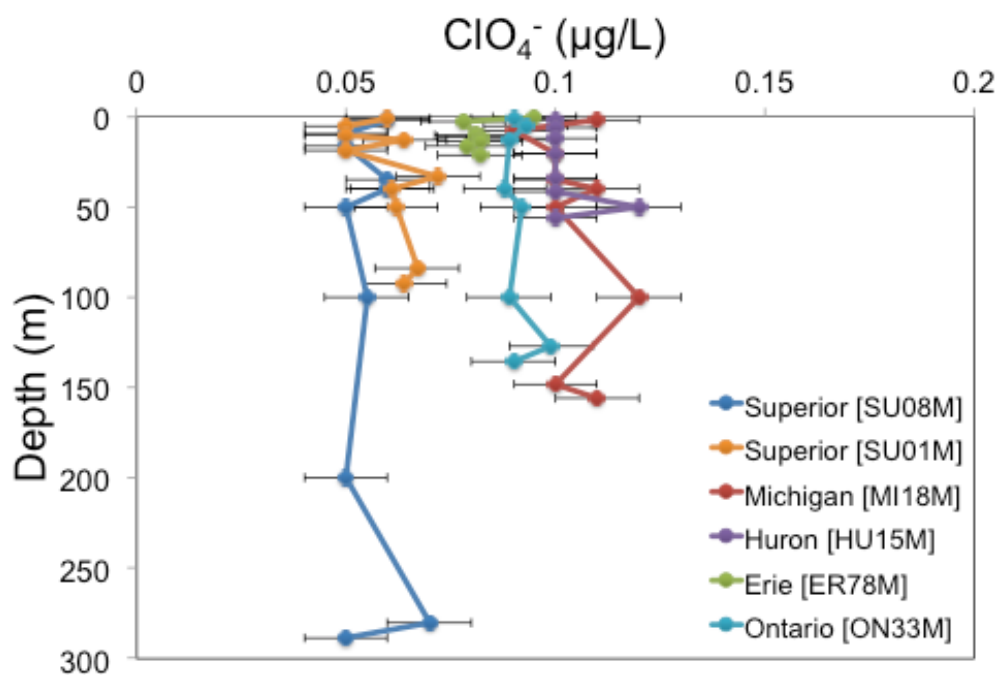


Figure 2.2.1. Perchlorate concentration vs. depth in the Great Lakes.

Table 2.2.2. Perchlorate concentrations in the water samples from the Great Lakes.

Lake	Date	Station	Depth (m)	ClO₄⁻ (µg/L)	Mean ClO₄⁻ (µg/L)
Superior	August, 2008	SU01M	1.5	0.06	
	August, 2008	SU01M	5.1	0.05	
	August, 2008	SU01M	10.5	0.05	
	August, 2008	SU01M	13.1	0.06	
	August, 2008	SU01M	18.8	0.05	
	August, 2008	SU01M	33	0.07	
	August, 2008	SU01M	40.2	0.06	
	August, 2008	SU01M	50.1	0.06	
	August, 2008	SU01M	84.1	0.07	
	August, 2008	SU01M	92.6	0.06	
	August, 2008	SU08M	1.6	0.06	
	August, 2008	SU08M	10	0.05	
	August, 2008	SU08M	16.1	0.05	
	August, 2008	SU08M	35	0.06	
	August, 2008	SU08M	39.9	0.06	
	August, 2008	SU08M	50	0.05	
	August, 2008	SU08M	99.9	0.06	
	August, 2008	SU08M	200	0.05	
	August, 2008	SU08M	280.4	0.07	
	August, 2008	SU08M	288.5	0.05	0.06 ± 0.01
Michigan	August, 2007	MI18M	1.6	0.11	
	August, 2007	MI18M	8.3	0.09	
	August, 2007	MI18M	20.5	0.10	
	August, 2007	MI18M	35.1	0.10	
	August, 2007	MI18M	40.3	0.11	

	August, 2007	MI18M	50	0.10	
	August, 2007	MI18M	100	0.12	
	August, 2007	MI18M	147.9	0.10	
	August, 2007	MI18M	156	0.11	
	August, 2007	MI27M INT	0	0.10	
	August, 2007	MI11 INT	0	0.09	
	August, 2007	MI17 INT	0	0.10	
	August, 2007	MI23 INT	0	0.10	
	August, 2007	MI19 SURF	Surface	0.10	
	August, 2007	MI17 SURF	Surface	0.10	
	August, 2007	MI32 SURF	Surface	0.10	
	August, 2007	MI34 SURF	Surface	0.10	
	August, 2008	MI18M	Sea Chest ^a	0.11	
	August, 2008	MI27M	Sea Chest	0.12	
	August, 2008	MI41M	Sea Chest	0.13	0.10 ± 0.01
Huron	August, 2007	HU15M	1.7	0.10	
	August, 2007	HU15M	6.1	0.10	
	August, 2007	HU15M	12	0.10	
	August, 2007	HU15M	20.4	0.10	
	August, 2007	HU15M	34.2	0.10	
	August, 2007	HU15M	42	0.10	
	August, 2007	HU15M	50	0.12	
	August, 2007	HU15M	56.4	0.10	
	August, 2007	HU32 INT	0	0.13	
	August, 2007	HU37 INT	0	0.11	
	August, 2007	HU53 INT	0	0.12	
	August, 2007	HU38 SURF	Surface	0.11	
	August, 2007	HU48 SURF	Surface	0.10	

	August, 2007	HU37 SURF	Surface	0.11	
	August, 2007	HU53 SURF	Surface	0.10	
	August, 2007	HU61 SURF	Surface	0.10	
	August, 2008	HU15M	Sea Chest	0.12	
	August, 2008	HU45M	Sea Chest	0.12	0.11 ± 0.01
Erie	August, 2008	ER78M	0	0.10	
	August, 2008	ER78M	2.5	0.08	
	August, 2008	ER78M	10.4	0.08	
	August, 2008	ER78M	11.4	0.08	
	August, 2008	ER78M	14	0.08	
	August, 2008	ER78M	16.4	0.08	
	August, 2008	ER78M	21.4	0.08	0.08 ± 0.01
Ontario	August, 2008	ON33M	1.5	0.09	
	August, 2008	ON33M	5	0.09	
	August, 2008	ON33M	12.7	0.09	
	August, 2008	ON33M	40.1	0.09	
	August, 2008	ON33M	50.1	0.09	
	August, 2008	ON33M	99.9	0.09	
	August, 2008	ON33M	127	0.10	
	August, 2008	ON33M	135.8	0.09	0.09 ± 0.01

^a The “sea chest” is a port through the ship’s hull about one meter below water level. Water was pumped continuously through this port up to the laboratory for sampling of perchlorate on 1-liter ion-exchange resin columns for isotopic analysis.

2.2.3.2 Perchlorate Isotopic Compositions

The isotopic compositions of ClO_4^- extracted from the Great Lakes provide constraints on possible source(s) and may indicate geochemical processes affecting ClO_4^- concentrations in the lakes. Values of $\delta^{37}\text{Cl}$ have a narrow range from +3.0 ‰ (Lake Ontario) to +4.0 ‰ (Lake Superior) (using the average values of the two Lake Superior samples), which is insignificant given the SIMS analytical error of ± 1.0 ‰. Values of $\delta^{18}\text{O}$ have a wider range from -4.1 ‰ (Lake Superior) to +4.0 ‰ (Lake Erie) (Table 2.2.1). Mass-independent oxygen isotopic variations are evident, with $\Delta^{17}\text{O}$ values ranging from +1.6 ‰ to +2.7 ‰. Lake Superior has a larger $\Delta^{17}\text{O}$ value (+2.7 ‰) than the other four lakes (+1.6 ‰ to +1.8 ‰). The overall ranges of

stable isotopic compositions of Great Lakes perchlorate resemble those of indigenous natural perchlorate measured in pre-industrial groundwaters of the western USA (Section 2.2.2; Jackson et al., 2010) indicating a predominantly natural source (Figure 2.2.2). However, the observed variations in oxygen isotope ratios may also indicate mixing with other sources, or possibly reactions such as biodegradation or oxygen exchange.

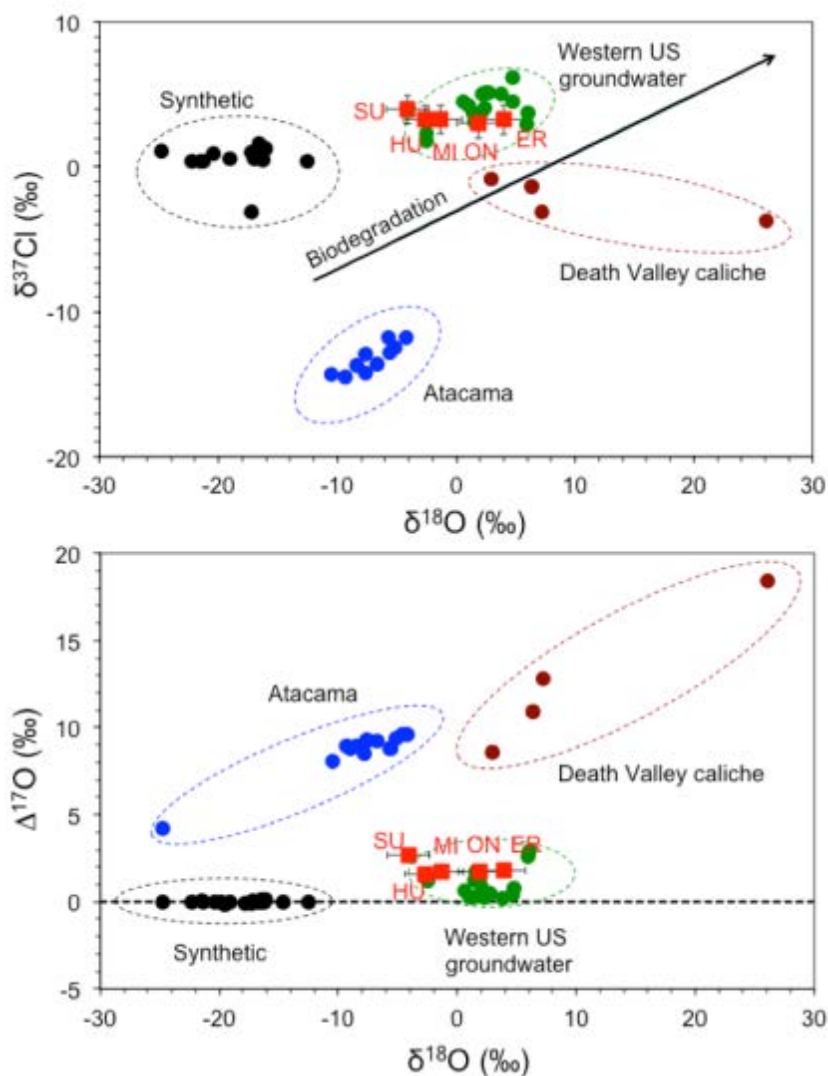


Figure 2.2.2. Diagrams showing $\delta^{37}\text{Cl}$ vs. $\delta^{18}\text{O}$ values (upper diagram) and $\Delta^{17}\text{O}$ vs. $\delta^{18}\text{O}$ values (lower diagram) for Great Lakes perchlorate samples. Published isotopic data from Atacama, Death Valley, western US groundwater and unsaturated zone, and synthetic perchlorates are also displayed on the graphs (Bao and Gu, 2004; Sturchio et al., 2006; Jackson et al., 2010; Hatzinger et al., 2013). Arrow in the upper diagram shows isotopic fractionation effect during biodegradation with a slope of 0.4 (Sturchio et al., 2007). The horizontal line in the lower diagram shows the mass dependent fractionation trend. Lake Superior values are the average of Superior R and Superior P values.

The $\delta^{18}\text{O}$ values of ClO_4^- from the Great Lakes are generally divided into two groups with Lakes Superior, Michigan and Huron having more negative $\delta^{18}\text{O}$ values (-4.1 ‰ to -1.3 ‰), and Lakes Erie and Ontario having more positive $\delta^{18}\text{O}$ values (+1.9 ‰ to +4.0 ‰). The spatial variability of the $\delta^{18}\text{O}$ values of perchlorate in the Great Lakes is similar to the spatial variability of the $\delta^{18}\text{O}$ values of H_2O (-9 ‰ to -6 ‰) in the Great Lakes, and in precipitation (-15 ‰ to -7 ‰) over the Great Lakes basin (IAEA/WMO, 2013; Longstaffe et al., 2011). This indicates that the oxygen isotopic ($\delta^{18}\text{O}$) variability of Great Lakes ClO_4^- could potentially reflect primary isotopic variability of atmospheric perchlorate in the region similar to the observed much larger range of isotopic values in Atacama and Death Valley perchlorates (Sturchio et al., 2006; Jackson et al., 2010; Section 2.2, this document).

Post depositional oxygen isotope exchange with the water in the Great Lakes could also affect ClO_4^- isotopic compositions. However, the experimentally measured rate of ClO_4^- -water oxygen isotope exchange is low; for example, a half-life of >4500 years at room temperature was found in a homogeneous perchloric acid solution by Hatzinger et al. (2011). This implies that such exchange must be catalyzed in natural settings if our results from the Great Lakes reflect the effects of oxygen exchange. Partial ClO_4^- -water oxygen exchange could thus account for the isotopic variation in perchlorate in the Great Lakes, along with other factors such as natural variability and mixing with other sources.

Chlorine-36 (^{36}Cl) is a cosmogenic radionuclide with a half-life of 301,000 years. Atmospheric ^{36}Cl is primarily produced by cosmic-ray spallation of ^{40}Ar (Lehmann et al., 1993; Lal et al., 1967). Isotopic abundance of ^{36}Cl in Great Lakes ClO_4^- decreases from west to east, from a high $^{36}\text{Cl}/\text{Cl}$ ratio of 6.7×10^{-11} in Lake Superior to a low ratio of 7.4×10^{-12} in Lake Ontario (Table 2.2.1). The $^{36}\text{Cl}/\text{Cl}$ ratio of perchlorate in Lake Superior is higher than that reported previously for any other location (Sturchio et al., 2009; Jackson et al., 2010; Section 2.2., this document)

Great Lakes ClO_4^- generally resembles that of indigenous natural ClO_4^- from the western USA in terms of $\delta^{37}\text{Cl}$ values and $^{36}\text{Cl}/\text{Cl}$ ratios (Figure 2.2.3). The isotopic composition of indigenous natural ClO_4^- in groundwater appears to be fairly consistent over a wide portion of North America, including West Texas, New Mexico, and Oregon (Sturchio et al., 2006, 2009; Jackson et al., 2010; Hatzinger et al., 2013; Section 2.2., this document) and similar isotopic composition is now also observed in ClO_4^- throughout the Great Lakes (Figures 2.2.2 and 2.2.3). Based on measurements performed to date, all pre-bomb indigenous natural ClO_4^- has high $^{36}\text{Cl}/\text{Cl}$ ratios relative to synthetic and Atacama ClO_4^- ; the highest $^{36}\text{Cl}/\text{Cl}$ ratios were found in indigenous ClO_4^- that may have incorporated bomb-pulse ^{36}Cl .³⁵ The relatively high $^{36}\text{Cl}/\text{Cl}$ ratios of perchlorate in the lakes having longer water residence times (Lakes Superior and Michigan, 180 yr and 110 yr respectively) are consistent with retention of bomb-pulse perchlorate. Nuclear weapon tests conducted on barges in the Pacific Ocean generated large amounts of ^{36}Cl by neutron activation of ^{35}Cl in seawater, and injected this ^{36}Cl into the stratosphere. The ^{36}Cl abundance in mid-latitude precipitation increased by as much as two to three orders of magnitude during the 1952 – 1964 period (Bentley et al., 1982; Heikkila et al., 2009). This period of

elevated atmospheric ^{36}Cl abundance occurred within the residence times of water contained in Lakes Superior and Michigan.

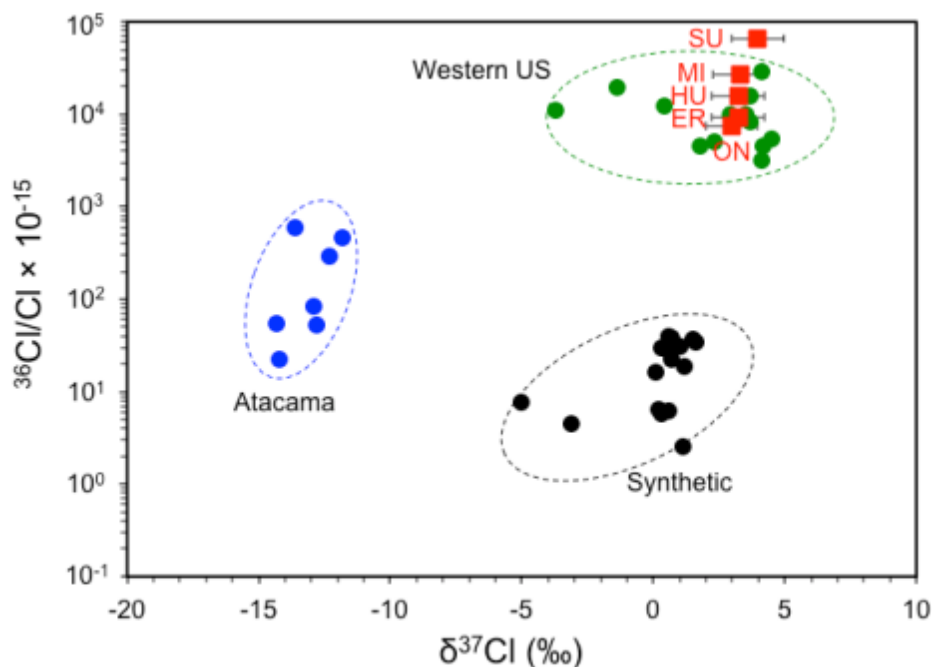


Figure 2.2.3. Diagram comparing $^{36}\text{Cl}/\text{Cl}$ vs. $\delta^{37}\text{Cl}$ values for perchlorate from the Great Lakes, in comparison with synthetic perchlorate, and natural perchlorate from Atacama (Chile) and the western USA. $^{36}\text{Cl}/\text{Cl}$ errors are smaller than data points. Lake Superior value is the average of Superior R and Superior P values.

2.2.3.3 Mass-Balance of Perchlorate in the Great Lakes

Measured ClO_4^- concentrations were used to build a mass-balance model for ClO_4^- in the Great Lakes. The model is similar to the mass-balance model of chloride in the Great Lakes developed by Chapra et al., (2009). The model treats the Great Lakes as a system of interconnected, well-mixed lakes. Our model assumes that the Great Lakes are in a steady state with each lake having a constant ClO_4^- concentration over time, whereby the total ClO_4^- mass entering each lake equals that leaving each lake. Likewise, we assume constant lake volumes because changes caused by short-term lake-level fluctuations are relatively small compared to total lake volumes. Physical parameters of the Great Lakes are summarized in Table 2.2.3 (Chapra et al., 2009; Quinn, 1982; GERL, 2012). These parameters were used in the calculations along with the average of the 1950 – 2008 monthly hydrologic data (Table 2.2.3) from the NOAA Great Lakes Environmental Research Laboratory.

Perchlorate fluxes out of the Great Lakes occur by outflow through the interconnected channels, diversion outflows, and by unknown processes that may include uptake and biodegradation.

Perchlorate input is from dry and wet atmospheric deposition (which are assumed to be equal), upstream inflow, and possibly from additional anthropogenic sources. It was assumed initially that all ClO_4^- deposited on the drainage basin of the Great Lakes is transferred into the lakes within one year. Perchlorate outflows and upstream inflows were estimated from the measured average ClO_4^- concentrations in the lakes, whereas ClO_4^- influx from the atmospheric deposition was estimated by using a value of twice the measured average ClO_4^- concentration of 14.1 ± 13.5 ng/L in rainwater (Rajagopalan et al., 2009).

Our ClO_4^- mass-balance model demonstrates that atmospheric deposition could account for the majority of the ClO_4^- fluxes in Lakes Superior, Michigan, Huron, and Ontario. However, some ClO_4^- loss is apparent in Lake Erie, where the influx of ClO_4^- is higher than its output (Table 2.2.4, Figure 2.2.4). Assuming conservatively that ClO_4^- enters Lake Erie only from Lake Huron, then Lake Erie outflow contains only about 82 % of the ClO_4^- from its inflow, indicating that at least 18 % of the ClO_4^- influx in Lake Erie is removed. In a more realistic scenario, in which perchlorate influx includes the atmospheric source as defined above, the total ClO_4^- removal occurring in Lake Erie would be about 26 %. In addition, any unaccounted ClO_4^- contribution from the anthropogenic sources would further increase the apparent ClO_4^- loss in Lake Erie.

Table 2.2.3. Physical parameters of the Great Lakes. Data from Chapra et al. (2009), Quinn (1982), GLERL (2012).

Lakes	Residence time (year)	Lake volume (km ³)	Surface Area (km ²)	Drainage area (km ²)	Over Lake Evaporation (km ³ /year)	Over Lake Precipitation (km ³ /year)	Over Land Precipitation (km ³ /year)
Superior	179.8	12,115	81,925	128,084	50	65	104
Michigan	110.2	4,947	57,291	115,804	38	47	96
Huron	21.3	3,567	59,560	132,208	39	51	117
Erie	2.7	499	25,404	60,602	24	24	56
Ontario	7.5	1,651	19,121	65,118	13	17	62

Table 2.2.4. Perchlorate mass-balance model results. Units are tonnes/year, except total ClO₄⁻ in tonnes.

Lakes	Atmospheric ClO ₄ ⁻ Input	Upstream ClO ₄ ⁻ Inflow	Total ClO ₄ ⁻ Input	ClO ₄ ⁻ Outflow	ClO ₄ ⁻ [Input–Outflow]	Total ClO ₄ ⁻ (tonne)
Superior	4.8 ± 4.6	n.a.	4.8 ± 4.6	4.2	0.6 ± 4.6	727
Michigan	4.0 ± 3.9	n.a.	4.0 ± 3.9	4.5	-0.5 ± 3.9	495
Huron	4.7 ± 4.5	8.4	13.1 ± 4.5	18.6	-5.5 ± 4.5	392
Erie	2.3 ± 2.2	19.2	21.5 ± 2.2	15.8	5.7 ± 2.2	40
Ontario	2.2 ± 2.1	15.8	18.0 ± 2.1	20.7	-2.7 ± 2.1	149

The apparent ClO_4^- removal in Lake Erie does not appear to cause significant isotope fractionation of oxygen and chlorine. In contrast, assuming Rayleigh-type fractionation according to the isotopic fractionation factors measured for microbial ClO_4^- reduction (Sturchio et al., 2007), a 20 % ClO_4^- reduction would cause about 9 ‰ increase in $\delta^{18}\text{O}$ and +3.5 ‰ increase in $\delta^{37}\text{Cl}$ while a 30 % reduction of ClO_4^- would increase the $\delta^{18}\text{O}$ and $\delta^{37}\text{Cl}$ values by about +14 ‰ and +5 ‰, respectively. However, complete biodegradation of ClO_4^- diffusing into the anaerobic sediments of Lake Erie (analogous to the “reactive microsites” model of Brandes and Devol (1997)) could be a plausible mechanism for ClO_4^- removal from Lake Erie without changing the isotopic composition of residual ClO_4^- . Lake Erie has a long history of seasonal hypoxia and sediments have high oxygen demand, resulting in anoxic conditions within 2 cm of the sediment-water interface (Matisoff et al., 2005) creating conditions conducive to microbial ClO_4^- reduction. Alternatively, if isotopic fractionation accompanies perchlorate removal, the ClO_4^- removed and that replaced by runoff input could fortuitously have similar stable isotopic compositions.

The mass-balance model also indicates possible minor ClO_4^- contributions from the drainage basins of Lakes Huron and Ontario. Perchlorate outflow exceeds inflow by at least 1.0 and 0.6 tonne/year (Table 2.2.4, Figure 2.2.4) in Lakes Huron and Ontario, respectively, indicating a possible ClO_4^- contribution from other sources not accounted by the atmospheric deposition of perchlorate when assuming a value of twice the ClO_4^- concentration of 14.1 ± 13.5 ng/L in rainwater. This strongly indicates that there might be a similar magnitude of ClO_4^- contribution from such unaccounted sources in Lake Erie since it is close to Lakes Huron and Ontario. However, the apparent ClO_4^- removal from Lake Erie is apparently much larger than the ClO_4^- influx from unaccounted sources.

2.2.3.4 ^{36}Cl Abundance of Perchlorate Formed During Atmospheric Bomb Tests.

Natural ClO_4^- of recent origin has relatively high $^{36}\text{Cl}/\text{Cl}$ ratios indicating an atmospheric source. Ratios of $^{36}\text{Cl}/\text{Cl}$ about $8,000 \times 10^{-15}$ were measured in ClO_4^- extracted from southwest US groundwater having ^{14}C ages of more than 10 ka (Sturchio et al., 2009). Perchlorate formed in the atmosphere during the period 1952-1964 when high quantities of bomb-produced ^{36}Cl were present could be expected to have much higher $^{36}\text{Cl}/\text{Cl}$ ratios compared with ClO_4^- that formed either before or after the bomb tests (Sturchio et al., 2009).

The relatively high $^{36}\text{ClO}_4^-$ abundances in Lakes Superior and Michigan may indicate the presence of ^{36}Cl -enriched ClO_4^- deposition during the period of elevated atmospheric ^{36}Cl activity following thermonuclear bomb tests in the Pacific Ocean. If we assume that the $^{36}\text{Cl}/\text{Cl}$ ratios of pre- and post-bomb ClO_4^- was $\sim 8,000 \times 10^{-15}$, based on measurements of pre-bomb groundwater perchlorate, then the ^{36}Cl abundance in atmospheric perchlorate formed during the bomb tests can be estimated from our data.

The $^{36}\text{ClO}_4^-$ abundances in the Great Lakes may have progressively increased from that of pre-bomb conditions by addition of ClO_4^- having anomalously high $^{36}\text{Cl}/\text{Cl}$ ratio that formed during

1950s and early 1960s, and peaked around mid 1960s when most of the bomb-produced ^{36}Cl atoms had been flushed out of the atmosphere due to the relatively short stratospheric residence time of two to three years (Bentley et al., 1982; Synal et al., 1990). We assume that the production and deposition rate of ClO_4^- remained constant, and only the isotopic abundance of ^{36}Cl changed in response to the transient bomb-pulse injection of ^{36}Cl into the stratosphere.

The fraction of initial water remaining in a lake at a given time can be approximated from the relationship $V_t/V = e^{-t/T}$, where V is the initial volume of the water mass at $t = 0$ (lake volume), V_t is the volume of the initial water mass remaining in the lake at any given time (t), and T is the residence time of the lake (Quinn, 1992). This equation assumes that the lake is fully mixed and ClO_4^- removal from the lake occurs only through the outflow. Lake Superior satisfies both criteria of being fully mixed and having ClO_4^- removal almost entirely through the outflow, which might not be the case in the lower lakes. Lake Superior also has the longest residence time (~ 180 yr from Table 2.2.3) indicating that most of the bomb-period water (and ClO_4^-) is still present within the lake.

Our estimate demonstrates that about 78 % of the water in Lake Superior at 2010 was also present in 1965 when the $^{36}\text{ClO}_4^-$ abundance was most likely the highest in Lake Superior. Since we assume that Lake Superior is fully mixed and ClO_4^- leaves the lake only through the outflow, the water fraction is roughly equivalent to the ClO_4^- fraction. Thus, Lake Superior ClO_4^- at 2010 was a mixture from ClO_4^- with elevated $^{36}\text{Cl}/\text{Cl}$ ratio from the 1965 peak period (78 %) and post-bomb atmospheric ClO_4^- with the $^{36}\text{Cl}/\text{Cl}$ ratio of about $8,000 \times 10^{-15}$ (22 %). The 1965 peak $^{36}\text{Cl}/\text{Cl}$ ratio of ClO_4^- in Lake Superior would have been about $83,000 \times 10^{-15}$. The estimate of the peak $^{36}\text{Cl}/\text{Cl}$ ratio at 1965 is relatively insensitive to the $^{36}\text{Cl}/\text{Cl}$ ratio of the post-bomb atmospheric ClO_4^- deposition, and it only varies by less than 3 % ($83,000 [\pm 2,000] \times 10^{-15}$) over a range of post-bomb $^{36}\text{Cl}/\text{Cl}$ ratios varying from $1,000 \times 10^{-15}$ to $15,000 \times 10^{-15}$. Finally, this peak ^{36}Cl abundance of ClO_4^- in Lake Superior at the end of the bomb-test period can be used to estimate the $^{36}\text{Cl}/\text{Cl}$ ratio of the total atmospheric ClO_4^- deposited during the bomb test period. Lake Superior ClO_4^- at 1965 was modeled as a mixture of pre-bomb (before 1952) ClO_4^- with the $^{36}\text{Cl}/\text{Cl}$ ratio of about $8,000 \times 10^{-15}$ (92.5 %) and ^{36}Cl -enriched ClO_4^- deposited during the thermonuclear bomb tests (7.5 %). In this case, our estimate of the $^{36}\text{Cl}/\text{Cl}$ ratio of ClO_4^- deposited during the thermonuclear bomb tests is about $1,000,000 \times 10^{-15}$. Sensitivity analysis demonstrates that the $^{36}\text{Cl}/\text{Cl}$ ratio of the bomb-period atmospheric ClO_4^- varies by about 11 % ($1,000,000 [\pm 110,000] \times 10^{-15}$) for a range of $^{36}\text{Cl}/\text{Cl}$ ratios in pre-bomb atmospheric ClO_4^- from $1,000 \times 10^{-15}$ to $15,000 \times 10^{-15}$. The ^{36}Cl abundance in natural ClO_4^- during the atmospheric thermonuclear bomb tests was about two orders of magnitude higher than that of indigenous natural ClO_4^- being deposited on the surface of the Earth (Sturchio et al., 2009; Jackson et al., 2010; Section 2.2, this document)

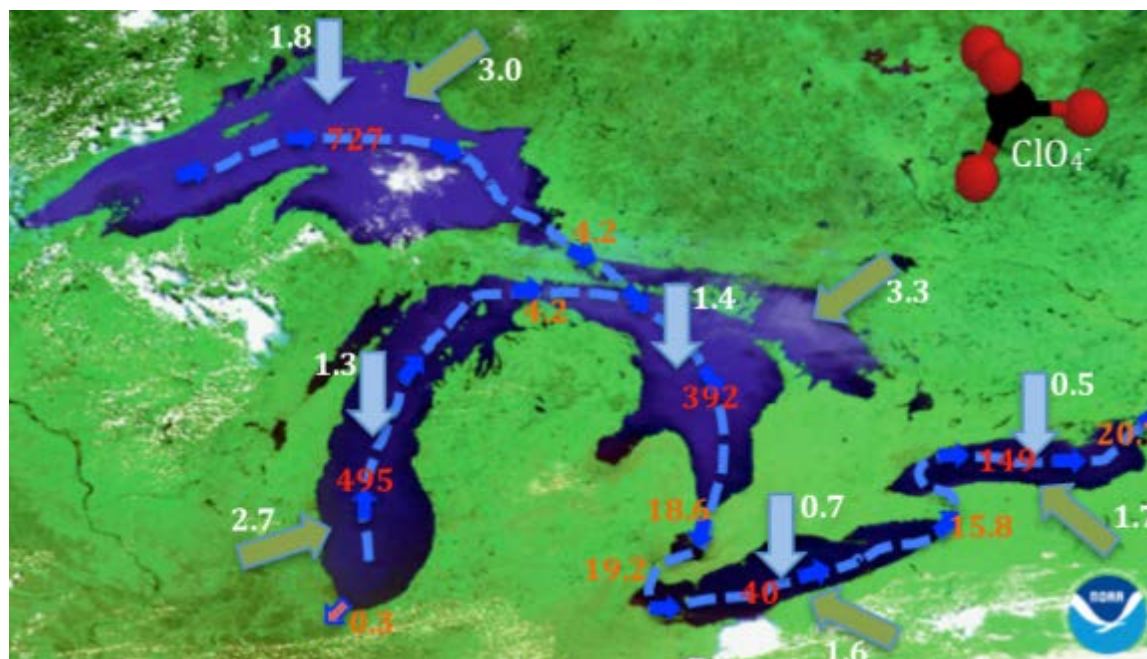


Figure 2.2.4. Estimated perchlorate fluxes in the Great Lakes. Red numbers represent total perchlorate inventories in each lake (tonne), white numbers next to the arrows represent perchlorate fluxes (tonne/year) from direct atmospheric deposition and from the drainage basins when assuming 14.1 ng/L ClO_4^- concentrations in the rainwater, and orange numbers represent ClO_4^- outflows from the lakes (tonne/year).

2.3 Occurrence of Natural Perchlorate and Relationship with Nitrate in Arid and Semi-Arid Environments Worldwide

2.3.1 Background

Here we present new data for natural ClO_4^- occurrences in selected globally distributed settings and an overview of the factors controlling ClO_4^- accumulation in the environment. We measured indigenous ClO_4^- concentrations in soil/caliche and groundwater samples from a variety of arid and semi-arid locations in Antarctica, Chile, China, southern Africa, United Arab Emirates (UAE), and the U.S. We also investigated the relationship between ClO_4^- and co-occurring Cl^- and NO_3^- as well as the sources and sinks of NO_3^- based on isotope data ($\delta^{15}\text{N}$, $\delta^{18}\text{O}$, and $\Delta^{17}\text{O}$). Our objectives were to evaluate the occurrence and fate of ClO_4^- in arid environments and the relationship of ClO_4^- to the better studied atmospherically deposited species NO_3^- and Cl^- as a means to understand the prevalent processes that affect the accumulation of these species over various time scales. We developed a conceptual model of ClO_4^- occurrence in relation to NO_3^- that incorporates the overall impact of biological processes to the co-occurrence of these important oxy-anions. Our results firmly establish the widespread global occurrence of ClO_4^- , provide insights about environmental conditions controlling its distribution, and appear to indicate a new approach for evaluating arid-region biogeochemistry with particular relevance to NO_3^- processing and Cl^- cycling. Our results also may contribute to understanding the prevalence of ClO_4^- on Mars and its implications to the co-occurrence of NO_3^- and possible extraterrestrial biologic impacts on these species (Stern et al., 2015). This work significantly expands that presented in Section 2.2, which focused primarily on the southwestern US.

Soil, unsaturated subsoil, caliche-type salt deposits, and groundwater samples were collected for this study or obtained from archived samples of previous studies from sites in the U.S., Southern Africa (Namibia, South Africa, and Botswana), UAE, China, Chile, and Antarctica (Figure 2.3.1). Sample sites are described below and summarized in Tables 2.3.1 and 2.3.2. All samples were analyzed for Cl^- , NO_3^- , and ClO_4^- concentrations and a subset was evaluated for NO_3^- stable isotopic composition as described below.

2.3.2 Site and Sample Descriptions

2.3.2.1 United States

Mojave Desert-Soil

Near surface soil samples (composites) from areas of desert pavement and subsoil samples from discrete depths were collected in the northern Mojave Desert near the U.S. Geological Survey (USGS) Amargosa Desert Research Site (Figure 2.3.1) (Andraski et al., 2014). The Amargosa Desert, in the Basin and Range Province, is bounded by block-faulted mountains composed of Paleozoic metamorphic rocks and Tertiary volcanic rocks. Moderate to steep sloping alluvial fans near the foot of the mountains and the valley floor have sparse, mixed vegetation dominated by creosote bush (*Larrea tridentata*). Discrete-depth soil and/or salt-rich caliche were also

collected from three sites (Bully Hill, Confidence Hills, Saratoga Hills) in the southern Death Valley region. The Death Valley sites are unvegetated clay hills formed from steeply tilted sedimentary beds and were previously studied for their unusual surface concentrations of NO_3^- and more recently for co-occurring ClO_4^- (Ericksen et al., 1988; Böhlke et al., 1997; Michalski et al., 2004; Jackson et al., 2010; Lybrand et al., 2013). We also obtained archived (filtered and aerated) soil leachates from previous studies of indigenous NO_3^- in the Rainbow Hills and Fort Irwin Basin in the western Mojave Desert (Densmore and Böhlke, 2000; Böhlke et al., 1997). The Mojave Desert sites receive variable rainfall but generally less than 10 cm/year.

Edwards Aquifer-Groundwater

Groundwater samples were collected from the San Antonio segment of the fractured karstic Edwards aquifer in Texas, (U.S.) as part of the USGS National Water-Quality Assessment Program (Figure 2.3.1) (Musgrove et al., 2010). Groundwater samples were collected in accordance with procedures described in Koterba and others (1995) and in the USGS National Field Manual. Water samples were collected from public-supply wells in 2004-05 and from a combination of public, domestic, stock, and commercial supply and monitoring wells in 2006. Public-supply well depths ranged from about 65 to 716 m; domestic, commercial, and stock well depths ranged from 24 to 152 m; and monitoring-well depths ranged from 55 to 98 m. The climate is subtropical sub-humid. Mean annual precipitation decreases across the region from 86 cm/year in the east to 56 cm/year in the west (Bomar, 1994). Groundwater from the sampled portion of the Edwards aquifer was recharged predominantly within approximately the past 50 years and mixed extensively in the subsurface, and the whole aquifer is susceptible to anthropogenic impacts (Musgrove et al., 2010).

Albuquerque Basin-Groundwater

In the Albuquerque (ABQ) Basin, New Mexico, U.S., groundwater samples were collected from public-supply wells in 2005 and from public-supply and monitoring wells in 2007-2009 (Figure 2.3.1). Public-supply well depths ranged from about 65 to 630 m and monitoring-well depths ranged from about 80 to 360 m. Groundwater samples were collected in accordance with USGS procedures cited above. The climate is semiarid, with potential evaporation substantially exceeding mean annual precipitation (22.1 cm/year at Albuquerque during 1914-2010). The ABQ alluvial basin consists largely of unconsolidated to moderately consolidated deposits of sand, gravel, silt, and clay. The age of most groundwater in the basin is on the order of thousands of years (Plummer et al., 2004; Bexfield et al., 2011).

2.3.2.2 Southern Africa-Soil and Groundwater

Soil samples collected in southern Africa were primarily from the hyper-arid Central Namib gravel plains (Figure 2.3.1). Samples represent composites (0-30 cm depth) from locations in an area covering ~150 km north to south and up to 85 km west to east from the coast. Rainfall for all sites is below 10 cm/year and may be as low as 0 cm/year. The eastern-most soil samples were from a calcrete-rich substrate and include the Zebra Pan, a small recharge playa. The central and western soil samples were from gypcrete-rich pediment characterized by lag gravel,

fog precipitation, and lichen growth, and they include a sample from Eisfeld, a saline discharge spring and playa. Samples from Goanikontes were taken at a 20 m high escarpment and include top (A), middle (B) and bottom (C) slopes. A small set of Namibia water samples (springs, potholes, and one groundwater sample) were also obtained from the same region. Additional soil samples were obtained from saline playa surfaces in South Africa (Kalahari Desert; Haskenpan, Koppieskraal and Nolokey) and in Botswana (Makgadikgadi).

2.3.2.2 United Arab Emirates (UAE)—Soil and Groundwater

Soil and groundwater samples were collected from a number of sites in the UAE (Emirate of Abu Dhabi). Soil-surface (0-30 cm) composite samples were from undisturbed areas and discrete-depth samples were from two hand-dug pits in the coastal Sabkha. Groundwater samples were collected from production wells (n=12), monitoring wells (n=3), and shallow hand-dug pits (n=2). Groundwater samples were collected from wells near agricultural areas of Mohayer, Ghayathi, and Liwa. Soil samples were collected from the coastal Sabkha, Matti, and Gayathi regions. The climate is subtropical arid. Rainfall varies across the UAE with reported modern (1966-1998) rainfall ranging from 7-13 cm/year, with a high potential evaporation rate of about 2-3 m/year (Sherif et al., 2014).

2.3.2.5 Atacama Desert-Soil/Caliche

Surface-soil samples (0-30 cm composites) were collected along an elevational transect east of Antofagasta, Chile, extending from the Baquedano nitrate mining district in the ‘absolute desert’ (~1300 m) (i.e., a plant-free landscape) to the tussock steppe grasslands of the Western Andes Cordillera (4200 m) (Figure 2.3.1). Discrete-depth samples were collected from existing or fresh hand excavated pits within 25-75 km of the coast along a 450 km north-south transect. Additional discrete-depth samples were collected from open faces within an active nitrate mine. Atacama NO_3^- mineral deposits are considered to have accumulated over a period of the order of 10^6 to 10^7 years (Pérez-Fodich et al., 2014). The Atacama Desert is a hyperarid cold desert with estimates of average annual rainfall less than 0.01 cm/year with large stretches of absolute desert.

2.3.2.6 China-Soil and Groundwater

Turpan-Hami-Caliche

Caliche-type salt-rich samples were obtained from three sub-basins (Kumutage, Wuzongbulake, and Xiacaohu) in the Turpan-Hami Depressions, an area of fault-bounded troughs that descend to below sea level in northwestern China (Figure 2.3.1). Samples from Kumutage are from a vertical profile (0-2 m depth), whereas samples from the other basins are from unknown depths. These sites are associated with recently described massive NO_3^- deposits (Qin et al., 2012). The NO_3^- from this region has a wide range of stable isotopic composition, ranging from predominantly un-cycled atmospheric to predominantly biogenic NO_3^- . The deposits are estimated to be < 260 k years old (Qin et al., 2012). Climate in the region is hyper-arid, with precipitation < 1.5 cm/year.

Loess Plateau-Groundwater

Archived (filtered and refrigerated) water samples were obtained from a previous study evaluating groundwater recharge in the central Loess Plateau in Shaanxi Province, China (Gates et al., 2011). Samples were originally collected in 2008. The sampled area has an elevation of ~1,000-2,000 m above sea level. Approximately 20% of the catchment land area is cultivated (primarily dryland wheat farming). Mean annual rainfall is ~50 cm/year. Groundwater is > 100 m deep in upland areas and discharges into incised valleys. The samples were collected from springs over a range of elevations (1,036-1,231 m).

Badain Jaran-Groundwater

Archived (filtered and refrigerated) groundwater samples were obtained from a previous study of shallow wells and springs located near the margin between the Badain Jaran dune field and Yabulai Mountains, Gurinai Grass Land, and Xugue Lake area (Figure 2.3.1) (Gates et al., 2008a,b). The area is sparsely settled and contains only limited vegetative cover on unconsolidated sand dunes interspersed with groundwater-fed lakes of varying salinity. The dune area is underlain by a shallow surficial aquifer that is locally confined in some areas. Previous studies indicate groundwater recharge occurs largely at higher elevations near the margins of the basin. The area is considered a cold continental desert with average (1956-1999) precipitation of 8.4 cm/year (Gates et al., 2008a).

2.3.2.7 Antarctica-Soil

Discrete depth samples were collected from shallow hand dug pits in University Valley (1600m), which is a perched valley above Beacon Valley in the Quartermain Range of the McMurdo Dry Valley (MDV) region of Antarctica (Figure 2.3.1). University Valley and nearby valleys contain elevated concentrations of NO_3^- primarily of atmospheric origin (Michalski et al., 2005) as well as elevated concentrations of ClO_4^- (Kounaves et al., 2010). University Valley is located in a hyper-arid region of the MDV and receives a current water equivalent precipitation of less than 5 cm/year.

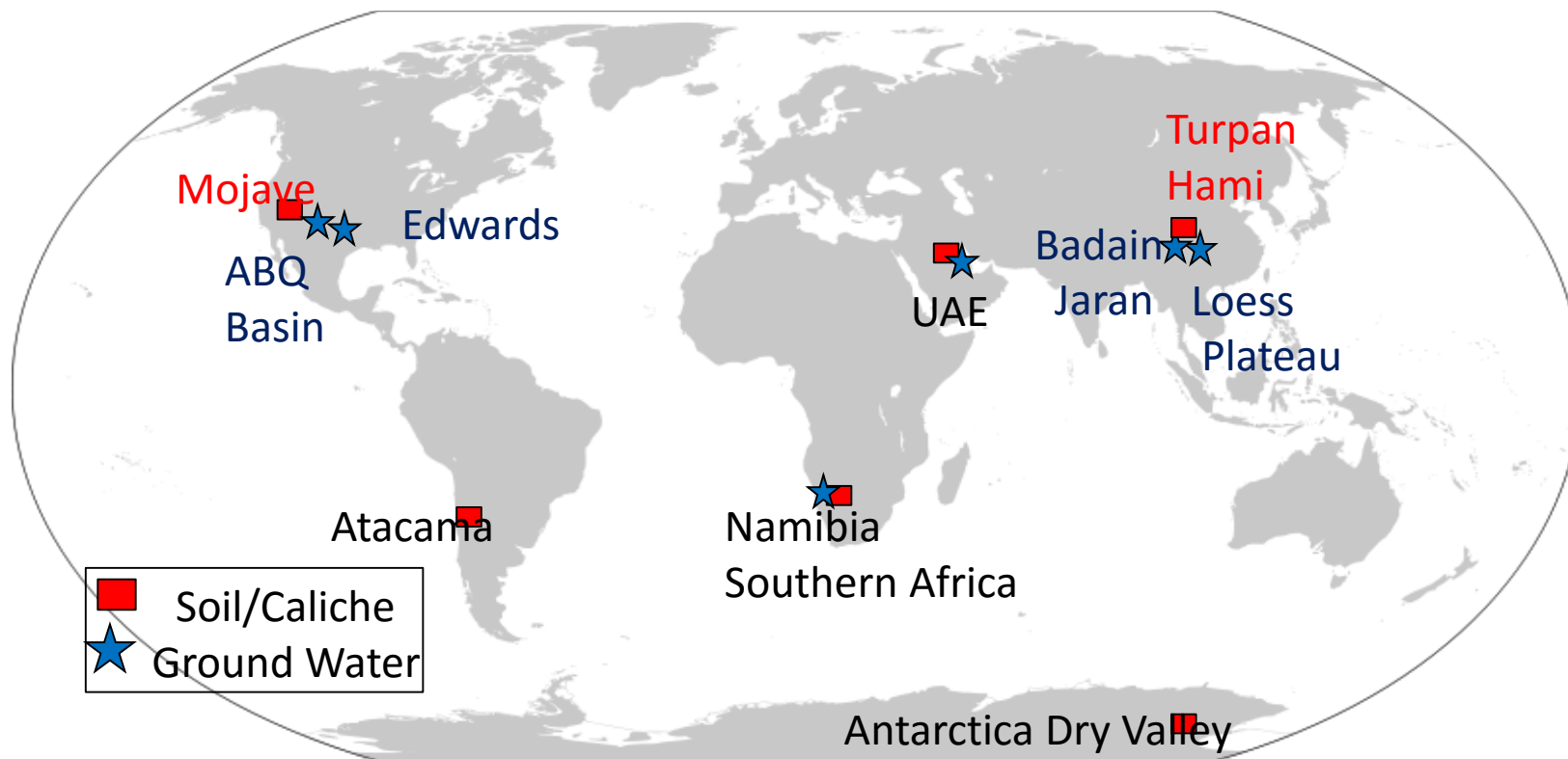


Figure 2.3.1. Map of Sample Locations

Table 2.3.1. Locations, sample types, summary statistics for ClO₄⁻, NO₃⁻, and Cl⁻ in groundwater and deposition sample sets. Molar ratios are averages of log-transformed ratios. r and P values are for linear regressions (see Figure 2.3.2)

Location	Site	Sample Type	Molar Ratio			NO ₃ and ClO ₄		Cl and ClO ₄		Cl and NO ₃	
			NO ₃ /ClO ₄	Cl/ClO ₄	Cl/N O ₃	r	P	r	P	r	P
All GW			24,000	240,000	15	0.98	<0.001	0.87	<.001	0.92	<.001
United States	Edwards Aquifer	Public Supply/ Monitoring	22,000	96,000	4.3	0.22	0.04	0.27	0.01	-.07	0.46
	Albuquerque Basin	Supply/ Monitoring	22,000	300,000	14	0.82	<.001	0.22	0.13	0.05	0.69
China	Loess Plateau	Springs	11,000	47,000	5.4	0.95	<0.001	0.15	0.69	0.35	0.33
	Badain Jaran	Shallow Wells/Springs	61,000	1,000,000	17	0.57	0.01	0.37	0.11	0.20	0.4
Namibia		Springs/well	29,000	2,300,000	81	0.91	<0.001	0.89	0.001	0.96	<.001
UAE		Supply and Monitoring Wells	22,000	550,000	25	0.98	<0.001	0.95	<.001	0.94	<.001
Deposition											
United States ¹	18 sites across U.S.	Wet Deposition	100,000	35,000	0.34	0.7	<0.001	0.52	<0.01	.5 ³	.01
United States ²	Mojave	Total Deposition	22,000	6,600	0.33	0.89	<0.01	0.84	<.01	0.89	<.01

Table 2.3.2. Locations, sample types, summary statistics for ClO₄⁻, NO₃⁻, and Cl⁻ in soil/caliche sample sets. Molar ratios are averages of log-transformed ratios. R and P values are for linear regressions (see Figure 2.3.5).

Location	Site	Sample Type	Sample Depth Range (m)	Molar Ratio			NO ₃ and ClO ₄		Cl and ClO ₄		Cl and NO ₃	
				NO ₃ /ClO ₄	Cl/ClO ₄	Cl/NO ₃	r	P	r	P	r	P
United States-Mojave	Total			85000	580000	6.7	0.66	<.001	0.18	0.06	0.42	<.001
	Saratoga Hills	Profile	0-0.4	114000	7400000	65	0.14	0.84	-0.56	0.33	-.08	0.9
	Bully Hill	Profile	0-0.9	240000	300000	1.3	0.87	0.06	.79	0.06	.98	.002
	Confidence Hills	Profile	0-1.0	115000	7400000	65	0.89	0.02	0.23	0.66	0.47	0.35
	Confidence Hills	Profile	0-0.3	41000	530000	13	0.98	.002	0.08	0.89	0.04	0.95
	Confidence Hills	Profile	0-0.7	25000	6300000	174	0.99	<0.001	0.72	0.17	0.97	0.03
	Confidence Hills	Profile	0-0.3	110000	141000	1.3	0.28	0.72	0.24	0.76	0.77	0.23
	Confidence Hills	Profile	0-0.4	91000	480000	5.2	0.30	0.62	-0.31	0.61	0.80	0.1
	Desert Pavement	Composite	0-0.3	86000	100000	1.2	0.90	0.01	0.81	0.05	0.96	0.002
	Desert Pavement	Profile	0-0.6	72000	77000	1.3	0.99	<.001	0.99	<.001	0.99	<0.001
	Subsurface Salt Bulge	Profile	0-16	40000	190000	4.6	0.92	<.001	0.64	0.001	0.75	<.001
	Rainbow Hills	Grab	0-4	230000	216000	1.0	0.99	0.002	0.99	.001	0.99	0.01
	Fort Irwin	Profile		216000	709000	3.53	0.61	0.2	0.04	0.93	0.59	0.22
Southern Africa	Total			120000	2700000	22	0.79	<.001	-.01	0.96	<0.08	0.67
	Namibia	Composite	0-0.3	96000	730000	7.3	0.81	<.001	0.07	0.77	-0.05	0.82
	South Africa	Composite	0-0.3	150000	650000	4.4	0.99	0.06	0.93	0.25	0.96	.18
	Botswana	Composite	0-0.3	125000	41000000	330	0.96	<.001	0.52	.23	0.53	.23
UAE				21000	870000	42	0.99	<.001	0.54	.11	0.25	0.40
	Soils	Composite	0-0.3	14000	19000	1.1	0.87	0.05	0.03	.96	0.41	0.36
	Sabkha	Composite	0-1	28000	1700000	82	0.99	<.001	0.15	.81	-0.12	0.8
Atacama	Total			1400	1500	1.1	0.63	<.001	0.26	.006	0.66	<.001
	AT6	Profile	0-1.5	2200	4700	2.3	0.74	0.002	0.59	.02	0.48	0.08
	AT8	Profile	0-2.0	570	1500	2.7	0.65	0.002	0.53	.02	0.52	0.02
	AT9	Profile	0-1.9	730	1100	1.5	0.91	<.001	0.61	.08	0.38	0.31
	AT16	Profile	0-0.7	13000	1300	0.1	0.98	<.001	0.48	.33	-0.50	0.31
	AT18	Profile	0-3.0	1600	1200	0.7	0.77	<.001	0.74	.002	0.93	<0.001
	Mine	Profile	0-3.0	550	615	1.1	0.32	0.22	0.86	<.001	0.93	<0.001
	Transect	Composite	0-.3	1000	2200	2.1	0.93	<.001	-0.1	.69	0.2	0.44
China	Turpan-Hami	Grab	<2	12000	190000	17	0.61	0.05	-.29	0.39	-0.56	0.07
Antarctica McMurdo Dry Valleys- University Valley	Total		<0.7	14,000	7200	0.35	0.78	<.001	0.81	<.001	0.75	<.001
	1	Profile	0-.36	11,000	4,600	0.46	0.83	<.001	0.72	.002	0.66	0.006
	2	Profile	0-.40	20,000	6,700	0.34	0.99	<.001	0.99	<.001	0.99	<0001
	3	Profile	0-.56	7,900	5,000	0.66	0.98	<.001	0.99	<.001	0.97	<.001
	4	Profile	0-.66	11,000	8,100	0.87	0.86	<.001	0.98	<.001	0.79	0.004
	5	Profile	0-.66	19,000	10,000	0.68	0.75	0.03	0.97	<.001	0.77	0.03
	7	Profile	0-.16	13,000	8,100	0.64	0.98	0.004	0.82	.09	0.76	0.13

2.3.3 Materials and Methods

2.3.3.1 Soil Extraction Methods

Soluble salts from soil samples were extracted by mixing the soil with Milli-Q water at a 5:1 ratio (mass of water: mass of soil) and shaking for 24 h. The samples were centrifuged for 10 minutes, after which the supernatant was decanted and filtered (0.2 μm). All extraction sets were accompanied by an extraction duplicate and extraction sample spike (soil + known amount of ClO_4^- spike), extraction blank (DDI water only), and extraction spike (known amount of ClO_4^- spike). Moisture contents of samples were determined by drying at 105 $^\circ\text{C}$ for 24 hours. Sub-samples of some extracts were preserved at pH~11 for analysis of NO_3^- stable isotopic composition.

2.3.3.2 Analytical Methods

Analysis of soil extracts and groundwater for ClO_4^- , NO_3^- , Cl^- , and NO_3^- stable isotopic composition has been described previously (Section 2.2; Jackson et al., 2010). Briefly, ClO_4^- was quantified using an ion chromatograph-tandem mass spectrometry technique (IC-MS/MS) that consisted of a GP50 pump, CD25 conductivity detector, AS40 automated sampler and Dionex IonPac AS16 (250 X 2 mm) analytical column. The IC system was coupled with an Applied Biosystems – MDS SCIEX API 2000TM triple quadrupole mass spectrometer equipped with a Turbo-IonSprayTM source. A 45 mM hydroxide (NaOH) eluent at 0.3 ml min^{-1} was followed by 90% acetonitrile (0.3 ml min^{-1}) as a post-column solvent. To overcome matrix effects, all samples were spiked with an oxygen-isotope (^{18}O) labeled ClO_4^- internal standard. A 25 μL loop was used for sample loading with a 0.0005 μM level of quantification. Chloride and NO_3^- were analyzed following EPA Method 300.0 using a Dionex LC20, an IonPac AS14A column (4 X 250 mm), 8 mM Na_2CO_3 /1 mM NaHCO_3 eluent, and an Anion Atlas electrolytic suppressor. The limit of detection (LOD) of Cl^- and NO_3^- were 1.4 μM and 3.5 μM , respectively. Individual sample quantification limits were based on the final dilution of the sample extract.

$\delta^{15}\text{N}$ and $\delta^{18}\text{O}$ in NO_3^- were measured by continuous-flow isotope-ratio mass spectrometry on N_2O produced from NO_3^- by bacterial reduction (Sigman et al., 2001; Casciotti et al., 2002; Coplen et al., 2004). The data were calibrated by analyzing NO_3^- isotopic reference materials as samples and normalizing to $\delta^{15}\text{N}$ and $\delta^{18}\text{O}$ reference values (Böhlke et al., 2003; Jackson et al., 2010). For samples with elevated $\Delta^{17}\text{O}$ of NO_3^- , $\delta^{15}\text{N}$ values determined by the bacterial N_2O method using conventional normalization equations may be slightly higher than true values (Sigman et al., 2001; Böhlke et al., 2003; Coplen et al., 2004). $\delta^{15}\text{N}$ values reported here were not adjusted for this effect because $\Delta^{17}\text{O}$ values were not measured in all samples. True $\delta^{15}\text{N}$ values could be lower than reported values by varying amounts ranging from 0 ‰ for biogenic NO_3^- with $\delta^{18}\text{O}$ and $\Delta^{17}\text{O}$ near 0 ‰ to around 1.6 ‰ for atmospheric NO_3^- from Antarctica with the highest $\delta^{18}\text{O}$ and $\Delta^{17}\text{O}$ values.

For selected samples, the $\Delta^{17}\text{O}$ value of NO_3^- was measured by dual-inlet isotope-ratio analysis of O_2 produced by off-line partial decomposition of AgNO_3 (modified from Michalski et al.,

2002). NO_3^- was isolated from mixed salt solutions by trapping on large-volume AG1X8 ion-exchange resin columns, followed by gradual elution with 0.5 M KCl to separate anions (Hannon et al., 2008). The KCl-KNO₃ eluent was passed through AG-MP50 cation-exchange resin columns in the Ag form to remove Cl and exchange K for Ag, then freeze dried to produce AgNO₃ salt. The AgNO₃ was heated under vacuum at 520°C while connected to a 5A° mol-sieve trap cooled with liquid N₂ to collect O₂, which was then isolated and transferred to the mass spectrometer and analyzed against tank O₂. Measured $\Delta^{17}\text{O}$ values of NO_3^- isotopic reference materials RSIL-N11 and USGS35 prepared as AgNO₃ were indistinguishable from reported values of -0.2 and +21.1 ‰, respectively, as defined in Böhlke et al. (2003).

2.3.4 Data Analysis

Average molar ratios were calculated by averaging log-transformed individual sample ratios and then back transforming to standard notation. This was done to reduce the impact of individual samples with order of magnitude differences in ratios. Regression analysis was performed on data as presented in figures and significance was designated as $P < 0.05$.

2.3.5 Results and Discussion

Results are summarized for all samples in Figures 2.3.2 and 2.3.3 and Tables 2.3.1 and 2.3.2 to highlight major global patterns and processes affecting the distribution of ClO_4^- and NO_3^- . Results for individual sites and sample types are then presented in more detail in Figures 2.3.4 and 2.3.5 to facilitate discussion of local patterns, controls, and exceptions to the global patterns.

2.3.5.1 Global Patterns of ClO_4^- , NO_3^- Concentrations and NO_3^- Isotopes

Combined data from this study indicate the global occurrence of ClO_4^- and positive correlation between NO_3^- and ClO_4^- concentrations in oxic groundwaters (Figures 2.3.2, Table 2.3.1), and in soils and caliches (Figure 2.3.3, Table 2.3.2), in arid and semi-arid environments. Previous work has largely attributed the source of indigenous natural ClO_4^- to atmospheric production and subsequent deposition (Section 2.1 and 2.2; Rajagopalan et al., 2009; Jackson et al., 2010). Excluding the Atacama site, our results are generally consistent with this assertion based on similarities between site $\text{NO}_3^-/\text{ClO}_4^-$ ratios and those previously reported. Atmospheric deposition data include wet deposition at 18 sites located across the conterminous U.S., Alaska, and Puerto Rico using weekly samples collected over 3 years (Rajagopalan et al., 2009) and total atmospheric deposition (wet plus dry including dust) collected over a 6 year period at the Amargosa Desert Research Site, Nevada (Andraski et al., 2014). The average molar ratios of $\text{NO}_3^-/\text{ClO}_4^-$ in wet deposition ranged over ~one order of magnitude, while $\text{Cl}^-/\text{ClO}_4^-$ ratios varied over 2 orders of magnitude and were significantly related to distance from a coast. $\text{NO}_3^-/\text{ClO}_4^-$ and $\text{Cl}^-/\text{ClO}_4^-$ molar ratios in total deposition were lower than in wet deposition and the NO_3^- was largely unaltered atmospheric, based on stable isotope ratios (Figures 2.3.2, 2.3.3, 2.3.6; Table 2.3.1).

In contrast to the relatively good correlation between NO_3^- and ClO_4^- at most sites, concentrations of Cl^- appear to be relatively poorly correlated with either NO_3^- or ClO_4^- for most sites (Figures 2.3.4 and 2.3.5). Most samples had relatively high $\text{Cl}^-/\text{NO}_3^-$ and $\text{Cl}^-/\text{ClO}_4^-$ ratios

compared to those of modern precipitation and total deposition in North America (Figure 2.3.7). Local high deposition fluxes of marine (seasalt) Cl^- could account for some, but not all of these differences. Additional sources of Cl^- unrelated to the Cl^- deposited with ClO_4^- and NO_3^- could include local Cl^- atmospheric inputs remobilized from salt flats, upwelling of saline groundwater, and run-on of Cl^- laden water. Alternatively, high $\text{Cl}^-/\text{NO}_3^-$ and $\text{Cl}^-/\text{ClO}_4^-$ ratios could indicate simultaneous net loss of NO_3^- and ClO_4^- as a result of microbial reduction where moisture and organic matter were present (Nozawa-Inoue et al., 2005). This could have occurred during episodic events, defined as locally reducing conditions during individual precipitation wetting events that led to the depletion of oxyanions during the accumulation period of the current oxyanions. Cl^- remaining after such episodic reduction is hereafter referred to as “episodic Cl^- ”. Alternatively, oxyanions could have been depleted relative to Cl^- during prolonged periods of wetter climate in the past prior to the accumulation period of the observed oxyanions. For this case, we hereafter refer to atmospheric Cl^- not associated with the current NO_3^- and ClO_4^- as “non-co-deposited Cl^- ”.

Isotope data indicate sources of NO_3^- from these sites varied from essentially 100% unaltered atmospheric to 100% biogenic, where biogenic NO_3^- could be derived from various N sources including recycled atmospheric NO_3^- (Figure 2.3.6). Collectively, isotopic analyses of NO_3^- are consistent with two major factors affecting $\delta^{15}\text{N}$ and $\delta^{18}\text{O}$ of NO_3^- : (1) variation in the relative proportions of atmospheric NO_3^- (low $\delta^{15}\text{N}$, high $\delta^{18}\text{O}$) and biogenic NO_3^- (high $\delta^{15}\text{N}$, low $\delta^{18}\text{O}$), yielding an overall negative correlation between $\delta^{15}\text{N}$ and $\delta^{18}\text{O}$, and (2) variation in the isotope fractionation effect of NO_3^- reduction, yielding local positive correlations between $\delta^{15}\text{N}$ and $\delta^{18}\text{O}$ at some sites. NO_3^- reduction can occur in the unsaturated zone and/or in groundwater after recharge. In addition, minor variations in $\delta^{18}\text{O}$ of biogenic NO_3^- may be related to local $\delta^{18}\text{O}$ of meteoric water during nitrification, and N cycling in soils and plants can cause local or regional variation in the $\delta^{15}\text{N}$ values of organic matter that is subject to nitrification (Handley et al., 1999; Amundson et al., 2003; McMahon and Böhlke, 2006). Isotopic variations caused by N cycling and NO_3^- reduction effects appear to be most prevalent at sites with relatively large fractions of biogenic NO_3^- , such that the combined effects of these major processes give a roughly triangular shape to the collection of isotope data in Figure 2.3.6 with the exception of Antarctica, which has anomalously low $\delta^{15}\text{N}$.

Clearly, patterns and processes are complex and each site is unique. Nevertheless, to facilitate discussion of individual sites and sample types, we present the following conceptual model relating relative concentrations of ClO_4^- and NO_3^- with the isotopic indicators of NO_3^- sources, based on the assumption that atmospheric sources ultimately are important for both ClO_4^- and NO_3^- . Assuming no net gains or losses of ClO_4^- other than atmospheric deposition, relations between $\text{NO}_3^-/\text{ClO}_4^-$ ratios and NO_3^- $\delta^{18}\text{O}$ values can be explored using a mixing model with three bounding cases (Figure 2.3.8): 1) deposition and preservation of atmospheric NO_3^- with no addition of biogenic NO_3^- ; 2) preservation of atmospheric NO_3^- with addition of biogenic NO_3^- produced by nitrification of reduced N from either fixed N_2 , atmospheric NH_4^+ , or accumulated organic matter (Figure 2.3.8 black dashed lines); and 3) assimilation of atmospheric NO_3^- and regeneration with biogenic NO_3^- with no net gain or loss of N (Figure 2.3.8 red dashed lines). In

this model, we have excluded the case of significant simultaneous NO_3^- and ClO_4^- reduction or NO_3^- reduction alone, which are alternative possibilities discussed below. For the Mojave and Atacama sites, ClO_4^- stable isotope data can be used to exclude large amounts of biological reduction (Jackson et al., 2010). We have not ruled out the possibility of abiotic O exchange with H_2O as an alternative to nitrification as a way of lowering $\delta^{18}\text{O}$ of atmospheric NO_3^- , but there is no direct evidence for such exchange in these environments, whereas there is evidence that lower NO_3^- $\delta^{18}\text{O}$ values are associated with increasing soil biologic activity.

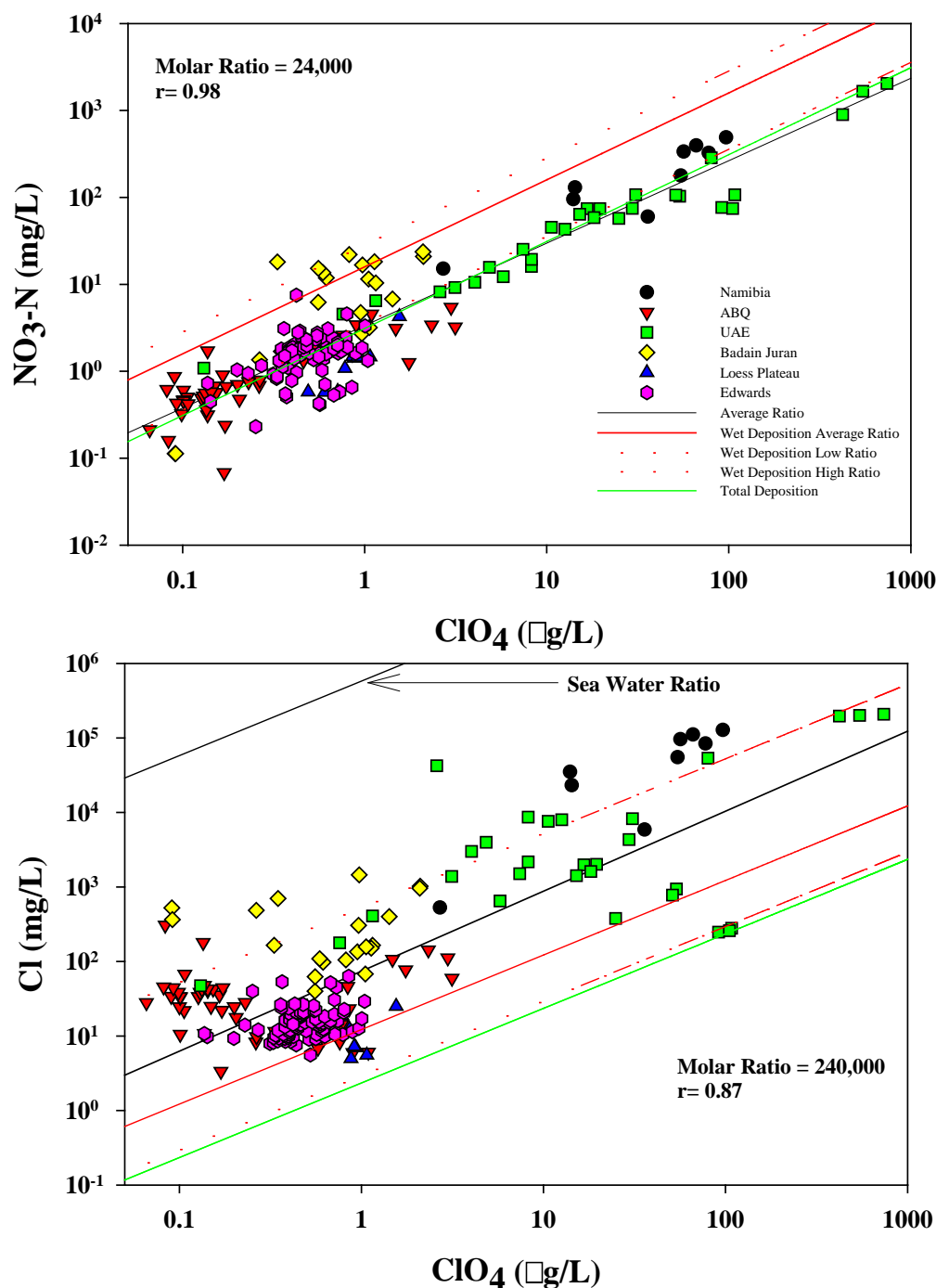


Figure 2.3.2. Relations among ClO_4^- , NO_3^- , and Cl^- concentrations in groundwater. Ratios for all groundwater samples are shown by solid black lines. Average ratios in U.S. wet deposition are shown as solid red lines, and minimum and maximum average site ratios are shown as dashed lines. Ratios for wet deposition include 18 sites located across the conterminous U.S., as well as Alaska, and Puerto Rico for weekly samples over a three year period (Rajagopalan et al., 2009). The total deposition ratio (green line) represents the 6 year average of quarterly samples (Andraski et al., 2014).

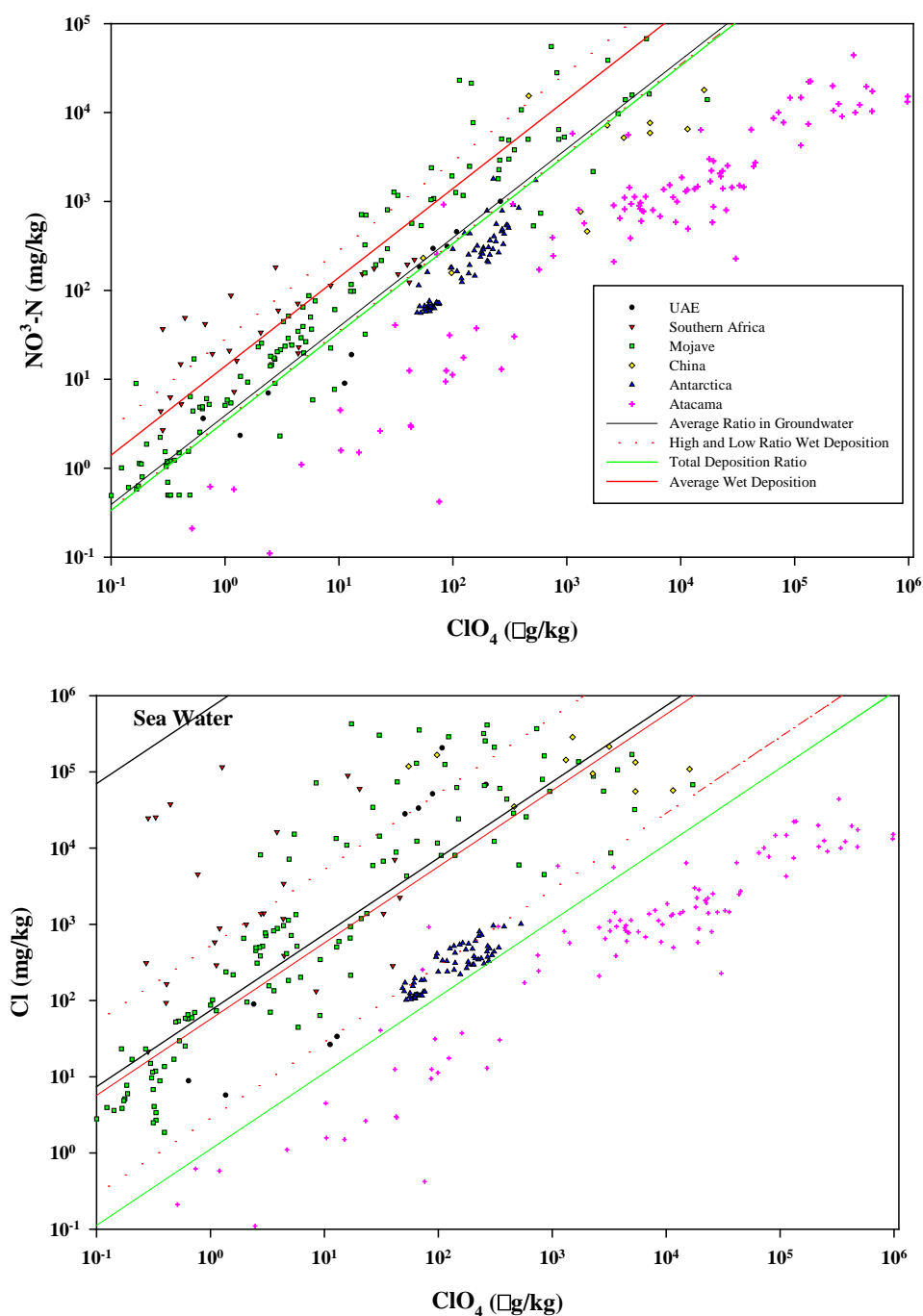


Figure 2.3.3. Relations between concentrations of ClO_4^- and NO_3^- and Cl^- for all soils and caliches. Average ratio in wet deposition is shown as solid red lines, and average minimum and maximum ratios for all sites are shown as dashed lines. Ratios for wet deposition include 18 sites located across the conterminous U.S., Alaska, and Puerto Rico for weekly samples over a three year period (Rajagopalan et al., 2009). The total deposition ratio (green line) represents the 6 year average of quarterly samples (Andraski et al., 2014).

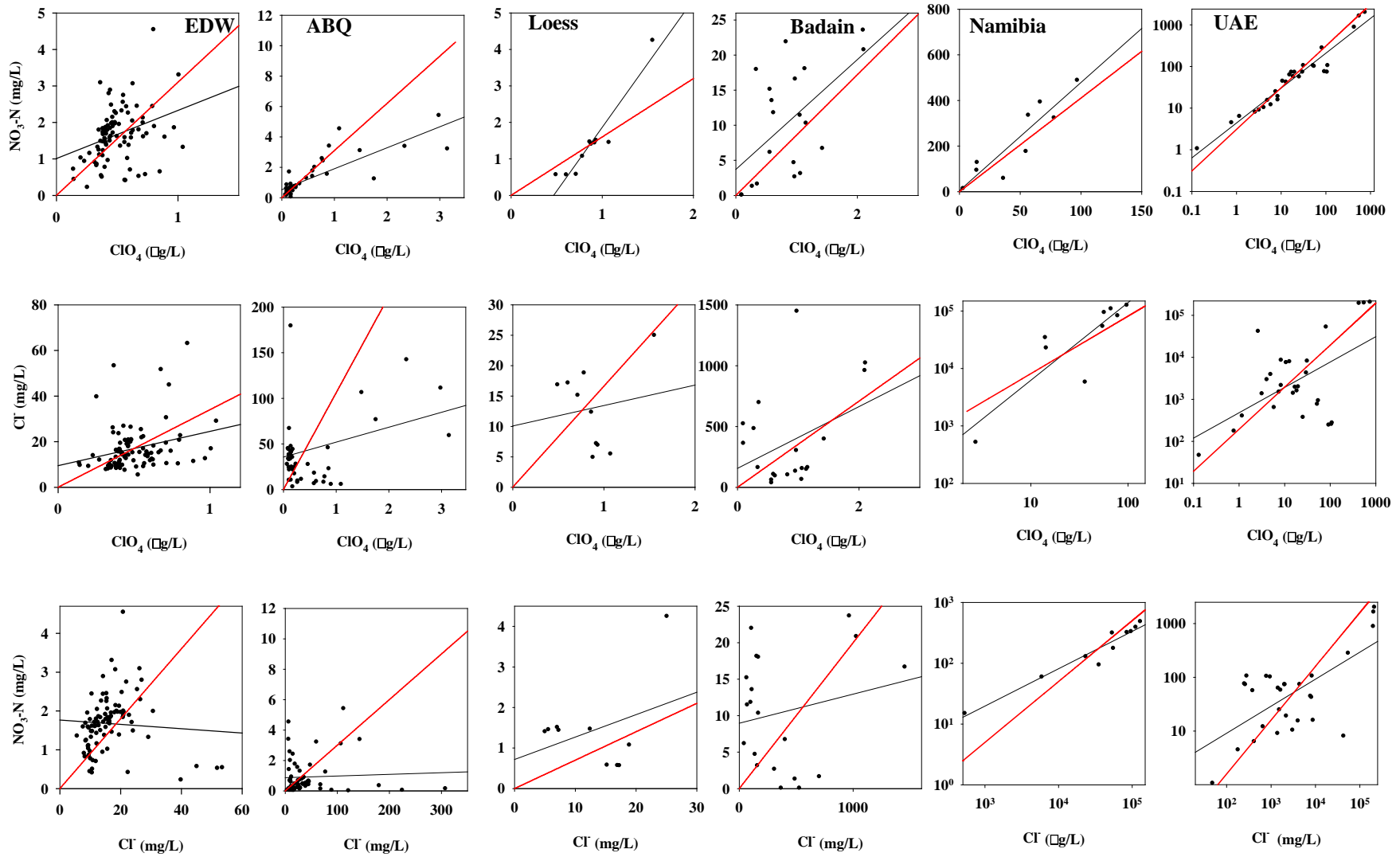


Figure 2.3.4. Relations among ClO_4^- , NO_3^- , and Cl^- in groundwater from arid and semi-arid locations. Solid black lines represent linear regressions of concentration data; red lines represent averages of log-transformed ratios. Correlation coefficients and P values are listed in Table 2.3.1.

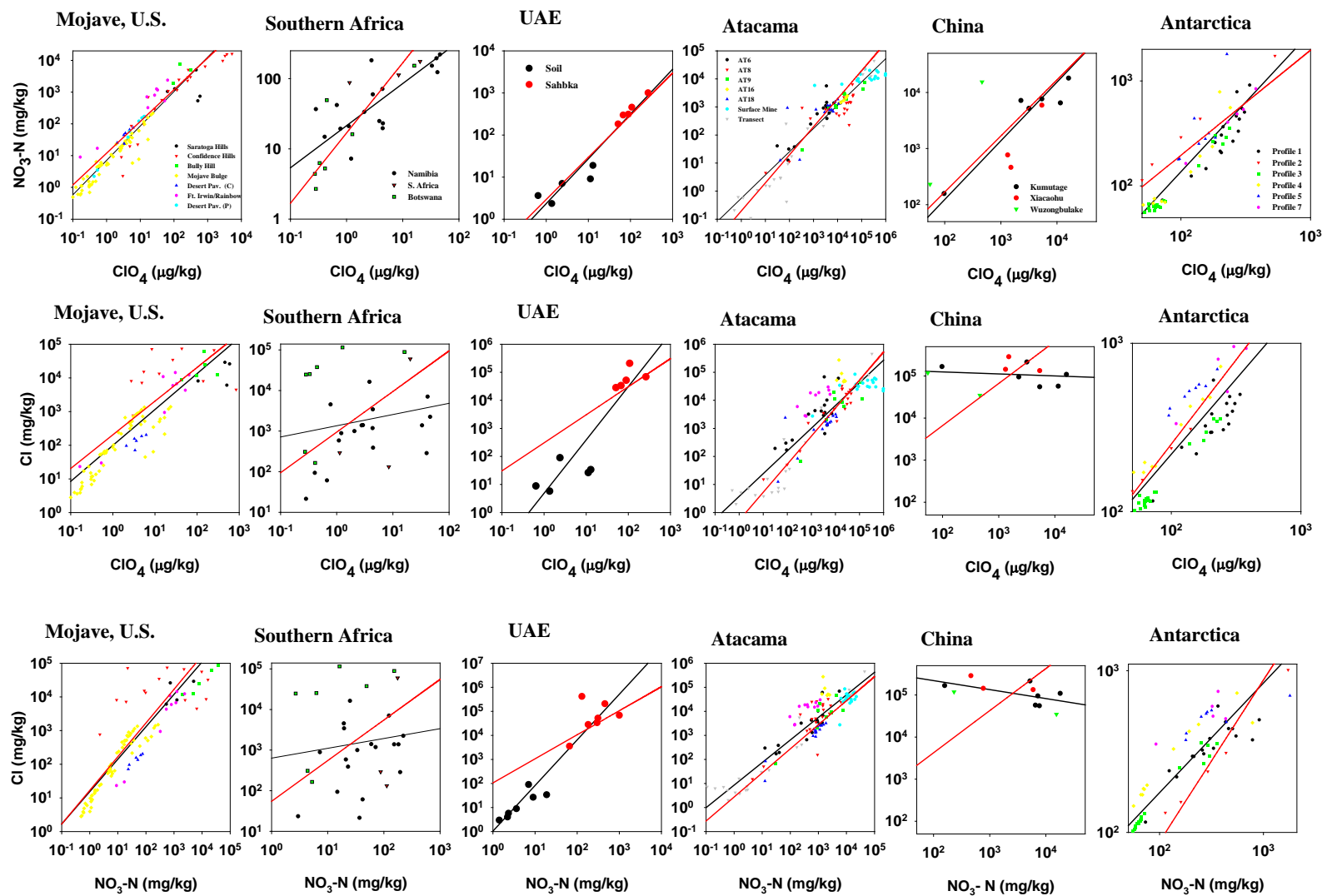


Figure 2.3.5. Relations among ClO_4^- , NO_3^- , and Cl^- concentrations in soils and caliches from arid and semi-arid locations. Solid black lines represent linear regressions of concentration data; red lines represent averages of log –transformed ratios. Correlation coefficients and P values are listed in Table 2.3.2.

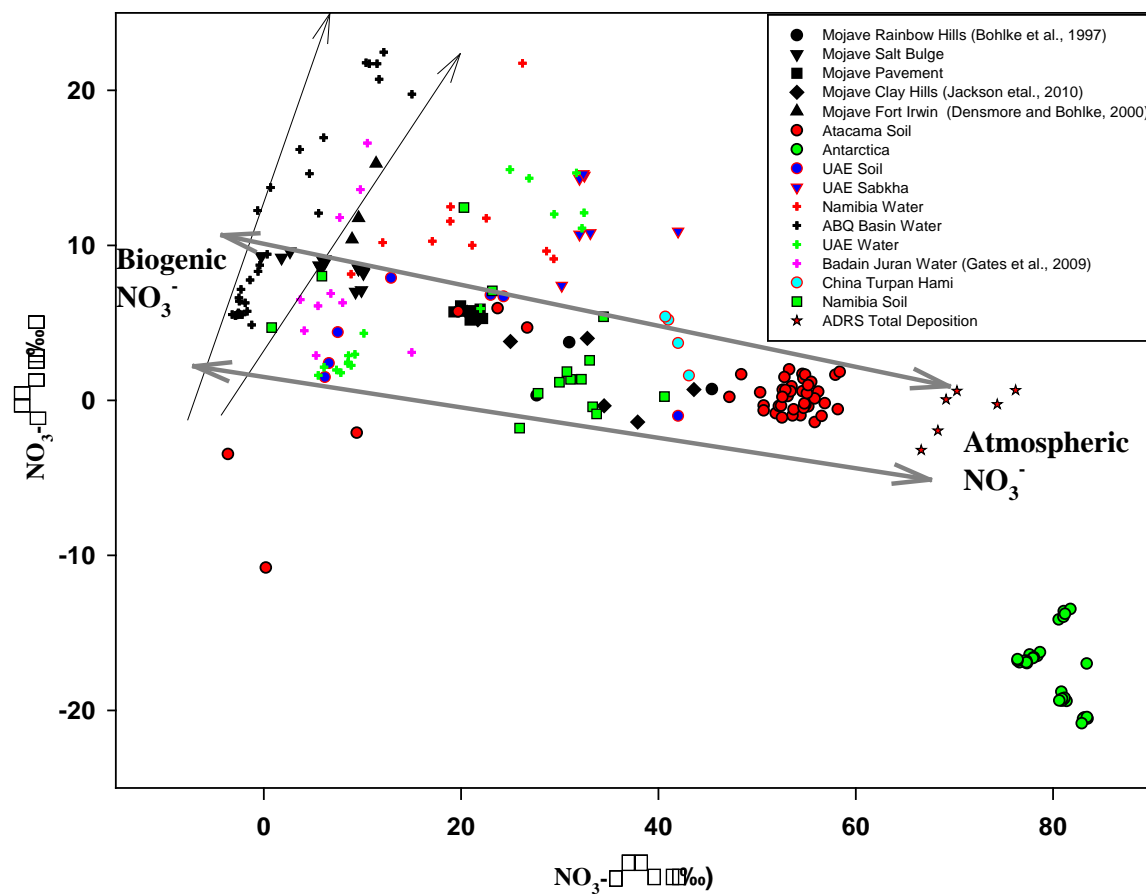


Figure 2.3.6. Relation between $\delta^{15}\text{N}$ and $\delta^{18}\text{O}$ of NO_3^- in groundwater and leachate from soil and caliche samples. Black arrows represent the range of slopes reported previously for isotopic fractionation due to denitrification and grey arrows represent general trends in mixing ratios of atmospheric and biogenic NO_3^- .

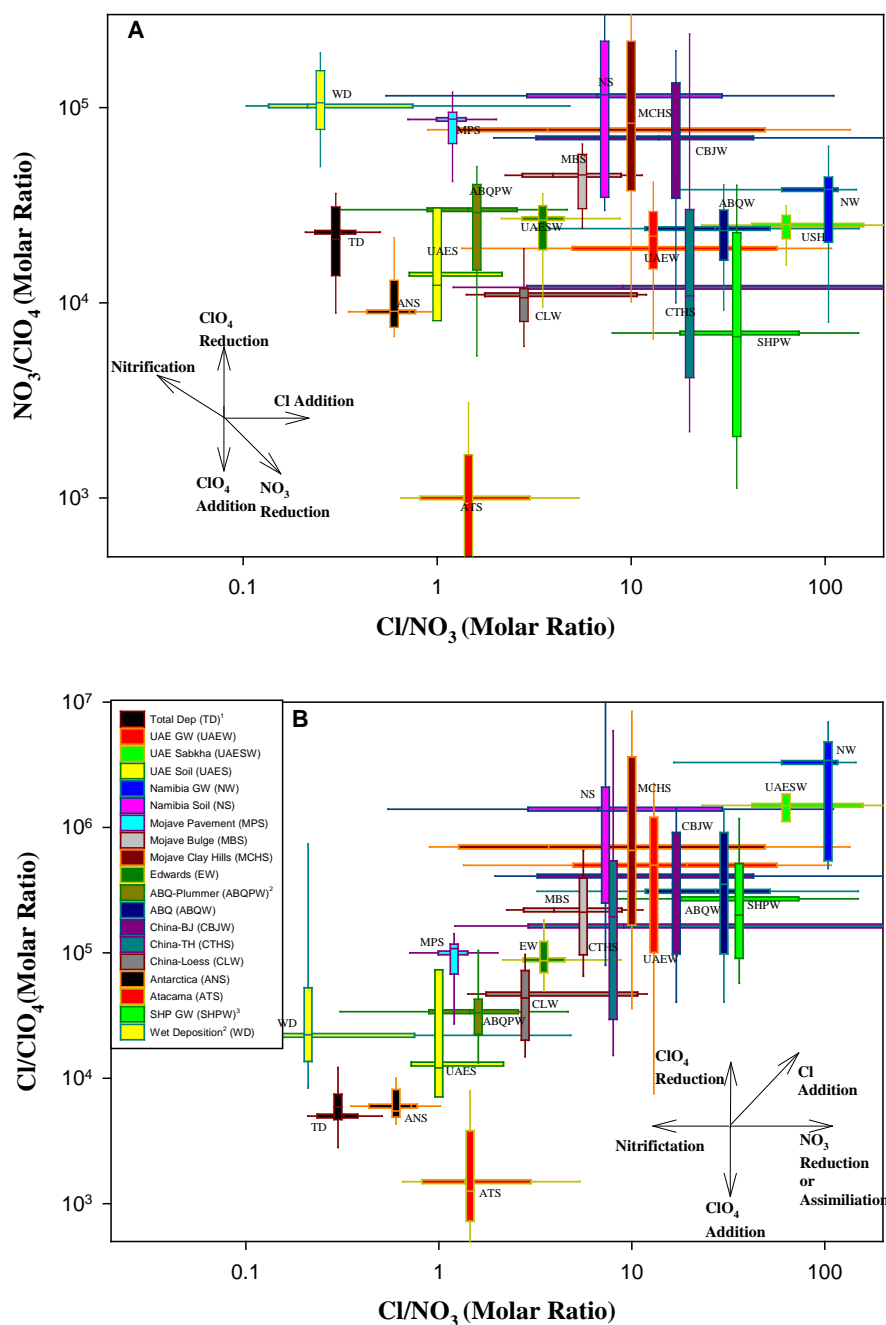


Figure 2.3.7. Variation of (A) NO₃/ClO₄ or (B) Cl/CIO₄ ratios with respect to Cl/NO₃ ratios in soils and groundwaters from arid and semi-arid locations as well as wet and dry deposition in North America. Box plots represent the 25th and 75th percentile values and extended lines from boxes represent the 90th and 10th percentiles. Arrows indicate hypothetical qualitative trajectories that could be caused by various processes. (¹Andraski et al., 2104; ²Plummer et al., 2006; ³Rajagopalan et al., 2006).

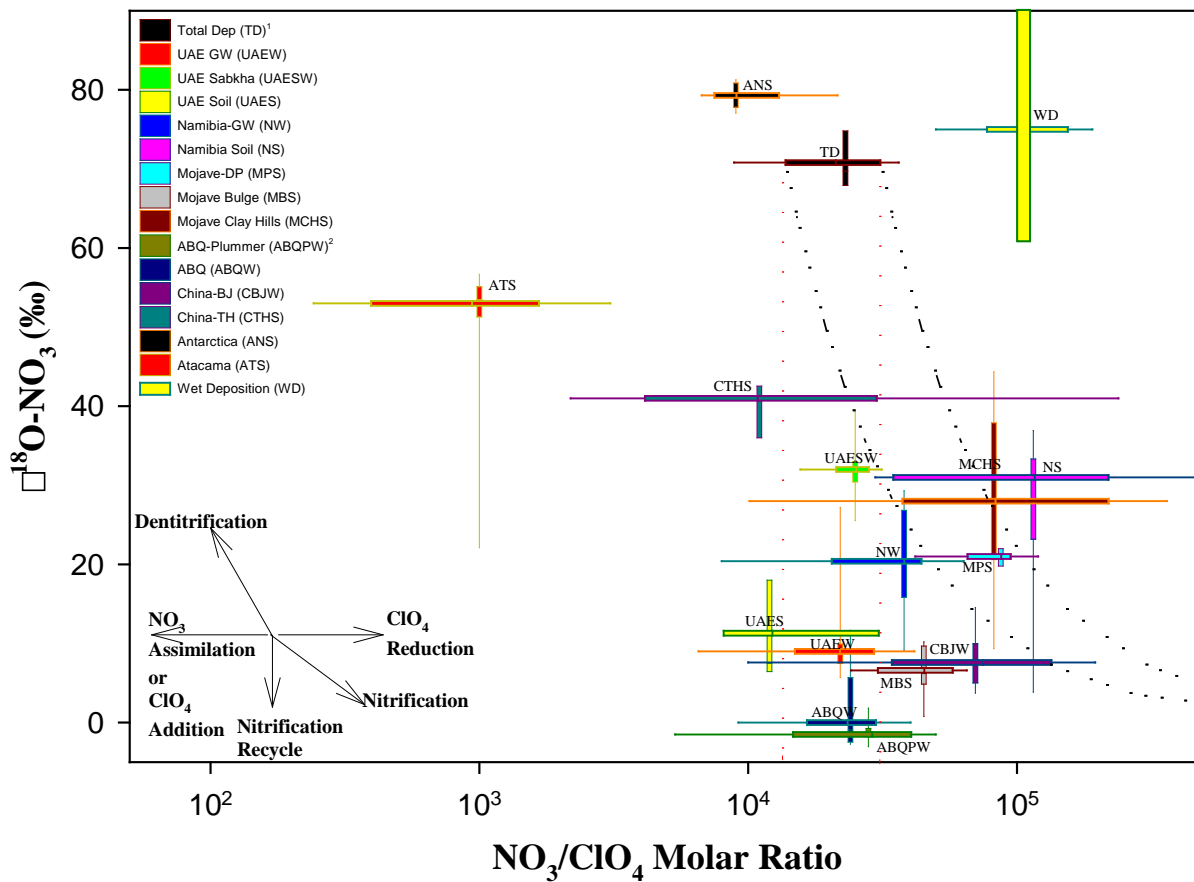


Figure 2.3.8. Relation between $\delta^{18}\text{O}$ of NO_3^- and bulk NO_3/ClO_4 ratios in soils and groundwaters from arid and semi-arid locations as well as wet and dry deposition in North America. Box plots represent the 25th and 75th percentile values and extended lines from boxes represent the 90th and 10th percentiles. Dashed curves originating at total deposition indicate hypothetical trends caused by either: 1 (red lines) atmospheric NO_3 assimilation, mineralization, and nitrification with no net loss or gain of N; or 2 (black curve) addition of biogenic NO_3 to uncycled atmospheric NO_3 , assuming in both cases ClO_4 is unaffected. Arrows in the lower left corner indicate hypothetical qualitative trajectories that could be caused by various processes. (¹Andraski et al., 2014; ²Plummer et al., 2006).

2.3.5.2 Groundwater Results

Groundwater Overview

The ClO_4^- concentrations in groundwater samples varied over four orders of magnitude, whereas the $\text{NO}_3^-/\text{ClO}_4^-$ molar ratios were remarkably constant (average = 24,000) and almost identical to that of total atmospheric deposition in the Amargosa Desert (Figure 2.3.2). This is true despite the geographic diversity of arid and semi-arid locations and isotopic evidence for varying degrees of biologic N cycling in soils or plants prior to recharge at these sites (Figure 2.3.6 and 2.3.8). Isotopic evidence for varying NO_3^- reduction in groundwater was not associated with substantial variation of $\text{NO}_3^-/\text{ClO}_4^-$ ratios. However, it should be noted that the variation in $\text{NO}_3^-/\text{ClO}_4^-$ ratios within most sites could be sufficient to accommodate substantial (>50%) NO_3^- losses. $\text{Cl}^-/\text{ClO}_4^-$ ratios were much more variable and for most sites these constituents were not correlated (Figure 2.3.2; Table 2.3.1). The lack of correlation and much larger $\text{Cl}^-/\text{ClO}_4^-$ ratios compared to total deposition for non-coastal sites supports addition of Cl^- from non-atmospheric sources, “episodic Cl^- ” or “non-co-deposited Cl^- ” in many cases.

Albuquerque Basin, U.S. (ABQ)

ClO_4^- concentrations in ABQ groundwater samples ($n=63$) varied over a relatively narrow range (< 0.05 ($n=22$) to $3.1 \mu\text{g/L}$) and concentrations were similar to those previously reported for this aquifer system (Plummer et al., 2006) (Figure 2.3.4). While some wells may have been influenced by anthropogenic activities, many were not impacted based on groundwater ages (Plummer et al., 2006; Bexfield et al., 2011). For the 41 samples with detectable ClO_4^- , NO_3^- and ClO_4^- were correlated ($r = 0.82$) but there was no correlation between Cl^- and either ClO_4^- or NO_3^- ($r = 0.22$ and 0.05 , respectively) (Table 2.3.1 and Figure 2.3.4). The average $\text{NO}_3^-/\text{ClO}_4^-$ and $\text{Cl}^-/\text{ClO}_4^-$ molar ratios were 22,000 and 300,000, respectively.

A subset ($n= 30$) of ABQ groundwater samples was also evaluated for NO_3^- stable isotopic composition ($\delta^{15}\text{N}$ and $\delta^{18}\text{O}$) (Bexfield et al., 2011). NO_3^- in the aquifer appears to be almost completely biogenic and NO_3^- in a number of wells may have been impacted by denitrification given the linear trend, correlation ($r = 0.90$) and slope (1.05) of some $\delta^{15}\text{N}$ and $\delta^{18}\text{O}$ data pairs (Figure 2.3.6) (Granger et al., 2008). These results are consistent with previous findings (Plummer et al., 2006). NO_3^- stable isotope data were available for 9 of the 22 samples with ClO_4^- concentrations below the reporting limit ($0.05 \mu\text{g/L}$). Of these, the $\delta^{15}\text{N}$ and $\delta^{18}\text{O}$ values of all but one exhibited evidence of denitrification. These data could indicate ClO_4^- reduction was associated with partial NO_3^- reduction in some parts of the system. For water samples ($n = 21$) with detectable ClO_4^- and NO_3^- , and with NO_3^- stable isotope data, $\delta^{18}\text{O}$ values of NO_3^- were relatively low ($< 1 \text{ ‰}$ for all but 2 samples) and there was no apparent relation between $\text{NO}_3^-/\text{ClO}_4^-$ molar ratios and $\delta^{18}\text{O}$ or $\delta^{15}\text{N}$ values that would indicate substantial NO_3^- reduction or ClO_4^- reduction. Dissolved O_2 concentrations were highly variable ($< 0.1\text{--}7 \text{ mg/L}$) but there was no apparent relationship with NO_3^- or ClO_4^- concentrations. Jackson et al., (2010) reported

similar NO_3^- isotopic composition ($\delta^{18}\text{O} \sim -1 \text{ ‰}$) and $\text{NO}_3^-/\text{ClO}_4^-$ ratios (18,000 and 28,000) for two oxic groundwater samples from the ABQ basin.

$\text{NO}_3^-/\text{ClO}_4^-$ ratios and NO_3^- stable isotopic compositions of ABQ groundwaters are consistent with a model of atmospheric deposition and subsequent recycling of NO_3^- with no net addition of NO_3^- (Figure 2.3.8), but with substantial addition of Cl^- (Figure 2.3.7). The source of the Cl^- could originally be from non-atmospheric sources, “episodic Cl^- ”, or “non-co-deposited Cl^- ” (as previously defined). For the “episodic Cl^- ” case, NO_3^- and ClO_4^- would have to have been reduced substantially (~ 2 orders of magnitude), which is not supported by available isotope data for NO_3^- (Figure 2.3.6) or ClO_4^- (Jackson et al., 2010).

Edwards Aquifer, U.S.

ClO_4^- concentrations in Edwards Aquifer samples ($n=92$) varied over a narrow range (< 0.05 ($n=2$) to $1.0 \text{ } \mu\text{g/L}$). No information is available regarding the source of the ClO_4^- in this system and it is possible that some groundwater is impacted by anthropogenic NO_3^- and ClO_4^- . NO_3^- and ClO_4^- were marginally correlated ($r=0.22$), as were Cl^- and ClO_4^- ($r=0.27$) but no significant relation exists between Cl^- and NO_3^- (Table 2.3.1 and Figure 2.3.4). The average $\text{NO}_3^-/\text{ClO}_4^-$ molar ratio (22,000) was the same as that for the ABQ basin, but the average $\text{Cl}^-/\text{ClO}_4^-$ molar ratio (96,000) was less than that for the ABQ basin. The stable isotopic compositions of NO_3^- are not available for samples evaluated for ClO_4^- concentrations. Other studies have evaluated the stable isotopic composition of NO_3^- in the same segment of the Edwards Aquifer and concluded that the NO_3^- is predominately biogenic with no evidence of denitrification based on either the isotope data or excess N_2 gas (Musgrove et al., 2010). Similar to the ABQ basin, the data could be consistent with a model in which atmospheric NO_3^- deposition largely was replaced by biogenic NO_3^- in recharge with no net loss or gain, and with addition of Cl^- ($\sim 10\times$) from sources other than atmospheric co-deposition (Figure 2.3.7).

Loess Plateau, China

ClO_4^- concentrations in Loess Plateau groundwater samples ($n=10$) varied over a range ($0.6\text{--}1.6 \text{ } \mu\text{g/L}$) similar to those for the ABQ basin and Edwards Aquifer (Figure 2.3.4). NO_3^- and ClO_4^- concentrations were correlated ($r=0.95$) but Cl^- was not correlated with either ClO_4^- or NO_3^- (Table 2.3.1). The $\text{NO}_3^-/\text{ClO}_4^-$ and $\text{Cl}^-/\text{ClO}_4^-$ molar ratios were the lowest of any groundwater evaluated ($\sim 11,000$ and $47,000$, respectively). No data are available concerning the age of the groundwater or the origin of the NO_3^- but the $\text{NO}_3^-/\text{ClO}_4^-$ ratios are less and $\text{Cl}^-/\text{ClO}_4^-$ ratios greater than in measured deposition (Figure 2.3.2 and 2.3.7). Although agriculture was a common land use in the region, sampled groundwater was not highly enriched in NO_3^- . Irrigation was almost absent in the area. It is not possible to discuss the origin or subsequent fate of NO_3^- due to the absence of NO_3^- isotope data, but the relation between NO_3^- and ClO_4^- is similar to that in other geographically distant sites.

Badain Jaran, China

ClO_4^- concentrations in groundwater samples ($n=20$) ranged from 0.3 to 2.1 $\mu\text{g/L}$ and were correlated with NO_3^- ($r = 0.57$) (Figure 2.3.4, Table 2.3.1) but Cl^- was not correlated with ClO_4^- or NO_3^- . The average $\text{NO}_3^-/\text{ClO}_4^-$ molar ratio (61,000) was the highest of any of the groundwater locations. Given the remoteness of the location, lack of intensive agriculture, and age of at least some of the groundwater evaluated, it is likely the ClO_4^- is indigenous (Gates et al., 2008a,b). NO_3^- in this system previously has been attributed to nitrification of NH_4^+ derived from atmospheric deposition or from mineralization of organic matter produced by nitrogen fixation or biologic assimilation of atmospheric N. In a few samples, NO_3^- may have been partially reduced through denitrification and a few samples with elevated $\delta^{18}\text{O}$ and low $\delta^{15}\text{N}$ of NO_3^- may have minor unaltered atmospheric components (Gates et al., 2008a). Our samples represent a subset of those analyzed by Gates et al., (2008a). Of the 20 samples we evaluated for ClO_4^- , NO_3^- stable isotope data were available for 10 (Figure 2.3.6). Six samples previously identified as most likely to contain NO_3^- impacted by denitrification have $\text{NO}_3^-/\text{ClO}_4^-$ molar ratios that are not significantly lower than the overall average (i.e., do not appear to indicate substantial preferential NO_3^- loss). Three samples appear to be impacted by denitrification based on relatively low $\text{NO}_3^-/\text{Cl}^-$ ratios and elevated $\delta^{15}\text{N}$ and $\delta^{18}\text{O}$ values (Gates et al., 2008a). However, even for these samples the ratio of $\text{NO}_3^-/\text{ClO}_4^-$ is not consistently lower than the overall average.

NO_3^- and ClO_4^- occurrence are consistent with atmospheric deposition and at least partial preservation of the atmospheric NO_3^- with substantial dilution (replacement and addition) by biogenic NO_3^- based on slightly elevated $\delta^{18}\text{O}$ and elevated $\text{NO}_3^-/\text{ClO}_4^-$ ratios (Figure 2.3.18). $\text{Cl}^-/\text{ClO}_4^-$ and $\text{Cl}^-/\text{NO}_3^-$ ratios support large ($\sim 100\text{X}$) inputs of local, “episodic”, or “non-co-deposited atmospheric Cl^- ”, similar to the ABQ aquifer (Figure 2.3.7).

Namibia

ClO_4^- concentrations in Namibia groundwater samples ($n = 10$) ranged from 2.7-97 $\mu\text{g/L}$ (Figure 2.3.4). ClO_4^- was correlated with NO_3^- and Cl^- ($r = 0.91$ and 0.89 , respectively) and as such NO_3^- and Cl^- were also correlated ($r=0.96$) (Table 1). Given the remote location of the sample sites, high concentrations of ClO_4^- and NO_3^- , and NO_3^- isotopic composition, the ClO_4^- and NO_3^- are considered to be natural. The average $\text{NO}_3^-/\text{ClO}_4^-$ ratio (29,000) was similar to those in all other groundwaters evaluated excluding the Badain Jaran, while the average $\text{Cl}^-/\text{ClO}_4^-$ molar ratio was much higher (2,300,000). Stable isotope data indicate NO_3^- in the Namibia samples was predominantly biogenic, but included substantial unaltered atmospheric components based on elevated $\Delta^{17}\text{O}$ values in some samples (1.1 to 5.9 ‰; $n = 5$). The NO_3^- also appears to have been variably affected by NO_3^- reduction based on elevated $\delta^{18}\text{O}$ and $\delta^{15}\text{N}$ values (Figure 2.3.6) and higher $\delta^{18}\text{O}$ values than expected from biogenic-atmospheric mixtures based on the $\Delta^{17}\text{O}$ values.

Factors affecting the Namibia groundwater could be similar to those at the Badain Juran site (atmospheric deposition with conservation of the atmospheric component and dilution by

biogenic NO_3^-) but altered by some denitrification (Figure 2.3.8). High $\text{Cl}^-/\text{ClO}_4^-$ ratios could be due to high local Cl^- deposition fluxes considering the coastal proximity, as values overlap with the high end of the range for wet deposition from US coastal locations. This is supported by the significant correlation between Cl^- and ClO_4^- for this site but not others, and by the similar $\text{Cl}^-/\text{ClO}_4^-$ ratios in surface soils (Figure 2.3.7).

UAE

Maximum ClO_4^- concentrations for UAE groundwater were the highest of any groundwater evaluated (Figure 2.3.4). Highest concentrations (500-740 $\mu\text{g/L}$) occurred in sabkha areas ($n = 5$) but concentrations in some inland fresh groundwater ($n=20$) were also elevated (0.1 to 108 $\mu\text{g/L}$), similar to the concentration range for Namibia groundwater. ClO_4^- and NO_3^- were well correlated with each other ($r = 0.98$) and with Cl^- (Table 1). The average $\text{NO}_3^-/\text{ClO}_4^-$ molar ratio (22,000) was similar to those for the Edwards, ABQ, and Namibia sites (22,000, 23,000, and 29,000, respectively) (Table 2.3.1). The NO_3^- in most ($n=10$) of the fresh-water samples (production wells) for which NO_3^- stable isotope data are available ($n=12$) appears to be predominantly biogenic, with little evidence of NO_3^- reduction ($\delta^{15}\text{N} \sim 2 - 6 \text{‰}$ and $\delta^{18}\text{O} \sim 5 - 10 \text{‰}$; Figure 2.3.6). In contrast, all of the sabkha locations and two of the fresh-water well samples had a substantial unaltered atmospheric component with variable impacts from NO_3^- reduction based on $\delta^{18}\text{O}$ and $\delta^{15}\text{N}$ of NO_3^- (Figure 2.3.6) as well as $\Delta^{17}\text{O}$ of NO_3^- (8 to 8.5‰) in a subset of the sabkha samples.

The sabkha data are consistent with evapo-concentration of deposition with some dilution by biogenic NO_3^- and only limited loss of the atmospheric NO_3^- component if the impact of NO_3^- reduction indicated by isotope data is taken into account. $\text{Cl}^-/\text{ClO}_4^-$ ratios were elevated and variable, possibly reflecting variable marine, atmospheric, and subsurface salt sources, and are generally similar to Namibia groundwater values, consistent with the coastal location and correlation between Cl^- and ClO_4^- (Table 2.3.1, Figure 2.3.7). UAE non-sabkha groundwater is more consistent with NO_3^- cycling rather than simple dilution (addition only) by biogenic NO_3^- . $\text{Cl}^-/\text{ClO}_4^-$ ratios are similar to sabkha samples but much higher than for UAE surface soil samples (see below) suggesting that atmospheric deposition may not be the dominant source of the Cl^- .

2.3.5.3 Soil and Caliche Results

Soil and Caliche Overview

ClO_4^- concentrations in soils/caliches for all sites vary over a larger range (0.1 to $10^6 \mu\text{g/kg}$) than those in groundwater (Figure 2.3.2 and 2.3.3). Similarly, $\text{NO}_3^-/\text{ClO}_4^-$ ratios appear to be more variable in soils/caliches than in groundwater (Figure 2.3.2 and 2.3.3). In part, these contrasts may be related to the fact that soil/caliche samples are likely to exhibit local heterogeneity caused by selective crystallization, re-dissolution, and redistribution of salts during infiltration, whereas groundwater is more likely to represent spatially and temporally integrated samples of

infiltrated salts. Nonetheless, there are clear relations between soil and groundwater NO_3^- and ClO_4^- concentrations within sites and between sites.

Overall there appear to be major groupings of $\text{NO}_3^-/\text{ClO}_4^-$ molar ratios that include 1) Mojave soil/caliche (85,000) and southern Africa soil (120,000); 2) all groundwater (24,000) and UAE soil (21,000); 3) Antarctica soil (14,000) and China–Turpan Hami soil/caliche (12,000); and 4) Atacama soils/caliches (1,400) (Figure 2.3.7). The first group (Mojave and southern Africa soil) ratios are similar to the average ratio ($\sim 100,000$) in wet deposition (Rajagopalan et al., 2009). The ratios of the second group (all groundwaters and UAE soil) are essentially identical to the ratio in total deposition at the Amargosa Desert Research Site (22,000) (Andraski et al., 2014). The third group (Antarctica and Turpan Hami) has lower ratios but are still similar to that in total atmospheric deposition, while the Atacama ratio is an order of magnitude lower and unique. The last two groups, with the lowest $\text{NO}_3^-/\text{ClO}_4^-$ ratio, are also the most arid. Soil $\text{Cl}^-/\text{ClO}_4^-$ ratios are much more variable than $\text{NO}_3^-/\text{ClO}_4^-$ ratios, as in the groundwater sample sets; only the Antarctica and Atacama soil data sets exhibit a clear relation between Cl^- and ClO_4^- . Each site is discussed below in more detail in order of the major groupings and generally from more biologically active to less biologically active.

Mojave Desert

Soil samples were collected from three different environments (surface of clay hills, valley floor desert pavement, and deep sub-surface salt bulge), all in a relatively small but geographically diverse area of the Mojave Desert (Figure 2.3.1). These samples do not represent “typical” soils but rather were chosen for their known accumulations of salts. Concentrations of ClO_4^- in these samples ranged from a low of $0.1 \mu\text{g/kg}$ (salt bulge) to a high of $5,500 \mu\text{g/kg}$ (Confidence Hills) (Figure 2.3.5). Samples (0-1m) from the clay hills of southern Death Valley (Confidence Hills, Bully Hill, and Saratoga Hills) had the highest known concentrations of indigenous ClO_4^- in the U.S., and were similar to those described in previous studies (Jackson et al., 2010; Lydbrand et al., 2013). Discrete-depth samples from a subsurface salt bulge have a wide range of ClO_4^- concentrations (0.1 to $20 \mu\text{g/kg}$), similar to other reported southwestern U.S. subsurface salt bulges (Rao et al., 2007). Near-surface samples from desert pavement on the Amargosa Desert valley floor contain concentrations of ClO_4^- similar to those in the nearby subsurface salt bulge. For comparison, a set ($n=48$) of composite (0-30 cm) samples collected in a pre-defined grid covering a 0.1 km^2 hill-slope area of a nearby knoll was reported to have an average ClO_4^- concentration of $3.0 \pm 2.6 \mu\text{g/kg}$ with a range of 0.8 to $11.8 \mu\text{g/kg}$ (Andraski et al., 2014).

ClO_4^- concentrations for all sites in the Mojave Desert are significantly correlated with NO_3^- ($r = 0.66$) but not with Cl^- ($r = 0.18$) (Table 2.3.2, Figure 2.3.5). ClO_4^- and NO_3^- concentrations from individual profiles in and near the Death Valley clay hills were generally but not always significantly correlated. In addition, for the spatially varying desert pavement composite, desert pavement profile, and subsurface salt bulge, concentrations of ClO_4^- and NO_3^- were correlated (r

= 0.90, 0.99, and 0.92, respectively). ClO_4^- was not correlated with Cl^- in the Mojave sample sets except for the subsurface salt bulge, desert pavement sites, and samples from Rainbow Hills. Cl^- and NO_3^- were also correlated for many of the same locations for which ClO_4^- and NO_3^- were correlated. A previous study found a significant but weaker relationship between NO_3^- and ClO_4^- in samples from the clay hills including some of the same locations reported here (Lybrand et al., 2013). One possible reason for the lower degree of correlation in the Lybrand study may have been the relatively high reportable ClO_4^- detection limit (165 $\mu\text{g/kg}$).

The molar ratios of $\text{NO}_3^-/\text{ClO}_4^-$ for all Mojave locations varied from 25,000 to 240,000 with an overall average of 85,000 (Table 2.3.2). $\text{NO}_3^-/\text{ClO}_4^-$ molar ratios were most variable in the clay hills samples, while the desert pavement and sub-surface salt bulge $\text{NO}_3^-/\text{ClO}_4^-$ ratios were more uniform (40,000 to 86,000). These ratios are similar to those reported for other salt bulges in the arid southwestern U.S. (30,000 - 51,000, 27,000, and 218,000 for depth profiles from the Chihuahuan Desert, Amargosa Desert, and Yucca Flats, respectively) (Rao et al., 2007). Mojave Desert soil $\text{NO}_3^-/\text{ClO}_4^-$ molar ratios are generally higher than the average ratio in total deposition at the Amargosa Desert Research Site (Andraski et al., 2014). The total deposition sample site was co-located with the desert pavement and sub-surface salt-bulge sites and within ~ 100 km of the remaining Mojave sites. In contrast to the relatively similar average $\text{NO}_3^-/\text{ClO}_4^-$ ratios in Mojave sample sets, average $\text{Cl}^-/\text{ClO}_4^-$ ratios varied over two orders of magnitude (77,000 to 7,400,000), indicating processes other than evapo-concentration affected anion ratios in the region.

Stable isotope data for NO_3^- ($\delta^{18}\text{O}$, $\Delta^{17}\text{O}$, and $\delta^{15}\text{N}$) in samples from the Death Valley clay hills and Rainbow Hills previously demonstrated that the NO_3^- is partially (20-50%) atmospheric in origin and partially biogenic, with no evidence of substantial isotope effect from NO_3^- reduction (Böhlke et al., 1997; Michalski et al., 2004; Jackson et al., 2010; Lybrand et al., 2013). NO_3^- in soil samples from Irwin Basin was mainly biogenic (Figure 2.3.6) (Densmore and Böhlke, 2000). The $\delta^{18}\text{O}$ and $\delta^{15}\text{N}$ of NO_3^- in samples from the desert salt bulge support a largely biogenic source of NO_3^- while those in samples from near-by desert pavement appear to have a substantial (up to ~20%) atmospheric component (Figure 2.3.6) (Andraski et al., 2014).

$\text{NO}_3^-/\text{ClO}_4^-$ ratios and NO_3^- stable isotope ratios for samples from the Mojave clay hills are consistent with a model of atmospheric deposition and addition of biogenic NO_3^- without significant recycling (Figure 2.3.8), and with substantial addition of Cl^- (Figure 2.3.7) from “episodic Cl^- ”, “non-co-deposited Cl^- ” sources or local non-atmospheric sources, consistent with the sedimentary host rocks and lack of plant life on the hills. Samples from the deep bulge are more similar to groundwater, indicating a largely recycled NO_3^- component consistent with N that infiltrated through the active soil zone. Samples of desert pavement are intermediate to the other two sample sets reflecting limited recycling of the atmospheric NO_3^- component and addition of biogenic NO_3^- .

The relatively low $\text{NO}_3^-/\text{ClO}_4^-$ ratios in the salt bulge and groundwaters may indicate that soil processes tend to decrease NO_3^- relative to ClO_4^- . The decrease in the $\text{NO}_3^-/\text{ClO}_4^-$ ratio could be due to episodic microbial reduction, though soils in these arid environments are generally well aerated. Another possibility could be uptake and assimilation of NO_3^- by plants and accumulation as organic N. A recent study suggested that while both ClO_4^- and NO_3^- are taken up by desert plants, the ClO_4^- can remain unprocessed and recycled back to the soils while NO_3^- is largely fixed within the plant tissue (Andraski et al., 2014). The similar low $\text{NO}_3^-/\text{ClO}_4^-$ ratio for groundwaters and deep salt bulge, given the complete loss of the original atmospheric NO_3^- component, suggests that in arid and semi-arid areas there is an upper limit to the amount of oxidized N that escapes from the biologically active vadose zone and that long term fluxes of NO_3^- may be somewhat regulated. Only in cases of extreme aridity or surface features (e.g. desert pavement), which limit infiltration, do ratios increase from NO_3^- addition in the relative absence of assimilation and gas loss.

Southern Africa

In contrast to the Mojave sample sites, southern Africa soil sample sites were not selected based on known salt accumulations. ClO_4^- concentrations varied from 0.2 to 45 $\mu\text{g/kg}$, with no relation to surface feature (pan, fan, or vertical profile) (Figure 2.3.5). Samples from Botswana and South Africa playa surfaces were similar to those from Namibia. For both the Namibia and Botswana sites, as well as the combined data set, ClO_4^- and NO_3^- concentrations were correlated (Table 2.3.2, Figure 2.3.5). Similar to the Mojave Desert samples, there were no significant correlations between Cl^- and ClO_4^- or Cl^- and NO_3^- . Average molar ratios of $\text{NO}_3^-/\text{ClO}_4^-$ were similar for the three sites (96,000, 150,000, and 125,000) with an average ratio of 120,000 (Table 2.3.2), significantly greater than Namibia groundwater samples. Site average $\text{Cl}^-/\text{ClO}_4^-$ ratios were much more variable (650,000 - 41,000,000). NO_3^- in the Namibia surface soils contained a greater unaltered atmospheric NO_3^- component (20 - 50%) than groundwater from Namibia (Figure 2.3.6), and was intermediate to Mojave Desert pavement and clay hill samples (Figure 2.3.8). $\text{NO}_3^-/\text{ClO}_4^-$ ratios largely overlap with ratios of the Mojave Desert sample sets (e.g. clay hills and desert pavement) but are higher than ratios for Namibia groundwater (Figure 2.3.8).

Overall, the Namibia soil data set appears to resemble the Mojave clay hills data set, consistent with a largely preserved atmospheric component with addition of biogenic NO_3^- (Figure 2.3.8). While the unusually high $\text{Cl}^-/\text{ClO}_4^-$ ratios in the Namibia samples could in part be due the coastal proximity, the lack of correlation between Cl^- and NO_3^- or ClO_4^- indicates local, “episodic”, or ‘non-co-deposited Cl^- ’ sources may be important, similar to the Mojave Clay hills (Figure 2.3.7).

UAE

Sample sites in the UAE represent both typical soil and sabkha sediment. Soil ClO_4^- concentrations (n=7) ranged from <0.1 (n=2) to 13 $\mu\text{g/kg}$ and those for sabkha sediment (n=7) were generally higher (0.1 < (n = 2) to 262 $\mu\text{g/kg}$). ClO_4^- and NO_3^- were correlated for both soil (r

= 0.87) and sabkha sediments ($r = 0.97$) with an overall correlation coefficient of 0.99 (Table 2.3.2 and Figure 2.3.5). Cl^- and ClO_4^- were not correlated, nor were NO_3^- and Cl^- . $\text{NO}_3^-/\text{ClO}_4^-$ molar ratios were similar in soils and sabkha sediments (14,000 and 28,000, respectively), while Cl/ClO_4^- ratios were much more variable (19,000 and 1,700,000, respectively). Isotope data indicate the source of NO_3^- in the soil samples is mainly biogenic except for two samples that may have around 20-50% unaltered atmospheric NO_3^- , both of which had very low NO_3^- and ClO_4^- concentrations (Figure 2.3.6). NO_3^- in the sabkha samples apparently had substantial fractions of unaltered atmospheric NO_3^- (approximately 20-50 %), and it also exhibited isotopic evidence of NO_3^- reduction. $\text{NO}_3^-/\text{ClO}_4^-$ molar ratios in UAE soil and sabkha samples were similar to those in UAE groundwater (22,000) and Amargosa Desert total deposition (22,000) (Figure 2.3.8).

The $\text{NO}_3^-/\text{ClO}_4^-$ ratios and NO_3^- isotopic compositions of the soil samples are consistent with substantial NO_3^- recycling, perhaps consistent with relatively high local precipitation, similar to UAE groundwater (Figure 2.3.8). Sabkha samples are more consistent with biogenic addition and limited recycling, given the large unaltered atmospheric component and higher $\text{NO}_3^-/\text{ClO}_4^-$ ratios and expected impact of NO_3^- reduction. Interestingly, UAE soil Cl/ClO_4^- ratios are near Mojave total deposition values and an order of magnitude lower than UAE groundwater values despite the similar $\text{NO}_3^-/\text{ClO}_4^-$ ratios and proximity to the coast. The lack of correlation between soil Cl^- and ClO_4^- , but strong correlation for groundwater coupled with higher ClO_4^- concentrations in groundwater than soil, suggest that the groundwater Cl^- , NO_3^- , and ClO_4^- were not simply derived from concentrated infiltration but rather may indicate dissolution of stored salts in the subsurface or that the groundwater was not recharged locally.

China, Turpan-Hami

High concentrations of ClO_4^- (~100 to 16,000 $\mu\text{g}/\text{kg}$) were present in a relatively small set ($n = 11$) of samples from three sites in the vicinity of recently described massive NO_3^- deposits of northern China (Qin et al., 2012; Li et al., 2010). Concentrations of ClO_4^- were similar to those in the Mojave clay hills samples and ~1-2 orders of magnitude lower than the majority of samples from the Atacama NO_3^- deposits, even though the NO_3^- concentrations were similar between the Atacama and China deposits (Figure 2.3.5). Turpan-Hami NO_3^- has been attributed largely to long-term atmospheric deposition, based on elevated $\Delta^{17}\text{O}$ (5-20‰) and $\delta^{18}\text{O}$ (30-60‰) values (Qin et al., 2012; Li et al., 2010), which are intermediate to NO_3^- from the Mojave clay hills and Atacama Desert. Previously reported ranges of $\delta^{18}\text{O}$ and $\Delta^{17}\text{O}$ indicate the Turpan-Hami NO_3^- is approximately 25-75% unaltered atmospheric. Data from the current study indicate similar atmospheric components (Figure 2.3.6). NO_3^- and ClO_4^- were correlated ($r = 0.61$) but Cl^- and ClO_4^- , and Cl^- and NO_3^- , were not. Cl^- concentration varied relatively little, while NO_3^- and ClO_4^- concentrations varied over 2 orders of magnitude (Figure 2.3.5). Molar ratios of $\text{NO}_3^-/\text{ClO}_4^-$ were generally lower than ratios for the Mojave Desert sites and for Mojave total atmospheric

deposition, but the overall average ratio was still ~1 order of magnitude greater than the Atacama ratio, although the ranges do overlap (Figure 2.3.7).

Given the large unaltered atmospheric NO_3^- component and the relatively low $\text{NO}_3^-/\text{ClO}_4^-$ ratio in the Turpan-Hami samples, it would appear that there has not been much net addition of biogenic NO_3^- (Figure 2.3.8). Compared to the Mojave total deposition anion ratios and NO_3^- isotope values, the Turpan-Hami data are consistent with partial recycling of the atmospheric NO_3^- component. However given the extreme aridity and lack of vegetation, an alternative explanation may be that the Mojave total deposition $\text{NO}_3^-/\text{ClO}_4^-$ ratios do not represent Turpan-Hami deposition ratios. For example, a lower contribution from wet deposition with higher $\text{NO}_3^-/\text{ClO}_4^-$ might reduce the total deposition $\text{NO}_3^-/\text{ClO}_4^-$ ratio and thus allow for biogenic addition without recycling. Similar to the Mojave, there also appears to be a substantial component of Cl^- unrelated to co-deposited NO_3^- and ClO_4^- (Figure 2.3.7).

Antarctica, University Valley

ClO_4^- concentrations varied over a relatively narrow range (50-500 $\mu\text{g/kg}$); variations with depth were similar in magnitude to variations among locations (Figure 2.3.5). These concentrations are similar to those previously reported for University Valley and Beacon Valley (Kounaves et al., 2010). Concentrations were higher than those of surface soils from other sites, excluding the samples from the Mojave clay hills, Atacama, and China Turpan-Hami. Concentrations of NO_3^- and ClO_4^- were correlated ($r = 0.83 - 0.99$) in all profiles, as were concentrations of Cl^- with ClO_4^- ($r = 0.72 - 0.99$) and NO_3^- ($r = 0.64 - 0.99$) with the exception of profile 7 (Table 2.3.2). Average molar ratios were similar among sites 7,900 - 20,000; 4,600 - 10,000; and 0.34 - 0.87, for $\text{NO}_3^-/\text{ClO}_4^-$, Cl/ClO_4^- , and Cl/NO_3^- respectively. The $\text{NO}_3^-/\text{ClO}_4^-$ molar ratios were similar to those of Turpan-Hami samples, but an order of magnitude higher than Atacama ratios. The Cl/NO_3^- molar ratios for the Antarctica sites were lower than for all other sites, but the Cl/ClO_4^- ratios for the Atacama sites were lower than those for University Valley (Figure 2.3.7).

NO_3^- in soils from the McMurdo Dry Valley region of Antarctica previously has been attributed to atmospheric deposition with no biogenic component based on extremely high $\delta^{18}\text{O}$ (>70‰) and $\Delta^{17}\text{O}$ values (>29‰) (Michalski et al., 2005). NO_3^- in Antarctica soil samples analyzed in this study had a similar $\delta^{18}\text{O}$ range (76-84‰) (Figure 2.3.6). This site represents the extreme end of low biological activity both due to the very few degree days above 0°C as well as the limited precipitation. NO_3^- deposition in Antarctica is somewhat unique and NO_3^- can also be subject to a number of isotopically fractionating abiotic processes (e.g. photolysis and volatilization) on snow and ice (e.g. Grannas et al., 2007 and Frey et al., 2009). Our soil samples do not appear to exhibit anomalous concentration ratios or NO_3^- isotopic compositions that might reflect post-depositional transformations. The ratios of $\text{NO}_3^-/\text{ClO}_4^-$ and Cl/ClO_4^- , and NO_3^- isotopic compositions, coupled with strong correlations among all three species, support an unaltered

atmospheric source consistent with the cold hyper-arid conditions and almost complete lack of biological activity (Figure 2.3.8).

Atacama

ClO_4^- concentrations ($n=102$) in Atacama soil/caliche samples ranged from a minimum of $0.5 \mu\text{g/kg}$ to a maximum of $1 \times 10^6 \mu\text{g/kg}$ (Figure 2.3.5). The vast majority of profile samples (AT) collected in the central depression contained ClO_4^- at concentrations that exceed those for all other sites evaluated in this study. Surface soil composites acquired along an east-west elevation transect vary in concentration; approximately 50% of the samples (those located above 2500 m elevation, east of the central depression and absolute desert where vegetation is present) had concentrations similar to those for the Mojave, southern Africa, and UAE sites. Spatial location (both altitude and geographic coordinates) is likely an important determinant of ClO_4^- concentration due to rainfall and evapotranspiration effects, but the associated discussion is beyond the scope of this paper.

For all profiles, surface composites, and the combined data set, NO_3^- and ClO_4^- were correlated except for the mine samples (Table 2.3.2). In general, correlation coefficients were lower for the relation between Cl^- and ClO_4^- compared to NO_3^- and ClO_4^- but still generally significant, and as such NO_3^- and Cl^- were generally correlated. $\text{NO}_3^-/\text{ClO}_4^-$ molar ratios (550-2,200) were at least an order of magnitude lower than at other sites evaluated in this study, with one exception (site AT16, where $\text{NO}_3^-/\text{ClO}_4^- = 13,000$). All the Atacama $\text{NO}_3^-/\text{ClO}_4^-$ ratios were below the minimum ratios reported for wet and total deposition in North America (Rajagopalan et al., 2009 Andraski et al., 2014). Previous studies indicate the source of NO_3^- in the Atacama caliche deposits is largely atmospheric ($> 50\%$) (Böhlke et al., 1997; Michalski et al., 2004) and the stable isotopic compositions of samples evaluated in this study generally were consistent with this, except for a few of the surface soil composites far from the central depression in which NO_3^- appears to be mainly biogenic (Figure 2.3.6). $\text{Cl}^-/\text{ClO}_4^-$ molar ratios for the Atacama sites were similar to each other in magnitude and variability (615 -4,700) and were lower than at other sites evaluated in this study (Table 2.3.2).

The Atacama Desert is the location with the longest record of aridity and the most extreme aridity under present conditions, and this is reflected by the predominantly atmospheric source of NO_3^- with only limited biogenic NO_3^- (Böhlke et al., 1997; Michalski et al., 2004). The average Atacama soil $\text{NO}_3^-/\text{ClO}_4^-$ ratio is at least one order of magnitude lower than all other measured deposition, soil/caliche, and groundwater ratios (Figure 2.3.8). We exclude the possibility that the low ratio compared to other sites was caused by loss of ClO_4^- at all other sites based on the stable isotopic composition of ClO_4^- in the Mojave (Jackson et al., 2010) as well as other unpublished data for Antarctica and Turpin-Hami. There was also limited or no evidence for biological reduction in most of the sites studied. The low ratio is not likely caused by net loss of NO_3^- by denitrification or plant assimilation, given the hyper-arid conditions. The low ratio

could be due to regionally low NO_3^- deposition flux or high ClO_4^- deposition flux. Both of these species are considered to be at least partly atmospheric in origin based on elevated $\Delta^{17}\text{O}$ values as well as ^{36}Cl content of ClO_4^- (Bao and Gu, 2004; Michalski et al., 2004; Sturchio et al., 2009; Jackson et al., 2010). Regionally low NO_3^- production does not seem likely as the overall average $\text{Cl}^-/\text{NO}_3^-$ molar ratio (1.1) is the fourth lowest of all locations and matches reasonably well with reported deposition ratios for the Atacama (0.74) (Ewing et al., 2006). An anomaly in the deposition flux of ClO_4^- presumably would require a mechanism to localize atmospheric production, as other sites in the southern hemisphere do not have such low $\text{NO}_3^-/\text{ClO}_4^-$ ratios. Atacama ClO_4^- has a unique isotopic composition compared to other reported natural ClO_4^- from Mojave, Rio Grande Basin, and Southern High Plains (Böhlke et al., 2005; Jackson et al., 2010; Sturchio et al., 2011). The unique isotopic composition (low $\delta^{37}\text{Cl}$, $\delta^{18}\text{O}$, and $^{36}\text{Cl}/\text{Cl}$) could be related to an additional unknown production mechanism which could also explain the very low ratios of $\text{NO}_3^-/\text{ClO}_4^-$. Alternatively, given the duration of hyper-arid conditions in the Atacama (> 2 million years), the relative enrichment and unique isotopic composition of ClO_4^- could be a reflection of atmospheric conditions that are no longer present. The age of the ClO_4^- in the Atacama has been estimated to be at least 750,000 years for the youngest samples, with a mean age of 3-8 million years based on $^{36}\text{Cl}/\text{Cl}$ ratios in ClO_4^- (Sturchio et al., 2009). This suggests that almost all of the Atacama ClO_4^- is older than 300,000 years, and thus predates the estimated time period over which ClO_4^- was deposited at other terrestrial locations.

2.3.5.4 Implications of $\text{Cl}^-/\text{NO}_3^-/\text{ClO}_4^-$ Global Correlations

The global consistency of $\text{NO}_3^-/\text{ClO}_4^-$ ratios in all locations other than the Atacama is in contrast to the more variable $\text{Cl}^-/\text{NO}_3^-$ and $\text{Cl}^-/\text{ClO}_4^-$ ratios (Figure 2.3.7). $\text{Cl}^-/\text{NO}_3^-$ ratios are commonly used to evaluate N and/or NO_3^- gains/losses in various ecosystems. Co-variation of $\text{Cl}^-/\text{NO}_3^-$ and $\text{Cl}^-/\text{ClO}_4^-$ ratios illustrated in Figure 2.3.7 indicates large variations in Cl^- are related to processes that either (1) do not affect NO_3^- or ClO_4^- , or (2) affect both NO_3^- and ClO_4^- similarly. Atmospheric deposition plots at the low end of the correlated data array in Figure 2.3.7, indicating that many soils, caliches, unsaturated salt bulges, and groundwaters in arid and semi-arid regions have $\text{NO}_3^-/\text{ClO}_4^-$ ratios similar to atmospheric deposition ratios, whereas $\text{Cl}^-/\text{NO}_3^-$ and $\text{Cl}^-/\text{ClO}_4^-$ ratios of terrestrial samples are systematically higher than deposition ratios. For the deposition data summarized in this paper (U.S. wet deposition (WD) and Mojave total deposition (TD)), the $\text{Cl}^-/\text{NO}_3^-$ molar ratios (0.33 and 0.61 for WD and TD, respectively) are similar to that previously estimated from oxic groundwater data for the Middle Rio Grande Basin ($\text{Cl}^-/\text{NO}_3^- = 0.27$) (Plummer et al., 2006) as well as that calculated using reported data (2000-2010) for total deposition from 95 sites across the U.S. ($\text{Cl}^-/\text{NO}_3^- = 0.29$; $n=892$) (CASTNET, 2014).

Cl^- concentrations in atmospheric deposition can vary independently of the concentrations of constituents with atmospheric sources. For example, Rajagopalan et al. (2006) reported mean values of $\text{Cl}^-/\text{NO}_3^-$ and $\text{Cl}^-/\text{ClO}_4^-$ in wet deposition at different sites across the U.S. varied by 2

orders of magnitude and much of the variation was related to distance from the coast, presumably reflecting variation in the sea-salt component relative to other components of the Cl^- deposition. Similarly, continental-scale studies of $^{36}\text{Cl}/\text{Cl}$ ratios in pre-anthropogenic groundwater in the U.S. and modern atmospheric deposition in Europe indicated maximum coastal marine Cl^- enrichment factors on the order of 20-40 (Davis et al., 2003; Johnston and McDermott, 2008). Varying deposition ratios could account for some of the regional terrestrial variation illustrated in Figure 2.3.7, but probably not all of it, and presumably would not cause almost all terrestrial samples to be relatively enriched in Cl^- . The $\text{Cl}^-/\text{NO}_3^-$ ratios of soil/caliche and groundwater samples vary over 3 orders of magnitude, with little relation to distance from the coast, although some of the highest $\text{Cl}^-/\text{NO}_3^-$ ratios are from areas near coasts (e.g., Namibia and UAE). The highest wet deposition $\text{Cl}^-/\text{NO}_3^-$ ratio observed by Rajagopalan et al., (2006) for 4 coastal sites (<50km) was 17 (Puerto Rico) while the other 3 coastal sites had ratios <4.

The array of data extending from atmospheric deposition toward higher $\text{Cl}^-/\text{NO}_3^-$ and $\text{Cl}^-/\text{ClO}_4^-$ ratios (Figure 2.3.7), and the lack of a relation between the increase in $\text{Cl}^-/\text{NO}_3^-$ ratio and the $\text{NO}_3^-/\text{ClO}_4^-$ ratio (Figure 2.3.7) suggests that either Cl^- at most sites has been supplemented by sources unrelated to the source of the original co-deposited NO_3^- or ClO_4^- , or that both NO_3^- and ClO_4^- were equally lost in these systems as previously described. Partial microbial reduction of NO_3^- is supported by isotope data at some sites (Figure 2.3.6). However, NO_3^- isotopes at most sites appear to be relatively unfractionated and some indicate substantial unaltered atmospheric NO_3^- . For ClO_4^- and NO_3^- to be lost due to episodic reduction without apparent isotope effect would require complete loss at micro-sites and as much as 99% total loss to account for the magnitude of change in the $\text{Cl}^-/\text{NO}_3^-$ ratios, which is considered improbable given the current aridity of most locations in this study. However, as previously mentioned, it is possible that some sites with elevated Cl^- concentrations contain atmospheric Cl^- that accumulated during previous wetter periods that supported biological reduction of NO_3^- and ClO_4^- (non-co-deposited Cl^-).

Another possible confounding factor may be the potential de-coupling of Cl^- and NO_3^- or ClO_4^- transport. Local redistribution of salts by selective crystallization, dissolution, and infiltration might have separated NO_3^- and ClO_4^- from Cl^- at the scale of individual samples or vertical profiles. Also, we have observed that at least some plants uptake ClO_4^- and NO_3^- proportionally while excluding Cl^- (Andraski et al., 2014). Biologic assimilation could be responsible for substantial N sequestration in persistent organic matter, and release of N gases (e.g., NH_4 , N_2O , N_2) during remineralization, nitrification, or denitrification, could also lead to elevated $\text{Cl}^-/\text{NO}_3^-$ ratios in soils and recharging groundwaters, but existing data do not support similar losses of ClO_4^- due to plant uptake (Andraski et al., 2014, Tan et al., 2004b, 2006). It is emphasized that the Atacama Desert occupies a unique position in all of the figures that present data from this study, which can only be achieved by assuming a localized *in-situ* production mechanism or

unknown variation in the deposition ratios over million-year time scales that would not be recorded at the other sites.

2.3.6 Conclusions

ClO_4^- is globally distributed in soil and groundwater in arid and semi-arid regions on Earth at concentrations ranging from 10^{-1} to 10^6 $\mu\text{g/kg}$. Generally, the ClO_4^- concentration in these regions increases with aridity index, but also depends on the duration of arid conditions. In many arid and semi-arid areas, NO_3^- and ClO_4^- co-occur at consistent ratios ($\text{NO}_3^-/\text{ClO}_4^-$) that vary between $\sim 10^4$ and $\sim 10^5$. These ratios are largely preserved in hyper-arid areas that support little or no biological activity (e.g. plants or bacteria), but can be altered in areas with more active biological processes including N_2 fixation, N mineralization, nitrification, denitrification, and microbial ClO_4^- reduction. At first approximation, relatively constant $\text{NO}_3^-/\text{ClO}_4^-$ ratios in desert environments are consistent with global atmospheric sources, and with dry deposition as a major controlling factor.

In contrast, much larger ranges of $\text{Cl}^-/\text{ClO}_4^-$ and $\text{Cl}^-/\text{NO}_3^-$ ratios indicate Cl^- varies independently from both ClO_4^- and NO_3^- . This is likely due to variation of sea salt Cl^- in deposition, plus variable addition of Cl^- from dust or subsurface sedimentary and evaporitic sources, and possibly excess Cl^- accumulation during past wetter periods of NO_3^- and ClO_4^- reduction. The general lack of correlation between Cl^- and ClO_4^- or NO_3^- implies that Cl^- is not a good indicator of co-deposition and should be used with care when interpreting oxy-anion cycling and mass balances in arid systems.

In general, the co-occurrence of ClO_4^- and NO_3^- in arid and semi-arid locations, and associated variations in the isotopic composition of the NO_3^- , are consistent with a conceptual model of atmospheric origin, global co-deposition, and variable alteration of the NO_3^- pool by biogenic addition, assimilation, and/or recycling on the surface. Preservation of the atmospheric deposition $\text{NO}_3^-/\text{ClO}_4^-$ ratio in unsaturated-zone accumulations and groundwater in areas where biological activity is substantial and on-going appears to indicate limits to net gains and losses of N through biological processes in soils between deposition inputs and infiltration outputs.

Measurements of ClO_4^- concentration in desert regions could be useful for interpreting major anion cycles and processes, particularly with respect to the less-conserved NO_3^- pool. If more accurate local measures of deposition can be obtained, then ClO_4^- surface accumulations in conjunction with NO_3^- isotopic composition could be useful in evaluating the duration of arid conditions that led to such accumulations, and potentially also the extent of biological processes and nitrogen mass transfers.

The Atacama Desert appears to be unique compared to other arid and semi-arid locations. There, exceptional enrichment in ClO_4^- compared to Cl^- or NO_3^- , accompanied by unique ClO_4^- isotopic

characteristics (Bao and Gu, 2004; Böhlke et al., 2005; Jackson et al., 2010), may reflect an unusually efficient, but yet unknown, *in situ* production mechanism, regionally elevated atmospheric ClO_4^- production rates, or higher ClO_4^- production rates in pre-Pleistocene times.

In the absence of microbial reduction, ClO_4^- can persist in many environmental conditions. On early Earth, prior to the onset of microbial ClO_4^- reduction, ClO_4^- concentrations could have been much higher than currently observed. However, the net impact of microbial ClO_4^- reduction on the global chlorine biogeochemical cycle remains unconstrained.

Elevated concentrations of ClO_4^- reported on the surface of Mars, and its enrichment with respect to Cl^- and NO_3^- , could reveal important clues regarding the climatic, hydrologic, and potentially biologic evolution of the planet. Given the highly conserved ratio of $\text{NO}_3^-/\text{ClO}_4^-$ in non-biologically active areas on Earth, it may be possible to use alterations of this ratio as a biomarker on Mars.

2.4 Perchlorate and Chlorate in the Ice-Covered Lakes of McMurdo Dry Valleys, Antarctica.

2.4.1 Background

In section 2.3, we summarized data concerning ClO_4^- concentrations in Antarctica soils in conjunction with a worldwide overview of natural anion concentrations and relationships in soils and groundwater. In this section, we provide the data concerning ClO_4^- and ClO_3^- in ice-covered lakes in Antarctica.

Ice-covered lakes are the main sites for biological activity in the McMurdo Dry Valleys (MDV) of Antarctica, and represent one of the most pristine aquatic ecosystems on Earth. These lakes have been extensively studied in relation to their physical structure, ecology, and biogeochemistry (e.g. Green and Lyons, 2009 and references therein). Most of the ice-covered lakes in the MDV contain both oxic and anoxic zones within the water column, although several lakes are oxic throughout. Lake water temperatures are always close to 0°C , and the water columns are characterized by relatively low biological productivity. In all cases, the lakes are perennially ice-covered, which influences all physical, chemical, and biological processes. The deep waters of the east lobe of Lake Bonney rank among the most saline aqueous environments on our planet with very limited or no microbial activity, while other lakes contain essentially fresh water and support diverse and widespread photosynthetic microbial mats, as well as chemolithotrophic and heterotrophic processes such as nitrification, sulfur oxidation, denitrification, and sulfate reduction (Voytek et al., 1999, Green and Lyons, 2009).

Many major and trace element geochemical and biogeochemical processes have been evaluated in these lakes (e.g., Lee et al., 2004), but no information is available concerning the occurrence, distribution and fate of ClO_3^- and ClO_4^- . The purpose of this task was to measure ClO_4^- and ClO_3^- levels in ice-covered lakes of the MDV, and to evaluate whether these species were being reduced by bacteria capable of (per)chlorate reduction. Results are discussed with regard to the ecology, chemical evolution, and history of lakes in the MDV.

2.4.2 Materials and Methods

ClO_4^- , ClO_3^- , NO_3^- , SO_4^{2-} , and Cl^- concentrations were measured for samples from a number of surface water bodies (e.g. streams, creeks, ponds; see Table 2.4.1) and 4 ice-covered lakes within the MDV: Lake Bonney (East and West Lobe), Lake Hoare, and Lake Fryxell in Taylor Valley and Lake Miers in the Miers Valley. All samples were obtained from the Long Term Ecological Research group (LTER) using techniques previously outlined (<http://www.lternet.edu/sites/mcm/>). Samples were collected in either December of 2008 (Lake Fryxell and Miers) or 2009 (Lake Hoare and Bonney). Samples were filtered (GF/F filter) within 6-8 hours of collection and stored frozen.

2.4.3 Analysis

Major anions (Cl^- , NO_3^- , and SO_4^{2-}) were analyzed by ion chromatography as described previously in this report. Anion concentration distribution within the lakes is well documented but was evaluated here to demonstrate consistency with past efforts and to evaluate ClO_4^- and ClO_3^- concentrations with respect to other anions on a consistent set of samples. ClO_4^- and ClO_3^- concentrations were separately measured by IC-MS/MS as previously described in this report following the method detailed in Rao et al., (2007 and 2010b). The MDL was 2 ng/L for both ClO_3^- and ClO_4^- , while the MRL for these samples was 50 ng/L. Samples were analyzed in batches of 8 including an analytical duplicate and spike. The errors in duplicate samples were less than $\pm 10\%$ and the spike recoveries were between 90 and 110 %. Samples with elevated Cl^- ($>10,000$ mg/L) or SO_4^{2-} (>1000 mg/L) were either diluted prior to analysis or in some cases pre-cleaned using On-Guard™ II Ag or Ba cartridges (Dionex).

2.4.4 Modeling

Two simple models were used to evaluate ClO_4^- , ClO_3^- , and SO_4^{2-} concentrations relative to the conserved species Cl^- in order to establish if non-transport related processes (e.g. bacterial reduction and evapoconcentration) were affecting the distribution of these species with depth in the water column. For Lakes Hoare, Miers, and Fryxell, for which the source of salts in the lakes is glacier and snow melt augmented by chemical weathering and possibly input of relic seawater for the hypolimnion of Lake Fryxell (Lyons et al., 1998 and 2000), we assumed that in the absence of sinks all anions should increase in concentration proportional to Cl^- . For each species we calculated the mass ratio with respect to Cl^- (e.g. $\text{ClO}_4^-/\text{Cl}^-$) at the depth closest to the bottom of the lake ice. This ratio was then multiplied by the Cl^- concentration at lower depths to determine the expected concentration of each species as shown below.

$$C_{Dx} = C_{Ds}/\text{Cl}^-_{Ds} \times \text{Cl}^-_{Dx}$$

Where C_{Dx} and C_{Ds} are the concentration of ClO_4^- , ClO_3^- , or SO_4^{2-} at depth X and the surface, respectively; and Cl^-_{Ds} and Cl^-_{Dx} are the concentrations of Cl^- at depth X and the surface, respectively. For Lake Bonney, for which the salts are attributed to both surface inflow and relic seawater (Lyons et al., 2005), we used a simple two component mixing model. We calculated the mixing ratio of surface and water from 35m (deepest depth) to produce the observed Cl^- profile using a simple mass balance

$$\text{Cl}^-_{Dx} = f_{Dx} \text{Cl}^-_{Ds} + f^{35}_{Dx} \text{Cl}^-_{35}$$

where f_{Dx} and f^{35}_{Dx} are the fraction of surface water and water at 35m respectively at any depth Dx , Cl^-_{35} is the concentration at 35m and all other variables are previously defined. The values of f_{Dx} and f^{35}_{Dx} determined for each depth using Cl^- were then used to calculate the concentration of

ClO_4^- , ClO_3^- , or SO_4^{2-} using the same mass balance but substituting the concentrations of each species for Cl^- at the surface and at 35m to predict the concentration at intermediate depths. Modeled results are only used to highlight processes impacting oxyanions relative to Cl^- . The modeled concentrations are plotted as dashed lines on the figures presenting the concentration distribution with depth for each Lake.

2.4.5 Results and Discussion

2.4.5.1 Surface Waters in Wright and Taylor Valley

The permanently ice-covered lakes in the MDV are supplied by glacial melt and include streams, creeks, and the Onyx River that feed various lakes as well as ponds (Figure 2.4.1). ClO_4^- concentrations in a subset of these water bodies ranged from 0.05-8.1 $\mu\text{g/l}$ but were generally less than 0.5 (45/49 samples) with an overall average of 0.19 $\mu\text{g/l}$ excluding one outlier (Parera Pond) (Table 1). Of the samples that exceeded 0.5 $\mu\text{g/l}$ all but one (Parera Pond) were in streams that feed Fryxell Lake. Only two samples (Green Creek and Blood Falls) were below the detection limit (0.05 $\mu\text{g/l}$). In most cases, we report concentrations for multiple samples from the same water body, taken at either different dates and/or different locations. In these instances, concentrations are generally within a factor of 2 of each other. Most ClO_3^- and ClO_4^- concentrations in surface waters of the MDV are higher than those reported for wet precipitation from North America (average = 0.014 $\mu\text{g/L}$) (Rajagopalan et al., 2009) or in ice cores from Wyoming ($0.0002 < 0.009 \mu\text{g/L}$), Yukon Territory ($0.0002 < - 0.002 \mu\text{g/L}$), and the Devon Ice Cap ($0.001\text{-}0.015 \mu\text{g/L}$) (Rao et al., 2012; Furdui and Tomassini, 2010). The higher concentrations in the MDV surface water are not surprising given that they include both dry and wet deposition from glacier melt, which may have experienced evapo-concentration due to ice sublimation as well as input from dissolution of salts from the surrounding catchment. ClO_3^- concentrations in the non-lake surface water bodies were similar to ClO_4^- with concentrations ranging from <0.05 to 15.5 $\mu\text{g/l}$ and an overall average excluding Goldman Pond of 0.25 $\mu\text{g/l}$ (Table 2.4.1). Little information is available concerning ClO_3^- in the environment but ratios of $\text{ClO}_3^-/\text{ClO}_4^-$ in North American precipitation and evaporites from the Mojave, Atacama and Namibia Deserts generally plot close to a 1:1 (W/W) ratio line (Rao et al., 2010b) and ice core samples from the Devon Island Ice Cap have an average ratio (W/W) of 3.8 ± 2.9 (Furdui and Tomassini, 2010). Samples from Taylor and Wright Valleys have an average ratio (W/W) of 1.7 ± 1.1 similar to other reported samples.

2.4.5.2 Ice-covered lakes in Taylor and Miers Valley

Lake Hoare

Lake Hoare is a fresh water lake ponded by the Canada Glacier (Figure 2.4.1). The lake water is relatively young ~1000-2500 yr and the source of Cl^- and other salts is attributed to snow and glacial melt, as well as weathering of minerals and dissolution of dust on melting glaciers (Lyons et al., 1998; Lyons et al., 2005; Voytek et al., 1999). The lake is uniformly oxidic (~20 mg O_2/l) to

a depth of ~17m at which point oxygen sharply decreases to near 0 at the sediment interface (Clocksin et al., 2007). There is a chlorophyll-a peak at 15m and NO_3^- is below detection ($<0.5 \mu\text{g N/l}$) above 15m and increases due to nitrification below 15m reaching a maximum of $\sim 112 \mu\text{gN/l}$ (Voytek et al., 1999). Microbial analysis indicates that nitrifiers are present at all depths and of the eight isolates obtained all were obligate aerobes (Clocksin et al., 2007 and Voytek et al., 1999). The presence ($\sim 0.7 \text{ mg/l}$) of H_2S near the sediment-water interface clearly indicates anoxic processes are occurring near the sediment water interface (Clocksin et al., 2007).

Our results show that ClO_4^- and ClO_3^- in Lake Hoare are present throughout the water column at concentrations ranging from 0.1 to 0.3 and 0.15 to $0.42 \mu\text{g/l}$, respectively (Figure 2.4.2). Concentrations were lowest near the surface and at the sediment interface with a peak concentration near 10m. As previously reported, Cl^- concentrations decrease exponentially towards the surface. SO_4^{2-} follows a similar trend increasing proportionally to Cl^- with the exception of the deepest sample (30m) consistent with the presence of H_2S at the same depth. Neither ClO_4^- nor ClO_3^- concentrations increase proportionally to Cl^- , although the concentrations do initially increase.

This relationship with Cl^- is further highlighted by the predicted concentrations (dashed lines Figure 2.4.2) of these species using a simple model based on maintaining the initial ratios of each species relative to Cl^- in the lake surface water with depth. The ratios of SO_4^{2-} to Cl^- are largely conserved with depth except as discussed near the sediment water interface. SO_4^{2-} reduction has apparently not been extensive enough to impact the concentration of SO_4^{2-} in the majority of the lake profile (Figure 2.4.2). The ratio of ClO_4^- and ClO_3^- to Cl^- in the lake surface water are close to the measured values in stream input to Lake Hoare (Figure 2.4.3). Predicted concentrations of ClO_3^- and ClO_4^- based on Cl^- concentration with depth are up to an order of magnitude higher than measured concentrations indicating a depletion of ClO_x^- for all depths below the surface water.

The concentration of ClO_4^- and ClO_3^- can likely be explained by a similar process as SO_4^{2-} . Like NO_3^- both ClO_4^- and ClO_3^- are only reduced at oxygen concentrations below $\sim 1 \text{ mg/l}$. Therefore given the elevated O_2 concentrations throughout the lake depth, ClO_4^- and ClO_3^- are unlikely to be reduced in the bulk lake water. However, as sulfate reduction is clearly occurring in the lake sediment the conditions exist to support ClO_x^- reduction. Both ClO_4^- and ClO_3^- are utilized as electron acceptors prior to SO_4^{2-} , and consequently the upper portions of the sediment should support ClO_x^- reduction. The very large differences in concentrations of SO_4^{2-} and ClO_x^- ($\text{SO}_4^{2-}/\text{ClO}_x^- > 10,000$) explain the difference in ClO_x^- depth profiles compared to SO_4^{2-} . The relatively low organic matter input to the sediments sustains relatively low rates of electron acceptor (O_2 , NO_3^- , SO_4^{2-}) reduction, but given the ratio of SO_4^{2-} to ClO_x^- this rate would lead to the rapid consumption of ClO_x^- but a negligible decrease in SO_4^{2-} concentration. This would eventually

lead to a depleted ClO_x^- concentration profile relative to Cl^- throughout most of the depth of the lake as observed. Hence, one implication of the data presented here is that ClO_x species can be used as a very sensitive marker for microbial activity in the water column of ice-covered lakes. Finally, the presence of trace amounts of NO_3^- at lower depths suggests that it is being produced in excess of the consumption rate.

East Lobe Lake Bonney

Lake Bonney is the largest lake in Taylor Valley with a maximum depth of ~40m (Green and Lyons, 2009). It has two lobes (west and east) that have had very different evolutionary histories (Matsubaya et al., 1972; Poreda et al., 2004). In the East Lobe (EL), the surface water is fresh (~0.6g TDS/l) to highly saline at depth (~273 g TDS/l). Both lobes are vertically stabilized by the strong salt gradients in the lake (Spigel and Priscu, 1998). The lake has existed in some form for a minimum of 300,000 years and the hypolimnion has been attributed to a Tertiary period marine fjord (Hendy, 2000; Lyons et al., 2005). The EL geochemistry has been modified due to the loss of ice cover in the mid-Holocene which reformed ~200 years ago. The loss of the ice cover led to cryo-concentration causing precipitation of various salts leading to a thick deposit of NaCl on the surface sediments. The lake geochemistry has been further modified by input from the west lobe due to overflow and input from glacier inflow including weathering products. Dissolved Organic Carbon (DOC) increases with depth reaching a maximum of 30 mg/l and is attributed to primary production in the lake, evapoconcentration (Green and Lyons, 2009) and subglacial flow from the Taylor Glacier (Mikucki et al. 2004).

The biogeochemistry of the EL is to some extent not fully understood. Oxygen is above saturation (~20mg/l) above 20m and rapidly declines to suboxic concentrations (<1 mg/l) across the chemocline (20-23m). Dissolved inorganic nitrogen (NO_3^- , NO_2^- , NH_4^+) rapidly increases below the chemocline reaching stable maximums (2.4, 0.6, and 3.7 mg-N/l, respectively) at a depth ~30m and below (Priscu et al., 2008). Dissolved N_2O in EL increases similarly below the chemocline and declines rapidly (<1uM) below 30m. The anomalously elevated concentrations of NO_3^- and NO_2^- under suboxic conditions in the deep water are not understood, but multiple studies indicate that denitrification is either not occurring or is occurring at such low rates as to have minimal impact (Priscu et al., 2006, 2008; Ward and Priscu, 1997). Factors contributing to the lack of denitrification activity include the elevated TDS, low temperatures, and elevated redox potential (>400mV) (Ward et al., 2005; Ward and Priscu, 1997). Isotopic studies of ^{15}N and ^{18}O in N_2O in concert with genomic studies suggest the origin of the N_2O was due to nitrification and the current profiles are attributed to a legacy of a former biogeochemical condition that have been preserved due to the extreme stability of the lake (Priscu et al., 2008). Sulfate concentrations increase with depth but the ratio of $\text{SO}_4^{2-}/\text{Cl}^-$ decreases from the surface to the top of the chemocline (~20m) below which it remains reasonably constant. Given the elevated redox condition, the presence of NO_3^- , NO_2^- , as well as the lack of any H_2S , the

reduction in ratio is most likely due to precipitation of a SO_4^{2-} mineral phase in the hypersaline waters rather than sulfate reduction.

ClO_4^- concentration increases with depth in the EL of Lake Bonney (0.46 to 8.3 $\mu\text{g/l}$ at the surface and 35m, respectively) (Figure 2.4.4). The increase in ClO_4^- concentration is proportional to the increase in Cl^- concentration ($r^2=0.99$) over the entire water column. ClO_4^- and SO_4^{2-} concentrations are predicted accurately with a simple mixing model of concentrations at the surface and 35m (Dashed lines Figure 2.4.4). The $\text{ClO}_4^-/\text{Cl}^-$ molar ratio (5×10^{-7}) at the shallowest depth (4m) is less than the ratio in Taylor Valley surface streams (4×10^{-6}) and decreases with depth to a relatively constant value of $\sim 6 \times 10^{-9}$ at 35m (Figure 2.4.3). The ratio at 35 m is still substantially enriched compared to seawater 3.0×10^{-10} which is considered the major source of salts in the EL. It is possible that water below 18m became enriched in ClO_4^- relative to Cl^- from *in situ* precipitation of NaCl which is reported to be at least 1.6m and up to 10m thick in EL sediments (Hendy et al., 1977). Cl^- concentrations reach a maximum at 24m and remain constant at lower depths (Lyons et al., 2005). ClO_4^- would not precipitate given its low concentrations relative to other anions and its very high solubility. There is no evidence (such as a selective loss of ClO_4^- at depth with respect to Cl^-) of biological reduction of ClO_4^- which is not unexpected given the stability of NO_3^- and NO_2^- at depth and the noted lack of any significant nitrate reduction (Priscu et al., 2008, Ward et al., 2005, Ward and Priscu, 1997). All of this suggests the ClO_4^- concentration profiles and $\text{ClO}_4^-/\text{Cl}^-$ ratio profiles are a product of dilution of evapoconcentrated seawater by surface inflow and subsequent diffusion which is consistent with the proposed history of the EL. The origin of ClO_4^- in the EL could be a mix of surface water inflow and seawater, although it is currently not possible to determine if the ClO_4^- in the original seawater is still present. It is possible the east lobe could have experienced conditions that supported ClO_4^- reduction in the distant past given the estimated age of isolation of the seawater 1.7-5.1Ma. Regardless, the ClO_4^- must be reasonably old as the concentration at 35 m is at least $\sim 70\times$ the average Taylor Valley stream concentration and $170\times$ seawater concentrations.

Table 2.4.1. ClO_3^- , ClO_4^- , Cl^- and SO_4^{2-} concentrations in surface waters of the Dry Valleys.

Valley	Basin	Water Body	Date	ClO_4^-	ClO_3^-	Cl^-	SO_4^{2-}
				$\mu\text{g/L}$		mg/l	
Taylor Valley	E. Bonney	Priscu	12/2009	0.07	0.20	10.7	5.4
		Priscu	12/2008	0.15	0.35	9.8	6.3
		Priscu	01/2009	0.47	0.47	43.0	11.3
	W. Bonney	Lawson	01/2009	0.14	0.18	8.22	5.4
		Lawson	12/2008	0.25	0.17	5.7	3.6
		Lawson	12/2009	0.18	0.25	4.9	3.5
		Blood Falls	12/2008	< 0.05	< 0.05		
	Fryxell	Aiken	12/2009	0.18	0.21	12.8	3.6
		Aiken	12/2009	0.12	< 0.1	7.1	3.2
		Canada	01/2009	0.06	.55	2.4	2.4
		Canada	12/2009	0.09	<0.1	2.2	3.3
		Canada	01/2010	0.06	0.25	1.7	2.2
		Canada	12/2008	0.13	0.11	4.0	3.9
		Common Wealth*	12/2008	0.10	0.21	4.7	2.2
		Crescent	12/2008	0.51	0.48	14.1	6.6
		Delta	01/2009	0.34	0.25	9.1	6.0
		Delta	01/2010	0.16	0.11	15.4	6.8
		Delta	12/2008	0.19	0.22	18.9	6.4
		Fryxell Pond	01/2010	0.13	0.48	8.4	3.3
		Green	01/2009	< 0.05	< 0.05	4.0	0.6
		Green	01/2010	0.09	0.35	1.4	0.7
		Green	12/2008	0.06	< 0.1	2.3	0.9
		Green	01/2009	0.05	0.15	2.7	0.9
		Harnish	01/2009	0.7	0.22	13.7	7.8
		Howard Pond	01/2010	0.11	0.20	8.0	3.9
		Huey	01/2009	0.21	0.26	10.3	12.3
		Huey	12/2008	0.43	0.43	10.3	12.1
		Lost Seal	12/2008	0.18	0.07	12.6	5.4
		Lost Seal	01/2010	0.07	<0.1	7.9	3.6
		Lost Seal	12/2008	0.51	0.24	12.7	5.9
		Von Guerard	01/2009	0.16	0.05	6.1	3.2
		Von Guerard	12/2008	0.49	< 0.1	6.8	3.8
		Von Guerard	01/2010	0.01	<0.1	61.7	13.7
	Hoare	Andersen	12/2008	0.1	<0.05	2.8	3.8
		Andersen	12/2009	0.09	<0.1	1.9	2.2
		Andersen	12/2008	0.07	<0.1	3.1	5.4
		Andersen	12/2008	0.18	0.17	14.2	11.1
		House	12/2008	0.10	<0.05	3.1	2.7
		House	12/2008	0.13	0.11	3.6	3.5
		House	12/2008	0.09	0.21	6.6	3.1
		House	12/2009	0.08	<0.1	2.4	2.3
		Wharton	12/2009	0.11	<0.1	2.0	1.6
		Parera Pond	01/2010	8.1	15.5	1300	198
Wright	Vanda	Onyx	12/2009	0.08	0.39	5.2	2.5
		Onyx	11/2009	0.13	0.16	6.8	3.4
		Onyx	01/2009	0.08	0.43	4.9	2.6
		Onyx	01/2009	0.13	0.28	8.0	4.8
		Onyx	12/2008	0.06	<0.1	8.9	2.7
		Onyx	12/2008	0.20	0.34	7.9	5.1
		Onyx	01/2010	0.17	0.18	5.9	3.9

*Common Wealth stream does not feed Lake Fryxell but Common Wealth Glacier, its source, does provide inflow to Lake Fryxell and so it was grouped in this basin.

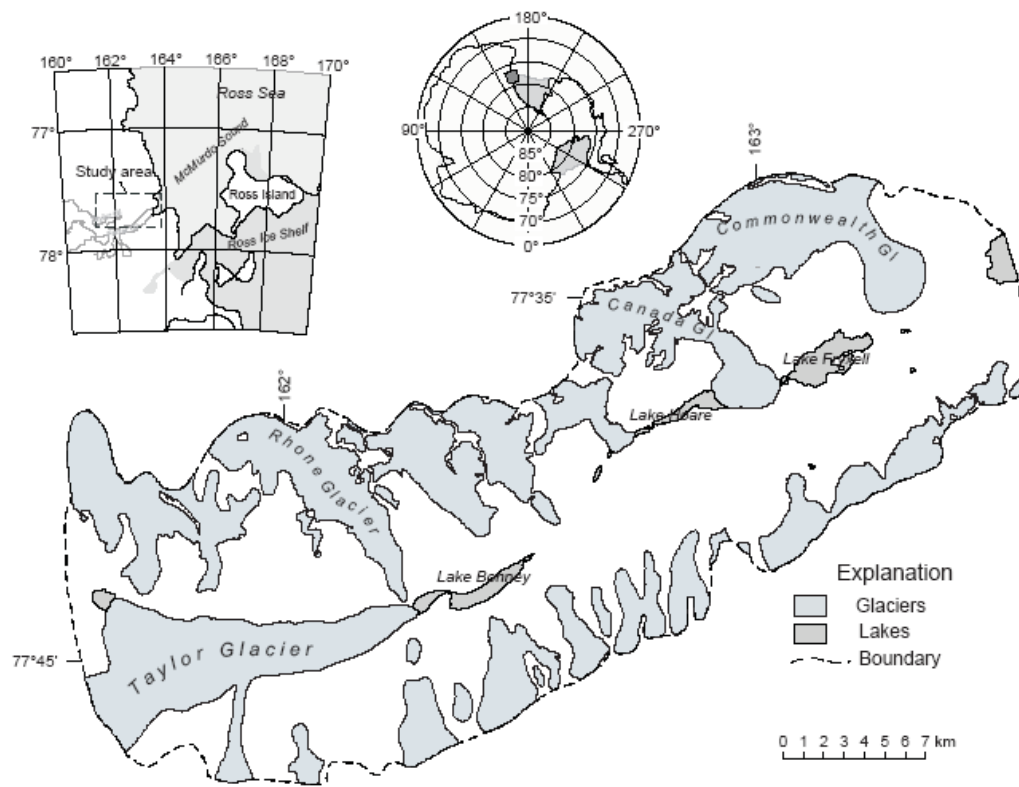


Figure 2.4.1. Map of Taylor Valley, Antarctica showing the locations of Lake Fryxell, Lake Bonney, and Lake Hoare. Adapted from Lyons et al., (2005).

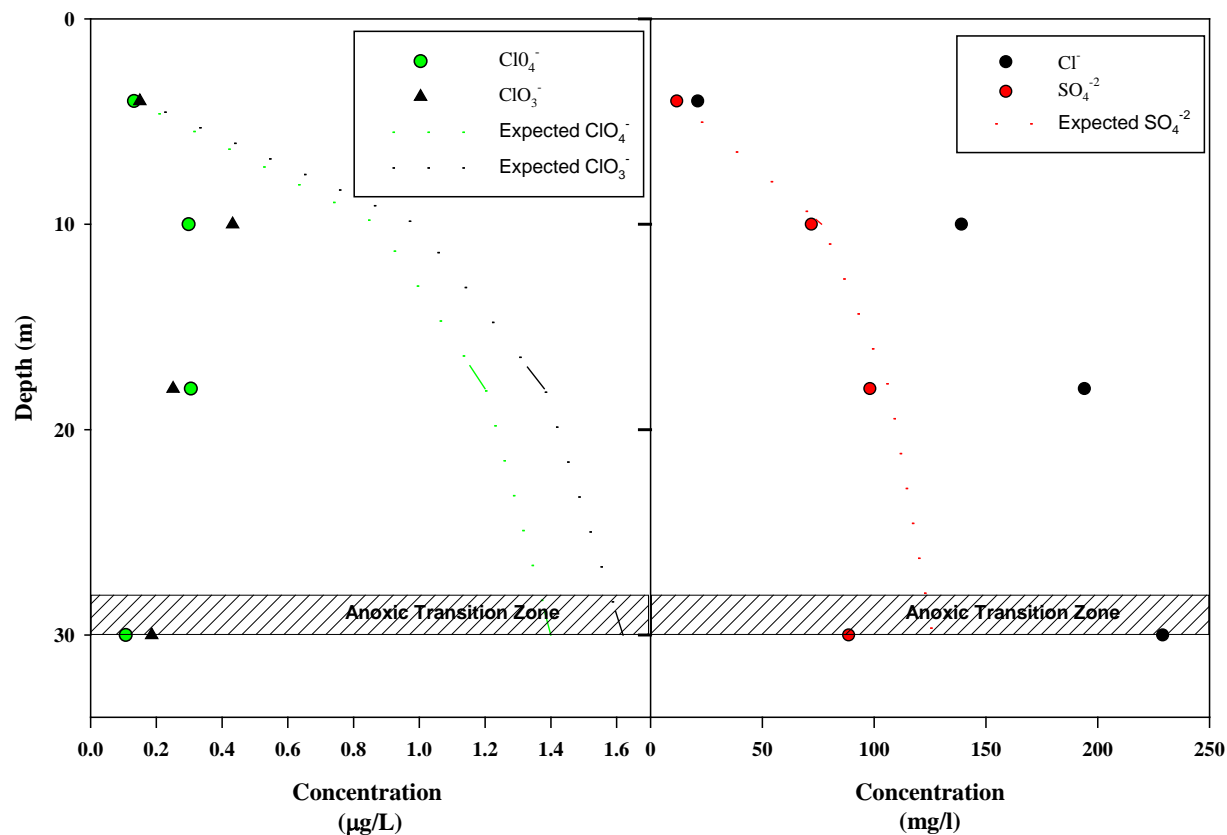


Figure 2.4.2. Concentration profiles of ClO_4^- and ClO_3^- , Cl^- and SO_4^{2-} in Lake Hoare, December 2009. Dashed lines represent modeled concentrations based on maintaining surface water ratios of ClO_3^- , ClO_4^- and SO_4^{2-} relative to Cl^- throughout the lake depth.

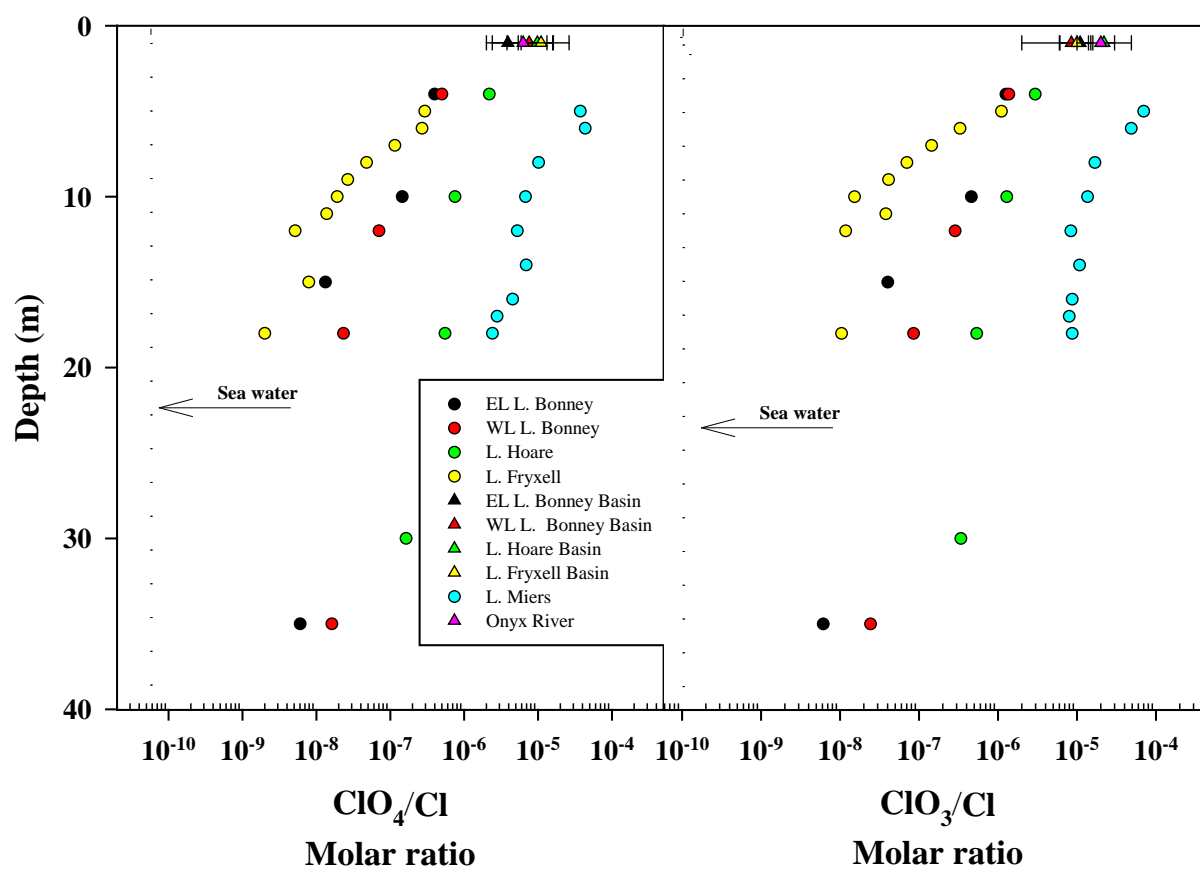


Figure 2.4.3. Molar ratios of $\text{ClO}_4^-/\text{Cl}^-$ and $\text{ClO}_3^-/\text{Cl}^-$ with depth in MCM lakes and feed waters for lake basins in Taylor Valley and the Onyx River in Wright Valley. The black dashed line in each figure represents the ratio in seawater sampled at McMurdo Station.

In contrast to ClO_4^- , ClO_3^- is not as conservative with respect to Cl^- concentration. ClO_3^- concentration does increase with depth (1.1 and 10.5 $\mu\text{g/l}$ at 4m and 35m, respectively) but the increase is proportional to Cl^- only to a depth of 18m (Figure 2.4.4). This is highlighted by evaluating the relationship between ClO_3^- and ClO_4^- (Figure 2.4.5) which is highly correlated ($R=0.97$) up to a depth of 18m. The predicted $\text{ClO}_3^-/\text{ClO}_4^-$ ratio (3.1) is very similar to the ratio in Taylor Valley surface streams (2.2). However, the sample point at 35m is clearly depleted in ClO_3^- relative to ClO_4^- . Modeled ClO_3^- concentrations at 4, 12, and 18m are well predicted based on the two parts mixing model and using the predicted ClO_3^- concentration at 35m based on the ClO_4^- concentration. $\text{ClO}_3^-/\text{Cl}^-$ molar ratios in EL surface water (1×10^{-6}) are similar to streams throughout Taylor Valley and are still well above seawater ratios (1×10^{-10}) even with the apparent reduction of ClO_3^- at 35m. What is clear is that at least at 35m some loss of ClO_3^- relative to ClO_4^- has occurred. This could be due to low level ClO_3^- reduction by low level nitrate reductase activity. While NO_3^- and NO_2^- concentrations appear to be temporally stable at 35m and denitrification is reported to be either absent or at most occurring at insignificant rates (Priscu et al., 2008; Ward et al., 2005; Ward and Priscu, 1997), it is still possible that ClO_3^- has been reduced. ClO_3^- concentrations are only 0.1 and 0.3% of the molar concentrations of NO_3^- and NO_2^- , respectively and therefore reduction rates too small to impact bulk NO_3^- and NO_2^- could have an impact on ClO_3^- concentrations over long periods. Whether this reduction is ongoing or simply a fossil of previous conditions in the EL is unknown.

West Lobe Lake Bonney

The West Lobe (WL) is much smaller than the EL and exchanges water with the EL down to 13m at which depth a sill separates the deeper waters of the east and west lobes. The water quality above the sill layer is therefore similar between the two lobes but the deeper depths are distinct presumably due to their separate evolutionary histories. The WL has apparently not ever lost its ice cover (Hendy et al., 1977; Matsubaya et al., 1979). The source of the deeper water is also attributed to seawater which has been cryo-concentrated but to a lesser extent (144 g/l) due to the presence of the ice cover (Lyons et al., 2005), and from subglacial outflow from the Taylor Glacier (Mikucki et al. 2004 and 2009). A number of lines of evidence suggest that the water may be quite old. The biogeochemistry of the WL follows a more conventional redox profile (Lee et al. 2004). Oxygen concentrations are supersaturated above 13m and decline rapidly to less than 1 mg/l at ~25m. NO_3^- , NO_2^- , and N_2O all peak in or near the chemocline (15-18m) and then rapidly decline below the oxycline due to denitrification (Voytek et al., 1999; Priscu et al., 1996; Ward and Priscu, 1997). Ammonium and DOC concentrations steadily increase below the chemocline but hydrogen sulfide is not present (Green and Lyons, 2009; Voytek et al., 1999; Downes et al., 1995).

Concentration profiles of ClO_4^- and ClO_3^- are similar to the EL except at the lowest sampling depth (35m) at which concentrations are ~5 and 8X lower even though Cl^- is only 2X lower

(Figure 2.4.6). $\text{ClO}_4^-/\text{Cl}^-$ and $\text{ClO}_3^-/\text{Cl}^-$ ratios are also similar for comparable depths (Figure 2.4.3). The loss of ClO_3^- relative to ClO_4^- is also similar to the EL (Figure 2.4.5). Predicted concentrations based on the two component mixing model are reasonably similar to measured values for SO_4^{2-} and ClO_4^- , although some loss of ClO_4^- has occurred at 35m. Predicted concentrations of ClO_3^- are similar for depths above 35m if the concentration at 35m is predicted from the ClO_4^- concentration and expected ratio of $\text{ClO}_3^-/\text{ClO}_4^-$ from Figure 2.4.5. ClO_4^- concentration at 35m and the ratio from Figure 2.4.5 is used to predict the ClO_3^- concentration at 35m rather than the measured concentration. The differences between the EL and WL are likely due to the biological reduction of ClO_4^- , ClO_3^- and NO_3^- at depth in the WL as opposed to only ClO_3^- in the EL. The WL has an active denitrification zone below 18m and NO_3^- , NO_2^- and N_2O are completely reduced by 30m (Voytek et al., 1999; Priscu et al., 1996, Priscu 1997). Taken together this implies that loss of ClO_4^- and ClO_3^- was active in the past but has now ceased or that loss commenced in the relatively near past compared to the age of the lake. Otherwise, we would expect much lower concentrations of both species at depth especially with respect to ClO_4^- which is only slightly depleted with respect to Cl^- .

Lake Fryxell

The geochemistry of Lake Fryxell has recently been reviewed by Green and Lyons (2009). TDS varies from near fresh water at the surface (0.99g/l) to brackish (7.8g/l) water at depths below the oxicleine (~9.5m) where high levels of hydrogen sulfide exist. The lake has been subject to a number of draw down and refill events (Wagner et al., 2006). The conserved Cl^- profile steadily increases with depth and has previously been attributed to diffusion of Cl^- from the sediment to the surface (Green and Lyons, 2009). At depths above ~9m the water is supersaturated with O_2 and between ~9-11m a chemocline exists in which O_2 is rapidly depleted and in which chlorophyll-a reaches a concentration maximum (Priscu, 1995). SO_4^{2-} slowly increases with depth to a maximum at ~11-12m and then rapidly decreases to below 0.1mM at the sediment water interface. H_2S reaches a maximum (1.4mM) at the sediment water interface and declines steadily to 9m above which it is not present (Karr et al., 2005; Sattley and Madigan, 2006; Aiken et al., 1996). An active sulfur oxidizing population is present with a population maximum within the chemocline but extending into the anoxic depths. DOC distribution is similar to Cl^- with a minimum at the surface (~3.0 mg/l) and a maximum (31.2 mg/l) at the sediment water interface. Like Cl^- the distribution of DOC is attributed to diffusion from the sediment of degraded and relic sediment organic matter, and new input from surface water inflow (Aiken et al., 1996). NH_4^+ was reported to be near the detection limit from the surface to the bottom of the chemocline, below which the concentration steadily increases to a maximum (5.6 mg-N/l) at the sediment water interface. NO_3^- was below detection for all depths and NO_2^- was present at trace concentrations (<0.0042 mg-N/L) at 7m and below 15m (Voytek et al., 1999).

Concentrations of both ClO_4^- and ClO_3^- increase slightly from 5m to a maximum at 7m and then decline steadily to just below the chemocline at 10m below which they remain relatively constant (Figure 2.4.7). Concentrations at depths above 9m are generally similar to surface water concentrations in Taylor Valley (Table 2.4.1). The ratio of ClO_4^-/Cl and ClO_3^-/Cl are the lowest of all the lakes, likely due to both the addition of Cl^- from the sediment and strongly reducing conditions below 11m that facilitate ClO_4^- and ClO_3^- bacterial reduction. Predicted concentrations based on surface water ratios of $\text{ClO}_4^-/\text{Cl}^-$ and $\text{ClO}_3^-/\text{Cl}^-$ over estimate both ClO_4^- and ClO_3^- concentrations at depths below 6m. SO_4^{2-} concentrations are likewise over predicted at depths below the chemocline. Collectively, these results in concert with the complete lack of NO_3^- and NO_2^- below the chemocline (Priscu and Ward, 1999, Priscu 1997) suggests that ClO_4^- and ClO_3^- are actively being reduced. These data further imply that ClO_4^- and ClO_3^- were either not present during the last lake drawdown (~1000Ka) or were consumed since the lake has been refilled. The ClO_3^- and ClO_4^- concentration profile appear to reflect a surface source, distribution by diffusion, and consumption at depth below 11m.

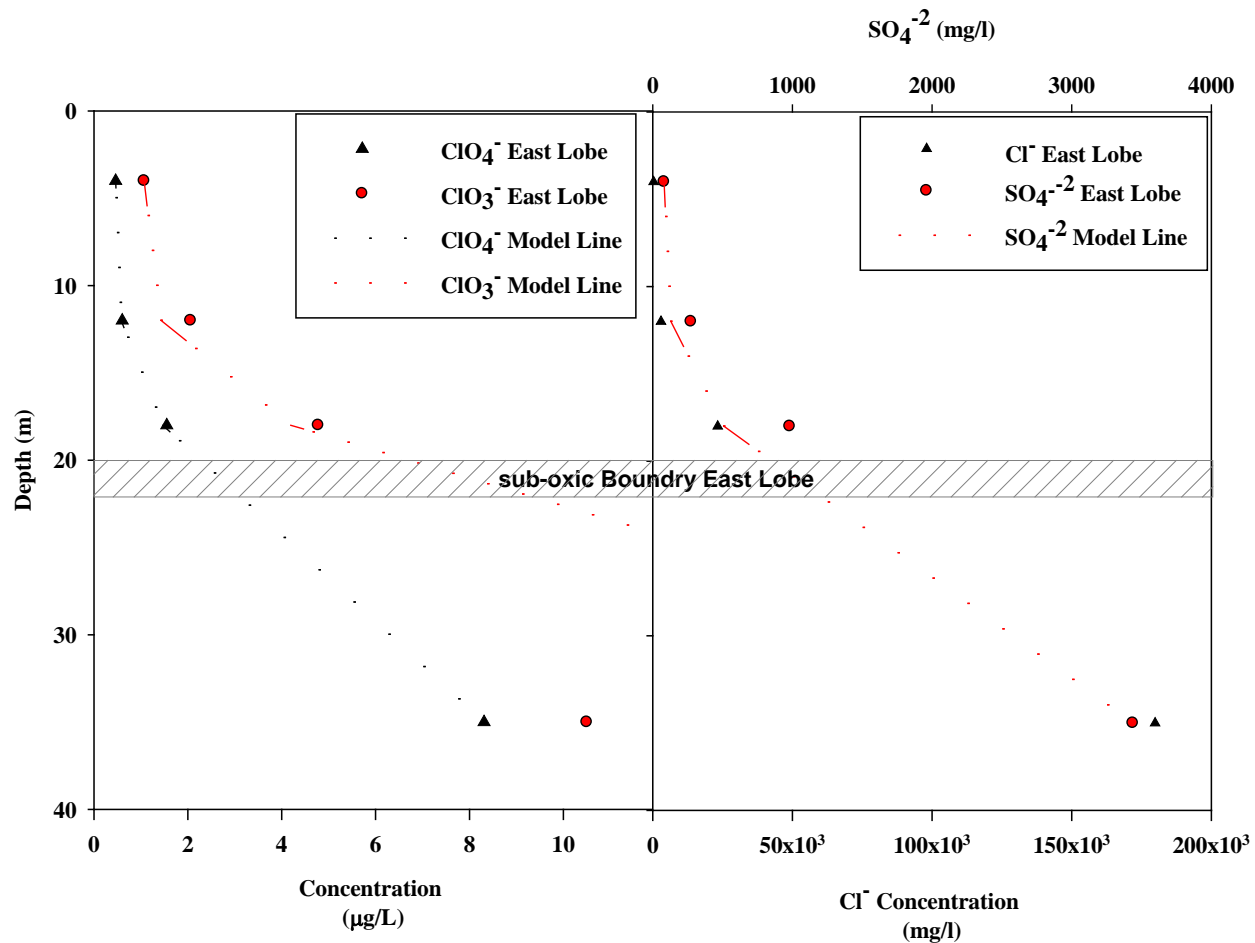


Figure 2.4.4. Concentration profiles of ClO_4^- and ClO_3^- , Cl^- and SO_4^{2-} in the EL of Lake Bonney, December 2009. Dashed lines represent modeled concentrations based on a two part mixing model of concentrations at the surface and 35m except for ClO_3^- for which the concentration at 35m is predicted from the ClO_4^- concentration using the ratio from Figure 2.4.5. See text for further explanation.

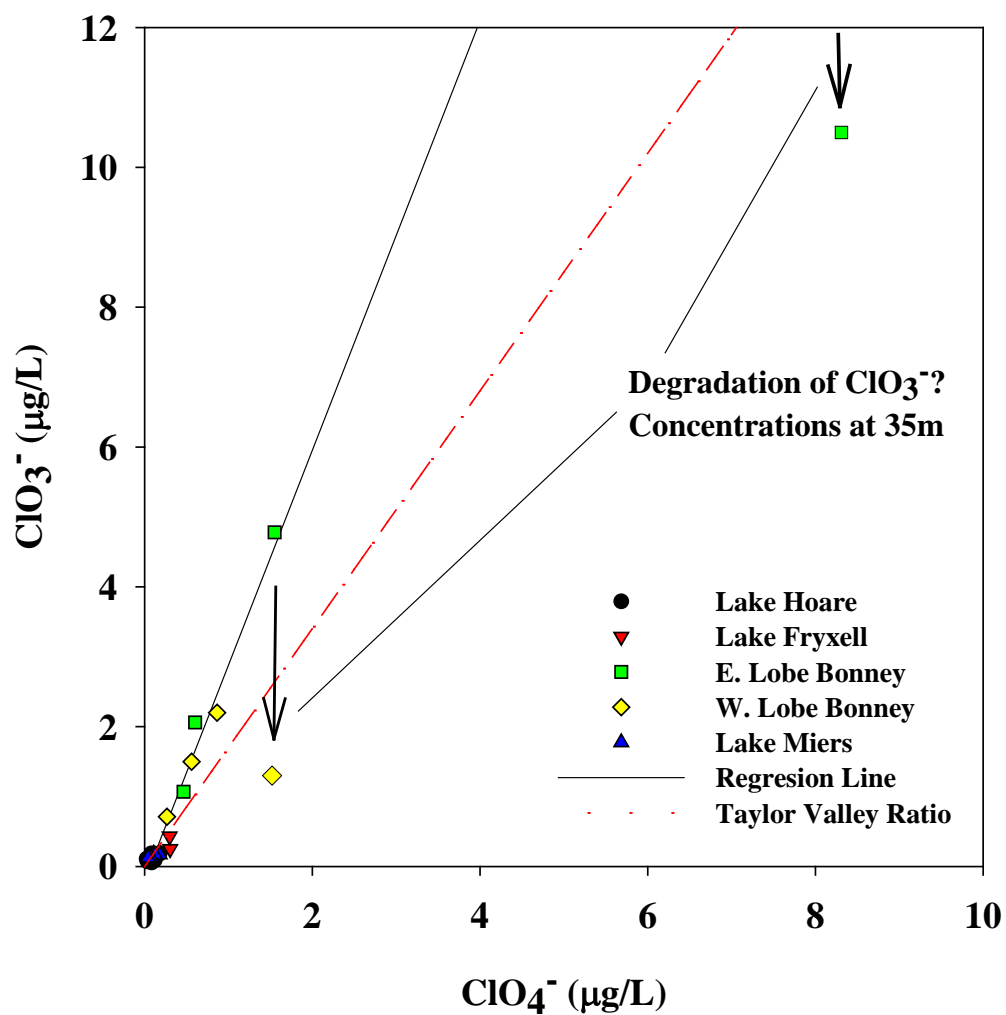


Figure 2.4.5. Relationship of ClO₃⁻ and ClO₄⁻ concentration in Dry Valley Lakes. The solid black line represents the regression line ($r^2 = 0.97$ and ratio = 3.1) and the red dashed line represents ratio of ClO₃⁻ and ClO₄⁻ in streams of Taylor Valley.

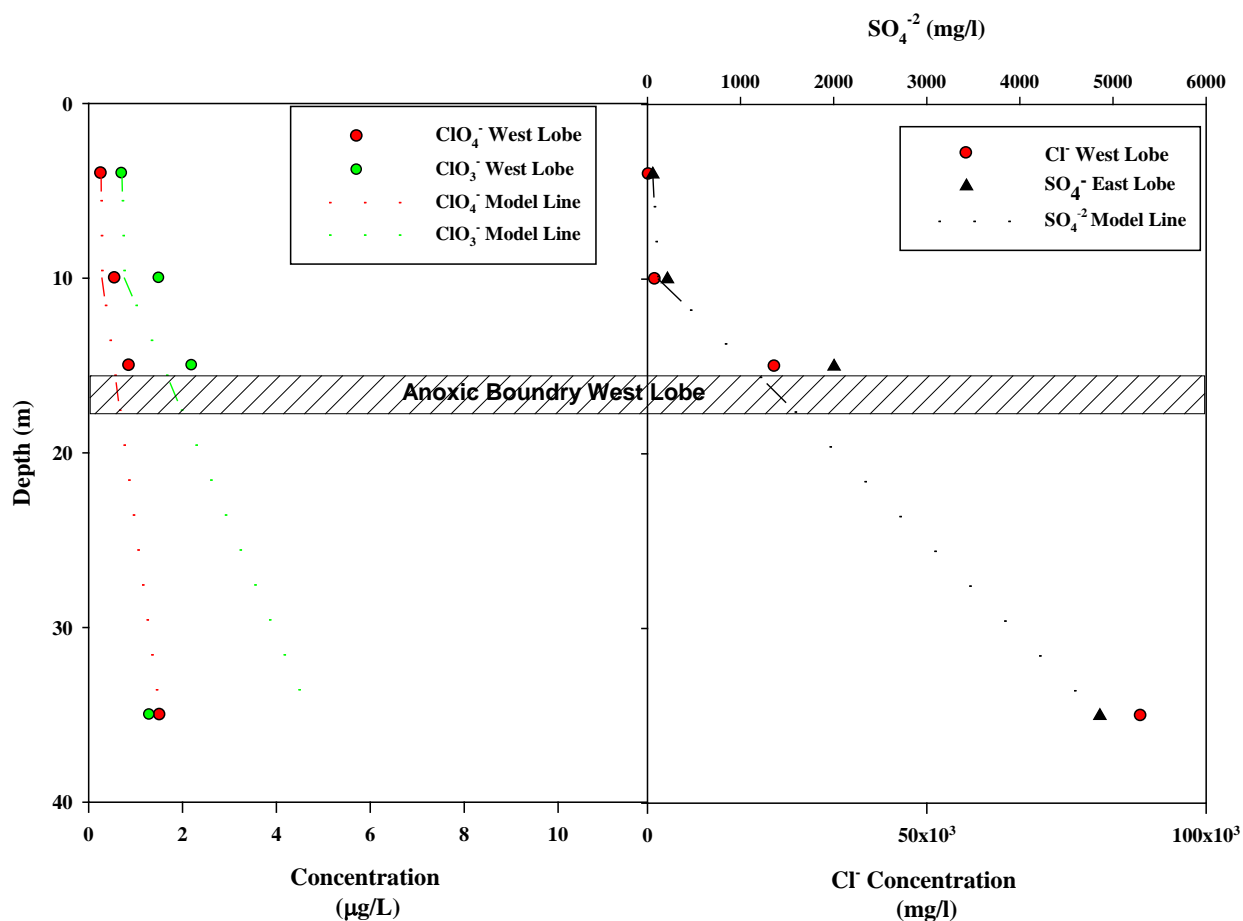


Figure 2.4.6. Concentration profiles of ClO_4^- and ClO_3^- , Cl^- and SO_4^{2-} in the WL of Lake Bonney, December 2009. Dashed lines represent modeled concentrations based on a two part mixing model of concentrations at the surface and 35m except for ClO_3^- for which the concentration at 35m is predicted from the ClO_4^- concentration using the ratio from Figure 2.4.5. See text for more explanation.

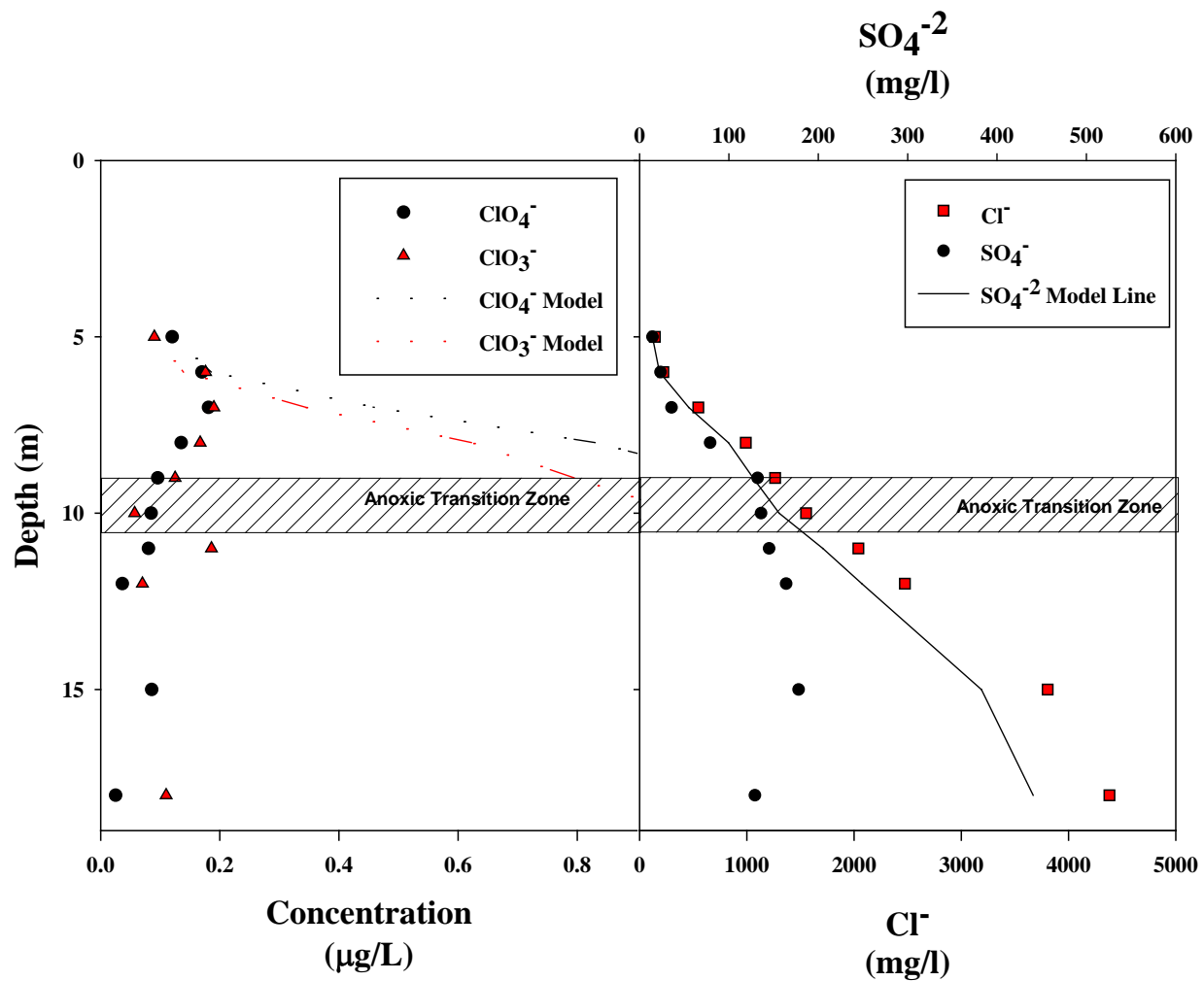


Figure 2.4.7. Concentration profiles of ClO_4^- and ClO_3^- , Cl^- and SO_4^{2-} in Lake Fryxell, December 2008. Dashed lines represent modeled concentrations based on maintaining surface water ratios of ClO_3^- , ClO_4^- and SO_4^{2-} relative to Cl^- throughout the lake depth.

Lake Miers

Lake Miers is relatively unstudied compared to other MDV lakes. It is much younger (<300 years) and is the only lake with both hydraulic inflow and outflow and, as such, its chemistry resembles glacier meltwater. The lake is oxic throughout its depth but approaches anoxic conditions at the sediment water interface. Nitrification rates while not directly measured are believed to be very low and NO_3^- and NO_2^- are essentially constant with depth (<0.03 and 0.002 mg-N/l, respectively) (Voytek et al., 1999). ClO_3^- and ClO_4^- concentrations are essentially constant with depth with exception of depths below 14m where ClO_4^- concentrations decrease (Figure 2.4.8). Chloride increases with depth until 12m below the surface beyond which it remains relatively constant. $\text{ClO}_3^-/\text{Cl}^-$ and $\text{ClO}_4^-/\text{Cl}^-$ ratios in surface water are near but above Taylor Valley surface water and consistently decrease with depth (Figure 2.4.4). While the lake is oxic, the reduction in SO_4^{2-} below 14m strongly suggests that the sediments may support anoxic processes. This would be congruent with the reduction in $\text{ClO}_4^-/\text{Cl}^-$ and $\text{ClO}_3^-/\text{Cl}^-$ ratios.

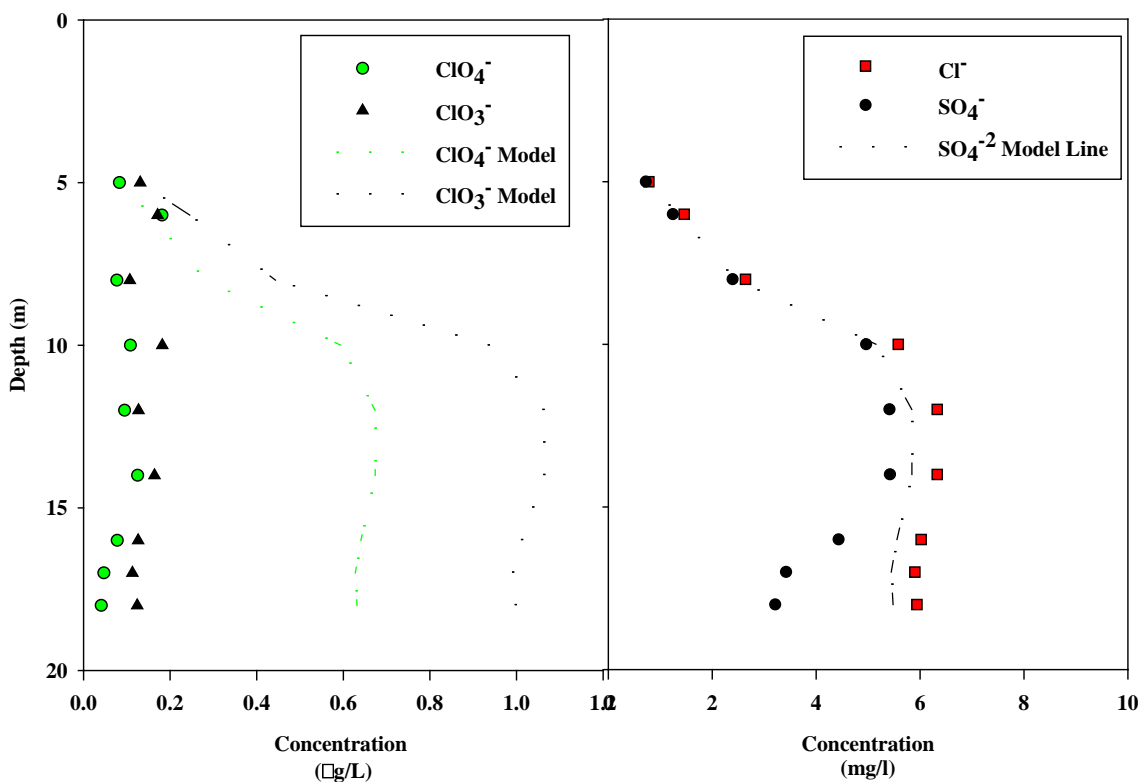


Figure 2.4.8. Concentration profiles of ClO_4^- and ClO_3^- , Cl^- and SO_4^{2-} in Lake Miers, December 2008. Dashed lines represent modeled concentrations based on maintaining surface water ratios of ClO_3^- , ClO_4^- and SO_4^{2-} relative to Cl^- .

2.4.6 Summary and Conclusions

ClO_3^- and ClO_4^- are present throughout the water columns of the MDV lakes and other surface water bodies in the area. Concentrations among surface water bodies are generally similar reflecting a common atmospheric source. Variations in streams are likely due to site-specific processes, such as the degree of evaporative concentration and the differential input of salts due to leaching of soils and aeolian materials and subsequent inflow to streams. The concentrations of ClO_3^- and ClO_4^- in the ice-covered lakes are dependent on both the total evaporative concentration that has occurred as well as the biological activity within each lake. The two relatively young lakes (Miers and Hoare), have ClO_3^- and ClO_4^- concentrations and ratios of $\text{ClO}_3^-/\text{Cl}^-$ and $\text{ClO}_4^-/\text{Cl}^-$ in surface waters that are similar to source streams, but suggest ClO_3^- and ClO_4^- reduction at depth or in the sediments. Lake Fryxell has ClO_3^- and ClO_4^- concentrations similar to input streams but $\text{ClO}_3^-/\text{Cl}^-$ and $\text{ClO}_4^-/\text{Cl}^-$ ratios much lower due to the large Cl^- source in bottom sediments due to its complete evaporation in the past. Based on the paucity of ClO_3^- and ClO_4^- in the deep waters, this lake appears to have supported ClO_3^- and ClO_4^- reduction at least back to the last draw down event. ClO_3^- and ClO_4^- concentrations in Lake Bonney are the highest of all the lakes reflecting the lake's greater age and concentration of Cl^- . Similar to NO_3^- , ClO_4^- appears to be stable in the East Lobe and its concentration is highly correlated to Cl^- concentration. It is even possible that some ClO_4^- at depth is a remnant of the initial seawater that formed Lake Bonney. In the West Lobe ClO_3^- and ClO_4^- appear stable at depths above the chemocline but have or are experiencing reduction at the deepest depth similar to NO_3^- . Finally the concentrations of ClO_3^- and ClO_4^- are well correlated except in cases where reduction has occurred.

These lakes provide an excellent case study for ClO_3^- and ClO_4^- biotransformation in pristine extreme environments. Given their low concentrations, high solubility, and lack of any *in situ* generation mechanisms, they may offer a sensitive means to study ongoing biological activity in the lakes, and the addition of ClO_4^- stable isotope evaluation could provide further clues as to the geochemical history of the lake water. Finally, ClO_3^- and ClO_4^- biogeochemistry in Antarctic ice-covered lakes may represent an excellent analog for similar processes in ice-covered lakes on Mars in the past (McKay and Davis, 1991), or even in more recent times, especially given the discovery of relatively large amounts of ClO_4^- in the Martian soil (Hecht et al., 2009).

2.5 Evaluate Cl and O Stable Isotope Signatures of UV and O₃ Generated Perchlorate

2.5.1 Background

As previously described, natural production of ClO₄⁻ has been linked to atmospheric processes involving the oxidation of Cl and oxy-chlorine (ClO_x) species by ultraviolet (UV) radiation and ozone (O₃) (Kang et al., 2006, 2008, 2009; Rao et al., 2010, Wang et al., 2011). The pathways for ClO₄⁻ formation are ambiguous and not well-defined, this more so for production of ClO₄⁻ by O₃ oxidation than by photo-oxidation, of which there have been more proposed pathways. Although the actual ClO₄⁻ production pathways are still unknown, studies by our group and others (Rao et al., 2010, 2012; Kang et al., 2009) have identified some of the reactants responsible for ClO₄⁻ formation by both UV and O₃ as well as some of the suspected intermediates and other major products. Formation of the ClO₄⁻ is considered dependent upon many factors including: exposure time, mass of reactant, pH, type of system (dry vs. aqueous), surface material, and in the case of UV, the light source (wavelength) (Kang et al., 2006, 2008, 2009; Rao et al., 2010, Wang et al., 2011). Along with oxidation of oxy-chlorine species, production of ClO₄⁻ has also been observed as a result of reactions involving chlorine monoxide (ClO) and chlorine dioxide (ClO₂) radicals on the surface of sulfuric acid (Jaegl et al., 1996). The factors affecting ClO₄⁻ formation can all contribute to fractionation effects that can lead to the variation observed in natural ClO₄⁻ isotopic compositions.

At present there are no studies related to the potential for different ClO₄⁻ formation pathways to produce distinct variations in ClO₄⁻ isotopic composition. The purpose of this study was to evaluate the potential for different formation processes to impact the stable isotopic composition of ClO₄⁻ produced from UV or O₃ oxidation of Cl and oxy-chlorine species. Isotopic compositions for water (H₂O), O₃, ClO₄⁻, starting materials, and major end products were determined. The isotopic data were compared to the known groups of natural ClO₄⁻ isotopic compositions to determine if different ClO₄⁻ formation processes contribute to the variation in natural ClO₄⁻ isotopic compositions observed.

2.5.2 Methods

2.5.2.1 Preparation of Reactant Species

Aqueous solutions of hypochlorite (OCl⁻), Cl⁻, and chlorite (ClO₂⁻) were prepared from calcium hypochlorite (Ca(OCl)₂; available chlorine ~65%, Sigma-Aldrich), sodium chloride (NaCl; ACS reagent, 99 + %; Sigma-Aldrich), and sodium chlorite (NaClO₂; technical grade, 80 %; Sigma-Aldrich) salts. All Ca(OCl)₂ solutions were filtered through a 0.2μm filter (PVDF Membrane, Millipore) before being used in the O₃ and photo-oxidation experiments. Concentrations for reactant species were based on ClO₄⁻ yields from previous studies (Kang et al., 2008; Rao et al., 2010, 2012; Wang et al., 2011).

The aqueous chlorine dioxide (ClO_2) solutions were prepared according to a standard iodometric method (SMEWW, 1998) by use of a gas generating and absorption system, with minor modifications (Figure 2.5.1). The aspirator flask was filled with 300 mL distilled deionized (DDI) water, the gas-generating bottle with 750 mL DDI water and 10 g NaClO_2 , the two scrubber bottles (used to capture impurities) with flaked NaClO_2 crystals, and the collecting bottle with 1500 mL DDI water. The collecting bottle was wrapped in aluminum foil to avoid the penetration of light in order to minimize the photodegradation of ClO_2 (aq). Before being connected to the gas-generating and absorption system the collecting bottle was chilled in the freezer and then placed in a bucket of ice so that better dissolution of ClO_2 occurred. The ClO_2 was generated by bubbling a smooth current of purified compressed air through the system and by adding 2 mL of H_2SO_4 in 5 mL increments through 5 minute intervals.

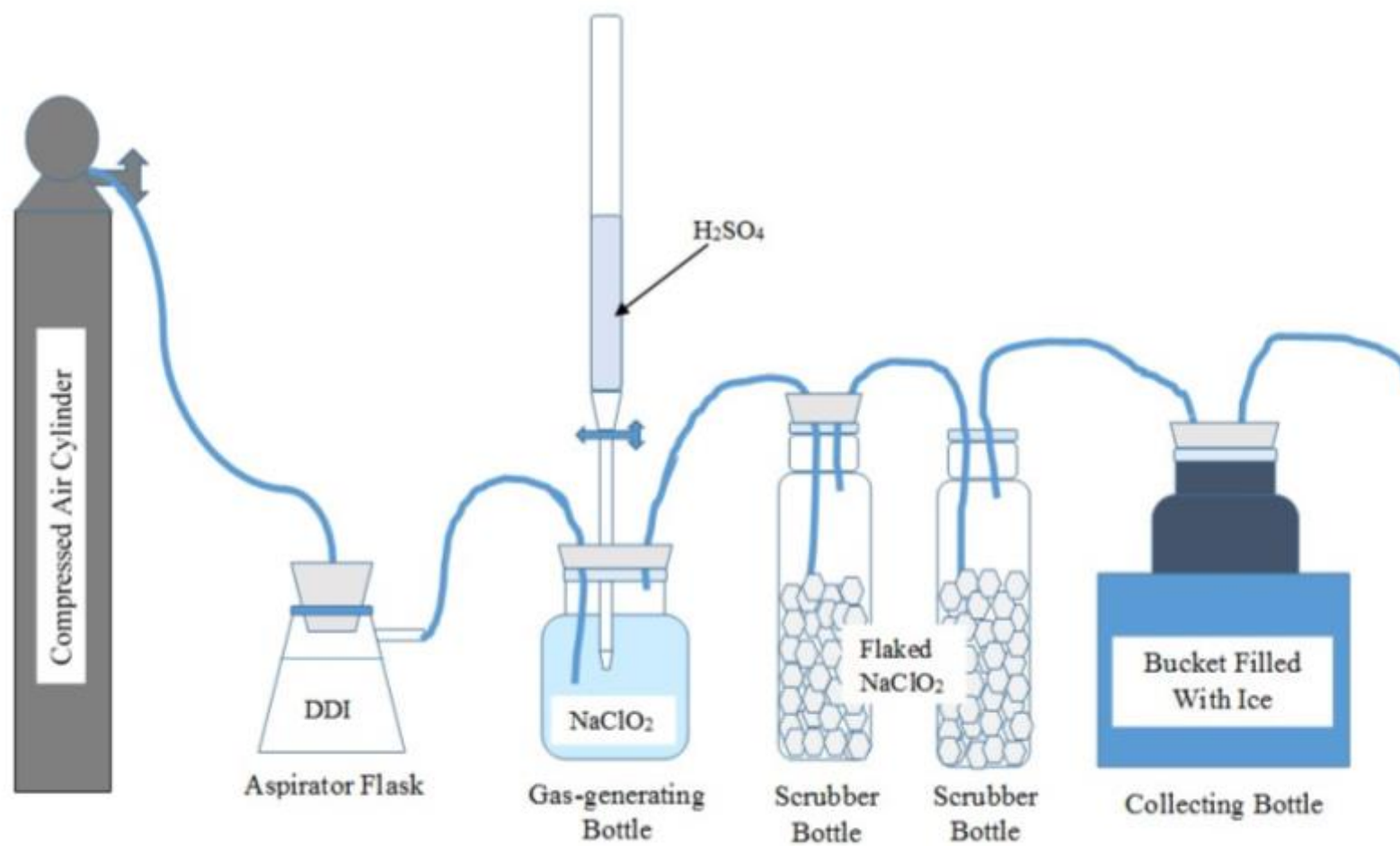


Figure 2.5.1 Chlorine dioxide gas-generating absorption system.

2.5.2.2 Ozone Experiments

Ozone experiments were conducted according to methods by Rao et al., 2010 with minor modifications. Ozone was produced by passing pure oxygen (O_2 -purity > 99.999%) through an adjustable corona discharge O_3 generator (Model OL80W, Ozone Services) and was bubbled through aqueous solutions of ClO_2 , ClO_2^- , OCl^- , and Cl^- (Table 2.5.1 and Figure 2.5.2)

Table 2.5.1. Experimental Conditions for O_3 oxidation of various Cl/ClO_x species.

Replicate #	Reactant Species	Species Mass (mg)	Volume (L)	Exposure Time
1	Dry Cl^-	514 041	N/A	~ 1 month
1	Cl^- (aq)	211 200	32	~ 9 months
2	Cl^- (aq)	747 000	18	~ 9 months
1	OCl^- (aq)	13 000	1.8	~ 1 day
2	OCl^- (aq)	8 640	0.5	~ 1 day
3	OCl^- (aq)	11 782*	0.5	~ 1 day
1	ClO_2^- (aq)	4 650	0.5	~ 2 – 20 hrs
2	ClO_2^- (aq)	4 133	0.5	~ 2 – 20 hrs
1	ClO_2 (aq)	38	0.5	~ 1.5 hrs
2	ClO_2 (aq)	71	1	~ 1.5 hrs

* Value is an approximation as solution was measured long after it was made

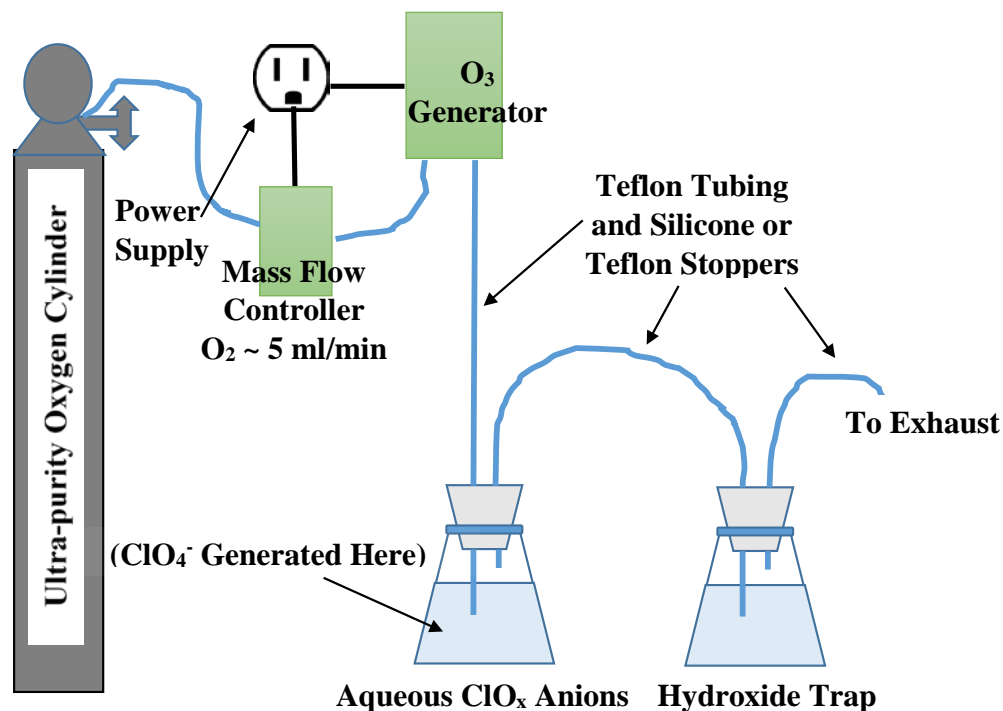


Figure 2.5.2. Experimental set-up for aqueous O_3 oxidation experiments.

Generation of ClO_4^- by O_3 oxidation of dry Cl^- ($NaCl$; Certified ACS, $\geq 99\%$; Fisher Chemical) was also performed. Ozone was passed through approximately 50 glass tubes containing ± 10 grams $NaCl$ each and connected in series by Teflon tubing (Figure 2.5.3). The flow rate of O_3 was maintained throughout the experiments by a gas flow controller (Model GFC-17; Aalborg) set closely at 5 mL/min. All experiments, minus the dry Cl^- , were performed in duplicate (Table 2.5.1). Starting and ending solutions were analyzed for Cl^- , OCl^- , ClO_2^- , ClO_2 , ClO_3^- , and ClO_4^- .

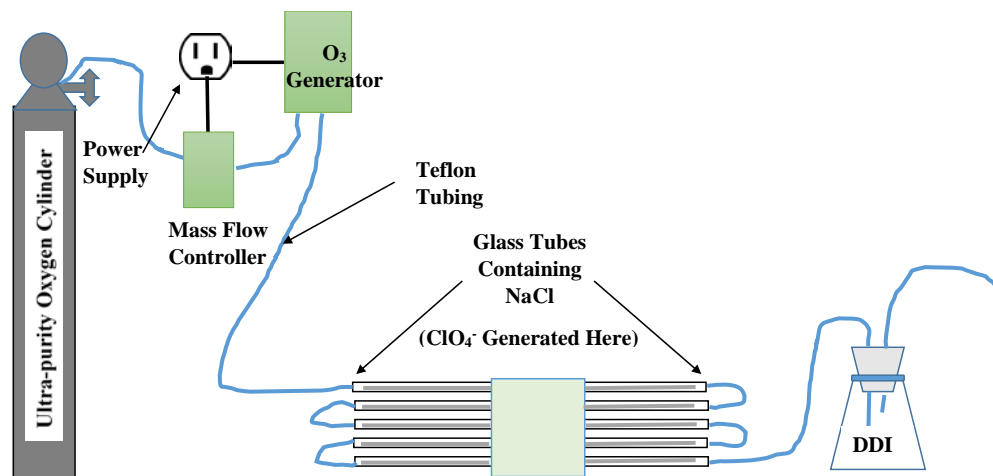


Figure 2.5.3. Experimental set-up for O₃ oxidation of dry Cl⁻.

2.5.2.3 UV Experiments

UV experiments were conducted according to methods by Rao et al., 2012b with minor modifications. Aqueous solutions of OCl^- , ClO_2^- , and ClO_2 were irradiated with UV light ($\lambda = 350 \text{ nm}$) using a Rayonet photochemical chamber (Model RPR-200; Southern New England Ultraviolet Co., Brandford, CT) equipped with 8 UV lamps (Table 2.5.2 and Figure 2.5.4). Erlenmeyer flasks containing the solutions and stoppered with silicone caps were placed inside the photochemical chamber until complete conversion of the reactant species (OCl^- , ClO_2^- , and ClO_2) was observed. All experiments were performed in duplicate and starting and ending solutions were analyzed for Cl^- , OCl^- , ClO_2^- , ClO_2 , ClO_3^- , and ClO_4^- .

Table 2.5.2. Experimental conditions for UV oxidation of various ClO_x species.

Replicate #	Reactant Species	Species Mass (mg)	Volume (L)	Wavelength λ	Exposure Time
1	OCl^- (aq)	20 000	0.8	350 nm	~ 5 – 10 hrs
2	OCl^- (aq)	36 000	1	350 nm	~ 5 – 10 hrs
1	ClO_2^- (aq)	8 000	0.3	350 nm	~ 1 – 3 hrs
2	ClO_2^- (aq)	10 000	1	350 nm	~ 1 – 3 hrs
1	ClO_2 (aq)	2 664	37	350 nm	~ 30 min – 3 hrs
2	ClO_2 (aq)	1 941	23.7	350 nm	~ 30 min – 3 hrs

* Value is an approximation as solution was measured long after it was made

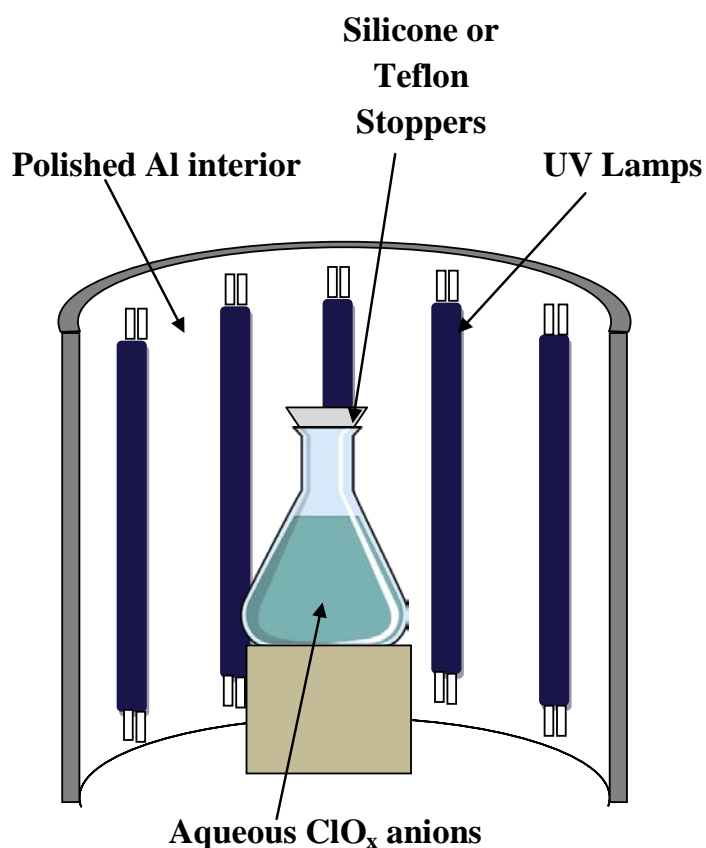


Figure 2.5.4. Experimental set-up for UV oxidation experiments using the Rayonet photochemical chamber.

2.5.2.4 Sample Analysis

Perchlorate and ClO_3^- concentrations in starting and ending solutions were determined using sequential ion chromatography-mass spectroscopy/mass spectroscopy (IC-MS/MS) as described in Rao et al. (2007). Concentrations of Cl^- and ClO_2^- were determined using ion-chromatography (IC) (Dionex LC20 enclosure) following U.S. EPA Methods 300.0 (USEPA, 1993) and 326.0 (Thomas et al., 2013) with minor modifications. Chloride was analyzed using a Dionex IonPac AS14A column (4 x 250 mm) and an 8 mM sodium carbonate (Na_2CO_3)/1 mM sodium bicarbonate (NaHCO_3) eluent while ClO_2^- was analyzed using a Dionex AS9-HC column and a 9 mM Na_2CO_3 eluent. The limit of detection (LOD) for Cl^- and ClO_2^- was 0.5 mg/L.

Hypochlorite was measured as total Cl_2 ($\text{total Cl}_2 = \text{Cl}_2 + \text{HOCl} + \text{OCl}^-$) by buffering solution samples at pH 8.5 and spiking them with excess iodide (I^-) to produce a tri-iodide species (I_3^-) that could be measured using a spectrophotometer (DU[®] Series 700, Beckman Coulter[®]) at 351 nm ($\epsilon = 2.54 \pm 0.02 \times 10^4 \text{ M}^{-1}\text{cm}^{-1}$). The reaction stoichiometry between Cl_2 and I_3^- was used to determine OCl^- concentration. The ClO_2 in solutions was determined by both UV spectrometry at 359 nm ($\epsilon = 1230 \pm 10 \text{ M}^{-1}\text{cm}^{-1}$) and iodometric titration with 0.025 N sodium thiosulfate ($\text{Na}_2\text{S}_2\text{O}_3$) (SMEWW, 1998)

2.5.2.5 Perchlorate Extraction and Purification

All ending solutions were passed through a Purolite[®] A530E resin column at a constant flow rate until at least 2 mg of ClO_4^- was collected (Gu et al., 2011). Ending solutions containing high amounts of ClO_3^- were first reduced so that their presence did not interfere with the uptake of ClO_4^- by the resin column. Reduction was achieved by first purging the solutions with helium (He) to remove any remaining oxidants and then by adding elemental nickel (Ni) and purging the solutions with hydrogen gas (H_2) to reduce the high level species. Resin columns were preserved with hydrochloric acid (HCl) at a pH of 2 and were sent to Oak Ridge National Laboratory for elution and purification, as described in Gu et al. (2011) and Hatzinger et al. (2011).

The elution process consisted of removing the Purolite[®] A530E resin containing the absorbed ClO_4^- from the column, rinsing it with ultrapure DDI water in an ultrasonic bath, transferring it into a preparative glass chromatography column (100 mL volume), and then washing it approximately with 5 bed volumes (BV) of 4 M HCl to remove any absorbed impurities (i.e. NO_3^- , organics, carbonates) (Hatzinger et al., 2011). The adsorbed ClO_4^- was eluted from the preparative glass column with a combination of 1 M FeCl_3 and 4 M HCl. The FeCl_3 -HCl eluent solution (containing the eluted ClO_4^-) contains high concentrations of organics, Fe, and other anions aside from ClO_4^- , the eluent solution was neutralized with NaOH (pH ~ 9 – 10) to precipitate out the Fe and other impurities (Hatzinger et al., 2011). These precipitates were washed and centrifuged to collect a clear supernatant solution that was evaporated using a

vacuum concentration system to form precipitates (removed through filtration) until the ClO_4^- concentration in solution was in excess of 3 mg/mL. The ClO_4^- from the remaining purified solution was crystallized as cesium perchlorate (CsClO_4) by adding CsCl . A detailed version of the elution and purification method is described in Hatzinger et al. (2011).

2.5.2.6 Isotope Ratio Analyses

Oxygen isotope analyses were performed at the Reston Stable Isotope Laboratory of the U.S. Geological Survey in Reston, VA by high-temperature conversion of the purified ClO_4^- salt (CsClO_4) to CO that was measured in continuous-flow mode by isotope-ratio mass spectrometry (CO-CFIRMS) and on O_2 produced by in vacuo decomposition of the ClO_4^- salt (CsClO_4) analyzed in dual-inlet mode by isotope-ratio mass spectrometry (O2-DIIRMS) (Sturchio et al., 2007, 2011; Böhlke et al., 2005; Bao and Gu, 2004; Hatzinger et al., 2011). Oxygen isotope ratios are reported in units of $\delta^{18}\text{O}$, $\delta^{17}\text{O}$, and $\Delta^{17}\text{O}$ in terms of per mil (‰), defined as the deviation from the Vienna Standard Mean Ocean Water ($\delta^{18}\text{O}_{\text{VSMOW}} = 0.0\text{‰}$) (Equations 1-3).

$$\delta^{18}\text{O} = \left[\frac{\left[\frac{n(^{18}\text{O})}{n(^{16}\text{O})} \right]_{\text{sample}}}{\left[\frac{n(^{18}\text{O})}{n(^{16}\text{O})} \right]_{\text{VSMOW}}} - 1 \right] \times 1000 \quad (1)$$

$$\delta^{17}\text{O} = \left[\frac{\left[\frac{n(^{17}\text{O})}{n(^{16}\text{O})} \right]_{\text{sample}}}{\left[\frac{n(^{17}\text{O})}{n(^{16}\text{O})} \right]_{\text{VSMOW}}} - 1 \right] \times 1000 \quad (2)$$

$$\Delta^{17}\text{O} = k = \left(\left[\frac{(1 + \delta^{17}\text{O})}{(1 + \delta^{18}\text{O})^\lambda} \right] - 1 \right) \times 1000 \quad (3)$$

Chlorine isotope ratios were analyzed at the Environmental Isotope Geochemistry Laboratory of the University of Illinois at Chicago by conversion of the CsClO_4 salt into methyl chloride (CH_3Cl) gas that was measured by ion-ratio mass spectrometry (IRMS) (Sturchio et al., 2007, 2011; Böhlke et al., 2005; Hatzinger et al., 2011). Perchlorate Cl isotope ratios are all reported in units of $\delta^{37}\text{Cl}$ in terms of per mil (‰), defined as the deviation from that of Standard Mean Ocean Chloride (SMOC) (Equation 4).

$$\delta^{37}\text{Cl} = \left(\frac{\left[\frac{n(^{37}\text{Cl})}{n(^{35}\text{Cl})} \right]_{\text{sample}}}{\left[\frac{n(^{37}\text{Cl})}{n(^{35}\text{Cl})} \right]_{\text{SMOC}}} - 1 \right) \times 1000 \quad (4)$$

2.5.3 Results

2.5.3.1 Mass Balance and Product Yields

A mass balance on initial and final amounts of Cl of ClO_x species for UV and O_3 mediated ClO_4^- generation experiments resulted in a Cl recovery of 81-116%, with one exception (Table 2.5.3). For one of three replicate experiments in which OCl^- was oxidized by O_3 , the total Cl recovery was only 31%. It is unclear whether the missing or excess Cl is related to analytical error due to the high concentrations of some species compared to others, or in the case of missing Cl perhaps due to production of Cl containing gasses that escaped the system (e.g. ClO_2).

Production yields for ClO_x species detected in final solutions were also evaluated (Table 2.5.3). ClO_4^- production yields for the majority of experiments were within an order of magnitude of each other (0.01 – 0.15 %). The exceptions were the O_3 aqueous and dry Cl^- experiments, which had the lowest ClO_4^- yields (note that not all Cl^- was reacted), and the O_3 - ClO_2 (aq) and one UV- ClO_2^- experiment(s), which had the highest ClO_4^- yields. It is unclear as to why one of the UV- ClO_2^- replicates had a ClO_4^- yield 10-fold higher than the other, but it could be related to this treatment's higher initial ClO_2^- concentration as suggested by Kang et al. (2006) and Rao et al. (2012b). This UV- ClO_2^- replicate also had a different product distribution than its replicate, suggesting that the difference in ClO_4^- yields may be due to different production mechanisms.

Oxidation of aqueous solutions of all starting ClO_x species produced Cl^- and ClO_3^- as major products with substantially smaller ClO_4^- yields. Cl^- was the dominant product for UV and O_3 mediated oxidation of OCl^- and UV mediated oxidation of ClO_2^- . ClO_3^- was the major product for O_3 mediated oxidation of ClO_2^- and UV and O_3 mediated oxidation of ClO_2 (aq). Except for the case of oxidation of solutions of ClO_2^- or ClO_2 (aq) by O_3 for which the ClO_3^- yield was > 80 %, yields of Cl^- and ClO_3^- generally were within a factor of 2–3 for O_3 and UV mediated oxidation of aqueous solutions (Table 2.5.3). However, final products from the oxidation of Cl^- as a dry solid or in aqueous solution could not be evaluated as the majority of the Cl^- was unreacted at the end of the oxidation period. As such, a better representation of the product distribution for the O_3 - Cl^- (aqueous and dry) experiments would be the final molar $\text{ClO}_4^-/\text{ClO}_3^-$ ratio, which for our study was estimated to be 0.0002 – 0.0003 and 5 for the aqueous and dry experiments, respectively. The O_3 oxidation of dry Cl^- was the only experimental condition for which ClO_4^- was produced in excess of ClO_3^- . Although the experimental conditions for our UV

and O₃ experiments were not the same as in previous studies, most of our yields were comparable to those reported in the same studies (Kang et al., 2006, 2008; Rao et al., 2010, 2012b; Wang et al., 2011).

Table 2.5.3. Cl amounts in ClO_x species of initial and final solutions, Cl mass balance, and product yields for UV and O₃ experiments.

Ozone Experiments																			
Initial Solution								Final Solution					Mass Balance		Product Yields*				
Reactant Species	Cl ⁻ mmol	OCl ⁻ mmol	ClO ₂ ⁻ mmol	ClO ₂ (aq) mmol	ClO ₃ ⁻ mmol	ClO ₄ ⁻ mmol	in ClO _x mmol	Cl ⁻ mmol	OCl ⁻ mmol	ClO ₂ ⁻ mmol	ClO ₃ ⁻ mmol	ClO ₄ ⁻ mmol	Total Cl in ClO _x mmol	% Cl Accounted	Cl ⁻ Yield %	OCl ⁻ Yield %	ClO ₂ ⁻ Yield %	ClO ₃ ⁻ Yield %	ClO ₄ ⁻ Yield %
1-OCl ⁻	140.8	252.7	< 0.55	NM	11.2	0.0005	404.7	300.4	< 0.06	< 0.55	52.6	0.09	353.1	87.2	63.17	-99.98	0.00	16.36	0.04
2-OCl ⁻	37.2	167.9	< 0.55	NM	1.5	0.0001	206.7	54.4	0.16	< 0.55	9.6	0.02	64.1	31.0	10.20	-99.91	0.00	4.77	0.01
3-OCl ⁻	41.2	39.0	< 0.55	NM	1.7	0.0002	81.9	81.3	0.32	< 0.55	12.5	0.03	94.1	114.9	102.68	-99.19	0.09	27.67	0.07
1-Cl ⁻	5957.7	< 0.06	< 0.55	NM	< 0.60	0.0004	5957.7	5867.4	< 0.06	< 0.55	222.4	0.05	6089.9	102.2	-1.52	0.00	0.00	3.72	< 0.001
1-Cl ⁻	21071.9	< 0.06	< 0.55	NM	< 0.60	0.0005	21071.9	21071.9	< 0.06	< 0.55	94.9	0.03	21166.9	100.5	0.00	0.00	0.00	0.45	< 0.001
1-ClO ₂ ⁻	18.2	NM	68.9	NM	0.86	0.0001	88.0	31.2	NM	< 0.55	65.9	0.06	97.2	110.5	18.92	0.00	-99.63	94.36	0.09
1-ClO ₂ ⁻	19.2	< 0.06	61.3	NM	< 0.60	< 0.0001	80.4	27.7	< 0.06	< 0.55	60.5	0.07	88.3	109.7	13.88	< 0.003	-99.94	98.07	0.11
1-Dry Cl ⁻	14500.4	NM	NM	NM	NM	NM	14500.4	12646.0	NM	NM	< 0.60	0.04	12646.0	87.2	-12.79	0.00	0.00	< 0.0001	< 0.001
1-ClO ₂ (aq)	NM	< 0.06	< 0.55	0.57	< 0.60	< 0.0001	0.57	NM	NM	NM	< 0.60	0.02	0.02	3.9	0.00	-1.03	-0.52	83.25	3.89
2-ClO ₂ (aq)	< 0.03	< 0.06	< 0.55	1.06	< 0.60	< 0.0001	1.1	< 0.03	< 0.06	< 0.55	0.85	0.03	0.88	82.9	0.00	1.47	0.00	80.02	2.74

UV Experiments																			
Initial Solution								Final Solution					Mass Balance		Product Yields*				
Reactant Species	Cl ⁻ mmol	OCl ⁻ mmol	ClO ₂ ⁻ mmol	ClO ₂ (aq) mmol	ClO ₃ ⁻ mmol	ClO ₄ ⁻ mmol	in ClO _x mmol	Cl ⁻ mmol	OCl ⁻ mmol	ClO ₂ ⁻ mmol	ClO ₃ ⁻ mmol	ClO ₄ ⁻ mmol	Total Cl in ClO _x mmol	% Cl Accounted	Cl ⁻ Yield %	OCl ⁻ Yield %	ClO ₂ ⁻ Yield %	ClO ₃ ⁻ Yield %	ClO ₄ ⁻ Yield %
1-OCl ⁻	216.64	388.73	< 0.55	NM	17.26	0.00080	622.6	521.86	< 0.06	< 0.55	117.44	0.52	639.82	102.8	78.52	-99.99	0.00	25.77	0.13
2-OCl ⁻	389.96	699.71	< 0.55	NM	31.06	0.00145	1120.7	729.48	< 0.06	< 0.55	177.59	0.35	907.42	81.0	48.52	-100.00	-0.05	20.94	0.05
1-ClO ₂ ⁻	37.17	< 0.06	118.61	NM	0.68	0.00322	156.5	119.83	< 0.06	< 0.55	59.67	0.18	179.68	114.8	69.69	0.00	-98.75	49.74	0.15
2-ClO ₂ ⁻	46.46	< 0.06	148.26	NM	0.85	0.00402	195.6	109.31	< 0.06	< 0.55	70.10	2.45	181.86	93.0	42.39	0.01	-99.95	46.71	1.65
1-ClO ₂ (aq)	3.05	< 0.06	3.44	39.50	< 0.60	0.00179	46.0	14.92	< 0.06	< 0.55	25.98	0.02	40.91	89.0	30.06	0.00	-7.31	64.60	0.03
2-ClO ₂ (aq)	0.67	< 0.06	< 0.55	28.77	< 0.60	0.00260	29.4	10.80	< 0.06	< 0.55	13.53	0.02	24.35	82.7	35.23	-0.01	-0.50	45.13	0.05

NM = Not measured

N/Y = No Yield

* Product Yields were calculated using the following equation: : Product Yield = (Final ClO_x^y-Initial ClO_x^y)/Main Reactant ClO_x^y

2.5.3.2 Ozone Experiment Isotopes

Dry Chloride

The $\delta^{37}\text{Cl}$ values of the initial dry Cl^- salt and the final solution total Cl were indistinguishable (-0.1‰) (Figure 2.5.5). This is because the reactants and products were essentially composed of all Cl^- and only a small amount of initial Cl^- reacted. ClO_4^- had $\delta^{37}\text{Cl}$ values $\sim 3.5\text{‰}$ lower than those of initial and final total Cl and Cl^- .

$\delta^{18}\text{O}$ and $\Delta^{17}\text{O}$ values of ClO_4^- in the final solution were $+21\text{‰}$ and $+33\text{‰}$, respectively. $\delta^{18}\text{O}$ values of final total Cl compounds (ClO_3^- and ClO_4^-) could not be measured because of high total Cl/O ratios.

Aqueous Chloride

Initial total Cl ($\approx \text{Cl}^-$), final total Cl ($\text{Cl}^- + \text{ClO}_3^- + \text{ClO}_4^-$), and final Cl^- had similar $\delta^{37}\text{Cl}$ values in both aqueous Cl^- experiments (Figure 2.5.6). ClO_4^- had $\delta^{37}\text{Cl}$ values $\sim 7\text{‰}$ higher than those of initial and final total Cl and Cl^- .

The $\delta^{18}\text{O}$ values of final total O ($\approx \text{ClO}_3^-$) were $\sim 60 - 75\text{‰}$ lower than those of ClO_4^- . The $\Delta^{17}\text{O}$ values of final total O ($\approx \text{ClO}_3^-$) were greater than zero but much lower ($\sim 25\text{‰}$ to 28‰) than ClO_4^- $\Delta^{17}\text{O}$ values.

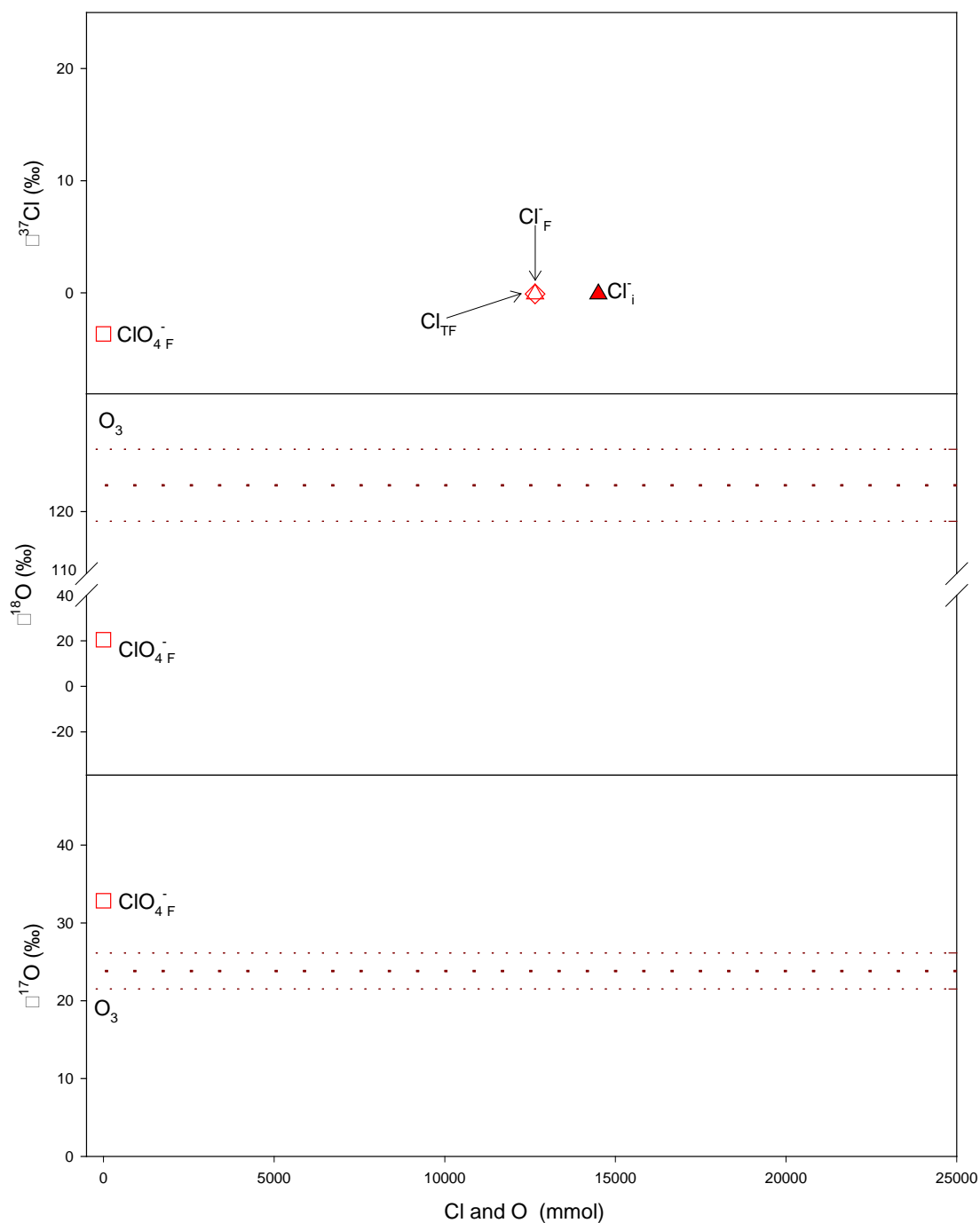


Figure 2.5.5. Stable isotopic composition of initial and final species for O_3 oxidized dry Cl^- . Replicate experiments are represented by the different colors and different symbols represent the Cl and O of ClO_x species present in initial and final solutions, where T_I = total initial, T_F = total final, I =initial, and F =final. Note that the horizontal axis indicates the amount of Cl (for $\delta^{37}\text{Cl}$) and the amount of O (for $\delta^{18}\text{O}$ and $\Delta^{17}\text{O}$) in the initial and final experimental solutions.

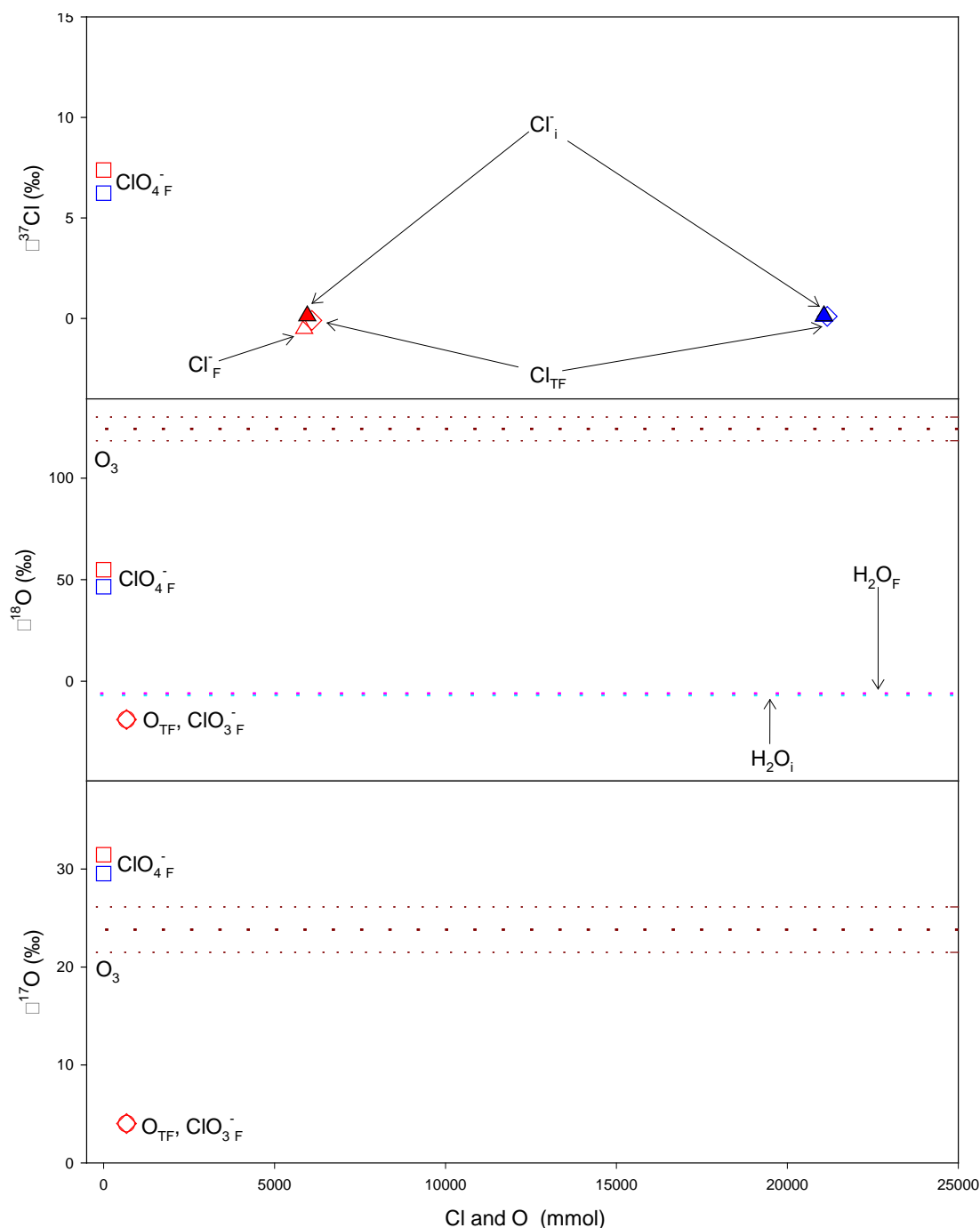


Figure 2.5.6. Stable isotopic composition of initial and final species for O_3 oxidized solutions of Cl^- (aq). Replicate experiments are represented by the different colors and different symbols represent the Cl and O of ClO_x species present in initial and final solutions, where T_i = total initial, T_F = total final, I = initial, and F = final. Note that the horizontal axis indicates the amount of Cl (for $\delta^{37}\text{Cl}$) and the amount of O (for $\delta^{18}\text{O}$ and $\delta^{17}\text{O}$) in the initial and final experimental solutions.

Hypochlorite

Not all initial and final $\delta^{37}\text{Cl}$, $\delta^{18}\text{O}$, and $\Delta^{17}\text{O}$ values were measured for each O_3 oxidized replicate OCl^- experiment (Figure 2.5.7). The $\delta^{37}\text{Cl}$ value (+ 2.56 ‰) of the initial total Cl ($\text{Cl}^- + \text{ClO}_3^- + \text{ClO}_4^-$) was similar (< 2.5 ‰) to the final total Cl ($\text{OCl}^- + \text{Cl}^-$), initial Cl^- , and final Cl^- $\delta^{37}\text{Cl}$ values. Compared to initial total Cl ($\text{OCl}^- + \text{Cl}^-$), the estimated $\delta^{37}\text{Cl}$ value (using a mass balance) for produced ClO_3^- and the $\delta^{37}\text{Cl}$ values of ClO_4^- of all the experiments were on average ~ 15 ‰ higher.

Final total O $\delta^{18}\text{O}$ values were similar between all replicates as were final ClO_4^- $\delta^{18}\text{O}$ values, which were (32 ‰ – 47 ‰) higher than the final total O (essentially all ClO_3^-). Initial total O $\delta^{18}\text{O}$ values of two of the replicate experiments were similar and only slightly lower than final ClO_4^- $\delta^{18}\text{O}$ values. However, the third replicate experiment had a much lower initial total O $\delta^{18}\text{O}$ value (~ 24 ‰), which is odd given the similar $\delta^{18}\text{O}$ values for the final total O for all treatments and for final ClO_4^- for all treatments. This may suggest that the very low initial total $\delta^{18}\text{O}$ values for the third replicate may be invalid. $\Delta^{17}\text{O}$ values were similar for initial total O ($\text{OCl}^- + \text{ClO}_3^-$) and final total O ($\approx \text{ClO}_3^-$), with less than 1.5 ‰ variation. On the contrary, ClO_4^- $\Delta^{17}\text{O}$ values were much higher (15 ‰ – 20 ‰) compared to final ClO_3^- and initial and final total O.

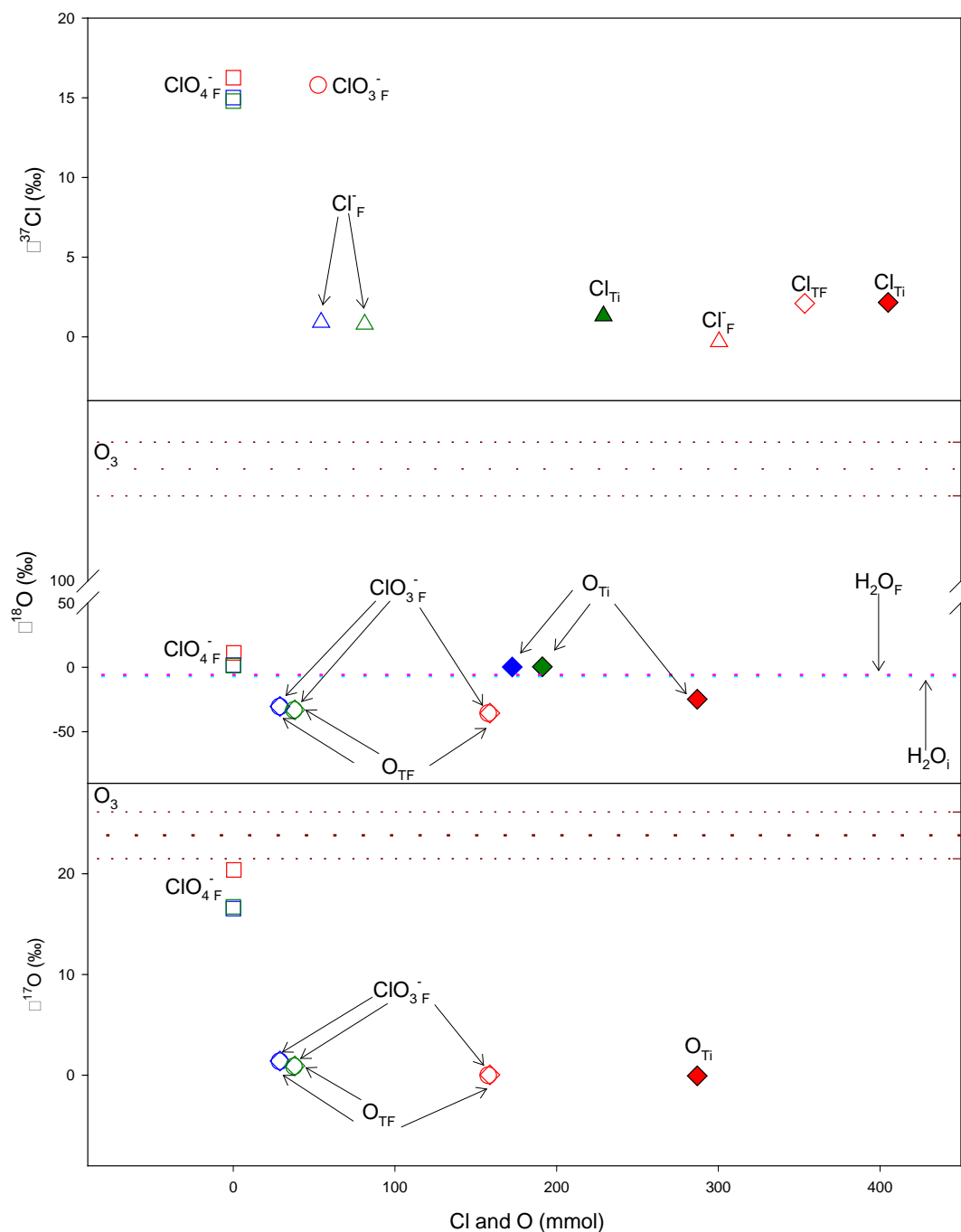


Figure 2.5.7. Stable isotopic composition of initial and final species for O_3 oxidized solutions of OCl^- (aq). Replicate experiments are represented by the different colors and different symbols represent the Cl and O of ClO_x species present in initial and final solutions, where T_I = total initial, T_F = total final, I = initial, and F = final. Note that the horizontal axis indicates the amount of Cl (for $\delta^{37}\text{Cl}$) and the amount of O (for $\delta^{18}\text{O}$ and $\Delta^{17}\text{O}$) in the initial and final experimental solutions.

Chlorite

The $\delta^{37}\text{Cl}$ values of initial total Cl ($\text{ClO}_2^- + \text{Cl}^-$) and final total Cl ($\text{Cl}^- + \text{ClO}_3^-$) were similar ($< 0.5\text{‰}$) for all ClO_2^- replicates (Figure 2.5.8). Likewise, $\delta^{37}\text{Cl}$ values of initial and final Cl^- were similar to one another ($< 2\text{‰}$ difference), but were lower than the $\delta^{37}\text{Cl}$ values of the initial total Cl ($\text{ClO}_2^- + \text{Cl}^-$) by $4\text{‰} - 6\text{‰}$. Estimated (by mass balance) $\delta^{37}\text{Cl}$ values for initial ClO_2^- and final ClO_3^- were similar to each other and higher than initial total Cl $\delta^{37}\text{Cl}$ values by $1.5\text{‰} - 2\text{‰}$. $\delta^{37}\text{Cl}$ values of ClO_4^- ($+5\text{‰} - +6\text{‰}$) were higher than all other species.

Total O in the initial solution ($\approx \text{ClO}_2^-$) and final solution ($\approx \text{ClO}_3^-$) had similar $\delta^{18}\text{O}$ values, but these $\delta^{18}\text{O}$ values were lower ($\sim 3\text{‰} - 6\text{‰}$) than those of produced ClO_4^- . In the initial solution the $\Delta^{17}\text{O}$ values of total O ($\approx \text{ClO}_2^-$) were lower than the $\Delta^{17}\text{O}$ values of the total O ($\approx \text{ClO}_3^-$) and ClO_4^- in final solution by $\sim 3\text{‰}$ and 12‰ , respectively.

Chlorine Dioxide

ClO_2 (aq) initial and final solution isotopes are not available, except for final ClO_4^- (Figure 2.5.9). The $\delta^{37}\text{Cl}$ value of ClO_4^- ($\sim +16\text{‰}$) was only determined for one experiment. The $\delta^{18}\text{O}$ value of ClO_4^- varied between the experiments, with one of the replicates being 4‰ higher in $\delta^{18}\text{O}$. $\Delta^{17}\text{O}$ values of ClO_4^- were similar between both experiments at approximately $+16.5\text{‰}$.

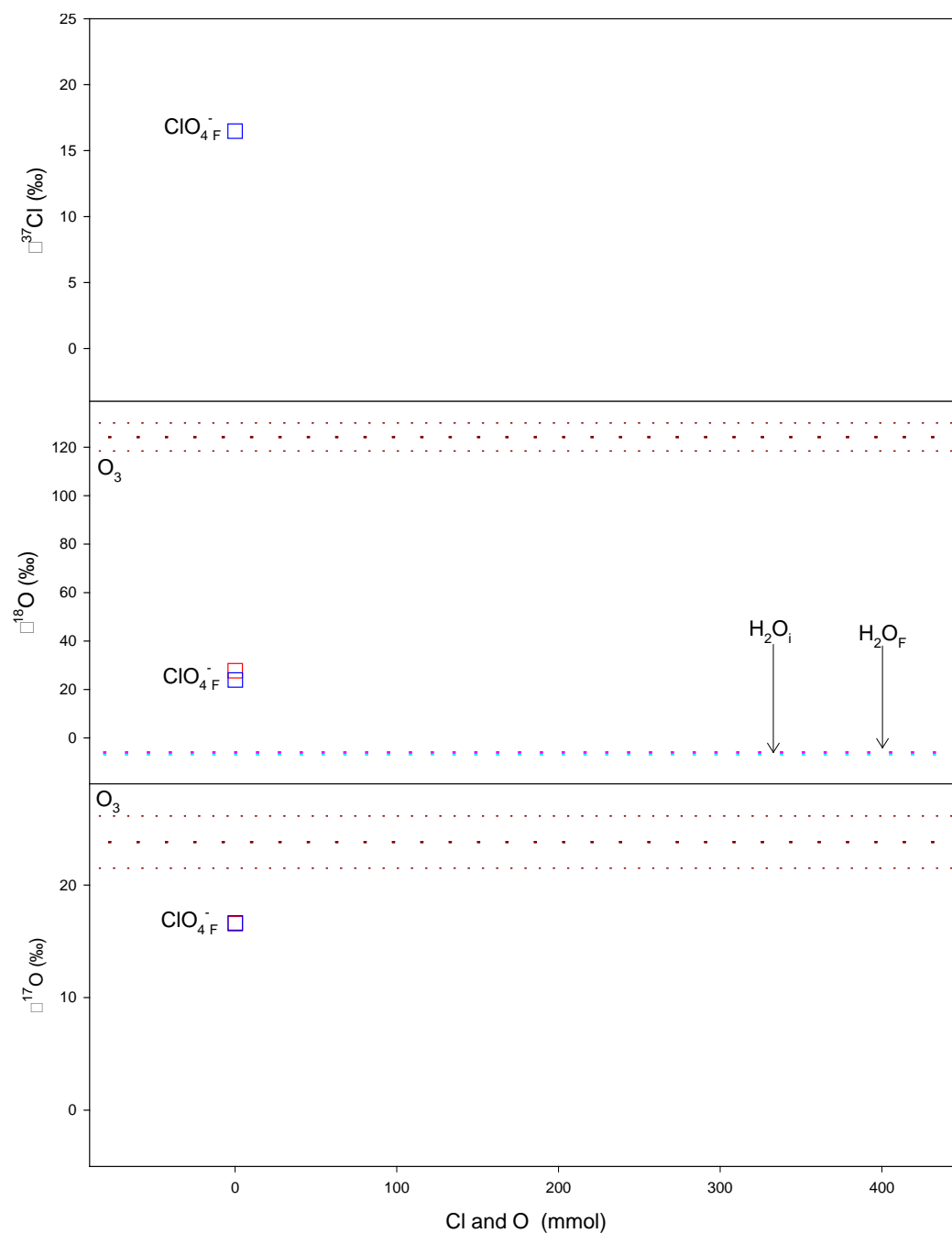


Figure 2.5.9. Stable isotopic composition of initial and final species for O_3 oxidized solutions of ClO_2 (aq). Replicate experiments are represented by the different colors and different symbols represent the Cl and O of ClO_x species present in initial and final solutions, where T_I = total initial, T_F = total final, I = initial, and F = final. Note that the horizontal axis indicates the amount of Cl (for $\delta^{37}\text{Cl}$) and the amount of O (for $\delta^{18}\text{O}$ and $\Delta^{17}\text{O}$) in the initial and final experimental solutions.

2.5.3.3 UV Experiment Isotopes

Hypochlorite

Regardless of the starting OCl^- mass and production yields, the isotopic compositions ($\delta^{37}\text{Cl}$, $\delta^{18}\text{O}$, and $\Delta^{17}\text{O}$) of the reactants and products from photolysis ($\lambda=350\text{ nm}$) of OCl^- solutions were essentially the same between both experiments (Figure 2.5.10). The $\delta^{37}\text{Cl}$ of initial total Cl ($\text{OCl}^- + \text{Cl}^- + \text{ClO}_3^-$), final total Cl ($\text{Cl}^- + \text{ClO}_3^- + \text{ClO}_4^-$), initial Cl^- , and final Cl^- did not vary ($< 1\text{ ‰}$). $\delta^{37}\text{Cl}$ in ClO_4^- and ClO_3^- (based on mass balance) were higher ($\sim 15\text{ ‰}$ and 2 ‰ , respectively) than initial and final total Cl or Cl^- .

The total O of ClO_x species in the final solution, which was almost solely composed of ClO_3^- , had $\delta^{18}\text{O}$ values approximately $11\text{ ‰} - 15\text{ ‰}$ lower than those of total O for the initial total ClO_x ($\sim \text{OCl}^- + \text{Cl}^-$). Contrarily, ClO_4^- $\delta^{18}\text{O}$ was 7 ‰ higher than $\delta^{18}\text{O}$ of initial total ClO_x ($\sim \text{OCl}^- + \text{Cl}^-$). $\Delta^{17}\text{O}$ values were essentially the same (-0.33 ‰ to $+0.45\text{ ‰}$) among all major species, both initial and final (ClO_4^- , ClO_3^- , and total O in ClO_x).

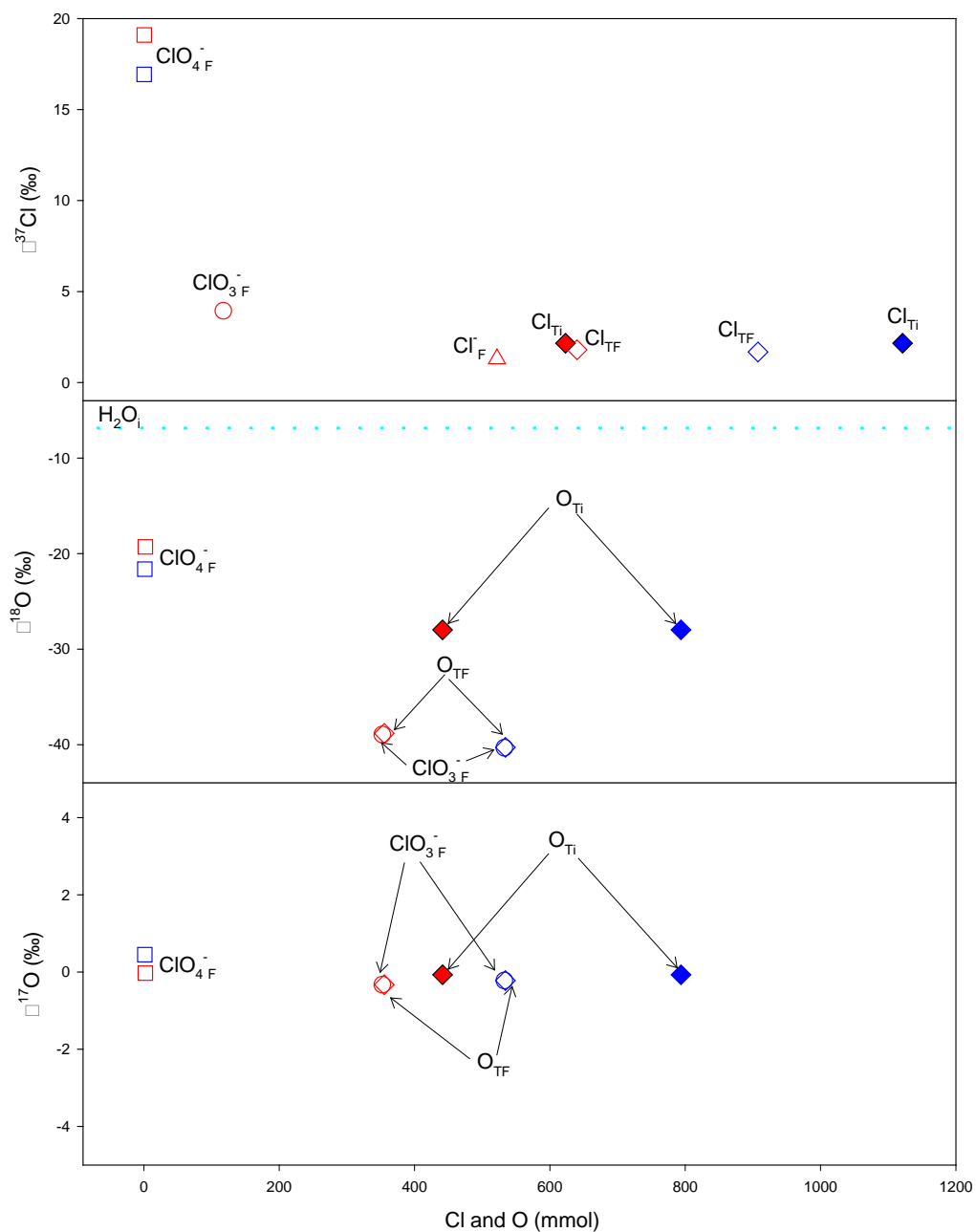


Figure 2.5.10. Stable isotopic composition of initial and final species for solutions of OCl^- (aq) exposed to 350 nm irradiation. Replicate experiments are represented by the different colors and different symbols represent the Cl and O of ClO_x species present in initial and final solutions, where T_I = total initial, T_F = total final, I = initial, and F = final. Note that the horizontal axis indicates the amount of Cl (for $\delta^{37}\text{Cl}$) and the amount of O (for $\delta^{18}\text{O}$ and $\Delta^{17}\text{O}$) in the initial and final experimental solutions.

Chlorite

There was little variation ($< \pm 2$ ‰) in the $\delta^{37}\text{Cl}$ values of initial total Cl ($\text{ClO}_3^- + \text{ClO}_2^- + \text{Cl}^-$), final total Cl ($\text{Cl}^- + \text{ClO}_3^- + \text{ClO}_4^-$), and final Cl^- for photolysis ($\lambda = 350$ nm) of ClO_2^- solutions (Figure 2.5.11). $\delta^{37}\text{Cl}$ values of ClO_4^- and estimated ClO_3^- (based on mass balance) were higher (~ 24 ‰ and 4 ‰, respectively) compared to final Cl^- and total Cl in initial and final solution.

There were small changes (< 3 ‰) in $\delta^{18}\text{O}$ values of initial total O ($\sim \text{ClO}_2^-$) and final total O, which was primarily composed of ClO_3^- . Compared to initial total O ($\sim \text{ClO}_2^-$), the $\delta^{18}\text{O}$ value for ClO_4^- was higher (~ 42 ‰) and estimated $\delta^{18}\text{O}$ value for ClO_3^- was lower (~ 3 ‰). No difference in $\Delta^{17}\text{O}$ values between initial ($\sim \text{ClO}_2^-$) and final total O ($\sim \text{ClO}_3^-$) was observed, but the $\Delta^{17}\text{O}$ value of ClO_4^- was smaller (< 2 ‰).

Chlorine Dioxide

Isotopic compositions of initial ClO_2 (aq) and final ClO_3^- (aq) were not able to be measured. The $\delta^{37}\text{Cl}$ values ($\sim +18$ ‰ and $+20$ ‰), $\delta^{18}\text{O}$ values ($\sim +9$ ‰ and $+13$ ‰), and $\Delta^{17}\text{O}$ values of ClO_4^- (~ 0 ‰) were similar between replicates (Figure 2.5.12).

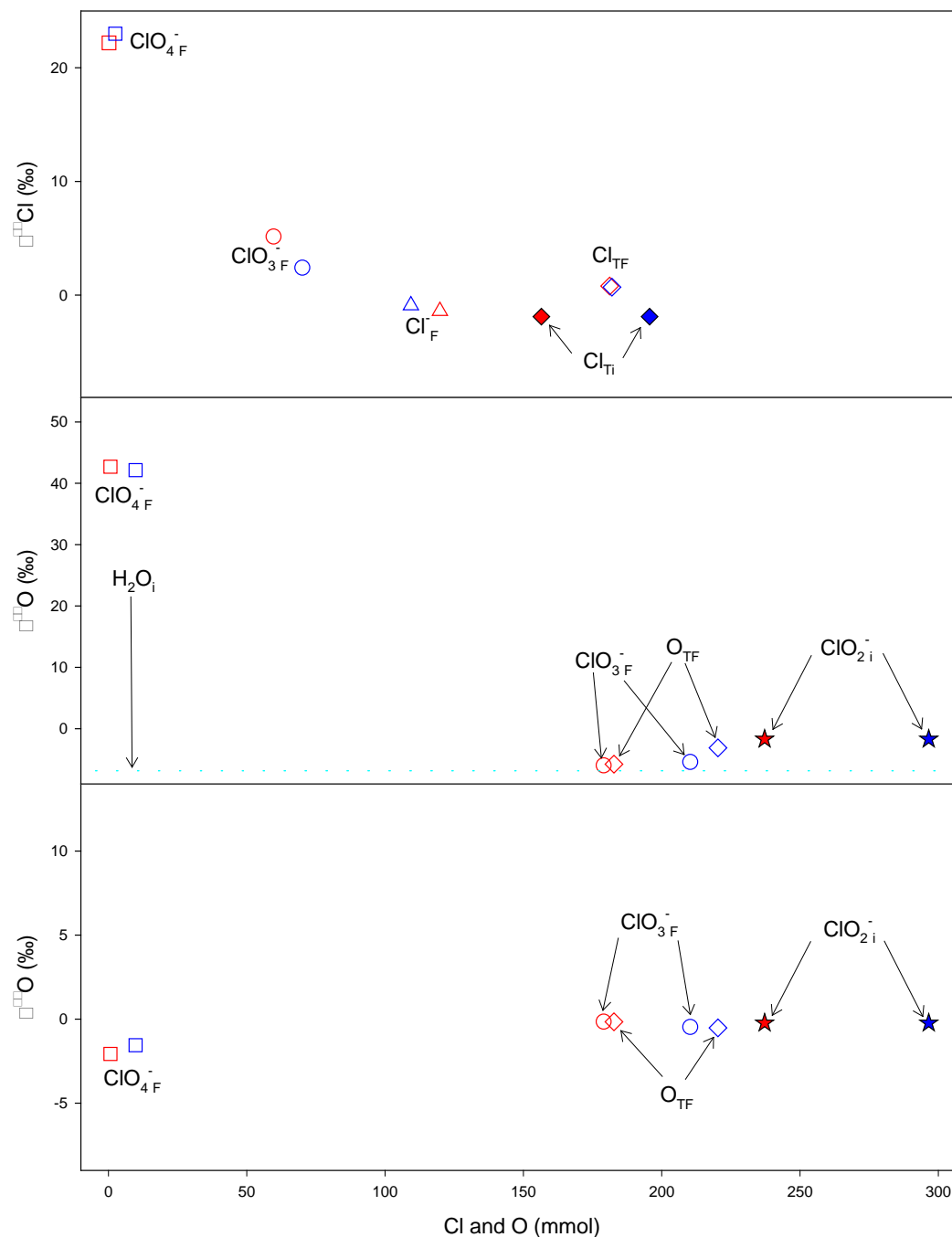


Figure 2.5.11. Stable isotopic composition of initial and final species for solutions of ClO_2^- (aq) exposed to 350 nm irradiation. Replicate experiments are represented by the different colors and different symbols represent the Cl and O of ClO_x species present in initial and final solutions, where T_1 = total initial, T_F = total final, I = initial, and F = final. Note that the horizontal axis indicates the amount of Cl (for $\delta^{37}\text{Cl}$) and the amount of O (for $\delta^{18}\text{O}$ and $\Delta^{17}\text{O}$) in the initial and final experimental solutions.

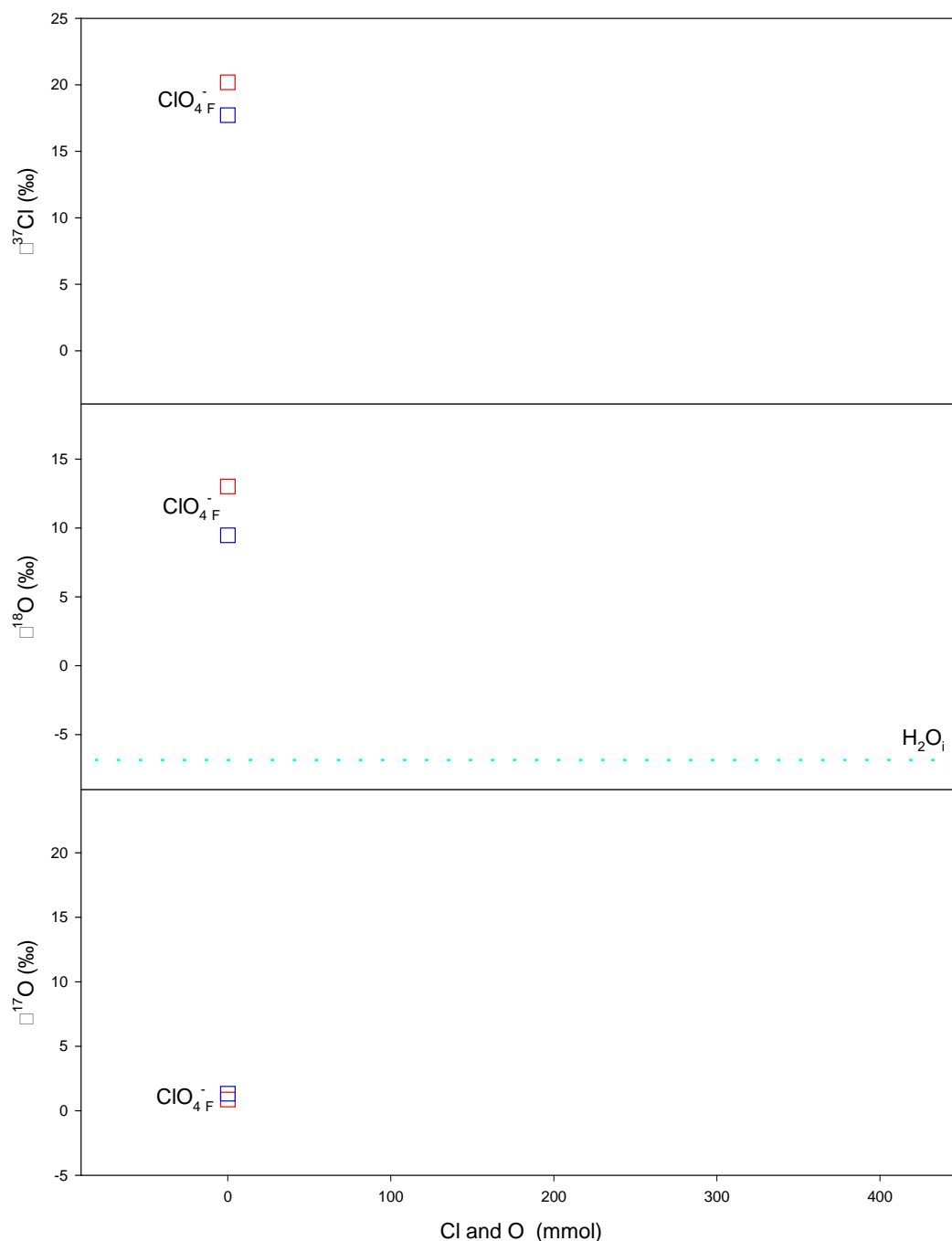


Figure 2.5.12. Stable isotopic composition of initial and final species for solutions of ClO_2 (aq) exposed to 350 nm irradiation. Replicate experiments are represented by the different colors and different symbols represent the Cl and O of ClO_x species present in initial and final solutions, where T_I = total initial, T_F = total final, I = initial, and F = final. Note that the horizontal axis indicates the amount of Cl (for $\delta^{37}\text{Cl}$) and the amount of O (for $\delta^{18}\text{O}$ and $\Delta^{17}\text{O}$) in the initial and final experimental solutions.

2.5.4 Discussion

2.5.4.1 Overall Observations

Perchlorate formed from UV and O₃ mediated oxidation processes generally had higher $\delta^{37}\text{Cl}$ and $\delta^{18}\text{O}$ values than all other ClO_x species (initial and final), with a few exceptions. In some cases, there was not enough O in the products for an IR-MS analysis to be made and in others, initial ClO_x species were simply not measured. In only one of the experiments (dry Cl⁻), for which ClO₄⁻ isotopes were measured, was the $\delta^{37}\text{Cl}$ of the initial Cl⁻ higher than in ClO₄⁻.

The same trend was observed for $\delta^{18}\text{O}$ values of produced ClO₄⁻ compared to those of the H₂O used in the experiments. With the exception of the UV OCl⁻ experiments, H₂O typically bore a lower $\delta^{18}\text{O}$ value than O in ClO₄⁻. The opposite was observed for the $\delta^{18}\text{O}$ of O₃ generated in the lab versus $\delta^{18}\text{O}$ of ClO₄⁻ from O₃ experiments. The $\delta^{18}\text{O}$ of O₃ (+ 124 ‰ ± 6 ‰) produced in the lab via the O₃ generator was always substantially higher than $\delta^{18}\text{O}$ of produced ClO₄⁻, for which the highest $\delta^{18}\text{O}$ value reported was ~ + 55 ‰.

The $\Delta^{17}\text{O}$ of ClO₄⁻ varied between the oxidation methods. In most cases, the $\Delta^{17}\text{O}$ values of ClO₄⁻ were below the $\Delta^{17}\text{O}$ value of lab generated O₃ (+ 24.5 ‰). The exceptions were the dry and aqueous Cl⁻ experiments for which values ranged from + 30 ‰ to + 33 ‰.

2.5.4.2 O₃ vs UV ClO₄⁻ Isotopes

There was a discernible difference between the $\Delta^{17}\text{O}$ of ClO₄⁻ produced by O₃ mediated processes and the $\Delta^{17}\text{O}$ of ClO₄⁻ produced by UV mediated processes (Figures 2.5.13 and 2.5.14). While the $\Delta^{17}\text{O}$ of UV ClO₄⁻ was typically around zero (- 1.55 ‰ to + 1.33 ‰), the $\Delta^{17}\text{O}$ of O₃ ClO₄⁻ (+12 ‰ to + 33 ‰) was substantially higher, indicating the source of O for oxidation of Cl in ClO_x precursor and intermediate species was different between UV and O₃ experiments.

Like $\Delta^{17}\text{O}$ of ClO₄⁻, ClO₄⁻ formed through O₃ mediated oxidation reactions tended to have higher $\delta^{18}\text{O}$ values than ClO₄⁻ formed through oxidation reactions produced by photolysis. The exception being the UV ClO₂⁻ experiment, which had a ClO₄⁻ with a higher $\delta^{18}\text{O}$ value than the ClO₄⁻ produced from O₃ oxidation of the same precursor species. In the case of $\delta^{37}\text{Cl}$, the $\delta^{37}\text{Cl}$ of UV produced ClO₄⁻ was always higher than the $\delta^{37}\text{Cl}$ of ClO₄⁻ produced from O₃ oxidation of the same precursor species.

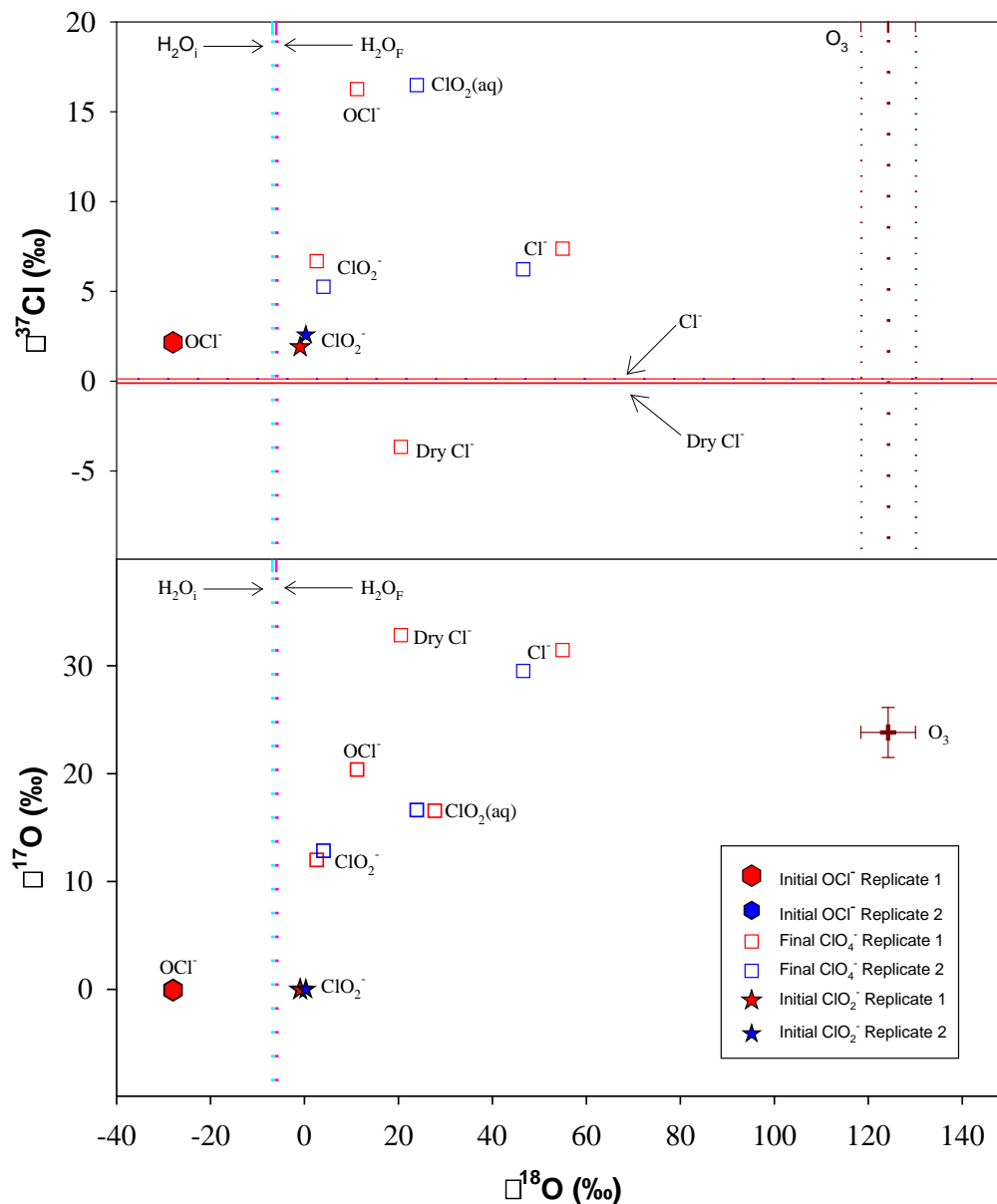


Figure 2.5.13. Stable isotopic compositions ($\delta^{37}\text{Cl}$, $\delta^{18}\text{O}$, $\Delta^{17}\text{O}$) of reactant species and final ClO_4^- for O_3 oxidized solutions. The vertical dashed light blue and pink lines represent the $\delta^{18}\text{O}$ value for initial and final H_2O , respectively. The thick dark maroon dashed line represents the average $\delta^{18}\text{O}$ value for O_3 and the thinner dashed lines represent the standard deviation from the average $\delta^{18}\text{O}$ value. Replicate experiments are represented by the different colors and different symbols represent the reactant species and ClO_4^- .

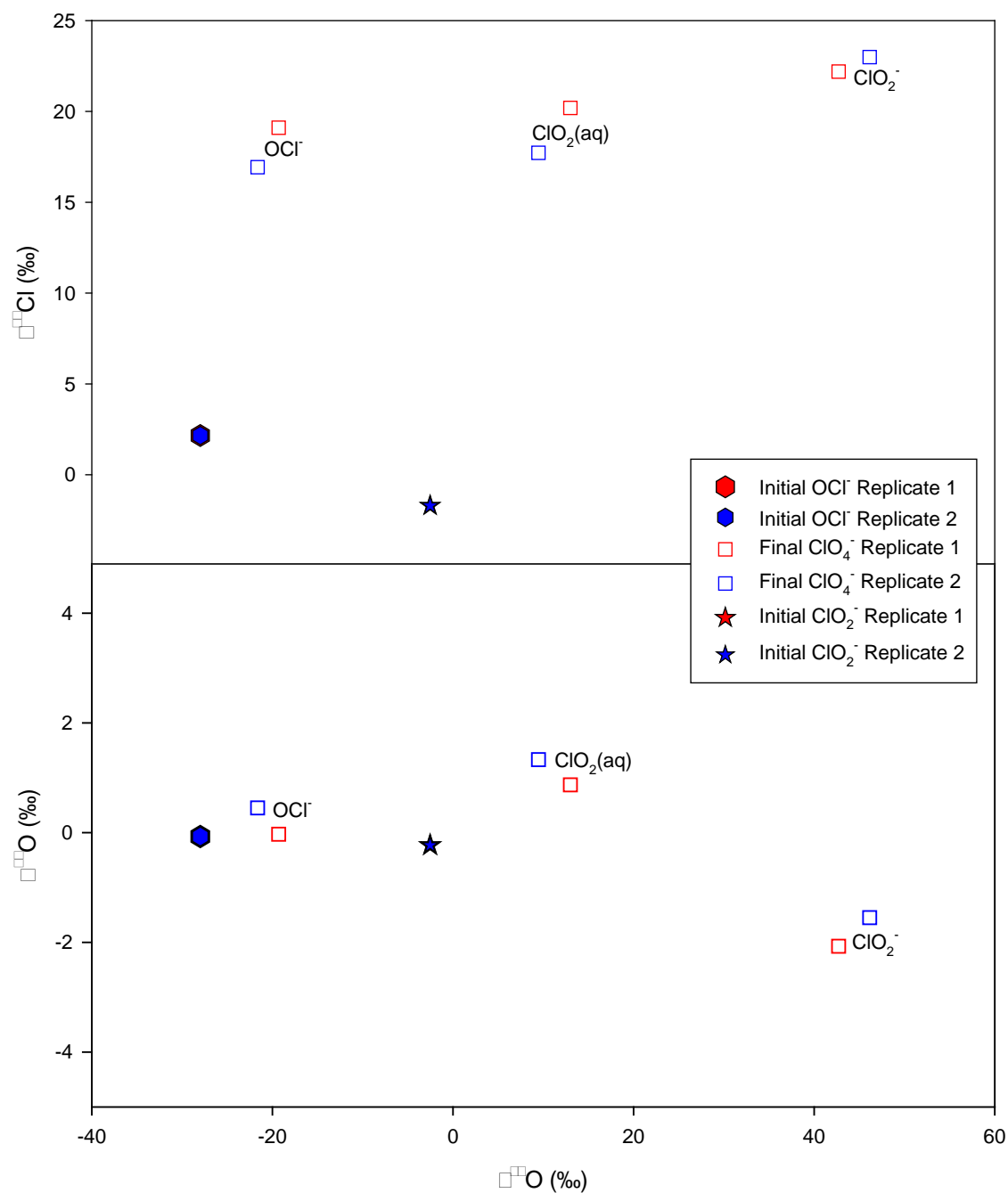


Figure 2.5.14. Stable isotopic composition ($\delta^{37}\text{Cl}$, $\delta^{18}\text{O}$, $\Delta^{17}\text{O}$) of reactant species and final ClO_4^- for UV oxidized solutions. Replicate experiments are represented by the different colors and different symbols represent the reactant species and ClO_4^- .

2.5.4.3 $\Delta^{17}\text{O}$ vs Precursor ClO_x Species

There appears to be an inverse relationship between $\Delta^{17}\text{O}$ values of ClO_4^- formed by O_3 mediated oxidation processes and the oxidation state of the Cl in the precursor ClO_x species (Figure 2.5.15). With the exception of the O_3 ClO_2^- experiments, $\Delta^{17}\text{O}$ values of ClO_4^- in O_3 experiments decreased with increasing oxidation state of ClO_x species (Figure 2.5.15f). This trend was not as obvious for the UV experiments (Figure 2.5.15c) as no experiments were conducted with Cl^- (aqueous or dry), but there was a consistency with behavior of $\Delta^{17}\text{O}$ values in ClO_4^- with the rest of the precursor species (OCl^- , ClO_2^- , and ClO_2) between both oxidation methods. In both UV and O_3 (not considering Cl^-), ClO_4^- formed from oxidation of ClO_2^- had the highest $\Delta^{17}\text{O}$ values, followed by ClO_4^- formed from OCl^- , and lastly ClO_4^- formed from ClO_2 . The $\Delta^{17}\text{O}$ values of ClO_4^- produced from UV experiments, however, were so close to zero that we cannot be sure that what we observed is actually a trend, or rather an error associated with the measurement method.

2.5.4.4 $\delta^{18}\text{O}$ vs Precursor ClO_x Species

The relationship between $\delta^{18}\text{O}$ values of ClO_4^- formed by O_3 mediated oxidation processes and the oxidation state of the Cl in the precursor ClO_x species parallels that of the $\Delta^{17}\text{O}$ values of ClO_4^- and oxidation state of the Cl in the precursor ClO_x species in O_3 experiments (Figure 2.5.15e). This seems logical as the mass-independent $\Delta^{17}\text{O}$ anomaly is calculated based on measured $\delta^{18}\text{O}$ and $\delta^{17}\text{O}$ values.

No connection was observed between oxidation state of the Cl in the precursor ClO_x species and $\delta^{18}\text{O}$ values of ClO_4^- in the UV experiments. Nevertheless, it should be noted that ClO_4^- formed from UV oxidation of ClO_2^- had exceedingly high $\delta^{18}\text{O}$ values, almost as high as those reported for ClO_4^- formed from O_3 oxidation of Cl^- (aq) (Figure 2.5.15b). On the contrary, $\Delta^{17}\text{O}$ values of ClO_4^- produced by UV oxidation of ClO_2^- were lower than any of the other UV experiments (Figure 2.5.12c).

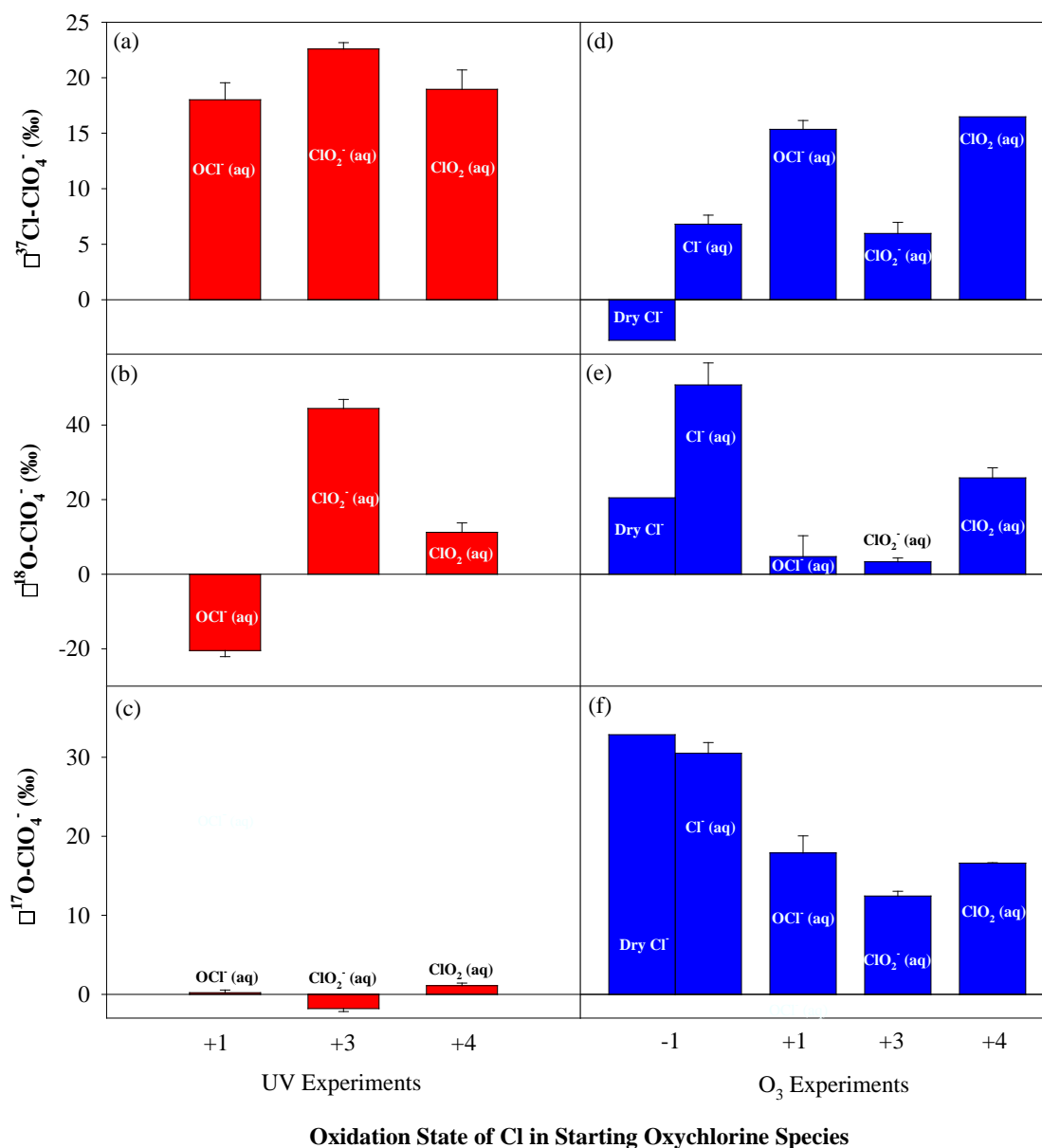


Figure 2.5.15. Relationship between $\delta^{37}\text{Cl}$ of final ClO_4^- produced by UV and O_3 mediated oxidation of Cl^- (s), Cl^- (aq), OCl^- (aq), ClO_2^- (aq), ClO_2 (aq) and the oxidation state of Cl in precursor ClO_x species. UV experiment data (red bars) are presented in graphs a, b, and c while the O_3 experiment data (blue bars) are presented in graphs d, e, and f. The name of the ClO_x species associated each bar is written on or on top of each bar. Data with no replicates do not include error bars.

2.5.4.5 $\delta^{37}\text{Cl}$ vs Precursor ClO_x Species

No interdependence was observed between $\delta^{37}\text{Cl}$ values of ClO_4^- formed from O_3 and UV mediated oxidation reactions with ClO_x species and the oxidation state of the Cl in the precursor ClO_x species. In the UV experiments, ClO_4^- formed from UV oxidation of ClO_2^- was enriched in $\delta^{37}\text{Cl}$ compared to ClO_4^- from UV oxidation of OCl^- and ClO_2 (aq) (Figure 2.5.15a). In contrast, the $\delta^{37}\text{Cl}$ of ClO_4^- formed from O_3 oxidation of ClO_2^- was depleted in $\delta^{37}\text{Cl}$ compared to ClO_4^- from UV oxidation Cl^- (aq), OCl^- , and ClO_2 (aq), but not dry Cl^- (Figure 2.5.15d). Although the Cl in both aqueous and dry Cl^- have the same oxidation number, O_3 oxidation of dry Cl^- resulted in ClO_4^- with negative $\delta^{37}\text{Cl}$ values, much lower than those of ClO_4^- formed from aqueous Cl^- or other species (OCl^- , ClO_2^- , ClO_2 (aq)) (Figure 2.5.15d).

2.5.4.6 Dry vs Aqueous Chloride

There was a clear difference between ClO_4^- formed from O_3 oxidation of dry Cl^- and Cl^- in aqueous solution (Figure 2.5.15). Perchlorate formed from O_3 oxidation of dry Cl^- was depleted in $\delta^{37}\text{Cl}$ and $\delta^{18}\text{O}$ compared to ClO_4^- formed from O_3 oxidation of Cl^- (aq), but was enriched in $\Delta^{17}\text{O}$. This is inconsistent with expected $\Delta^{17}\text{O}$ values of ClO_4^- from O_3 oxidation of dry Cl^- given the measured $\delta^{18}\text{O}$ values of the ClO_4^- . O_3 mediated oxidation reactions with dry Cl^- also yielded ClO_4^- containing the only negative $\delta^{37}\text{Cl}$ values measured in all of our experiments (including both O_3 and UV oxidation of ClO_x species). Based on these results, oxidation reactions occurring on solid surfaces do not fractionate species in the same way as they would if the species were dissolved in aqueous media.

2.5.4.7 ClO_3^- Isotopes

Estimated $\Delta^{17}\text{O}$ values of chlorate (based on mass balance) formed from both UV and O_3 processes were always lower than $\Delta^{17}\text{O}$ values of ClO_4^- . $\Delta^{17}\text{O}$ values of ClO_3^- from UV experiments were consistently below zero, whereas in the O_3 experiments $\Delta^{17}\text{O}$ of ClO_3^- were consistently above zero, but not by much (+ 0.8 ‰ to + 4 ‰). The small $\Delta^{17}\text{O}$ anomaly observed in the ClO_3^- produced by O_3 oxidation of ClO_x species suggests that although a minor contribution of $\text{O}_3\text{-O}$ exists in the formation of ClO_3^- , that O atoms in ClO_3^- are mostly not from O_3 . The limited contribution of $\text{O}_3\text{-O}$ in the ClO_3^- structure may be indicative of reaction mechanisms for which the early reaction steps are similar for both ClO_4^- and ClO_3^- formation, but then diverge later in the process to form ClO_4^- and ClO_3^- separately.

Calculated final product $\text{ClO}_3^-/\text{ClO}_4^-$ ratios in the O_3 experiments ranged from 0.18 – 4431, with the higher and lower end of this range corresponding to the O_3 oxidation of dry Cl^- and Cl^- (aq), respectively. Of the O_3 experiments for which ClO_3^- $\Delta^{17}\text{O}$ values were estimated (Cl^- (aq), OCl^- , and ClO_2^-), no clear trend was discernible between $\text{ClO}_3^-/\text{ClO}_4^-$ final product ratios and the $\Delta^{17}\text{O}$ values of ClO_3^- . A similarity was however, observed between ClO_4^- $\Delta^{17}\text{O}$ values and ClO_3^- $\Delta^{17}\text{O}$ values with respect to oxidation of Cl in precursor species and final $\text{ClO}_3^-/\text{ClO}_4^-$ ratios. Both

final $\text{ClO}_3^-/\text{ClO}_4^-$ ratios and $\Delta^{17}\text{O}$ values of ClO_4^- and ClO_3^- were highest for the O_3 $\text{Cl}^-(\text{aq})$ experiments, followed by those of the O_3 OCl^- experiments, and lastly the O_3 ClO_2^- experiments. This further suggests a model in which pathways with common initial reaction stages for ClO_3^- and ClO_4^- production exist.

2.5.4.8 Isotopic Characteristics of ClO_4^- and their Connection to Formation Pathways

The isotopic composition of precursor compounds involved in ClO_4^- formation via UV and O_3 processes and/or fractionation caused by isotope exchange reactions or kinetic processes could be used to explain our ClO_4^- isotope values. Isotope exchange involves reversible equilibrium reactions in which products can become either heavier or lighter than the original reactants, whereas kinetic processes are irreversible and generally result in products enriched in the lighter isotopes. The oxidation state of a species can also affect equilibrium reactions, with species having higher oxidation states often enriched in the heavier isotope (Kendall et al., 1998, 2008; Schauble et al., 2003). The $\delta^{37}\text{Cl}$ values of ClO_4^- formed from UV and O_3 oxidation processes indicate that the heavier ^{37}Cl isotope was preferentially accumulated in ClO_4^- compared to initial species and other final products, with the exception of two experiments (O_3 oxidation of dry Cl^- and OCl^-). These results could be indicative of equilibrium processes resulting in branching fractionation of intermediate species leading to accumulation of the heavier Cl isotope in the species with the higher oxidation state (ClO_4^-). The two exceptions (O_3 oxidation of dry Cl^- and OCl^-) may be indicative of kinetic isotope effects that cause enrichments of the heavier isotopes in the residual reactants. The difference in isotope compositions of ClO_4^- produced by O_3 oxidation of dry Cl^- versus those of aqueous Cl^- suggests that reactions involving ClO_x oxidation of solid compounds may not fractionate isotopes in the same way as $\text{ClO}_x(\text{aq})$ species. It is possible that one may be kinetically based whereas the other might be equilibrium based. $\Delta^{17}\text{O}$ values of ClO_4^- also suggest that ClO_4^- may be formed by more than one pathway and its isotopic composition may be the result of a mixture of the compositions of ClO_4^- formed by each distinct pathway.

2.5.4.9 Implications of ClO_4^- $\Delta^{17}\text{O}$ values in O_3 Experiments

Conclusions regarding the mechanisms responsible for the ClO_4^- isotopic compositions observed in our study were made by considering proposed alternative O_3 - ClO_x oxidation reactions and evaluating them with respect to which ClO_4^- formation pathways are plausible based on the $\Delta^{17}\text{O}$ values of the ClO_4^- produced in our O_3 experiments.

O_3 -Dry Chloride

It is difficult to evaluate the formation of ClO_4^- from O_3 oxidation of dry Cl^- as it is uncertain if reactions take place on the surface of the salt, on the glass surface, or in the gas phase; nor if water vapor in the O_2 cylinders or bound water on the solids plays a role in reactions leading to its formation.

The O₃ dry Cl⁻ experiment was the only experiment that resulted in a ClO₃⁻/ClO₄⁻ product molar ratio (0.18) less than 1. The O₃ oxidation of dry Cl⁻ produced ClO₄⁻ with the highest Δ¹⁷O values (+ 33 ‰), but the values were only slightly higher than ClO₄⁻ produced by O₃ oxidation of aqueous Cl⁻ (aq) (+ 29 ‰ to + 32 ‰). This suggests that not only does liquid H₂O not need to be present for the formation of ClO₄⁻ to occur but that all four O in ClO₄⁻ are sourced from O₃, as O₃ produced from the O₃ generator had a bulk Δ¹⁷O value of + 24.5 ‰.

From the proposed O₃-ClO_x oxidation reactions (Table 2.5.4), four pathways with different initial reaction sequences (Rxn's 1–3; Rxn's 1, 8–9; Rxn's 1, 8, and 10–11; and Rxn's 1, 3, 8, and 13) but with the same final reaction sequence (Rxn's 4 and 12) were identified that could produce ClO₄⁻ with four O from O₃ in the absence of water (Table 2.5.4; Figure 2.5.16). Due to missing reaction rates, little can be inferred regarding the ClO₄⁻ pathways proposed. Aside from ClO₄⁻, the only other detectible product was ClO₃⁻ for which we were able to identify at least one pathway that formed ClO₃⁻ without reactions involving H₂O (Figure 2.5.17). This pathway has the same initial reaction sequences as formation of ClO₄⁻ but a different final reaction (Table 2.5.4; Rxn 29). Due to the low mass of ClO₃⁻ produced, no ClO₃⁻ Δ¹⁷O values are available.

There has been much debate regarding the position (central vs terminal O atom) of the Δ¹⁷O anomaly in the O₃ molecule and whether it is preferentially transferred to other molecules during oxidation reactions (Berhanu et al., 2012; Bhattacharya et al., 2008; Lyons et al., 2001). Our ClO₄⁻ Δ¹⁷O values (+ 29 ‰ to + 32 ‰) being higher than those of the generated O₃ (+ 24.5 ‰) support the theory that terminal O atoms in O₃ are preferentially enriched in the Δ¹⁷O anomaly and that the terminal O atoms carrying the anomaly are preferentially incorporated into the ClO_x compounds. If we assume that site preference is on the terminal O atom and that the Δ¹⁷O of the terminal O atom is transferred to ClO₄⁻, then we could theoretically calculate the Δ¹⁷O values of ClO₄⁻ that we would expect if there was complete or partial preference of the heavy isotope on the terminal O atom of O₃ using Equation 5 (Bhattacharya et al., 2008; Lyons et al., 2001). Application of Equation 5 and assuming complete terminal O site preference would result in a ClO₄⁻ with a maximum Δ¹⁷O value of + 37 ‰. With no terminal site preference, the maximum Δ¹⁷O of ClO₄⁻ would be + 24.5 ‰. Our ClO₄⁻ Δ¹⁷O values (+ 29 ‰ to + 32 ‰) were between these two values, indicating there is at least some preferential incorporation of terminal O atoms from O₃ into ClO₄⁻.

$$\Delta^{17}O \text{ of terminal } O_3 \text{ atoms} = \frac{3}{2} \times \Delta^{17}O \text{ of bulk } O_3 \quad (5)$$

However, it is not possible to completely constrain site preference because it is also possible that the observed $\Delta^{17}\text{O}$ value of ClO_4^- from O_3 oxidation of dry Cl^- is less than the value for complete preference due to the addition of a small amount of ClO_4^- formed from reaction pathways incorporating three or less O from O_3 or partial O exchange during the reactions.

Table 2.5.4. Proposed reactions possibly leading to the formation of ClO_4^- via O_3 oxidation of ClO_x species.

Reaction #	Reaction	Reaction Rate	Method	Comments	Source
1	$\text{O}_3 + \text{Cl}^- \rightarrow \text{OCl}^-/\text{HOCl} + \text{O}_2$		Based on $\text{O}_3(\text{aq})$ depletion	pH > 3	Hoigné et al. (1985) Levanov et al. (2003)
2	$\text{O}_3 + \text{OCl}^- \rightarrow \text{O}_2 + \text{ClO}_2^-$	$K = 30 \text{ M}^{-1}\text{s}^{-1}$ (1985; 1996)	Based on $\text{O}_3(\text{aq})$ depletion		Hoigné et al. (1985) Siddiqui (1996)
3	$\text{O}_3 + \text{ClO}_2^- \leftrightarrow \text{O}_3^- + \text{ClO}_2$	$^a K_F = 8.2(4) \times 10^6 \text{ M}^{-1}\text{s}^{-1}$ (2002) $^b K_R = 1.8 \times 10^5 \text{ M}^{-1}\text{s}^{-1}$ (1984) $^c K_F = (4 \pm 1) \times 10^6 \text{ M}^{-1}\text{s}^{-1}$ (1985)	a Determined under pseudo-first order conditions using stopped flow spectrometry b Pulse Radiolysis c Pulse Radiolysis and Stopped Flow Spectrometry		Nicoson et al. (2002) Klaning et al. (1985) Bühler et al. (1984)
4	$\text{ClO}_2 + \text{O}_3 \rightarrow \text{ClO}_3 + \text{O}_2$	$K = (1.05 \pm 0.10) \times 10^3 \text{ M}^{-1}\text{s}^{-1}$ (1985)	Stopped flow spectroscopy of $\text{ClO}_2(\text{aq})$ and $\text{O}(\text{aq})$		Klaning et al. (1985)
5	$\text{ClO}_3 + \text{ClO}_3 \rightarrow \text{Cl}_2\text{O}_6$	$K = (4.5 \pm 0.8) \times 10^8 \text{ M}^{-1}\text{s}^{-1}$ (1997) $K = 3.7 \times 10^9 \text{ M}^{-1}\text{s}^{-1}$ (2005, 1989)	Calculated from Laser Photolysis of $\text{ClO}_3^-(\text{aq})$ (1997) Assumed diffusion control by using the expression of Smoluchowski and the Stokes-Einstein Equation (2005, 1989)	Estimated	Zuo et al. (1997) Quiroga and Perissinotti (2005) Sander et al. (1989)

6	$O_2ClOClO_3 + O_3 \rightarrow Cl_2O_7 + O_2$				Sander et al. (1989) Wiberg et al. (2001)
7	$Cl_2O_7 + H_2O \rightarrow 2ClO_4^- + 2H^+$				Wiberg et al. (2001)
8	$OH + HOCl \rightarrow OCl + H_2O$	$K=(1.4\pm0.1) \times 10^8 \text{ M}^{-1}\text{s}^{-1}$ (1997)	Pulse Radiolysis of HOCl and H ₂ SO ₄		Zuo et al. (1997)
9	$ClO + O_3 \rightarrow ClOO + O_2$				Vaida and Simon (1995)
10	$ClO + ClO \rightarrow Cl + ClOO$ OR $ClO + ClO \rightarrow Cl + OClO$				Sander et al. (1989)
11	$Cl + O_3 \rightarrow ClO + O_2$		Flash Photolysis	wavelength > 300 nm	Sander et al. (1989)
12	$ClO_3 + HO \rightarrow HClO_4$		Boron Doped Diamond Film Electrodes, speculated to occur in the stratosphere	Considered	Hubler et al. (2014) Simonatis and Heicklen (1975)
13	$OCl + HO \rightarrow HClO_2$		Boron Doped Diamond Film Electrodes	Considered	Hubler et al. (2014)
14	$O_2ClOClO_3 + H_2O \rightarrow ClO_3^- + ClO_4^- + 2H^+$	$K = 180 \text{ M}^{-1}\text{s}^{-1}$	Assumed attack of water on the more acidic chlorine	Adopted from previous studies	Quiroga and Perissinotti (2005) Wiberg et al. (2001)

15	$OCIO + ClO \rightarrow ClOClO_2$	$K = 7.4 \times 10^9 \text{ M}^{-1}\text{s}^{-1}$	Assumed diffusion control by using the expression of Smoluchoswski (Cite) and the Stokes-Einstein Equation	Estimated	Quiroga and Perissinotti (2005) Sander et al. (1989)
16	$Cl_2O_3 + O_3 \rightarrow Cl_2O_4$			Hypothesised Considered	
17	$Cl_2O_4 + H_2O \rightarrow HClO + ClO_4^- + H^+$	$K = 180 \text{ M}^{-1}\text{s}^{-1}$	Estimated		Quiroga and Perissinotti (2005) Wiberg et al. (2001)
18	$OCIO + Cl \rightarrow ClClO_2$	$K = 7.8 \times 10^9 \text{ M}^{-1}\text{s}^{-1}$	Assumed diffusion control by using the expression of Smoluchoswski and the Stokes-Einstein Equation	Estimated	Quiroga and Perissinotti (2005)
19	$Cl_2O_2 + O_3 \rightarrow Cl_2O_3$			Hypothesised Considered	
20	$OCIO + ClO_3 \rightarrow O_2ClOClO_2$	$K = 7.5 \times 10^9 \text{ M}^{-1}\text{s}^{-1}$	Assumed diffusion control by using the expression of Smoluchoswski and the Stokes-Einstein Equation	Estimated	Quiroga and Perissinotti (2005)
21	$O_2ClOClO_2 + H_2O \rightarrow 2ClO_3^- + 2H^+$ OR $O_3ClOClO + H_2O \rightarrow ClO_3^- + ClO_4^- + 2H^+$	$K_{ClO_3^-} = 180 \text{ M}^{-1}\text{s}^{-1}$ $K_{ClO_4^-} = ?$	Assumed attack of water on the more acidic chlorine	Adopted from previous studies	Quiroga and Perissinotti (2005)
22	$ClO + ClO_3 \rightarrow ClOClO_3$	$K = 7.5 \times 10^9$	Assumed diffusion control by using the expression of Smoluchoswski and the Stokes-Einstein Equation	Estimated Proposed	Quiroga and Perissinotti (2005) Sander et al. (1989)
23	$ClO + ClO + M \rightarrow ClOOC l + M$				von Hobe et al. (2009) Sander et al. (1989)

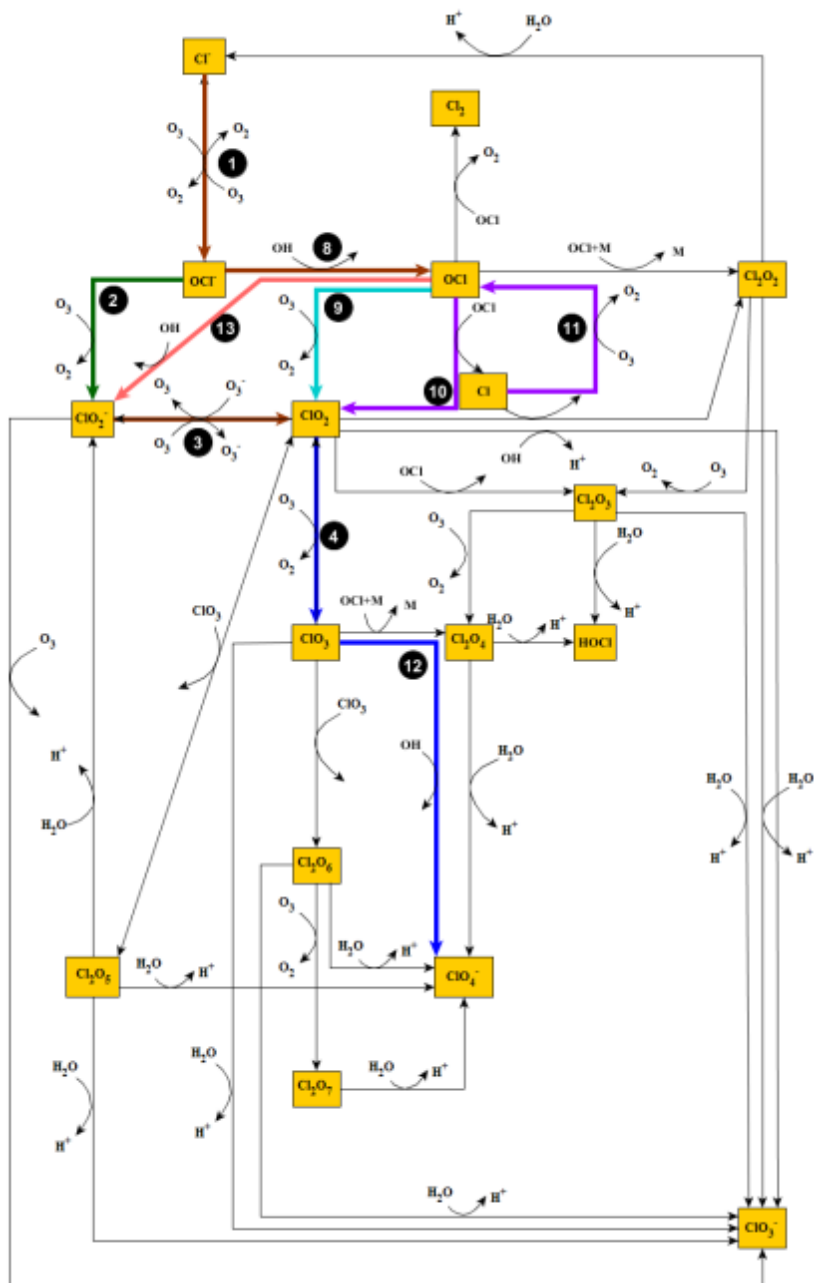


Figure 2.5.16. Combined final pathways determined responsible for ClO_4^- formation by O_3 oxidation of Cl^- (dry and aq). Note the thick forest dark red lines indicate the initial reactions that some of the species may share while the dark blue lines indicate the final reactions all pathways share. All other colored lines (green, pink, aqua, and blue) represent reactions unique to each of the four proposed pathways. All four pathways lead to the formation of one ClO_4^- molecule containing three O's from O_3 .

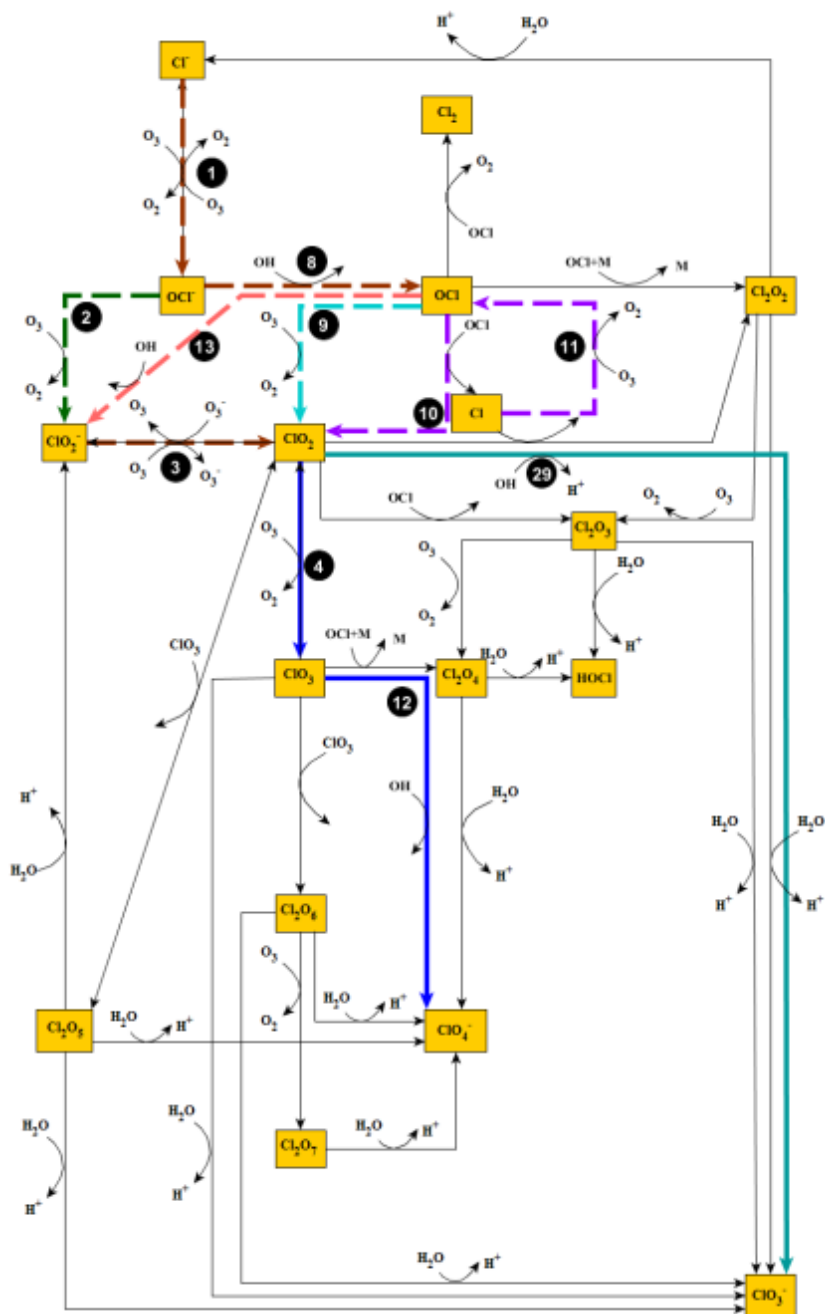


Figure 2.5.17. Combined final pathways determined responsible for ClO_4^- formation by O_3 oxidation of Cl^- including possible pathways for ClO_3^- formation (aq). Note the thick dashed lines indicate the initial reactions that are possibly shared between ClO_4^- and ClO_3^- pathways and the thick aqua lines represent the final reactions leading to ClO_3^- formation. Both ClO_3^- pathways lead to the formation of one ClO_3^- molecule containing one O from O_3 .

O₃-Aqueous Chloride

There are at least twenty-six possible pathways that could lead to the formation of ClO₄⁻ from O₃ oxidation of Cl⁻ (aq) (Appendix A: Figures A.1–A.26). Four speculated initial reaction sequences: [1] Rxn's 1– 3; [2] Rxn's 1, 8 – 9; [3] Rxn's 1, 8, 10 – 11; and [4] Rxn's 1, 3, 8, 13 and five final reaction sequences: [1] Rxn's 4 – 7; [2] Rxn's 4 and 12; [3] Rxn's 4 – 5 and 14; [4] Rxn's 4, 22, and 17; and [5] Rxn's 15 – 17 and Rxn's 20 – 21 were identified (Appendix A Figures A.1–A.26; Table 2.5.4). All pathways produced ClO₂ (aq) as an intermediate.

Our ClO₄⁻Δ¹⁷O values (+29 ‰ to + 32 ‰) suggest that the O₃ oxidation of Cl⁻ (aq) includes intermediate reactions that will lead to the formation of a ClO₄⁻ molecule with all or nearly all (depending on the final site preference value) O originating from O₃; therefore, any mechanisms resulting in a ClO₄⁻ with less than four O from O₃ were dismissed as plausible pathways (Appendix A: Figures A.9 – A.26). Excluding the pathways that do not result in transfer of four O from O₃ lowers the number of possible mechanisms from twenty-six to only eight, all of which require the formation of both ClO₂ (aq) and the ClO₃ radical (Appendix A: Figures A.1 – A.8). Of the eight remaining pathways (Appendix: Figures A.1 – A.8), four of them (Appendix A Figures A.1 – A.4) require the reaction of the ClO₃ radical with an OH radical and four of them (Appendix A: Figures A.5 – A.8) require the formation of the Cl₂O₇ species. The Cl₂O₇ species hydrolyzes to form two ClO₄⁻ molecules (Table 2.5.4; Rxn 7), one containing three and the other four O from O₃. It has been speculated that Cl₂O₇ is involved in the production of ClO₄⁻, but our ClO₄⁻-Δ¹⁷O values indicate that this may not be the case as only one of the two ClO₄⁻ molecules formed from hydrolysis of this intermediate species has a structure in which all O's originate from O₃. However, the unknown degree of site preference can allow for a limited amount of ClO₄⁻ with only three O from O₃ and thus it is possible that a mixture of the two ClO₄⁻ molecules produced from hydrolysis of the Cl₂O₇ species is in part responsible for the ClO₄⁻ formed in our Cl⁻ (aq) experiments. It might be unlikely that reactions involving the Cl₂O₇ species are responsible for substantial ClO₄⁻ production, unless unknown Cl₂O₇ reaction pathways exist that include transfer of an additional O from O₃ (e.g. O radical) rather than from water. However, given the high Δ¹⁷O value of ClO₄⁻ observed, it is possible that ClO₄⁻ is a result of mixing between branching pathways involving the OH radical and Cl₂O₇ species.

Elimination of the pathways involving the Cl₂O₇ species would reduce the number of plausible mechanisms responsible for ClO₄⁻ formation by O₃ oxidation of Cl⁻ (aq) to only four, all of which go through the same final reaction sequence (Table 2.5.4; Rxn's 4 and 12) involving the formation of a ClO₃ radical that is oxidized by an OH radical (simultaneously represented by Figure 2.5.16). Currently it is unclear as to whether the O in the OH radical originates from O₃ or has another origin. Our interpretation of the ClO₄⁻ Δ¹⁷O values along with the evaluation of the proposed pathways suggest that ClO₄⁻ with four O from O₃ is possibly mainly formed through a final oxidation reaction involving an OH radical and not through the Cl₂O₇

intermediate species, as suggested by others. If our analysis is correct then it would mean that the O in the OH radical most likely originates from O₃.

The $\Delta^{17}\text{O}$ values of ClO_3^- produced during ClO_4^- production from O₃ oxidation of Cl^- (aq) indicate that only one O in ClO_3^- could be derived from an O₃ molecule. This could occur through reactions that lead to the incorporation of a single O from O₃ or through a mixture of pathways that lead to zero to four O being incorporated from O₃. If ClO_4^- and ClO_3^- were formed from the same initial reactions (Rxn's 1–3; Rxn's 1, and 8–9; Rxn's 1, 8, and 10–11; and Rxn's 1, 3, 8, and 13); they alone would contribute at least two O from O₃ to the ClO_3^- molecules, with the final ClO_3^- containing anywhere from two to three O from O₃. Even pathways only sharing two of the initial reactions (Rxn's 1 and 8) would result in a ClO_3^- with two O from O₃ (Figure 2.5.18). In addition, none of the pathways that we identified as possible ClO_4^- formation mechanisms (Figure 2.5.16) produced ClO_3^- directly from the production of ClO_4^- , further indicating the independence of ClO_4^- from ClO_3^- pathways. A couple of factors could be responsible for ClO_3^- only having one O from O₃ including: (1) non O₃ related reactions that have not yet been identified and (2) oxygen exchange during equilibrium reactions. In support of the likelihood of independent ClO_3^- production pathways, $\text{ClO}_3^-/\text{ClO}_4^-$ molar ratios (3000–4400) are orders of magnitude higher than for dry oxidation of Cl^- even though ClO_4^- production was relatively similar. Based on the ratios we would expect that the major reactions lead to ClO_3^- formation and if so, based on our ClO_3^- $\Delta^{17}\text{O}$ values, we could speculate that the major source of oxidation for formation of ClO_3^- is not O₃, but rather another species. Given our relatively high $\text{ClO}_3^-/\text{ClO}_4^-$ molar ratios in our Cl^- (aq) experiments compared to those of O₃ oxidation of dry Cl^- , it is evident that hydrolysis reactions are not as important for ClO_4^- formation as they are for ClO_3^- . Our $\text{ClO}_3^-/\text{ClO}_4^-$ ratios in conjunction with our ClO_4^- $\Delta^{17}\text{O}$ values further suggest and support our theory that the involvement of O₃ in ClO_4^- formation mechanisms due to oxidation of Cl^- is not hindered by the presence of H₂O, but rather that H₂O may not be required for formation of ClO_4^- to occur.

It may be possible to determine the feasibility of the ClO_4^- and ClO_3^- pathways by evaluating the reaction rates involved, but not all reactions have reported reaction rates (Table 2.5.4). One key step in which reaction rates are known is the decomposition of the OCl^- species that when oxidized can either form ClO_2^- or the OCl radical (Table 2.5.4; Rxn's 2 and 8, respectively). The reaction rates for these two oxidation reactions indicate that the faster reaction leads to the formation of the OCl radical by means of an OH radical, whereas the slower reaction leads to formation of ClO_2^- by means of the O₃ molecule (Rxn's 8 and 2, respectively). Compared to other ClO_x species, Cl^- (dry and aqueous) reacted slowly and O₃ was unlimited, giving way for more reactions with O₃ to occur. Reactions 2 and 8 (Table 2.5.4) both imply that O₃ reactions occur much slower than reactions involving a non O₃ species and thus because major reactions are expected to form ClO_3^- , it is likely that pathways leading to ClO_3^- follow Reaction 8 (Table

2.5.4), which involves the OH radical, and pathways leading to ClO_4^- follow Reaction 2 (Table 2.5.4), which involves the O_3 molecule. The reactions for the decomposition of the ClO_2 species also support ClO_4^- being formed by slow reactions involving O_3 . In the ClO_4^- pathways identified (Figure 2.5.16), we propose that ClO_2 is oxidized to the ClO_3 radical by O_3 (Table 2.5.4; Rxn 4). This reaction is much slower compared to reactions that either lead to the formation of the Cl_2O_2 species (Table 2.5.4; Rxn 18), the formation of ClO_3^- (Table 2.5.4; Rxn 29), or the formation of the Cl_2O_3 species, indicating that the pathways we propose may well be the pathways responsible for ClO_4^- formation in this study.

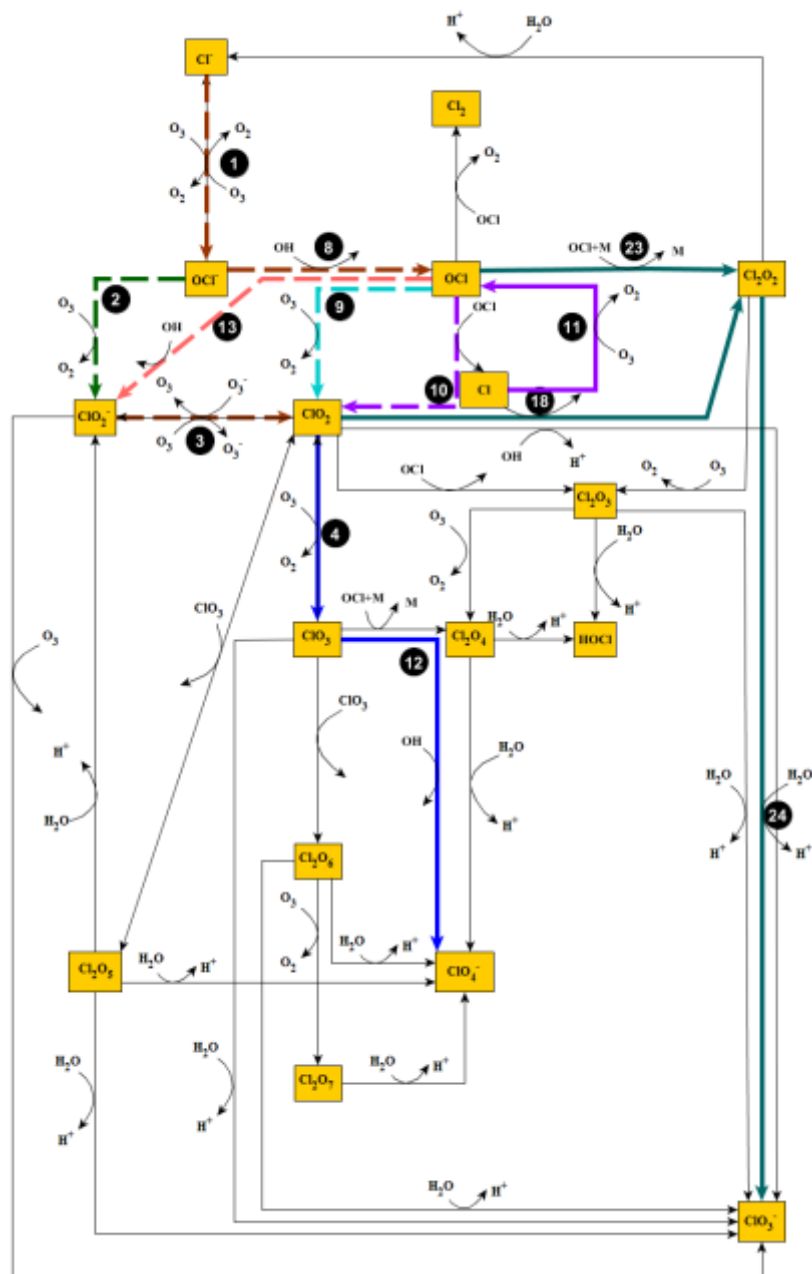


Figure 2.5.18. Combined final pathways determined responsible for ClO_4^- formation by O_3 oxidation of Cl^- (aq) including possible pathways for ClO_3^- formation. Note the thick dashed lines indicate the initial reactions that are possibly shared between ClO_4^- and ClO_3^- pathways and the thick aqua lines represent the final reactions leading to ClO_3^- formation. Both ClO_3^- pathways lead to the formation of one ClO_3^- molecule containing one O from O_3 .

O₃-Hypochlorite

With the exception of reaction 1 (Table 2.5.4), all mechanisms possibly leading to ClO₄⁻ production from O₃ oxidation of OCl⁻ (aq) (Appendix: Figures A.27 – A.49) were the same as the mechanisms identified leading to ClO₄⁻ formation from O₃ oxidation of Cl⁻ (aq). For further evaluation, these twenty-six mechanisms were divided into five groups: [1] pathways leading to ClO₄⁻ with only three O atoms from O₃ (Appendix: Figures A.27 – A.30), [2] pathways leading to production of two ClO₄⁻ molecules containing two and three O atoms from O₃, respectively (Appendix: Figures A.31 – A.34), [3] pathways leading to ClO₄⁻ with only two O atoms from O₃ (Appendix: Figures A.35 – A.39), [4] pathways involving the formation of the Cl₂O₅ intermediate species (Appendix: Figures A.40 – A.43), and [5] pathways involving reactions 16 and 19, reactions involving the oxidation of Cl₂O₃ into Cl₂O₄ and oxidation of Cl₂O₂ into Cl₂O₃ by O₃, respectively (Appendix: Figures A.44 – A.49). Assuming that the Δ¹⁷O values (+29 ‰ to +33‰) of ClO₄⁻ from the O₃-Cl⁻ (dry and aqueous) experiments can be used as a reference to determine site preference and reaction selectivity of terminal O atoms from O₃ into ClO₄⁻ we would expect that each O from O₃ would contribute about 8 ‰. Based on this assumption, our ClO₄⁻-Δ¹⁷O values produced from OCl⁻ (+ 16 ‰ to + 20 ‰) suggest that the O₃ oxidation of OCl⁻ (aq) results in a ClO₄⁻ molecule with at least two but less than three O from O₃, thus we were unable to eliminate pathways based on the number of O atoms derived from O₃ as the Δ¹⁷O values of our ClO₄⁻ could be the result of a combination of pathways yielding ClO₄⁻ having zero to four O from O₃. Furthermore, OCl⁻ is a direct product of the reaction between Cl⁻ and O₃ (Table 2.5.4: Rxn 1), thus it is also possible that OCl⁻ and Cl⁻ share the same pathway leading to the production of ClO₄⁻. Therefore, reductions in pathways were made by eliminating pathways with reactions and species that have not been observed or discussed in detail in literature.

The Cl₂O₅ species has two possible isomers (Table 2.5.4) and only one isomer will lead to the formation of ClO₄⁻ (Quiroga et al., 2005). Due to the lack of knowledge regarding the isomer structures of Cl₂O₅ and the likeliness of a mechanism forming ClO₃⁻ from the Cl₂O₅ species instead, all mechanisms involving Cl₂O₅ were regarded as being unlikely to account for ClO₄⁻ formed in our study (Appendix: Figures A.40 – A.43) (Quiroga et al., 2005). In addition, all pathways involving reactions 16 and 19, the formation of ClO₄⁻ from the reaction between OCl and ClO₃ radicals, were also eliminated as these reactions have not been demonstrated to exist and were only speculated to occur (Appendix: Figures A.44 – A.49). Exclusion of these pathways (Appendix: Figures A.40 – A.49) resulted in thirteen mechanisms (Appendix: Figures A.27 – A.39) capable of forming the ClO₄⁻ in our study, nine more than those identified for ClO₄⁻ formed from the O₃ oxidation of dry Cl⁻ (simultaneously represented in Figure 2.5.16). Similarly to O₃ oxidation of Cl⁻ (aq) the remaining pathways all require the formation of ClO₂ (aq) and a subsequent ClO₃ radical (simultaneously represented in Figure 2.5.19).

We could hypothetically theorize which pathways might be more important than others based on the rate of reaction of Cl^- versus that of OCl^- in the presence of O_3 . Complete decay of OCl^- happened in hours compared to Cl^- loss which took months and did not fully complete. Molar yields of ClO_4^- for the $\text{O}_3\text{-OCl}^-$ (0.01- 0.07 %) experiments were at least an order of magnitude higher than the molar yields of ClO_4^- from the $\text{O}_3\text{-Cl}^-$ (aq) experiments (< 0.001 %) even though the initial mass of Cl^- was two to three orders of magnitude higher than the initial molar mass of OCl^- (Table 2.5.3). Although the molar mass of transformed Cl^- was less (1.5 %) compared to transformed OCl^- (99.98 %), in the Cl^- experiments there was an excess amount of Cl^- and O_3 in solution as O_3 was being continuously input into the system, allowing for continuous reactions between Cl^- and O_3 to occur. Yet the rate of reaction between Cl^- and O_3 might have been much slower compared to the rate of reactions between Cl^- and other species. Due to the rate of reaction and input rate of O_3 for the oxidation of OCl^- , O_3 was likely limiting, perhaps facilitating reactions not involving O_3 and thus allowing alternate reactions (e.g. Rxn's 7, 14, 22, and 17) not observed in O_3 oxidation of Cl^- to occur (Figure 2.5.19; Table 2.5.4). Some of these reactions (Table 2.5.4; Rxn's 7, 14, and 7) are hydrolysis reactions, reactions which, as previously suggested, are not considered necessary for ClO_4^- to form from O_3 oxidation of Cl^- (aq). Based on this data, it is assumed that ClO_4^- production from O_3 oxidation of OCl^- is not entirely dependent on the same pathway as that of ClO_4^- from O_3 oxidation of Cl^- , but is rather a mixture of that pathway and other pathways not entirely dependent on O_3 or O_3 related oxidant reactions.

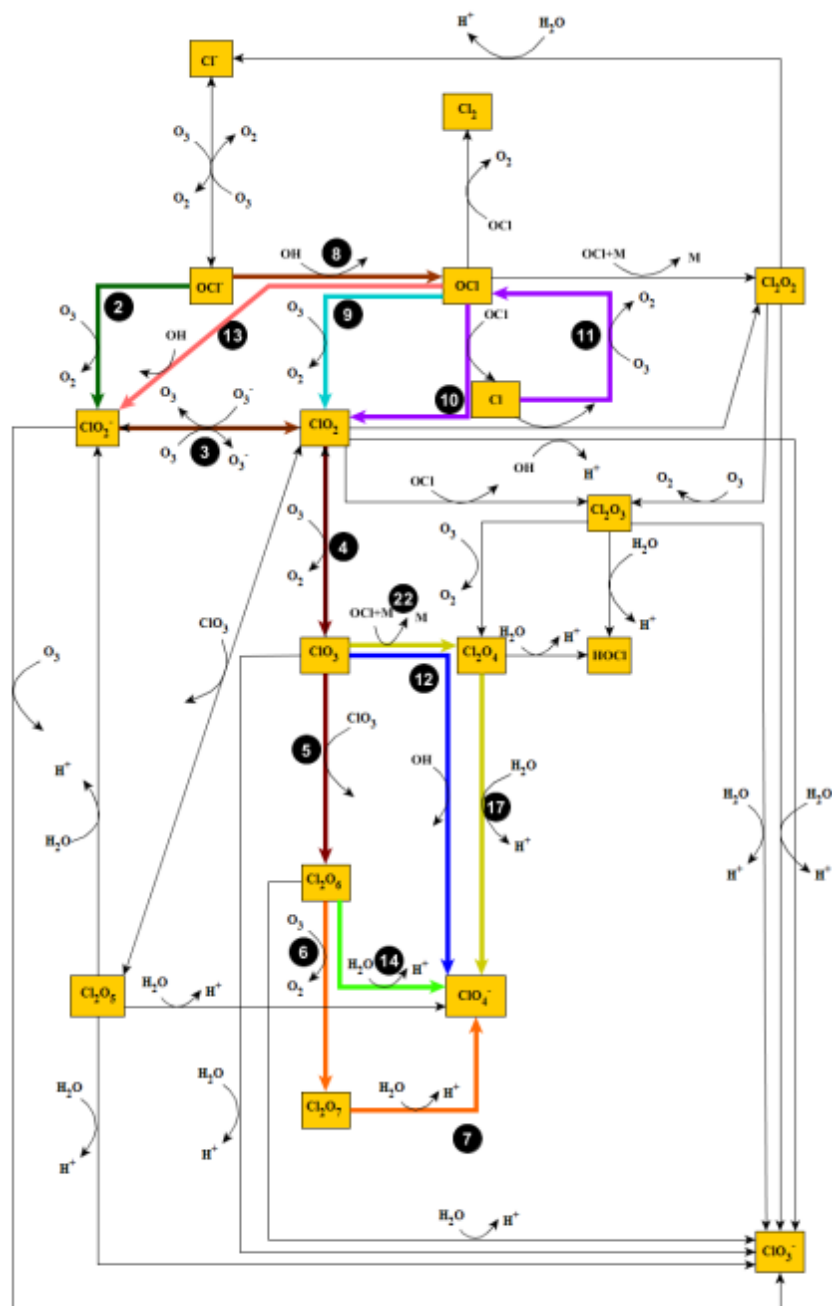


Figure 2.5.19. Combined final pathways determined responsible for ClO_4^- formation by O_3 oxidation of OCl^- (aq). Note the thick forest dark red lines indicate the reactions that some of the species may share while other colored lines represent reactions unique to each of the proposed pathways. All pathways lead to the formation of a ClO_4^- molecule containing either two or three O's from O_3 .

Our results for the OCl^- experiments further support the theory that formation of ClO_3^- may be independent of formation of ClO_4^- . $\Delta^{17}\text{O}$ values for ClO_3^- (-0.02 ‰ to + 1.37 ‰) indicate that the O in ClO_3^- is not primarily derived from O_3 (+ 24.5 ‰). Out of the thirteen possible pathways (Appendix: Figures A.27 – A.39), only two pathways (Appendix A: Figures A.35 – A.38) result in the formation of a ClO_3^- molecule along with ClO_4^- . These pathways would produce a ClO_3^- with two O atoms derived from O_3 and thus, cannot be responsible for ClO_3^- formation in our study. Three pathways (Figure 2.5.20), independent of ClO_4^- formation, were determined to be possible for formation of a ClO_3^- molecule with no O from O_3 . Given that reaction sequences that would form ClO_3^- during O_3 oxidation of Cl^- would form ClO_3^- with two O from O_3 (Figure 2.5.18), the ClO_3^- formed from O_3 oxidation of OCl^- is consistent as reaction 1 (Table 2.5.4) would be eliminated reducing the contribution of O from O_3 to near zero.

Final $\text{ClO}_3^-/\text{ClO}_4^-$ product ratios for O_3 oxidation of OCl^- (aq) (482-527) were not as high as those for O_3 oxidation of Cl^- (aq). These molar ratios indicate a higher production of ClO_3^- compared to ClO_4^- , supporting our hypothesis that ClO_4^- formation by O_3 oxidation of OCl^- may be independent of that of ClO_3^- . However, our product yields indicate that a significant amount of OCl^- is transformed to Cl^- , not ClO_3^- or ClO_4^- , suggesting that the main pathway rather leads to Cl^- not ClO_3^- (Table 2.5.3). This pathway may be the result of reaction 1 (Table 2.5.4), a back reaction involving the conversion of OCl^- to Cl^- .

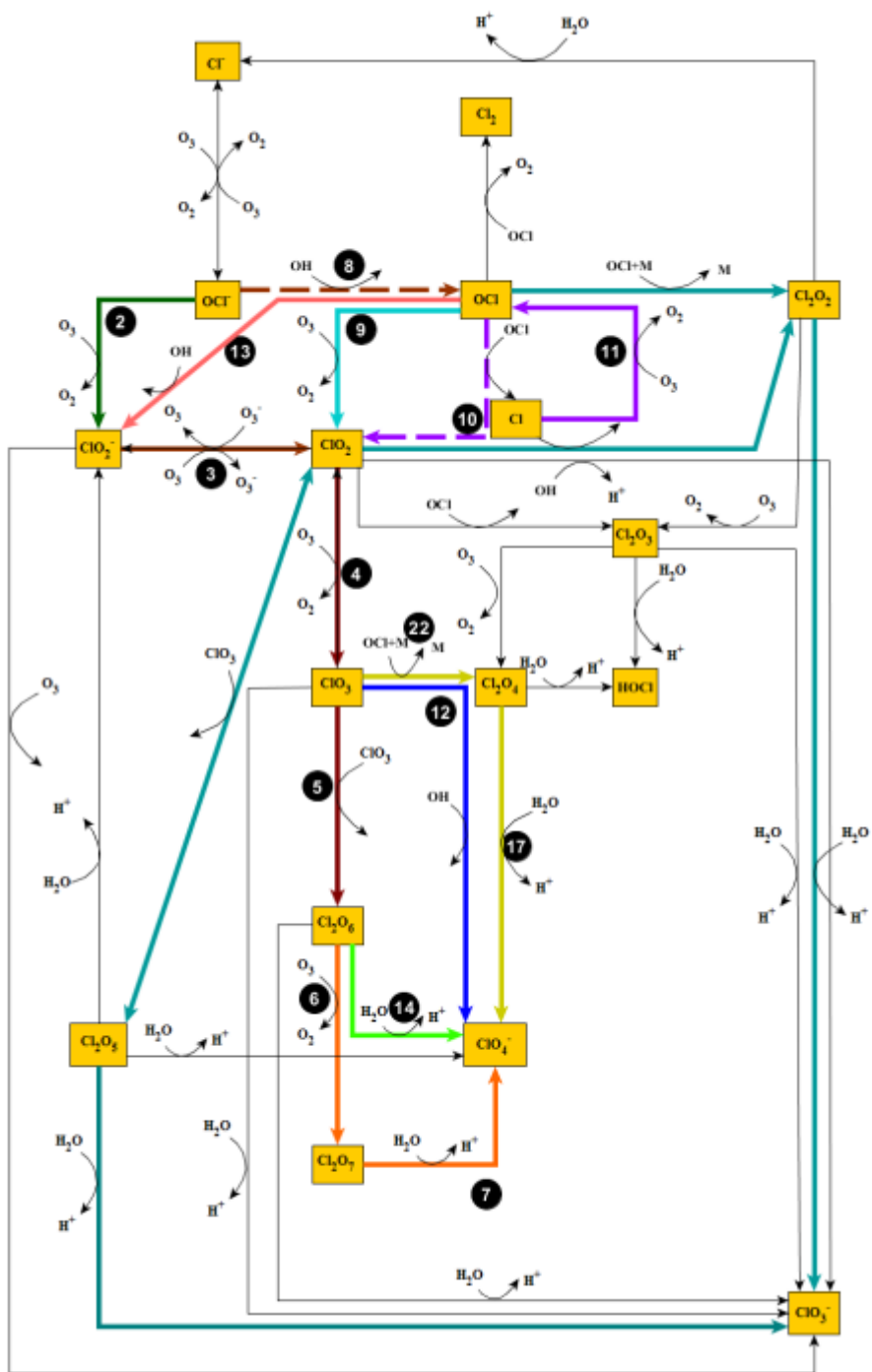


Figure 2.5.20. Combined final pathways determined responsible for ClO_4^- formation by O_3 oxidation of OCl^- including possible pathways for ClO_3^- formation (aq). Note the thick dashed lines indicate the initial reactions that are possibly shared between ClO_4^- and ClO_3^- pathways and the thick aqua lines represent the final reactions leading to ClO_3^- formation.

O₃-Chlorite

ClO₄⁻ produced from O₃ oxidation of ClO₂⁻ ($\Delta^{17}\text{O} = +12\text{‰}$ to $+13\text{‰}$) had a lower $\Delta^{17}\text{O}$ than ClO₄⁻ produced from OCl⁻ or Cl⁻. Using the $\Delta^{17}\text{O}$ values for ClO₄⁻ produced from O₃ oxidation of Cl⁻ (aq) ($+29\text{‰}$ to $+32\text{‰}$), for which all four O must come from O₃, as a reasonable approximation of the site preference value, we would expect that ClO₄⁻ incorporating two O from O₃ would have a $\Delta^{17}\text{O}$ value near the ranges of $+14.5\text{‰}$ to $+16\text{‰}$. This suggests that O₃ oxidation of ClO₂⁻ results in the transfer of two or less O from O₃.

A total of six mechanisms were postulated to form ClO₄⁻ from O₃ oxidation of ClO₂⁻ (aq) (Appendix A: Figures A.50 – A.55). All pathways starting from ClO₂⁻ produce ClO₄⁻ with one or two O from O₃. Two pathways (Appendix A: Figures A.54 and A.55) were eliminated because they either required formation of the Cl₂O₅ species or the formation of the Cl₂O₄ species by the oxidation of Cl₂O₃ by O₃ (Rxn 16; Table 2.5.4), a reaction we speculated could occur but has not been documented, leaving only four (Appendix: Figures A.50 – A.53) possible pathways (simultaneously represented in Figure 2.5.21). Two (Appendix A: Figures A.52 – A.53) of the four pathways produce a ClO₄⁻ with one O from O₃ and two (Appendix A: Figures A.50 – A.51) produce a ClO₄⁻ with two O's from O₃ (similar to that indicated by the $\Delta^{17}\text{O}$ values of ClO₄⁻).

The pathways (Appendix A: Figures A.50 – A.51) leading to ClO₄⁻ with two O from O₃ are consistent with the pathways observed for O₃ oxidation of Cl⁻ (aq) and OCl⁻ given the consistent decrease in $\Delta^{17}\text{O}$ of ClO₄⁻ indicating a loss of O transfer from each reaction step starting with O₃ oxidation of Cl⁻ (aq). In the Cl⁻ (aq) pathway, the first reaction donates an O to Cl⁻ from O₃ (Rxn 1; Table 2.5.4) and any subsequent reactions (Rxn 2 or Rxn's 8 and 13; Table 2.5.4) add an additional O, derived from O₃, to OCl⁻ to form ClO₂⁻.

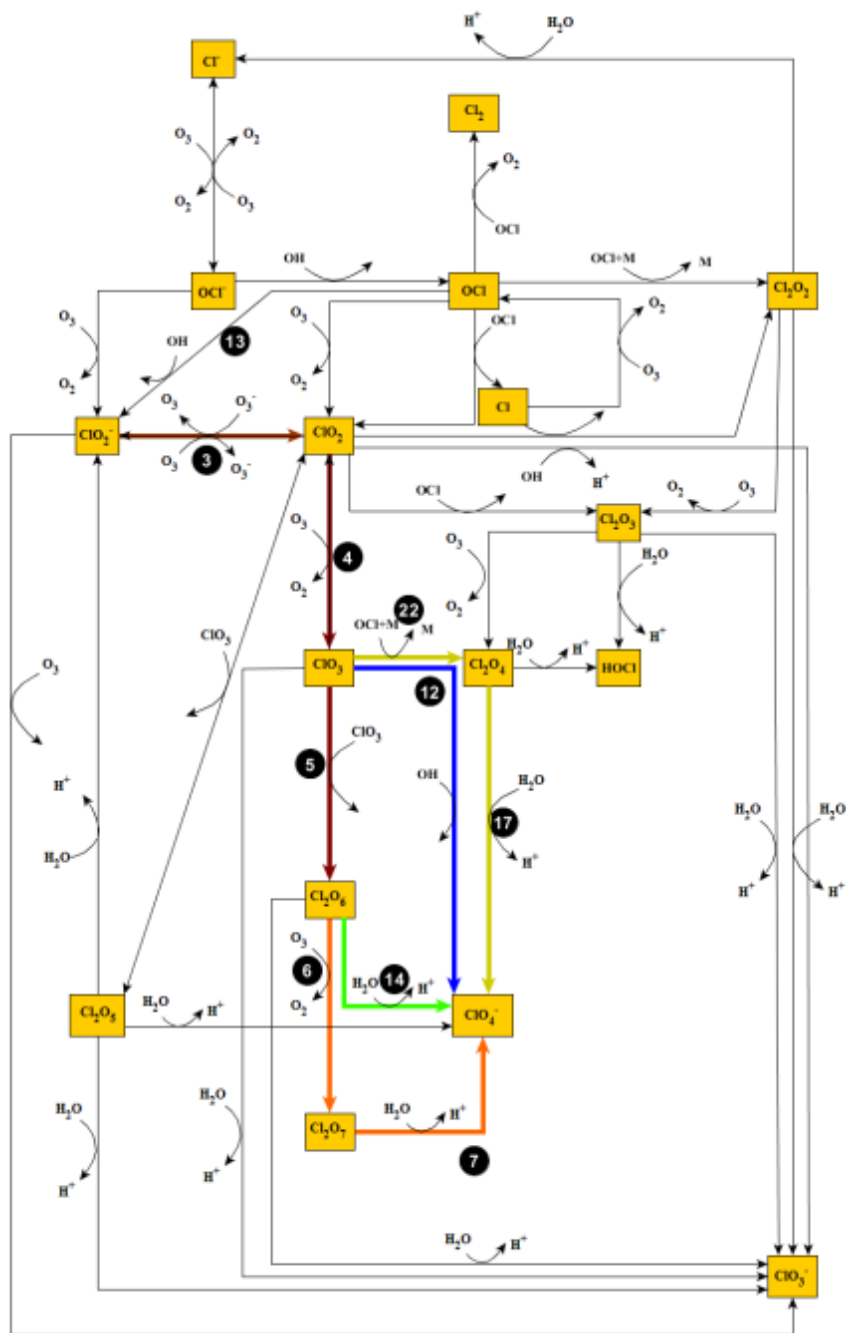


Figure 2.5.21. Combined final pathways determined responsible for ClO_4^- formation by O_3 oxidation of ClO_2^- (aq). Note the thick forest dark red lines indicate the reactions that some of the species may share while other colored lines represent reactions unique to each of the proposed pathways. All pathways lead to the formation of a ClO_4^- molecule containing either one or two O's from O_3 .

ClO_3^- was the major product of the $\text{O}_3\text{-ClO}_2^-$ experiments and in accordance with the previous ClO_3^- - $\Delta^{17}\text{O}$ values of the Cl^- (aq) and OCl^- (aq) experiments, $\Delta^{17}\text{O}$ values (+ 3 ‰ to + 4 ‰) of ClO_3^- formed from O_3 oxidation of ClO_2^- suggest that ClO_3^- formation pathways may be independent of those of ClO_4^- as only about half of one O in ClO_3^- is derived from O_3 . This is further supported by the $\text{ClO}_3^-/\text{ClO}_4^-$ molar ratios (902 – 1111) which indicate that the main pathway would lead to ClO_3^- formation and the minor pathways to ClO_4^- . Four pathways (Figure 2.5.22) were proposed as possibly leading to the ClO_3^- produced in our ClO_2^- (aq) experiments. Three pathways share the initial reaction (Reaction 3: formation of ClO_2 (aq)) with the ClO_4^- pathways, but then diverge into separate reaction sequences to produce ClO_3^- (Figure 2.5.22). All reactions proposed to occur after reaction 3 that lead to ClO_3^- formation are fast (Rxn's 15 and 29; Table 3.4) compared to reaction 4, which leads to ClO_4^- formation (Figure 2.5.22; Table 2.5.4), indicating that our proposed mechanisms for ClO_4^- and ClO_3^- formation might be correct. Out of the four ClO_3^- pathways proposed, two of the pathways (those involving Rxn's 26 and 27; Table 2.5.4 and Figure 2.5.22) form a ClO_3^- molecule with one O from O_3 and the other two pathways (those involving Rxn's 20 – 21 and 29; Table 2.5.4; Figure 2.5.22) form a ClO_3^- molecule with possibly zero O from O_3 depending on where the O from O_3 is located in the Cl_2O_5 structure and whether the O in the OH radical is derived from the O_3 molecule. These pathways suggest that ClO_3^- formed from O_3 oxidation of ClO_2^- may be the result of a mixture of different formation mechanisms (Table 2.5.4).

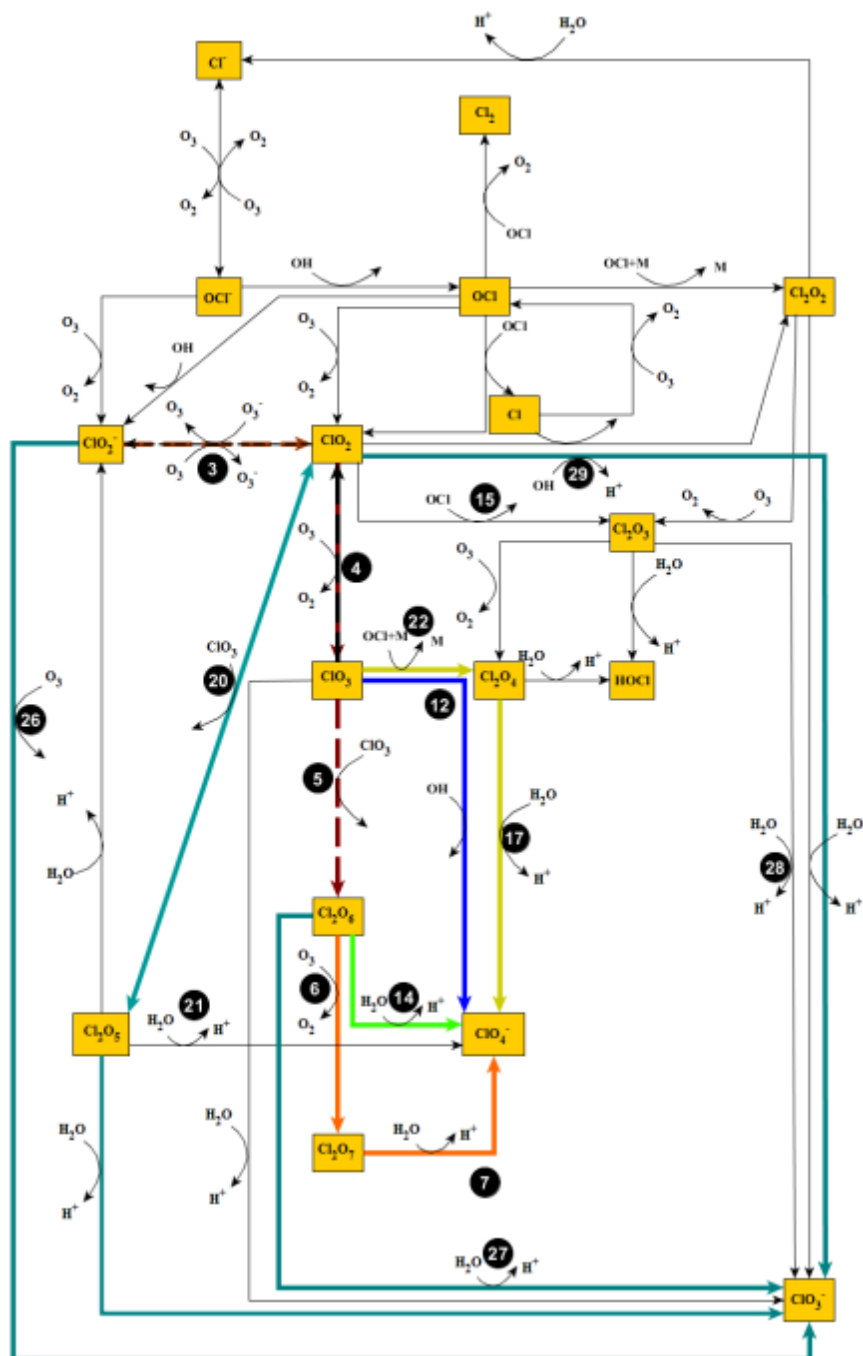


Figure 2.5.22. Combined final pathways determined responsible for ClO_4^- formation by O_3 oxidation of ClO_2^- including possible pathways for ClO_3^- formation (aq). Note the thick dashed lines indicate the initial reactions that are possibly shared between ClO_4^- and ClO_3^- pathways and the thick aqua lines represent the final reactions leading to ClO_3^- formation.

O₃-Chlorine Dioxide

The proposed mechanisms for the formation of ClO_4^- from molecular O_3 and ClO_2 (aq) are summarized in Appendix A Figures A.56 – A.61 and either produce a ClO_4^- with one or two O from O_3 . ClO_4^- produced from O_3 oxidation of ClO_2 (aq) had $\Delta^{17}\text{O}$ values (+16 ‰ to + 17 ‰) similar, yet slightly less than oxidation of OCl^- and higher than oxidation of ClO_2^- . Assuming our estimated value for the site preference are correct based on ClO_4^- produced from O_3 oxidation of Cl^- (e.g. $\text{O} \approx 8$ ‰), all pathways producing a ClO_4^- with less than two O from O_3 were eliminated as possible ClO_4^- formation pathways (Appendix A: Figures A.57 – A.61), thus resulting in only one possible pathway (Figure 2.5.23), consistent with the most likely pathways described previously.

A reason for the slightly higher $\Delta^{17}\text{O}$ value for ClO_4^- produced from ClO_2 (aq) compared to ClO_2^- is unclear but perhaps is due to variation in the site preference value. The transformation of ClO_2^- to ClO_2 (aq) does not involve an O transfer. Perhaps the much higher concentration (60 – 69 mmol) of reactant in the ClO_2^- oxidation experiment compared to ClO_2 (aq) (0.5 – 1.1 mmol) experiment produced an effect on the site preference value. The oxidation of ClO_2^- (rapid reaction) may have resulted in O_3 limitations, while for ClO_2 (aq) oxidation (also rapid) O_3 may not have been limiting due to the lower reactant concentration. The yield of ClO_4^- for both ClO_2 (aq) and ClO_2^- were the highest for all experiments although they were twenty to thirty fold higher for ClO_2 (aq) than ClO_2^- .

The $\text{ClO}_3^-/\text{ClO}_4^-$ molar ratios (21-30) for O_3 oxidation of ClO_2 (aq) were lower compared to those of the ClO_2^- (aq) and even the Cl^- (aq) (3022 – 4431) and OCl^- (482 – 569) experiments, supporting the previous postulations that ClO_3^- production is due to reactions unrelated to ClO_4^- production and that major ClO_3^- pathways may diverge from those of ClO_4^- early in the reaction sequence. Aside from ClO_4^- , ClO_3^- was the only other species produced in the ClO_2 (aq) experiments, but without isotopic data for ClO_3^- , we were unable to determine the mechanisms involved in ClO_3^- formation.

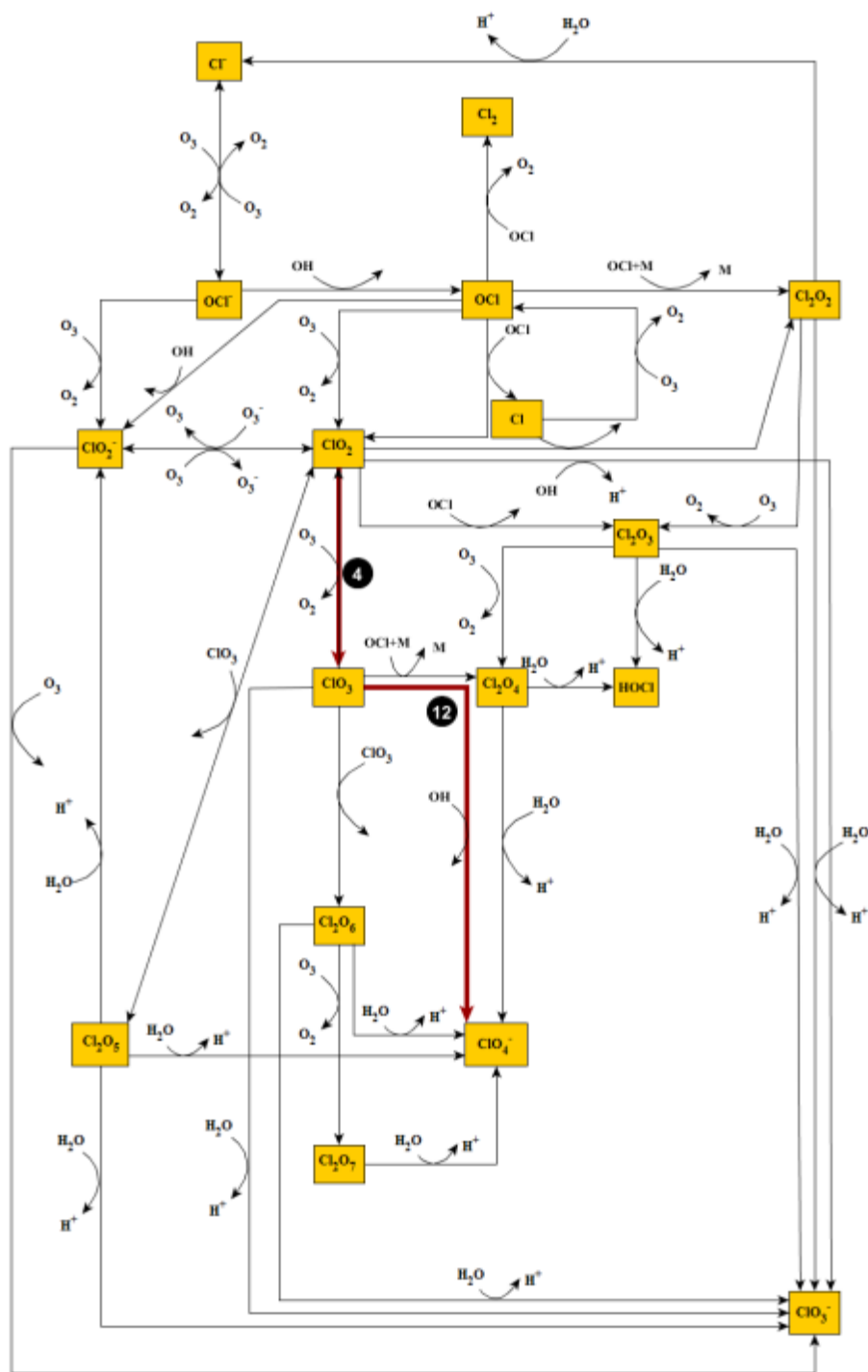


Figure 2.5.23. O_3 oxidation of ClO_2 (aq). Note the thick maroon lines indicate the pathway leading to the formation of the ClO_4^- and black solid circles represent reaction number from Table 2.5.4. This pathway leads to the formation one ClO_4^- molecule containing two O from O_3 .

2.5.4.10 Overall Conclusions Based on $\Delta^{17}\text{O}$ of O_3 Experiments

The $\Delta^{17}\text{O}$ values of ClO_4^- produced by O_3 oxidation of ClO_x species provide a better understanding of the role the O_3 molecule plays in the transfer of O atoms into produced ClO_4^- as well as help to identify key reactions involved in ClO_4^- formation. There was a consistent decrease in O atoms incorporated from O_3 into ClO_4^- with increasing oxidation state of Cl as the reactant species, with the exception of $\text{ClO}_2(\text{aq})$. The ClO_4^- pathways proposed for O_3 oxidation of Cl^- , OCl^- , and ClO_2^- are consistent with these observations as they account for the loss of O_3 O atoms through each initial reaction step: Cl^- to OCl^- (Rxn 1; Table 2.5.4) and OCl^- to ClO_2^- (Rxn 2; Table 2.5.4). Moreover, regardless of the reactant species (Cl^- , OCl^- , ClO_2^- , or $\text{ClO}_2(\text{aq})$) all ClO_4^- pathways include the ClO_2 and the ClO_3 radical. Because $\text{ClO}_2(\text{aq})$ is a required intermediate, the generation pathway must include Reactions 4 (Table 2.5.4), the oxidation of ClO_2 to ClO_3 .

The $\Delta^{17}\text{O}$ values of ClO_3^- compared to those of ClO_4^- also indicate that ClO_4^- and ClO_3^- are formed through independent pathways. ClO_3^- was the main species produced, indicating that major reactions of O_3 with ClO_x produce ClO_3^- , not ClO_4^- . Although not all reaction rates for reactions in our proposed pathways are known, there are reaction rates for the decay of OCl^- and $\text{ClO}_2(\text{aq})$ (Rxn's 2, 4, 8, 15, 18, and 29; Table 2.5.4) that indicated that the slower reaction (Rxn 4, Table 2.5.4) is the one likely responsible for ClO_4^- formation.

2.5.4.11 $\Delta^{17}\text{O}$ in UV Experiments

UV-Hypochlorite

The reactions involved in the photodecomposition of OCl^- are well-known and possible ClO_4^- formation mechanisms have been proposed from them (Kang et al., 2006; Buxton et al., 1972a,b). These ClO_4^- mechanisms have been compiled into one diagram (Figure 2.5.24) and are dependent upon the wavelength (253.7 nm and 313 nm, or 365 nm) at which initial photolysis of OCl^- occurs (Figure 2.5.24; Rxn's 1-3). Three pathways (Figure 2.5.24; [1] Rxn sequence: 1, 4-5, 25, 30, and 41-43, [2] Rxn sequence: 1, 4-6, 26, 30, and 41-43, [3] Rxn sequence: 1, 4-6, 20, 30, and 41-43) are possible at low wavelengths (253.7 and 313 nm) and depend on Cl atoms to oxidize OCl^- , while two pathways (Figure 2.5.24; [1] Rxn sequence: 3, 13, 17, 21, 30, and 41-43, [2] Rxn sequence: 3, 13, 20, 30, and 41-43) are predominant at a higher wavelength (365 nm) and depend on the ground state $\text{O}(^3\text{P})$ atom to oxidize OCl^- .

The low $\Delta^{17}\text{O}$ values (- 0.0 ‰ and + 0.5 ‰) of ClO_4^- formed from UV oxidation of OCl^- indicated no involvement of O_3 and thus, it was determined that pathways leading to ClO_4^- did not form O_3 and therefore, could not be postulated on the basis of the number of O atoms coming from the O_3 molecule. However, because UV experiments were conducted at a wavelength of 350 nm, the pathways most likely involved in production of ClO_4^- are believed to be the two

involving the oxidation of OCl^- by the ground state $\text{O}(^3\text{P})$ atom (Figure 2.5.24; [1] Rxn sequence: 3, 13, 17, 21, 30, and 41-43, [2] Rxn sequence: 3, 13, 20, 30, and 41-43). Similar to the pathways for O_3 oxidation of OCl^- , the formation of two key intermediate species was found necessary for ClO_4^- production in the UV experiments: ClO_2 and the ClO_3 radical (Figure 2.5.24). The only uncertainty associated with the two $\text{O}(^3\text{P})$ - ClO_4^- pathways is as to which reactions are responsible for the formation of ClO_2 : Rxn's 17 and 21 or Rxn 20 (Figure 2.5.24). The reactions following ClO_2 formation, which included oxidation of ClO_2 into the ClO_3 radical (Rxn's 30 and 41), the reaction between two ClO_3 radicals to produce Cl_2O_6 (Rxn 42), and the hydrolysis of the Cl_2O_6 species (Rxn 43) were common and deemed necessary for the production of ClO_4^- in all the UV mechanisms proposed.

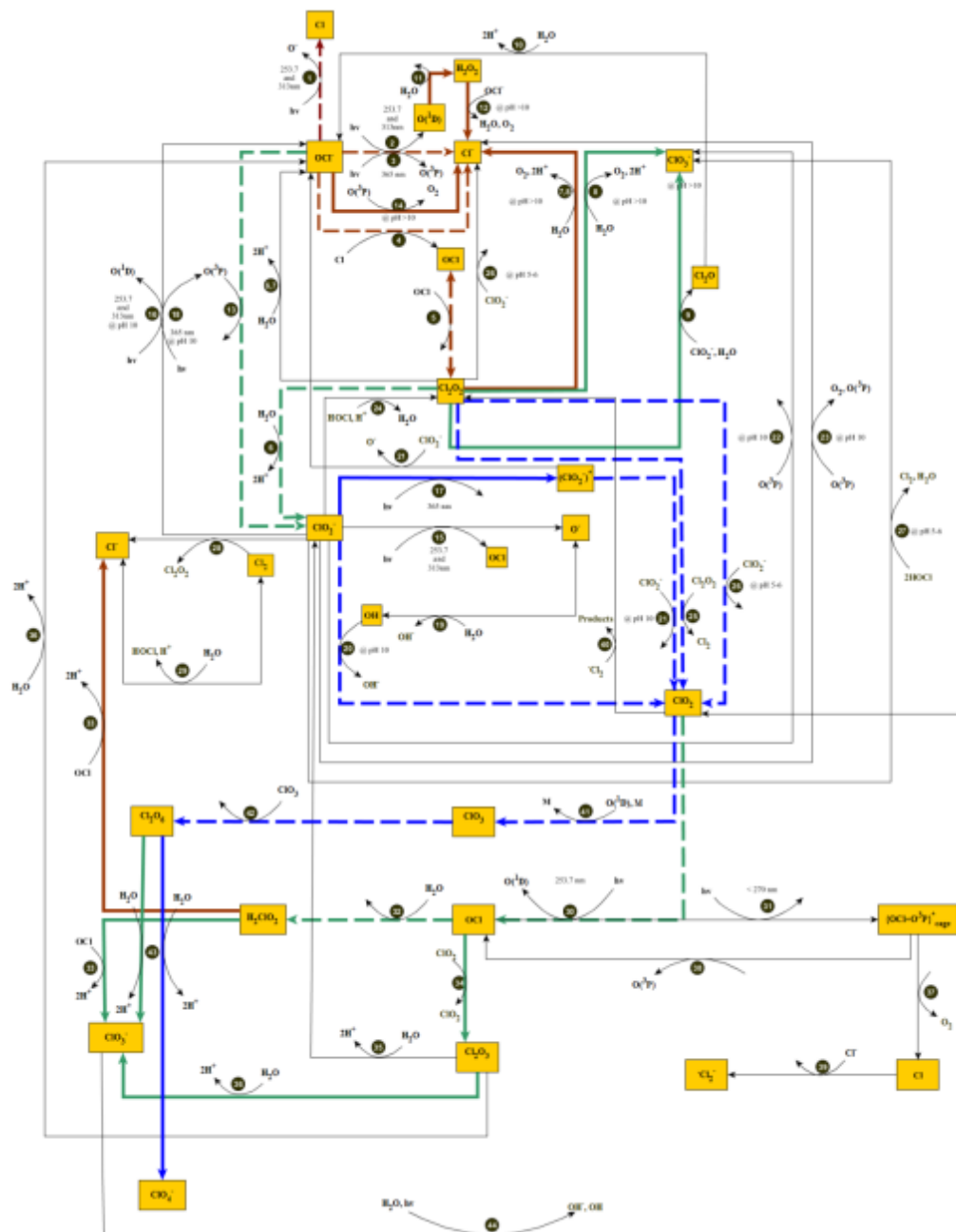


Figure 2.5.24. UV oxidation of OCl^- (aq). Note the thick red lines indicate the pathways leading to the formation of Cl^- , the thick aqua lines indicate the pathways leading to formation of ClO_3^- , and the thick blue lines indicate the pathways leading to the formation of ClO_4^- . The solid lines indicate reactions specific only to the anion produced, the dashed lines indicate shared reactions between pathways leading to either two or all three anions, and the black solid circles represent reaction numbers corresponding to reactions listed.

UV-Chlorite

Photodecomposition pathways of ClO_2^- have also been previously proposed and are summarized in Figure 2.5.25 (Kang et al., 2006). Determination of the exact pathway(s) responsible for ClO_4^- formation from UV oxidation of ClO_2^- is not possible based on the number of O atoms from O_3 as the $\Delta^{17}\text{O}$ values of ClO_4^- produced were below zero ($\sim -2\text{‰}$), indicating that UV pathways are mass-dependent processes and that O_3 was not a major source of O in ClO_4^- . The photolysis of ClO_2^- was observed at a wavelength of 350 nm and thus the ClO_4^- pathways proposed only include reactions occurring at longer wavelengths (365 nm) (Figure 2.5.25; Rxn's 17 and 18). All preferred UV ClO_4^- pathways lead to the formation of the ClO_2 molecule which undergoes the same final reaction sequence (Figure 2.5.25; Rxn's 30, and 41 – 43) as the pathways for UV oxidation of OCl^- (Figure 2.5.24) to produce ClO_4^- .

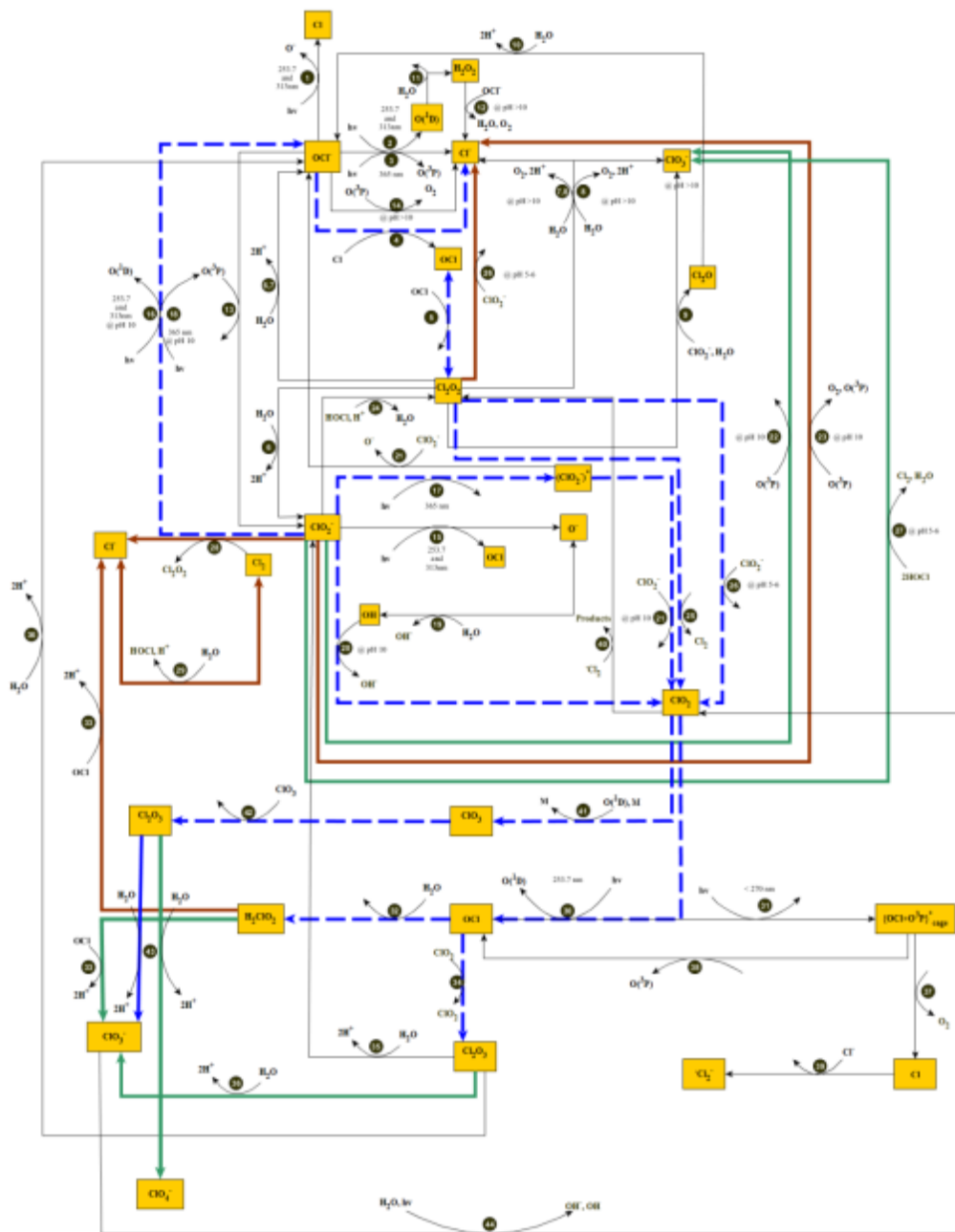


Figure 2.5.25. UV oxidation of ClO_2^- (aq). Note the thick red lines indicate the pathways leading to the formation of Cl^- , the thick aqua lines indicate the pathways leading to formation of ClO_3^- , and the thick blue lines indicate the pathways leading to the formation of ClO_4^- . The solid lines indicate reactions specific only to the anion produced, the dashed lines indicate shared reactions between pathways leading to either two or all three anions, and the black solid circles represent reaction numbers corresponding to reactions listed.

UV-Chlorine Dioxide

$\Delta^{17}\text{O}$ values of ClO_4^- formed from the photodecomposition of ClO_2 (aq) (+ 0.9 ‰ and + 1.3 ‰) were higher than those of ClO_4^- from the OCl^- and ClO_2^- experiments indicating either an unusual mass-dependent process or possibly that O_3 was generated by the UV reactions. These $\Delta^{17}\text{O}$ values provide further evidence indicating that ClO_4^- produced from UV pathways is most likely due to mass dependent fractionation processes and thus cannot be formulated on the basis of O derived from O_3 . Based on what we know regarding UV oxidation of OCl^- and ClO_2^- , only one pathway was determined possible for the formation of ClO_4^- from UV oxidation of ClO_2 (aq) (Figure 2.5.26; Rxn sequence: 30 and 41-43). This pathway requires the formation of the ClO_3 radical (rxn 41) and the Cl_2O_6 species (rxn 42).

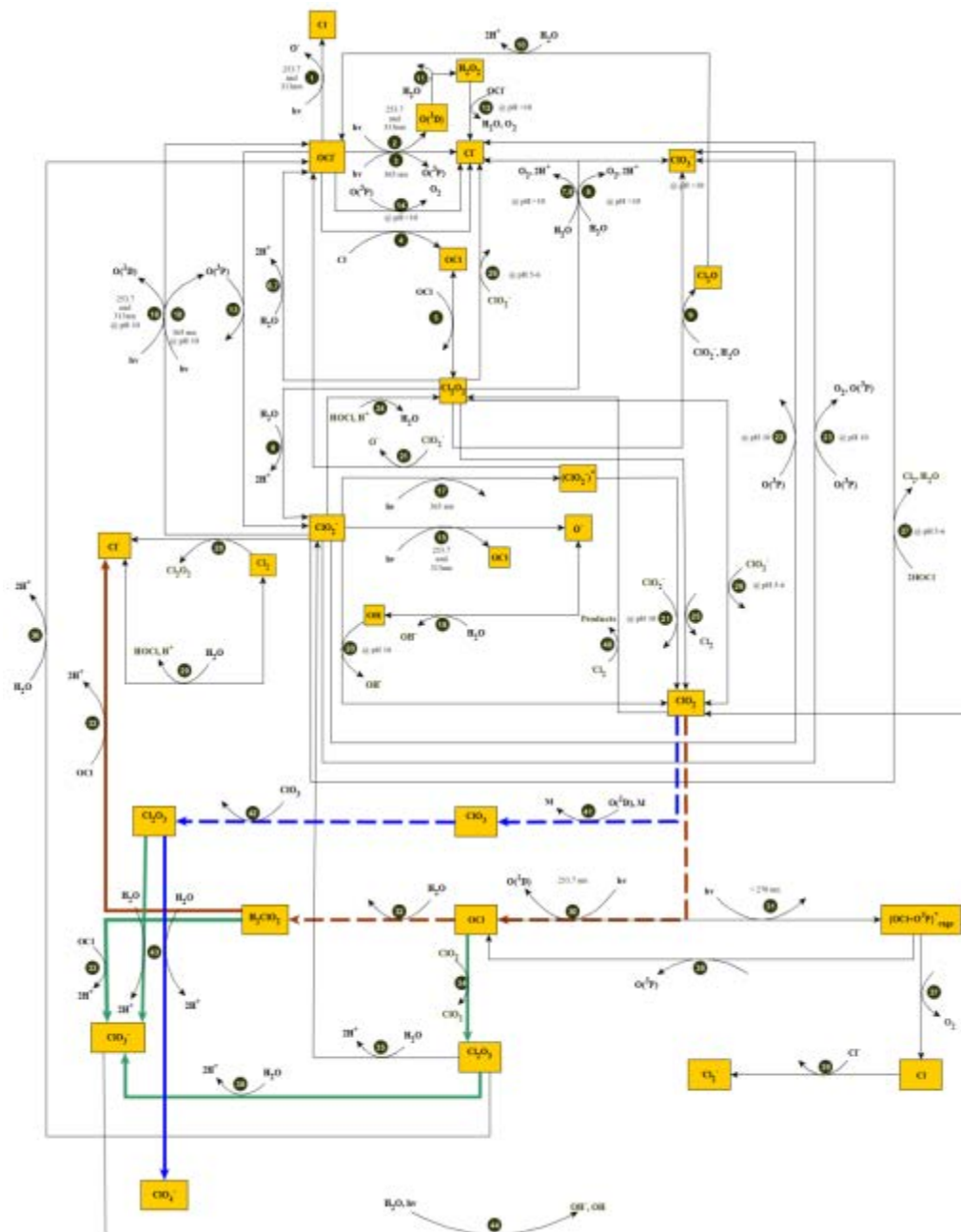


Figure 2.5.26. UV oxidation of ClO_2 (aq). Note the thick red lines indicate the pathways leading to the formation of Cl^- , the thick aqua lines indicate the pathways leading to formation of ClO_3^- , and the thick blue lines indicate the pathways leading to the formation of ClO_4^- . The solid lines indicate reactions specific only to the anion produced, the dashed lines indicate shared reactions between pathways leading to either two or all three anions, and the black solid circles represent reaction numbers corresponding to reactions listed.

2.5.4.12 Implications of $\delta^{18}\text{O}$ and $\Delta^{17}\text{O}$

Expected Relationship Between $\delta^{18}\text{O}$ and $\Delta^{17}\text{O}$ Values of ClO_4^-

For all experiments (UV and O_3) in which O isotopes were measured, the $\delta^{18}\text{O}$ values of ClO_4^- were much higher than the initial total reactant ClO_x species, bulk water, and produced ClO_3^- (the only other final ClO_x species (Figures 2.5.5 – 2.5.12). With the exception of $\delta^{18}\text{O}$ values of ClO_4^- from the oxidation of ClO_2 (aq), in the O_3 experiments, the $\Delta^{17}\text{O}$ and $\delta^{18}\text{O}$ values of ClO_4^- increased as oxidation state of Cl in reactant ClO_x species (ClO_2^- , OCl^- , and Cl^- , respectively) decreased, whereas in the UV experiments, as expected, no trend was observed between $\Delta^{17}\text{O}$ and $\delta^{18}\text{O}$ values (Figures 2.5.13 – 2.5.15). The increase in $\delta^{18}\text{O}$ values with increasing number of O incorporated from O_3 is expected. The $\delta^{18}\text{O}$ values for experiments involving O_3 should be proportional to the number of O atoms incorporated from O_3 , although the relationship may not be linear given possible variation in the $\delta^{18}\text{O}$ values of other O sources and possible impacts of exchange and/or fractionation. Interpretations of the $\delta^{18}\text{O}$ values of ClO_4^- formed from each individual reactant ClO_x species for both oxidation methods (O_3 and UV) were attempted by evaluating the likelihood of these three factors. Where possible (O_3 experiments) we attempted to evaluate the possible impact of O from other sources by using the expected number of O atoms from O_3 and other sources and applying an isotope mass balance.

O_3 -Dry Chloride

The O_3 oxidation of dry Cl^- produced ClO_4^- with the highest $\Delta^{17}\text{O}$ values (~33 ‰) which indicated most, if not all, O in ClO_4^- is from O_3 depending on the final site preference value. If all the O were sourced from O_3 , then $\delta^{18}\text{O}$ values of ClO_4^- should have been near + 124 ‰, assuming no fractionation effects. The lower $\delta^{18}\text{O}$ values (+ 20.5 ‰) indicate that either some of the O came from a source with very negative values, that some O exchanged with an O source for which the equilibrium value is very negative, or that the O incorporated from O_3 was fractionated. Assuming that O_3 had a final $\Delta^{17}\text{O}$ site preference value of + 7 ‰, the maximum possible, it was determined (Equations 6 and 7) that a maximum of 10 % O from ClO_4^- could have come from a source other than O_3 .

Although caution was taken to remove H_2O in the reaction tubes used in the dry Cl^- experiments, there is a possibility that some moisture remained in the tubes resulting in interactions between H_2O and ClO_x species. If moisture was involved then four O sources for ClO_4^- would have been available: O_3 , H_2O , OH radical, and O_2 . However, O_2 is not an oxidant in any of the ClO_4^- production pathways from O_3 oxidation of Cl^- (aq) and we assume that the O from the OH radical is from O_3 , thus they were not considered further in our mixing evaluation.

Bulk water used in the experiment had a $\delta^{18}\text{O}$ value of - 6.9 ‰, the lowest of the known O sources, but residual H_2O on the salt would likely be much heavier. Therefore, even assuming

that the source of O was bulk water and using the maximum % of O that could come from water based on the maximum site preference value and the $\delta^{18}\text{O}$ mass balance (Equations 6 and 8) would result in a ClO_4^- with a $\delta^{18}\text{O}$ value (+ 111 ‰) higher than the $\delta^{18}\text{O}$ value measured for ClO_4^- (+ 20.5 ‰) (Figure 2.5.27). For mixing to have been responsible 79 % (3.16) of the O atoms in ClO_4^- would have to be from H_2O and only 21 % (0.84) from O_3 , therefore, contribution of O atoms from other sources cannot account for the $\delta^{18}\text{O}$ value of ClO_4^- from O_3 oxidation of dry Cl^- . We do not have any information on possible O equilibrium exchange values and therefore, cannot evaluate their potential to account for the observed $\delta^{18}\text{O}$ ClO_4^- values, but they would have to be substantially more negative than bulk H_2O . Given the above discussion, it appears that the most likely explanation for the relatively low observed $\delta^{18}\text{O}$ values, given the $\Delta^{17}\text{O}$ values, is the impact of mass dependent fractionation during ClO_4^- formation.

$$\begin{array}{l} \% \text{ O from } \text{H}_2\text{O} + \% \text{ O from } \text{O}_3 = \\ 1 \end{array} \quad (6)$$

$$(\% \text{ O from } \text{H}_2\text{O} \times \Delta^{17}\text{O of } \text{H}_2\text{O}) + (\% \text{ O from } \text{O}_3 \times \Delta^{17}\text{O of } \text{O}_3) = \Delta^{17}\text{O of } \text{ClO}_4^- \quad (7)$$

$$(\% \text{ O from } \text{H}_2\text{O} \times \delta^{18}\text{O of } \text{H}_2\text{O}) + (\% \text{ O from } \text{O}_3 \times \delta^{18}\text{O of } \text{O}_3) = \delta^{18}\text{O of } \text{ClO}_4^- \quad (8)$$

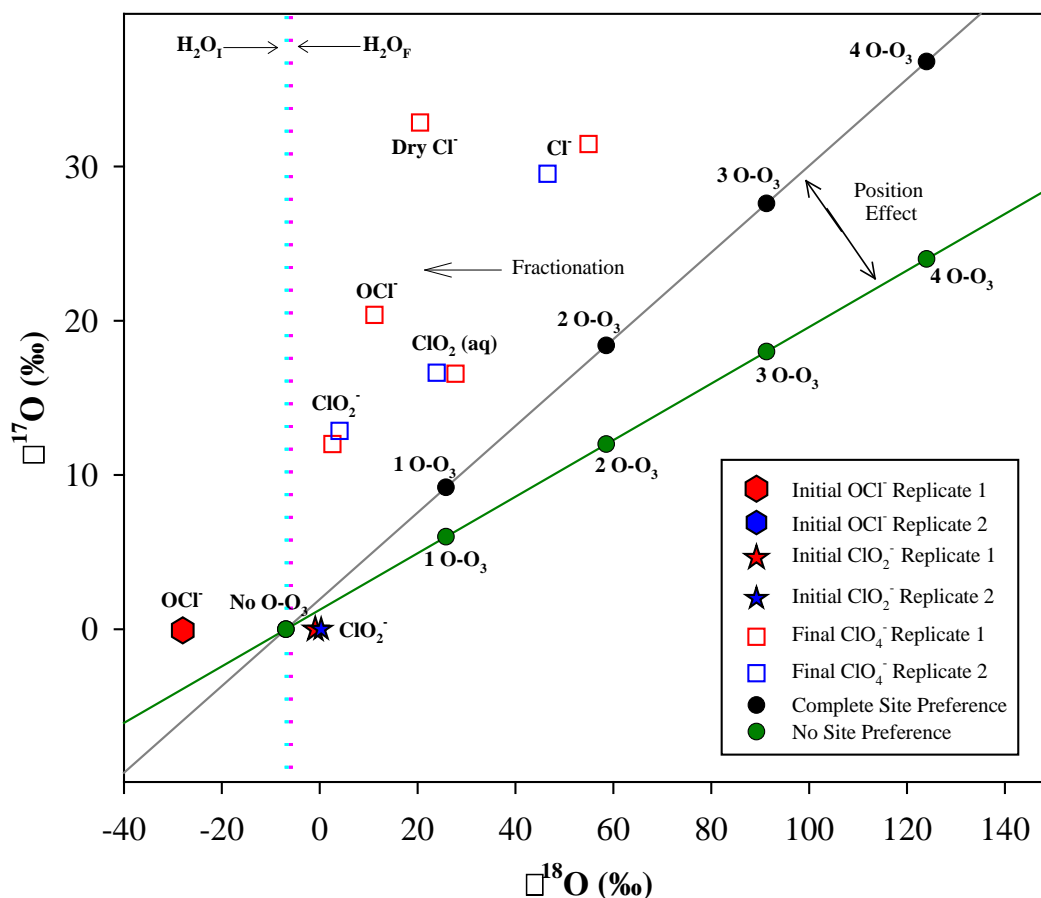


Figure 2.5.27. Stable O isotopic compositions ($\delta^{18}\text{O}$ and $\Delta^{17}\text{O}$) of reactant species and final ClO_4^- for O_3 oxidized ClO_x solutions including expected $\delta^{18}\text{O}$ and $\Delta^{17}\text{O}$ of ClO_4^- formed from the mixture of H_2O and O_3 (with complete site preference of the heavy O isotope in the terminal O atoms of O_3) (black circles) and expected $\delta^{18}\text{O}$ and $\Delta^{17}\text{O}$ of ClO_4^- formed from the mixture of H_2O and O_3 (with no site preference of the heavy O isotope in the terminal O atoms of O_3) (green circles). The replicate experiments are represented by the different colors (blue and red). The species label next to the final ClO_4^- symbols indicates the species oxidized corresponding to that ClO_4^- .

O_3 -Chloride (aq)

Similar to dry Cl^- , $\Delta^{17}\text{O}$ values of ClO_4^- from the Cl^- (aq) experiments (+ 29 ‰ and + 32 ‰) also indicated that nearly all O atoms in ClO_4^- were from O_3 , depending on the final $\Delta^{17}\text{O}$ site preference value of O_3 . The ClO_4^- $\delta^{18}\text{O}$ values were however higher (~ 25.5 – 34.5 ‰) than those of ClO_4^- from the dry Cl^- experiments but they were still lower (~ 69 – 78 ‰) than what would be expected (~ + 124 ‰) assuming no fractionation effects. Assuming that O_3 had a final $\Delta^{17}\text{O}$ site preference value of + 37 ‰, the maximum possible, it was determined using a $\Delta^{17}\text{O}$

mass balance that between 13– 21% of O in ClO_4^- could come from H_2O and the other 79 – 87 % from O_3 (Equations 6 and 7). It was determined through a $\delta^{18}\text{O}$ mass balance that even assuming the maximum % of O that could come from H_2O (21%) would result in a ClO_4^- with a $\delta^{18}\text{O}$ value of + 97 ‰, a value much greater than the ClO_4^- $\delta^{18}\text{O}$ values observed (+ 46 ‰ to + 55 ‰) (Figure 2.5.27). Therefore it was concluded that mixing of O sources most likely does not account for the $\delta^{18}\text{O}$ values of ClO_4^- formed from O_3 oxidation of Cl^- (aq), but that given the little that is known regarding O exchange between ClO_x species, that mass-dependent fractionation effects are the most likely explanation for the $\delta^{18}\text{O}$ values of ClO_4^- .

O₃-Hypochlorite

The $\Delta^{17}\text{O}$ values of ClO_4^- from O_3 oxidation of OCl^- (+ 16 ‰, + 17 ‰, and + 20 ‰) indicated that, assuming a $\Delta^{17}\text{O}$ site preference value of + 32 ‰ for O_3 based on the Cl^- oxidation experiments, two to three O in ClO_4^- come from O_3 . The ClO_4^- $\delta^{18}\text{O}$ values observed (+ 1 ‰, + 2 ‰, and +11‰) were much lower than those of O_3 (+ 124 ‰), but higher than those of H_2O (- 6.9 ‰) and initial total O (- 28 ‰), all of which are species considered as O sources available for ClO_4^- formation. Because less than 5 % of the initial total O was attributed to a species other than OCl^- , the $\delta^{18}\text{O}$ values of initial total O were considered to be the same for OCl^- (- 28 ‰).

To evaluate whether mixing of O sources could account for the ClO_4^- $\delta^{18}\text{O}$ values observed, a mass balance on $\Delta^{17}\text{O}$ values of OCl^- (-0.07 ‰ to + 0.4 ‰) (assuming the original O in the reactant OCl^- species was transferred into final ClO_4^-), O_3 (assuming a maximum possible $\Delta^{17}\text{O}$ site preference value of + 37 ‰), and H_2O (0 ‰) was performed. Assuming that 25 % of the O in ClO_4^- came from OCl^- , the mass balance indicates that 19.5 – 30 % of O came from H_2O , and 45 – 55.5 % of O came from O_3 (Equations 9 and 10). Assuming the minimum % of O that could come from OCl^- (25 %) and the maximum % that could come from H_2O (30 %), it was determined through a $\delta^{18}\text{O}$ mass balance that ClO_4^- should exhibit a $\delta^{18}\text{O}$ value near + 47 ‰, a value much higher than the ClO_4^- $\delta^{18}\text{O}$ values observed (+ 1 ‰, + 2 ‰, and + 11 ‰).

Given these results, it is unlikely that mixing of O_3 with other O sources (OCl^- and H_2O) alone is responsible for the $\delta^{18}\text{O}$ values of ClO_4^- formed from O_3 oxidation of OCl^- . Therefore, based on $\Delta^{17}\text{O}$ values indicating only partial contribution of O_3 -O atoms into ClO_4^- and the mixing calculations, we conclude that the other most likely explanation for the observed ClO_4^- $\delta^{18}\text{O}$ values is the impact of mass dependent fractionation during ClO_4^- formation.

$$\% \text{ O from } \text{H}_2\text{O} + \% \text{ O from } \text{O}_3 + \% \text{ O from } \text{OCl}^- = 1 \quad (9)$$

$$(\% \text{ O from } H_2O \times \Delta^{17}O \text{ of } H_2O) + (\% \text{ O from } O_3 \times \Delta^{17}O \text{ of } O_3) + (\% \text{ O from } OCl^- \times \Delta^{17}O) = \Delta^{17}O \text{ of } ClO_4^- \quad (10)$$

$$(\% \text{ O from } H_2O \times \delta^{18}O \text{ of } H_2O) + (\% \text{ O from } O_3 \times \delta^{18}O \text{ of } O_3) + (\% \text{ O from } OCl^- \times \delta^{18}O) = \delta^{18}O \text{ of } ClO_4^- \quad (11)$$

O₃-Chlorite

The O₃ oxidation of ClO₂⁻ produced ClO₄⁻ with the lowest Δ¹⁷O values (+ 12 ‰ and + 13 ‰) which indicated that two or less O in ClO₄⁻ is from O₃, depending on the final site preference value of O₃. Assuming a Δ¹⁷O site preference value of + 37 ‰ for O₃, the maximum possible and the measured Δ¹⁷O of H₂O (0‰) and ClO₂⁻ (+ 0.0 ‰) (assuming that the original O in the reactant ClO₂⁻ species was transferred into the final ClO₄⁻ structure), a mass balance determined that 15 – 17 % of O came from H₂O, and 33–35 % of O came from O₃ (Equations 12 and 13). Out of the three O sources available (ClO₂⁻, H₂O, and O₃), bulk water has the lowest δ¹⁸O value (- 6.9 ‰). Assuming the maximum % of O that could come from water (17 %), based on the Δ¹⁷O mass balance, and the assumed 50 % of O that came from ClO₂⁻, we would expect a ClO₄⁻ with a δ¹⁸O value near + 39 ‰, a value considerably greater than the measured ClO₄⁻ δ¹⁸O values (+ 2 ‰ and + 4 ‰). The ClO₄⁻ Δ¹⁷O values indicate that another O source other than O₃ is involved in the formation of ClO₄⁻, but given the mass balance results it appears that mixing alone cannot be responsible for the δ¹⁸O values observed. Given previous results for other oxidized species (Cl⁻ and OCl⁻) the most likely explanation is that mass dependent fractionation and mixing of O from the original ClO₂⁻ were both responsible for the δ¹⁸O values of ClO₄⁻ from O₃ oxidation of ClO₂⁻.

$$\% \text{ O from } H_2O + \% \text{ O from } O_3 + \% \text{ O from } ClO_2^- = 1 \quad (12)$$

$$(\% \text{ O from } H_2O \times \Delta^{17}O \text{ of } H_2O) + (\% \text{ O from } O_3 \times \Delta^{17}O \text{ of } O_3) + (\% \text{ O from } ClO_2^- \times \Delta^{17}O) = \Delta^{17}O \text{ of } ClO_4^- \quad (13)$$

$$(\% \text{ O from } H_2O \times \delta^{18}O \text{ of } H_2O) + (\% \text{ O from } O_3 \times \delta^{18}O \text{ of } O_3) + (\% \text{ O from } ClO_2^- \times \delta^{18}O) = \delta^{18}O \text{ of } ClO_4^- \quad (14)$$

O₃-Chlorine Dioxide

The $\Delta^{17}\text{O}$ values of ClO_4^- from O_3 oxidation of ClO_2 (aq) (+16 to +17 ‰) were similar to those of ClO_4^- from O_3 oxidation of OCl^- (+16, +17, and +20‰) but were somewhat higher than those of ClO_4^- from O_3 oxidation of ClO_2^- (+ 12 ‰ and + 13 ‰). However, the $\delta^{18}\text{O}$ values of ClO_4^- formed in the ClO_2 (aq) experiments (+ 23 ‰ to + 28 ‰) were higher than the $\delta^{18}\text{O}$ values of ClO_4^- from both O_3 oxidation of OCl^- and ClO_2^- : (+ 1 ‰, + 2 ‰, and + 11 ‰) and (+ 2 ‰ and + 4 ‰), respectively. It is not possible to evaluate the likelihood of O source mixing, fractionation, and/or O exchange in the ClO_2 (aq) experiments as ^{18}O isotopes for the starting ClO_2 (aq) were not measured.

UV-Hypochlorite

Photodecomposition of OCl^- produced a ClO_4^- with near zero $\Delta^{17}\text{O}$ values (-0.0 ‰ to + 0.5 ‰) and the lowest $\delta^{18}\text{O}$ values (- 19 ‰ to - 22 ‰) out of all the UV experiments. ClO_4^- pathways proposed for UV oxidation of OCl^- (Figure 2.5.24) indicate at least five O sources are available for ClO_4^- formation: initial OCl^- , $\text{O}(^3\text{P})$, OH, OCl , and H_2O . Initial OCl^- and H_2O had low $\delta^{18}\text{O}$ values (-28 ‰ and -6.9‰, respectively), but the $\Delta^{17}\text{O}$ and $\delta^{18}\text{O}$ values of $\text{O}(^3\text{P})$, OH, and OCl are not available, thus a proper evaluation of the percentage of O in ClO_4^- from the different O sources cannot be made.

UV-Chlorite

The photolysis of ClO_2^- led to the production of ClO_4^- with $\Delta^{17}\text{O}$ values relatively close to zero (- 1 ‰ to -2 ‰) but with high $\delta^{18}\text{O}$ values (+ 42 ‰ to + 46 ‰). Only three O sources were identified in the proposed ClO_4^- mechanisms (Figure 2.5.25) as available for ClO_4^- formation from UV exposure to ClO_2^- : initial ClO_2^- , the OCl radical, and H_2O . Because there is lack of information related to the $\delta^{18}\text{O}$ values of the OCl radical, that might have been an intermediate product in the experiment, it is not possible to determine the likelihood of mixing between these three O sources. However, because the $\delta^{18}\text{O}$ values of initial ClO_2^- (- 2.5 ‰) and H_2O (- 6.9 ‰) were both below zero it can be deduced that for the ClO_4^- formed to be a result of mixing of the O sources, the $\delta^{18}\text{O}$ value of the OCl radical would have to be higher than the $\delta^{18}\text{O}$ values of the ClO_4^- reagent or that there was substantial O isotope fractionation.

UV-Chlorine Dioxide

The photodecomposition of ClO_2 (aq) resulted in ClO_4^- with $\Delta^{17}\text{O}$ values near zero (+ 0.9 ‰ and +1.3‰) and with $\delta^{18}\text{O}$ values (+ 9 ‰ to +13 ‰) higher than those of the OCl^- experiments (- 19‰ to -22‰) but lower than those of the ClO_2^- experiments (+ 42 ‰ to + 46 ‰). Two initial O sources were available in the UV ClO_2 (aq) experiments: initial ClO_2 (aq) and H_2O . The $\delta^{18}\text{O}$ values for initial ClO_2 are not available and thus a proper evaluation of mixing of the O sources cannot be made. One conclusion that can be drawn is that the $\delta^{18}\text{O}$ values of initial ClO_2 (aq)

would have to be higher than the $\delta^{18}\text{O}$ values of H_2O and ClO_4^- for mixing to be responsible for the ClO_4^- $\delta^{18}\text{O}$ values.

2.5.4.13 Fractionation

There was not enough information in the UV experiments to form a thorough evaluation of the $\delta^{18}\text{O}$ values of ClO_4^- formed from oxidation of all ClO_x species (OCl^- , ClO_2^- , and $\text{ClO}_2(\text{aq})$), but given the mixing $\delta^{18}\text{O}$ results, it appears that the $\delta^{18}\text{O}$ values for ClO_4^- in the O_3 experiments are in line with simple mass-dependent fractionation where ClO_4^- gets lighter than would be expected given the maximum $\Delta^{17}\text{O}$ site preference value of O_3 (+ 37 ‰). It is possible that ClO_4^- $\delta^{18}\text{O}$ values in O_3 experiments were lower due the continuous input of O_3 into the reaction vessels. Fractionation would dictate that the lighter O isotope would react first and thus continuous input would purge out the already reacted O_3 , allowing for a cycle of the lighter O isotope of the new O_3 to keep reacting.

Kinetic isotope fractionation would result in a large fractionation effect, depending on the pathway leading to ClO_4^- , the reaction rates of reactions involved, and the bonds of species being broken or formed in each reaction (Kendal et al., 2011). Not all reaction rates for reactions in the proposed ClO_4^- formation mechanisms (Figure 2.5.16–2.5.23) are known and reaction sequences are speculative, thus it is not possible to determine if $\delta^{18}\text{O}$ values of ClO_4^- resulted from kinetic fractionation and/or equilibrium isotope exchange reactions.

Implications of $\delta^{37}\text{Cl}$

With the exception of the O_3 dry Cl^- experiments the $\delta^{37}\text{Cl}$ values of ClO_4^- formed in both aqueous UV and O_3 experiments were higher than the $\delta^{37}\text{Cl}$ values of the source species (Cl^- , OCl^- , ClO_2^- , and ClO_2) (Figures 2.5.5–2.5.12). The $\delta^{37}\text{Cl}$ values of ClO_4^- formed in the UV experiments were generally higher than the $\delta^{37}\text{Cl}$ values of ClO_4^- produced in the O_3 experiments, but ClO_4^- $\delta^{37}\text{Cl}$ values from the different photolyzed ClO_x species were similar to one another (Figure 2.5.15). In the O_3 experiments the $\delta^{37}\text{Cl}$ values of ClO_4^- appear to be roughly correlated with the oxidation state of the Cl in the reactant species, with the only exception being the $\delta^{37}\text{Cl}$ values of ClO_4^- from the ClO_2^- experiments.

The high $\delta^{37}\text{Cl}$ values of ClO_4^- produced in the UV and O_3 experiments may have been influenced by equilibrium or kinetic fractionations between different aqueous ClO_x species. Mixing calculations are not possible due to the lack of ^{37}Cl isotope data for all possible Cl sources in both UV and O_3 experiments, but it is hypothesized that because $\delta^{37}\text{Cl}$ values of ClO_4^- produced in all aqueous O_3 and UV experiments were relatively high, that the $\delta^{37}\text{Cl}$ values of the Cl sources would need to be relatively high as well for mixing to have occurred while in the O_3

dry Cl^- experiment, the $\delta^{37}\text{Cl}$ values of the Cl source would be expected to be below zero. Given that our source Cl was typically near zero, it is unlikely that it had an impact on our $\delta^{37}\text{Cl}$ values.

Kinetic Cl isotope fractionation factors related to photodecomposition or O_3 oxidation of Cl^- , OCl^- , ClO_2^- , and ClO_2 have not been experimentally determined. Schauble et al.⁴⁹ determined that under equilibrium conditions at 298 K, $\delta^{37}\text{Cl}$ values of coexisting ClO_x species were possibly correlated with Cl oxidation state: Cl^{-1} , Cl^0 , Cl^{+1} , Cl^{+2} , Cl^{+3} , Cl^{+4} , and Cl^{+7} can concentrate ^{37}Cl approximately by +2.5 ‰ to +6 ‰, +7 ‰, +7 ‰ to +9 ‰, +10 ‰, +27 ‰, and +75 ‰, respectively. Any reversible reaction in the proposed ClO_4^- mechanisms for either UV or O_3 processes (Figures 2.5.16–2.5.26) has the potential to have experienced equilibrium isotope exchange. Although it is not known if the proposed reversible reactions (Table 2.5.4: Rxns 1, 3 – 4; and UV Rxn's 5 and 26) reached full equilibrium, even if only partial equilibrium occurred, the $\delta^{37}\text{Cl}$ values of ClO_4^- produced in the aqueous UV (+17 ‰ to +23 ‰) and O_3 (+5 ‰ to +17 ‰) experiments might be reasonable given the Cl isotope fractionations calculated by Schauble et al, 2003.

It is possible that some of the proposed reactions may have created intermediate species that were then consumed by multiple branching reactions with different isotope effects, continuously getting heavier and thus forming heavier ClO_4^- . One example of this is reaction 4 (Table 2.5.4) from the O_3 proposed mechanisms, a reaction for which no forward or reverse reaction rates are known. If ClO_2 was converted to ClO_3 with relatively little kinetic isotope fractionation while also being consumed by another reaction with a larger kinetic fractionation, the $\delta^{37}\text{Cl}$ of ClO_3 could increase rapidly and thus produce ClO_4^- with high $\delta^{37}\text{Cl}$ values. This is purely hypothesized but illustrates that high $\delta^{37}\text{Cl}$ ClO_4^- could be produced in a complex reaction network.

Schauble et al., 2003 also suggested that under equilibrium some molecules could have different affinities for the heavier isotopes, thus it is also possible that molecules that break apart to form two or more species could result in one product species being heavier than the other, depending on the location of the heavy isotope. This would be more applicable to the UV experiments as all ClO_4^- pathways proposed go through the same final reaction sequence (Figures 2.5.24–2.5.26; rxn's 41–43) that ends up in the Cl_2O_6 species being hydrolyzed to produce ClO_4^- and ClO_3^- . In this reaction (Rxn 43) the ^{37}Cl isotope may be located in the Cl_2O_6 species in such a way that when hydrolyzed, always ends up in ClO_4^- . Once formed ClO_4^- is not known to further react thus we do not know if this phenomenon is possible outside of equilibrium.

Given the high $\delta^{37}\text{Cl}$ values of ClO_4^- from the aqueous UV and O_3 experiments and the low $\delta^{37}\text{Cl}$ values of ClO_4^- from the O_3 dry Cl^- experiments, it appears that heterogeneous surfaces can undergo different isotope fractionation processes than do homogenous surfaces. The low $\delta^{37}\text{Cl}$

value of ClO_4^- produced from Cl^- in the dry UV experiments implies kinetic fractionations were more important than equilibrium effects in the dry system.

Relation to Natural ClO_4^-

All ClO_4^- generated in the UV and O_3 aqueous experiments was as heavy as or heavier in $\delta^{37}\text{Cl}$ than natural ClO_4^- (Figure 2.5.28). Our ClO_4^- $\delta^{37}\text{Cl}$ isotope data further suggest that aqueous production mechanisms produce ClO_4^- that is enriched in ^{37}Cl whereas dry production mechanisms produce ClO_4^- depleted in ^{37}Cl . Given this information, if aqueous reactions were solely responsible for ClO_4^- production in the atmosphere and for natural ClO_4^- , then it would mean that precursor species, prior to ClO_4^- formation, would need to have considerably lower $\delta^{37}\text{Cl}$ values than Atacama ClO_4^- , which has the lowest reported $\delta^{37}\text{Cl}$ values of any substance on Earth (Böhlke et al., 2005). Although it is possible that an unknown precursor species exists on Earth that is much lighter in $\delta^{37}\text{Cl}$ than Atacama ClO_4^- , it is difficult to conceive an atmospheric production process that is purely dependent upon aqueous reactions. Given the lower $\delta^{37}\text{Cl}$ values of ClO_4^- from the O_3 dry Cl^- experiments and those of natural ClO_4^- , it is more likely that natural ClO_4^- is a result of dry (heterogeneous) atmospheric reactions (Figure 2.5.28). Dry production mechanisms could potentially start with a precursor species with high $\delta^{37}\text{Cl}$ values, as high as those reported for species found on Earth, and would end up producing a ClO_4^- with lower $\delta^{37}\text{Cl}$ values, a finding that is more consistent with the reported $\delta^{37}\text{Cl}$ values of natural ClO_4^- .

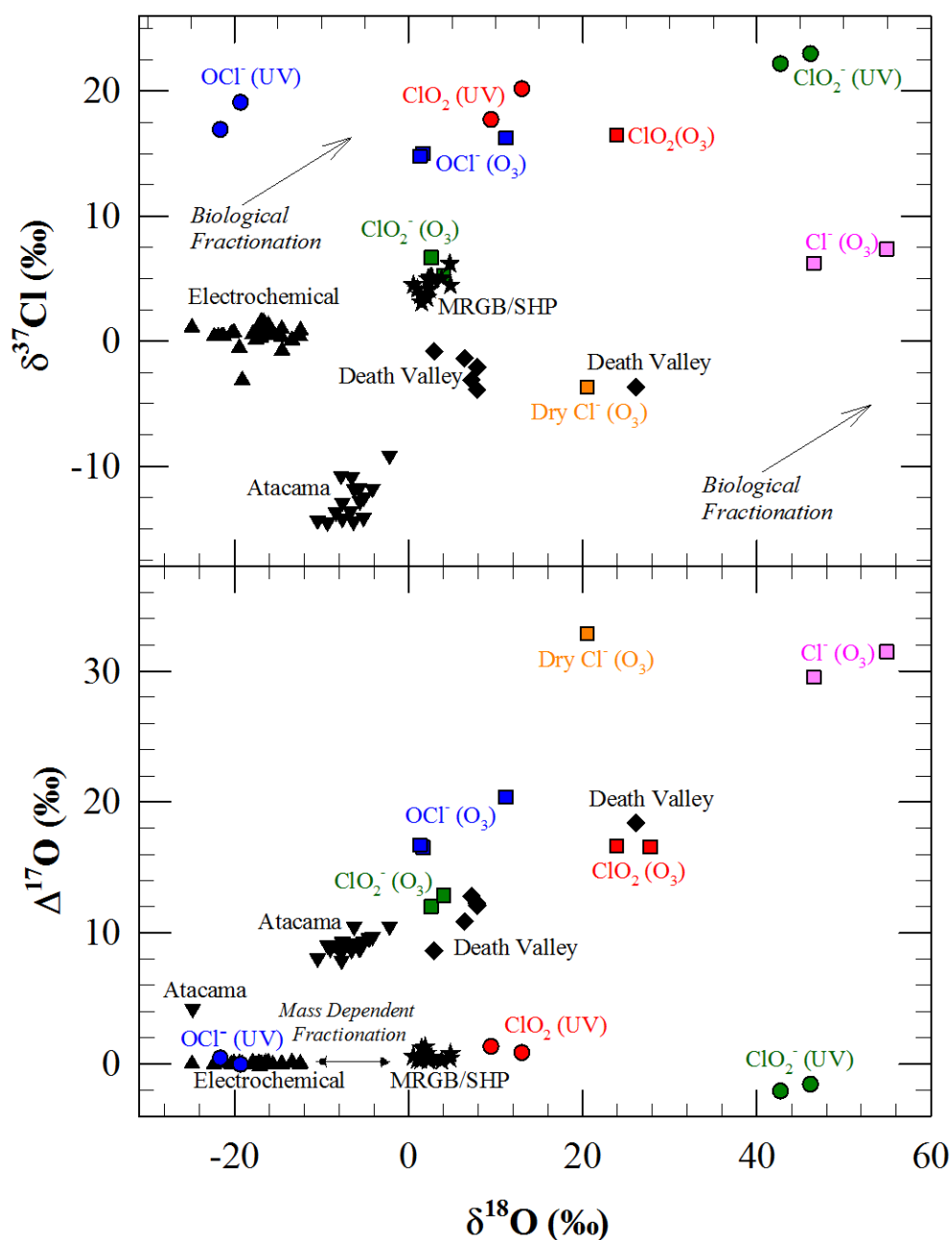


Figure 2.5.28. Summary of isotope data for ClO_4^- produced in the O_3 (square symbols) and UV (circle symbols) generation experiments. Species labels next to the ClO_4^- symbols represent the precursor species from which ClO_4^- was produced. Generation data is displayed with previously published isotope data for ClO_4^- produced electrochemically (Böhlke et al., 2005) or found in natural samples from: (1) SHP and MRGB of western Texas and central New Mexico (Jackson et. al., 2010; Section 2.2 this report; Böhlke et al., 2005), respectively, (2) Atacama Desert, Chile (Böhlke et al., 2005, Bao and Gu, 2004) and (3) Death Valley (Jackson et. al., 2010; Section 2.1 and 2.3 this report).

All the $\delta^{18}\text{O}$ and $\Delta^{17}\text{O}$ values of ClO_4^- produced in the O_3 experiments fell along a diagonal, positive line indicating different mixing reactions between O_3 and other O sources along with possible fractionation and/or isotope exchange (Figure 2.5.28). Our O_3 experiment $\delta^{18}\text{O}$ and $\Delta^{17}\text{O}$ isotope data is consistent with the trend observed between $\delta^{18}\text{O}$ and $\Delta^{17}\text{O}$ values of ClO_4^- found in Death Valley and the Atacama caliche, indicating that ClO_4^- in these regions consistent with O_3 production mechanisms (Figure 2.5.28). ClO_4^- from the UV experiments did not have positive $\Delta^{17}\text{O}$ values but the $\delta^{18}\text{O}$ values largely bracketed the $\delta^{18}\text{O}$ values observed for MRGB/SHP ClO_4^- , indicating that indigenous ClO_4^- in this region could be consistent with UV production mechanisms (Figure 2.5.28). Coincidentally, natural ClO_4^- that is consistent with O_3 production mechanisms (Atacama and Death Valley) had negative $\delta^{37}\text{Cl}$ values while natural ClO_4^- that is consistent with UV mechanisms (MRGB/SHP) had positive $\delta^{37}\text{Cl}$ values. Because concentrations and isotopic compositions of precursor species likely vary in the Earth's atmosphere, we cannot account for which precursor species was actually responsible for each type of natural ClO_4^- found on Earth.

Uncertainty Related to $\Delta^{17}\text{O}$ and $\delta^{18}\text{O}$ Measurements

Oxygen isotopes ratios in our study were analyzed using two IRMS methods: (1) the CO continuous-flow isotope-ratio mass spectrometry (CO-CFIRMS) method which is used to measure $\delta^{18}\text{O}$ and (2) the O_2 dual-inlet isotope-ratio mass spectrometry (O2-DIIRMS) method which is used to measure $\delta^{17}\text{O}$ and $\delta^{18}\text{O}$ (Bohlke et al., 2016). The average difference between $\delta^{18}\text{O}$ values from each method was 1.55 ± 1.29 ‰. Only the $\delta^{18}\text{O}$ values obtained from the O2-DIIRMS method were reported and used for $\Delta^{17}\text{O}$ calculations in this study as $\delta^{18}\text{O}$ values from the CO-CFIRMS method were not available for all species.

$\Delta^{17}\text{O}$ values are also considered an effect of different equations and different coefficients/exponents (λ) (Table 2.5.5). Many definitions of $\Delta^{17}\text{O}$ have been formulated, with the coefficient (λ) ranging from 0.50 – 0.53 depending on the type of conditions and processes being observed, and can result in different $\Delta^{17}\text{O}$ values (Table 2.5.5) (Miller et al., 2002; Cliff et al., 1997; Farquhar et al., 1999; Luz et al., 2005). In our study we adopted the definition of Miller et al., 2002 and assumed a λ value of 0.525. Because $\Delta^{17}\text{O}$ variations in values of ClO_4^- from the UV experiments are small, we must consider the variability in $\Delta^{17}\text{O}$ values of ClO_4^- had we used other definitions. The $\Delta^{17}\text{O}$ values of ClO_4^- calculated using different definitions of $\Delta^{17}\text{O}$ and λ range of 0.50 – 0.53 are reported in Table 2.5.5 and indicate that the photodecomposition of OCl^- might be the only process associated with solely mass-dependent fractionation, as it was the only experiment for which replicates had values near zero (greater than -0.5 ‰ but less than 0.5‰). Regardless of the definition, it appears that $\Delta^{17}\text{O}$ values of ClO_4^- from the UV ClO_2^- and ClO_2 (aq) experiments are truly negative and positive, respectively, indicating some mass-independent fractionation (Table 2.5.5).

Table 2.5.5. Calculated $\Delta^{17}\text{O}$ values of ClO_4^- produced in the UV experiments using the coefficient (λ) range of 0.50 – 0.53 in the various definitions of $\Delta^{17}\text{O}$.

Definition/Equation	Reference	Possible Range in $\Delta^{17}\text{O}$ Values of ClO_4^- in UV Experiments (‰)					
		OCI^-		ClO_2^-		ClO_2	
		Rep 1	Rep 2	Rep 1	Rep 2	Rep 1	Rep 2
^b $\Delta^{17}\text{O} = k = \frac{(1 + \delta^{17}\text{O})}{(1 + \delta^{18}\text{O})^k} - 1$	Miller, 2002	(-0.52) – (+0.07)	(-0.10) – (+0.56)	(-1.02) – (-2.28)	(-0.43) – (-1.78)	(+1.20) – (+0.81)	(+1.57) – (+1.28)
^a $\Delta^{17}\text{O} = \delta^{17}\text{O} - (\lambda \times \delta^{18}\text{O})$	Cliff and Thiemens, 1997 Thiemens, 1999	(-0.56) – (+0.02)	(-0.15) – (+0.49)	(-1.27) – (-2.55)	(-0.70) – (-2.08)	(+1.19) – (+0.79)	(+1.56) – (+1.28)
^a $\Delta^{17}\text{O} = (1 + \delta^{17}\text{O}) - (1 + \delta^{18}\text{O})^\lambda$	Farquhar et al., 1999	(-0.51) – (+0.07)	(-0.10) – (+0.55)	(-1.04) – (-2.32)	(-0.44) – (-1.82)	(+1.21) – (+0.82)	(+1.58) – (+1.29)
^b $^{17}\Delta = \ln(k + 1) = \ln(1 + \delta^{17}\text{O}) - \lambda \times \ln(1 + \delta^{18}\text{O})$	Luz and Barkan, 2005	(-0.52) – (+0.07)	(-0.10) – (+0.56)	(-1.02) – (-2.28)	(-0.43) – (-1.78)	(+1.20) – (+0.81)	(+1.57) – (+1.28)

^a Traditional definition which indicates deviation from a point on reference mass-dependent fractionation (MDF) line (Farquhar et al., 1999; Miller, 2002; Assonov and Brenninkmeijer, 2005)

^b This definition characterizes a specific mass-dependent fractionation (MDF) line, where $^{17}\Delta$ is the ordinate intercept (Miller, 2002; Luz and Barkan, 2005; Assonov and Brenninkmeijer, 2005)

2.5.5 Conclusions

This study presents proposed reaction mechanisms for the formation of ClO_4^- , with distinct isotopic compositions ($\delta^{37}\text{Cl}$, $\delta^{18}\text{O}$, and $\Delta^{17}\text{O}$), via O_3 oxidation and UV photolysis. While no new UV production pathways were introduced, we were able to partially constrain O_3 formation pathways based on the number of O atoms in ClO_4^- coming from O_3 , as indicated by $\Delta^{17}\text{O}$ values. The mechanisms proposed are ambiguous and there is still much information missing related to the intermediate species as well as the reaction rates for most of the reactions proposed.

Our findings suggest that ClO_4^- formed from oxidation (UV and O_3) of various ClO_x species is a result of mixing between ClO_4^- formed from branching pathways along with some fractionation, with UV ClO_4^- isotope data suggesting mass-dependent fractionation and O_3 ClO_4^- isotope data being more consistent with mass-independent variation. There is also evidence to suggest that oxidation of ClO_x species on a heterogeneous (dry) surface has different fractionation effects than oxidation of fully aqueous ClO_x species.

From the $\Delta^{17}\text{O}$ values of ClO_4^- formed in the O_3 experiments we were able to show a large O_3 position effect, indicating that the heavy isotope is preferentially located in the terminal O atoms in O_3 and that the terminal O atoms were preferentially incorporated into ClO_x compounds. $\Delta^{17}\text{O}$ values of ClO_4^- were approximately related to the number of O atoms added from O_3 and indicated a stepwise reduction in the contribution of O atoms from O_3 into ClO_4^- based on increasing oxidation state of Cl in precursor species. In addition, the $\Delta^{17}\text{O}$ data for the O_3 experiments indicated large quantities of ClO_3^- were produced by a process that was not involved in production of ClO_4^- , meaning that ClO_3^- was not the major precursor for ClO_4^- in the O_3 experiments. The $\delta^{37}\text{Cl}$ of ClO_4^- was generally higher than precursor $\delta^{37}\text{Cl}$ values in all experiments and was possibly a result of partial equilibrium reactions.

Although our experiments may not reflect natural conditions, they were successful in producing Cl and O isotopic variations in ClO_4^- that incorporate much of the reported variation in nature. The low $\delta^{37}\text{Cl}$ in Atacama ClO_4^- was not reproduced, but all other variations were. All other isotopic data suggests that ClO_4^- indigenous to Atacama and Death Valley and ClO_4^- from MRGB/SHP are consistent with an O_3 and a UV related ClO_4^- mechanism, respectively. Unfortunately we cannot determine which precursor species were involved in the formation of ClO_4^- in each of these regions. Our experiments showed that final ClO_4^- isotopic composition is dependent on the precursor species oxidized and given the global variations in precursor species in this planetary system, we cannot say for sure if ClO_4^- formed through mechanisms in our atmosphere would be the same. The reaction rates and intermediate species proposed to be involved in ClO_4^- formation require further study mixing, isotope exchange, and/or fractionation may be important during the formation process. More generation experiments involving

oxidation of other precursor species other than Cl^- , on a heterogeneous surface or gas phase would provide additional information to resolve ambiguities such as $\delta^{37}\text{Cl}$ of Atacama ClO_4^- .

2.6 Evaluation of Bacterial Production of Perchlorate

2.6.1 Background

One potential production mechanism for natural ClO_4^- that has not been previously evaluated is microbiological generation. Nitrifying bacteria generate nitrate through the oxidation of NH_4 (e.g., *Nitrosomonas* spp.) and NO_2^- (e.g., *Nitrobacter* spp.) (Paerl, 1997). During this well-studied process, NH_4 serves as a microbial electron donor and oxygen as an electron acceptor (Capone, 1997). There are also anaerobic oxidation processes by which NO_3^- is biologically generated from reduced nitrogen species. Moreover, a class of widely occurring haloperoxidase enzymes produced by specific fungi, algae, and bacteria are known to oxidize Cl^- to hypochlorous acid (HClO) (Griffin, 1991; Vilter, 1995). This could represent an initial biological step in the production of natural ClO_4^- in some environments (possibly followed by additional photochemical or biological reactions). We should also note that the oxygen isotope ratios reported for ClO_4^- in West Texas are similar to those of biologically generated NO_3^- , which incorporates O from H_2O and O_2 during microbial oxidation of NH_4 (Hollocher et al., 1983; Kumar et al., 1983; Amberger and Schmidt, 1987; Böhlke et al., 2005). Thus, isotopic evidence supports the possibility of biologically generated ClO_4^- . During this task, we evaluated whether microbial generation of ClO_4^- (as well as HClO , ClO_2^- , and ClO_3^-) is possible in an aerobic environment.

2.6.2 Initial Studies using Haloperoxidase Enzymes and Natural Sunlight

Experiments were conducted to evaluate whether specific haloperoxidase enzymes could produce ClO_4^- during the oxidation of chloride (Cl^-), both in the presence and absence of ultraviolet (UV) light from natural sunlight. Haloperoxidases combine hydrogen peroxide (H_2O_2) with halides (e.g., Cl^- , I^- , Br^-) to form corresponding hypohalous acids (e.g., HClO from Cl^-) (Griffin, 1991; Vilter, 1995). Various microbial and plant species utilize this reaction as a protection mechanism from microbial pathogens (i.e., via acid formation) and as a means to chemically decompose complex polymers (Butler and Carter-Franklin, 2004). Initial experiments were conducted to determine if specific haloperoxidase enzymes could produce ClO_4^- during the oxidation of Cl^- , both in the presence and absence of UV light. Follow-on studies were conducted to better refine conditions of ClO_4^- generation. To our knowledge the potential for these enzymes to produce ClO_4^- , either as a minor side reaction, or through the subsequent interaction of the biologically-generated HClO with UV light, has never been evaluated

2.6.2.1 Methods

Enzymes and buffer

Two different haloperoxidase enzymes were initially tested. The first enzyme was a vanadium-based chloroperoxidase (VCP) derived from *Curvularia inaequalis*. A small aliquot of dried (~3 mg) VCP was provided to CB&I as gift by Tatyana Polenova at the University of Delaware. The entirety of this enzyme was suspended in 30 μ l of assay buffer (see below). Only enough enzyme was available for a single experiment. The units of activity/ml for this preparation was not available. The second enzyme used was a iron-based chloroperoxidase derived from the filamentous fungus *Caldariomyces fumago* (FCP). This well-studied haloperoxidase was obtained from Sigma-Aldrich (St. Louis, MO). For initial experiments, this enzyme was suspended in assay buffer to an activity level of 7,000 units/ml. The assay buffer was prepared by first running distilled water through a column bed filled with Purolite A530E ion exchange resin to remove traces of ClO_4^- from the laboratory water. Potassium phosphate (100 mM) and potassium chloride (50 mM) were then added to the water and the pH was adjusted to 5.0 with HCl.

Experimental design

A standard enzyme reaction consisted of 7,000 units of enzyme/ml assay buffer with 20 mM H_2O_2 . The reactions were performed in 3 ml volumes ~5 ml quartz tubes (which do not block UV light) sealed with screw caps with a Teflon liner. In general, the enzyme was added as the final step. Deviations from this standard setup are noted in the results as appropriate. A number of controls were utilized to define the baseline level of ClO_4^- in the test samples. The individual components (buffer, H_2O_2 , and diluted enzyme) were analyzed separately. Furthermore, mixtures of the components (buffer + enzyme and buffer + H_2O_2) were also prepared and analyzed. Once all the additions were made, some samples were placed in the dark and incubated at 37°C, and others were incubated outdoors in direct sunlight for UV exposure. The temperature of the UV-exposed samples varied with the daily conditions. During the four initial experiments conducted, the influence of enzyme type, enzyme concentration, UV exposure, and H_2O_2 concentration on the enzymatic production of ClO_4^- were assessed. Results are detailed below.

Analysis

At the conclusion of each experiment, samples were analyzed for ClO_4^- in the laboratory of Andrew Jackson at Texas Tech University using IC/MS/MS as described previously in this report. The detection limit for ClO_4^- by this technique is ~ 0.05 $\mu\text{g/L}$.

2.6.2.2 Results and Discussion

All of the components that comprise the complete reaction mixture were analyzed for the presence of ClO_4^- as separate entities (buffer, H_2O_2 , and the enzyme mix diluted in water). The H_2O_2 had the highest levels of ClO_4^- (1.88 $\mu\text{g/L}$), while the diluted enzyme and buffer had much

lower concentrations (0.33 and 0.08 $\mu\text{g/L}$ respectively). The contribution of ClO_4^- from the H_2O_2 in the reaction mixture is $\sim 1000\times$ less than the reported concentration due to dilution (i.e., only 0.002 $\mu\text{g/L}$). Based on the initial results, the background ClO_4^- concentration in the typical reaction mixture should equal $\sim 0.4 \mu\text{g/L}$ or less.

In the initial study with vanadium chloroperoxidase (VCP), production of ClO_4^- was not apparent when samples were incubated in the dark, but there was an increase in ClO_4^- in those incubated for ~ 8 h in sunlight (Table 2.6.1). The mean ClO_4^- concentration in the samples exposed to UV light (Full rxn – light in Table 2.6.1) was 0.86 $\mu\text{g/L}$ whereas that in the samples remaining in the dark was 0.32 $\mu\text{g/L}$, which is similar to the control samples run for the study. It should be noted, however, that there was appreciable variability in the UV exposed samples, and the results were not statistically different from other samples. No additional enzyme was available to repeat this study.

In the subsequent experiments, Sigma-Aldrich fungal iron chloroperoxidase (FCP) enzyme was used. In the initial study, production of ClO_4^- was evaluated in the presence and absence of UV light (Table 2.6.2). These data again showed significant variability among treatments, with mean ClO_4^- concentrations ranging from 0.3 to 0.8 $\mu\text{g/L}$. The enzyme reaction performed in sunlight yielded higher ClO_4^- than that performed in the dark ($0.61 \pm 0.09 \mu\text{g/L}$ vs $0.27 \pm 0.08 \mu\text{g/L}$, respectively), but both values were lower than that with buffer and H_2O_2 alone (i.e., no enzyme) at $0.76 \pm 0.46 \mu\text{g/L}$. In a subsequent study, the influence of H_2O_2 concentration on ClO_4^- production was evaluated. All reactions were exposed to sunlight for ~ 8 h. As shown in Table 2.6.3, the ClO_4^- concentrations ranging from ~ 1 to 4 $\mu\text{g/L}$ in this study, which is appreciably higher than in the two previous studies. However, the samples again showed significant variability between replicates. A control sample without enzyme or not exposed to sunlight was not tested in this case.

Table 2.6.1. Evaluation of perchlorate production from H₂O₂ and Cl⁻ with vanadium chloroperoxidase (VCP).

Sample	PC [ppb]	Range	N=
Buffer + enzyme - dark	0.31	0.19	2
Buffer + enzyme - light	0.30	0.18	2
Buffer + H ₂ O ₂ - dark	0.35	0.25	2
Buffer + H ₂ O ₂ - light	0.34	0.23	2
Full rxn - dark	0.32	0	2
Full rxn - light	0.86	0.6	2

Table 2.6.2. Evaluation of the influence of UV on perchlorate production by fungal iron chloroperoxidase.

Sample	ClO ₄ ⁻ [µg/L]	Range	N
Buffer + Enzyme	0.42	0.26	3
Buffer + H ₂ O ₂	0.76	0.46	3
Full rxn - dark	0.27	0.08	3
Full rxn - light	0.61	0.09	3

Table 2.6.3. Evaluation of the influence of H₂O₂ concentration on perchlorate production by fungal iron chloroperoxidase.

Sample	ClO ₄ ⁻ [µg/L]	Range	N
0.5 mM H ₂ O ₂	1.02	0.41	2
2.5mM H ₂ O ₂	2.2	1.2	2
12.5 mM H ₂ O ₂	3.96	2.9	2
62.5 mM H ₂ O ₂	2.85	3.3	2

All samples were exposed to sunlight and contained 7,000 units of enzyme

2.6.3 Controlled Studies using Haloperoxidase Enzymes, Produced UV and Sunlight

In previous studies, two haloperoxidase enzymes were tested for their ability to produce ClO_4^- in the presence/absence of sunlight and H_2O_2 . The data showed high variability, but provided some indication that ClO_4^- production was possible in samples incubated in sunlight with chloroperoxidase enzyme and H_2O_2 . During these studies, the key sources of variability were hypothesized to be as follows: (1) incubation outdoors in sunlight as a source of UV without temperature control and, (2) addition of high concentrations of hydrogen peroxide in batch, as excess may cause destruction of the enzymatically-generated HClO (or ClO^\cdot), which can subsequently be photochemically converted to ClO_4^- by UV (see Chapter 2.1 reactions with *hypochlorite* + UV). Additional studies were subsequently conducted under better controlled conditions in order to reduce variability. In particular, a Rayonet photochemical reactor was utilized in the laboratory to better control UV exposure time, UV wavelength, and reaction temperature. In addition, H_2O_2 was added to the samples continuously at a low concentration using a laboratory syringe pump in order to minimize excess.

An assay was conducted with monochlorodimedone to evaluate the activity of the various chloroperoxidase enzymes. In the presence of hydrogen peroxide, chloroperoxidase enzymes have been observed to convert monochlorodimedone to dichlorodimedone, which can then be monitored via spectroscopic analysis (Hager et al., 1966).

2.6.3.1 Materials and Methods: Perchlorate Formation Assays

Enzymes

The following enzymes were used in these studies: Chloroperoxidase from *Caldariomyces fumago* (10,717 U/mL) was obtained from Sigma-Aldrich (St. Louis, MO) and from Bio-Research Products, Inc (21,972 U/mL; North Liberty, IA); and soybean peroxidase (1,356 U/mg) was obtained from Bio-Research Products, Inc. (North Liberty, IA).

Buffers

Phosphate buffer was made using water purified via a Barnstead UV filtration system (Barnstead, Dubuque, IA), which was then further treated to remove any trace ClO_4^- by passing it through a column packed with Purolite A530E resin (Purolite, Bala Cynwyd, PA). The original buffer consisted of 100 mM potassium phosphate, dibasic (Fisher, Fair Lawn, NJ) plus 50 mM potassium chloride (Sigma-Aldrich). The phosphate buffer was later modified, with the modified buffer consisted of 10 mM potassium phosphate, dibasic, and 50 mM potassium chloride. The buffer pH was adjusted to pH 3.0, 5.0, or 7.0 using pure phosphoric acid (Fisher).

Experimental Design: UV Reactor. Triplicate chloroperoxidase enzyme assays were performed simultaneously by placing three quartz test tubes in a RAYONET photochemical chamber

reactor (Southern New England Ultra Violet Company, Branford, CT) equipped with two 300 nm UV bulbs. Tubes were placed approximately 45 mm away from the UV bulbs. Each tube contained an aliquot of peroxidase enzyme plus 2 mL phosphate buffer. Two lengths of Teflon® tubing were placed into each tube until they reached the bottom of the tube. One length of Teflon® tubing was attached to a peristaltic pump and was used to slowly bubble air through the buffer. The other length of Teflon® tubing was attached to a 20 mL plastic syringe containing buffer plus H₂O₂, which was metered into the test tubes at a rate of 0.083 mL/h (1 mL every 12 h). Experiments were conducted for 24 hours each. Samples were stored at 4°C until analysis.

Experimental Treatments

Experiments were performed in both 100 mM and 10 mM phosphate buffer at pH 3, pH 5, and pH 7. Controls consisted of experiments performed in the absence of H₂O₂, in the absence of enzyme, and in the absence of light (i.e., in the dark).

Sample Preparation. Upon initial sample analysis (see below), it was determined that the high levels of phosphate in the original buffer (containing 100 mM potassium phosphate) caused some interference with ClO₄⁻ analysis. A procedure was thus performed to reduce the amount of phosphate in the samples. First, the pH of the sample was raised to greater than pH 10 using a concentrated (10 N) sodium hydroxide solution. Twenty microliters of 5 M calcium chloride was then added per mL of sample. This caused the immediate precipitation of solid calcium phosphate, which was then removed from the samples by filtration through a 0.2 micron filter.

Experimental Design: Natural Sunlight

100 mM phosphate buffer was used in these studies as described above, except that buffer pH was adjusted to 2.75. A benchtop rotary shaker was placed outside in direct sunlight for UV exposure. A plastic tub containing ice packs was placed on the shaker. Eight 55 mm diameter quartz petri dishes (Technical Glass Products, Painesville, OH) were placed on top of the ice packs. Each dish contained 5 mL 100mM phosphate buffer, hydrogen peroxide (final concentration 0.5 - 2 mM), and chloroperoxidase enzyme (final concentration 0.2 µg/mL). A quartz glass lid was placed on each dish, and four of the dishes were covered with aluminum foil to serve as no sunlight (i.e., dark) controls. The shaker was operated at 50 rpm for a period of four hours. Thermometers were used to measure both the temperature on the ice packs and the ambient outside temperature. Samples were removed at 2 h and 4 h and analyzed for perchlorate as previously described.

2.6.3.2 Materials and Methods: Monochlorodimedone (MCD) Assays

Buffers and Solutions

100 mM phosphate buffer was as described above for the sunlight studies, with the buffer pH was adjusted to 2.75. MCD solution was made by adding 3.62 mg of MCD (Bio-Research) per

mL to a 95% ethanol solution (e.g. 95% ethanol, 5% water). Peroxide solution consisted of 0.06 M hydrogen peroxide (Fisher) in water.

Experimental Procedure

A quartz cuvette containing 1 mL of phosphate buffer (100 or 10 mM) containing MCD (final concentration 0.0181 mg/mL) and H₂O₂ (final concentration 0.5 - 2 mM) was placed in the chamber of a Thermo Spectronic Genesys 2 Spectrophotometer (Thermo Scientific, Waltham, MA). The spectrophotometer was set to measure absorbance at 278 nm (A₂₇₈) every 5 sec. Chloroperoxidase enzyme (Bio Research; final concentration 1 µg/mL) was added immediately after absorbance measurements were initiated. A negative control experiment was performed in which enzyme was omitted (i.e., no enzyme control).

2.6.3.3 Results and Discussion

UV Light Source Experiments

Results of experiments performed using artificially generated UV light are presented in Table 2.6.4. Perchlorate levels in the experimental treatments were similar to those detected in the buffer alone, indicating that no significant ClO₄⁻ formation occurred. The background ClO₄⁻ concentration observed in the buffer is most likely a contaminant present in the phosphoric acid used to adjust the pH of the buffer.

MCD Assays

Results of MCD assays are presented in Figure 2.6.1. A rapid decrease in absorbance was observed when 2 mM peroxide and 100 mM phosphate buffer was used, indicating a reduction in monochlorodimedone concentrations as it is converted to dichlorodimedone (Hager et al., 1966). Significant decreases in A₂₇₈ were also observed when 2 mM peroxide and 0.01 M phosphate buffer (i.e., 1/10 strength phosphate buffer) and 1 mM phosphate buffer and 0.01 M phosphate buffer (i.e., 1/10 strength phosphate buffer and ½ strength peroxide) were used. MCD disappearance was significantly diminished when peroxide concentrations of 50 mM or less were used.

Natural Sunlight Experiments

Results of experiments performed using natural sunlight are presented in Table 2.6.5. Perchlorate levels in the experimental treatments (i.e., those exposed to natural sunlight) were similar to those detected in the controls, which were not exposed to light, indicating that no significant ClO₄⁻ formation was detected.

The results of the MCD assays indicated that the peroxidase enzymes being used in these studies were active under the study conditions used (i.e., at the testing buffer concentrations and pH),

and that their activity was rapid, with optimal MCD degradation occurring within the first 10 minutes of incubation. However, despite this, no significant ClO_4^- was formed when assays were exposed either to artificial UV light or to natural sunlight. The reason for this failure to produce ClO_4^- is unclear, but possible reasons include the inability of the peroxidase enzymes tested to produce significant hypochlorous acid, or rapid breakdown of that acid under test conditions before UV-mediated conversion to ClO_4^- . The chloroperoxidase experiments were concluded at this point. It is possible that low levels of ClO_4^- are generated via this mechanism in nature, but unlikely that this is a significant source of natural ClO_4^- in the environment.

Table 2.6.4. Perchlorate levels ($\mu\text{g/L}$) in UV light experiments.

		Perchlorate ($\mu\text{g/L}$)						
Buffer Used	pH	ClO_4^- in Buffer	Control Treatments			Experimental Treatments		
			No UV control	No enzyme control	No peroxide control	Fumago CPO (Sigma)	Fumago CPO (BR)	SBP (BR)
100 mM PO_4 buffer	5	$0.18 \pm 0.16^{* \wedge}$	ND	ND	ND	$0.23 \pm 0.28^*$	$0.14 \pm 0.12^*$	<0.26
100 mM PO_4 buffer	7	$0.48 \pm 0.59^{* \wedge}$	ND	ND	ND	$0.35 \pm 0.49^*$	$0.55 \pm 0.61^*$	$0.19 \pm 0.21^*$
10 mM PO_4 buffer	3	$3.44 \pm 0.03^{\wedge}$	ND	ND	ND	3.78 ± 0.04	ND	3.75 ± 0.11
10 mM PO_4 buffer	5	$0.15 \pm 0.15^*$	0.28 ± 0.01	0.41 ± 0.18	0.36 ± 0.13	0.70 ± 0.60	ND	0.42 ± 0.09
10 mM PO_4 buffer	7	<0.25	ND	ND	ND	$0.53 \pm 0.81^*$	ND	0.46 ± 0.18

Values are the average of triplicate samples +/- 1 standard deviation unless otherwise indicated
 *Value includes both detected and non-detected values. For non-detected values, one-fourth of the PQL was used in calculations
[^]Values are the average of duplicate samples +/- 1 standard deviation

Table 2.6.5. Perchlorate levels ($\mu\text{g/L}$) in natural sunlight experiments.

	2 hours		4 hours		sample temperature ($^{\circ}\text{C}$)
	Light	Dark	Light	Dark	
samples on ice	0.37 ± 0.03	0.35 ± 0.04	0.39 ± 0.07	0.39 ± 0.02	17 ± 5
samples at ambient temperature	0.45 ± 0.08	0.66 ± 0.15	0.60 ± 0.05	0.57 ± 0.04	39 ± 9

Perchlorate values in $\mu\text{g/L}$
 Perchlorate values are the average of duplicate values +/- one standard deviation

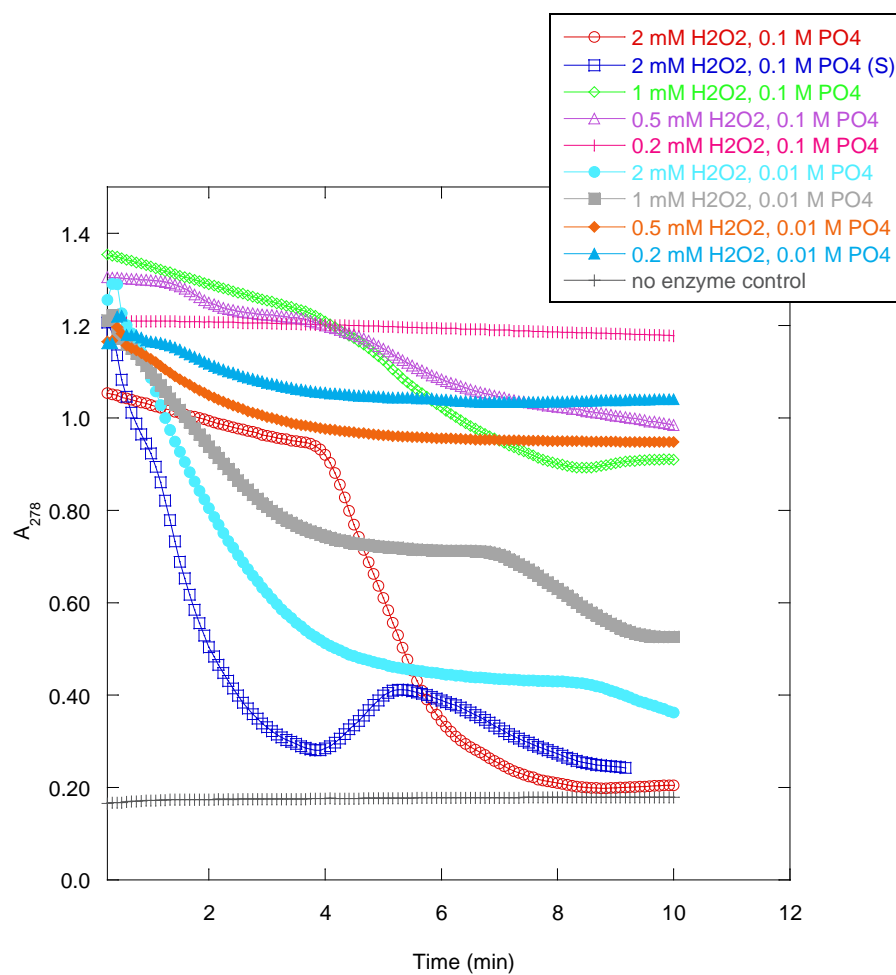


Figure 2.6.1. Results of MCD assays. Decreases in A_{278} indicate the loss of monochlorodimedone as it is converted to dichlorodimedone (Hager et al., 1966).

2.6.4 Perchlorate Formation under Nitrifying Conditions

2.6.4.1 Background

The potential for ClO_4^- generation by nitrifying bacteria was tested in a series of laboratory studies. The goal was to determine if ClO_4^- could be produced aerobically under nitrifying conditions from ClO^- , ClO_2^- , or ClO_3^- as precursors (i.e., like NO_3^- is produced from NH_4 and NO_2^- by nitrifying bacteria).

2.6.4.2 Material and Methods

Enrichment cultures for nitrifiers were obtained from sewage sludge (Ewing, NJ wastewater treatment plant), West Texas surface soils, and a freshwater fish tank. One gram of soil or 1 mL of sludge/water was inoculated into 100 mL of Winogradsky's medium (with NH_4 from $(\text{NH}_4)_2\text{SO}_4$ as a sole N source) designed for isolation of nitrifiers (Atlas, 1995). Periodically, samples were tested for NO_2^- and NO_3^- levels via colorimetric test strips. After 3 days of incubation, colorimetric analysis indicated the formation of NO_2^- and NO_3^- in the flask containing sewage sludge. After six days of incubation, colorimetric analysis indicated depletion of NO_2^- and formation of NO_3^- in this same flask. Nitrate production continued to increase between six and ten days of incubation. This culture was passed into fresh Winogradsky's medium, and production of NO_2^- and NO_3^- again was observed within 10 days of passing. The culture was passed a third and fourth time, with the same results. Nitrite and nitrate formation also occurred in samples from West Texas soils and fish tank water.

Based on the results from the nitrification enrichments, the sewage sludge enrichment in Winogradsky's medium was selected for use as the inoculum for ClO_4^- formation studies. Rates and extents of NO_3^- formation were highest in this media. The Winogradsky's medium was supplemented with 2 mg/L ClO_3^- , 2mg/L ClO_2^- , 2 mg/L ClO^- , or no chlorinated compounds (i.e., unsupplemented); chloride-free Winogradsky's medium (i.e., Winogradsky's medium made as described above except that sodium chloride was omitted); and NH_4 -free Winogradsky's medium (i.e., Winogradsky's medium made as described above except that $(\text{NH}_4)_2\text{SO}_4$ was omitted) supplemented with 2 mg/L ClO_3^- , 2mg/L ClO_2^- , 2 mg/L ClO^- , or unsupplemented. Fifty mL of each media was placed into a 125 mL flask. Prior to inoculation, 10 mL aliquots were removed and filtered through a 0.2 micron syringe filter for analysis of anions (media baseline) (Cl^- , NO_2^- (as N), SO_4^- , NO_3^- (as N), ClO_3^- , PO_4^{2-} , and ClO_2^-) via EPA Method 300.0.

2.6.4.3 Results and Discussion

Significant NO_3^- formation was observed in unamended Winogradsky's medium, medium supplemented with 2 mg/L ClO_3^- , and Cl^- - free medium. In these three treatments, NO_3^- levels increased from ~ 45 mg/L (± 0.6 ; $n=3$) to 287 mg/L (± 2 ; $n=3$) in two weeks, confirming that nitrification was occurring. Low-level NO_3^- formation was also observed in NH_4 -free Winogradsky's medium supplemented with 2 mg/L ClO_3^- or 2 mg/L ClO_2^- ; in these treatments

NO_3^- concentrations increased from $\sim 46 \text{ mg/L}$ (± 0.6 , $n=2$) to 71 mg/L (± 0.4 , $n=2$) in two weeks. Interestingly, ClO_3^- was degraded below detectable limits (less than 0.5 mg/L) under aerobic conditions within 2 weeks in Winogradsky's medium. However, ClO_4^- was not detected in these samples over the course of the study (ClO_4^- detection limit was $25 \text{ }\mu\text{g/L}$). ClO_2^- concentrations were reduced to 0.35 mg/L within 2 weeks in Winogradsky's medium supplemented with ClO_2^- , but again ClO_4^- was not detected.

The loss of ClO_3^- under aerobic, nitrifying conditions is interesting. The only chlorine oxyanion that is more oxidized than ClO_3^- is ClO_4^- , but no ClO_4^- was generated during the reaction. It is possible that the loss of ClO_3^- in the system was reductive (i.e., the ClO_3^- was reduced to chloride), and coupled to the oxidation of NH_4 or NO_2^- . A similar process was recently proposed for the bacterium *Candidatus Nitrospira defluvii* (Maixner et al., 2008), when this nitrifying organism was observed to contain the gene chlorite dismutase, which would serve to dismutate (to Cl^- and O) any ClO_2^- formed during ClO_3^- reduction, and thus mitigate toxicity of this product. Aerobic destruction of ClO_3^- may be important for understanding the mass balance of chlorine oxyanions (e.g., concentrations of ClO_3^- vs ClO_4^-) in arid environments if this process occurs routinely. However, the absence of any ClO_4^- generation suggests that nitrifying strains do not produce ClO_4^- from Cl^- , ClO_2^- or ClO_3^- , at least in the enrichments tested during these studies.

2.6.5 Perchlorate Formation Tests Using *Starkeya novella* and West Texas Soil Enrichments

2.6.5.1 Background

The bacterial strain *Starkeya novella* (formerly *Thiobacillus novellus*) has been shown to oxidize thiosulfate (Kappler et al, 2001) via a Cytochrome c oxidoreductase that catalyzes the direct oxidation of sulfite to sulfate (Kappler et al, 2000). Based on the ability of this strain to oxidize $\text{Na}_2\text{S}_2\text{O}_3$ to SO_4 , we tested *Starkeya novella* ATCC 8093 and unidentified strain TSP69, a strain enriched and isolated in our lab from West Texas soil, for the ability to oxidize ClO_3^- to ClO_4^- .

2.6.5.2 Bacterial Strains and Culture Conditions

Starkeya novella ATCC # 8093 was purchased from the American Type Culture Collection (Manassas, VA), and was cultured in DSMZ Medium 69: *Thiobacillus novellus* medium (http://www.dsmz.de/microorganisms/medium/pdf/DSMZ_Medium_69.pdf). Unidentified strain TSP69 was isolated from West Texas soil inoculated and serially passed into DSMZ Medium 69 (Atlas, 1995).

Several variations of this medium were used, including unadjusted/neutral pH, as well as substituting sodium sulfite or sodium phosphite for sodium thiosulfate. Cultures were given additional thiosulfate, sulfite, or phosphite up to three times per week. After 2 passes into fresh media, cultures were streaked onto agar plates. All cultures, regardless of pH or O_3 -containing compound, were shown to be pure cultures that were morphologically the same. One culture, grown on sodium thiosulfate at neutral pH, was chosen for further study.

2.6.5.3 Perchlorate Formation Study Methods and Procedures

Media. The variations of DSMZ Medium 69 used in this study can be seen in Table 2.6.6.

Table 2.6.6. Variations of DSMZ Medium 69 used in the perchlorate formation studies.

Variation #	O₃-containing compound (5 mM)	Perchlorate precursor (0.1 mM)
1	Sodium thiosulfate	Chlorate (as sodium chlorate)
2	Sodium thiosulfate	Chlorite (as sodium chlorite)
3	Sodium sulfite	Chlorate (as sodium chlorate)
4	Sodium sulfite	Chlorite (as sodium chlorite)
5	Sodium phosphite	Chlorate (as sodium chlorate)
6	Sodium phosphite	Chlorite (as sodium chlorite)
7	None	Chlorate (as sodium chlorate)
8	None	Chlorite (as sodium chlorite)
9	Sodium thiosulfate	None
10	Sodium sulfite	None
11	Sodium phosphite	None

One flask of each media type was inoculated with either *Starkeya novella* or strain TSP69, or was left uninoculated to serve as a no cell control. Flasks were placed in an incubator/shaker operating at room temperature (approximately 22-23°C). Flasks were sampled weekly as follows. Flasks were removed from the shaker. Ten mL was removed aseptically and filtered through a 0.2 µm filter for perchlorate analysis. The volume removed was then replaced with fresh sterile medium and the flasks were replaced in the incubator. All samples were refrigerated until being shipped on ice to Texas Tech for ClO₄⁻ analysis as previously described.

2.6.5.4 Results and Discussion

Cultures grown on thiosulfate exhibited the most growth, followed by those grown on sulfite, as evidenced by visual inspection. Cultures grown on phosphite exhibited significantly less growth than those grown on the sulfur-containing compounds. Samples were chosen for ClO₄⁻ analysis based on the amount of growth observed (i.e., samples from flasks exhibiting the most growth were chosen for further analysis). Analysis was also performed on the appropriate controls. Results of ClO₄⁻ analysis are provided in Table 2.6.7. The data showed no significantly enhanced ClO₄⁻ production in any set of live samples compared to uninoculated controls.

To confirm these results, (i.e., that no significant ClO₄⁻ production was observed), selected culture conditions were repeated in a second experiment. Variations # 4, 5, 6, 10, 11, and 12 were set up in duplicate, and variations 22-30 were set up singularly as controls. Cultures were incubated, sampled, and fed as described above, except that sampling and feeding was performed every 3 weeks (i.e., at T=3 weeks and 6 weeks). No ClO₄⁻ generation was documented.

Table 2.6.7. Perchlorate concentrations ($\mu\text{g/L}$) in studies with *Starkeya novella* and TSP69.

Time		Media components				Inoculants		
date	days	thiosulfate	sulfite	chlorate	chlorite	TSP 69	<i>Starkeya novella</i>	Uninoculated
2/15/2012	7	X		X		ND	ND	ND
2/22/2012	14	X		X		0.145	0.152	0.123
2/29/2012	21	X		X		0.223	0.246	0.247
3/8/2012	29	X		X		0.344	0.339	0.341
2/15/2012	7	X			X	ND	ND	0.044
2/22/2012	14	X			X	0.041	0.029	0.027
2/29/2012	21	X			X	0.085	0.088	0.096
3/8/2012	29	X			X	0.241	0.190	0.176
2/15/2012	7		X	X		0.108	ND	0.100
2/22/2012	14		X	X		0.130	0.141	0.132
2/29/2012	21		X	X		0.238	0.239	0.226
3/8/2012	29		X	X		0.368	0.356	0.285
2/15/2012	7			X		0.096	0.088	ND
2/22/2012	14			X		0.147	0.140	0.138
2/29/2012	21			X		0.259	0.262	0.264
3/8/2012	29			X		0.296	0.341	0.361
2/15/2012	7				X	0.064	0.050	0.050
2/22/2012	14				X	0.041	0.038	0.029
2/29/2012	21				X	ND	0.077	0.093
3/8/2012	29				X	0.146	0.197	0.173
2/15/2012	7	X				0.067	0.040	0.036
2/22/2012	14	X				0.029	0.008	0.014
2/29/2012	21	X				0.056	0.052	0.050
3/8/2012	29	X				0.067	0.092	0.047

2.7 Evaluate the Accumulation of ClO_4^- in Plants and their Role in Ozone-Mediated Production of ClO_4^-

2.7.1 ClO_4^- Accumulation at Environmentally-Relevant O_3 Concentrations.

2.7.1.1 Background

The role of tropospheric O_3 in the origin of non-anthropogenic ClO_4^- remains unclear. Tropospheric O_3 has increased in concentration since pre-industrial times (Vingarzan, 2004; Stevenson et al., 2006). Current levels of ambient O_3 are injurious to crop species and to native vegetation (Avnery et al., 2011a,b; Booker et al., 2009; USEPA, 2012). High concentrations of O_3 have been shown experimentally to produce ClO_4^- from Cl^- in both aqueous solution and in dry systems (Dasgupta et al., 2005; Kang et al., 2006, 2008; Rao et al., 2010). Stable isotopic composition of some indigenous ClO_4^- in the US and Chile exhibits a significant $\Delta^{17}\text{O}$ anomaly, suggesting some production of natural ClO_4^- through O_3 mediated oxidation reactions. However, other sources appear to have a small O_3 mediated contribution (Böhlke et al., 2005; Jackson et al., 2010). Our preliminary evidence (Burkey et al., unpublished) shows that O_3 -sensitive and O_3 -tolerant genotypes of snap bean (*Phaseolus vulgaris*) accumulate foliar ClO_4^- under field conditions, and the role of contrasting O_3 environments is currently being evaluated. Through abscission and litter turnover this would represent an unaccounted source of ClO_4^- in the environment.

Plants, particularly in arid environments, may contain abundant chloride in their tissues; display a vast array of hydrated internal and external reaction surfaces; and catalyze a multitude of redox reactions that could be involved in biosynthesis of ClO_4^- . These factors, the ubiquitous distribution of plants, and the post-industrial increase in O_3 exposure are consistent with the possibility that tropospheric O_3 may induce biosynthesis of ClO_4^- from Cl^- in plants. This would represent a novel source of ClO_4^- in the environment.

We present the results of a series of experimental exposures to environmentally relevant concentrations of O_3 of a broad range of contrasting food, feed and fiber species under controlled conditions. We test the hypotheses that (1) exposure of plants to O_3 leads to foliar biosynthesis of ClO_4^- in young, physiologically active leaves, that (2) such exposure leads to accumulation of ClO_4^- in older, senescing leaves, and that (3) contrasting plant species exhibit little foliar ClO_4^- at low O_3 exposure.

2.7.1.2 Materials and Methods

Plant Material

We chose a range of plants of economic importance, used for human consumption, animal feed, or fiber. These species represent diverse classes of crop species, leafy green vegetable row crops and extensively cultivated grain and forage crops, warm season and cool season crops, and both C₃ and C₄ species.

The C₃ species were spinach (*Spinacia oleracea* cv. Bloomsdale Long Standing; Ferry Morse Seed Co., Fulton KY), lettuce (*Lactuca sativa* cv. Romaine, Parris Island Cos; Ferry Morse Seed Co., Fulton KY), broccoli (*Brassica oleracea* cv. De Cicco, Ferry Morse Seed Co., Fulton KY), soybean (*Glycine max* cv. Disoy; Ferry Morse Seed Co., Fulton KY), Pima cotton (*Gossypium barbadense* cv. Phytogen 800, Dow AgroScience, Indianapolis IN and cv. S-6, J.G. Boswell Company, Corcoran CA; foundation seed stock), and bush bean (*Phaseolus vulgaris* cv. Bush Blue Lake 156; Ferry Morse Seed Co., Fulton KY). The C₄ species were sorghum (*Sorghum bicolor* cv. 4662, Pioneer Seed Co., Johnston IA), sugarcane (*Saccharum officinarum* x *S. spontaneum* hybrid cv. Elephant; Grantz and Vu, 2009; Grantz et al. 2012), and maize (*Zea mays* cv. Golden Cross Bantam (hybrid); Ferry Morse Seed Co., Fulton KY).

Seed (stalk cuttings in the case of sugarcane) were planted in moist commercial potting mix (Earthgro Potting Soil; Scotts Company, Marysville, OH) in 10 cm square pots. After emergence, pots were thinned to 1 plant per pot. Plants were grown in a research greenhouse at Kearney Research and Extension Center (103 msl; 36.598 N 119.503 W). Irrigation was provided daily through a drip emitter in each pot. A complete (N-P-K; 24-8-16) fertilizer solution was administered twice weekly (2.9 g L⁻¹, Miracle Gro, Scotts Miracle-Gro Products Inc., Port Washington, NY) through the same emitters. Both irrigation and fertilizer were applied until substantial drainage through the potting medium occurred, to avoid accumulation of salts or fertilizer in the soil (Grantz et al., 2010). Pots retained 68.9 mL of solution against drainage.

Plants were grown from germination until harvest in one of nine continuously stirred, Teflon lined tank reactors (CSTRs; Heck et al., 1978; Grantz et al., 2010) located in the greenhouse. Growth temperature was 15-30 °C, illuminated with natural sunlight (approximately 300 μmol m⁻² s⁻¹ PPFD; 400 – 700 nm at plant level) near solar noon.

Ozone Exposure

Plants were exposed to environmentally relevant O₃ concentrations (12 hour means nominally 4, 59, and 114 ppb; 8 h means of 4, 75 and 150 ppb, and daily maxima near solar noon of 4, 89 and 163 ppb) from emergence in the CSTRs. Exposures were imposed as daily half-sine wave, 7 days per week. O₃ was provided to the CSTRs by corona discharge (Model SGC-11, Pacific O₃ Technology, Brentwood, CA) from purified oxygen (Series ATF-15, Model 1242, SeQual Technologies Inc., San Diego CA). Feedback for the O₃ generator was provided by the exit

stream of a single exposure chamber, monitored with an ultraviolet O₃ monitor (ThermoElectron Model 41C), with other CSTRs controlled by ratio of O₃ flow rate (Grantz et al., 2010). Each CSTR was monitored every 15 min, independently of the control system, with a separate ThermoElectron Model 41C. All monitors were calibrated against a factory certified calibration unit (Model 306; 2B Technologies; Boulder CO). Air with the desired O₃ concentration was introduced at one complete air exchange per minute.

Perchlorate Determination

Plants were harvested at about 9 weeks after germination. Species varied with their specific rate of development, but all runs within a species were harvested at precisely the same plant age. Roots were washed in cool water to remove the potting medium. Leaves, roots and stems were separated and immediately frozen at -20 °C. Older leaves, senescing or recently abscised, were gathered separately and treated similarly.

Samples of unused planting media and fertilizer were collected and stored at -20 °C in zip-lock polyethylene bags. The surface 1 cm of soil was sampled following plant harvest and treated similarly. Irrigation water was sampled directly from the emitters of the drip irrigation system into plastic, screw-top vials and immediately frozen at -20 °C. Samples were shipped on dry ice to the analytical laboratory for ClO₄⁻ analysis.

Soil samples were extracted using Milli-Q water at a 2:1 mass ratio (water: soil) by shaking for 24 hours. The samples were centrifuged for 10 minutes and the supernatant decanted and filtered through a 0.2 micron Nylon membrane (ion chromatography (IC)-certified Acrodisc syringe filter). All extraction sets were accompanied by an extraction duplicate, an extraction spike (soil + known amount of added ClO₄⁻), and an extraction blank (DDI water only). The moisture content of parallel samples was determined by drying at 105 °C for 24 hours. The final filtered extract was analyzed for major anions and ClO₄⁻.

Plant leaf samples were pre-dried (105° C for 12 hrs) and approximately 1 gm placed in a 45-mL capacity centrifuge tube to which 25 mL of Milli-Q water was added. The centrifuge tubes, containing the samples, were boiled for 1 hr (water bath temperature ~ 99 °C) and centrifuged at 5000 rpm for 5 minutes. A 2 mL aliquot of the supernatant was gently transferred into a plastic bottle containing 1.0 ± 0.1 g of activated alumina. The alumina-extract mixture was diluted by adding 18 mL of DDI water, capped, and held at 3 °C for 8 hrs. The suspension was then re-centrifuged at 5000 rpm for 5 minutes, and the final supernatant filtered (0.2 micron) and passed through a pre-cleaned and activated OnGuard® RP cartridge (Dionex Corporation). The extraction procedure was repeated for the extraction duplicate, spike and blank (DDI). The final solution was then diluted and analyzed for ClO₄⁻.

Perchlorate in the resulting solutions was quantified by IC-MS/MS at Texas Tech University as described in previous sections of this report. To overcome matrix effects all samples were spiked with an oxygen-isotope (^{18}O) labeled ClO_4^- internal standard. The method detection limit (MDL) for ClO_4^- was $0.01\ \mu\text{M}$. ClO_4^- content of tissue, potting medium, and fertilizer is reported as ($\mu\text{g (kg dry wt)}^{-1}$). ClO_4^- content of irrigation water and fertilizer solution is reported as ($\mu\text{g L}^{-1}$).

Ozone Flux

Stomatal conductance of young, healthy, fully expanded leaves (leaf 0 and leaf 2) was determined with a porometer (LI 1600; LiCor Inc., Lincoln NE USA or AP4; Delta T Devices, Cambridge UK). Measurements were determined on both classes of leaves at 2 hour intervals throughout the day, and on 2 occasions at 14 day intervals. Values were averaged from these 4 leaves as an estimate of stomatal conductance over time, developmental age, and leaf position. Conductance was converted from water vapor to O_3 (Massman and Grantz, 1995) and multiplied by mean O_3 concentration over the surrounding two hour period. The products were summed diurnally over daylight hours and over the lifespan (germination to harvest) of each species to yield cumulative flux, or dose.

Statistical Analysis

CSTRs were arrayed in three blocks parallel to windows and cooling fans. Plants were randomly assigned to individual exposure chambers. One CSTR per block was exposed to each of the three O_3 concentrations, with the CSTR taken as the unit of replication in a Randomized Complete Block Design. Two runs were conducted with each species ($n=6$) except for broccoli ($n=9$), Pima Cotton ($n=9$; as data for two closely related cultivars were combined), and spinach ($n=3$). Neither blocks nor runs were significant, and data were pooled. Older leaves were not available at harvest for all species. Stomatal conductance and flux calculations were not available for all runs, but were available for all species.

Values of ClO_4^- were normalized by basal values observed at 4 ppb O_3 for consideration of the relationship between accumulation and potential sensitivity of ClO_4^- contents to O_3 exposure. For comparison of responses of tissue ClO_4^- content to O_3 exposure vs. O_3 dose, ClO_4^- values were normalized within each species by the median value of ClO_4^- across all O_3 exposures.

Each species was analyzed independently for response to O_3 exposure. Basal ClO_4^- content of all species at low O_3 concentration was subjected to independent analysis by ANOVA with reduced degrees of freedom to evaluate differences in accumulation between species. Analyses were conducted using SAS v. 9.3 (SAS Institute Inc.; Cary NC, 2002). Means separation ($P < 0.05$) by Duncan's Multiple Range Test and standard errors of the means were performed with PROC GLM and PROC MEANS. To address a potential positive relationship between variances and means in some data sets, the data were analyzed in their native form by ANOVA, and again after

transformation as the square root. Neither yielded significant differences and only the native analysis is presented. Linear regression analyses of relationships between perchlorate and ozone exposure and concentration were performed using PROC REG.

2.7.1.3 Results

Sources of Perchlorate

The plants were irrigated with water containing very little ClO_4^- (Table 2.7.1). Similarly, the commercial potting mix exhibited relatively low ClO_4^- content. The commercial fertilizer applied to all species contained substantial amounts of ClO_4^- on a dry weight basis (Table 2.7.1), but only $3.6 \mu\text{g ClO}_4^- \text{ L}^{-1}$ in the dilute irrigation solution. Over the approximate 9 weeks of plant growth, each pot received a total of approximately $4.4 \mu\text{g ClO}_4^-$ from the fertilizer that was applied twice weekly, and an additional $2.6 \mu\text{g ClO}_4^-$ in irrigation water applied daily. These provided the principal source for ClO_4^- accumulation from the growth medium (Table 2.7.1).

Perchlorate Accumulation

Large interspecific differences were observed in foliar concentrations of ClO_4^- averaged across all O_3 exposures (Figure 2.7.1; Table 2.7.2). These appear to reflect physiological differences in uptake or exclusion of ClO_4^- present in the growth medium. Spinach accumulated approximately $700 \mu\text{g (kg dry wt)}^{-1}$, the highest level observed, while sugarcane accumulated less than $100 \mu\text{g kg}^{-1}$. Other species were intermediate, with young leaf contents lying generally between $150\text{--}250 \mu\text{g kg}^{-1}$. On average, plants accumulated about 7% of the applied ClO_4^- over their lifespan, much of the remainder being lost to drainage.

The results were similar for older, senescing leaves (Table 2.7.3) although ClO_4^- was accumulated to much higher levels in these leaves. Young leaves of broccoli exhibited contents near $400 \mu\text{g kg}^{-1}$ (Table 2.7.2) whereas older leaves averaged slightly over $1000 \mu\text{g kg}^{-1}$ (Table 2.7.3). For sugarcane, the corresponding values were about $50 \mu\text{g kg}^{-1}$ for young leaves (Table 2.7.2) but $>100 \mu\text{g kg}^{-1}$ for older leaves (Table 2.7.3). Averaged over all species, older leaves accumulated more than twice the ClO_4^- as younger leaves ($>500 \mu\text{g kg}^{-1}$ vs. $<250 \mu\text{g kg}^{-1}$).

Effect of Ozone Exposure on Perchlorate Accumulation

There was no consistent effect of O_3 exposure on foliar content of ClO_4^- in young leaves. Five of nine species exhibited a decline in ClO_4^- content with increasing O_3 exposure while for the remaining four species ClO_4^- content increased with O_3 exposure. In no species was this response significant (Table 2.7.2) and even with the additional statistical power of combining all species ($n=68$), the mean response across all species was not significantly related to O_3 exposure (Table 2.7.2). The same absence of relationship with O_3 exposure was observed in older leaves, despite the greater overall accumulation of ClO_4^- (Table 2.7.3).

Basal accumulation of ClO_4^- at low O_3 was not predictive of the effect of elevated O_3 , on ClO_4^- in young leaves, whether significant or not (Figure 2.7.2; Table 2.7.4). This was the case for absolute changes in ClO_4^- between low and moderate O_3 and between low and higher O_3

exposures (Figure 2.7.2A; triangles, squares, respectively). The relationship was not improved by normalization of the values associated with O₃ exposure by basal ClO₄⁻ content (Figure 2.7.2B).

We considered whether O₃-induced foliar biosynthesis of ClO₄⁻ might occur, yet not be reflected in leaf contents due to transport to the rhizosphere. However, there was no relationship between ClO₄⁻ in the top level of the potting medium and basal accumulation of ClO₄⁻ at 4 ppb O₃ (Table 2.7.4). Similarly, there was no significant relationship between O₃ exposure of plant and potting medium and surface content of ClO₄⁻ (Table 2.7.4). However, a multiple range test of ClO₄⁻ in the surface layer of the growth medium of unused potting medium, potting medium exposed at 4 ppb O₃, and potting medium exposed at 114 ppb O₃ (Table 2.7.5) suggested a positive association between ClO₄⁻ and O₃. The potting medium exposed to the highest and lowest O₃ concentrations did not differ in ClO₄⁻ content, and that exposed to the lowest O₃ did not differ from the unused medium. However, there was a significant difference between unused potting medium and that exposed to the highest O₃ concentration.

Table 2.7.1. ClO_4^- content of unused irrigation water, potting medium, and fertilizer.

Material	n	Perchlorate Content	S.E.	Range
Irrigation Water	11	0.61 ($\mu\text{g L}^{-1}$)	± 0.053	0.33 – 0.81
Potting Medium	12	3.78 ($\mu\text{g (kg dry wt)}^{-1}$)	± 0.72	0.43-6.41
Fertilizer (granular)	6	1270 ($\mu\text{g (kg dry wt)}^{-1}$)	± 89.3	1090-1700
(asapplied)		3.55 ($\mu\text{g L}^{-1}$)	± 0.25	

Table 2.7.2. Perchlorate content ($\mu\text{g kg}^{-1}$) of young leaves of a range of crop species as a function of O_3 exposure (ppb, 12 hr mean) sampled at the time of final harvest.
There were no significant differences between O_3 exposures ($P < 0.05$) within any species, nor within the pooled data.

Species	n	O_3 Exposure (ppb)	Perchlorate Content ($\mu\text{g kg}^{-1}$)	S.E.	Range
Bush Bean	6	4	155	± 31.3	72.1-294
	6	59	160	± 19.0	110-225
	6	114	204	± 15.4	130-236
Broccoli	9	4	380	± 41.4	234-653
	7	59	349	± 75.0	42.1-672
	9	114	528	± 86.1	68.3-927
Lettuce	9	4	223	± 89.0	65.8-926
	9	59	145	± 26.3	56.2-279
	9	114	151	± 20.1	81.3-250
Maize	6	4	173	± 54.1	15.0-371
	5	59	85	± 10.2	50.1-114
	6	114	123	± 38.3	23.9-295
Pima Cotton	18	4	290	± 40.2	33.4-544
	18	59	218	± 24.8	75.5-416
	18	114	218	± 36.3	58.6-590
Sorghum	6	4	177	± 38.4	87.5-328
	6	59	182	± 20.6	128-267
	5	114	369	± 110.3	84.2-598
Soybean	5	4	222	± 39.8	136-366
	6	59	218	± 16.8	164-284
	6	114	186	± 24.7	123-294
Spinach	3	4	766	± 84.5	670-934
	2	59	568	± 110.6	458-679
	3	114	686	± 31.8	622-719
Sugarcane	6	4	42.5	± 6.2	30.6-71.4
	6	59	61.0	± 19.0	6.67-132
	6	114	54.6	± 15.3	15.0-122
All Species	68	4	255	± 24.8	15.00-934
	65	59	199	± 17.0	6.67-679
	68	114	255	± 26.1	15.0-927

Table 2.7.3. Perchlorate content of older, senescing leaves of a range of crop species as a function of O₃ exposure (ppb, 12 hr mean) sampled at the time of final harvest.

There were no significant differences between O₃ exposures ($P < 0.05$) within any species, nor within the pooled data.

Species	n	O ₃ Exposure (ppb)	Perchlorate Content (µg kg ⁻¹)	S.E.	Range
Broccoli	9	4	1730	± 970	312-9450
	8	59	765	± 123	423-1430
	8	114	945	± 170	417-1960
Lettuce	2	4	337	± 188	150-525
	3	59	430	± 171	165-750
	9	114	319	± 62.5	188-750
Maize	6	4	87.0	± 19.8	51.5-184
	6	59	85.1	± 14.0	17.4-110
	5	114	77.4	± 11.6	54.9-120
Pima Cotton	12	4	435	± 133	97.5-1320
	17	59	352	± 74.6	78.1-1280
	18	114	549	± 170	70.3-2330
Sorghum	3	4	238	± 11.8	214-250
	3	59	527	± 166.4	348-860
	3	114	463	± 77.3	375-617
Sugarcane	3	4	131	± 22.7	104-176
	3	59	85.7	± 16.0	58.4-114
	6	114	95.4	± 7.94	72.1-125
All Species	35	4	660	± 267	51.5-9450
	40	59	394	± 55.2	17.4-1432
	49	114	462	± 78.7	54.9-2330

Table 2.7.4. Perchlorate content ($\mu\text{g (kg dry wt)}^{-1}$) of potting medium after use for plant growth by a range of crop species, sampled at the time of final harvest (mean \pm S.E.), as a function of O_3 exposure (ppb, 12 hr mean). There were no significant differences between O_3 exposures ($P < 0.05$) within any species, nor within the pooled data.

Species	n	O_3 Exposure (ppb)	Perchlorate Content ($\mu\text{g kg}^{-1}$)	S.E.	Range
Broccoli	6	4	5.68	± 0.40	5.00-7.61
	6	59	6.09	± 0.26	5.38-7.07
	6	114	6.2	± 0.39	4.62-7.31
Bush Bean	3	4	6.98	± 0.08	6.88-7.14
	3	59	6.53	± 0.2	6.15-6.82
	3	114	6.14	± 0.25	5.88-6.64
Lettuce	6	4	6.13	± 0.27	5.49-7.34
	6	59	5.7	± 0.21	5.07-6.36
	6	114	7.32	± 1.08	6.00-12.63
Maize	3	4	0.51	± 0.05	0.43-0.60
	1	59	2.8	na	2.80-2.80
	3	114	0.44	± 0.06	0.37-0.55
Pima Cotton	9	4	1.38	0.29	0.65-2.87
	8	59	3.44	2.02	0.69-17.5
	9	114	4.49	2.03	1.03-18.6
Sorghum	3	4	7.79	± 0.88	6.70-9.52
	3	59	7.16	± 0.09	6.98-7.25
	3	114	8.65	± 1.32	7.32-11.3
Soybean	3	4	6.96	± 0.31	6.47-7.54
	3	59	6.65	± 0.61	5.54-7.65
	3	114	6.41	± 0.25	5.95-6.82
Spinach	3	4	5.73	± 0.21	5.34-6.07
	3	59	6.05	± 0.87	4.59-7.60
	3	114	6.26	± 0.17	5.93-6.49
Sugarcane	3	4	10.7	± 3.18	4.53-15.1
	3	59	7.55	± 0.43	6.81-8.31
	3	114	9.31	± 1.83	5.70-11.6
All Species	39	4	5.11	± 0.53	0.43-15.1
	36	59	5.63	± 0.50	0.69-17.5
	39	114	5.98	± 0.61	0.37-18.6

Table 2.7.5. Perchlorate content ($\mu\text{g (kg dry wt)}^{-1}$) of potting medium before and after use for plant growth, sampled directly from the commercial container or from pots of all species at the time of final harvest (mean \pm S.E.), as a function of O_3 exposure (ppb, 12 hr mean). Means followed by different letters were significantly different ($P < 0.05$).

O_3 Exposure (ppb)	n	Perchlorate Content ($\mu\text{g kg}^{-1}$)	S.E.	Range ($\mu\text{g kg}^{-1}$)
na	12	3.78 a	± 0.72	0.43-6.41
4	39	5.11 ab	± 0.53	0.43-15.1
114	39	5.98 b	± 0.61	0.37-18.6

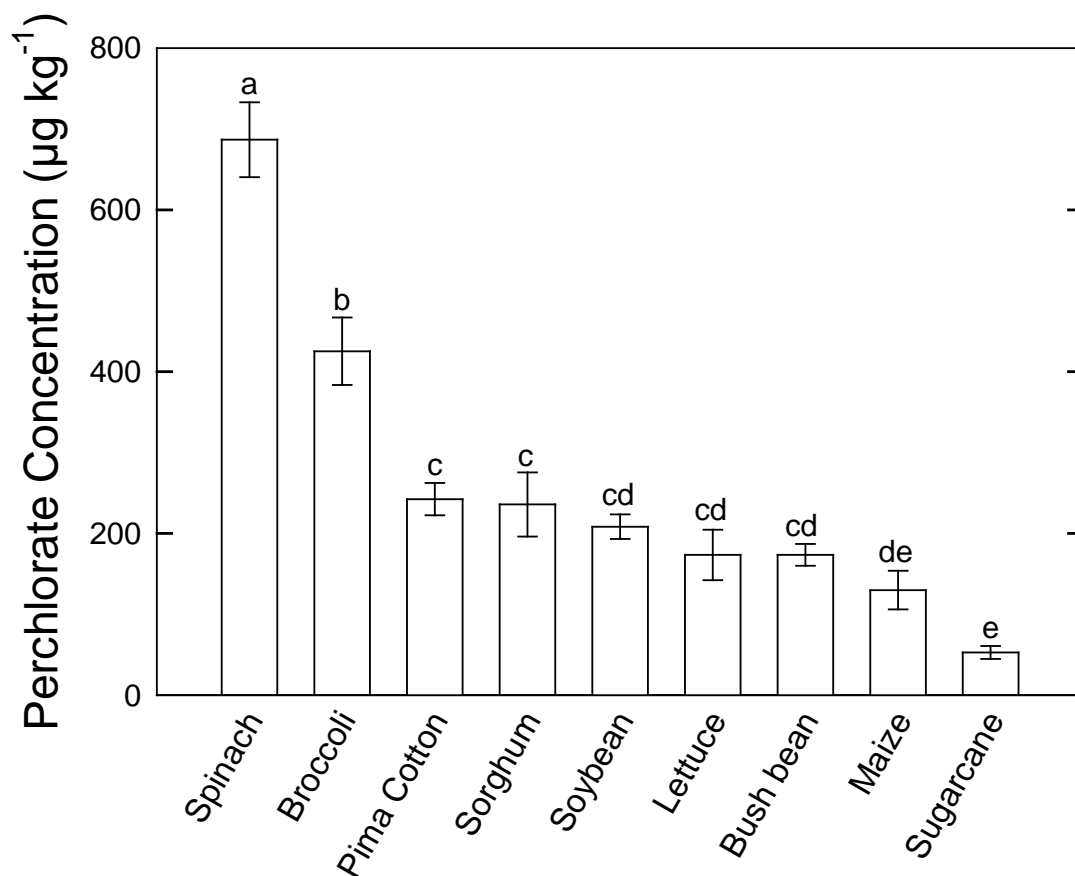


Figure 2.7.1. Inter-specific differences in perchlorate content ($\mu\text{g (kg dry wt)}^{-1}$) of youngest fully expanded leaves of a range of crop species (mean over all O_3 exposures \pm SE). Bars with different letters differ at $P < 0.05$.

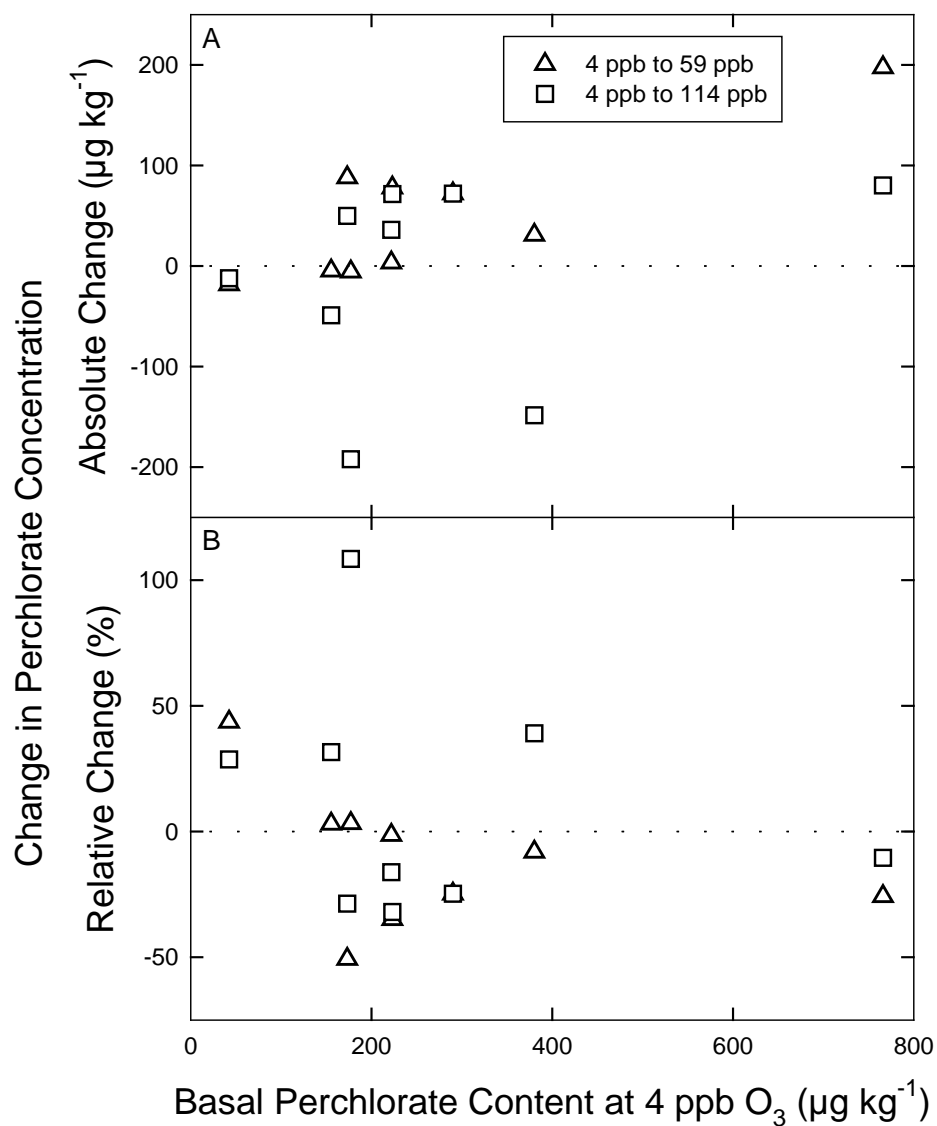


Figure 2.7.2. There was no significant relationship between basal perchlorate content (at 4 ppb O₃) and the change in ClO₄⁻ content (unitless) between 4 and 59 ppb O₃ (circles) and between 4 and 114 ppb (squares) of youngest fully expanded leaves of a range of crop species.

Role of Ozone Metrics

We evaluated whether the lack of response of foliar ClO_4^- content in young and older leaves to O_3 exposure was associated with a failure of the exposure protocol. This was not supported by the observation that these plants exhibited a highly significant reduction in above ground biomass at the highest O_3 exposure (data not shown).

We also considered whether the use of O_3 concentration could be an inadequate metric of O_3 exposure. The lack of relationship between foliar ClO_4^- and O_3 was not improved by use of cumulative stomatal uptake of O_3 (O_3 dose) rather than O_3 concentration (O_3 exposure). A linear regression analysis of the subset of young leaf data for which stomatal conductance was available (Fig. 2.7.3) revealed a non-significant relationship between normalized ClO_4^- and O_3 exposure (Fig. 2.7.3A), consistent with the results of the ANOVA with young leaves (Table 2.7.2). The relationship was not improved when ClO_4^- was considered as a function of O_3 dose (Fig. 2.7.3B).

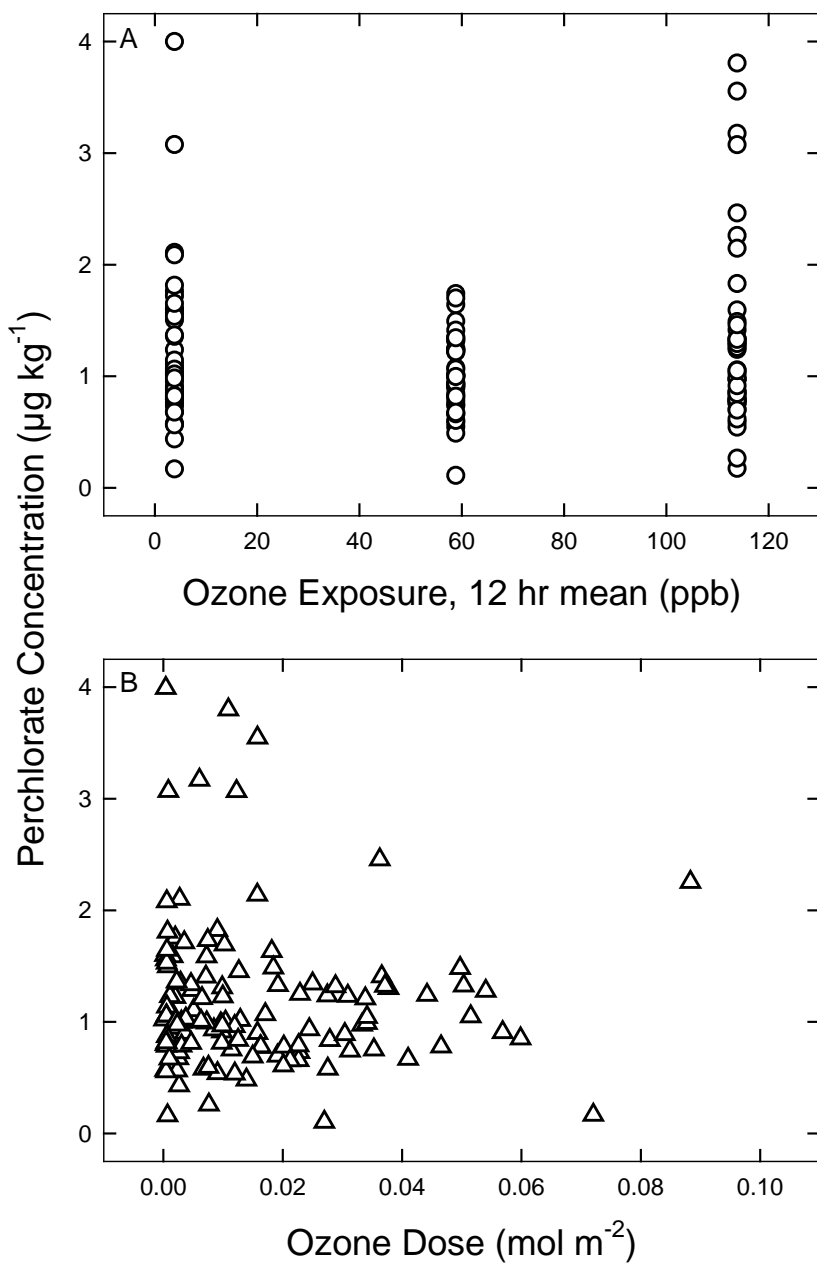


Figure 2.7.3. There was no significant relationship between O_3 exposure (A; $r^2 = 0.0034$) or O_3 dose (cumulative flux; B; $r^2=0.0018$) and ClO_4^- content of young leaves normalized by the median ClO_4^- content of each species shown in Figure 2.7.1 for which O_3 flux data were available.

2.7.1.4 Discussion

Perchlorate Accumulation

The plants in the current study exhibited a range of accumulation factors for ClO_4^- in the growth medium. This is consistent with previous studies showing that plants accumulate ClO_4^- with bioconcentration factors of up to two orders of magnitude (Tan et al., 2004, 2005; Urbansky et al., 2000; van Aken and Schnoor, 2002).

Uptake of ClO_4^- has been observed in many species, including in cottonwood (*Populus deltoids*, hybrid *Populus*), *Eucalyptus cineria*, willow (*Salix nigra*) (Nzengung et al., 1999) and in tamarisk (*Tamarix ramosissima*) (Urbansky et al., 2000a), cucumber (*Cucumis sativus*), lettuce, and soybean (Yu et al., 2004; Yang and Her, 2011), and many others. The high tissue contents observed in spinach (about $700 \mu\text{g kg}^{-1}$) are consistent with previous reports for leafy green food crops.

In our study this ClO_4^- was contributed mostly by the commercial fertilizer. Although ClO_4^- from this material did not accumulate significantly in the potting medium, it was apparently available during and following the twice weekly application. Under field conditions diverse plant species demonstrated a substantial capacity for phyto-accumulation of ClO_4^- (Tan et al., 2004; Yu et al., 2004; Jackson et al., 2005), with the magnitude of uptake related to the distance from streams draining ClO_4^- contaminated watersheds and to the duration of exposure (Tan et al., 2004; 2005). This capacity for uptake suggests that phytoremediation of contaminated watersheds may be feasible. Our data and these previous studies indicate that this phyto-accumulation, rather than biosynthesis, appears to account for the appearance of ClO_4^- in the human food supply.

The contrasting accumulation characteristics among species in this and previous studies appear to reflect physiological differences in uptake or exclusion by roots of ClO_4^- present in the growth medium. Phytoaccumulation of ClO_4^- occurs in transpiring leaves, apparently due to transport in the xylem transpiration stream (Seyfferth et al., 2007). Accumulation in leaf tissue has been effectively modeled using growth and passive (i.e. first order) uptake kinetics (Seyfferth et al., 2008a; Sundberg et al., 2003). In the present and previous studies, root and stem tissue of all species exhibited very low ClO_4^- contents relative to leaves (Vogt and Jackson, 2010). Bioaccumulation was considerably higher in leaves than in pods or fruits of soybean and tomato (Jackson et al., 2006).

In the juvenile plants used in the present study it was relatively simple to distinguish young, healthy, fully expanded leaves from the older and senescing cohort. Under these conditions we demonstrate that the older leaf population also accumulated ClO_4^- , and to a considerably greater extent than the younger leaves. It is not known if this reflects the greater age of the leaf for accumulation by transpiration, or a physiological sequestering of this xenobiotic in older leaves

soon to be shed from the plant body. In any case, over all species the older leaves accumulated more than twice as much ClO_4^- as younger leaves. This represents a potent mechanism for concentrating ClO_4^- from the rhizosphere to the soil surface.

Effect of Ozone Exposure on Perchlorate Accumulation

O_3 exposure had a nearly random effect on foliar content of ClO_4^- in both young and older leaves. Approximately half of experimental species exhibited a decline in ClO_4^- content with increasing O_3 exposure, while the other half exhibited an increase. These trends were not significant in any individual species nor in the combined, all-species, data set.

Our attempts to improve the power of the test of O_3 effects were not successful. Basal accumulation of ClO_4^- , indicative of favorable uptake / unfavorable exclusion properties of root membranes, was not predictive of the effect of O_3 on ClO_4^- content of young leaves. This putative relationship was tested at moderate and at higher O_3 exposures without success. Similarly, various normalization procedures, seeking to remove the undue influence of high baseline values of ClO_4^- in the accumulating species did not improve relationships between O_3 exposure and changes in tissue ClO_4^- .

The O_3 exposure protocol and its representation as O_3 concentration was adequate to induce a substantial decline in above ground biomass in these plants, suggesting that the test could have identified O_3 -induced biosynthesis of ClO_4^- if it had occurred. The uptake of ClO_4^- observed in this study is not without potential consequence for plants. Millimolar concentrations of ClO_4^- in irrigation water reduced photosynthetic electron transport and induced antioxidant metabolism in tobacco and *Arabidopsis* (Hamissou 2011). As ClO_4^- is not significantly metabolized in plants (Seyfferth et al., 2008a; Susarla et al., 2000a) it is unclear whether this induction of ascorbate peroxidase and superoxide dismutase reflects the strongly oxidizing nature of ClO_4^- , or a non-specific toxic effect of this xenobiotic. In either case, we can conclude from the present data that the growth inhibition associated with O_3 exposure is not a consequence of enhanced tissue accumulation of ClO_4^- , but rather reflects the phytotoxicity of O_3 , itself. The data were clear in indicating that ambient and near ambient concentrations of O_3 did not lead to increased tissue contents of ClO_4^- .

Alternative Sinks

We observed bioconcentration of ClO_4^- in older, senescing and abscised leaves. In more mature canopy conditions this would serve to shed ClO_4^- from the plant and distribute it onto the soil surface. As we collected these leaves either prior to abscission or soon afterwards and prior to decomposition or leaching, this mechanism did not apply in the present study.

The soil surface and any Cl^- in the irrigation water or fertilizer were exposed directly to O_3 in the CSTRs. There was some indication that direct exposure of the growth medium to the highest O_3 concentration may have led to accumulation of ClO_4^- in the surface layer. Averaged over all species there was a modest but non-significant relationship with increasing O_3 exposure, but a significant difference between unused potting medium and medium exposed to the highest O_3 . This suggests that ClO_4^- content in the soil surface may increase with exposure to O_3 , presumably due to oxidation of Cl^- in the soil, as demonstrated experimentally at higher O_3 concentrations with Cl^- coated sand (Kang et al., 2008) and soil (Dasgupta et al., 2005). Our results were observed without artificial enhancement of the Cl^- content, at near ambient O_3 concentrations, and over relatively brief exposure periods relative to geologic time. This potentially important conclusion requires confirmation, but if reproducible and applicable under field conditions, this mechanism would contribute to ClO_4^- present in the environment.

The clear absence of O_3 -sensitivity of ClO_4^- in young leaves could have indicated a robust translocation to roots and exudation into the rhizosphere. However, we observed no relationship between foliar accumulation of ClO_4^- and its content in the potting medium. Retranslocation to stems or roots has not been detected in previous studies (Vogt and Jackson, 2010), consistent with high concentrations of ClO_4^- in leaf laminae and considerably lower concentrations in the rest of the plant. This was the case in the current study, and in *Polygonum spp.* (smartweed) in which leaves accumulated up to $800 \mu\text{g (kg dwt)}^{-1}$, while roots and stems accumulated only $100\text{--}150 \mu\text{g (kg dwt)}^{-1}$ (Tan et al., 2006). Neither exudation to non-contaminated media nor reductive metabolism are significant sinks for phytoaccumulated ClO_4^- , (van Aken and Schnoor, 2002), though some metabolites were detected in *Populus*.

2.7.1.5 Conclusions

The ubiquitous distribution of vegetation and rising concentrations of tropospheric O_3 provided a tempting hypothesis to explain the quantitatively and spatially inadequate emission inventory for ClO_4^- in the environment. We show that a broad range of crop species accumulate ClO_4^- from the growth medium, differing widely in their effectiveness in bioconcentration. Foliar ClO_4^- concentration was greatest in older leaves, which ultimately contribute to the litter layer, suggesting that scavenging of ClO_4^- from deeper soil horizons could lead to redistribution on the soil surface. However, we found no evidence that exposure of leaves to ambient O_3 induces any increase in tissue contents of ClO_4^- . We found an increasing trend in soil surface ClO_4^- with increasing O_3 , and a significant difference between potting medium exposed to high O_3 and unexposed medium. The environmental significance of this result is not known. These results demonstrate that current ambient concentrations of O_3 in most locations do not lead to increased phyto-accumulation nor biosynthesis of ClO_4^- . They do not disprove the hypothesis that such plant activity could be induced by the higher O_3 concentrations observed in some areas of the developing world and during stratospheric incursions, or in potential future atmospheres.

2.7.2 ClO₄⁻ Accumulation at Elevated O₃ Concentrations

2.7.2.1 Background

In the previous Section (2.7.1), we demonstrated that low to moderate concentrations of O₃ (0–114 nL L⁻¹, 12 hr mean) did not increase foliar ClO₄⁻, despite large interspecific differences in ClO₄⁻ uptake from the growth medium. However, these previous data did not disprove the hypothesis that much higher concentrations of O₃, such as that observed during stratosphere-troposphere folding events or during O₃ episodes in emerging mega-cities, might stimulate O₃ synthesis or accumulation in plants. Here we test the hypothesis that exposure of plants to environmentally plausible, but very high, concentrations of O₃ may lead to accumulation of ClO₄⁻ in plant leaf tissue or in the soil surrounding the plants.

2.7.2.2 Material and Methods

Plant Material

We examined 5 crops: the C₃ dicotyledonous species, soybean (*Glycine max* cv. Disoy; Ferry Morse Seed Co., Fulton KY), Pima cotton (*Gossypium barbadense* cv. S-6, J.G. Boswell Company, Corcoran CA; foundation seed stock), and bush bean (*Phaseolus vulgaris* cv. Bush Blue Lake 156; Ferry Morse Seed Co., Fulton KY), and the C₄ monocotyledonous species, sorghum (*Sorghum bicolor* cv. 4662, Pioneer Seed Co., Johnston IA), and maize (*Zea mays* cv. Golden Cross Bantam (hybrid); Ferry Morse Seed Co., Fulton KY). Some of these cultivars are known to be relatively sensitive to O₃, while the sensitivity of others has not been evaluated.

Seeds were planted in moist potting mix (Earthgro Potting Soil; Scotts Company, Marysville, OH) and subsequently thinned to 1 plant per pot (10 cm x 10 cm x 13 cm). Plants were grown under greenhouse conditions at Kearney Research and Extension Center (103 msl; 36.598 N 119.503 W) with daily drip irrigation and twice weekly application of a complete fertilizer solution (2.9 g L⁻¹, Miracle Gro, Scotts Miracle-Gro Products Inc., Port Washington, NY). These plants were exposed to relatively low amounts of ClO₄⁻ in their growth environment. The ClO₄⁻ content of the fertilizer was 3.55 ± 0.25 µg L⁻¹, and that of the potting soil and irrigation water were 3.77 ± 0.72 µg and 0.61 ± 0.05 µg L⁻¹ (kg dry wt)⁻¹, respectively (Section 2.6; Grantz et al., 2014). Pots retained 68.9 mL of solution against drainage so that over 9 weeks of growth, each plant had access to approximately 7 µg ClO₄⁻, the principal substrate for ClO₄⁻ accumulation.

Ozone Exposure

Plants were grown from germination through harvest in Teflon greenhouse exposure chambers (CSTRs; Section 2.7.1; Heck et al., 1978; Grantz et al., 2010; 2014). Growth temperature was 15–30 °C, illumination with natural sunlight was about 300 µmol m⁻² s⁻¹ PPFD at plant level, reflecting shading by both the greenhouse structure and the CSTR. Air with appropriate O₃ concentrations (12 hour means nominally 4, 102, and 204 nL L⁻¹; daily maxima near solar noon

of 4, 160 and 320 nL L⁻¹) was introduced at one complete air exchange per minute into each CSTR.

O₃ was produced by corona discharge (Model SGC-11, Pacific O₃ Technology, Brentwood, CA) from a feedstock of purified oxygen (Series ATF-15, Model 1242, SeQual Technologies Inc., San Diego CA). O₃ concentration followed a half-sine wave during daylight hours, 7 days week⁻¹, with voltage to the O₃ generator regulated by feedback from the exit stream of a master CSTR using an ozone monitor (Model 41C; Thermo Electron Corp.; Franklin MA, USA) calibrated against an O₃ calibration unit (Model 306; 2B Technologies, Boulder, CO, USA). The remaining CSTRs were controlled proportionally (Grantz et al., 2010) and monitored independently (Model 41C).

O₃ flux into the leaves was determined from bi-hourly measurements of stomatal conductance of the youngest fully expanded leaf and of the leaf two insertion levels older, using a porometer (AP4; Delta T Devices, Cambridge UK). Values are means of the two leaves, replicated in 3 CSTRs at each ozone concentration and over 2 runs with different sets of plants (n = 6). To calculate O₃ flux, conductance was converted from water vapor to O₃ using the ratio of diffusivities (Massman and Grantz, 1995; Massman, 1998), and multiplied by mean O₃ concentration during the 2 hour period centered on the conductance measurement. O₃ dose was calculated as flux summed over all daylight hours from germination to harvest.

Perchlorate Determination

All healthy leaves and the surface 5 cm of potting soil were collected at 9 weeks after planting and immediately frozen at -20 °C for shipping on dry ice to Texas Tech University for determination of ClO_4^- by ion chromatograph-tandem mass spectrometer (IC-MS/MS) as previously described in this report.

Samples were dried to constant weight (105° C; 12 hrs) and 1 g placed in a centrifuge tube with 25 mL of Milli-Q water, immersed in boiling water for 1 h, then centrifuged at 5000 rpm for 5 minutes. The supernatant (2 ml) was added to 1.0 ± 0.1 g of activated alumina, and diluted with 18 mL of DDI water, held at 3 °C for 8 h, then centrifuged at 5000 rpm for 5 minutes. The supernatant was filtered (0.2 micron), passed through a pre-cleaned and activated OnGuard® RP cartridge (Dionex Corporation; Sunnyvale CA), then diluted.

All extraction sets were accompanied by an extraction duplicate, an extraction spike (sample + known amount of added ClO_4^-), and an extraction blank (DDI water only). Samples were spiked with an oxygen-isotope (^{18}O) labeled ClO_4^- internal standard, then loaded into a 25 μL pre-concentrating loop. This was connected to the IC-MS/MS, with a GP50 pump, CD25 conductivity detector, AS40 automated sampler and Dionex IonPac AS16 (250 X 2 mm) analytical column, followed by an Applied Biosystems - MDS SCIEX API 2000® triple quadrupole mass spectrometer with a Turbo-IonSpray™ source. The eluent was 45 mM sodium hydroxide (NaOH) followed by 90% acetonitrile as a post-column solvent (both at 0.3 ml min⁻¹). The method detection limit (MDL) was 0.01 μM ClO_4^- .

Statistical Analysis

CSTRs were arrayed in three blocks parallel to windows and cooling fans, to isolate location effects. One CSTR per block was exposed to each of the three O_3 concentrations. Two runs were conducted with each species (n=6). The individual CSTR was taken as the unit of replication. Block and run were not significant and were pooled.

The relationship between ClO_4^- and O_3 exposure was evaluated independently for each species and for all species pooled, by regression analysis (SAS v. 9.3; PROC REG; SAS Institute, 2002). The relationship between ClO_4^- and O_3 dose was evaluated similarly, using both native ClO_4^- data and ClO_4^- data normalized within each species by the median value of ClO_4^- determined in each species over all O_3 exposures.

Basal ClO_4^- content of all species at low O_3 concentration was subjected to independent analysis by ANOVA (PROC GLM and PROC MEANS), with means separation by Duncan's Multiple

Range Test. Significant differences were identified at $P < 0.05$. Means are presented with standard errors of the means.

2.7.2.3 Results and Discussion

Species Differences in Perchlorate Uptake

There was considerable interspecific variability in the capacity for accumulation of ClO_4^- from the rhizosphere (Table 2.7.6). The large capacity to accumulate ClO_4^- from the environment in some species has been observed in other systems (Grantz et al., 2014; Jackson et al., 2005; Nzengung et al., 1999; Tan et al., 2004, 2005; Urbansky et al., 2000, 2000a; van Aken and Schnoor, 2002; Yu et al., 2004; Yang and Her, 2011). This capacity, in species including cottonwood (*Populus spp.* hybrids), *Eucalyptus cineria*, willow (*Salix nigra*), tamarisk (*Tamarix ramosissima*), cucumber (*Cucumis sativus*), lettuce (*Lactuca sativa*), and soybean (*Glycine max*), among others, has implications for bioremediation of contaminated soils and aquifers. Among the species examined here, foliar contents of ClO_4^- at low O_3 ranged from about $130 \pm 16 \mu\text{g (kg dry wt)}^{-1}$ (range $87 - 205 \mu\text{g (kg dry wt)}^{-1}$) in Pima cotton to over $500 \pm 191 \mu\text{g (kg dry wt)}^{-1}$ (range $252 - 1469 \mu\text{g (kg dry wt)}^{-1}$) in young leaves of soybean (Table 2.7.6). In our previous study described in Section 2.7.1, spinach (*Spinacia oleracea*) accumulated over $700 \mu\text{g (kg dry wt)}^{-1}$, while sugarcane (*Saccharum spp.*, hybrid) accumulated less than $100 \mu\text{g (kg dry wt)}^{-1}$.

These species differences reflect physiological differences in uptake/exclusion of ClO_4^- present in the growth medium. In both studies, plants accumulated less than 10% of the available ClO_4^- over the entire study period, but exhibited bioconcentration factors of up to two orders of magnitude. Accumulation of ClO_4^- was greater in older than in younger leaves as described in Section 2.7.1, reflecting the greater duration of uptake. ClO_4^- in the foliage is attributed to transpiration and deposition at the distributed sites of evaporation. In willow (*Salix nigra*) uptake was linear with transpiration rate (Nzengung et al., 1999) until a state of tissue saturation reduced net uptake to zero. In diverse types of lettuce (*Lactuca sativa*), the transpiring outer leaves contained an order of magnitude greater ClO_4^- than the sheltered inner leaves (Ha et al., 2013). Re-translocation of ClO_4^- has not been reported.

Root and stem tissue exhibit very low ClO_4^- contents relative to leaves, as observed in the present study (not shown; Grantz, et al., 2014) and in other species (Vogt and Jackson, 2010). In smartweed (*Polygonum spp.*), leaves accumulated up to $800 \mu\text{g (kg dry wt)}^{-1}$, while roots and stems contained less than $150 \mu\text{g (kg dry wt)}^{-1}$ (Tan et al., 2006).

Accumulation of ClO_4^- from the rhizosphere, its sequestration in older leaf cohorts, and their subsequent abscission, represents a possible mechanism of transporting and concentrating rhizosphere ClO_4^- to the soil surface (Section 2.7.1; Grantz et al., 2014). Under natural conditions and longer time frames this mechanism may be significant, but in the short term

experiments described here was not observed. Soil surface ClO_4^- values ranged from 6.2 to 8.4 $\mu\text{g (kg dry wt)}^{-1}$ (Table 2.7.7) at the highest O_3 exposure, similar to the values observed previously at lower O_3 (Table 2.7.4 in Section 2.7.1 and Table 2.7.7 herein). There was no relationship between plant capacity for ClO_4^- accumulation and the ClO_4^- content of the surface soil.

Table 2.7.6. Perchlorate concentration ($\mu\text{g (kg dry wt)}^{-1}$) of young leaves of contrasting crop species exposed to filtered air. Values followed by the same letter do not differ at $P < 0.05$.

Species	O_3 Exposure (nL L^{-1})	n	Perchlorate Content ($\mu\text{g (kg dry wt)}^{-1}$)	S.E.	Range
Soybean	4	6	524.54 a	± 190.88	251.90-1469.00
Bush bean	4	6	307.90 a,b	± 95.60	119.50-678.30
Maize	4	6	160.33 b	± 76.49	30.00-514.10
Sorghum	4	6	134.34 b	± 13.18	90.21-174.10
Pima Cotton	4	6	133.86 b	± 16.37	86.64-205.10

Table 2.7.7. Perchlorate concentration ($\mu\text{g (kg dry wt)}^{-1}$) of potting medium used for plant growth by contrasting crop species exposed to high O_3 . Values followed by the same letter do not differ at $P < 0.05$.

Species	O_3 Exposure (nL L^{-1})	n	Perchlorate Content ($\mu\text{g (kg dry wt)}^{-1}$)	S.E.	Range
Soybean	204	4	8.39 a	± 2.77	4.86-16.64
Bush bean	204	4	5.92 a	± 0.48	4.97-7.24
Maize	204	4	7.74 a	± 2.07	4.44-13.80
Sorghum	204	4	6.89 a	± 1.41	4.53-10.60
Pima Cotton	204	4	6.20 a	± 0.18	5.84-6.71

O₃ Impacts on ClO₄⁻ Accumulation

The soil surface and any Cl⁻ in the irrigation water or fertilizer near the surface were exposed directly to O₃. Soil surface enhancement of ClO₄⁻ could occur with increasing O₃ exposure due to soil surface reactions. The average soil surface ClO₄⁻ concentration, over all species at the highest O₃ (204 nL L⁻¹), was $7.03 \pm 0.70 \mu\text{g (kg dry wt)}^{-1}$, significantly greater than the ClO₄⁻ concentration of $3.77 \pm 0.72 \mu\text{g (kg dry wt)}^{-1}$ observed at the lowest O₃, and greater than that observed in the unused potting medium (Fig. 2.7.4). The unused potting mix (sampled directly from an unopened container) was non-significantly lower than that exposed to the low O₃, indicating that placement of the plant and soil in the CSTR, even in the absence of appreciable O₃, may have caused an increase in ClO₄⁻ due to unknown heterogeneous surface reactions.

The ClO₄⁻ concentration of surface soil increased linearly with increasing O₃ exposure (Fig. 2.7.4). A similar trend was observed in our previous study described in Section 2.7.1. The short exposure period in both of our experiments suggests that over longer time periods exposure of the soil surface to environmental O₃ could lead to environmentally significant accumulation of ClO₄⁻. Soil ClO₄⁻ does not appear to be attributable to retranslocation from leaves to root exudates. Such exudation of phytoaccumulated ClO₄⁻ was not observed into ClO₄⁻-free media in *Populus* (van Aken and Schnoor, 2002).

In contrast to the soil surface, there was no effect of O₃ exposure on foliar content of ClO₄⁻ in young leaves of any of the 5 crop species considered (not shown). Combining the data for all species increased the sample size substantially. This analysis also revealed no significant relationship between O₃ exposure and foliar ClO₄⁻ accumulation (Fig. 2.7.5).

Stomatal Responses and O₃ Dose

The use of O₃ concentration as a metric of O₃ exposure has limitations, associated with temporal shifts between stomatal opening and elevated ambient O₃ concentrations (Massman et al., 2000). This is addressed by use of measured or calculated uptake or flux of O₃ into the leaf, (i.e. O₃ dose) (Grunhage et al., 1997). Here, we directly measured stomatal conductance (g_s) over the diel timecourse, in sorghum (Fig. 2.7.6A) and bush bean (Fig. 2.7.6B) and several other species (Table 2.7.8). O₃ exposure had a strongly inhibitory effect on g_s , a commonly observed response that represents an active plant defense mechanism against oxidant injury (Massman et al., 2000). The observed values of g_s are lower than commonly observed with these species under higher light field conditions.

The daily mean g_s declined linearly with O₃ exposure in sorghum and bush bean (Fig. 2.7.6C, and D). The decline was proportional at the intermediate O₃ exposure in these species. In soybean and cotton (Table 2.7.8), exposure to 102 nL L⁻¹ induced a somewhat greater than proportional reduction in g_s , relative to 204 nL L⁻¹ O₃, resulting in a somewhat concave response

curve (not shown). In contrast, maize exhibited a slightly convex response curve. Reduction of mean conductance was between 28% and 83% at the highest O₃.

With simultaneous measurement of O₃ concentration, we calculated flux of O₃ directly (Section 2.7.1; Grantz et al., 2014). Ozone-induced reduction in stomatal conductance reduced the relative increase in O₃ dose compared with the increase in concentration, at intermediate and high exposures relative to the low [O₃]. Averaged over all species, the increase in ozone concentration was 20.4- and 40.8-fold, respectively, whereas the increase in dose was only 14.1- and 18.8-fold (not shown). No relationship between foliar ClO₄⁻ and O₃ concentration was found (Fig. 2.7.5) and no relationship was found by use of O₃ dose, in any species (not shown) nor in the pooled data (Fig. 2.7.7A), despite a wide range of dosage achieved. A similar absence of relationships, both between foliar ClO₄⁻ and O₃ concentration and between ClO₄⁻ and O₃ dose, was observed at lower O₃ concentrations in both young and old leaf cohorts in the previous study (Section 2.7.1). The flux metric did not contribute to identification of meaningful relationships in either case.

Normalization of the data within each species by its median value (Fig. 2.7.7B) did not strengthen the statistical relationship, also as observed in the earlier study.

Table. 2.7.8. Effect of exposure to ozone on stomatal conductance in contrasting species. Average of midday values (12:00 – 14:00).

Species	n	g_s at 4 nL L ⁻¹ (mol m ⁻² s ⁻¹)	S.E.	% g_s reduction relative to g_s at 4 nL L ⁻¹	
				100 nL L ⁻¹	204 nL L ⁻¹
Soybean	18	0.14 b	. ± 0.020	27%	29%
Bush bean	18	0.13 b	± 0.027	39% *	63% *
Maize	18	0.055 c	± 0.0084	16%	73% *
Sorghum	20	0.082 bc	± 0.0093	18%	33% *
Pima Cotton	12	0.29 a	± 0.032	79% *	83% *

(*) significant at $P < .05$.

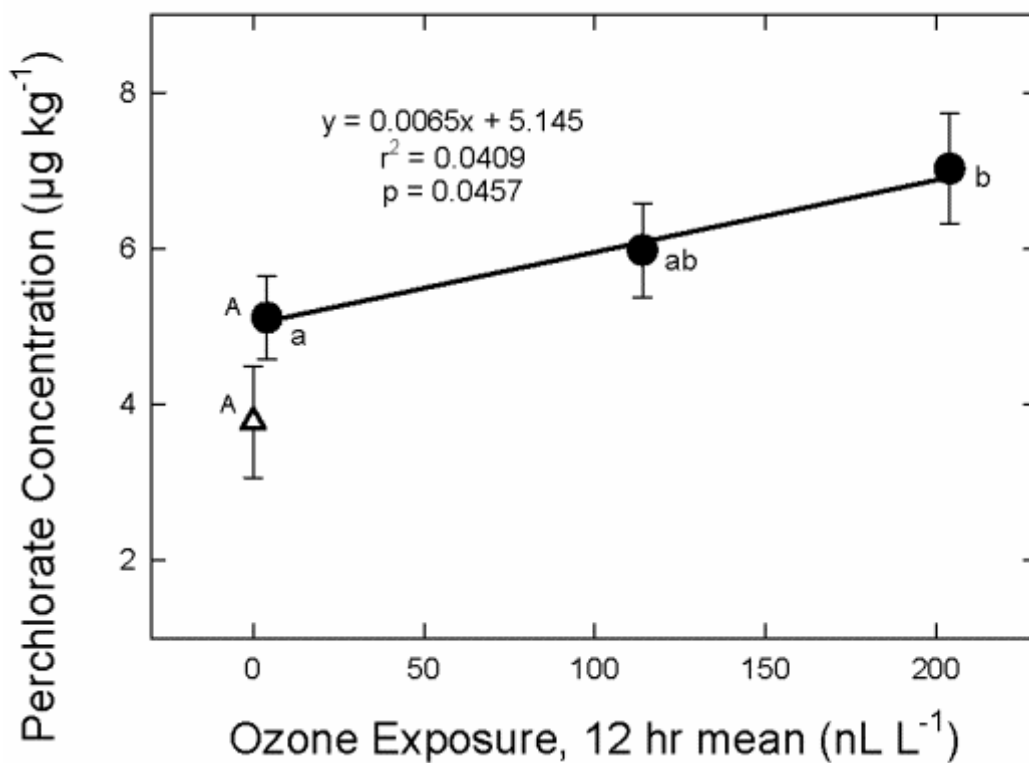


Figure 2.7.4. Significant relationship between perchlorate concentration ($\mu\text{g (kg dry wt)}^{-1}$) of potting medium exposed in the CSTRs and O_3 exposure (nL L^{-1} ; 12 hr mean; $r^2 = 0.99$; $P = 0.0714$). The data for unused medium and medium exposed to 4 and $114 \text{ nL L}^{-1} \text{ O}_3$ are from Grantz et al. (2014). Means followed by different letters are significantly different ($P < 0.05$).

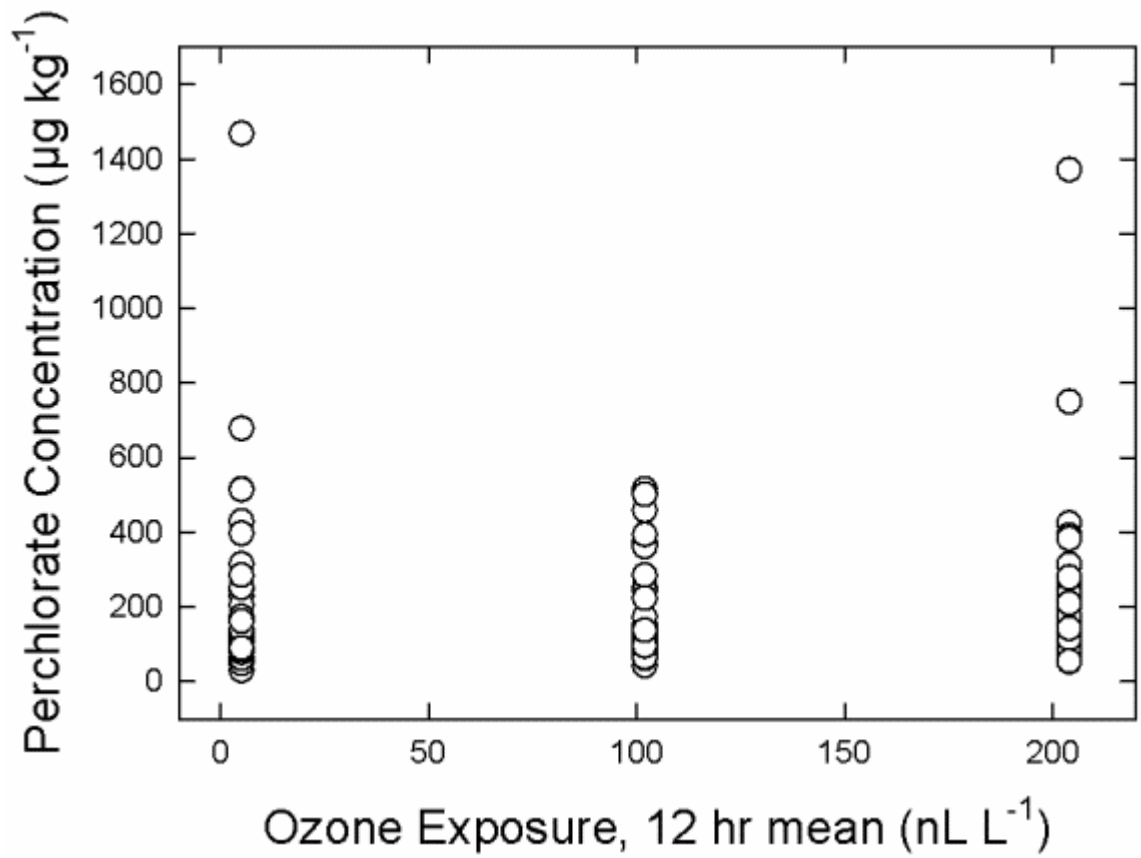


Figure 2.7.5. No relationship between perchlorate concentration ($\mu\text{g (kg dry wt)}^{-1}$) of young leaves and O_3 exposure.

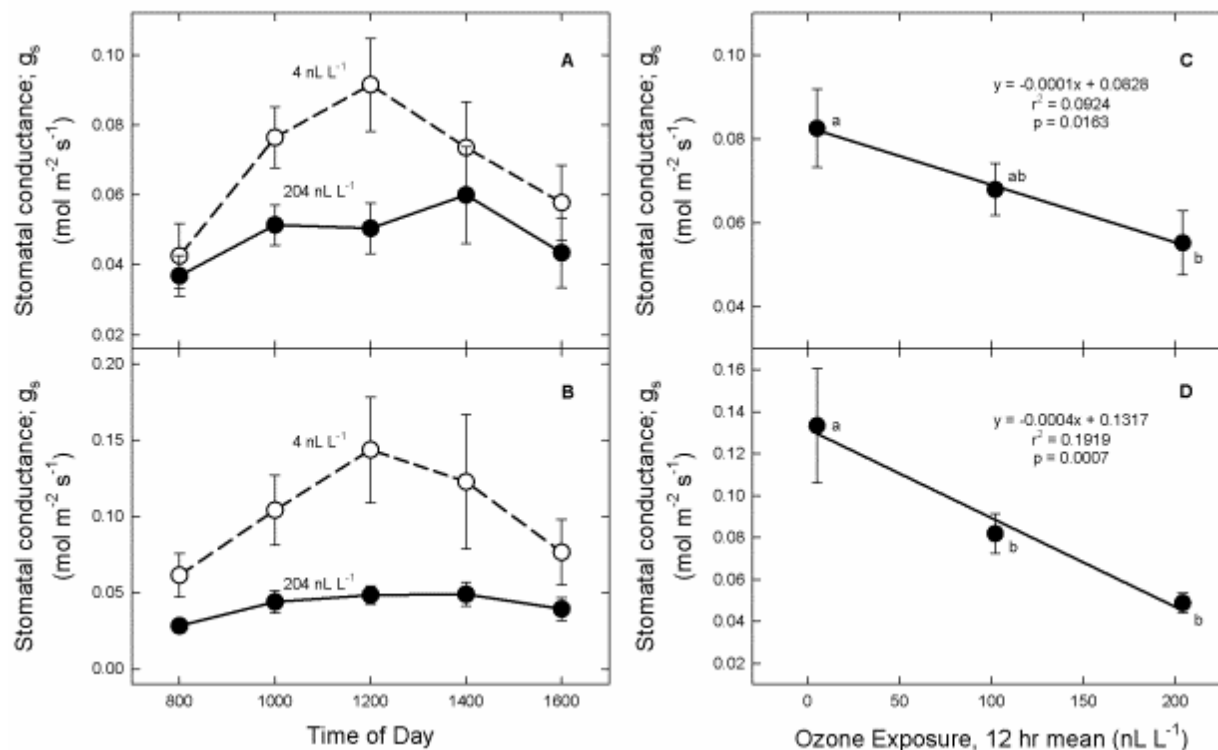


Figure 2.7.6. Effect of O_3 exposure on stomatal conductance (g_s). (A,B) Diel course of g_s in (A) sorghum and (B) bush bean at low (open symbols) and high (closed symbols) O_3 exposure. (C,D) Relationship between g_s of (C) sorghum and (D) bush bean (average of midday values, 12:00 – 14:00), and ozone exposure. Means followed by different letters are significantly different ($P < 0.05$).

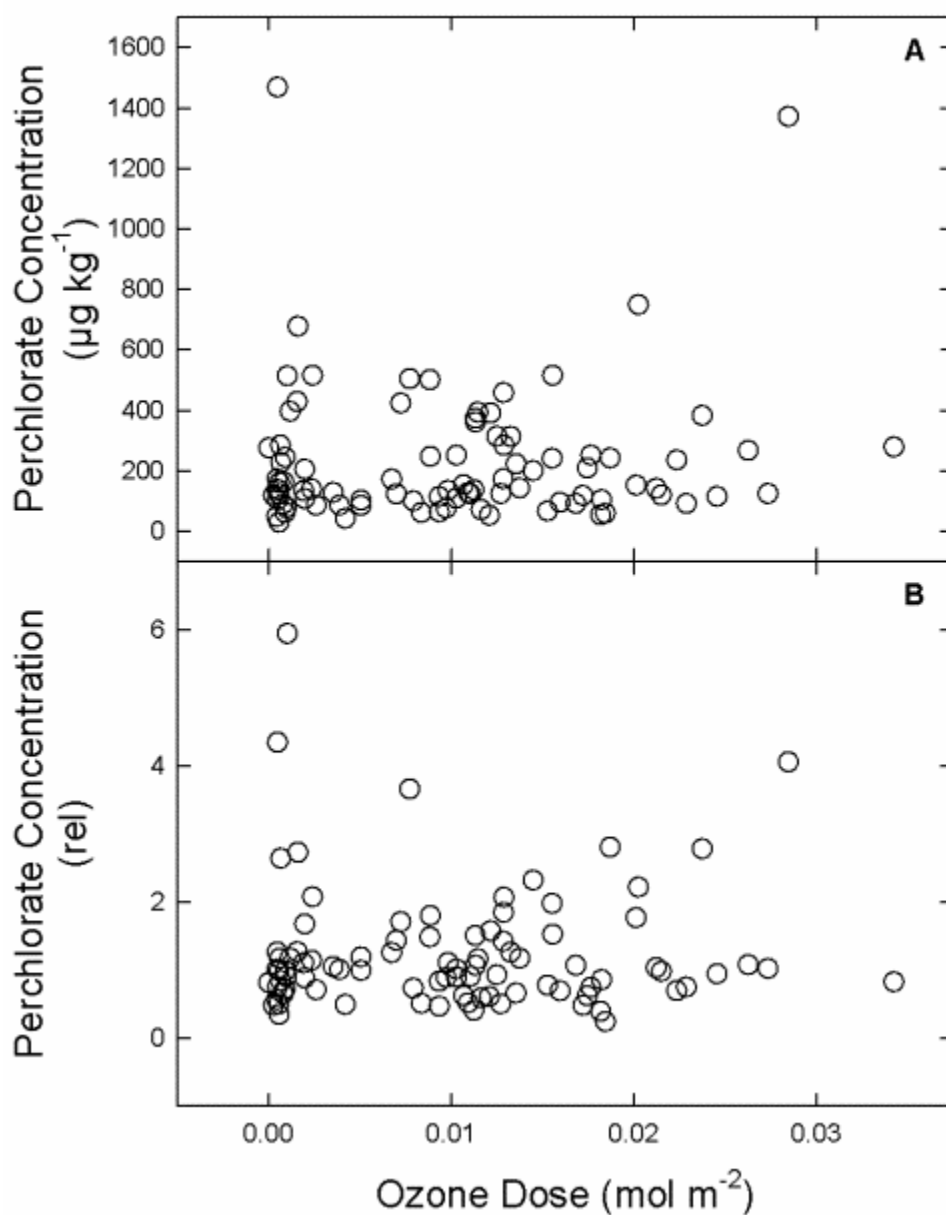


Figure 2.7.7. No relationship between (A) perchlorate concentration of young leaves ($\mu\text{g (kg dry wt)}^{-1}$) and O_3 dose; or (B) perchlorate concentration (unitless) normalized by the median concentration over all O_3 within each species, and O_3 dose.

2.7.2.4 Conclusions

The ubiquitous distribution of vegetation, rising concentrations of tropospheric O_3 , and occasional bursts of very high O_3 associated with stratospheric intrusion, combined with evidence that O_3 facilitates conversion of Cl^- to ClO_4^- under laboratory and field conditions, suggested that O_3 -exposed vegetation may contribute to the emission inventory for ClO_4^- in the environment. We show that contrasting crop species all accumulate ClO_4^- from the growth medium, but with different bioconcentration factors. We further show that exposure to very high O_3 up to 320 nL L^{-1} , hourly maximum, daily for 9 weeks, provided no evidence that foliar contents of ClO_4^- were related to O_3 exposure. There was no evidence that this relationship was strengthened by use of the measured uptake of O_3 into the leaf interior (O_3 flux or dose). These results are fully consistent with earlier results at more moderate concentrations of O_3 . We found a trend of increasing soil surface content of ClO_4^- with increasing O_3 in both studies. The consistency between studies and the environmental significance of this potential source of ClO_4^- suggest that this putative soil pathway deserves further investigation. As the concentrations of O_3 used in these studies are at or above those observed even during extreme events of tropopause folding and in polluted mega-cities in the developing world, we conclude that O_3 -exposed vegetation is not likely to be a significant source of environmental ClO_4^- .

2.8 Effect of Plant Uptake on Stable Isotope Composition of ClO_4^-

2.8.1 Background

A process which could affect ClO_4^- isotopes is plant uptake; however, its impact on ClO_4^- isotopic compositions is not yet clear. It is possible that plants could change the ClO_4^- isotopic composition through a variety of mechanisms including: transport carriers in the root; diffusion limitations through the root; reduction of ClO_4^- by plant reductases, translocation within the plant, and non-specific exchange of O between ClO_4^- and H_2O or other compounds catalyzed by plant compounds.

Uptake of ClO_4^- in plants has been studied extensively in both soil and hydroponic exposure experiments (Section 2.7; Sanchez et al., 2005a,b; Van Aken and Schnoor, 2002; Urbansky et al., 2000; Smith et al., 2004; Seyfferth et al., 2007, 2008 a,b; Yu et al., 2004; Nzengung et al., 1999, 2003, 2004; Tan et al., 2004a,b, 2006; Suslara et al., 2000; Ha et al., 2011; Voogt et al., 2010; Marschner, 1995). Most studies indicate ClO_4^- accumulation is species and genotype-dependent and most of the ClO_4^- accumulation occurs in transpiring tissues with large surface areas (e.g. leaves) (Sanchez et al., 2005a,b; Smith et al., 2004; Seyfferth et al., 2007, 2008 a,b; Nzengung et al., 1999; Voogt et al., 2010). From positive relations between the mass of ClO_4^- entering the plant and the amount of water being transpired, it is inferred that uptake of ClO_4^- is at least partially through passive transport, but demonstrated competition for uptake between ClO_4^- and other anions like NO_3^- and HCO_3^- from soil or water indicates that transport is not purely a passive process and that transport proteins may also facilitate transfer of ClO_4^- into plant cells (Seyfferth et al., 2008 a,b; Tan et al., 2006; Suslara et al., 2000; Voogt et al., 2010; Marschner, 1995; Farquhar et al., 1989). In contrast to NO_3^- and HCO_3^- other anions such as Cl^- , SO_4^{2-} , I^- , IO_3^- are not reported to interfere with ClO_4^- uptake (Seyfferth et al., 2008 ;Voogt et al., 2010; Marschner, 1995). The influence of NO_3^- on ClO_4^- uptake indicates that a similar uptake mechanism exists for both anions. Plant transporters are selective for specific anions on the basis of physicochemical properties, thus similarities in the properties of ClO_4^- and NO_3^- may cause competition for a common carrier protein or metabolic pathway within the plant tissue (Seyfferth et al., 2008; Farquhar et al., 1989).

It is well known that physiological and physicochemical processes (fixation, assimilation, and diffusion) in plants can cause isotopic fractionation of carbon ($^{13}\text{C}/^{12}\text{C}$) and nitrogen ($^{15}\text{N}/^{14}\text{N}$); (Evans, 2001; Mariotti et al., 1982; Tcherkez et al., 2006; Karsh et al., 2012). By analogy, intracellular processing of ClO_4^- within plants could also affect ClO_4^- isotope compositions. Isotopic discrimination occurs when NO_3^- is reduced and assimilated in plant tissue by the nitrate reductase enzyme, causing an increase in both $\delta^{15}\text{N}$ and $\delta^{18}\text{O}$ of the residual NO_3^- (Andraski et al., 2014). Although processes by which ClO_4^- might be metabolized within plants are unknown, considering that ClO_4^- and NO_3^- might share the same uptake mechanism, it is possible that ClO_4^-

may be subjected to reduction and isotopic fractionation in plants by action of a catalyst similar to nitrate reductase. At least one study (Van Aken et al., 2002) indicated ClO_4^- reduction in plants. Such processes in plants could affect the isotopic characteristics of ClO_4^- returned to soils and groundwaters if residual ClO_4^- is released back into the environment, which appears likely (Van Aken et al., 2002; Nzengung et al., 2004; Susalara et al., 2000; Laursen et al., 2013). Improved understanding of such processes could be useful for interpreting origins of environmental ClO_4^- and NO_3^- . The relative abundance and isotopic composition of ClO_4^- and NO_3^- in plants could also provide evidence about fertilizer sources used to grow commercial plant products (e.g. Mihailova et al., 2014; Hatzinger et al., 2011).

In this task, controlled experiments were conducted to develop procedures for analyzing the isotopic composition of ClO_4^- extracted from plants and to determine whether isotopic exchange or fractionation (by transport or degradation) might alter the isotopic composition of ClO_4^- accumulating in plants. This was accomplished by comparing the stable isotopic compositions of ClO_4^- accumulated in hydroponically grown snap bean plants (*Phaseolus vulgaris* L.) with those of the starting reference materials and growth solutions. Results were interpreted in part by contrasting the isotopic fractionation of ClO_4^- and NO_3^- in the same experiments. This is important because isotopic fractionation effects of enzymatic reactions may not fully be expressed in residual reactants (i.e. in heterogeneous systems where reactions are transport-limited). Therefore, a lack of observable isotope effects in extractable ClO_4^- might not be a reliable indicator of ClO_4^- stability unless extractable NO_3^- exhibited substantial fractionation effects. We also evaluated ClO_4^- isotopic composition in plants and source water for field-grown snap beans to validate the applicability of our methods in a more realistic setting. In order to demonstrate how our methods can be used to identify sources of ClO_4^- in the food chain, we analyzed commercially grown spinach and snap bean plants exposed only to background concentrations of ClO_4^- .

2.8.2 Materials and Methods

2.8.2.1 Hydroponic Experimental Design

Hydroponic greenhouse studies were conducted at the Texas Tech University Greenhouse Complex in Lubbock, TX. Snap beans (*Phaseolus vulgaris* L.) were grown hydroponically in nutrient solutions containing either normal synthetic reagent ClO_4^- or isotopically labeled ClO_4^- . Plants were harvested at maturity, when bean pods were full grown and flowering ceased. Plants were divided into roots, stems, leaves, and bean pods and each compartment was evaluated for ClO_4^- , NO_3^- , Cl^- uptake. Isotopic analyses were performed on ClO_4^- and NO_3^- in bean leaves and growth solutions. Details are described below.

Two hydroponic experiments were conducted with multiple treatments in each experiment (Table 2.8.1). Treatments generally consisted of plants grown in nutrient solutions containing ClO_4^- (0.01, 2, and 10 mg/L) along with NO_3^- and other ions. Two control treatments were also evaluated. One control contained no plants and 1 mg/L ClO_4^- and the other contained plants and had no ClO_4^- . The ClO_4^- for the 0.01, 1, and 10 mg/L exposures was supplied from a 98% sodium perchlorate (NaClO_4) lab reagent (ACROS Organics) while the ClO_4^- used in the 2 mg/L exposure was supplied from an isotopically labeled KClO_4 reagent (USGS38) distributed by the USGS (Reston, VA). All treatments were evaluated to determine the amount of ClO_4^- and NO_3^- lost from solution over time and the amount of ClO_4^- and NO_3^- accumulated in plant tissue, while a subset of treatments (1 mg/L no plants control, 2 mg/L ClO_4^- , and 10 mg/L ClO_4^-) were evaluated for stable isotopes.

Table 2.8.1 Summary of initial experimental conditions for ClO_4^- treatments in experiment 1 and 2. Experiment 1 was conducted during the months of October and December while experiment 2 was conducted during April and May.

Parameter	Experiment 1				Experiment 2			
	ClO_4^- Treatments (mg/L)				ClO_4^- Treatments (mg/L)			
	0	1	2	10	0	1	0.01	10
Cl (mg/L)	1.2 (0)	1.0 (0)	1.3 (0.4)	1.7 (0.3)	103 (0)	105 (0)	108 (1)	108 (3)
NO_3^- -N (mg/L)	274 (0)	268 (0)	274 (3)	264 (13)	237 (0)	240 (0)	237 (2)	235 (4)
PO_4^{3-} (mg/L)	48 (0)	46 (0)	72 (17)	59 (23)	72 (0)	74 (0)	76 (5)	70 (1)
SO_4^{2-} (mg/L)	117 (0)	110 (0)	116 (2)	113 (9)	130 (0)	137 (0)	144 (12)	142 (15)
# tubs (replicates)	1	1	4	2	1	1	2	2
Plants per tub	6	0	6	6	4	0	4	4

Anion concentrations reported are the means of the replicates for each ClO_4^- treatment. Standard errors of the means are indicated in parenthesis (e.g. Mean (\pm SD)).

Snap bean (*Phaseolus vulgaris* L.) seeds were sown in small rockwool cubes presoaked in reverse osmosis (RO) water. The seeds were watered daily with RO water until full germination (presence of 4-5 leaves, ~ 3 weeks) was achieved. During the germination period, the small rockwool cubes were transferred to larger rockwool cubes. Polypropylene/polyethylene opaque tubs measuring 52.7cm \times 36.87cm \times 33.3cm and pre-rinsed with RO water three times were filled with 32 L and 34L (for experiment 1 and experiment 2, respectively) of a standard nutrient solution that was made by the methods of a previous study (Marschner, 1995) with minor modifications (Table 2.8.1). Prior to transfer of the plants to the growth tubs, the pH of the nutrient solution was adjusted to 5.5- 6.1 by addition of HNO_3 . The rockwool cubes containing plants were then positioned on the lids of the tubs, which were then secured to the tubs with the plant roots hanging into the nutrient solution and plants exposed to air. Rockwool cubes were covered with aluminum foil to prevent algae growth. Commercial aquarium pumps supplied air to maintain bulk oxic conditions in solution for the duration of the experiments.

Once germination reached the 4-5 leaf stage (~15-18 days), plants were exposed to ClO_4^- by addition of a concentrated solution in selected tubs. The water level in each tub was maintained by adding RO water weekly. Growth solution samples from each tub were collected every two to three days and refrigerated immediately until they could be analyzed. Electrical conductivity and pH were also measured two to three times weekly. To maintain pH between 5.5 and 6.1, 3M KOH was added as needed. After some weeks, insects became apparent and leaves were treated

using Safer Soap (AgroCrop Sciences). Eventually, insects became so problematic the plants were sprayed with Orthonex (an organophosphate insecticide).

Snap bean plants were harvested 62-65 days after germination, corresponding to 38 days of ClO_4^- exposure. The bean pods, leaves, stems, and roots from each treatment were separated, weighed, and then placed in labeled plastic bags. The plastic bags were placed in a freezer until processed. The growth solution and rockwool cubes in which the plants were grown were also weighed and frozen until processed.

2.8.2.2 Sampling and Processing of Hydroponic Solutions

The plant solute extraction method of Ellington and Evans, (2000) was used in these experiments with minor modifications. Leaves, bean pods, stems, and roots were separated into approximately 20, 5, 6, and 10 g fresh weight (FW) portions, respectively. Each portion of leaves, bean pods, stems, and roots were placed in containers (vials) with 200, 25, 25, and 20 mL of distilled deionized (DDI) water, respectively. Water/plant tissue mixtures were boiled for 30-60 minutes in a precision boiler set at 99°C. The boiled extracts were centrifuged and the supernatant was decanted into containers (vials) with activated alumina (Al_2O_3) and placed in the refrigerator overnight. Each leaf aqueous extract was then vacuum filtered using GF/F 47 mm Whatman™ filters. The bean pod, stem, and root extracts were filtered using syringe Whatman™ filters. From each tissue extraction solution, a small volume was separated and cleaned by passing the aqueous extract through a (0.2 μm) syringe filter and a Dionex RP cartridge. Cleaned samples from each treatment were analyzed for ClO_4^- , Cl^- , NO_3^- -N, SO_4^{2-} , and PO_4^{3-} and a small volume was set aside and preserved for NO_3^- isotopic analysis by raising the pH to 11-12 using 50% w/w NaOH. The remaining filtered supernatants for each tub in each treatment were pooled together to make one extraction solution per treatment for ClO_4^- isotopic analysis. The pooled leaf extracts for each treatment as well as the remaining nutrient solutions, excluding the 0.01 mg/L and no ClO_4^- control plant extraction and growth solutions, were pumped through Purolite A-530E resin columns to capture the ClO_4^- (Gu et al., 2011). Columns were preserved with 0.1 N HCl and stored at 4°C until processing.

2.8.2.3 Snap Bean Field Studies

Ozone-sensitive (S156) and tolerant (R123) snap bean genotypes described previously (Burkey et al., 2005) were grown in field plots during the summers of 2009 – 2011 at two locations to provide bulk leaf tissue for extraction and isotopic analysis of ClO_4^- . The first site was located at the USDA-ARS Air Quality field site 5 km south of Raleigh, NC (Lat: 35°43'59" N; Long: 78°41'2" W) and the second site was located at the Long Island Horticultural Research & Extension Center, Riverhead, NY (Lat: 40°57'36" N; Long: 72°43'12" W). For each location in each year, three separate plots consisting of 500 linear feet of row were established as three experimental blocks with each block consisting of one S156 plot and one R123 plot (randomized

complete block design). Fields were cultivated before planting and a '10-10-10 Extra' fertilizer blend (Carolina Eastern-Vail, Niverville, NY) was applied at a rate of 500 lbs/acre by broadcast and incorporated into the soil prior to planting. Approximately 1500 seeds were sown per plot in late May or early June each year at both sites. Plots were provided water equivalent to at least 1 inch of rain per week by either natural rainfall or supplemental drip irrigation from wells located at each site. In preliminary tests, well water at the NC site was found to contain a relatively high concentration ClO_4^- ($\sim 5 \mu\text{g/L}$). In this case, a Purolite® A-530E resin filter was used to reduce ClO_4^- levels. Irrigation water at the NY site was found to contain ~ 0.3 ppb ClO_4^- , and filtering was not deemed necessary. At 45-55 days after planting at the developmental stage where vegetative biomass was near maximum, leaf tissue was manually harvested from each plot, placed in mesh bags, and dried at 60°C . Dried leaf tissue was stored in large plastic bags to exclude moisture and prevent contamination and then shipped to Texas Tech University for ClO_4^- extraction and purification.

Field grown snap bean leaves were extracted two times for 48 hours in large 55-gallon barrels using reverse osmosis water to which the pH was reduced to 2 using HCl. Leaves were removed from solution and the solution was pumped through a $0.45 \mu\text{m}$ filter and Purolite® A-530E resin columns. The resin columns were stored at 4°C until processed for ClO_4^- isotopes.

2.8.2.4 Sampling and Processing of Spinach

Thirty-eight (38) kg of fresh spinach leaves in pre-packaged plastic bags was purchased from a supermarket in Lubbock, Texas. Spinach sold by the supplier was conventionally grown by the NewStar Fresh Foods Limited Liability Company in the Salinas Valley, California region from April through October and the Yuma, Arizona region from November through March. The spinach was purchased in early November and thus it is not known which location the spinach was from. The spinach was frozen to rupture the plant cell walls and facilitate ion extraction.

Solutes were extracted using a spinach to water ratio of 0.28 by weight (19 kg /84 kg). The leaves were mixed thoroughly in the water and were allowed to extract overnight. Leaves were then removed from the solutions and the extraction solution was pumped through a $0.45 \mu\text{m}$ filter and Purolite A-530E resin column. The extraction column was preserved with HCl at a pH ≤ 2 .

2.8.2.5 Sample Analyses

Concentrations of ClO_4^- and major anions (Cl^- , NO_3^- , SO_4^{2-} , PO_4^{3-}) in hydroponic solutions and plant extracts were measured at Texas Tech University using sequential ion chromatography-mass spectroscopy-mass spectroscopy (IC-MS/MS) with a reporting limit of $0.05 \mu\text{g/L}$ (ClO_4^-) and ion chromatography (EPA Method 300.0) with a reporting limit of 0.5 mg/L (other anions) as previously described in this report. The ClO_4^- in the resin columns was extracted and purified

at Oak Ridge National Laboratory using procedures described previously (Hatzinger et al., 2011; Gu et al., 2011). Purified ClO_4^- was shipped to the USGS in Reston Virginia for analysis of $\delta^{18}\text{O}$, $\delta^{17}\text{O}$, and $\Delta^{17}\text{O}$ of O_2 produced by decomposition of ClO_4^- and the Cl^- residue from the decomposed ClO_4^- was analyzed for $\delta^{37}\text{Cl}$ at the University of Illinois at Chicago (Hatzinger et al., 2011). The NO_3^- stable isotope ratios ($\delta^{18}\text{O}$, $\delta^{15}\text{N}$) of hydroponic solutions and plant extracts were also analyzed at the USGS in Reston, Virginia (Sigman et al., 2001; Casciotti et al., 2002; Böhlke et al., 2003, 2007). Isotopic reference materials and calibration values for ClO_4^- and NO_3^- were from Böhlke et al. (2009) and Böhlke et al. (2003), respectively. Selected samples were analyzed for NO_2^- concentration and isotopic composition, as NO_2^- can interfere with NO_3^- isotopic analysis (Böhlke et al., 2007).

2.8.3 Results

2.8.3.1 Hydroponic Study

Changes in the Growth Solutions

Substantial water loss occurred in both hydroponic experiments (Figure 2.8.1). This loss was attributed mainly to transpiration, as the cumulative volume of growth solution lost in treatments with no plants was less than 10% of the initial volume compared to a cumulative loss greater than 96 % of the initial volume in treatments with plants (Figure 2.8.1). Within each experiment the volume of solution transpired by plant treatments was similar regardless of the presence or absence of ClO_4^- , but the volume transpired in experiment 2 was approximately twice that of experiment 1 (Figure 2.8.1). Experiment 1 was conducted during the months of October and December and experiment 2 during the months of April and May when temperatures were higher, possibly contributing to higher transpiration in experiment 2. Individual tubs contained more plants in experiment 1, but plant mass was 2-4 fold higher in experiment 2, possibly contributing to more overall transpiration in experiment 2.

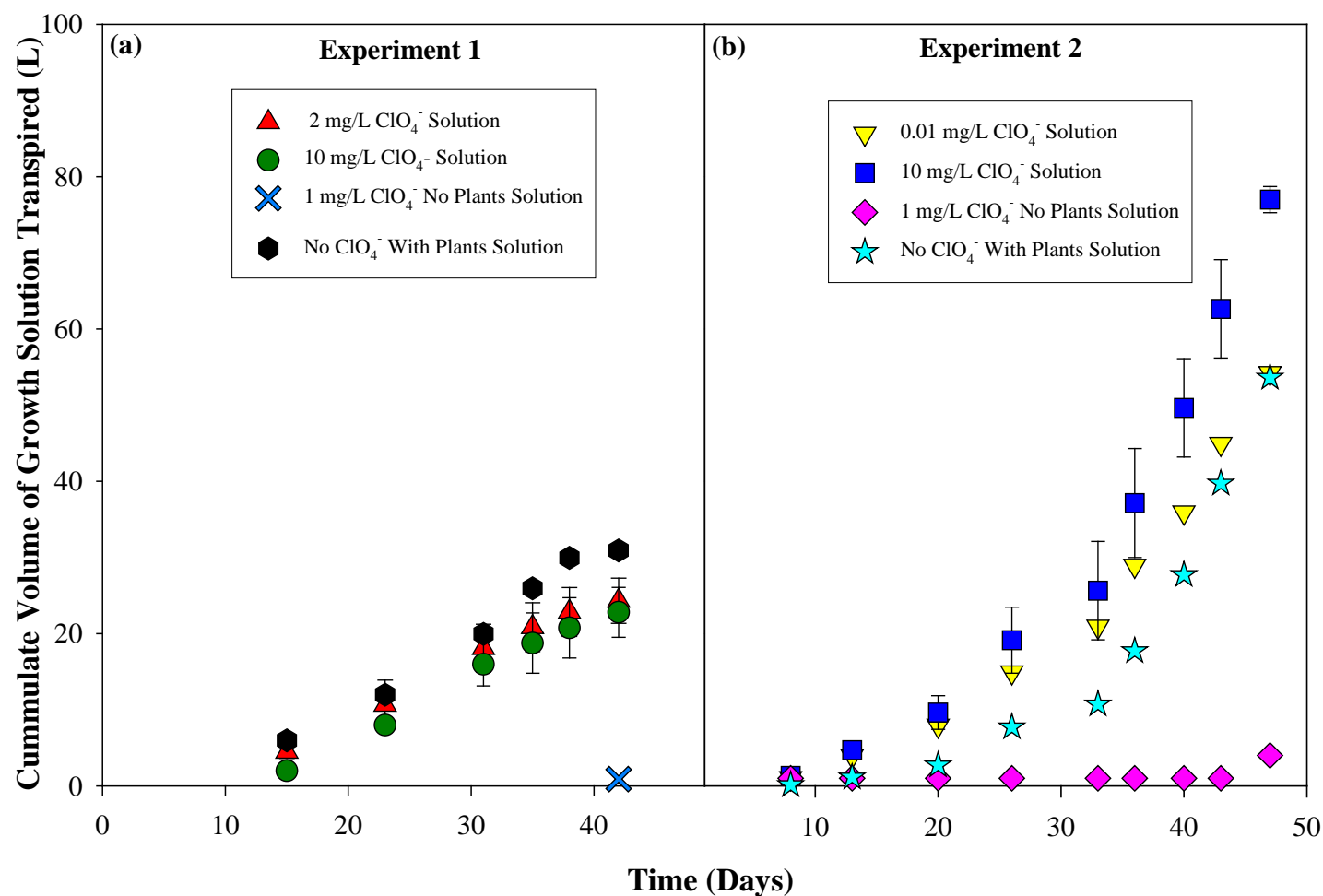


Figure 2.8.1. Cumulative volume of growth solution uptaken by pooled replicate treatments in both experiments.

Cumulative volume refers to the overall volume of nutrient solution uptaken by the snap bean plants in each treatment from time of exposure to nutrient solution to time of harvest. Values plotted are average values of the replicates in each treatment. No replicate is available for the control treatments or for the 0.01 mg/L ClO_4^- treatment.

As DDI water was added to replace transpired water, ClO_4^- concentrations in the hydroponic tubs generally should have not changed as a result of dilution, but they were affected by selective uptake into plants. Therefore, our results are reported on a mass basis hereafter. As in previous studies (Van Aken et al., 2002; Seyfferth et al., 2007; Tan et al., 2006), ClO_4^- mass in hydroponic solutions of treatments with plants decreased gradually over time in a non-linear fashion (Figure 2.8.2a and 2.8.2d). On a cumulative mass loss basis, our results indicate an overall loss of 60-80% of the initial ClO_4^- from solution (Figure 2.8.2a and 2.8.2d). The fractional mass loss of ClO_4^- from solution was independent of initial ClO_4^- concentration, but there was a larger overall decrease in ClO_4^- solution mass in experiment 2, which had higher transpiration loss of water (Figure 2.8.2d and Table 2.8.2). There was an unexplained decrease (~20%) in ClO_4^- solution mass in treatments with no plants in experiment 1, but not experiment 2. Linear correlations that were independent of initial ClO_4^- treatment concentration ($r^2 = 0.82$ and 0.95 for 2 mg/L and 10 mg/L ClO_4^- , respectively, $P < 0.05$) were observed between the amount of solution transpired and the fraction of ClO_4^- solution mass loss in experiment 2 (Figure 2.8.3a). Insufficient time points were available to evaluate such correlations in the first experiments. Our results support previous work (Seyfferth et al., 2007; Tan et al., 2004) that suggests ClO_4^- mass lost from solution is directly proportional to the volume of transpired water, but less than the predicted amount based on water uptake and the concentration in solution.

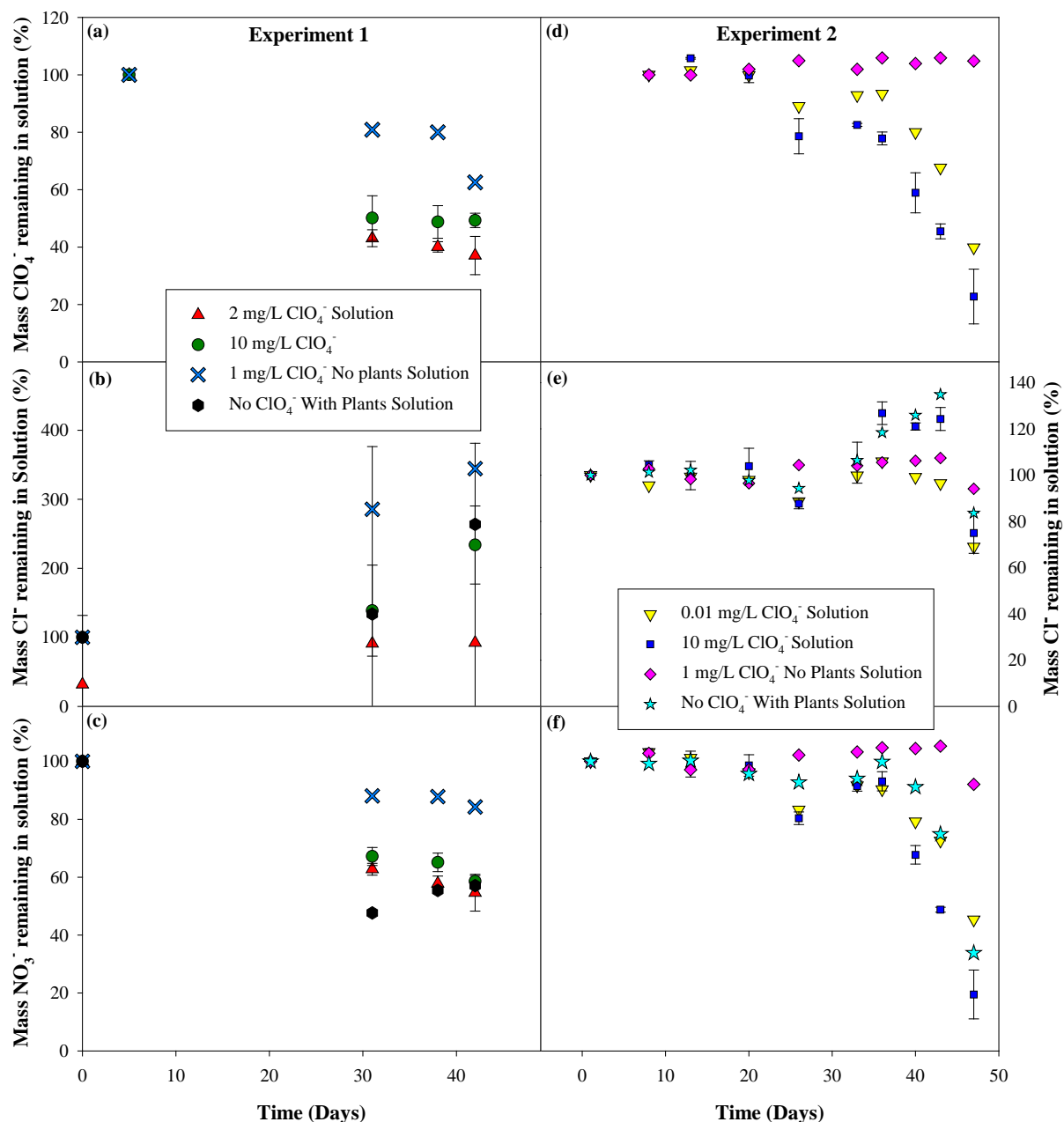


Figure 2.8.2. Fraction of ClO_4^- , Cl^- , and NO_3^- mass remaining in nutrient solutions at the time of harvest. Values reported are the average of pooled replicates in each treatment. Experiment 1 data is represented in graph panels (a), (b), and (c) while experiment 2 data is represented in panels (d), (e), and (f). No replicate is available for the control treatments or for the 0.01 mg/L ClO_4^- treatment.

Like ClO_4^- , the NO_3^- concentrations in solutions of treatments with plants decreased gradually over time in a non-linear fashion and there was smaller NO_3^- loss (< 20% of total NO_3^-) in the no plant treatments (Figure 2.8.2c and 2.8.2f and Table 2.8.2). The NO_3^- fractional mass loss was linearly correlated ($P < 0.05$) with the amount of solution transpired regardless of initial ClO_4^- treatment concentration ($r^2 = 0.76, 0.83, 0.86$ for 0, 0.01, and 10 mg/L ClO_4^- , respectively) (Figure 2.8.3c). Both NO_3^- and ClO_4^- had similar uptake rates as % mass/L transpired (-0.8683 ± 0.15 to -0.9912 ± 0.21) and (-0.97 ± 0.08 to -1.02 ± 0.17), respectively, supporting a similar uptake mechanism, as also suggested previously by other studies (Seyfferth et al., 2008; Marschner, 1995).

In contrast to ClO_4^- and NO_3^- , Cl^- mass in solution remained relatively constant (~ 80-120%) throughout the experiment regardless of initial ClO_4^- treatment concentration and presence or absence of plants (Figure 2.8.2e). There was no correlation between mass of Cl^- removed from solution and the amount of solution transpired ($r^2 = 0.0001-0.2255$, $P > 0.05$ for all treatments combined) (Figure 2.8.3b). Although Cl^- clearly was accumulated in plants, the amount taken up was small compared to the amount in solution (high – Cl^- in experiment 2) or small compared to analytical uncertainty (low – Cl^- in experiment 1).

Table 2.8.2. Average ClO_4^- , NO_3^- , Cl^- and total-N fractional mass distribution in growth solution and snap bean plant tissue.

Parameter	Experiment 1: ClO_4^- Treatments (mg/L)				Experiment 2: ClO_4^- Treatments (mg/L)			
	0	1	2	10	0	0.01	1	10
% ClO_4^- mass of initial total ClO_4^- mass (SD)								
Final Solution	N/A	62.5(0.0)	37.1(6.7)	49.3(2.5)	N/A	39.8(0.0)	104.8(0.0)	22.8(9.6)
Leaves	N/A	N/A	16.3(1.7)	17.9(7.2)	N/A	41.4(0.0)	N/A	53.7(6.5)
Bean Pods	N/A	N/A	4.1(0.5)	4.9(0.4)	N/A	2.2(0.0)	N/A	7.3(0.6)
Stems	N/A	N/A	0.26(0.04)	0.29(0.07)	N/A	1.3(0.0)	N/A	0.98(0.18)
Roots	N/A	N/A	0.22(0.09)	0.24(0.09)	N/A	0.9(0.0)	N/A	0.59(0.02)
Rockwool	N/A	N/A	0.11(0.01)	0.15(0.00)	N/A	NM	N/A	NM
Unaccounted	N/A	37.5(0.0)	42.0(7.3)	27.3(4.4)	N/A	14.3(0.0)	-4.8(0.0)	19.8(3.4)
% NO_3^- mass of initial total NO_3^- mass (SD)								
Final Solution	57.1(0.0)	84.3(0.0)	54.7(6.4)	58.6(2.1)	33.8(0.0)	45.3(0.0)	92.0(0.0)	19.5(8.4)
Leaves	0.45(0.0)	N/A	0.49(0.08)	0.29(0.14)	4.0(0.0)	1.4(0.0)	N/A	1.9(1.7)
Bean Pods	0.45(0.0)	N/A	0.41(0.03)	0.36(0.01)	0.26(0.0)	0.6(0.0)	N/A	1.3(0.7)
Stems	0.52(0.0)	N/A	0.61(0.15)	0.4(0.0)	1.4(0.0)	1.2(0.0)	N/A	1.7(0.2)
Roots	0.31(0.0)	N/A	0.33(0.10)	0.27(0.10)	4.6(0.0)	2.4(0.0)	N/A	3.3(0.3)
Rockwool	NM	NM	NM	NM	NM	NM	NM	NM
Unaccounted	41.2(0.0)	15.7(0.0)	43.5(6.4)	40.1(1.8)	55.8(0.0)	49.1(0.0)	8.0(0.0)	72.3(6.9)
% Cl^- mass of initial total Cl^- mass (SD)								
Final Solution	N/A	N/A	N/A	N/A	78.2(0.0)	77.3(0.0)	101.0(0.0)	73.0(13.0)
Leaves	N/A	N/A	N/A	N/A	2.0(0.0)	5.8(0.0)	N/A	3.9(1.3)
Bean Pods	N/A	N/A	N/A	N/A	0.85(0.0)	2.0(0.0)	N/A	3.0(1.8)
Stems	N/A	N/A	N/A	N/A	3.6(0.0)	4.7(0.0)	N/A	4.6(2.8)
Roots	N/A	N/A	N/A	N/A	2.0(0.0)	1.3(0.0)	N/A	1.6(1.0)
Rockwool	N/A	N/A	N/A	N/A	NM	NM	N/A	NM
Unaccounted	N/A	N/A	N/A	N/A	13.2(0.0)	8.6(0.0)	-1.0(0)	13.6(9.6)
% total-N mass of Initial total-N mass (SD)								
Final Solution	57.1(0.0)	84.3(0.0)	54.7(6.4)	58.6(2.1)	NM	NM	NM	NM
Leaves	12.8(0.0)	N/A	10.8(1.6)	13.8(3.9)	NM	NM	NM	NM
Bean Pods	14.3(0.0)	N/A	13.8(1.0)	12.4(1.6)	NM	NM	NM	NM
Stems	3.8(0.0)	N/A	3.9(0.9)	3.2(0.9)	NM	NM	NM	NM
Roots	2.7(0.0)	N/A	3.1(1.6)	2.7(1.0)	NM	NM	NM	NM
Rockwool	NM	NM	NM	NM	NM	NM	NM	NM
Unaccounted	9.4(0.0)	15.7(0.0)	14.3(6.0)	9.3(5.3)	NM	NM	NM	NM

NM = Not Measured

N/A = Not Applicable

(SD) = Standard deviation

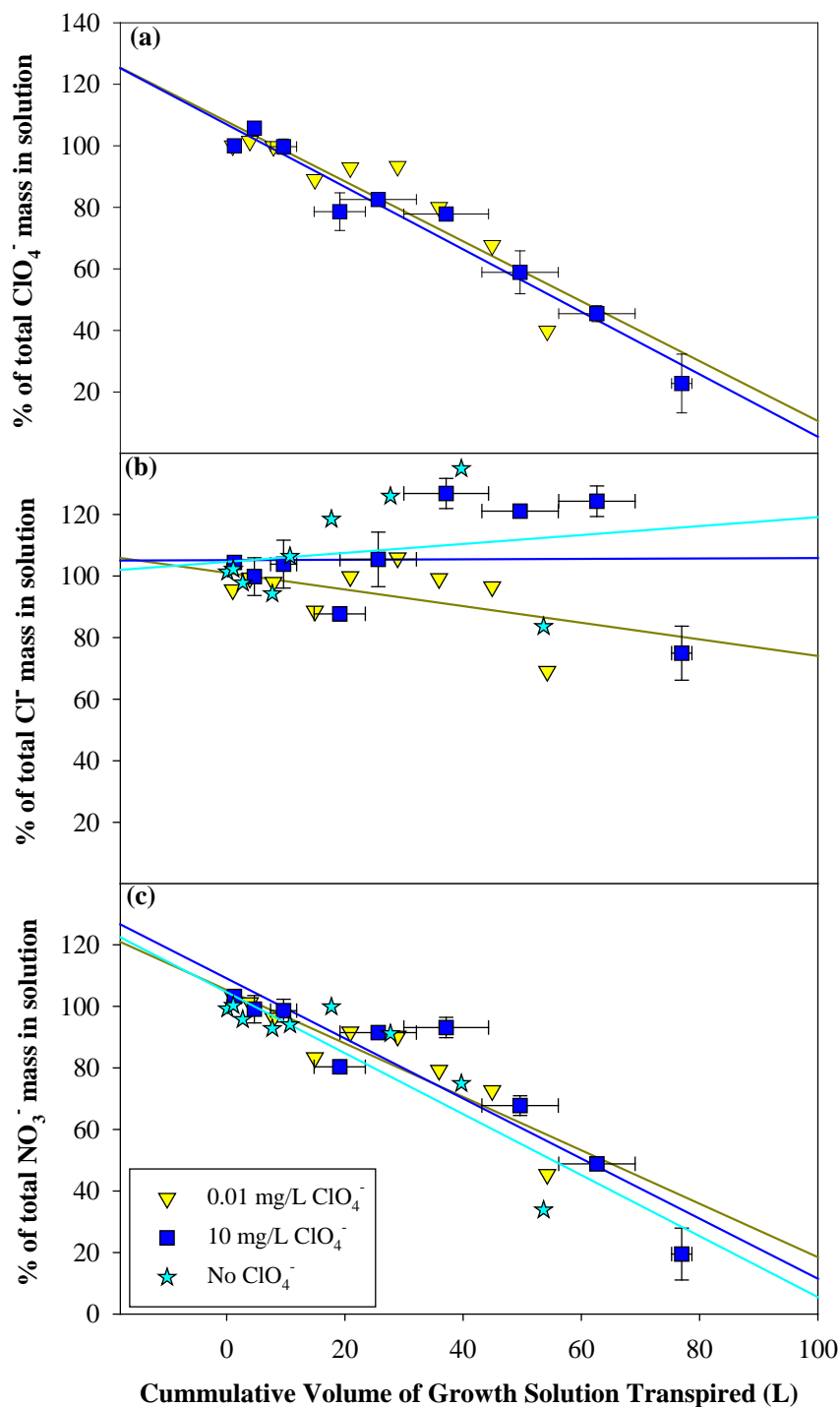


Figure 2.8.3. Relationship between fraction of total (a) ClO_4^- , (b) Cl^- , and (c) NO_3^- mass lost from solution and cumulative volume of solution transpired over the course of experiment 2. The grayish yellow regression lines correspond to the 0.01 mg/L ClO_4^- treatment, the dark blue regression lines correspond to the 10 mg/L ClO_4^- treatment, and the aqua blue regression lines correspond to the no ClO_4^- with plants treatment. Not enough data was collected for an analysis of experiment 1. No replicate is available for the 0.01 mg/L treatment.

Anion Distributions and Bioconcentration Factors

Whole plants were sectioned and solutes were extracted from plant tissue to determine how much ClO_4^- from solution had accumulated in the plant. Plant uptake of ClO_4^- was proportional to exposure concentration in both experiments, but more ClO_4^- mass was accumulated in experiment 2 for the same exposure concentrations, likely because of more total loss of H_2O by transpiration in experiment 2. To facilitate comparisons, leaf bioconcentration factors (BCF) were calculated using Equation 1.

$$BCF = \frac{\text{Ion mass per plant fresh weight at harvest (mg/kg)}}{\text{Initial ion concentration in solution (mg/L)}} \quad (1)$$

Combined results of both experiments yielded ClO_4^- BCF values of 66 ± 0 , 64 ± 3 , and 63 ± 11 L/kg fresh weight (FW) for the 0.01, 2, and 10 mg/L ClO_4^- treatments, respectively. Our BCF values were higher than those reported for lettuce (2-25 L/kg; Seyfferth et al., 2007) but within the range of those reported for spinach (17-102 L/kg; Voogt et al., 2010). The distribution of ClO_4^- between the different plant parts was independent of ClO_4^- exposure concentration in both experiments (Table 2.8.2). Of the ClO_4^- found in the plant, the majority was located in leaves (77-90%), a finding consistent with past studies (Jackson et al., 2005; Seyfferth et al., 2007, 2008; Nzengung et al., 2003, 2004; Voogt et al., 2010). The next largest accumulation of ClO_4^- was detected in bean pods (4-21%), followed by stems (1.2-2.8%), and then roots (1-2%). A mass balance was performed to determine the fate of ClO_4^- lost from solution. Approximately 27.3 ± 4.4 to $42.0 \pm 7.3\%$ and 14.3 ± 0.0 to $19.8 \pm 3.4\%$ of the initial ClO_4^- mass was unaccounted for in experiment 1 and experiment 2, respectively (Table 2.8.2). The solute extraction procedure was applied to the rockwool cubes in which snap bean seeds were sown at the end of experiment 1 to determine if they were a possible sink for missing ClO_4^- , but the amount of ClO_4^- recovered was negligible compared to the amount unrecovered (Table 2.8.2).

BCF values were also calculated for NO_3^- in both experiments (1.56 ± 0.76 , 0.49 ± 0 , 1.38 ± 0.11 , and 1.40 ± 0.63 L/kg for 0, 0.01, 2, and 10 mg/L ClO_4^- , respectively), but these values are not meaningful as most of the NO_3^- was converted within plants to organic N. Only a small amount of NO_3^- was detected in plant tissues, with the accumulation being higher in the experiment 2, which had higher transpiration (Table 2.8.2). Fractional mass of plant NO_3^- was relatively similar among different plant tissues. Much of the NO_3^- lost from solution ($\sim 15.7 \pm 0$ to $43.5 \pm 6.4\%$ and 8.0 ± 0 to $72.3 \pm 6.9\%$ in experiment 1 and experiment 2, respectively) was recoverable as N in plant tissues, as indicated by the near-quantitative recovery of the initial total-N (Table 2.8.2). Experiment 1 BCF average values for total-N were 158, 181, and 159 for 0, 2, and 10 mg/L ClO_4^- treatments, respectively.

The BCF values for Cl^- (1.85, 8.76, and 3.74 L/kg for the 0, 0.01, and 10 mg/L ClO_4^- treatments in the second experiment, respectively) were much lower than those for ClO_4^- indicating that

plants selectively uptake ClO_4^- as opposed to Cl^- . Plants did not accumulate much Cl^- , but of the Cl^- in the plant, Cl^- percent mass was distributed similarly between leaves and stems (24-43%) and between bean pods and roots (10-24%). The fraction of Cl^- mass recovered in the snap bean plant and the Cl^- mass not accounted for were comparable (~ 9-15%) (Table 2.8.2).

Perchlorate Isotopes

The role of plant uptake on ClO_4^- isotopic composition was determined by evaluating the isotopic composition of solution and plant leaf ClO_4^- . To minimize ambiguity in the results, two sources of ClO_4^- were used in the experiments: a normal synthetic NaClO_4 lab reagent and a KClO_4 salt that was depleted in ^{37}Cl and enriched in ^{18}O and ^{17}O (USGS38, with large positive $\Delta^{17}\text{O}$). With few exceptions, leaf and solution ClO_4^- isotopic composition ($\delta^{37}\text{Cl}$, $\delta^{18}\text{O}$, $\Delta^{17}\text{O}$) were not consistently different from each other in both experiments using both ClO_4^- sources ($n = 4$ pairs) (Figure 2.8.4). For most experiments using isotopically anomalous ClO_4^- (Figure 2.8.4a and 2.8.4b), small differences between final growth solutions and leaf extracts were not systematically in one direction or the other, and likely represent small variations or impurities or isotope effects of sample preparation. One of the 2 mg/L ClO_4^- replicate treatments in experiment 1 had anomalously high $\delta^{18}\text{O}$ and relatively high $\delta^{37}\text{Cl}$ in leaf tissue, but not difference in $\Delta^{17}\text{O}$ (Figure 2.8.4a and 2.8.4b). That sample may have been isotopically fractionated slightly, but it is not known if the anomalous result was caused by plant processes or subsequent handling of the organic-rich extract. The NO_3^- extracted from that sample was not anomalous. For experiments with normal reagent ClO_4^- (Figure 2.8.4c and 2.8.4d), small apparent trends could be consistent with fractionation effects in growth solutions or plants, but overall variations were ≤ 1 ‰. Given typical uncertainties of approximately ± 0.5 to ± 1.0 ‰ due to combined effects of ClO_4^- extraction, purification, and isotopic analysis, these data indicate isotopic fractionation or exchange attributable to plant ClO_4^- uptake, plant ClO_4^- transformation, microbial ClO_4^- transformation, or isotopic exchange between ClO_4^- and other constituents during the experiments was generally insignificant.

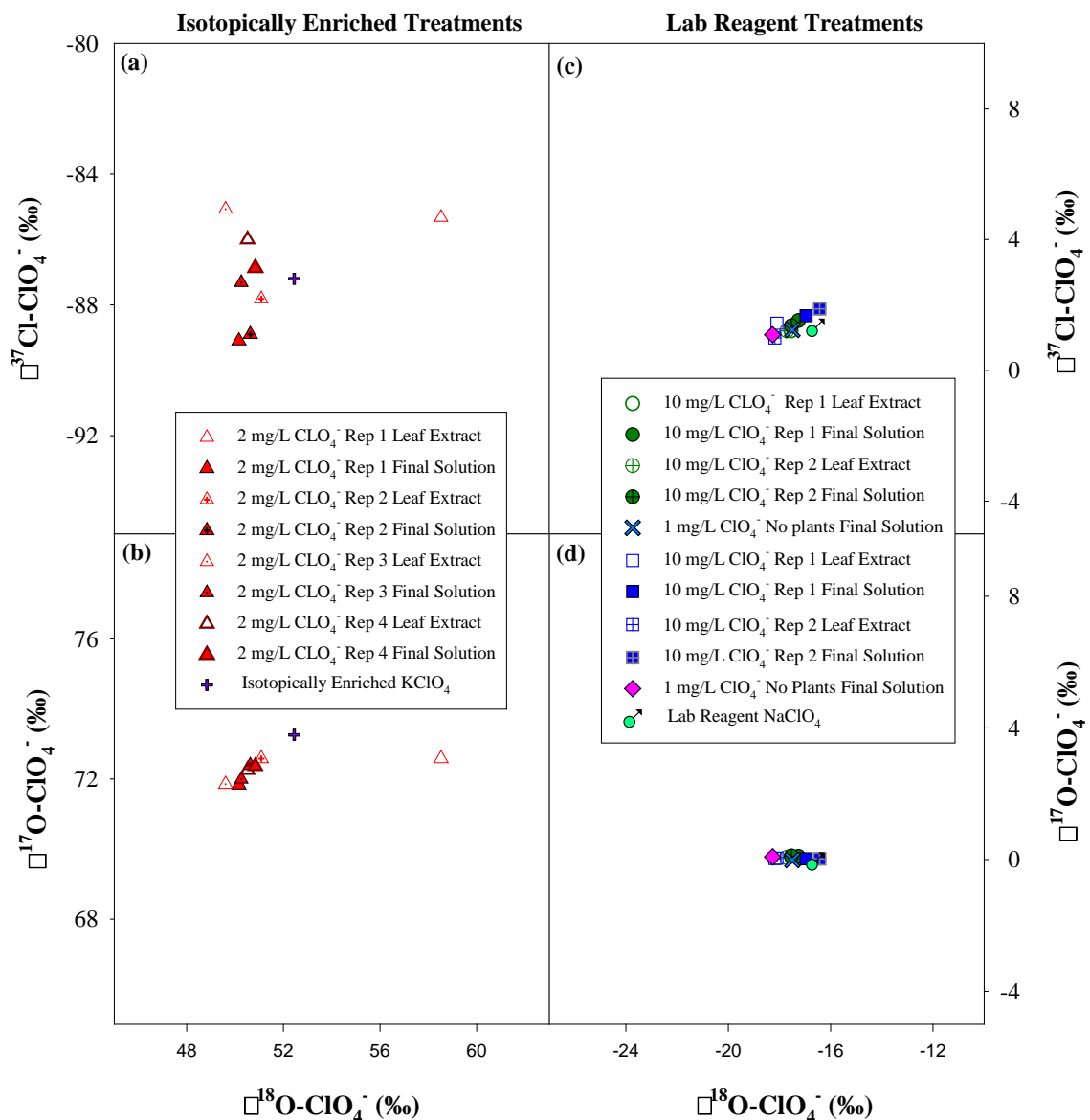


Figure 2.8.4. Stable ClO_4^- isotopic composition of nutrient solutions and leaf extracts of replicate treatments in experiment 1 and 2. Experiment 1 is represented by the red triangle, green circle, and light blue cross symbols, while experiment 2 is represented by the dark blue square and pink diamond symbols. $\delta^{37}\text{Cl}$, $\delta^{18}\text{O}$ (O2-DI), and $\Delta^{17}\text{O}$ values are referenced to 0 for SMOC, VSMOW, and VSMOW, respectively.

Nitrate Isotopes

Hydroponic solution NO_3^- $\delta^{15}\text{N}$ values appear to have increased slightly ($< 2 \text{ ‰}$) over time in both experiments for all treatments with plants but no increase was observed in control treatments without plants (Figure 2.8.5). In experiment 1, $\delta^{15}\text{N}$ increases were small but fairly constant throughout the growth period, whereas in experiment 2 the increases did not occur until mid-way through the growth period. In the two treatments with the largest $\delta^{15}\text{N}$ increases, $\delta^{18}\text{O}$ also increased significantly, whereas $\delta^{18}\text{O}$ variations in other treatments were within normal analytical uncertainties. Apparent isotope fractionation factors (ϵ) derived from residual NO_3^- in solution were of the order of -0.6 to -1.5 ‰ for $\epsilon(15/14)$ and -0.4 to -3.1 ‰ for $\epsilon(18/16)$ (Figure 2.8.6). Correlated increases in $\delta^{15}\text{N}$ and $\delta^{18}\text{O}$ in late stages of two treatments could indicate minor fractionation by plant uptake or NO_3^- reduction, but the apparent effects in solution were much smaller than those attributable to assimilation within the plants (Figure 2.8.5). Apparent $\epsilon^{15}\text{N}/\epsilon^{18}\text{O}$ values for NO_3^- in solution of around 0.5 - 0.6 (Figure 2.8.6f) were lower than most reported values for NO_3^- reduction ($\epsilon^{15}\text{N}/\epsilon^{18}\text{O} \approx 1$) and possibly more like those reported for NO_3^- transport from solution into plants (Needoba et al., 2003, 2004; Granger et al., 2010) though overall uncertainties are large.

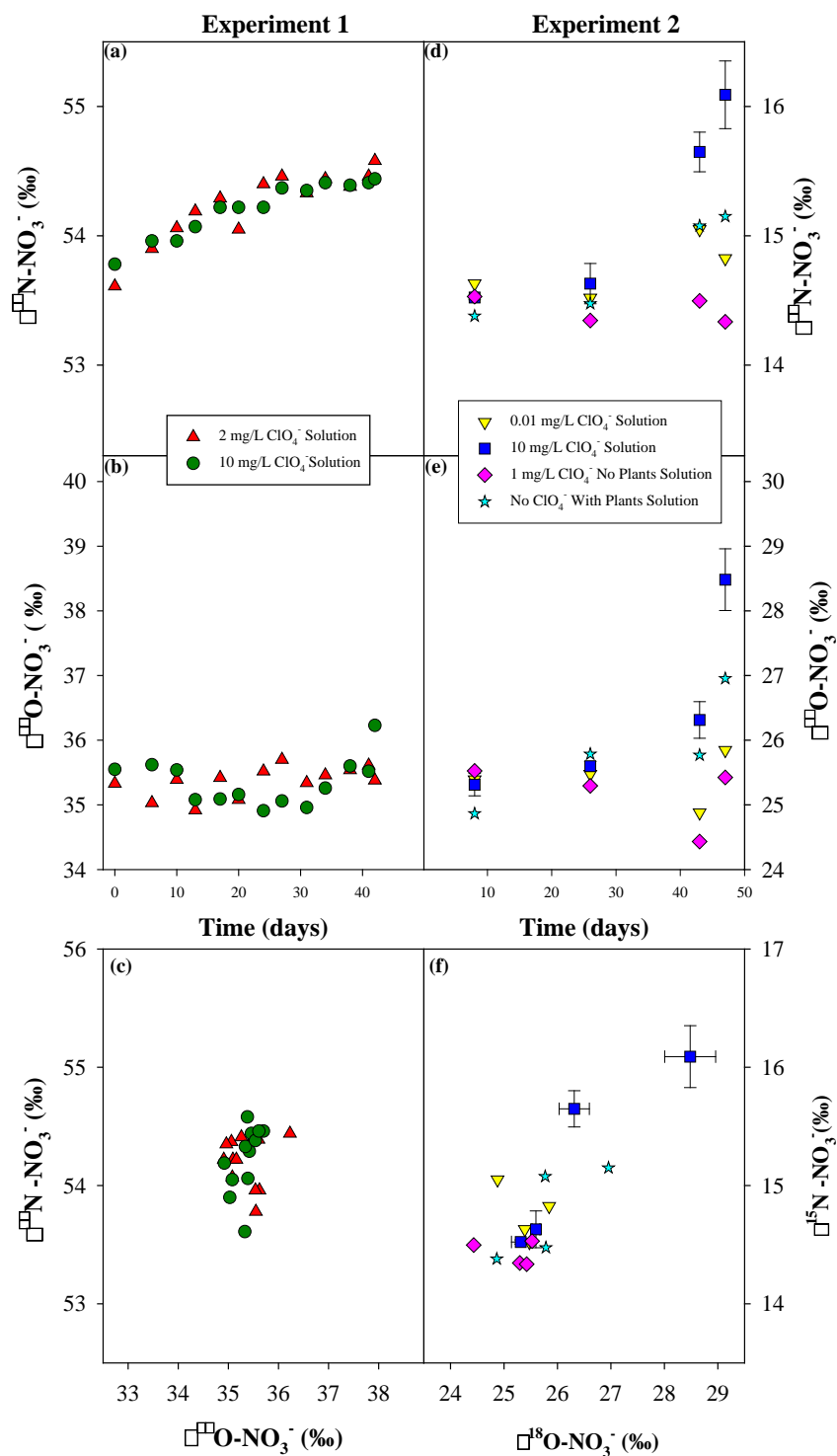


Figure 2.8.5. Stable isotopic composition of NO_3^- in nutrient solutions as a function of time for experiment 1 (a, b) and experiment 2 (d, e). Panels (c) and (f) show the corresponding relation between $\delta^{15}\text{N}$ and $\delta^{18}\text{O}$. Initial NO_3^- isotopic compositions differed between the experiments. Only a subset of solution samples was analyzed in experiment 2.

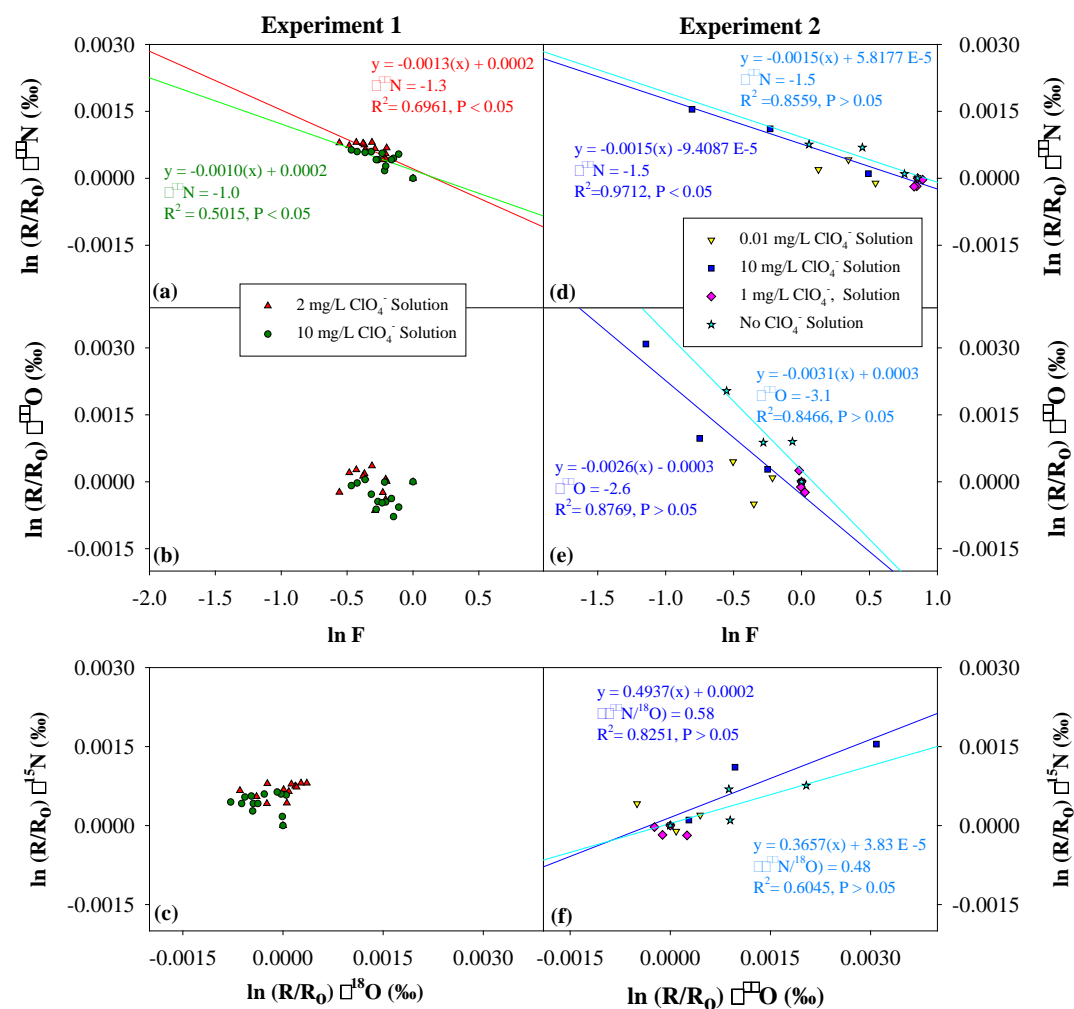


Figure 2.8.6 Rayleigh plots of the change in the $\delta^{15}\text{N}$ and $\delta^{18}\text{O}$ of NO_3^- in nutrient solutions of experiment 1(a, b, c) and experiment 2 (d, e, f). The colors of the regression lines and text are the same as those of the symbols for the treatments they represent (e.g. red = 2 mg/L ClO_4^-).

$\delta^{15}\text{N}$ and $\delta^{18}\text{O}$ values of NO_3^- extracted from leaves were higher than those in the hydroponic solutions (by about 10-20‰) (Figure 2.8.7). In both experiments there were linear ($P < 0.001$) correlations between $\delta^{15}\text{N}$ and $\delta^{18}\text{O}$ values of leaves and growth solutions with ratios ($\Delta^{15}\text{N}/\Delta^{18}\text{O}$) of 1.07 (experiment 1) and 1.04 (experiment 2), consistent with reported effects of NO_3^- reduction during assimilation by plants (Granger et al., 2004; Trull et al., 2008, DiFiore et al., 2009). This is supported by $\delta^{15}\text{N}$ measurements of plants from experiment 1. Total N- $\delta^{15}\text{N}$ varied by around 3.4 ‰ in different plant compartments (i.e. roots, stems, leaves, and bean pods). Highest $\delta^{15}\text{N}$ values were in stems ($\pm 34 \pm 3$ ‰) and lowest values were in roots ($\pm 29 \pm 4$ ‰). The weighted composite mean $\delta^{15}\text{N}$ value for whole plants in experiment 1 was $+31 \pm 4$ ‰. A mass balance on total N in Experiment 1 indicates that at least 84 – 91% of the total initial mass of total-N is accounted for in residual growth solutions and whole plant tissue (Table 2.8.2). In experiment 1, $\delta^{15}\text{N}$ values were $\sim +54$ ‰ for solution NO_3^- , $\sim +31$ ‰ for final plant tissue, and $\sim +72$ ‰ for final residual NO_3^- extracted from leaves. These results are quantitatively consistent with isotope effects dominated by internal NO_3^- reduction during assimilation. Plant total-N isotope data are not available for experiment 2, but isotopic contrasts between solution NO_3^- and leaf NO_3^- were similar to those in experiment 1, even though the NO_3^- reagents used in the experiments had different initial isotopic compositions (Figure 2.8.7).

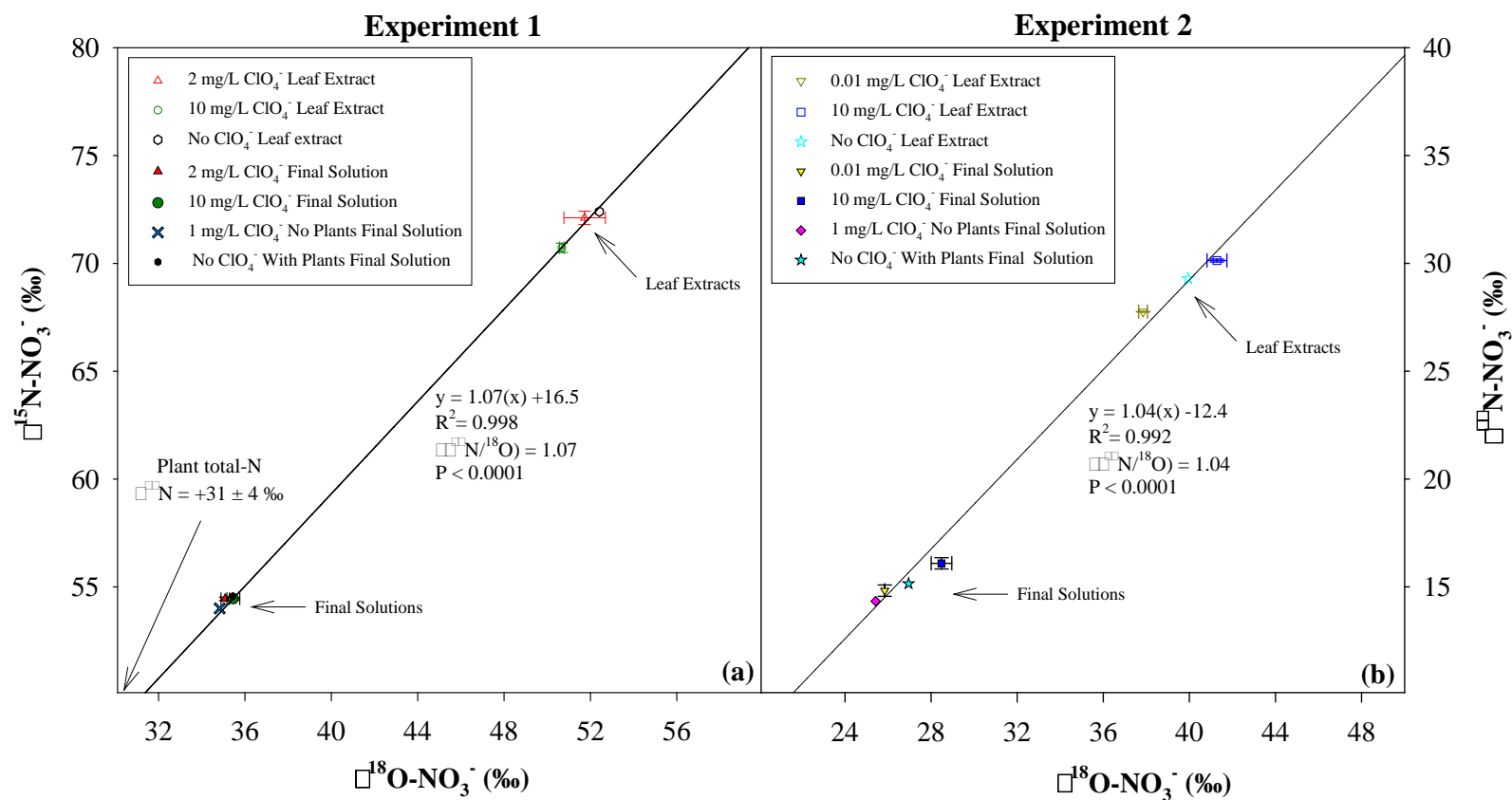


Figure 2.8.7. Stable isotopic composition of NO_3^- in final growth solutions (solid symbols) and leaf extracts (open symbols) of pooled replicate treatments in experiments 1 and 2. Plant total-N $\delta^{15}\text{N}$ was only measured in experiment 1.

2.8.3.2 Snap Bean Field Study Results

ClO_4^- isotopic values of field-grown snap beans from Raleigh, NC varied between years. The isotopic composition of plants grown in 2009 was intermediate and located on a two component mixing line between the isotopic composition of ClO_4^- in groundwater used for irrigation and the isotopic composition of indigenous ClO_4^- from groundwater in the US (Jackson et al., 2010) (Figure 2.8.8). In 2010, the isotopic composition of the snap beans was indistinguishable, given cumulative error terms ($< \pm 2\%$), to the isotopic composition of ClO_4^- in the groundwater. The isotopic composition of ClO_4^- in the groundwater was very similar to the composition of Atacama ClO_4^- , consistent with the elevated ClO_4^- concentrations and documented historical use of Chilean fertilizers. The difference in isotopic composition between years is qualitatively consistent with the variation in the mass of applied ClO_4^- from each source (groundwater and atmospheric deposition) between years based on variations in rainfall and ClO_4^- concentration in applied groundwater (Table 2.8.3).

Snap beans grown at Raleigh, NC received varying proportions of rainfall and groundwater in 2009 and 2010 (Table 2.8.3). Concentrations of ClO_4^- in applied groundwater also varied between 2009 and 2010 (0.6 and 2.2 $\mu\text{g/L}$, respectively), presumably due to exhaustion of the ion exchange column installed to remove ClO_4^- from applied groundwater (Table 2.8.3). The increase of applied ClO_4^- from groundwater is reflected in the $\sim 5\text{X}$ higher foliar ClO_4^- concentrations in 2010 (X and Y, respectively). The similarity between the snap bean and groundwater isotopic composition in 2010 is consistent with the much larger applied ClO_4^- mass from groundwater in 2010, (48 and 480 $\mu\text{g/m}^2\text{-yr}$ (growing season only), in 2009 and 2010, respectively) (Table 2.8.3). The intermediate isotopic composition of foliar ClO_4^- in 2009 is consistent with a larger contribution from indigenous ClO_4^- due to the order of magnitude decrease in groundwater applied ClO_4^- (i.e., containing Atacama ClO_4^-). Annual average ClO_4^- deposition rate in the US is $\sim 6.5 \mu\text{g/m}^2\text{-yr}$ with an unknown contribution from dry deposition ⁴

The ClO_4^- composition in snap beans from Long Island appears to reflect multiple sources, possibly dominated by indigenous ClO_4^- and Atacama ClO_4^- with a smaller contribution of manmade ClO_4^- (Figure 2.8.8). It is not possible to determine if the foliar ClO_4^- isotopic composition is consistent with the contributing sources as no data are available on the isotopic composition of the groundwater. Long Island groundwater has previously been shown to be a mix of indigenous and Atacama ClO_4^- and given the very low concentrations of ClO_4^- in the groundwater ($\sim 0.4 \mu\text{g/L}$), the isotopic data are not unreasonable (Böhlke et al., 2009). Regardless, we show that for field-grown plants even with background levels of foliar ClO_4^- , it is possible to evaluate foliar isotopic composition.

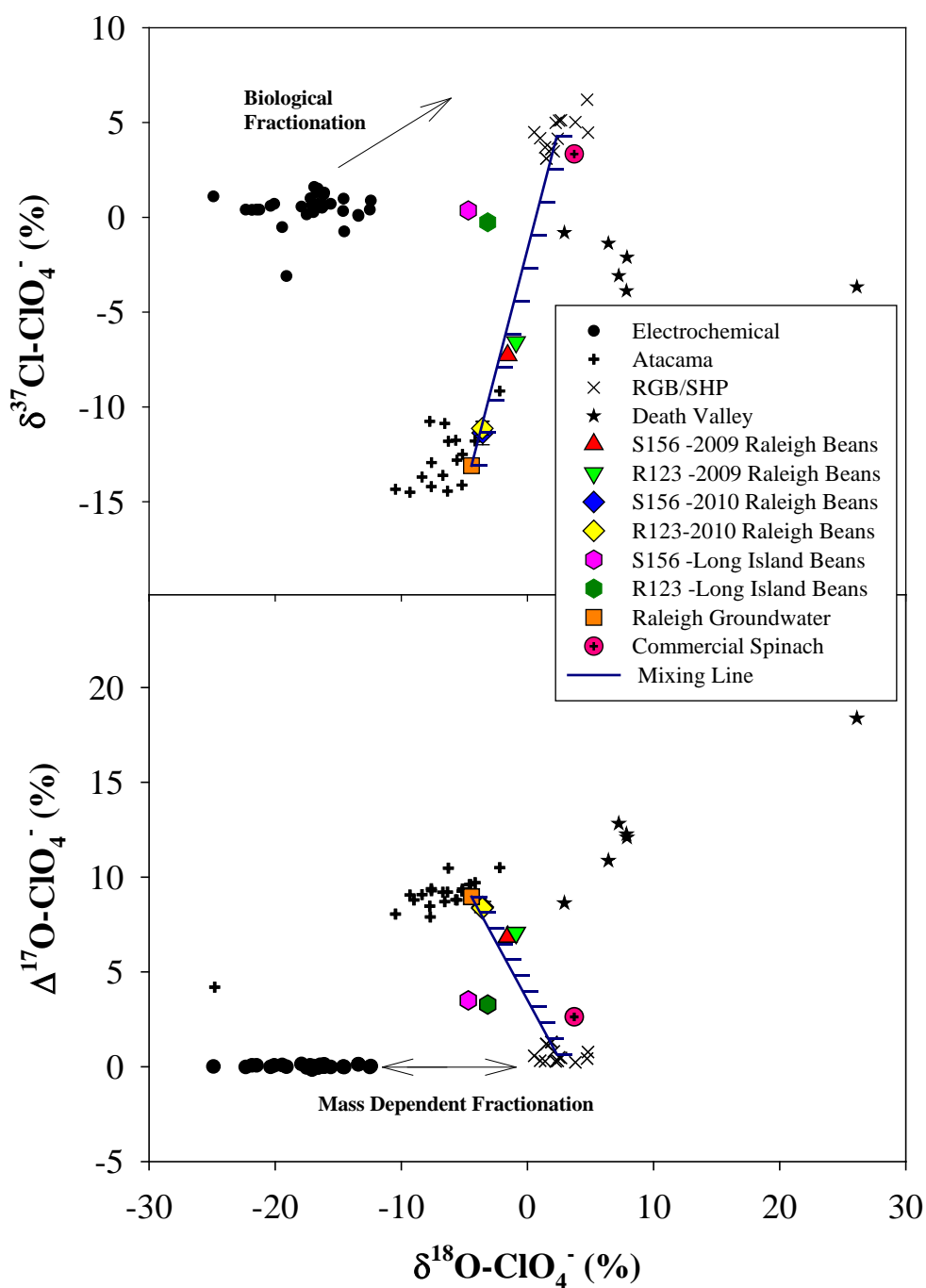


Figure 2.8.8. Summary of isotope data for ClO_4^- from Raleigh, NC and Long Island, NY field studies and commercial spinach displayed with previously published ClO_4^- isotope data from synthetic and natural sources from the Atacama Desert in Chile, Death Valley (DV), California, and the Southern High Plains (SHP) and Middle Rio Grande Basin (MRGB) of Texas and New Mexico (Jackson et al., 2010; Böhlke et al., 2005; Bao and Gu, 2004; Hatzinger et al., 2011). Symbols with error bars for the 2010 Raleigh bean S156 ($n = 3$) and R123 ($n = 2$) plots indicate average values (\pm standard deviation). The mixing line (dark blue) was calculated assuming a two-member source (Raleigh groundwater and RGB/SHP) isotopic mass

Table 2.8.3 Irrigation, rainfall, and foliage ClO_4^- data for the Raleigh, NC and Long Island, NY snap bean field studies. All values reported are mean values.

Year	Raleigh, NC							Long Island, NY						
	Foliar	Irrigation			Rainfall			Foliar	Irrigation			Rainfall		
	ClO_4^- ($\mu\text{g/kg}$)	Total Depth (cm)	ClO_4^- ($\mu\text{g/L}$)	ClO_4^- ($\mu\text{g/m}^2$)	Total Depth (cm)	ClO_4^- ($\mu\text{g/L}$)	ClO_4^- ($\mu\text{g/m}^2$)	ClO_4^- ($\mu\text{g/kg}$)	Total Depth (cm)	ClO_4^- ($\mu\text{g/L}$)	ClO_4^- ($\mu\text{g/m}^2$)	Total Depth (cm)	ClO_4^- ($\mu\text{g/L}$)	ClO_4^- ($\mu\text{g/m}^2$)
2009	1000	8.41	0.57	47.94	24.89	N/A	N/A							
2010	3000	21.53	2.23	480.12	14.25	N/A	N/A							

2.8.3.3 Spinach Study Results

We analyzed commercially grown spinach as a demonstration of our extraction and analysis procedures and to evaluate sources of ClO_4^- in food products. The spinach ClO_4^- isotopic composition: $\delta^{37}\text{Cl} = + 3.3 \text{ ‰}$, $\delta^{18}\text{O} = + 3.7 \text{ ‰}$, $\Delta^{17}\text{O} = + 2.6 \text{ ‰}$ was similar to isotopic compositions reported for indigenous natural ClO_4^- in soil and groundwater in the southwestern U.S. and surface waters of the Great Lakes, and to inferred isotopic values for groundwater in parts of southern California (Figure 2.8.8) (This report, Sections 2.2 & 2.3; Jackson et al., 2010; Böhlke et al., 2005; Hatzinger et al., 2015; Sturchio et al., 2006; Sturchio et al., 2014; Poghosyan et al., 2014).

2.8.4 Discussion

A number of processes could contribute to the observed range of natural ClO_4^- stable isotopic composition in soil and groundwater. Uptake of ClO_4^- by ion transporters, plant-catalyzed reduction, or oxygen exchange could all potentially cause isotopic fractionation. Snap bean plants were found to selectively uptake ClO_4^- relative to Cl^- , but not relative to NO_3^- , supporting a common ion transport mechanism for ClO_4^- and NO_3^- . The similarity in uptake rates (-0.87 and -0.97 ‰ mass/L) for ClO_4^- and NO_3^- , the strong correlation of anion uptake with volume of transpired solution, and the lower than predicted ClO_4^- mass accumulated in the plant (based on transpiration volume) are all consistent with findings from past studies (Seyfferth et al., 2008; Tan et al., 2006). This suggests that transport is through an ion carrier in roots that is specific to both NO_3^- and ClO_4^- but also dependent on transpiration rate (Seyfferth et al., 2008; Marschner, 1995).

No substantial differences were observed in the $\delta^{37}\text{Cl}$ and $\delta^{18}\text{O}$ values of ClO_4^- between the growth solutions and leaf extracts during the hydroponic experiments. There were small, but inconsistent changes in stable isotopic composition of NO_3^- in growth solutions. In experiment 1 a slight increase ($\sim 1 \text{ ‰}$) in $\delta^{15}\text{N-NO}_3^-$ but lack of measurable change in $\delta^{18}\text{O}$ could be consistent with fractionation. The effects of NO_3^- reduction or transport processes in the plant on $\delta^{18}\text{O}$ may not be as apparent as for $\delta^{15}\text{N}$ due to the difference in analytical uncertainty between the two ($\sim \pm 1 \text{ ‰}$ versus $\sim \pm 0.5 \text{ ‰}$, respectively). In experiment 2, small increases in $\delta^{15}\text{N}$ and $\delta^{18}\text{O}$ of NO_3^-

in two of the growth solutions, consistent with $\epsilon^{15}\text{N}$ values around -1.5 ‰ and $\epsilon^{15}\text{N}/\epsilon^{18}\text{O}$ of around 0.5 – 0.6 might have resulted from isotopic fractionation during uptake into the plants, or they might indicate microbial reduction of NO_3^- in solution. If bacterial NO_3^- reduction occurred, it does not appear to have been accompanied by substantial ClO_4^- reduction based on ClO_4^- isotopic compositions.

Although there was a substantial mass of ClO_4^- (27-42%) not accounted for in experiment 1, the lack of change in solution ClO_4^- stable isotopic composition compared to source material indicates ClO_4^- was not a major sink for ClO_4^- in growth solutions. If fractionation of ClO_4^- occurred during uptake, then the magnitude was too small to detect in these experiments and unlikely to be a significant factor for the variation in ClO_4^- stable isotopic composition observed in natural systems. However, it is possible that hydroponic studies may not fully reflect uptake processes in normal soil plant systems.

Plant-mediated transformation of ClO_4^- could also cause mass-dependent fractionation of ClO_4^- . While in experiment 1 approximately 27-42% of the ClO_4^- was unaccounted for, in experiment 2 and in other published studies, ClO_4^- generally appears to have been conserved in plant-water systems. In both experiments, essentially identical ClO_4^- stable isotopic composition in leaf tissue, growth solution, and source ClO_4^- makes it unlikely that substantial transformation of ClO_4^- occurred. Only one study, using hybrid poplar trees (*P. deltoids x nigra*) and radio labeled ClO_4^- ($^{36}\text{ClO}_4^-$), gave evidence of ClO_4^- metabolism within plant tissue (Van Aken et al., 2002). In that study approximately 10 – 34 % of the radioactivity (^{36}Cl) introduced as ClO_4^- was recovered as ClO_3^- , ClO_2^- , and Cl^- . Our results, and other published studies (Seyfferth et al., 2008; Nzengung et al., 2003; Tan et al., 2004; Suslara et al., 2000; Ha et al., 2011) suggest that plant-mediated transformation may not be common. Our results further indicate no measurable plant-mediated exchange of O occurred between ClO_4^- and other compounds such as H_2O (i.e., $\leq 1 - 2$ % exchange in a growing season).

In contrast to ClO_4^- , $\delta^{15}\text{N}$ of NO_3^- in plant tissue was fractionated substantially (~10-20‰), consistent with reported fractionation effects of NO_3^- assimilation in marine culture studies (~15-30‰) (Needoba et al., 2004; Granger et al., 2010; Ledgard et al., 1985; Schmidt and Medina, 1991). The $\epsilon^{15}\text{N}/\epsilon^{18}\text{O}$ ratios of 1.04 – 1.07 observed in our study support previous experimental studies indicating that isotopic fractionation by assimilatory nitrate reductase has an intrinsic $\epsilon^{15}\text{N}/\epsilon^{18}\text{O}$ ratio of approximately 1, regardless of the magnitudes of $\epsilon^{15}\text{N}$ and $\epsilon^{18}\text{O}$ values expressed (Karsh et al., 2012, 2014; Granger et al., 2004).

We also demonstrate that field-grown plants exposed to environmentally relevant ClO_4^- concentrations do not appear to affect foliar ClO_4^- isotopic composition. ClO_4^- extracted from snap beans grown in Raleigh varied somewhat isotopic composition between 2009 and 2010 based presumably on the source of irrigation water, but the stable isotope data clearly showed a

significant component of Chilean-type ClO_4^- , which was also the predominant source in local groundwater based on isotopic analysis. Commercial spinach had an isotopic composition similar to that of indigenous natural ClO_4^- from the SHP of West Texas and New Mexico as well as the U.S Great Lakes (Sections 2.2 & 2.3; Jackson et al., 2010; Böhlke et al., 2005; Hatzinger et al., 2015; Sturchio et al., 2006; Sturchio et al., 2014; Poghosyan et al., 2014). This result could indicate the spinach was exposed to natural ClO_4^- with a similar isotopic composition in soil or irrigation water in one or both of the potential source areas of the spinach (Arizona and southwestern California). The lower concentrations of ClO_4^- in spinach, compared to those in the hydroponic bean plants, are consistent with exposure to low level background ClO_4^- commonly found in groundwater (MRGB: 0.12 to 0.12 to 1.8 $\mu\text{g/L}$; SHP: ~0.1 to 200 $\mu\text{g/L}$) or soil (SHP: 3.3 $\mu\text{g/kg}$) (Jackson et al., 2010). Because the spinach ClO_4^- time of exposure likely was similar to time of plant exposure in the hydroponic studies, it might be concluded that time-related isotope effects were minimal and the spinach ClO_4^- isotopic composition represents the source ClO_4^- isotopic composition. However, it is also possible that ClO_4^- in spinach tissue was altered isotopically (e.g. reduction or oxygen exchange). If so, while the O isotopic composition of spinach ClO_4^- might be relatively independent of the source values, the Cl isotopic composition of spinach ClO_4^- might still reflect the source value, which would be consistent with an indigenous ClO_4^- source and not electrochemical or Atacama ClO_4^- .

Although only one composite sample of spinach was extracted, these results combined with those of the field and hydroponic studies suggest that it should be possible to evaluate the source of ClO_4^- in commercial produce and in other plant-based food products. This finding is important because most of the exposure to ClO_4^- in the U.S. population and likely the populations of many other countries is through ingestion of produce (Jackson et al., 2005, El Aribi et al., 2006, Sanchez et al., 2005a,b). Thus, isotopic ratio measurements of ClO_4^- in plant tissue may provide a direct method to distinguish the dominant sources of ClO_4^- in the U.S. and other food chains worldwide.

It is possible that hydroponic studies may not fully reflect uptake processes in normal soil-plant systems and that snap beans may not represent other plant types. However, our results indicate ClO_4^- uptake and accumulation can occur without significant net loss or isotope effects and that plant NO_3^- reduction systems efficiently exclude ClO_4^- , in contrast to some other NO_3^- reducing systems, such as bacteria (Hatzinger et al., 2009; Nerenberg et al., 2008; Maixner et al., 2008; Chaudhuri et al., 2002). These results suggest that isotopic characteristics of ClO_4^- in soils and groundwater may not be affected by plant uptake and release. Therefore, our results do not support the hypothesis that plant uptake is a major cause of variation in ClO_4^- stable isotopic composition observed in natural systems. Given the relatively large contribution of U.S. human exposure through food, further studies may be warranted to determine sources of ClO_4^- in the food chain, as well as to determine if other types of plants in other settings can alter the isotopic composition of ClO_4^- .

2.9 Publications

Some of the data and text presented herein was previously published in the following journal articles and dissertations. Sections from these articles are reprinted with permission as required.

1. Jackson, W.A., J.K. Böhlke, B. J. Andraski, L. Fahlquist, L. Bexfield, F.D. Eckardt, J. B. Gates, A.F. Davila, C.P. McKay, B. Rao, R. Sevanthi, S. Rajagopalan, N. Estrada, N. C. Sturchio, P.B. Hatzinger, T. A. Anderson, G. Orris, J. Betancourt, D. Stonestrom, C. Latorre, Y. Li, and G. Harvey. 2015. Global survey of perchlorate and nitrate co-occurrence in arid and semi-arid regions. *Geochim. Cosmochim. Acta* 164:502-522.
2. Poghosyan, A., N.C. Sturchio, C.G. Morrison, Y. Guan, J.M. Eiler, W.A. Jackson, P.B. Hatzinger. 2014. Perchlorate in the Great Lakes: Isotopic composition and origin. *Environ. Sci. Technol.* 48:11146-11153.
3. Jackson, W.A., J.K. Böhlke, B. Gu, P.B. Hatzinger and N.C. Sturchio. 2010. Isotopic composition and origin of indigenous natural perchlorate and co-occurring nitrate in the southwestern United States. *Environ. Sci. Technol.* 44:4869-4876.
4. Grantz, D.A., K.O. Burkey, W.A. Jackson, H-B Vu, M.T. McGrath, and G. Harvey. 2014. Perchlorate content of plant foliage reflects a wide range of species-dependent accumulation but not ozone-induced biosynthesis. *Environ. Pollut.* 184:690-696.
5. Grantz, D.A., A. Jackson, H-B Vu, K.O. Burkey, M.T. McGrath, and G. Harvey. 2014. High ozone increases soil perchlorate but does not affect foliar perchlorate content. *J. Environ. Qual.* 43:1460-1466.
6. Jackson, W.A., A. F. Davila, N. Estrada, W. Berry Lyons, J. D. Coates, J.C. Prisco. 2012. Perchlorate and chlorate biogeochemistry in ice-covered lakes of the McMurdo Dry Valleys, Antarctica. *Geochim. Cosmochim. Acta* 98: 19-30.
7. Estrada, N.L. 2015. Effects of Plant Uptake and UV and O₃ Production Mechanisms on Perchlorate Isotopic Composition and Possible Implications to Natural Perchlorate. Ph.D. Dissertation, Texas Tech University, 230 pg.

3.0 CONCLUSIONS and IMPLICATIONS FOR FUTURE RESEARCH

The results from a range of different laboratory studies evaluating ClO_4^- formation mechanisms confirm that there are multiple potential pathways of ClO_4^- generation from both UV-photolysis and O_3 -mediated oxidation of Cl^- and other ClO_x precursors. Laboratory studies were successful in producing Cl and O isotopic variations in ClO_4^- that incorporate much of the reported stable isotope variation in natural ClO_4^- . Only the characteristically low $\delta^{37}\text{Cl}$ values of Atacama ClO_4^- (Chile) were not reproduced and these remain enigmatic. Data indicate that final ClO_4^- isotopic composition is dependent on the precursor species oxidized. The reaction rates and intermediate species proposed to be involved in ClO_4^- formation require further study and additional experiments are required to resolve the reason for the low $\delta^{37}\text{Cl}$ values of Atacama ClO_4^- , but significant progress was made in constraining pathways of ClO_4^- production in nature by application of stable isotope analysis.

Worldwide soil and groundwater sampling data indicate that ClO_4^- is globally distributed in soil and groundwater in arid and semi-arid regions on Earth at concentrations ranging from 10^{-1} to 10^6 $\mu\text{g/kg}$. Generally, the ClO_4^- concentration in these regions increases with aridity index, but this also depends on the duration of arid conditions. In many arid and semi-arid areas, NO_3^- and ClO_4^- co-occur at consistent ratios ($\text{NO}_3^-/\text{ClO}_4^-$) that vary between $\sim 10^4$ and $\sim 10^5$. This is not the case for $\text{Cl}^-/\text{ClO}_4^-$ ratios, which vary widely among locations. The $\text{NO}_3^-/\text{ClO}_4^-$ ratios are largely preserved in hyper-arid areas that support little or no biological activity (e.g. plants or bacteria), but can be altered in areas with more active biological processes. In general, the co-occurrence of ClO_4^- and NO_3^- in arid and semi-arid locations, and associated variations in the isotopic composition of the NO_3^- , are consistent with a conceptual model of atmospheric origin, global co-deposition, and variable alteration of the NO_3^- pool by biogenic addition, assimilation, and/or recycling on the surface. The Atacama Desert appears to be unique compared to other arid and semi-arid locations. There, exceptional enrichment in ClO_4^- compared to Cl^- or NO_3^- , accompanied by unique ClO_4^- isotopic characteristics, may reflect an unusually efficient, but yet unknown, *in situ* production mechanism, regionally elevated atmospheric ClO_4^- production rates, or higher ClO_4^- production rates in pre-Pleistocene times. Further laboratory and field research is required to better understand and identify the conditions and/or processes that have led to the unique ClO_4^- isotopic characteristics and high relative ClO_4^- concentrations in the Atacama.

Stable isotope analysis of Cl and O and radioactive isotope analysis of ^{36}Cl in natural ClO_4^- confirmed and extended initial data suggesting that indigenous ClO_4^- sources in the southwestern U.S. show some isotopic variation by location and environment but remain isotopically distinct from synthetic and Atacama ClO_4^- when all relevant isotope ratios are considered. Perchlorate concentration and isotope analysis was conducted in all five of the North American Great Lakes. The data showed average ClO_4^- concentrations ranging from 0.05 to 0.13 $\mu\text{g/L}$ (varying by lake) with concentrations being nearly constant with depth. Interestingly, the overall ranges of stable isotopic compositions of Great Lakes ClO_4^- resemble those of indigenous natural ClO_4^- measured

in groundwaters of the western USA indicating a predominantly natural atmospheric source of ClO_4^- in all of the lakes.

ClO_4^- and ClO_3^- concentration profiles with depth were also collected from ice-covered lakes in the McMurdo Dry Valleys MDV of Antarctica. Sample quantities, however, were insufficient for stable isotope analysis. These lakes provide an excellent case study for ClO_3^- and ClO_4^- biotransformation in pristine extreme environments. Given their low concentrations, high solubility, and lack of any *in situ* generation mechanisms, ClO_3^- and ClO_4^- may offer a sensitive means to study ongoing biological activity in the lakes, and the addition of ClO_4^- stable isotope evaluation could provide further clues as to the geochemical history of the lake water. Finally, ClO_3^- and ClO_4^- biogeochemistry in Antarctic ice-covered lakes may represent an excellent analog for similar processes in ice-covered lakes on Mars in the past or even in more recent times, especially given the discovery of relatively large amounts of ClO_4^- in the Martian soil. Further research with Antarctic ClO_4^- samples, including isotopic analysis is recommended.

Several potential biological mechanisms of ClO_4^- generation were evaluated to determine if any could be a secondary source of this anion in the environment and to help explain the isotopic characteristics and variation in some natural ClO_4^- samples. Bacterial production of ClO_4^- was assessed using (1) various nitrifying cultures and enrichments that oxidize NH_4 to NO_3^- ; (2) natural haloperoxidase enzymes that are known to oxidize Cl^- to hypochlorous acid (HClO) and potentially to ClO_4^- (possibly via additional photochemical or biological reactions); and (3) organisms capable of oxidizing sulfite or phosphite. A variety of experiments were conducted with Cl^- or ClO_x precursors in the presence of different enzymes, organisms, and conditions as summarized above. While some ClO_4^- generation was initially indicated via haloperoxidase enzymes in the presence of UV light, this result was not consistent and is unlikely to account for significant ClO_4^- production. The other organisms and processes evaluated did not result in ClO_4^- formation.

A variety of plant species were also evaluated for their potential to accumulate and even generate ClO_4^- via O_3 -mediated processes. A broad range of crop species was observed to accumulate ClO_4^- from growth medium, and these species differed widely in their bioconcentration of the anion. Foliar ClO_4^- concentration was greatest in older leaves, which ultimately contribute to the litter layer, suggesting that scavenging of ClO_4^- from deeper soil horizons could lead to redistribution on the soil surface. However, there was no evidence that exposure of leaves to ambient O_3 or at significantly elevated O_3 induced any increase in tissue contents of ClO_4^- . The results indicate that O_3 does not lead to increased phyto-accumulation nor plant biosynthesis of ClO_4^- .

The impact of plant accumulation of ClO_4^- on Cl and O stable isotope values was also evaluated in both hydroponic laboratory studies and field crops grown in different parts of the U.S. In hydroponic studies with snap beans, no substantial differences were observed in the $\delta^{37}\text{Cl}$, $\delta^{18}\text{O}$, or $\Delta^{17}\text{O}$ values of ClO_4^- between the growth solutions and leaf extracts. In contrast to ClO_4^- , $\delta^{15}\text{N}$

of NO_3^- in plant tissue was fractionated substantially (~10-20‰). The $\epsilon^{15}\text{N}/\epsilon^{18}\text{O}$ ratios of 1.04 – 1.07 support previous experimental studies showing similar ratios via assimilatory nitrate reductase. The data indicate that plants do not metabolize and assimilate ClO_4^- similarly to NO_3^- .

Similar to hydroponically grown plants, field grown plants exposed to environmentally relevant ClO_4^- concentrations also did not appear to affect foliar ClO_4^- isotopic composition. ClO_4^- extracted from snap beans grown in Raleigh, NC varied somewhat in isotopic composition between two growing seasons based presumably on the source of irrigation water, but the stable isotope data clearly showed a significant component of Atacama-type ClO_4^- from past fertilizer use which was also the predominant source in local groundwater based on isotopic analysis. Commercial spinach was also extracted and analyzed for ClO_4^- stable isotopes. The spinach had an isotopic composition similar to that of indigenous natural ClO_4^- from the SHP as well as the Great Lakes. This result could indicate the spinach was exposed to natural ClO_4^- with a similar isotopic composition in soil or irrigation water in one or both of the potential source areas of the spinach (Arizona and southwestern California). Although this spinach that was extracted represents only one composite sample, these results combined with those of the field bean and hydroponic studies suggest that it should be possible to evaluate the dominant source of ClO_4^- (i.e., synthetic, Atacama, indigenous) in commercial produce and in other plant-based food products through stable isotope analysis of plant accumulated ClO_4^- . This finding is important because most of the exposure to ClO_4^- in the U.S. population and likely the populations of many other countries is through ingestion of produce. Additional research is warranted with a variety of food crops and products to confirm that ClO_4^- isotope signatures in vegetation reflect those in irrigation water and/or local soils and groundwater, thus allowing forensic determination of ClO_4^- sources in food crops.

Overall, the results of this project have provided important new information on natural ClO_4^- in the environment. Significant progress was made concerning potential mechanisms of its formation, isotopic characterization of natural ClO_4^- sources in groundwater, lakes, soils and plants, and its worldwide occurrence and accumulation in arid and semi-arid environments compared with that of NO_3^- , Cl^- , and other anions. The data support previous studies showing that natural and synthetic ClO_4^- can be differentiated by stable isotope methods, and suggest for the first time that the source(s) of ClO_4^- in food crops may be determined by isotopic analysis of ClO_4^- in plant tissue. While this project has provided a much more comprehensive understanding of natural ClO_4^- , significant research questions still remain, including whether natural ClO_4^- production mechanisms exist other than the UV and O_3 mediated processes identified in this and other studies, and whether isotopic exchange processes exist that alter the stable isotope signatures of produced ClO_4^- . A more thorough understanding of these factors could resolve remaining uncertainties concerning the observed range of stable isotope signatures of natural ClO_4^- , including the seemingly unique isotopic characteristics and relative concentrations of ClO_4^- in the Atacama Desert.

4.0 REFERENCES CITED

- Aiken, G., McKnight, D., Harnish, R., and Wershaw, R. 1996. Geochemistry of aquatic humic substances in the Lake Fryxell Basin, Antarctica. *Biogeochemistry* 34, 157-188.
- Amberger, A., and Schmidt, H.L. 1987. Natürliche Isotopengehalte von Nitrat als Indikatoren für dessen Herkunft: *Geochimica et Cosmochimica Acta*, 51:2699-2705.
- Avnery, S., D.L. Mauzerall, J. Liu, and L.W. Horowitz. 2011. Global crop yield reductions due to surface ozone exposure: 1. Year 2000 crop production losses and economic damage. *Atmospheric Environment* 45:2284-2296.
- Aziz, C. E.; Hatzinger, P. B. 2008. Perchlorate Sources, Source Identification, and Analytical Methods. *In* In Situ Bioremediation of Perchlorate in Groundwater; Stroo, H. F.; Ward, C. H., Eds. Springer: New York, 2008; pp 55-77.
- Aziz, C.; Borch, R.; Nicholson, P.; Cox, E. 2006. Alternative causes of wide-spread, low concentration perchlorate impacts to groundwater. *In* Perchlorate, Environmental Occurrence, Interactions and Treatment. Gu, B., Coates, J.D., Eds.; Springer: New York, pp 71- 92.
- Backus, S. M.; Klawuun, P.; Brown, S.; D'sa, I.; Sharp, S.; Surette, C.; Williams, D. J. 2005. Determination of perchlorate in selected surface waters in the Great Lakes Basin by HPLC/MS/MS. *Chemosphere* 61 (6), 834-43.
- Bao, H.; Gu, B. 2004. Natural perchlorate has a unique oxygen isotope signature. *Environ. Sci. Technol.* 38 (19), 5073-7.
- Batista, J. R.; McGarvey, F. X.; Vieira, A. R. 2000. The removal of perchlorate from waters using ion exchange resins. *In* Perchlorate in the Environment; Urbansky, E. T., Ed. Kluwer/Plenum: New York, pp 135-145.
- Bentley, H. W.; Phillips, F. M.; Davis, S. N.; Gifford, S.; Elmore, D.; Tubbs, L. E.; Gove, H. E. 1982. Thermonuclear Cl-36 Pulse in Natural-Water. *Nature*, 300 (5894), 737-740.
- Blake, R.E.; O'Neil, J.R.; and Garcia, G.A. 1997. Oxygen isotope systematics of biologically mediated reactions of phosphate: 1. Microbial degradation of organophosphorus compounds. *Geochim. Cosmochim. Acta* 61, 4411-4422.
- Blount, B.C., Pirkle JL, Osterloh J.D, Valentin-Blasini, L., and Caldwell, L. 2007. Urinary perchlorate and thyroid hormone levels in adolescent and adult men and women living in the United States *Environ. Health Persp.* 114: 1865-1871
- Böhlke, J. K.; Erickson, G. E.; Revesz, K. 1997. Stable isotope evidence for an atmospheric origin of desert nitrate deposits in northern Chile and southern California, U.S.A. *Chem. Geol.* 136, 135-152.

- Böhlke, J. K.; Sturchio, N. C.; Gu, B.; Horita, J.; Brown, G. M.; Jackson, W. A.; Batista, J.; Hatzinger, P. B. 2005. Perchlorate Isotope Forensics. *Anal. Chem.* 77 (23), 7838-7842.
- Böhlke, J.K.; Hatzinger, P.B.; Sturchio, N.C.; Abbene, I.J.; Mroczkowski, S.J. 2009. Atacama perchlorate as an agricultural contaminant in groundwater: Isotopic and chronologic evidence from Long Island, New York. *Environ. Sci. Technol.* 43, 5619-562.
- Böhlke, J.K.; Mroczkowski, S.J.; and Coplen, T.B. 2003. Oxygen isotopes in nitrate: new reference materials for ^{18}O : ^{17}O : ^{16}O measurements and observations on nitrate-water equilibration. *Rapid Comm. Mass Spec.*, 17, 1835-1846.
- Böhlke, J.K., S.J. Mroczkowski, N.C. Sturchio, L.J. Heraty, K. W. Richman, D.B. Sullivan, K.N. Griffith, B. Gu, and P.B. Hatzinger. Stable isotope analyses of oxygen (^{18}O : ^{17}O : ^{16}O) and chlorine (^{37}Cl : ^{35}Cl) in perchlorate: Reference materials, calibrations, and interferences. *Rapid. Comm. Mass Spect.* (in press; DOI: 10.1002/rcm.7751)
- Booker, F., Muntifering, R., McGrath, M., Burkey, K., Decoteau, D., Fiscus, E., Manning, W., Krupa, S., Chappelka, A., Grantz, D. 2009. The ozone component of global change: potential effects on agricultural and horticultural plant yield, product quality and interactions with invasive species. *Journal of Integrative Plant Biology* 51, 337-51.
- Brandes, J. A.; Devol, A. H. 1997. Isotopic fractionation of oxygen and nitrogen in coastal marine sediments. *Geochim. Cosmochim. Acta*, 61 (9), 1793-1801.
- Brown, G. M.; Gu, B. 2006. The Chemistry of Perchlorate in the Environment. In *Perchlorate: Environmental Occurrence, Interactions and Treatment*; Gu, B.; Coates, J.D., Eds.; Springer: New York, pp 17-47.
- Bunton, C.A.; Halevi, E.A.; Llewellyn, D.R. 1953. Oxygen exchange between nitric acid and water. Part III. Catalysis by nitrous acid. *J. Chem. Soc.* 5, 2653-2657.
- Burkey, K.O.; Miller, J.E.; Fiscus, E.L. 2005. Assessment of ambient ozone effects on vegetation using snap bean as a bio-indicator species. *J. Environ. Qual.* 34, 1081-1086.
- Burkey, K.O. and Eason, G. 2002. Ozone tolerance in snap bean is associated with elevated ascorbic acid in the leaf apoplast. *Physiologia Plantarum* 114: 387-394.
- Burkey, K.O. Eason, G., and Fiscus, E. L. 2003. Factors that affect leaf extracellular ascorbic acid content and redox status. *Physiologia Plantarum* 117: 51-57.
- Buxton, G. V.; Subhani, M. S. 1972. Radiation chemistry and photochemistry of oxychlorine Ions. Part 3. – Photodecomposition of aqueous solutions of chlorite ions. *J. Chem. Soc., Faraday Trans.* 1, 68, 970-977.
- Capone, D.G. 1997. Microbial Nitrogen Cycling. In *Manual of Environmental Microbiology*, ASM Press, Washington, D.C. pp. 334-342.
- Casciotti, K.L.; Böhlke, J.K.; McIlvin, M.R.; Mroczkowski, S.J.; Hannon, J.E. 2007. Oxygen isotopes in nitrite: analysis, calibration, and equilibration. *Anal. Chem.* 79, 2427-2436.

- Chaudhuri, S.K.; O'Connor, S.M.; Gustavson, R.L.; Achenbach, L.A.; Coates, J.D. 2002. Environmental factors that control microbial perchlorate reduction. *Appl. Environ. Microb.* 68 (9), 4425-4430.
- Chan, S.; Kilby, M. D. 2000. Thyroid hormone and central nervous system development. *J. Endocrinol.* 165, 1-8.
- Chapra, S. C.; Dove, A.; Rockwell, D. C. 2009. Great Lakes Chloride Trends: Long-Term Mass Balance and Loading Analysis. *J. Great Lakes Res.* 35 (2), 272-284.
- Chen, T. 1967. Spectrophotometric determination of microquantities of chlorate, chlorite, hypochlorite, and chloride in perchlorate. *Anal. Chem.* 39, 804-813.
- Clark, I.; Fritz, P. 1997. *Environmental Isotopes in Hydrology*; CRC Press LLC: New York.
- Cliff, S. S.; Thiemens, M. H. 1997. The $^{18}\text{O}/^{16}\text{O}$ and $^{17}\text{O}/^{16}\text{O}$ Ratios In Atmospheric Nitrous Oxide: A Mass-independent Anomaly. *Science*, 278 (5344), 1774-1776.
- Clocksinn, K.M., Jung, D.O., and Madigan, M.T. 2007. Cold-active chemoorganotrophic bacteria from permanently ice-covered Lake Hoare, McMurdo Dry Valleys, Antarctica. *Applied and Environmental Microbiology* 73, 3077-3083.
- Coates, J.D., and Achenbach, L.A. 2004. Microbial perchlorate reduction: Rocket-fuelled metabolism. *Nature Reviews Microbiology* 2, 569-580.
- Coates, J.D., and Achenbach, L.A., 2006. The microbiology of perchlorate reduction and its bioremediative application. In *Perchlorate, Environmental Occurrence, Interactions, and Treatment* (eds. B. Gu and J.D. Coates). Springer, New York, NY, pp.279-295.
- Coleman, M. L.; Ader, M.; Chaudhuri, S.; Coates, J. D. 2003. Microbial Isotopic Fractionation of Perchlorate Chlorine. *Appl. Environ. Microb.* 69 (8), 4997-5000.
- Cope, V.W., Miller, R.G., Fraser, R.T.M. 1967. Titanium (III) as a reductant in electron-transfer reactions. *Journal of the Chemical Society (A) Inorganic, Physical, Theoretical*; pages 301-306.
- Coplen, T. B. 1996. New guidelines for reporting stable hydrogen, carbon, and oxygen isotope-ratio data. *Geochim. Cosmochim. Acta* 60 (17), 3359-3360.
- Coplen, T.B.; Böhlke, J.K.; Casciotti, K.L. 2004. Using dual bacterial denitrification to improve $\delta^{15}\text{N}$ determinations of nitrates containing mass independent ^{17}O . *Rapid Com. Mass Spec.* 18, 245-250.
- Cosson, H.; Ernst, W. R. 1994. Photodecomposition of Chlorine Dioxide and Sodium Chlorite In Aqueous Solution by Irradiation With Ultraviolet Light. *Ind. Eng. Chem. Res.* 33 (6), 1468-1475.
- DasGupta, P. K.; Dyke, J. V.; Kirk, A. B.; Jackson, W. A. 2006. Perchlorate In the United States. Analysis of Relative Source Contributions to the Food Chain. *Environ. Sci. Technol.* 40 (21), 6608-6614.

- Dasgupta, P. K.; Martinelango, P. K.; Jackson, W. A.; Anderson, T. A.; Tian, K.; Tock, R. W.; Rajagopalan, S. 2005. The Origin of Naturally Occurring Perchlorate: The Role of Atmospheric Processes. *Environ. Sci. Technol.* 39 (6), 1569-1575.
- De Groot, G.N., and Stouthamer, A.H. 1969. Regulation of reductase formation in *Proteus mirabilis*. *Archives of Microbiology* 66, 220-233.
- DiFiore, P. J.; Sigman, D. M.; Dunbar, R. B. 2009. Upper ocean nitrogen fluxes in the polar antarctic zone: Constraints from the nitrogen and oxygen isotopes of nitrate. *Geochem. Geophys. Geosy.* 10 (11). DOI: 10.1029/2009GC002468.
- Domae, M.; Katsumara, Y.; Jiang, P.; Nagaishi, R.; Hasegawa, C.; Ishigure, K.; Yoshida, Y. 1994. Observation of ClO_3 radical in aqueous chlorate solution by pulse radiolysis. *J. Phys. Chem.* 98, 190-192.
- Dosch, R. G. 1968. Determination of perchlorate by precipitation with tetra-n-pentylammonium bromide. *Anal. Chem.* 40 (4), 829–831.
- Downes, M.T. and Priscu, J.C. 1995. Profiles of electrode potential and dissolved oxygen in lakes of the McMurdo Dry Valleys. *Antarctic Journal of the United States* 30, 305-307.
- Duke, F.R., and P.R. Quinney. 1954. The kinetics of reduction of perchlorate ion by Ti(III) in dilute solution. *Journal of the American Chemical Society* 76:3800-3803.
- El Aribi, H.; Le Blanc, Y. J. C.; Antonsen, S.; Sakuma, T. 2006. Analysis of Perchlorate in Foods and Beverages by Ion Chromatography Coupled With Tandem Mass Spectrometry (IC-ESI-MS/MS). *Anal. Chim. Acta* 567 (1), 39-47.
- Ellington, J. J.; Evans, J. J. 2000. Determination of perchlorate at parts-per-billion levels in plants by ion chromatography. *J. Chromatogr. A* 898 (2), 193-199.
- EPA, 1993. Determination of Inorganic Anions by Ion Chromatography, Method 300.0 Rev. 2.1 1993 (US Environmental Protection Agency: Cincinnati, OH). Available at http://www.epa.gov/waterscience/methods/method/files/300_0.pdf
- EPA, 2011. Drinking Water: Regulatory Determination on Perchlorate. U.S. Environmental Protection Agency (USEPA), 7762-7767.
- EPA, 2000. Great Lakes Ecological Protection and Restoration: Great Lakes Ecosystem Report 2000. Great Lakes National Program Office. Chicago, IL, EPA-905-R-01-001.
- EPA, 2008. Interim Drinking Water Health Advisory For Perchlorate Office of Science and Technology (EPA 822-R-08-025), Washington, DC.
- EPA, 2002. Perchlorate Environmental Contamination: Toxicological Review and Risk Characterization (External Review Draft). National Center for Environmental Assessment, Washington, DC.

- EPA, 1998. Perchlorate Environmental Contamination: Toxicological Review and Risk Characterization Based on Emerging Information (External Review Draft). National Center for Environmental Assessment, Washington, DC.
- Ericksen, G. E. 1983. The Chilean Nitrate Deposits. *Am. Sci.* 71 (4), 366-374.
- Ericksen, G. E. 1981. Geology and Origin of the Chilean Nitrate Deposits Geological Survey Professional Paper 1188, United States Government Printing Office, Washington, DC. 1981.
- Ericksen, G.E.; Hosterman, J.W.; St. Amand. 1988. Chemistry Mineralogy, and origin of the clay-hill nitrate deposits Amaragosa River Valley, Death Valley region, California, U.S.A. *Chem. Geol.* 67, 85-102
- Evans, R. D. 2001. Physiological Mechanisms Influencing Plant Nitrogen Isotope Composition. *Trends Plant Sci.* 2001, 6 (3), 121-126.
- Ewing, S. A.; Michalski, G.; Thiemens, M.; Quinn, R.; C.; Macalady, J. L.; Kohl, S.; Wankel, S. D.; Kendall, C.; McKay, C. P.; Amundson, R. 2007. Rainfall limit of the N cycle on Earth. *Global Biogeochem. Cycles* 21, GB3009, 1-12.
- Farquhar, G. D.; Ehleringer, J. R.; Hubick, K. T. 1989. Carbon Isotope Discrimination and Photosynthesis. *Annu. Rev. Plant Biol.* 40 (1), 503-537.
- Farquhar, J.; Thiemens, M. H.; Jackson, T. L. 1999. In $\Delta^{17}\text{O}$ Anomalies in Carbonate from Nakhla and Lafayette and $\Delta^{33}\text{S}$ Anomalies in Sulfur from Nakhla: Implications for Atmospheric Chemical Interactions with the Martian Regolith, 30th Annual Lunar and Planetary Science Conference, Houston, TX, March 15-29; abstract no. 1675.
- Fuller, K.; Shear, H.; Wittig, J. 1995. The Great Lakes : an environmental atlas and resource book (Chapter 2). 3rd ed. Great Lakes National Program Office, U.S. Environmental Protection Agency ; Government of Canada. Chicago, IL.; Toronto, Ont.
- Furdui, V.I., and Tomassini, F. 2010. Trends and sources of perchlorate in Arctic Snow. *Environ. Sci. Technol.* 44, 588-592.
- Furman, C. S.; Margerum, D. W. 1998. Mechanism of chlorine dioxide and chlorate ion formation from the reaction of hypobromous acid and chlorite ion. *Inorg. Chem.* 37, 4321-4327.
- GAO. 2010. Perchlorate: Occurrence Is Widespread but at Varying Levels; Federal Agencies Have Taken Some Actions to Respond to and Lessen Releases; GAO-10-769; U.S. Government Accountability Office (GAO): Washington, DC.
- GeoSyntec Consultants, 2005. Alternative Causes of Widespread Low Concentration Perchlorate. Impacts to Groundwater (CP-1429). Final Report Prepared for the Strategic Environmental Response and Development Program (SERDP), Arlington, VA.

- GLERL Great Lakes Monthly Hydrologic Data. 2012.
<http://www.glerl.noaa.gov/data/arc/hydro/mnth-hydro.html>, Ann Arbor, MI.
- Godon, A.; Jendryzejewski, N.; Eggenkamp, H. G. M.; Banks, D. A.; Ader, M.; Coleman, M. L.; Pineau, F. A 2004. Cross-calibration of chlorine isotopic measurements and suitability of seawater as the international reference material. *Chem. Geol.* 207 (1-2), 1-12.
- Granger, J.; Sigman, D. M.; Rohde, M. M.; Maldonado, M. T.; Tortell, P. D. 2010. N and O isotope effects during nitrate assimilation by unicellular prokaryotic and eukaryotic plankton cultures. *Geochim. Cosmochim. Acta.* 74 (3), 1030-1040.
- Granger, J.; Sigman, D. M.; Needoba, J. A.; Harrison, P. J. 2004. Coupled nitrogen and oxygen isotope fractionation of nitrate during assimilation by cultures of marine phytoplankton. *Limnol. and Oceanogr.* 49 (5), 1763-1773.
- Grantz, D.A., and H-B. Vu. 2009. O₃ Sensitivity in a potential C₄ bioenergy crop: sugarcane in California. *Crop Science* 49:643-650.
- Grantz, D.A., H-B. Vu, T.L. Tew, and J.C. Veremis, 2012. Sensitivity of gas exchange parameters to O₃ in diverse C₄ sugarcane hybrids. *Crop Science* 52:1-11.
- Grantz, D.A., K.O. Burkey, W.A. Jackson, H-B. Vu, M.T. McGrath, and G. Harvey. 2014. Perchlorate content of plant foliage reflects a wide range of species dependent accumulation but not ozone-induced biosynthesis. *Environmental Pollution* 184: 690-696.
- Grantz, D.A., Vu, H-B. 2009. O₃ Sensitivity in a potential C₄ bioenergy crop: sugarcane in California. *Crop Science* 49, 643-650.
- Grantz, D.A., Vu, H-B., Aguilar, C., Rea, M.A. 2010. No interaction between methyl jasmonate and ozone in pima cotton: Growth and allocation respond independently to both. *Plant Cell and Environment* 33, 717-728.
- Grantz, D.A., Vu, H-B., Tew, T.L., Veremis, J.C. 2012. Sensitivity of gas exchange parameters to o₃ in diverse C₄ sugarcane hybrids. *Crop Science* 52:1-11.
- Green, T.J.; Islam, M.; Canosa-Mas, C.; Marston, G.; Wayne, R.P. 2004. Higher oxides of chlorine: absorption cross-section of Cl₂O₆ and Cl₂O₄, the decomposition of Cl₂O₆, and the reactions of OClO with O and O₃. *J. Photochem. Photobiol. A: Chem.* 162, 353-370.
- Green, W.J., and Lyons, W.B. 2009. The saline lakes of the McMurdo Dry Valleys, *Antarctica. Aquatic Geochemistry* 15, 321-348.
- Greer, M. A.; Goodman, G.; Pleus, R. C.; Greer, S. E. 2002. Health Effects Assessment for Environmental Perchlorate Contamination: the Dose Response for Inhibition of Thyroidal Radioiodine Uptake in Humans. *Environ. Health Persp.* 110 (9), 927-937.

- Griffin, B.W. 1991. Chloroperoxidase: a review. *In* Peroxidases in chemistry and biology. Everse, J., Everse, K.E. and Grisham, M.B., (ed.), CRC Press, Boca Raton, vol. II, pp. 85-137.
- Grunhage, L., H.-J. Jager, H.-D. Haenel, K. Hanewald, and S. Krupa. 1997. PLANTIN (plant-atmosphere-interaction) II: Co-occurrence of high ambient ozone concentrations and factors limiting plant absorbed dose. *Environmental Pollution* 98: 51-60.
- Gu, B., G., Brown, G., Maya, L., Lance, M., Moyer, B. 2001. Regeneration of perchlorate loaded anion exchange resins by a novel tetrachloroferrate displacement technique. *Environ. Sci. Technol.* 35, 3363-3368.
- Gu, B., Böhlke, J.K., Sturchio, N.C., Hatzinger, P.B., Jackson, W.A., Beloso, A.D., Heraty, L.J., Bian, Y., Jiang, X., and Brown, G.M. 2011. Applications of selective ion exchange for perchlorate removal, recovery, and environmental forensics. 2011. In SenGupta, A. K., ed., *Ion Exchange and Solvent Extraction: A Series of Advances*: 20. Taylor & Francis, pp 117-144.
- Gu, B., Ku, Y., Brown, G. 2005. Sorption and Desorption of perchlorate and U(VI) by strong base anion exchange resins. *Environ. Sci. Technol.* 39, 901-907.
- Gu, B.; Brown, G. M.; Chiang, C. C. Treatment of perchlorate-contaminated groundwater using highly selective, regenerable ion-exchange technologies. *Environ. Sci. Technol.* 2007, 41 (17), 6277-82.
- Gu, B.; Brown, G. M.; Maya, L.; Lance, M. J.; Moyer, B. A. 2001. Regeneration of perchlorate (ClO_4^-)-loaded anion exchange resins by a novel tetrachloroferrate (FeCl_4^-) displacement technique. *Environ. Sci. Technol.* 35 (16), 3363-3368.
- Ha, W., D.L. Suarez and S.M. Lesch. 2013. Predicting perchlorate uptake in greenhouse lettuce from perchlorate, nitrate, and chloride irrigation water concentrations. *Journal of Environmental Quality* 42: 208-218.
- Ha, W.; Suarez, D. L.; Lesch, S. M. 2011. Perchlorate uptake in spinach as related to perchlorate, nitrate, and chloride concentrations in irrigation water. *Environ. Sci. Technol.* 45 (21), 9363-9371.
- Haag, W. R.; Hoigné, J. 1983. Ozonation of water containing chlorine or chloramines: Reaction products and kinetics. *Water Res.* 17 (10), 1397-1402.
- Hager, L.P., D.R. Morris, F.S. Brown, and H. Eberwein. 1966. Chloroperoxidase: II. Utilization of halogen anions. *J. Biol. Chem.* 241:1769-1777.
- Hamissou, M. 2011. Selected physiological and molecular responses of *Arabidopsis thaliana* and *Nicotiana tabacum* plants irrigated with perchlorate-containing water. *Asian Journal of Plant Sciences* 10:255-262.

- Hannon, J.E.; Böhlke, J.K.; Mroczkowski, S.J. 2008. Effects of nitrate and water on the oxygen isotopic analysis of barium sulfate precipitated from solution. *Rapid Com. Mass Spec.* 22, 4109-4120.
- Hart, E. J.; Sehested, K.; Holeman, J. 1983. Molar absorptivities of ultraviolet and visible bands of ozone in aqueous solutions. *Anal. Chem.* 55, 46-49.
- Hatzinger, P. B.; Böhlke, J. K.; Sturchio, N. C.; Gu, B.; Heraty, L. J.; Borden, R. C. 2009. Fractionation of stable isotopes in perchlorate and nitrate during in situ biodegradation in a sandy aquifer. *Environ. Chem.* 6 (1), 44-52.
- Hatzinger, P. B.; J.K. Böhlke; N.C. Sturchio; Gu, B. 2011. Guidance manual for forensic analysis of perchlorate in groundwater using chlorine and oxygen isotopic analyses. Environmental Security Technology Certification Program (ESTCP), ESTCP Project ER-200509.
- Hatzinger, P. B.; J.K. Böhlke; N.C. Sturchio; Gu, B. 2013. Validation of Chlorine and Oxygen Isotope Ratio Analysis To Differentiate Perchlorate Sources and To Document Perchlorate Biodegradation. Environmental Security Technology Certification Program (ESTCP) Final Report, ESTCP Project ER-200509.
- Hecht, M. H.; Kounaves, S. P.; Quinn, R. C.; West, S. J.; Young, S. M. M.; Ming, D. W.; D. C. Catling, D. C.; Clark, B. C.; Boynton, W. V.; Hoffman, J.; DeFlores, L. P.; Gospodinova, K.; Kapit, J.; Smith, P. H. 2009. Detection of perchlorate and the soluble chemistry of martian soil at the Phoenix Lander site. *Science* 325: 64-67.
- Heck, W.W., Philbeck, R.B., Denning, J.A. 1978. A continuous stirred tank reactor (CSTR) system for exposing plants to gaseous air pollutants. USDA, Pub. No. ARS-563 5-181, Washington D.C.
- Heikkilä, U.; Beer, J.; Feichter, J.; Alfimov, V.; Synal, H. A.; Schotterer, U.; Eichler, A.; Schwikowski, M.; Thompson, L. 2009. ³⁶Cl bomb peak: comparison of modeled and measured data. *Atmos. Chem. Phys.* 9 (12), 4145-4156.
- Hendy, C.H., Wilson, A.T., Popplewell, K.B., and House D.A. 1977. Dating of geochemical events in Lake Bonney, Antarctica and their relation to glacial and climatic changes. *New Zealand Journal of Geology and Geophysics* 20, 1103-1122.
- Hoering, T.C.; Ishimori, F.T.; McDonald, H.O. 1958. The oxygen exchange between oxy-anions and water. II. Chlorite, chlorate, and perchlorate ions. *J. Amer. Chem. Soc.* 80, 3876-3879.
- Hogue, C. 2003. Environmental Pollution: Rocket-fueled River. *Chem. Eng. News*, 81 (33), 37-46.

- Hoigné, J.; Bader, H.; Haag, W. R.; Staehelin, J. 1985. Rate constants of direct reactions of ozone with organic and inorganic compounds in water-III. Inorganic compounds and radicals. *Water Res.* 19 (8), 993-1004.
- Hollocher, T.C. 1984. Source of the oxygen atoms of nitrate in the oxidation of nitrite by *Nitrobacter agilis* and evidence against a P-O-N anhydride mechanism in oxidative phosphorylization: *Arch. Biochem. Biophys.* 233:721-727.
- Horváth, M., Bilitzky, L., Huttner, J. 1985. *Ozone*; Elsevier: New York.
- Hough, J. L. 1963. The prehistoric Great Lakes of North America. *American Scientist* 51 (1), 84-109.
- Hunter, W.J. 2001. Perchlorate is not a common contaminant of fertilizers. *Journal of Agronomy and Crop Science* 187:203-206.
- IAEA/WMO Global Network of Isotopes in Precipitation. 2013. The GNIP Database. <http://www.iaea.org/water>
- Impellitteri, C. A.; Saxe, J. P.; Schmitt, E. C.; Young, K. R. 2011. A survey on the temporal and spatial distribution of perchlorate in the Potomac River. *J. Environ. Monit.* 13 (8), 2277-2283.
- ITRC, 2005. Perchlorate: Overview of Issues, Status, and Remedial Options. Perchlorate -1. Interstate Technology & Regulatory Council, Perchlorate Team. Washington, D.C.
- Jackson, W. A.; Böhlke, J. K.; Gu, B.; Hatzinger, P. B.; Sturchio, N. C. 2010. Isotopic composition and origin of indigenous natural perchlorate and co-occurring nitrate in the southwestern United States. *Environ. Sci. Technol.* 44 (13), 4869-76.
- Jackson, W.A., Joseph, P.C., Patil, L.B., Tan, K., Smith, P.N., Yu, L., Anderson, T.A. 2005. Perchlorate accumulation in forage and edible vegetation. *Journal of Agricultural and Food Chemistry* 53, 369-373.
- Jaeglé, L.; Yung, Y. L.; Toon, G. C.; Sen, B.; Blavier, J.-F. L. 1996. Balloon observations of organic and inorganic chlorine in the stratosphere: The role of HClO₄ production on sulfate aerosol. *Geophys. Res. Lett.* 23 (14), 1749-1752.
- Jansen, M.; Schatte, G.; Tobais, K. M.; Willner, H. 1988. Properties of dichlorine hexaoxide in the gas phase and in low-temperature matrices. *Inorg. Chem.* 27, 1703-1706
- Johnson, D.G.; Jucks, K.W.; Traub, W.A.; Chance K.V. 2000. Isotopic composition of stratospheric ozone. *J. Geophys. Res-Atmos.* 105, 9025-9031
- Kang, N., Anderson, T.A., Rao, B., and Jackson, W.A. 2009. Characteristics of perchlorate formation via photodissociation of aqueous chlorite. *Environmental Chemistry* 6, 53-59.
- Kang, N., Anderson, W., Jackson W.A. 2006. Photochemical formation of perchlorate from aqueous oxychlorine anions. *Anal. Chim. Acta* 567, 48-56.

- Kang, N., Jackson, W.A., Dasgupta, P.K., Anderson, T.A. 2008. Perchlorate production by ozone oxidation of chloride in aqueous and dry systems. *Science of the Total Environment* 405, 301-309.
- Kappler, U., C.G. Friedrich, H.G. Truper, and C. Dahl. 2001. Evidence for two pathways of thiosulfate oxidation in *Starkeya novella* (formerly *Thiobacillus novellus*). *Arch. Microbiol.* 175:102-111.
- Kappler, U., B. Bennett, J. Rethmeier, G. Schwartz, R. Deutzmann, A. G. McEwan, and C. Dahl. 2000. Sulfite: Cytochrome c oxidoreductase from *Thiobacillus novellus*. *J. Biol. Chem.* 275:13202-13212.
- Karr, E.A., Sattley, W.M., Rice, M.R., Jung, D.O., Madigan, M.T., and Achenbach, L.A. 2005. Diversity and distribution of sulfate-reducing bacteria in permanently frozen Lake Fryxell, McMurdo Dry Valleys, Antarctica. *Appl. Environ. Microbiol.* 71, 6353-6359.
- Karsh, K. L.; Granger, J.; Kritee, K.; Sigman, D. M. 2012. Eukaryotic assimilatory nitrate reductase fractionates N and O isotopes with a ratio near unity. *Environ. Sci. Technol.* 46 (11), 5727-5735.
- Karsh, K.L.; Trull, T.W.; Sigman, D.M.; Thompson, P.A.; Granger, J. 2014. The contributions of nitrate uptake and efflux to isotope fractionation during algal nitrate assimilation. *Geochim. Cosmochim. Acta* 132, 391-412.
- Kendall, C.; Caldwell, E. A. 1998. Fundamentals of Isotope Geochemistry. In *Isotope Tracers in Catchment Hydrology*; Kendall, C.; McDonnell, J. J., Eds.; Elsevier Science B.V.: Amsterdam, pp 51-86.
- Kendall, C.; Doctor, D. H. 2011. Stable Isotope Applications in Hydrologic Studies. In *Isotope Geochemistry From the Treatise on Geochemistry*; Holland, H. D.; Turekian, K. K., Eds.; Elsevier Science: Italy, pp 181-226.
- Kirk, A. B.; Smith, E. E.; Tian, K.; Anderson, T. A.; Dasgupta, P. K. 2003. Perchlorate in milk. *Environ. Sci. Technol.* 37 (21), 4979-4981.
- Kläning, U. K.; Sehested, K. 1991. The primary process $\text{ClO}_3^- (+h\nu) \longleftrightarrow \text{ClO}^- + \text{O}_2$ in the photolysis of aqueous ClO_3^- solutions. *J. Phys. Chem.* 95, 740-743.
- Kläning, U. K.; Sehested, K.; Holeman, J. 1985. Standard Gibbs energy of formation of the hydroxyl radical in aqueous solution. Rate constants for the reaction $\text{ClO}_2^- + \text{O}_3 \longleftrightarrow \text{O}_3^- + \text{ClO}_2$. *J. Phys. Chem.* 89, 760-763.
- Kläning, U. K.; Wolff, T. 1985. Laser Flash Photolysis of HClO , ClO^- , HBrO , and BrO^- in aqueous solution. Reactions of Cl- and Br- atoms. *Ber. Bunsenges. Phys. Chem.* 89, 243-245.
- Kounaves, S. P.; Stroble, S. T.; Anderson, R. M.; Moore, Q.; Catling, D. C.; Douglas, S.; McKay, C. P.; Ming, D. W.; Smith, P. H.; Tamppari, L. K.; Zent, A. P. 2010. Discovery of natural

- perchlorate in the Antarctic dry valleys and its global implications. *Environ. Sci. Technol.* 44, 2360–2364.
- Kumar, S., Nicholas, D.J.D., and Williams, E.H. 1983. Definitive ^{15}N NMR evidence that water serves as a source of 'O' during nitrite oxidation by *Nitrobacter agilis*: *Fed. Europ. Biochem. Soc. (FEBS) Lett.*, 152:71-74.
- Lal, D.; Peters, B. 1967. Cosmic Ray Produced Radioactivity on the Earth. In *Kosmische Strahlung II / Cosmic Rays II*; Sitte, K., Ed. Springer: Berlin Heidelberg, 9, 551-612.
- Langford, A.O., J. Brioude, O.R. Cooper, C.J. Senff, R.J. Alvarez II, R.M. Hardesty, B.J. Johnson, and S.J. Oltmans. 2012. Stratospheric influence on surface ozone in the Los Angeles area during late spring and early summer of 2010. *Journal of Geophysical Research* 117: doi:10.1029/2011JD016766.
- Larson, G.; Schaetzl, R. 2001. Origin and Evolution of the Great Lakes. *J. Great Lakes Res.* 27 (4), 518–546.
- Ledgard, S. F.; Woo, K. C.; Bergersen, F. J. 1985. Isotopic fractionation during reduction of nitrate and nitrite by extracts of spinach leaves. *Funct. Plant Biol.* 12 (6), 631-640.
- Laursen, K. H.; Mihailova, A.; Kelly, S. D.; Epov, V. N.; Bérail, S.; Schjoerring, J. K.; Donard, O. F. X.; Larsen, E. H.; Pedentchouk, N.; Marca-Bell, A. D.; Halekoh, U.; Olesen, J. E.; Husted, S. 2013. Is it really organic? – Multi-isotopic analysis as a tool to discriminate between organic and conventional plants. *Food Chem.* 141 (3), 2812-2820.
- Lee P.A., Mikucki, J.A., Foreman, C. M., Priscu, J. C., DiTullio, G.R., Riseman, S. F., de Mora, S. J., Wolf C. F., and Kester, L. 2004. Thermodynamic constraints on microbially mediated processes in lakes of the McMurdo Dry Valleys, Antarctica. *Geomicrobiology Journal*, 21,1–17.
- Lehmann, B. E.; Davis, S. N.; Fabryka-Martin, J. T. 1993. Atmospheric and subsurface sources of stable and radioactive nuclides used for groundwater dating. *Water Resour. Res.* 29 (7), 2027-2040.
- Leung, A. M.; Pearce, E. N.; Braverman, L. E. 2010. Perchlorate, iodine and the thyroid. *Best Pract. Res. Cl. En.* 24, 133-141.
- Levanov, A. V.; Kuskov, I. V.; Zosimov, A. V.; Antipenko, E. E.; Lunin, V. V. 2003. Acid catalysis in reaction of ozone with chloride ions. *Kinetics and Catalysis.* 44 (6), 740-746.
- Lloyd, R.M., 1968. Oxygen isotope behavior in the sulfate-water system. *J. Geophys. Res.* 73, 6099-6110.
- Longstaffe, F. J.; Ayalon, A.; Hladyniuk, R.; Hyodo, A.; Macdonald, R.; St. Amour, N.; Crowe, A.; P., H. 2011. The Oxygen and Hydrogen Isotope Evolution of the Great Lakes. International Atomic Energy Association. IAEA-CN-186-INV002.

- Luz, B.; Barkan, E. 2005. The isotopic ratios $^{17}\text{O}/^{16}\text{O}$ and $^{18}\text{O}/^{16}\text{O}$ in molecular oxygen and their significance in biogeochemistry. *Geochim. Cosmochim. Acta* 69 (5), 1099-1110.
- Lyons, W.B., Fountain, A., Doran, P., Priscu, J.C., Neumann, K., and Welch, K.A. 2000. Importance of landscape position and legacy: the evolution of the lakes in Taylor Valley, Antarctica. *Freshwater Biology* 43, 355-367.
- Lyons, W.B., Tyler, S.W., Wharton, R.A., McKnight, D.M., and Vaughn, B.H. 1998. A Late Holocene desiccation of Lake Hoare and Lake Fryxell, McMurdo Dry Valleys, Antarctica. *Antarctic Science* 10, 247-256.
- Lyons, W.B., Welch, K.A., Snyder, G., Olesik, J., Graham, E.Y., Marion, G.M., and Poreda, R.J. 2005. Halogen geochemistry of the McMurdo dry valleys lakes, Antarctica: Clues to the origin of solutes and lake evolution. *Geochimica et Cosmochimica Acta* 69, 305-323.
- Maixner, F., Wagner, M., Lückner, S., Pelletier, E., Schmitz-Esser, S., Haeck, K., Spieck, E., Konrat, R., Le Paslier, D., and Daims, H. 2008. Environmental genomics reveals a functional chlorite dismutase in the nitrite-oxidizing bacterium '*Candidatus Nitrospira defluvii*'. *Environ. Microbiol.* 10, 3043-3056.
- Mariotti, A.; Mariotti, F.; Champigny, M.L.; Amarger, N.; Moyse, A. 1982. Nitrogen Isotope Fractionation Associated With Nitrate Reductase Activity and Uptake of NO_3^- by Pearl Millet. *Plant Physiol.* 69 (4), 880-884.
- Marschner, H. 1995. 2- Ion Uptake Mechanisms of Individual Cells and Roots: Short-Distance Transport. In *Mineral Nutrition of Higher Plants (Second Edition)*; Marschner, H., Ed.; Academic Press: London, pp 6-78.
- Massman, W. J., R. C. Musselman, A. S. Lefohn. 2000. A conceptual ozone dose-response model to develop a standard to protect vegetation. *Atmospheric Environment* 34: 745-759.
- Massman, W.J., 1998. A review of the molecular diffusivities of H_2O , CO_2 , CH_4 , CO , O_3 , SO_2 , NH_3 , N_2O , NO , AND NO_2 in air, O_2 and N_2 near STP. *Atmospheric Environment* 32, 1111-1127.
- Massman, W.J., and D.A. Grantz, 1995. Estimating canopy conductance to ozone uptake from observations of evapotranspiration at the canopy scale and at the leaf scale. *Global Change Biology* 1:183-198.
- Matisoff, G.; Neeson, T. M. 2005. Oxygen Concentration and Demand in Lake Erie Sediments. *J. Great Lakes Res.* 31, Supplement 2 (0), 284-295.
- Matsubaya, O., Sakai, H., Torri T., Burton, H., and Kerry, K. 1979. Antarctic saline lakes-stable isotope ratios, chemical compositions, and evolution. *Geochimica et Cosmochimica Acta* 43, 7-25.

- McElroy, J. A. 1990. Laser Photolysis Study of the Reaction of SO_4^- with Cl^- and the Subsequent Decay of Cl_2^- in Aqueous Solution. *J. Phys. Chem.* 94, 2435-2441.
- McKay, C.P. and Davis, W. 1991 Duration of liquid water habitats on early Mars. *Int. J. of Solar Sys. Studies*, 2: 214-221.
- McMahon, P.B.; Böhlke, J.K., 2006. Regional patterns in the isotopic composition of natural and anthropogenic nitrate in groundwater, high plains, U.S.A. *Environ. Sci. Technol.* **2006**, 40, 2965-2970.
- Michalski, G., Böhlke J.K., Thiemens, M. 2004. Long term atmospheric deposition as the source of nitrate and other salts in the Atacama Desert, Chile: New evidence from mass-independent oxygen isotopic compositions. *Geochimica Cosmochimica Acta* 68, 4023-4038.
- Michalski, G.; Savarino, J.; Böhlke, J.K. Thiemens, M.H. 2002. Determination of the total oxygen isotopic composition of nitrate and the calibration of a $\Delta^{17}\text{O}$ nitrate reference material. *Anal. Chem.* 74, 4989-4993.
- Michalski, G.; Scott, Z.; Kabiling, M.; Thiemens, M.H. 2003. First measurements and modeling of $\Delta^{17}\text{O}$ in atmospheric nitrate. *Geophys. Res. Lett.*, 30(16), ASC 14.1-14.4.
- Mihailova, A.; Pedentchouk, N.; Kelly, S. D. 2014. Stable isotope analysis of plant-derived nitrate—Novel method for discrimination between organically and conventionally grown vegetables. *Food Chem.* 154, 238-245.
- Mikucki, J.A., A. Pearson, D. T. Johnston, A.V. Turchyn, J. Farquhar, D.P. Schrag, A. D. Anbar, J. C. Priscu, P. A. Lee. 2009. A contemporary, microbially-maintained, ferrous subglacial 'ocean'. *Science*, 324:397
- Mikucki, J.A., C.M. Foreman, J.C. Priscu, W. B. Lyons, B. Sattler, and K. Welch. 2004. Geomicrobiology of Blood Falls: A Saline, Iron-rich Subglacial Feature of Taylor Glacier, Antarctica. *Aquatic Geochemistry*, 10:199-220.
- Miller, M. F. 2002. Isotopic Fractionation and the Quantification of ^{17}O Anomalies in the Oxygen Three-isotope System: An Appraisal and Geochemical Significance. *Geochim. Cosmochim. Acta.* 66 (11), 1881-1889.
- Mizutani, Y.; Rafter, T.A. 1969. Oxygen isotopic composition of sulphates: Pt. 3, Oxygen isotope fractionation in the bisulphate ion-water system. *New Zealand J. Sci.* 12, 54-59. 34.
- Morrison, C. 2009. A mass inventory of perchlorate in the Great Lakes hydrologic system. M.S. Thesis, University of Illinois at Chicago, Chicago, IL.
- Motzer, W. E. 2001. Perchlorate: Problems, detection, and solutions. *Environ. Forensics* 2 (4), 301-311.

- Murphy, D. M.; Thomson, D. S. 2000. Halogen Ions and NO^+ in the Mass Spectra of Aerosols in the Upper Troposphere and Lower Stratosphere. *Geophysical Res. Lett.* 27 (19), 3217-3220.
- National Academies, 2005. The National Academies of Sciences, Division of Earth and Life Studies. . Health Implications of Perchlorate Ingestion. The National Academies Press, Washington DC. Available online [<http://www.nap.edu/read/11202/chapter/1>].
- Needoba, J. A.; Waser, N. A.; Harrison, P. J.; Calvert, S. E. Nitrogen isotope fractionation in 12 species of marine phytoplankton during growth on nitrate. *Mar. Ecol. Prog. Ser.* 2003, 255, 81-91.
- Needoba, J. A.; Sigman, D. M.; Harrison, P. J. 2004. The mechanism of isotope fractionation during algal nitrate assimilation as illuminated by the $^{15}\text{N}/^{14}\text{N}$ of intracellular nitrate. *J. Phycol.*, 40 (3), 517-522.
- Nerenberg, R.; Kawagoshi, Y.; Rittmann, B.E. 2008. Microbial ecology of a perchlorate-reducing, hydrogen-based membrane biofilm reactor. *Water Res.* 42, 1151-1159.
- Nicoson, J. S.; Wang, L.; Becker, R. H.; Hartz, K. E. H.; Muller, C. E.; Margerum, D. W. 2002. Kinetics and mechanisms of the ozone/bromite and ozone/chlorite reactions. *Inorg. Chem.* 2002, 41 (11), 2975—2980.
- Noble, L.F. 1931. Nitrate deposits in southeastern California. U.S. Geological Survey Bulletin. 820, 108 pp.
- Noble, L.F.; Mansfield, G.R.; Gale, H.S. 1922. and Calkins, F.C. Nitrate deposits of the Amargosa Region, southeastern California. U.S. Geological Survey Bulletin. 724, 99 pp.
- Nzengung, V. A.; McCutcheon, S. C. 2003. Phytoremediation of Perchlorate. In Phytoremediation Transformation and Control of Contaminants; McCutcheon, S. C.; Schnoor, J. L., Eds.; John Wiley & Sons, Inc.: Hoboken, New Jersey.
- Nzengung, V. A.; Penning, H.; O'Niell, W. 2004. Mechanistic Changes During Phytoremediation of Perchlorate Under Different Root-zone Conditions. *Int. J. Phytoremediat.* 6 (1), 63-83.
- Nzengung, V. A.; Wang, C.; Harvey, G. 1999. Plant-mediated transformation of perchlorate into chloride. *Environ. Sci. Technol.* 33 (9), 1470-1478.
- Obvintseva, L. A.; Chibirova, F. K.; Kazakov, S. A.; Avetisov, A. K.; Srobkova, M. V.; Finogenova, N. V. 2003. Semiconductor sensors application for definition of factor of ozone heterogenous destruction on Teflon surface. *Sensors.* 3, 504-508.
- Paerl, H.W. 1997. Primary Productivity and Producers. In Manual of Environmental Microbiology, ASM Press, Washington, D.C. pp 252-262.

- Parker, D.R.; Seyfferth, A.L.; Reese, B.K. 2008. Perchlorate in groundwater: A synoptic survey of “pristine” sites in the conterminous United States. *Environ. Sci. Technol.* 42, 1465-1471
- Parthiban, S.; Raghunandan, B. N.; Sumathi, R. 1995. Ab initio study of the molecular structure and vibrational spectra of dichlorine hexoxide and its significance to stratospheric ozone depletion. *Chemical Physics.* 199, 183-193.
- Patterson, M.C., Samuelson, L., Somers, G., and Mays, A. 2000. Environmental control of stomatal conductance in forest trees of the Great Smoky Mountains National Park. *Environ. Pollut.*, 110:225-233.
- Pearson, R. 2008. Annual Report of the Great Lakes Regional Water Use Database - Representing 2008 Water Use Data. Great Lakes Commission. Issue No. 17 2010.
- Pfaff, J.D. 1993. US EPA Method 300.0, Methods for the Determination of Inorganic Substances in Environmental Samples, EPA-600/R-93-100, NTIS PB94-121811.
- Phillips, F. M. 1994. Environmental tracers for water movement in desert soils of the American southwest. *Soil Sci. Soc. Amer. J.* 58, 15-24.
- Plummer, L. N.; Böhlke, J. K.; Doughten, M. W. 2006. Perchlorate in Pleistocene and Holocene Groundwater in North-Central New Mexico. *Environ. Sci. Technol.* 40 (6), 1757-1763.
- Plummer, L.N.; Bexfield, L.M.; Anderholm, S.K.; Sanford, W.E.; Busenberg, E. 2004. Geochemical characterization of ground-water flow in the Santa Fe Group aquifer system, Middle Rio Grande Basin, New Mexico. U.S. Geological Survey, Water-Resources Investigations Report 03-4131,
- Poreda, R.J., Hunt, A.G., Lyons, W.B., and Welch, K.A. 2004. The helium isotopic chemistry of Lake Bonney, Taylor Valley, Antarctica: Timing of Late Holocene climate change in Antarctica. *Aquatic Geochemistry* 10, 353-371.
- Porterfield, S. P. 1994. Vulnerability of the Developing Brain to Thyroid Abnormalities: Environmental Insults to the Thyroid System. *Environ. Health Persp.* 102 (2), 125-130.
- Prasad, S. S.; Lee, T. J. 1994. Atmospheric Chemistry of the Reaction $\text{ClO} + \text{O}_2 \leftrightarrow \text{ClO} \cdot \text{O}_2$: Where it Stands, What Needs to be Done, and Why? *J. Geophys. Res-Atmos.* (1984–2012) 99 (D4), 8225-8230.
- Priscu, J.C. 1995. Phytoplankton nutrient deficiency in lakes of the McMurdo Dry Valleys, Antarctica. *Freshwater Biology* 34:215-227.
- Priscu, J.C. 1997. The biogeochemistry of nitrous oxide in permanently ice-covered lakes of the McMurdo Dry Valleys, Antarctica. *Global Change Biology* 3:301-305.
- Priscu, J.C., Christner, B.C., Dore, J.E., Westley, M.B., Popp, B.N., Casciotti, K.L., and Lyons, W.B. 2008. Supersaturated N_2O in a perennially ice-covered Antarctic lake: Molecular

- and stable isotopic evidence for a biogeochemical relict. *Limnology and Oceanography* 53, 2439-2450.
- Priscu, J.C., Downes, M.T., and McKay, C.P. 1996. Extreme supersaturation of nitrous oxide in a poorly ventilated Antarctic lake. *Limnology and Oceanography* 41, 1544-1551.
- Quinn, F. H. 1992. Hydraulic residence times for the Laurentian Great Lakes. *J. Great Lakes Res.* 18 (1), 22-28.
- Quiroga, S. L.; Perissinotti, L. J. 2005. Reduced mechanism for the 366 nm chlorine dioxide photodecomposition in N₂-saturated aqueous solutions. *J. Photochem. Photobiol. A: Chem.* 171, 59-67.
- Rajagopalan, S.; Anderson, T. A.; Fahlquist, L.; Rainwater, K. A.; Ridley, M.; Jackson, W. A. 2006. Widespread presence of naturally occurring perchlorate in High Plains of Texas and New Mexico. *Environ. Sci. Technol.* 2006, 40, 3156-3162.
- Rajagopalan, S.; Anderson, T.; Cox, S.; Harvey, G.; Cheng, Q.; Jackson, W. A. 2009. Perchlorate in wet deposition across North America. *Environ. Sci. Technol.* 43 (3), 616-622.
- Rao, B. Natural Perchlorate and Chlorate in the Environment: An Investigation of their Occurrence and Formation Processes. Ph.D. Dissertation, Texas Tech University, Lubbock, TX, 2010.
- Rao, B., Anderson, T.A., Redder, A., Jackson, W.A. 2010a. Perchlorate formation by ozone oxidation of aqueous chlorine/oxy-chlorine species: Role of Cl_xO_y radicals. *Environmental Science and Technology* 44, 2961–2967.
- Rao, B., Hatzinger, P.B., Böhlke, J.K., Sturchio, N.C., Andraski, B.J., Eckardt, F.D., and Jackson, W.A. 2010b. Natural chlorate in the environment: application of a new IC-ESI/MS/MS method with a Cl(18)O(3)(-) internal standard. *Environmental Science & Technology* 44, 8429-8434.
- Rao, B., S. Mohan, A. Neuber, and W.A Jackson. 2012a. Production of perchlorate by laboratory simulated lightning process. 223:275-287.
- Rao, B.; Estrada, N.; McGee, S.; Mangold, J.; Gu, B.; Jackson, W. A. 2012b. Perchlorate production by photodecomposition of aqueous chlorine solutions. *Environ. Sci. Technol.* 46 (21), 11635-11643.
- Rao, B.; Wake, C.; Anderson, T.; Jackson, W. 2012c. Perchlorate Depositional History as Recorded in North American Ice Cores from the Eclipse Icefield, Canada, and the Upper Fremont Glacier, USA. *Water Air Soil Pollut.* 223 (1), 181-188.
- Rao, B.; Anderson, T. A.; Orris, G. J.; Rainwater, K. A.; Rajagopalan, S.; Sandvig, R. M.; Scanlon, B. R.; Stonestrom, D. A.; Walvoord, M. A.; Jackson, W. A. 2007. Widespread

- Natural Perchlorate in Unsaturated Zones of the Southwest United States. *Environ. Sci. Technol.* 41 (13), 4522-4528.
- Rao, B.; Anderson, T.; Redder, A.; Jackson, W.A. 2010. Perchlorate formation by ozone oxidation of aqueous chlorine/oxy-chlorine species: Role of Cl_xO_y radicals. *Environ. Sci. Technol.*, 44, 2961-2967.
- Rheaume, S. J.; Williams, S. J.; Larsen, C. E.; Geological Survey (U.S.) 1995. United States Geological Survey : programs in the Great Lakes. Fact sheet (FS-056-95).
- Roldan, M.D., Reyes, F., Morenovivian, C., and Castillo, F. 1994. Chlorate and nitrate reduction in the phototrophic bacteria rhodobacter-capsulatus and rhodobacter-sphaeroides. *Current Microbiology* 29, 241-245.
- Sánchez, C. A.; Crump, K. S.; Krieger, R. I.; Khandaker, N. R.; Gibbs, J. P. 2005a. Perchlorate and nitrate in leafy vegetables of North America. *Environm. Sci. Technol.* 39 (24), 9391-9397.
- Sánchez, C. A.; Krieger, R. I.; Khandaker, N.; Moore, R. C.; Holts, K. C.; Neidel, L. L. 2005b. Accumulation and Perchlorate Exposure Potential of Lettuce Produced in the Lower Colorado River Region. *J. Agr. Food Chem.* 53 (13), 5479-5486.
- Sánchez, J.A., and F.J.G. Ayala. 2008. Recent Trend in Ozone Levels in the Metropolitan zone of Mexico City. *Journal of the Mexican Chemical Society* 52: 256-262.
- SAS Institute. 2002. SAS Users' Guide. SAS Institute. Cary NC.
- Sattley, W.M. and Madigan, M.T. 2006. Isolation, characterization, and ecology of cold-active, chemolithotrophic, sulfur-oxidizing bacteria from perennially ice-covered Lake Fryxell, Antarctica. *Applied and Environmental Microbiology* 72, 5562-5568.
- Schauble, E.A.; Rossman, G.R.; Taylor, H.P. 2003. Theoretical estimates of equilibrium chlorine-isotope fractionations. *Geochim. Cosmochim. Acta* 67, 3267-3281. 38.
- Schmidt, H. L.; Medina, R. Possibilities and scope of the double isotope effect method in the elucidation of mechanisms of enzyme catalyzed reactions. *Isotopenpraxis Isot. Environ. Healt. S.* 1991, 27 (1), 1-4.
- Seyfferth, A. L.; Parker, D. R. 2008. Chapter 2: Uptake and Fate of Perchlorate in Higher Plants. In *Advances in Agronomy*: Donald, L. S., Ed.; Academic Press: Vol. 99, pp 101-123.
- Seyfferth, A.L., and D.R Parker. 2007. Effects of genotype and transpiration rate on the uptake and accumulation of perchlorate (ClO_4^-) in lettuce. *Environmental Science and Technology* 41:3361-3367.
- Seyfferth, A.L., M.K. Henderson, and D.R. Parker. 2008a. Effects of common soil anions and pH on the uptake and accumulation of perchlorate in lettuce. *Plant and Soil* 302:139-148.

- Seyfferth, A.L., N.C. Sturchio, and D.R. Parker, 2008b. Is perchlorate metabolized or re-translocated within lettuce leaves? *Environmental Science and Technology* 42:9437-9442.
- Siddiqui, M. S. 1996. Chlorine-ozone interactions: Formation of chlorate. *Water Res.* 30 (9), 2160-2170.
- Sigman, D.M.; Casciotti, K.L.; Andreani, M.; Barford, C.; Galanter, M.; and Böhlke, J.K. 2001. A bacterial method for the nitrogen isotopic analysis of nitrate in seawater and freshwater. *Anal. Chem.*, 73, 4145-4153.
- Sigman, D.M.; Robinson, R.; Knapp, A.N.; van Green, A.; McCorkle, D.C.; Brandes, J.A.; Thunell, R.C. 2003. Distinguishing between water column and sedimentary denitrification in the Santa Barbara Basin using the stable isotopes of nitrate. *Geochem. Geophys. Geosy.* 4 (5), 1-20.
- Sigman, D.M.; Granger, J.; DiFiore, P.J.; Lehmann, M.M.; Ho, R.; Cane, G.; van Green, A. 2005. Coupled nitrogen and oxygen isotope measurements of nitrate along the Eastern North Pacific Margin. *Global Biogeochem. Cy.* 19, 1-14.
- Simonatis, C.; Heicklen, J. 1975. Perchloric acid: A possible sink for stratospheric chlorine. *Plant. Space. Sci.* 23, 1567-1569.
- Smith, P. N.; Theodorakis, C. W.; Anderson, T. A.; Kendall, R. J. 2001. Preliminary Assessment of Perchlorate In Ecological Receptors at the Longhorn Army Ammunition Plant (LHAAP), Karnack, Texas. *Ecotoxicology* 10 (5), 305-313.
- Smith, P. N.; Yu, L.; McMurry, S. T.; Anderson, T. A. 2004. Perchlorate in Water, Soil, Vegetation, and Rodents Collected From the Las Vegas Wash, Nevada, USA. *Environ. Pollut.* 132 (1), 121-127.
- Snyder, S. A.; Pleus, R. C.; Vanderford, B. J.; Holady, J. C. 2006. Perchlorate and Chlorate in Dietary Supplements and Flavor Enhancing Ingredients. *Anal. Chim. Acta* 567 (1), 26-32.
- Solomon, S.; Mount, G. H.; Sanders, R. W.; Jakoubek, R. O.; Schmeltekopf, A. L. 1988. Observations of the nighttime abundance of OClO in the winter stratosphere above Thule, Greenland. *Science*, 242, 4878, 550-555.
- Solomon, S.; Sanders, R. W.; Garcia, R. R.; Keys, J. G. 1993. Increased chlorine dioxide over Antarctica caused by volcanic aerosols from Mount Pinatubo. *Nature*, 363, 245-248.
- Solomon, S.; Sanders, R.W.; Carroll, M. A.; Schmeltekopf, A. L. 1989. Visible and near-ultraviolet spectroscopy at McMurdo Station, Antarctica 5. Observations of the diurnal variations of BrO and OClO. *J. Geophys. Res.*, 94(D9), 393-403
- Spigel, R.H. and Priscu J.C. 1998. Physical limnology of the McMurdo Dry Valley lakes, In. *Ecosystems Dynamics in a Polar Desert: The McMurdo Dry Valleys, Antarctica* (ed. J.C.

- Priscu), Antarctica Research Series 72, American Geophysical Union, Washington, D.C. pp.153-187.
- Srinivasan, A. and T. Viraraghavan. 2009. Perchlorate: Healthy effects and technologies for its removal from water resources. *International Journal of Environmental Research and Public Health* 6: 1418-1442.
- Stevenson, D. S., Dentener, F.J., Schultz, M.G., Ellingsen, K., van Noije, T.P.C., Wild, O., Zeng, G., Amann, M., Atherton, C.S., Bell, N., Bergmann, D.J., Bey, I., Butler, T., Cofala, J., Collins, W.J., Derwent, R.G., Doherty, R.M., Drevet, J., Eskes, H.J., Fiore, A.M., Gauss, M., Hauglustaine, D.A., Horowitz, L.W., Isaksen, I.S.A., Krol, M.C., Lamarque, J.-F., Lawrence, M.G., Montanaro, V., Muller, J.-F., Pitari, G., Prather, M.J., Pyle, J.A., Rast, S., Rodriguez, J.M., Sanderson, M.G., Savage, N.H., Shindell, D.T., Strahan, S.E., Sudo, K., Szopa, S. 2006. Multimodel ensemble simulations of present-day and near-future tropospheric ozone. *Journal of Geophysical Research* 111, D08301, doi: 10.1029/2005JD006338.
- Sturchio, N. C.; Beloso Jr, A.; Heraty, L. J.; Wheatcraft, S.; Schumer, R. 2014. Isotopic tracing of perchlorate sources in groundwater from Pomona, California. *Appl. Geochem.*, 43, 80-87.
- Sturchio, N. C.; Böhlke, J. K.; Gu, B.; Hatzinger, P. B.; Jackson, W. A. 2011. Isotopic Tracing of Perchlorate in the Environment. In *Handbook of Environmental Isotope Geochemistry*; Baskaran, M., Ed. Springer-Verlag Berlin Heidelberg: London, New York, Vol. 1, pp 437-452.
- Sturchio, N. C.; Böhlke, J. K.; Gu, B.; Horita, J.; Brown, G. M.; Beloso, A. D. J.; Patterson, L. J.; Hatzinger, P. B.; Jackson, W. A.; Batista, J. 2006. Stable isotopic composition of chlorine and oxygen in synthetic and natural perchlorate. In *Perchlorate: Environmental Occurrence, Interactions, and Treatment* Gu, B.; Coates, J. D., Eds. Springer: New York; pp 93-110.
- Sturchio, N. C.; Caffee, M.; Beloso, A. D., Jr.; Heraty, L. J.; Böhlke, J. K.; Hatzinger, P. B.; Jackson, W. A.; Gu, B.; Heikoop, J. M.; Dale, M. 2009. Chlorine-36 as a tracer of perchlorate origin. *Environ. Sci. Technol.* 43 (18), 6934-8.
- Sturchio, N. C.; Hatzinger, P. B.; Arkins, M. D.; Suh, C.; Heraty, L. J. 2003. Chlorine isotope fractionation during microbial reduction of perchlorate. *Environ. Sci. Technol.* 37 (17), 3859-3863.
- Sturchio, N. C.; Hoaglund, J. R., 3rd; Marroquin, R. J.; Beloso, A. D., Jr.; Heraty, L. J.; Bortz, S. E.; Patterson, T. L. 2012. Isotopic mapping of groundwater perchlorate plumes. *Groundwater* 50 (1), 94-102.
- Sturchio, N.C.; Böhlke, J.K.; Beloso, A.D.; Streger, S.H.; Heraty, L.J.; Hatzinger, P.B. 2007. Oxygen and chlorine isotopic fractionation during perchlorate biodegradation: Laboratory

- results and implications for forensics and natural attenuation. *Environ. Sci. Technol.* 41, 2796-2802.
- Sundberg, S.E., Ellington, J.J., Evans, J.J., Keys, D.A., Fisher, J.W. 2003. Accumulation of perchlorate in tobacco plants: development of a plant kinetic model. *The Journal of Environmental Monitoring* 5, 505-512.
- Susarla, S., T. Collette, W. Garrison, A. W. Wolfe, N. L. and McCutcheon, S. C. 1999. Perchlorate identification in fertilizers. *Environ. Sci. Technol.* 33, 3469-3472
- Susarla, S., Bacchus S.T., Harvey, G. McCutcheon S.C. 2000a. Uptake and transformation of perchlorate by vascular plants. *Toxicological and Environmental Chemistry* 74, 29-47.
- Susarla, S., T. Collette, W. Garrison, A. W. Wolfe, N. L. and McCutcheon, S. C. 2000b: Additions and corrections: "Perchlorate identification in fertilizers". *Environ. Sci. Technol.* 34, 224.
- Synal, H. A.; Beer, J.; Bonani, G.; Suter, M.; Wölfli, W. 1990. Atmospheric transport of bomb-produced ^{36}Cl . *Nucl. Instrum. Meth. B.* 52 (3-4), 483-488.
- Tan, K., Anderson, T.A., Jackson, W.A. 2005. A temporal and spatial variation of perchlorate in streambed sediments: Results from in-situ dialysis samplers. *Environmental Pollution* 136, 283-291.
- Tan, K., Anderson, T.A., Jones, M.W., Smith, P.N., Jackson, W.A. 2004. Accumulation of perchlorate in aquatic and terrestrial plants at a field scale. *Journal of Environmental Quality* 33, 1638-1646.
- Tan, K.; Anderson, T. A.; Jackson, W. A. 2006. Uptake and exudation behavior of perchlorate in smartweed. *Int. J. Phytoremediat.* 8 (1), 13-24.
- Tan, K.; Jackson, W. A.; Anderson, T. A.; Pardue, J. H. 2004. Fate of perchlorate-contaminated water In upflow wetlands. *Water Res.* 38 (19), 4173-4185.
- Tcherkez, G.; Farquhar, G. D. 2006. Viewpoint: Isotopic fractionation by plant nitrate reductase, twenty years later. *Funct. Plant Biol.* 33 (6), 531-537.
- Thiemens, M. H. 1999. Mass-independent isotope effects in planetary atmospheres and the early solar system. *Science* 283 (5400), 341-345.
- Trull, T. W.; Davies, D.; Casciotti, K. 2008. Insights into nutrient assimilation and export in naturally iron-fertilized waters of the Southern Ocean from nitrogen, carbon and oxygen isotopes. *Deep- Sea Res Pt II.* 55 (5-7), 820-840.
- Trumpolt, C. W.; Crain, M.; Cullison, G. D.; Flanagan, S. J. P.; Siegel, L.; Lathrop, S. 2005. Perchlorate: Sources, uses, and occurrences in the environment. *Remed. J.* 16 (1), 65-89.

- Urbansky, E. 2002. Perchlorate as an environmental contaminant. *Environ. Sci. Pollut. R.* 9 (3), 187-192.
- Urbansky, E. T. 1998. Perchlorate chemistry: Implications for analysis and remediation. *Bioremediation* 2 (2), 81-95.
- Urbansky, E. T.; Brown, S. K.; Magnuson, M. L.; Kelty, C. A. 2001. Perchlorate levels in samples of sodium nitrate fertilizer derived from Chilean caliche. *Environ. Pollut.* 112 (3), 299-302.
- Urbansky, E. T.; Collette, T.; Robarge, W. P.; Hall, W. L.; Skillen, J. M.; Kane, P. F. 2001. *Survey of Fertilizers and Related Materials for Perchlorate (ClO₄⁻): Final Report*; EPA/600/R-01/049; National Risk Management Research Laboratory: Cincinnati, OH.
- Urbansky, E. T.; Magnuson, M. L.; Kelty, C. A.; Brown, S. K. 2000. Perchlorate uptake by salt cedar (*Tamarix Ramosissima*) in the Las Vegas Wash riparian ecosystem. *Sci. Total Environ.* 256 (2-3), 227-232.
- Urbansky, E.T., and S.K Brown. 2003. Perchlorate retention and mobility in soils. *Journal of Environmental Monitoring* 5:455-462.
- Urbansky, E.T., M.L. Magnuson, C.A. Kelty, and S.K. Brown. 2000a. Perchlorate uptake by salt cedar (*Tamarix ramosissima*) in the Las Vegas Wash riparian ecosystem. *Science of the Total Environment* 256:227-232.
- Urbansky, E.T., M.L. Magnuson, C.A Kelty, B. Gu, and G.M. Brown. 2000b. Comment on: Perchlorate identification in fertilizers, and the subsequent addition/correction. *Environmental Science and Technology* 34:4452–4453.
- Urbansky, E.T.; Schock, M.R. Issues in managing the risks associated with perchlorate in drinking water. *J. Environ. Man.* 1999, 56, 79-95.
- USEPA, 2005. United States Protection Agency. EPA Dose for Perchlorate. Available online [https://yosemite.epa.gov/opa/admpress.nsf/d0cf6618525a9efb85257359003fb69d/c1a57d2077c4bfda85256fac005b8b32!OpenDocument].
- USFDA, U.S. Food and Drug Administration. 2008. 2004-2005 Exploratory survey data on perchlorate in food. [online] <http://www.cfsan.fda.gov/~dms/clo4data.html>.
- USGS, 2010. Reston Chlorofluorocarbon Laboratory and Reston Stable Isotope Laboratory, online: <http://water.usgs.gov/lab/> and <http://isotopes.usgs.gov/>.
- Van Aken, B.; Schnoor, J. L. 2002. Evidence of Perchlorate (ClO₄⁻) Reduction in Plant Tissues (Poplar Tree) Using Radio-Labeled ³⁶ClO₄⁻. *Environ. Sci. Technol.* 36 (12), 2783-2788.
- Vilter, H. 1995. Vanadium-dependent haloperoxidases. *Metal Ions Biol. Syst.* 31:325-362.
- Vingarzan, R. 2004. A review of surface ozone background levels and trends. *Atmospheric Environment* 38:3431-3442.

- Vogt, W., and W.A. Jackson. 2010. Perchlorate, nitrate, and iodine uptake and distribution in lettuce (*Lactuca sativa* L.) and potential impact on background levels in humans. *Journal of Agricultural and Food Chemistry*. 58:12192-12198.
- Voogt, W.; Jackson, W. A. Perchlorate, nitrate, and iodine uptake and distribution in lettuce (*Lactuca Sativa* L.) and potential impact on background levels in humans. *J. Agr. Food Chem.* 2010, 58 (23), 12192-12198.
- Voytek, M.A., Priscu, J.C., and Ward, B.B. 1999. The distribution and relative abundance of ammonia-oxidizing bacteria in lakes of the McMurdo Dry Valley, Antarctica. *Hydrobiologia* 401, 113-130.
- Wagner, B., Melles, M., Doran, P.T., Kenig, F., Forman, S.L., Pierau, R., and Allen, P. (2006) Glacial and postglacial sedimentation in the Fryxell Basin, Taylor Valley, southern Victoria Land, Antarctica. *Palaeogeography Palaeoclimatology Palaeoecology* 241, 320-337.
- Walvoord, M. A., Phillips, F. M., Tyler, S. W., and Hartsough, P. C. Deep arid system hydrodynamics 2. Application to paleohydrologic reconstruction using vadose zone profiles from the northern Mojave Desert. *Water Resour. Res.*, 2002, 38,271-2712.
- Wang, S. Heterogeneous Production of Perchlorate and Chlorate by Ozone oxidation of Cl₂. M.S.C.E. Thesis, Texas Tech University, August 2011.
- Ward, B.B., and Priscu, J.C. 1997. Detection and characterization of denitrifying bacteria from a permanently ice-covered Antarctic lake. *Hydrobiologia* 347, 57-68.
- Ward, B.B., Granger, J., Maldonado, M.T., Casciotti, K.L., Harris, S., and Wells, M.L. (2005) Denitrification in the hypolimnion of permanently ice-covered Lake Bonney, Antarctica. *Aquatic Microbial Ecology* 38, 295-307.
- Werner, R.A.; Schmidt, H.L. The in vivo nitrogen isotope discrimination among organic plant compounds. *Phytochemistry*. 2002, 61, 465-484.
- Wiberg, N., Eagleson, M., Aylett, B. J., Eds. *Inorganic Chemistry*, 1st, ed.; Academic Press: New York, 2001.
- Wolff, J. 1998. Perchlorate and the Thyroid Gland. *Pharmacol. Rev.* 50 (1), 89-105.
- Xu, J., J.Z. Ma¹, X.L. Zhang, X.B. Xu¹, X.F. Xu, W.L. Lin, Y. Wang, W. Meng, and Z.Q. Ma. 2011. Measurements of ozone and its precursors in Beijing during summertime: Impact of urban plumes on ozone pollution in downwind rural areas. *Atmospheric Chemistry and Physics* 11: 12241–12252.
- Yang, M., and N.Her. 2011. Perchlorate in soybean sprouts (*Glycine max* L. Merr.), water dropwort (*Oenanthe stolonifera* DC.), and Lotus (*Nelumbo nucifera* Gaertn.) root in South Korea. *Journal of Agricultural and Food Chemistry*. 59:7490-7495.

- Yu, L., Canas, J.E., Cobb, G.P., Jackson, W.A., Anderson, T.A. 2004. Uptake of perchlorate in terrestrial plants. *Ecotoxicology and Environmental Safety* 58, 44-49.
- Zeebe, R. E. 2010. A new value for the stable oxygen isotope fractionation between dissolved sulfate ion and water. *Geoch. Cosmochim. Acta*, 74, 818-828.
- Zeebe, R. E.; Wolf-Gladrow, D. A. 2001. Stable Isotope Fractionation. In *CO₂ In Seawater: Equilibrium, Kinetics, Isotopes*; Halpern, D., Ed.; Elsevier Inc.: New York, Vol. 65, pp 141-250.
- Zuo, Z.; Katsumura, Y.; Ueda, K.; Ishigure, K. 1997a. Laser photolysis study on reactions of sulfate radical and nitrate radical with chlorate ion in aqueous solutions. Formation and reduction potential of ClO₃[•] radical. *J. Chem. Soc., Faraday Trans.* 93 (4), 533-536.
- Zuo, Z.; Katsumura, Y.; Ueda, K.; Ishigure, K. 1997b. Reactions between some inorganic radicals and oxychlorides studied by pulse radiolysis and laser photolysis. *J. Chem. Soc., Faraday Trans.* 93 (10), 1885-1891.

Appendix A: Proposed Mechanisms of Perchlorate Formation

A.1 Proposed Pathways for O₃ Oxidation of Aqueous Chloride

A.1.1 ClO₄⁻ formed from ClO₃ oxidation by OH radical (Final Proposed Pathways)

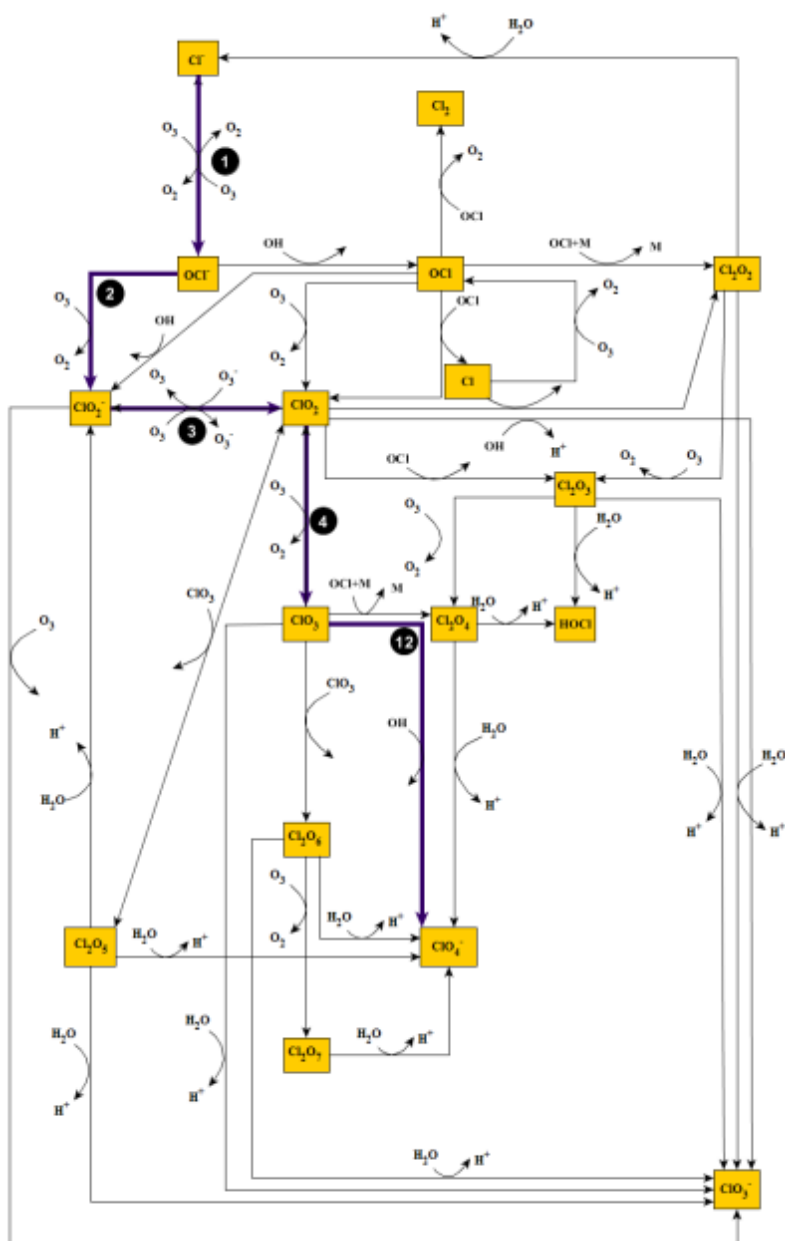


Figure A.1 Mechanism 1: O₃ oxidation of Cl⁻(aq). Note the thick purple lines indicate the pathway leading to the formation of the ClO₄⁻ and black solid circles represent reaction number from Table 3.4. This pathway leads to the formation of one ClO₄⁻ molecule containing all four O's from O₃.

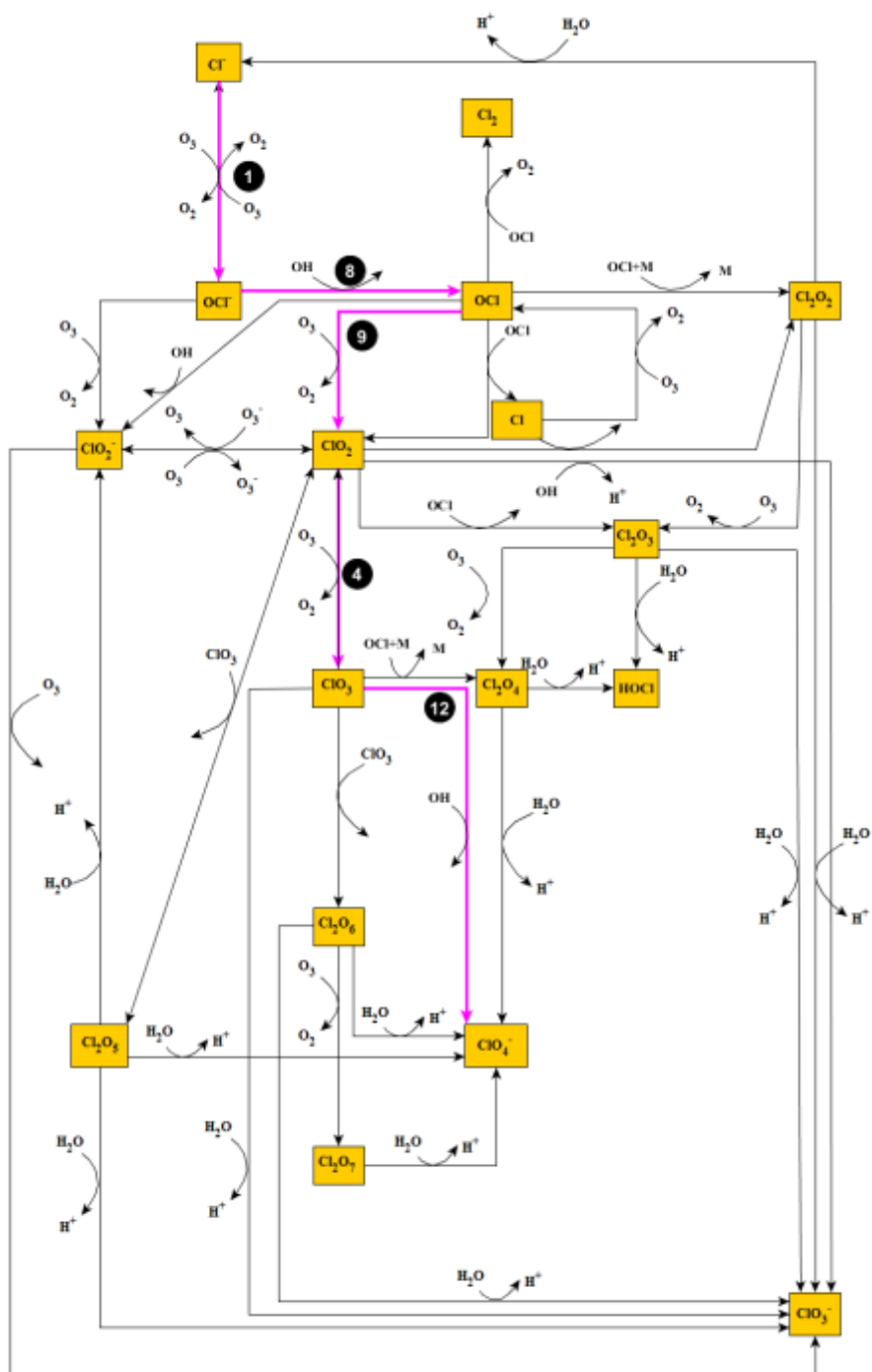


Figure A.2 Mechanism 2: O₃ oxidation of Cl⁻ (aq). Note the thick pink lines indicate the pathway leading to the formation of the ClO₄⁻ and black solid circles represent reaction number from Table 3.4. This pathway leads to the formation of one ClO₄⁻ molecule one containing four O's from O₃.

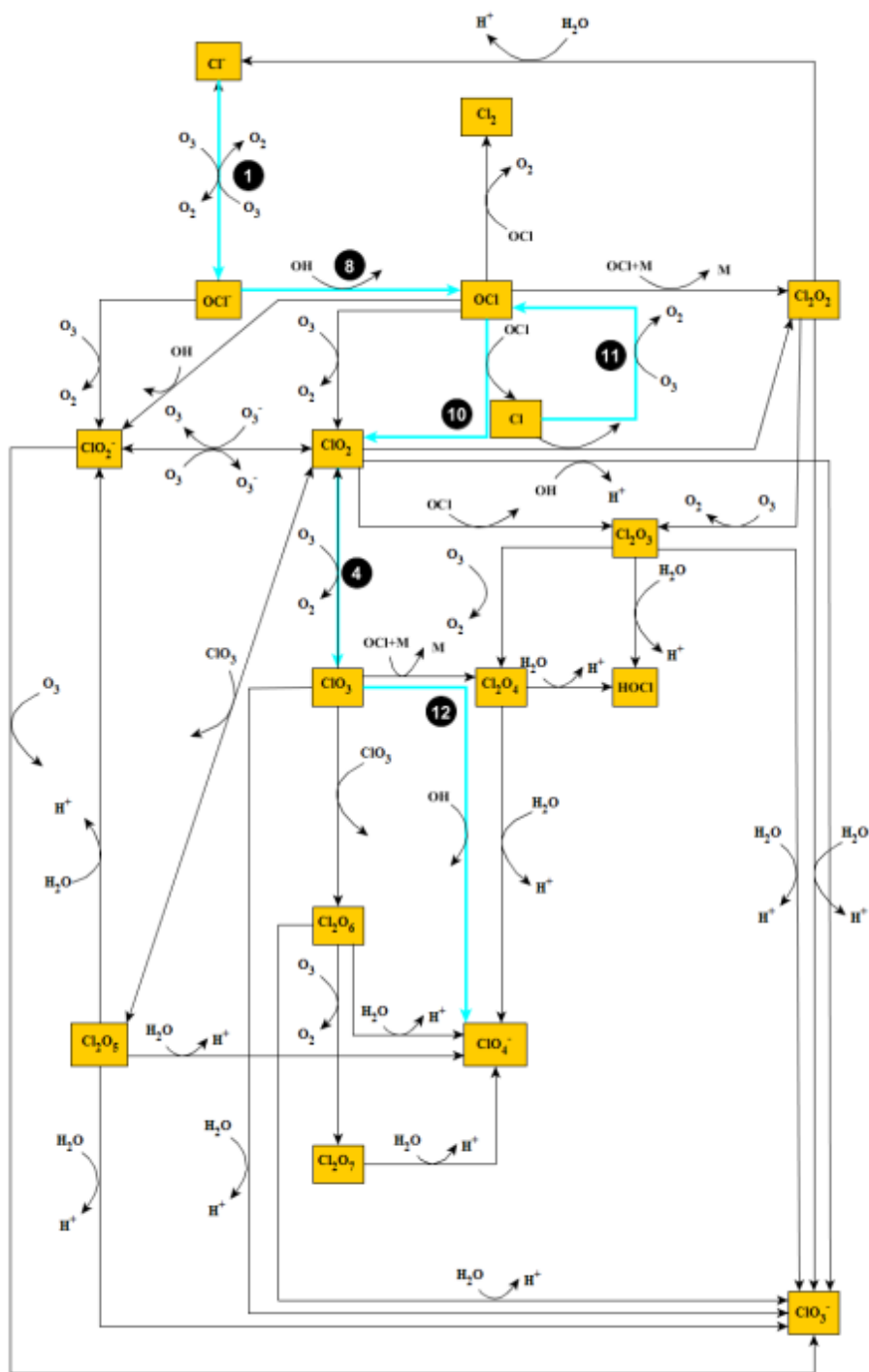


Figure A.3 Mechanism 3. O_3 oxidation of Cl^- (aq). Note the thick aqua blue lines indicate the pathway leading to the formation of the ClO_4^- and black solid circles represent reaction number from Table 3.4. This pathway leads to the formation of one ClO_4^- molecule containing all four O's from O_3 .

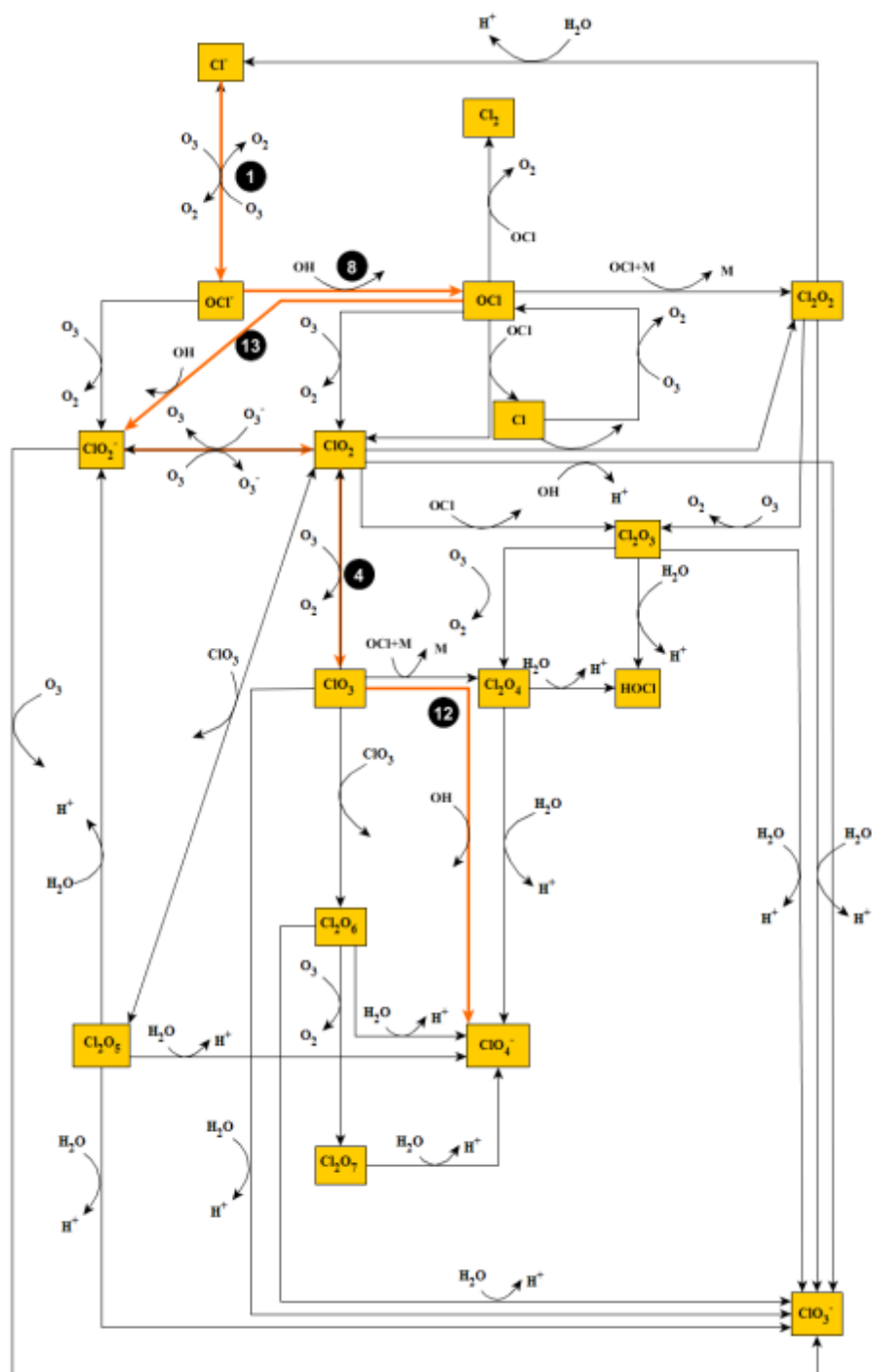


Figure A.4 Mechanism 4. O_3 oxidation of Cl^- (aq). Note the thick orange lines indicate the pathway leading to the formation of the ClO_4^- and black solid circles represent reaction number from Table 3.4. This pathway leads to the formation of one ClO_4^- molecule containing all four O's from O_3 .

A.1.2 ClO_4^- Formed from Hydrolysis of the Cl_2O_7 Species

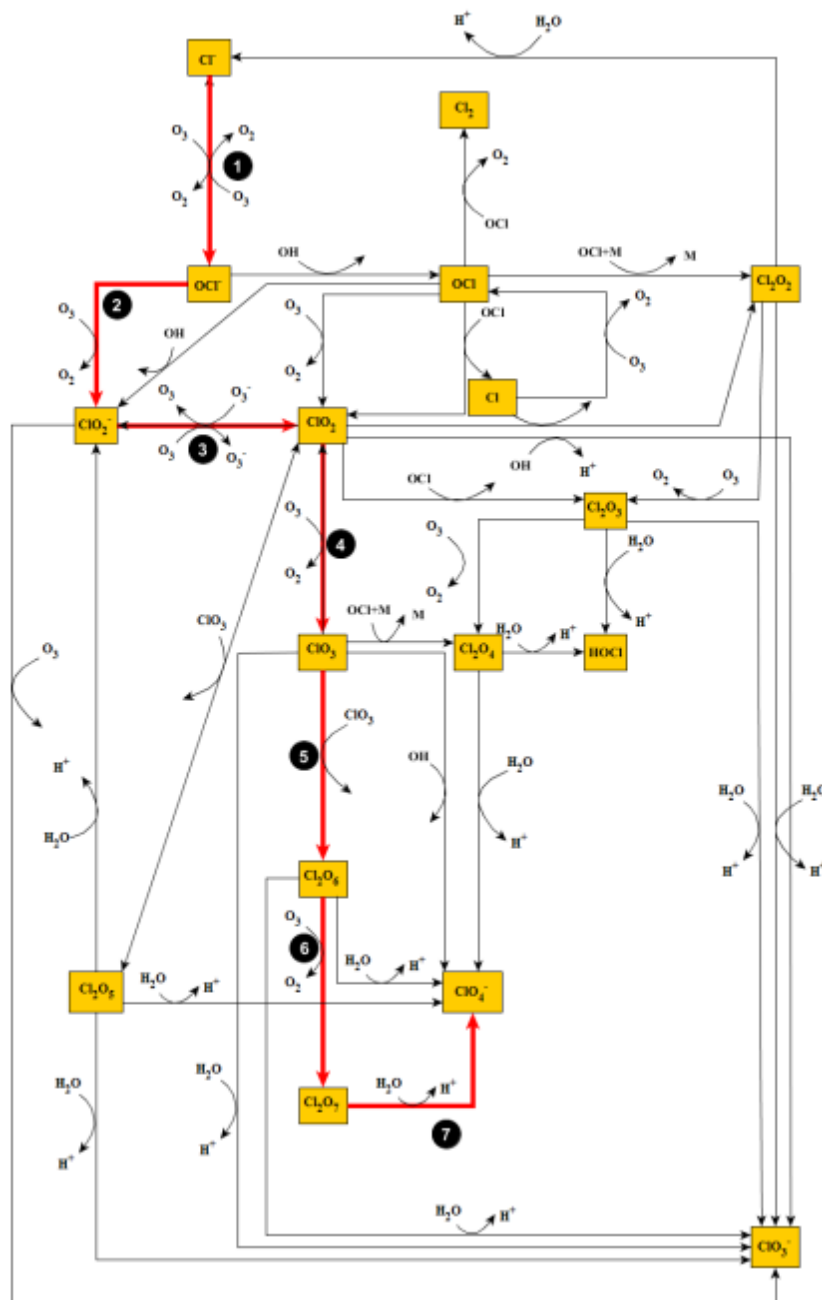


Figure A.5 Mechanism 5: O_3 oxidation of Cl^- (aq). Note the thick red lines indicate the pathway leading to the formation of the ClO_4^- and black solid circles represent reaction number from Table 3.4. This pathway leads to the formation of two ClO_4^- molecules, one with three O from O_3 and the other with four O from O_3 .

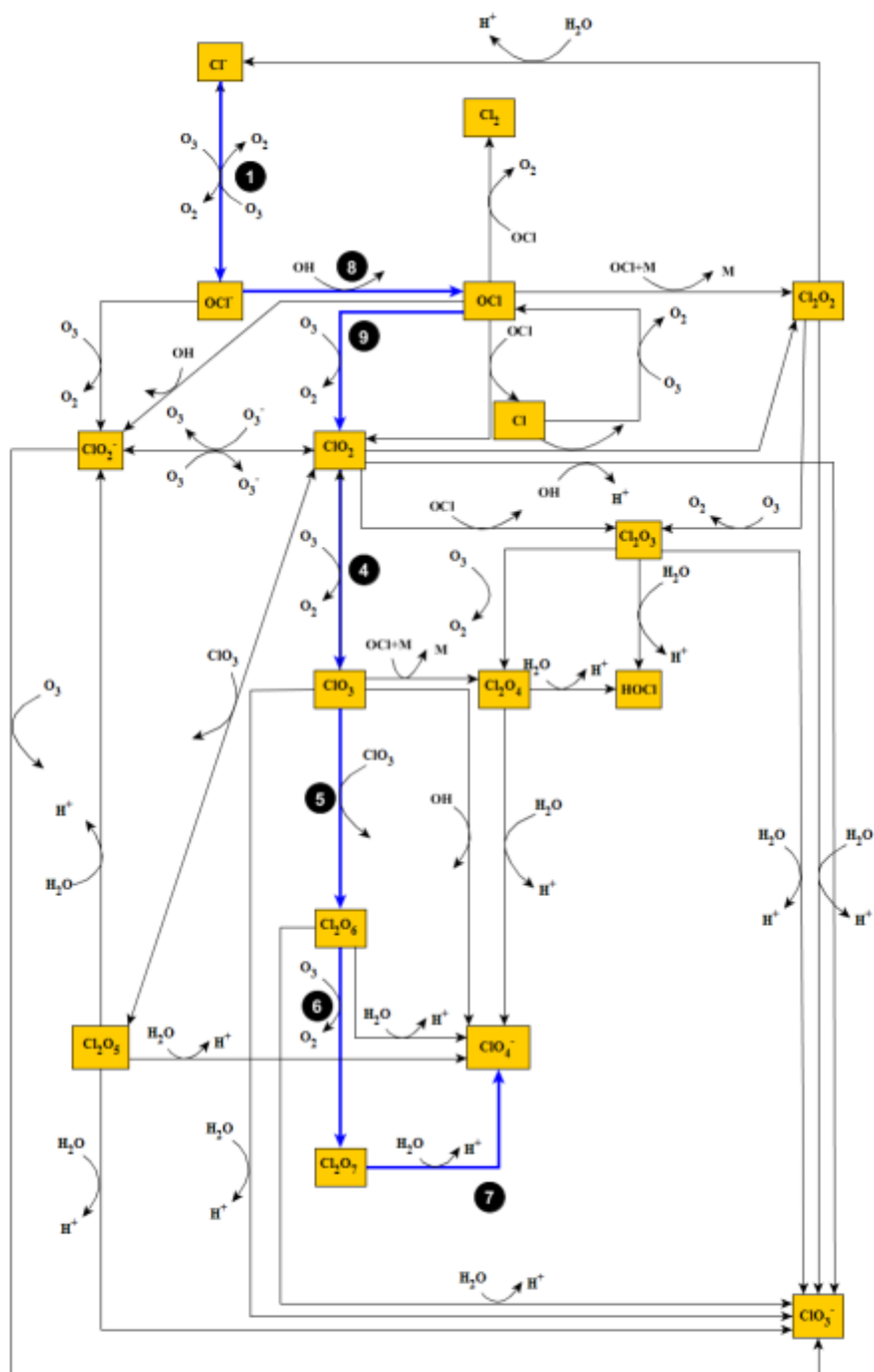


Figure A.6 Mechanism 6: O_3 oxidation of Cl^- (aq). Note the thick blue lines indicate the pathway leading to the formation of the ClO_4^- and black solid circles represent reaction number from Table 3.4. This pathway leads to the formation of two ClO_4^- molecules one containing three O's from O_3 and the other four O's from O_3 .

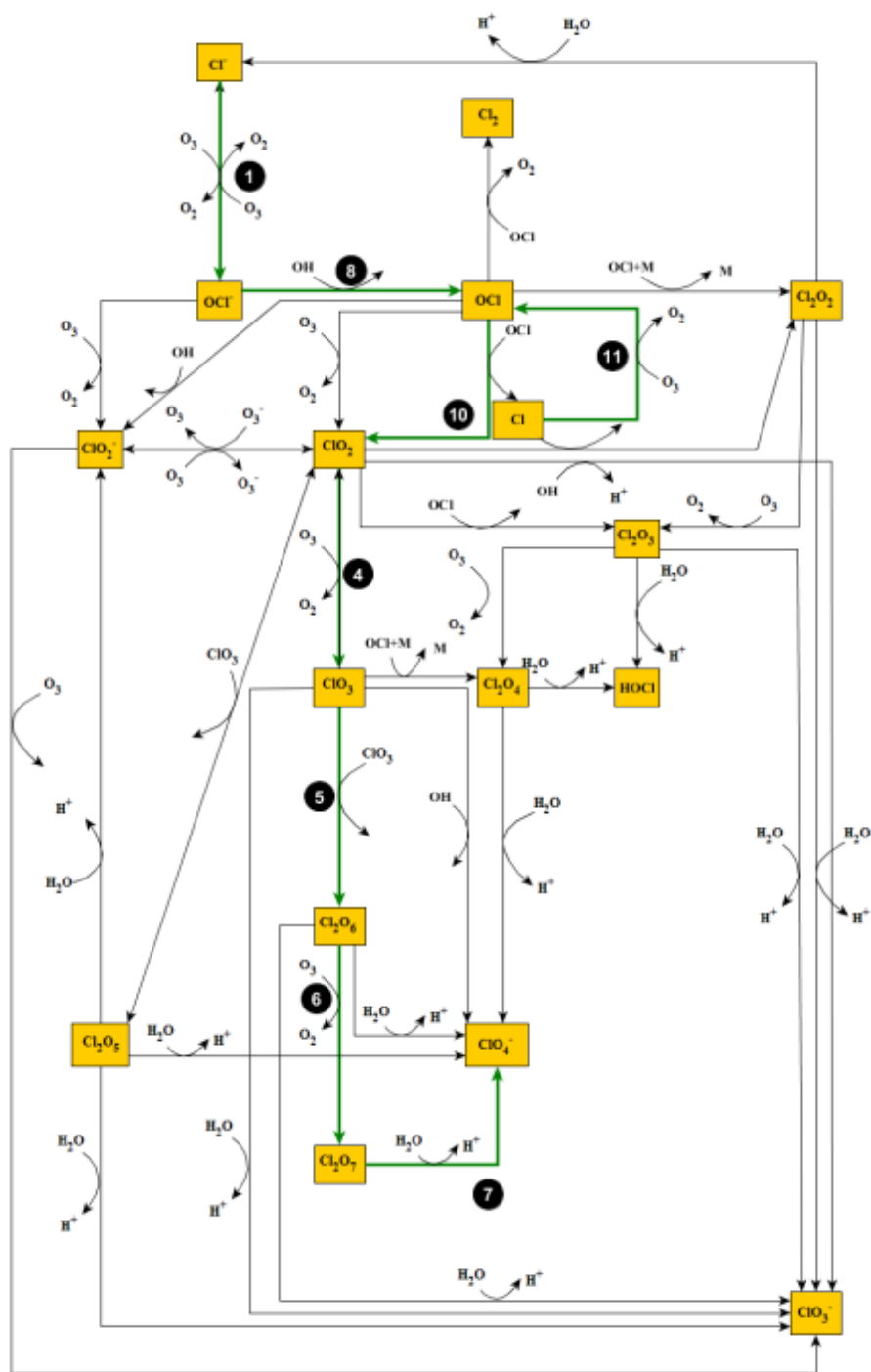


Figure A.7 Mechanism 7. O_3 oxidation of Cl^- (aq). Note the thick apple green lines indicate the pathway leading to the formation of the ClO_4^- and black solid circles represent reaction number from Table 3.4. This pathway leads to the formation of two ClO_4^- molecules, one with three O from O_3 and the other with four O from O_3 .

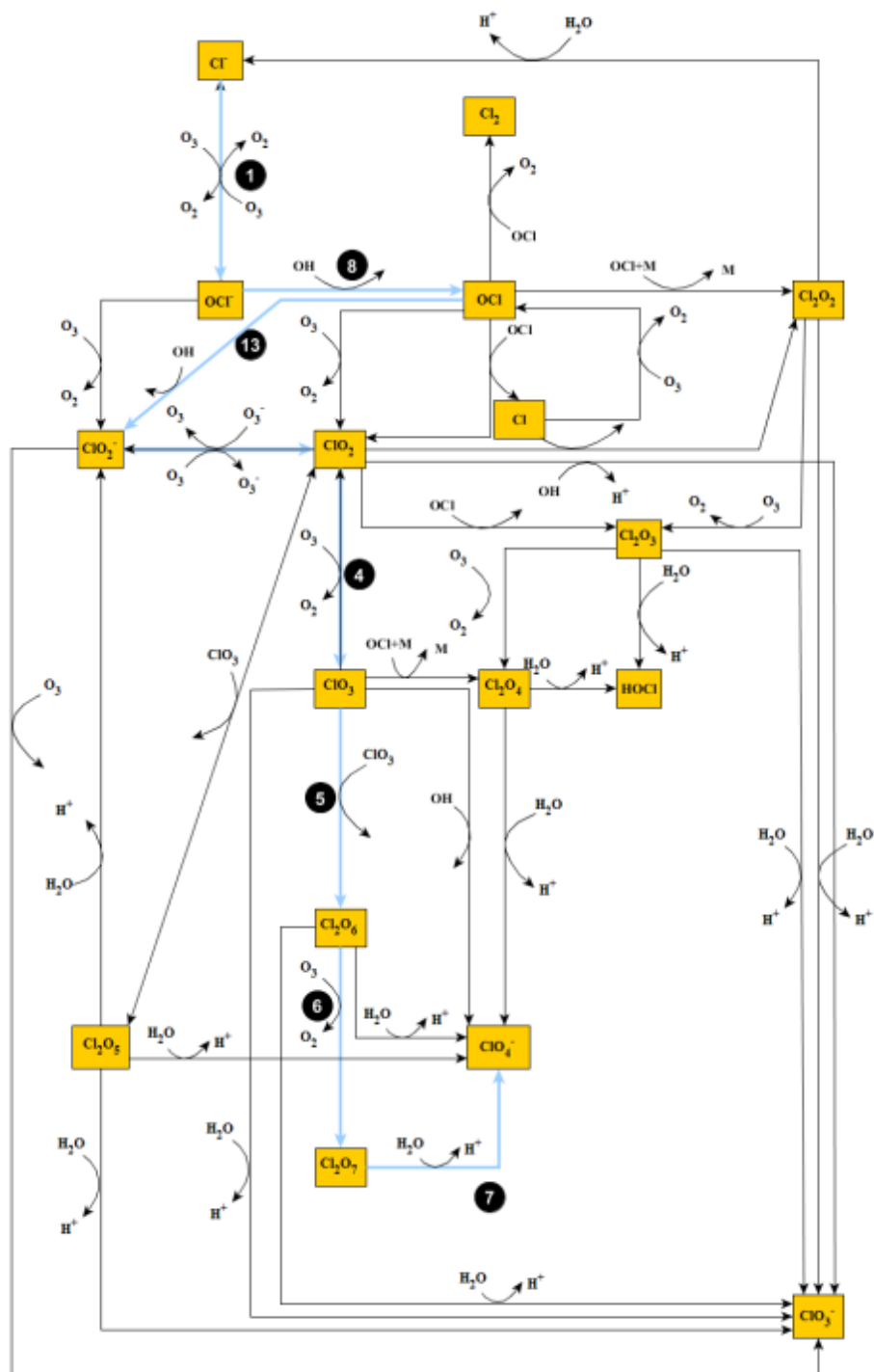


Figure A.8 Mechanism 8. O_3 oxidation of Cl^- (aq). Note the thick light blue lines indicate the pathway leading to the formation of the ClO_4^- and black solid circles represent reaction number from Table 3.4. This pathway leads to the formation of two ClO_4^- molecules, one with three O from O_3 and the other with four O from O_3 .

A.1.3 Pathways that Produce ClO_4^- with Only 3 O atoms from O_3

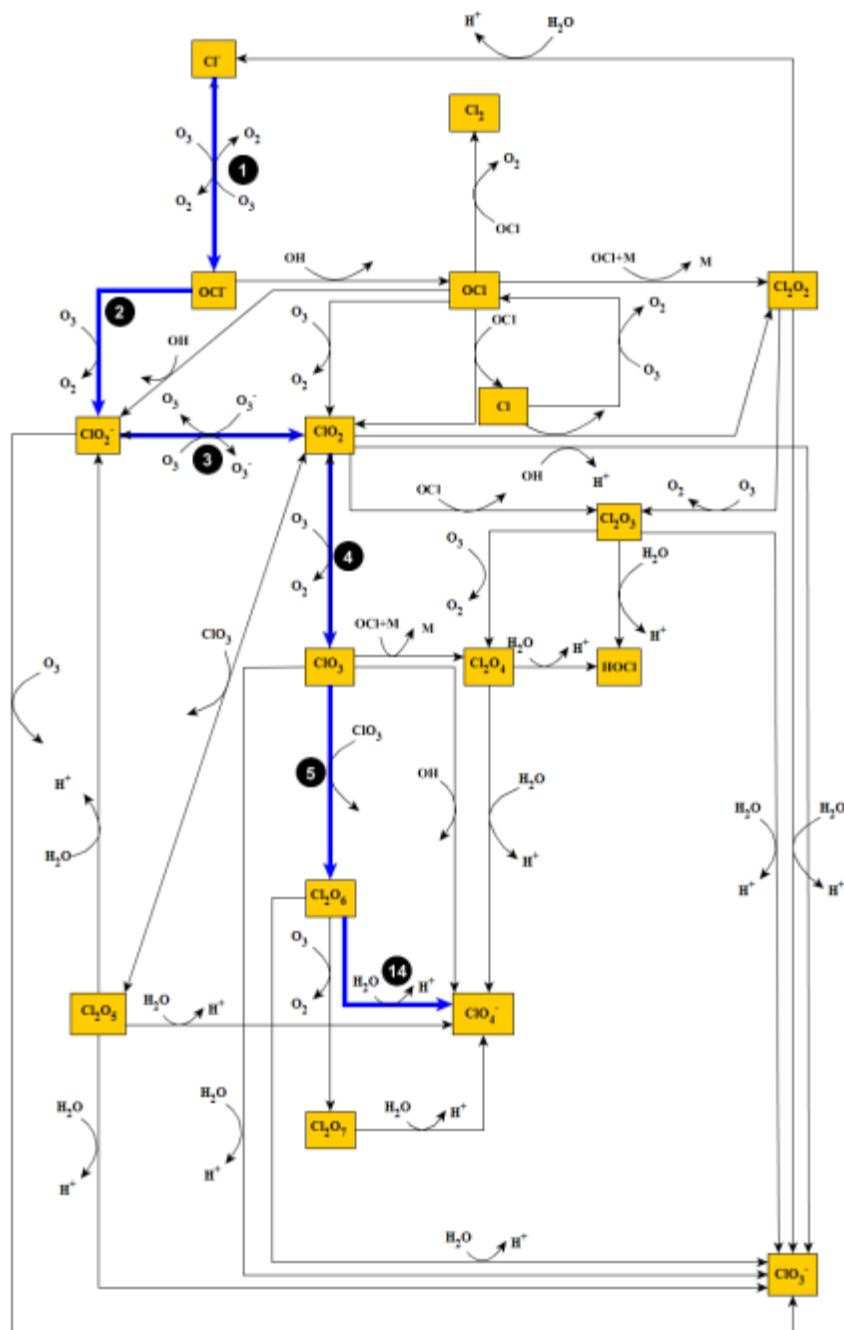


Figure A.9 Mechanism 9: O_3 oxidation of Cl^- (aq). Note the thick blue lines indicate the pathway leading to the formation of the ClO_4^- and black solid circles represent reaction number from Table 3.4. This pathway leads to the formation of one ClO_4^- molecule containing three O's from O_3 and a ClO_3^- molecule containing all three O's from O_3 .

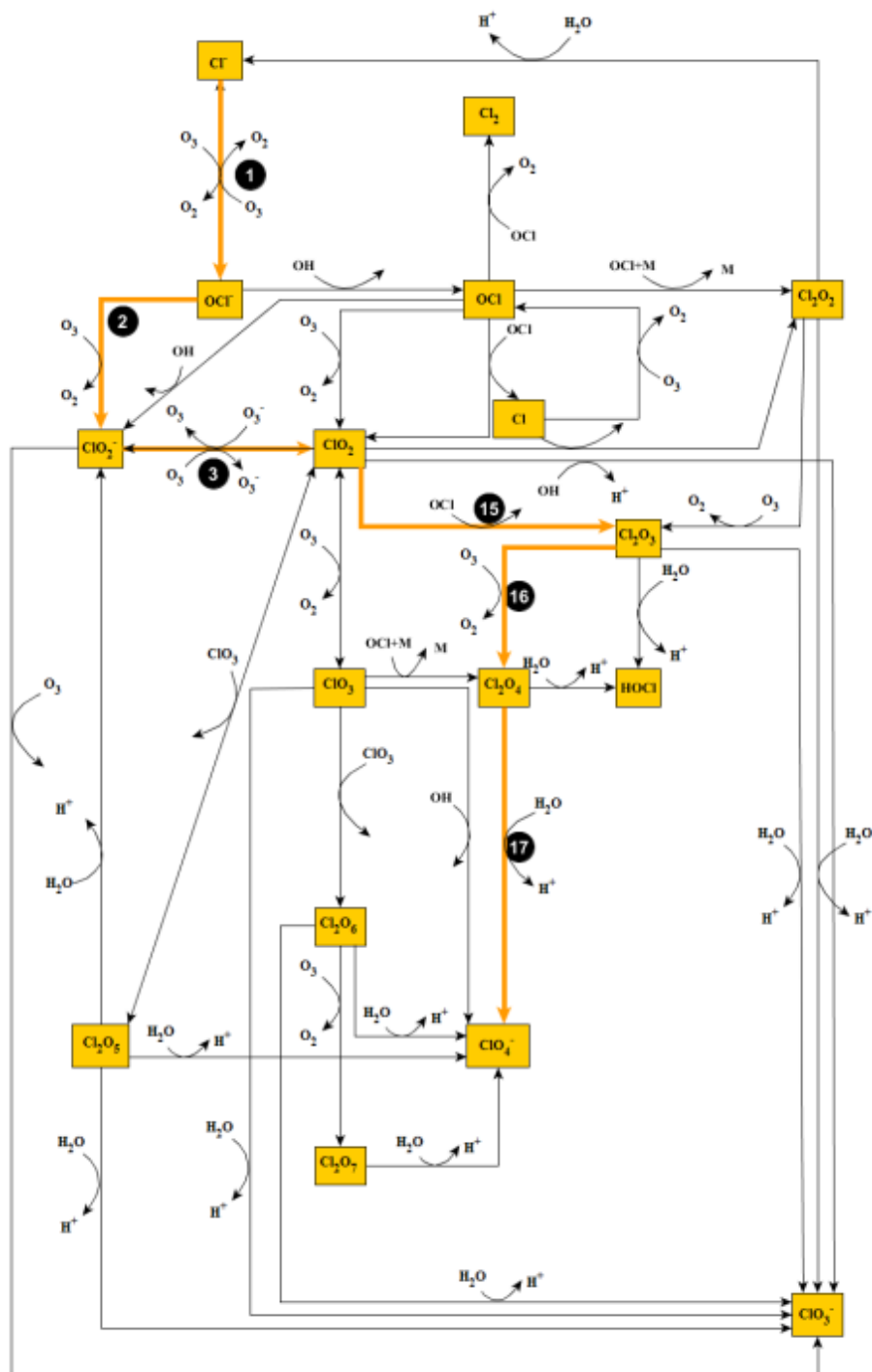


Figure A.11 Mechanism 11: O_3 oxidation of Cl^- (aq). Note the thick orange lines indicate the pathway leading to the formation of the ClO_4^- and black solid circles represent reaction number from Table 3.4. This pathway leads to the formation of one ClO_4^- molecule containing three O's from O_3 .

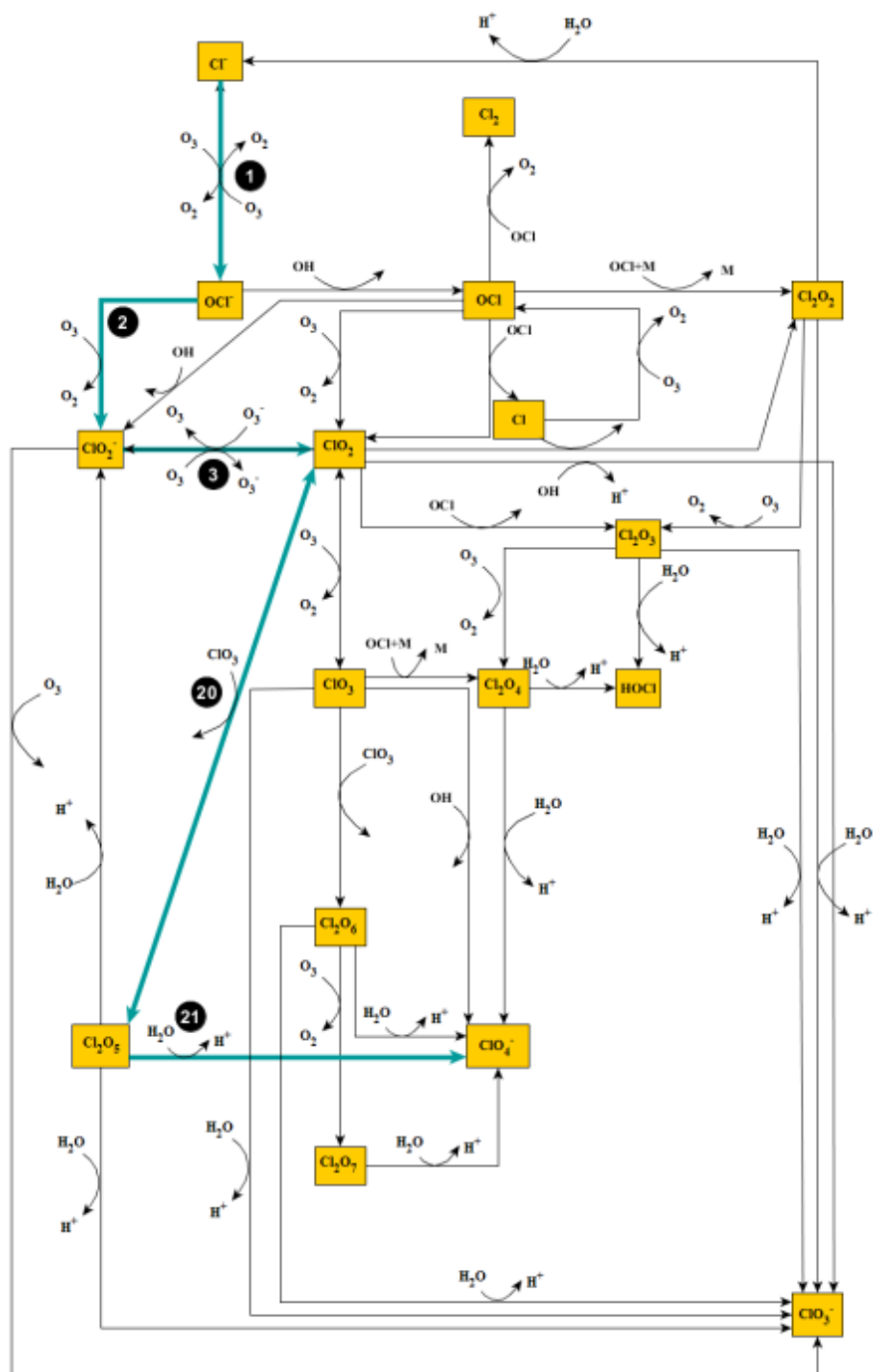


Figure A.12 Mechanism 12: O_3 oxidation of Cl^- (aq). Note the thick aquamarine lines indicate the pathway leading to the formation of the ClO_4^- and black solid circles represent reaction number from Table 3.4. This pathway leads to the formation of one ClO_4^- molecule containing three O's from O_3 .

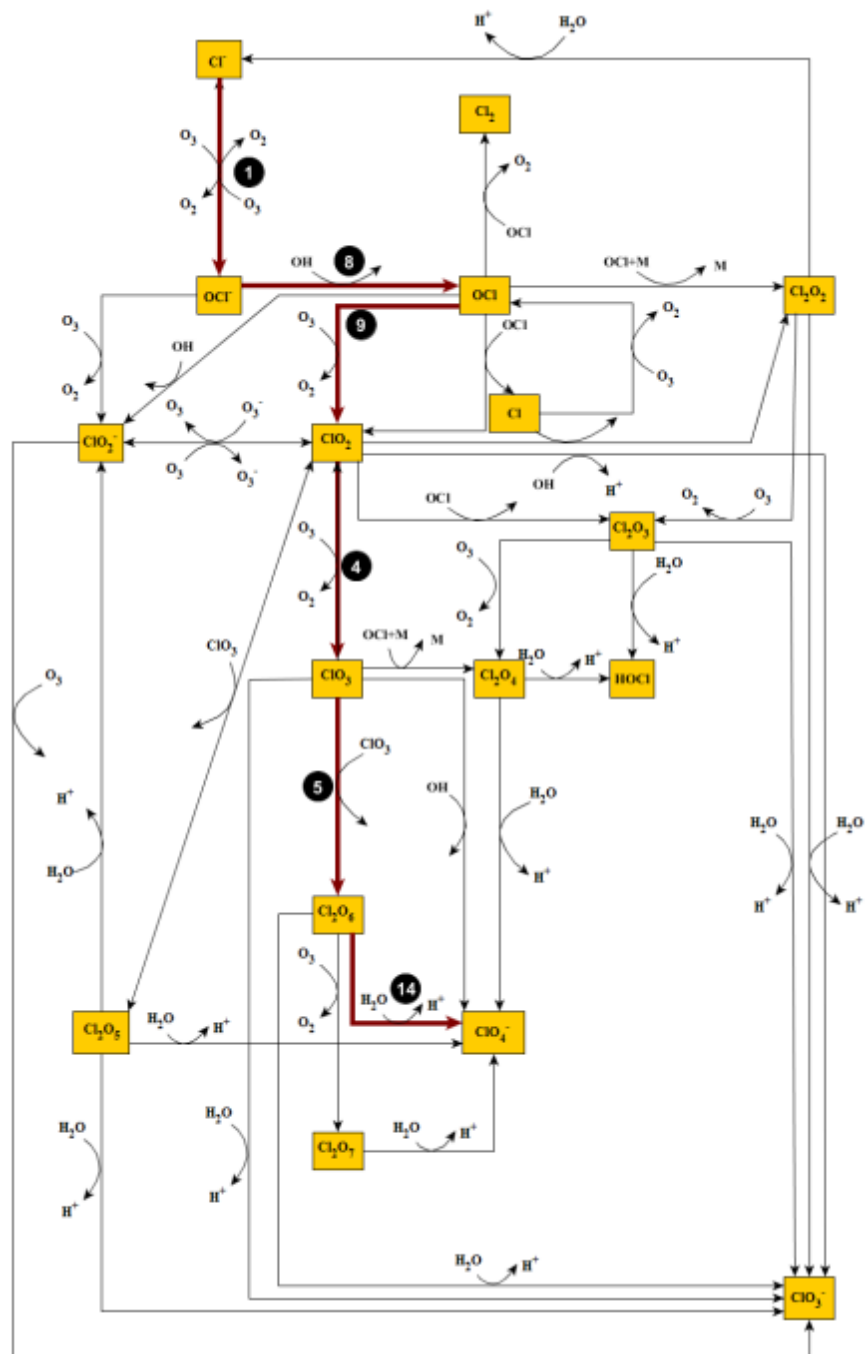


Figure A.13 Mechanism 13: O_3 oxidation of Cl^- (aq). Note the thick maroon lines indicate the pathway leading to the formation of the ClO_4^- and black solid circles represent reaction number from Table 3.4. This pathway leads to the formation of one ClO_4^- molecule containing three O's from O_3 and a ClO_3^- molecule containing all three O's from O_3 .

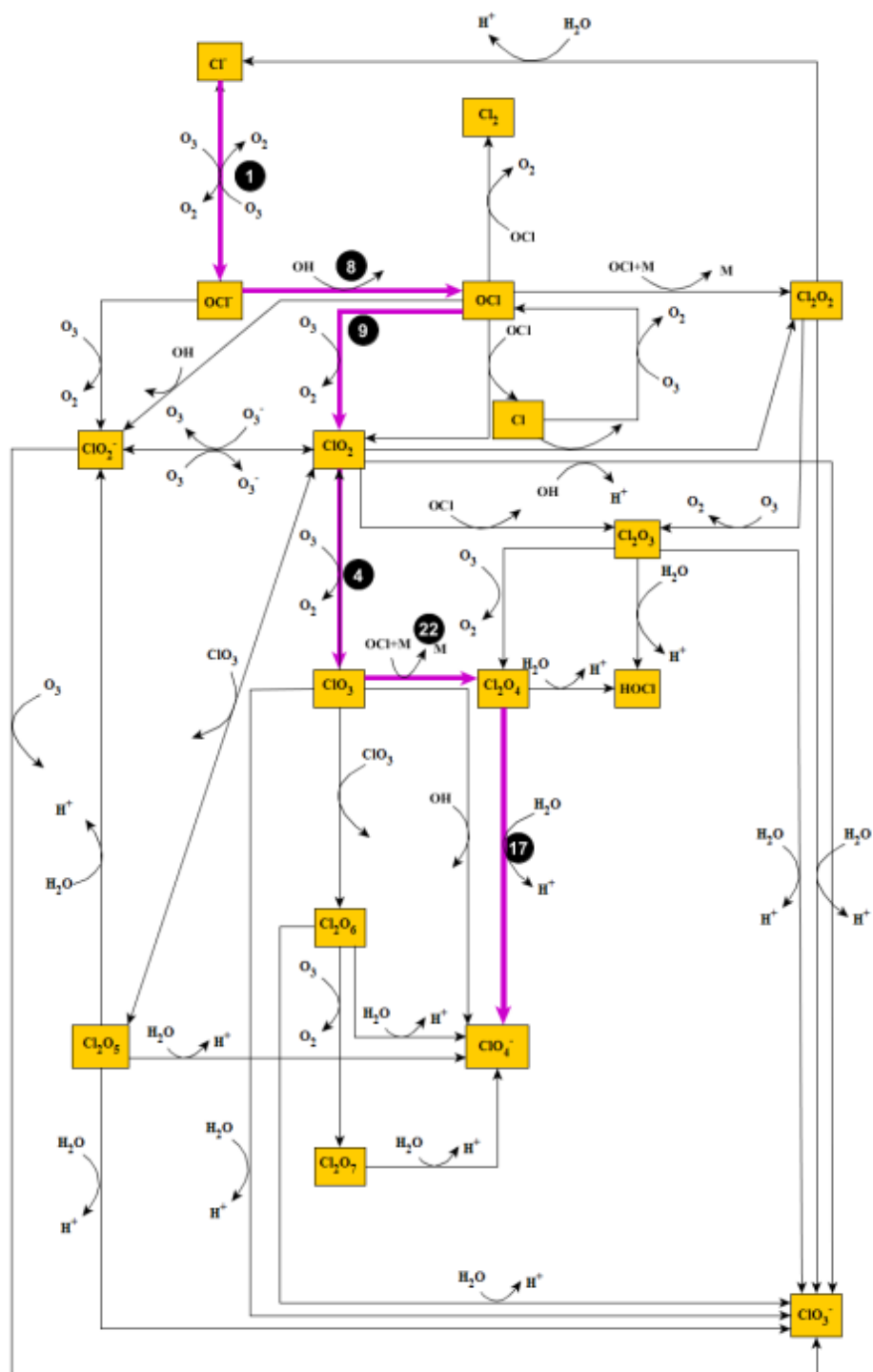


Figure A.14 Mechanism 14: O_3 oxidation of Cl^- (aq). Note the thick magenta lines indicate the pathway leading to the formation of the ClO_4^- and black solid circles represent reaction number from Table 3.4. This pathway leads to the formation of one ClO_4^- molecule containing three O's from O_3 .

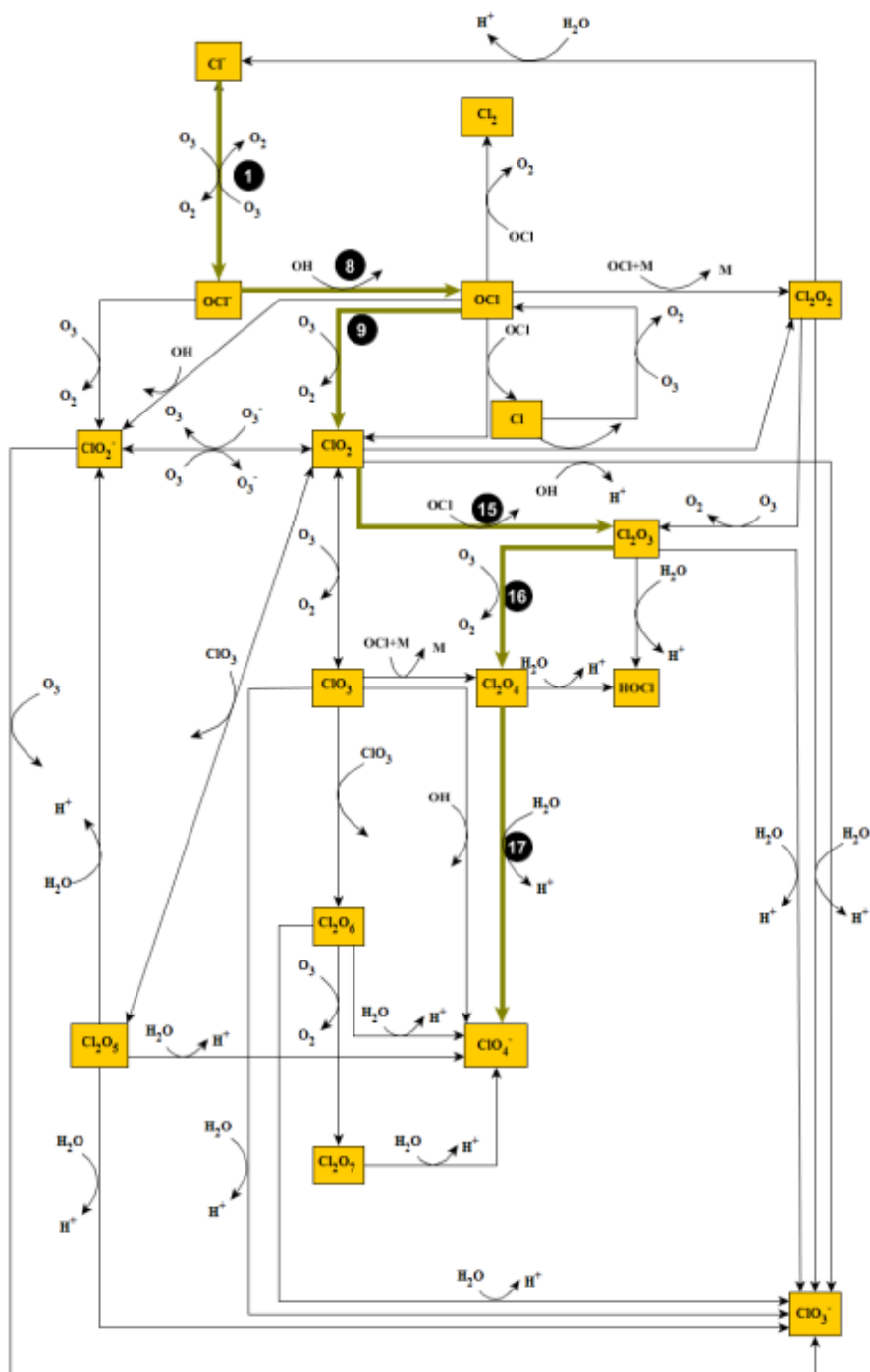


Figure A.15 Mechanism 15: O_3 oxidation of Cl^- (aq). Note the thick olive green lines indicate the pathway leading to the formation of the ClO_4^- and black solid circles represent reaction number from Table 3.4. This pathway leads to the formation of one ClO_4^- molecule containing three O's from O_3 .

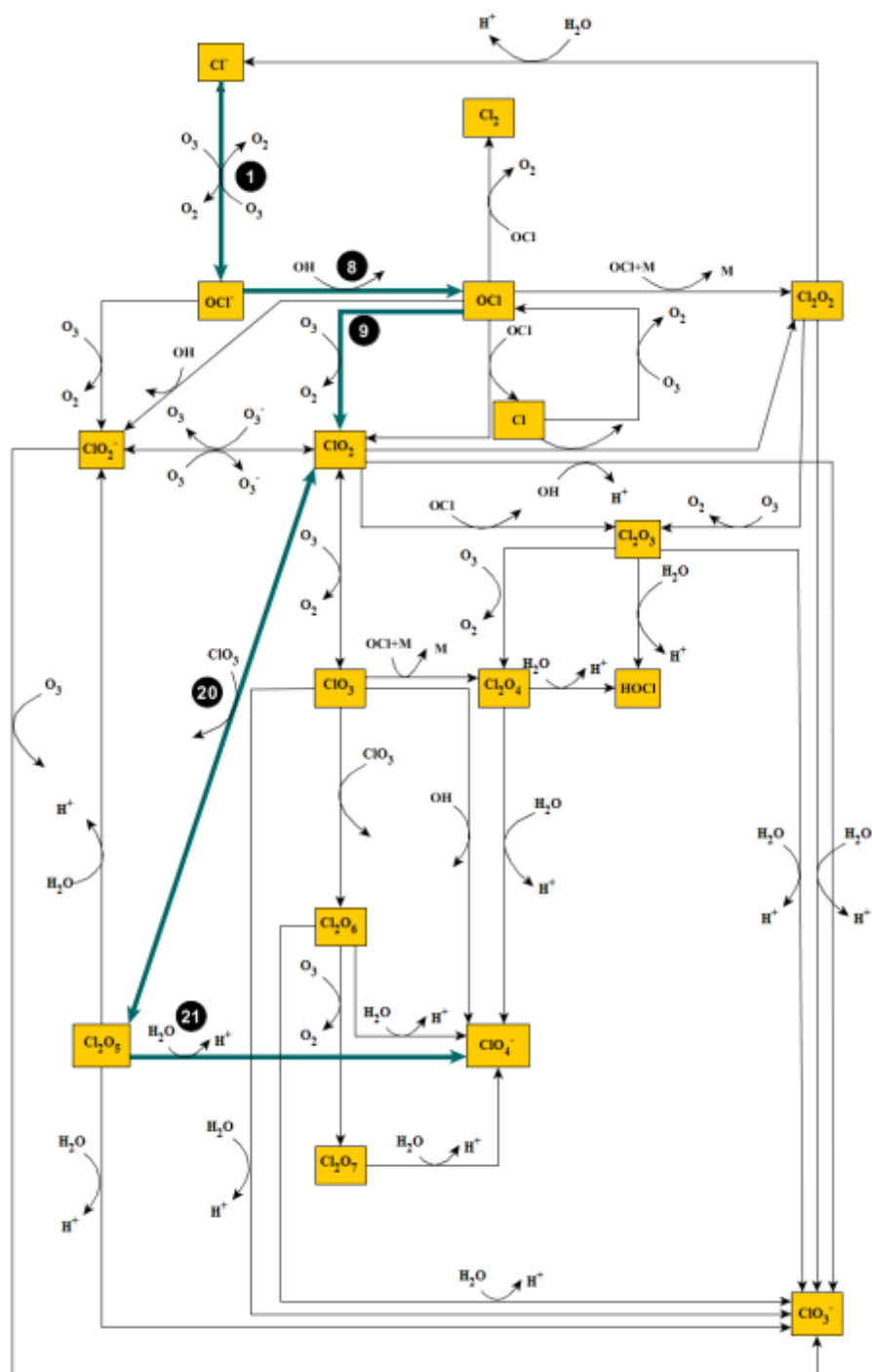


Figure A.16 Mechanism 16. O_3 oxidation of Cl^- (aq). Note the thick dark cyan lines indicate the pathway leading to the formation of the ClO_4^- and black solid circles represent reaction number from Table 3.4. This pathway leads to the formation of one ClO_4^- molecule containing three O's from O_3 .

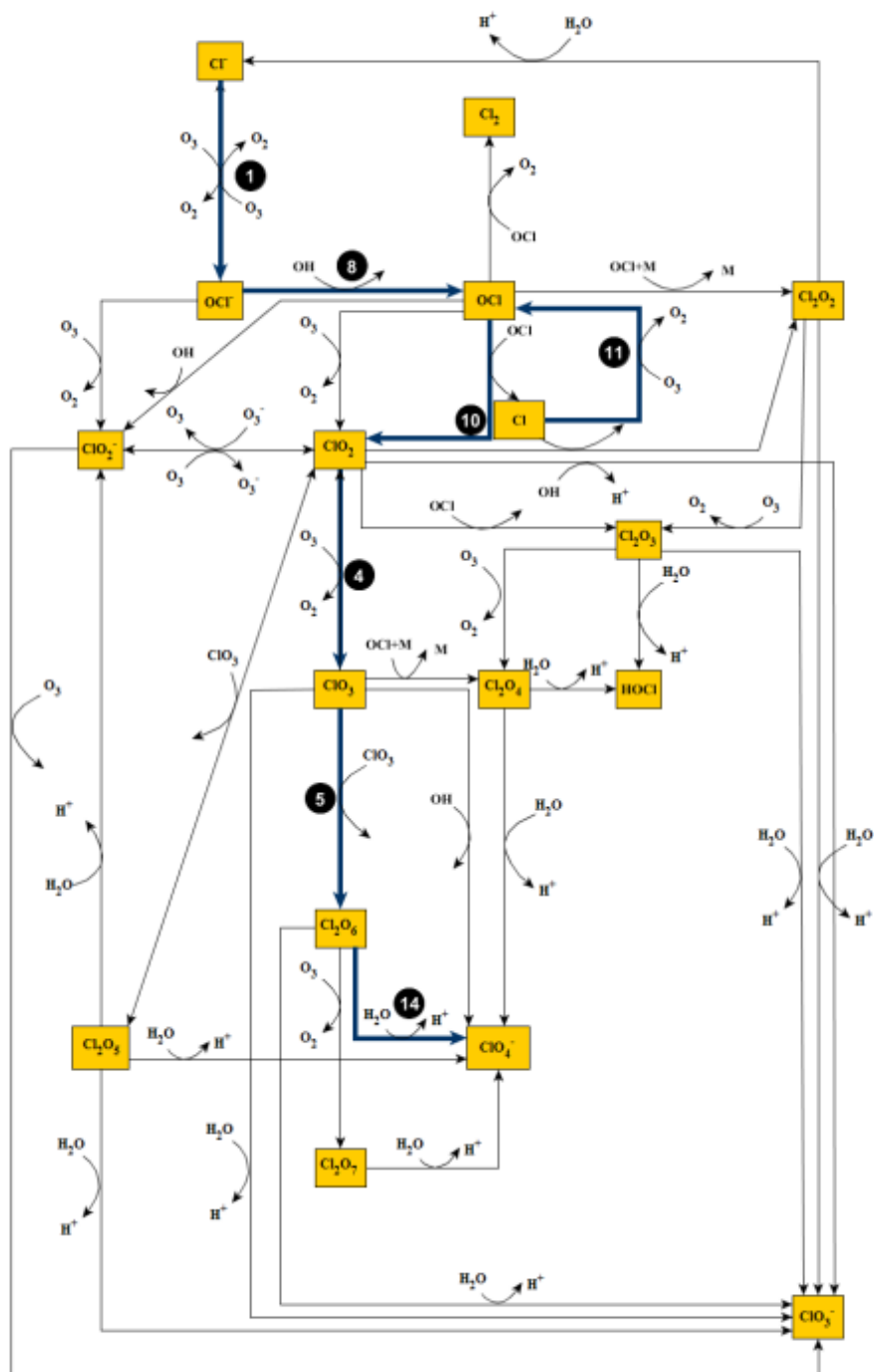


Figure A.17 Mechanism 17. O_3 oxidation of Cl^- (aq). Note the thick dark blue lines indicate the pathway leading to the formation of the ClO_4^- and black solid circles represent reaction number from Table 3.4. This pathway leads to the formation of one ClO_4^- molecule containing three O's from O_3 and a ClO_3^- molecule containing all three O's from O_3 .

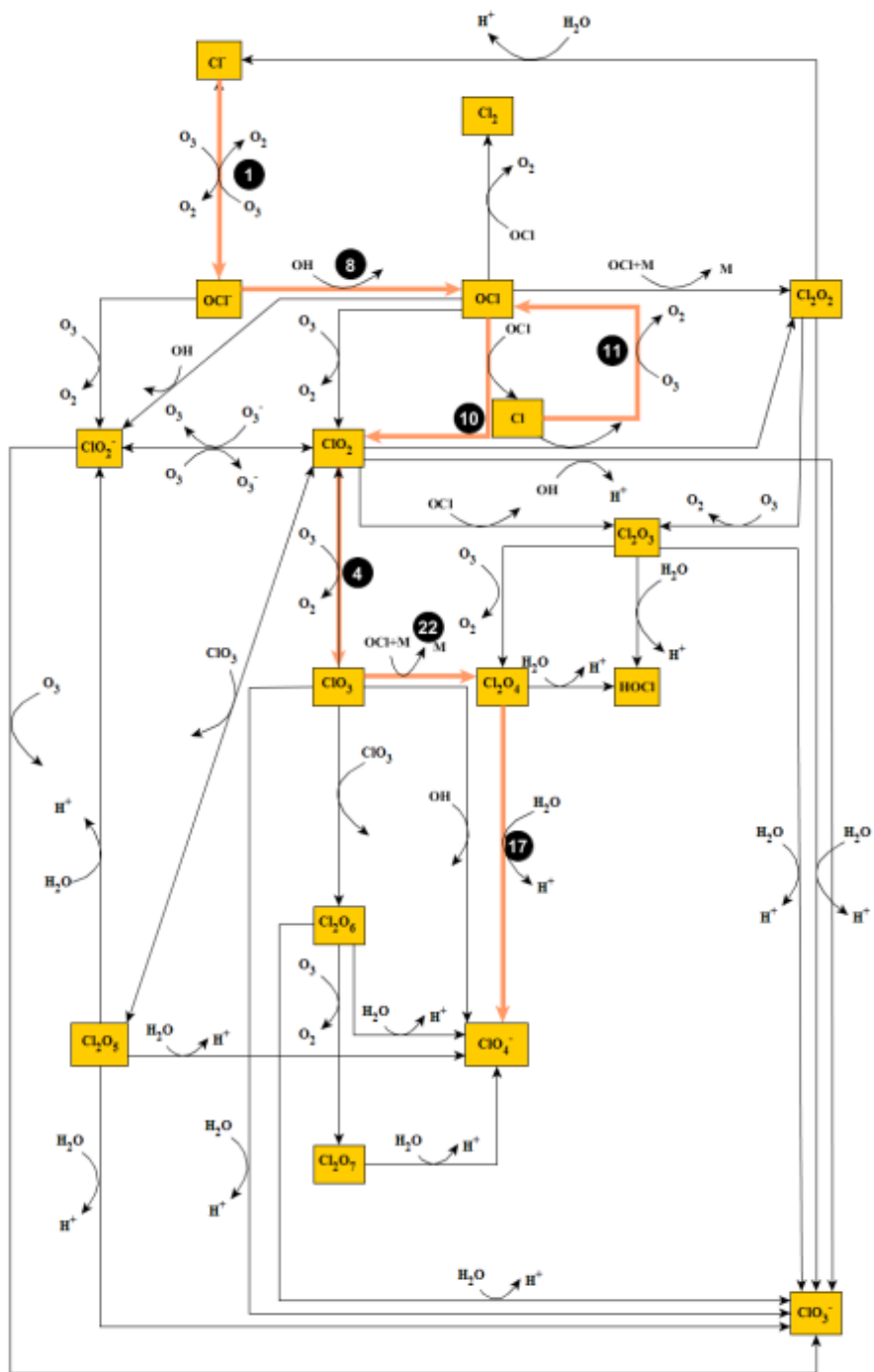


Figure A.18 Mechanism 18. O_3 oxidation of Cl^- (aq). Note the thick apricot lines indicate the pathway leading to the formation of the ClO_4^- and black solid circles represent reaction number from Table 3.4. This pathway leads to the formation of one ClO_4^- molecule containing three O's from O_3 .

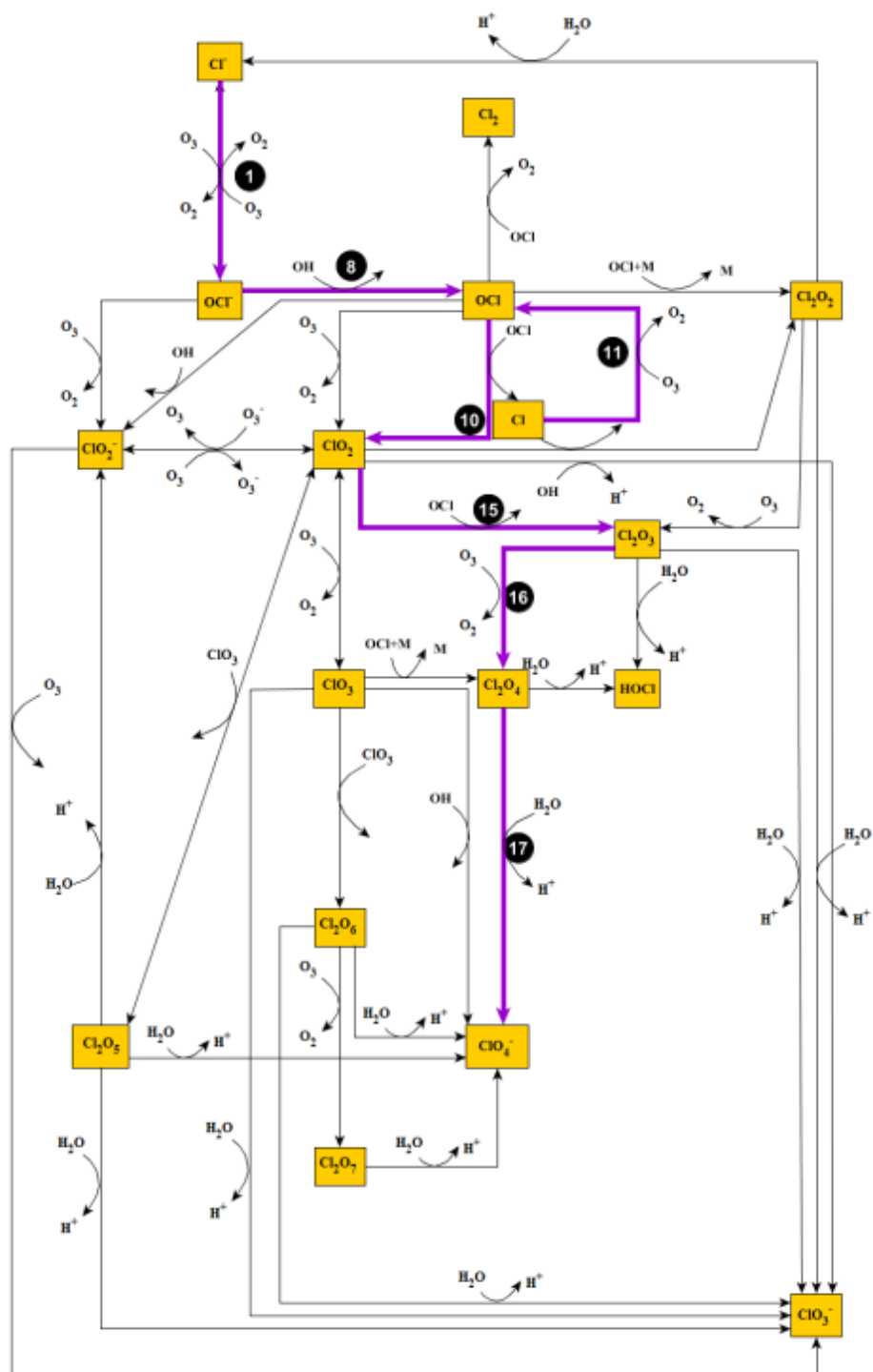


Figure A.19 Mechanism 19. O_3 oxidation of Cl^- (aq). Note the thick purple lines indicate the pathway leading to the formation of the ClO_4^- and black solid circles represent reaction number from Table 3.4. This pathway leads to the formation of one ClO_4^- molecule containing three O's from O_3 .

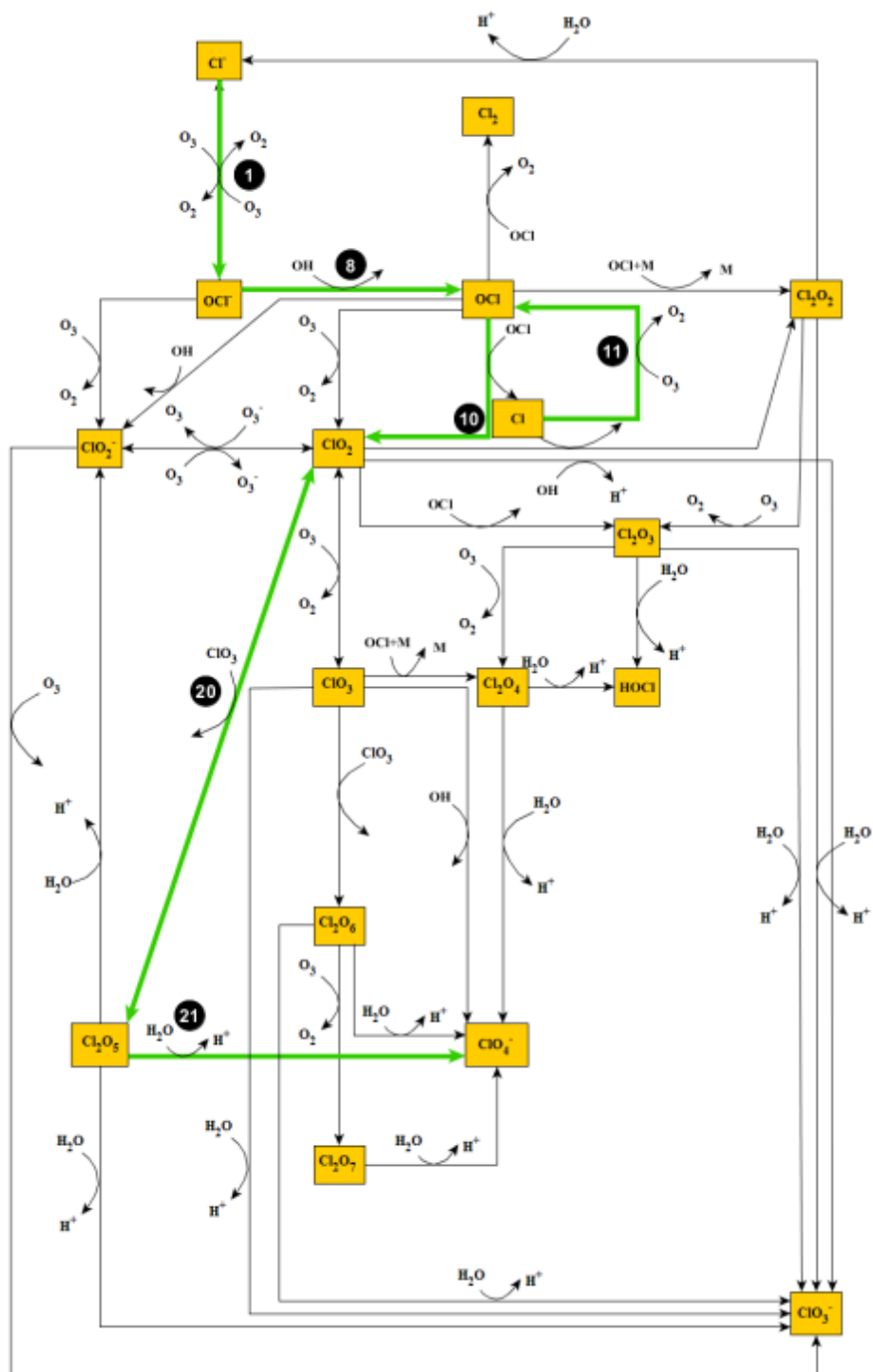


Figure A.20 Mechanism 20. O_3 oxidation of Cl^- (aq). Note the thick lime green lines indicate the pathway leading to the formation of the ClO_4^- and black solid circles represent reaction number from Table 3.4. This pathway leads to the formation of one ClO_4^- molecule containing three O's from O_3 .

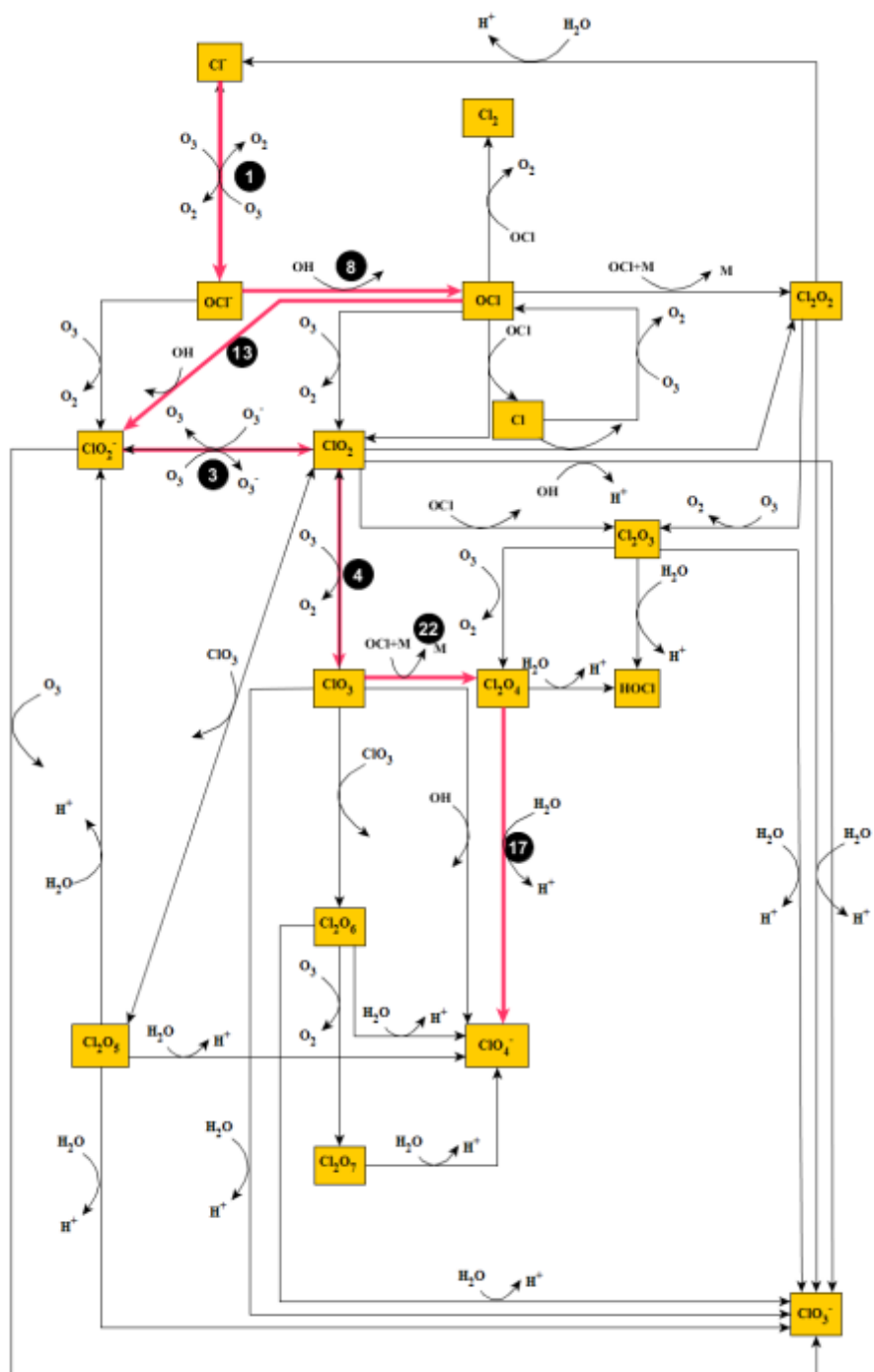


Figure A.22 Mechanism 22. O_3 oxidation of Cl^- (aq). Note the pink lines indicate the pathway leading to the formation of the ClO_4^- and black solid circles represent reaction number from Table 3.4. This pathway leads to the formation of one ClO_4^- molecule containing three O's from O_3 .

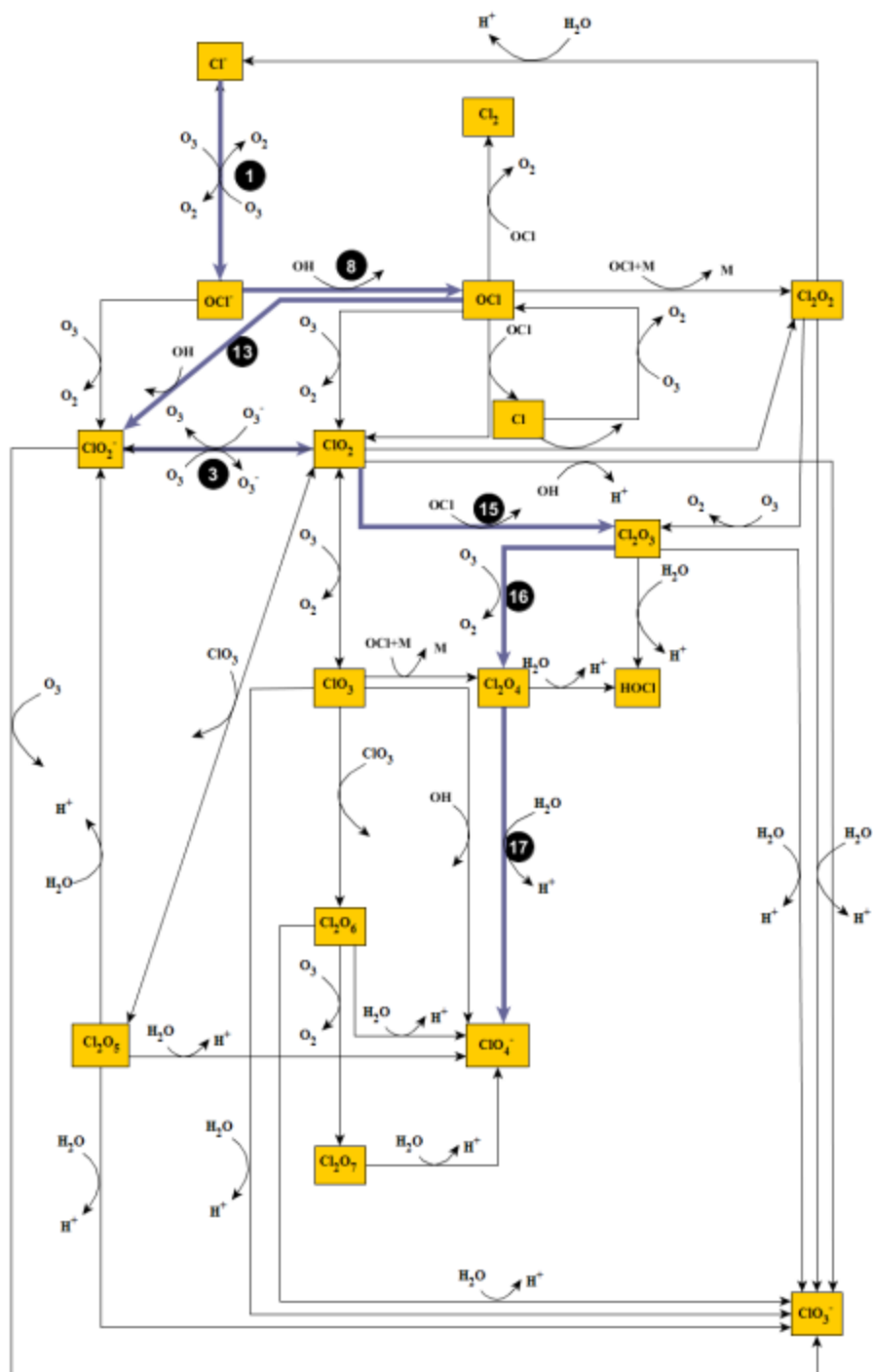


Figure A.23 Mechanism 23. O_3 oxidation of Cl^- (aq). Note the grayish purple lines indicate the pathway leading to the formation of the ClO_4^- and black solid circles represent reaction number from Table 3.4. This pathway leads to the formation of one ClO_4^- molecule containing three O's from O_3 .

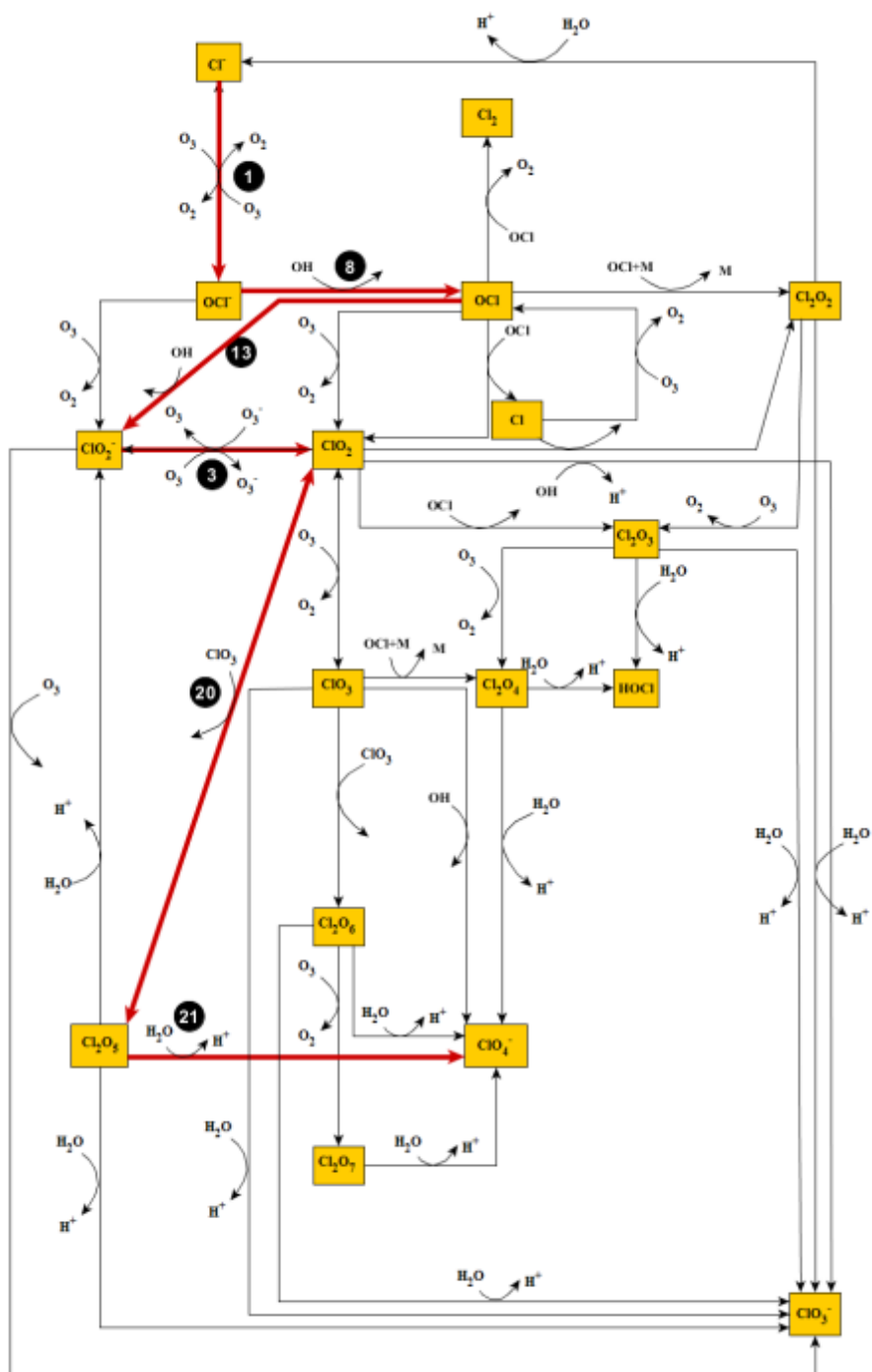


Figure A.24 Mechanism 24. O_3 oxidation of Cl^- (aq). Note the thick red lines indicate the pathway leading to the formation of the ClO_4^- and black solid circles represent reaction number from Table 3.4. This pathway leads to the formation of one ClO_4^- molecule containing three O's from O_3 .

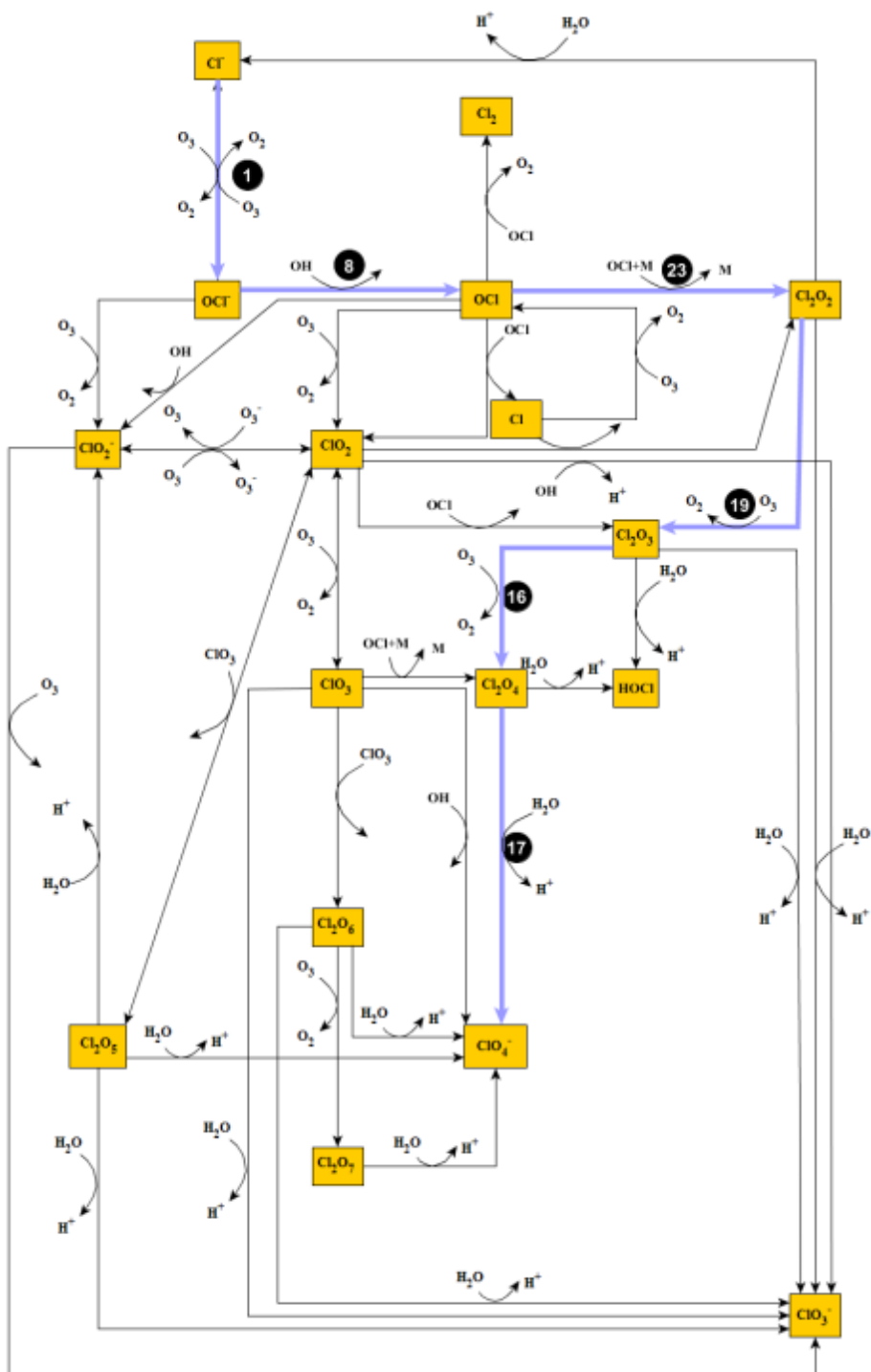


Figure A.25 Mechanism 25. O_3 oxidation of Cl^- (aq). Note the thick red lines indicate the pathway leading to the formation of the ClO_4^- and black solid circles represent reaction number from Table 3.4. This pathway leads to the formation of one ClO_4^- molecule containing three O's from O_3 .

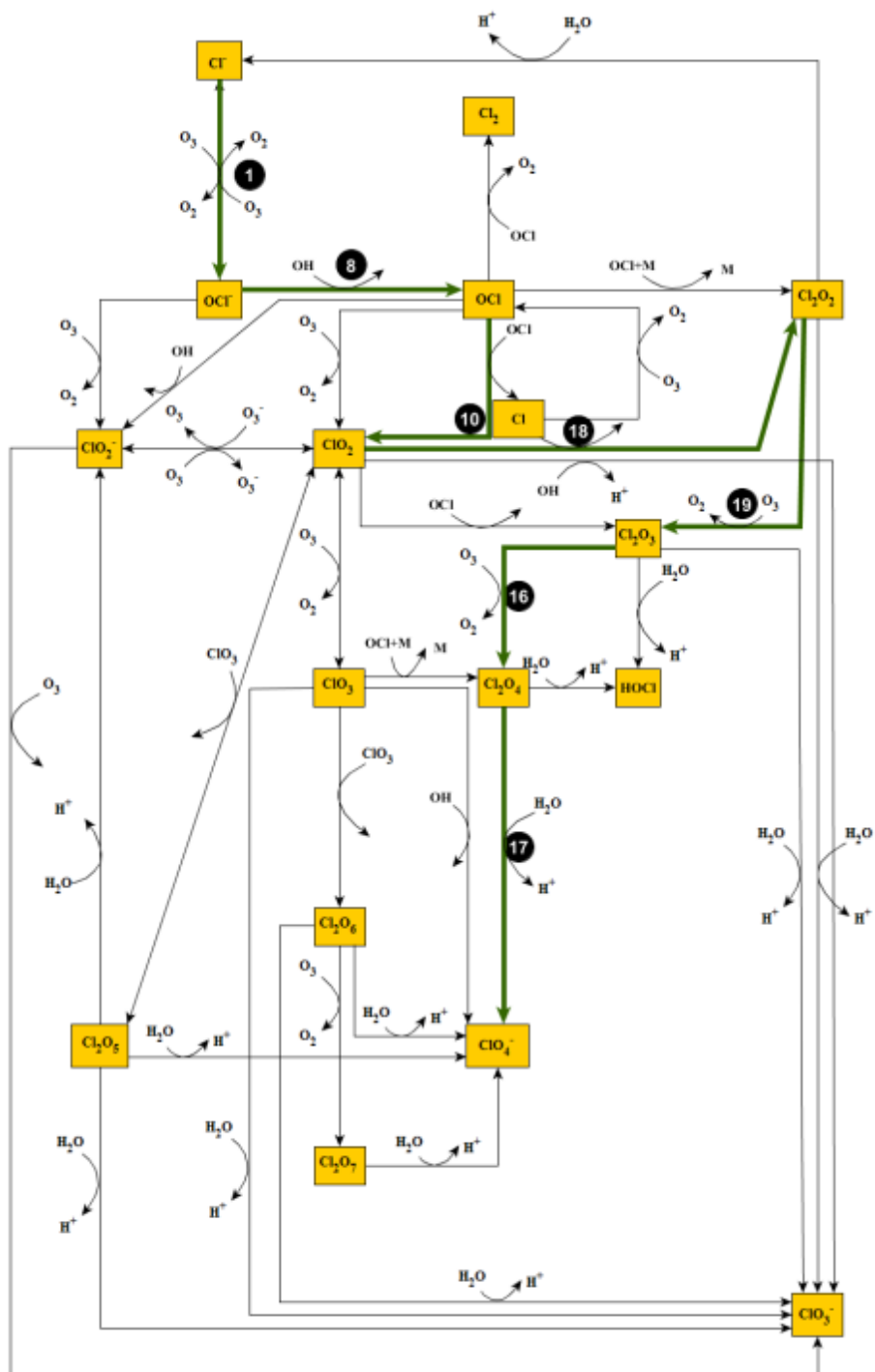


Figure A.26 Mechanism 26. O_3 oxidation of Cl^- (aq). Note the thick forest green lines indicate the pathway leading to the formation of the ClO_4^- and black solid circles represent reaction number from Table 3.4. This pathway leads to the formation of one ClO_4^- molecule containing three O's from O_3 .

A.2 Proposed Pathways for O₃ Oxidation of Hypochlorite (aq)

A.2.1 Pathways that Produce ClO₄⁻ with only three O's from O₃

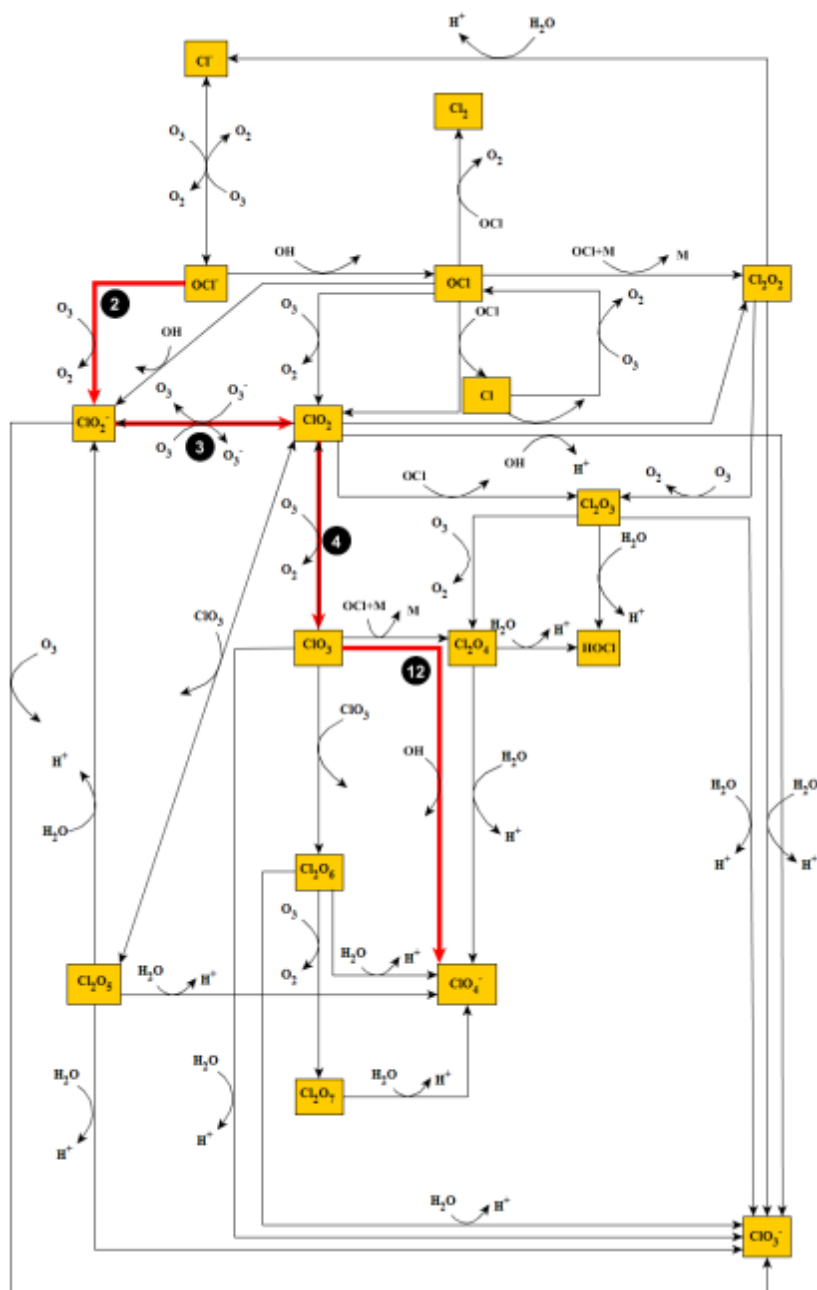


Figure A.27 Mechanism 1: O₃ oxidation of OCl⁻ (aq). Note the thick red lines indicate the pathway leading to the formation of the ClO₄⁻ and black solid circles represent reaction number from Table 3.4. This pathway leads to the formation of one ClO₄⁻ molecule with three O's from O₃.

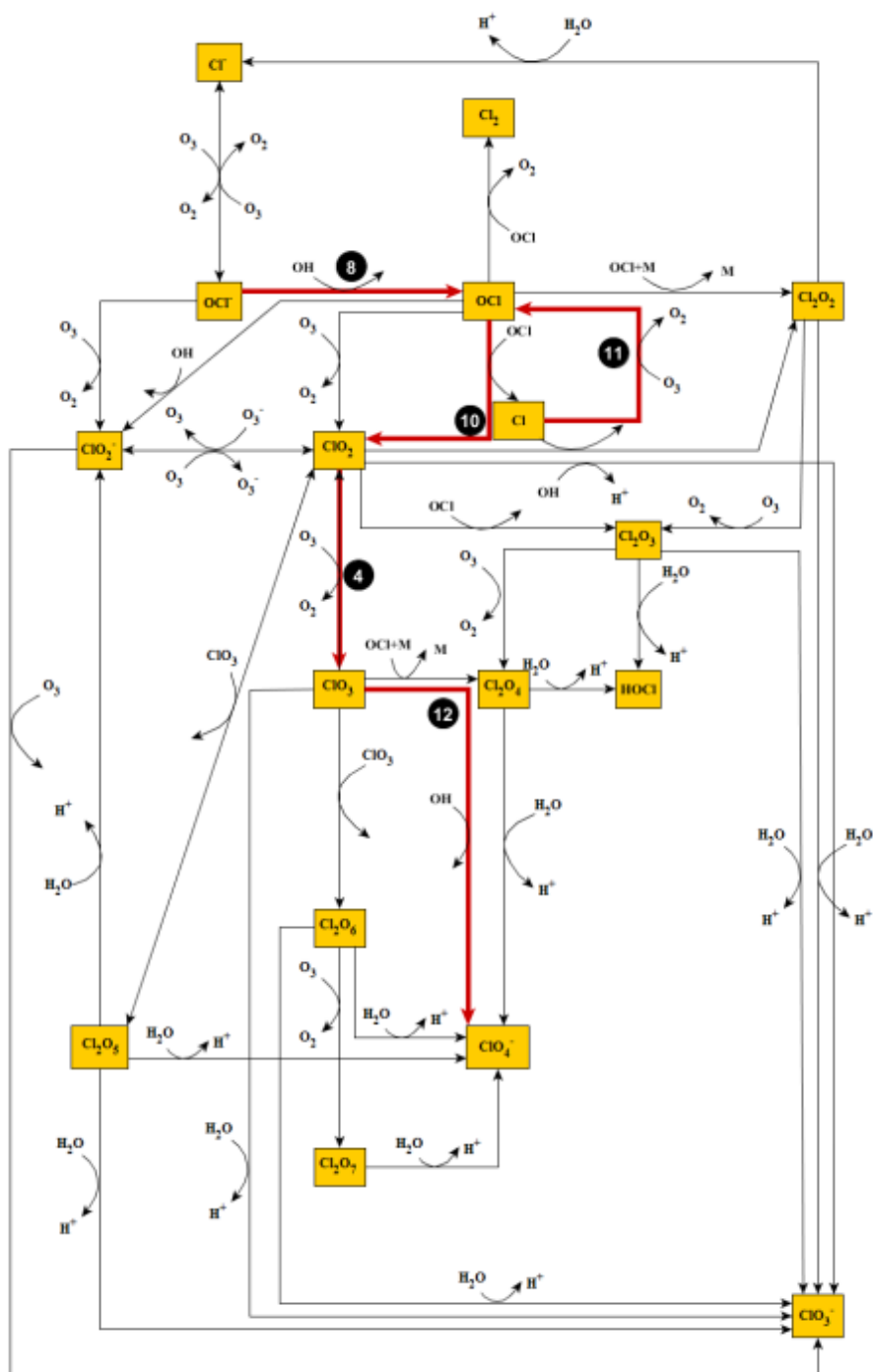


Figure A.28 Mechanism 2: O_3 oxidation of OCl^- (aq). Note the thick red lines indicate the pathway leading to the formation of the ClO_4^- and black solid circles represent reaction number from Table 3.4. This pathway leads to the formation of one ClO_4^- molecule containing three O's from O_3 .

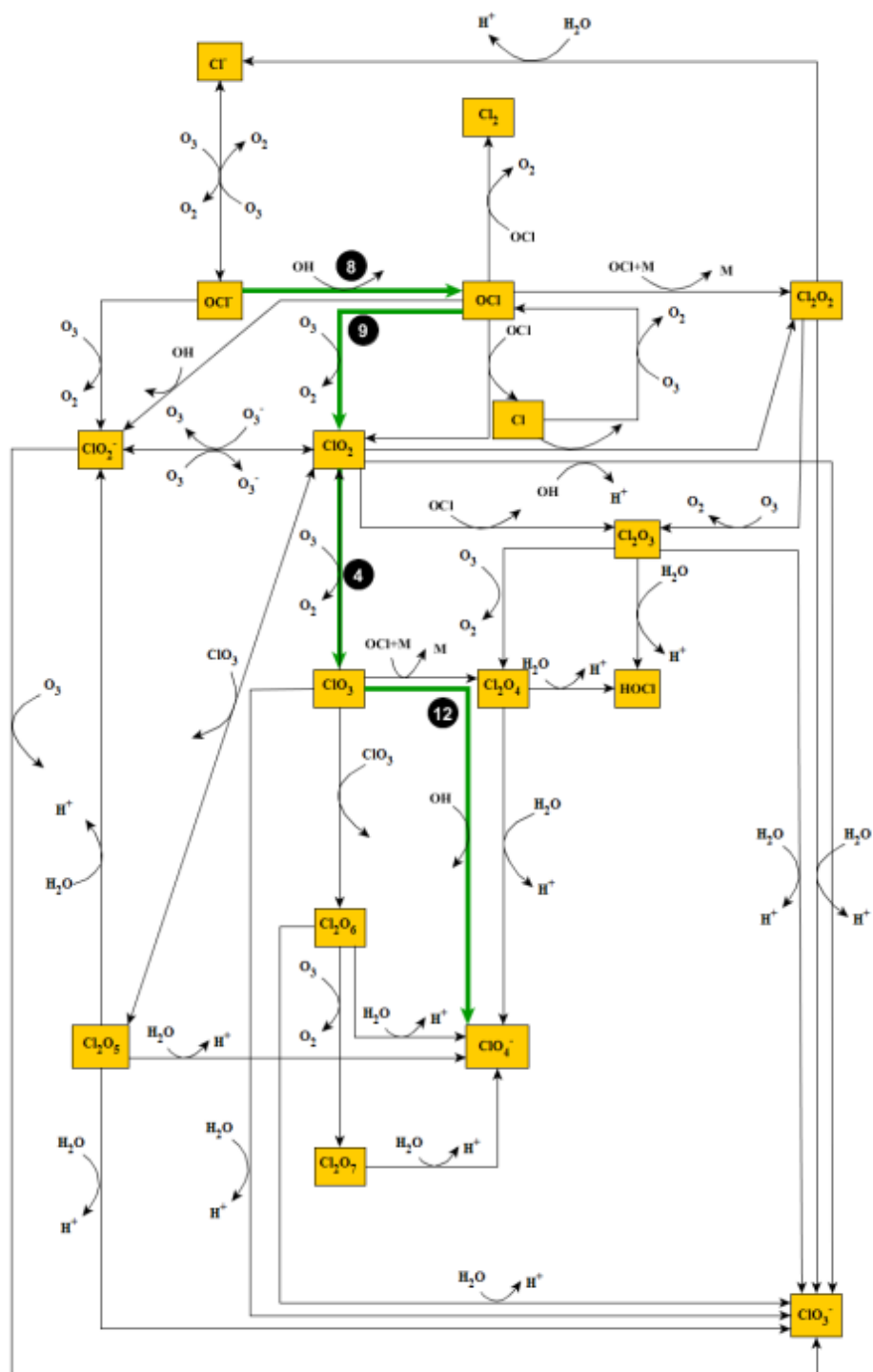


Figure A.29 Mechanism 3: O_3 oxidation of OCl^- (aq). Note the thick green lines indicate the pathway leading to the formation of the ClO_4^- and black solid circles represent reaction number from Table 3.4. This pathway leads to the formation of one ClO_4^- molecule containing three O's from O_3 .

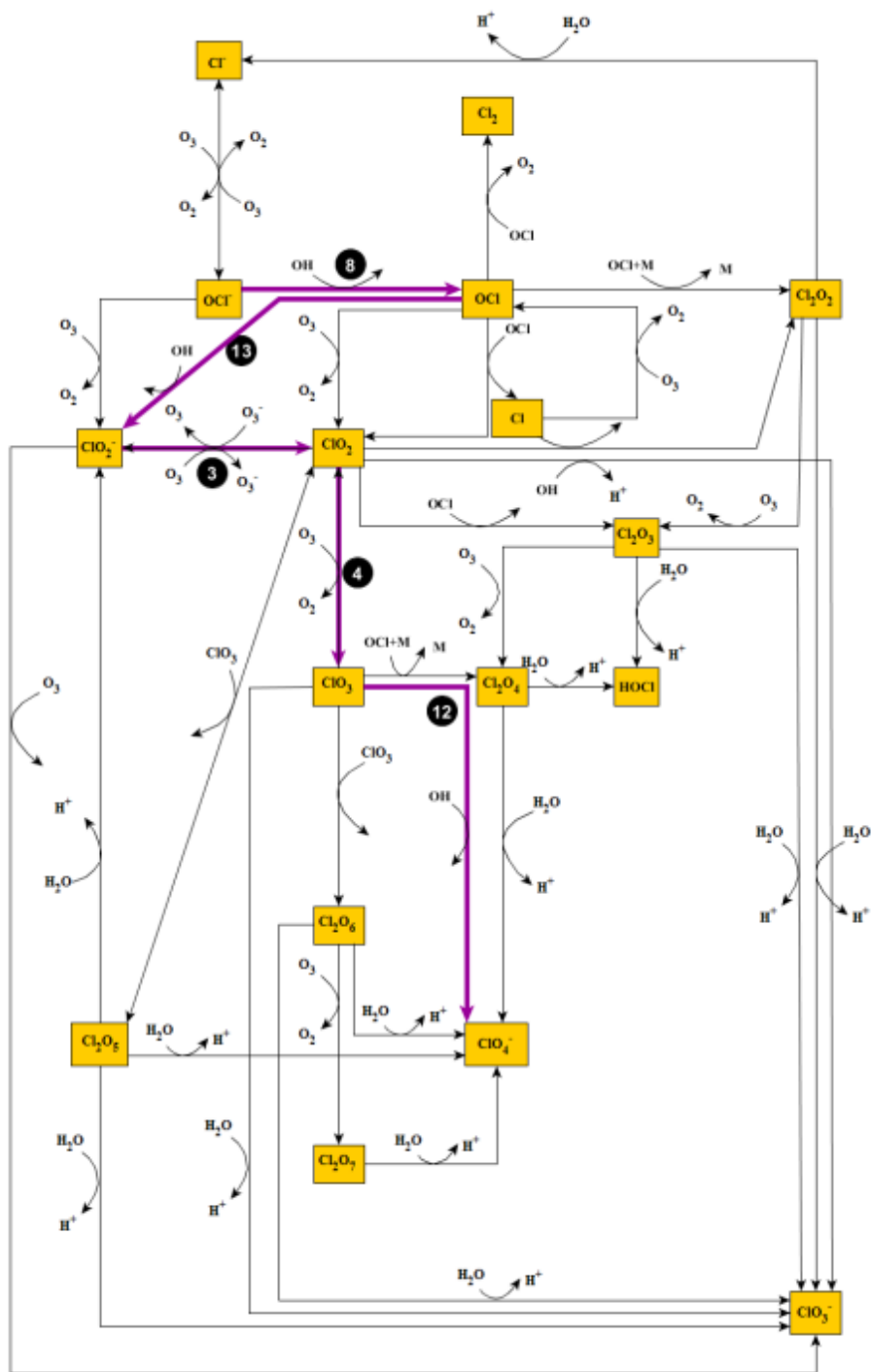


Figure A.30 Mechanism 4: O_3 oxidation of OCl^- (aq). Note the thick purple lines indicate the pathway leading to the formation of the ClO_4^- and black solid circles represent reaction number from Table 3.4. This pathway leads to the formation of one ClO_4^- molecule containing three O's from O_3 .

A.2.1 Pathways that Produce ClO_4^- with two and three O's from O_3

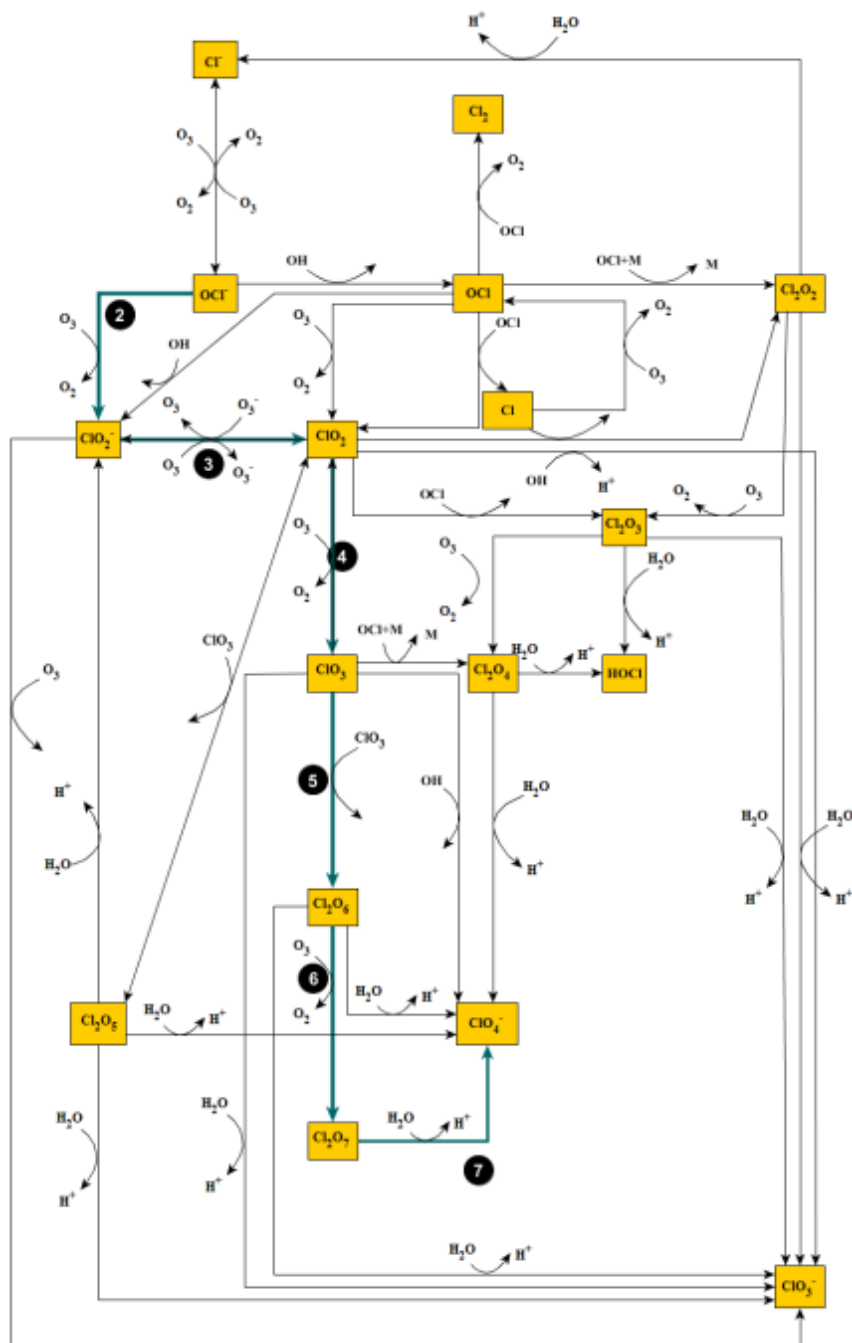


Figure A.31 Mechanism 5: O_3 oxidation of OCl^- (aq). Note the thick dark aqua lines indicate the pathway leading to the formation of the ClO_4^- and black solid circles represent reaction number from Table 3.4. This pathway leads to the formation of two ClO_4^- molecules, one with three O from O_3 and the other with two O from O_3 .

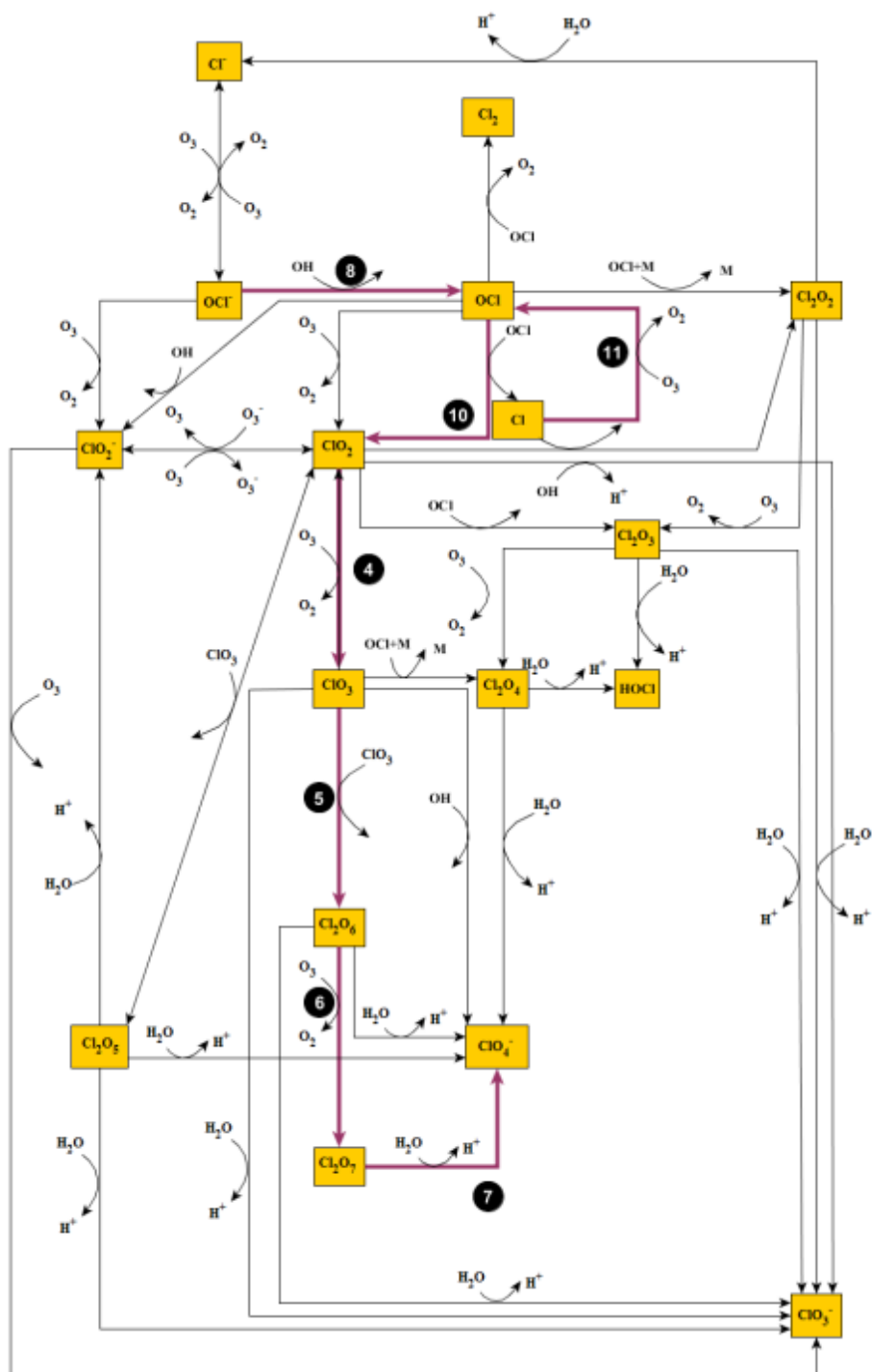


Figure A.32 Mechanism 6: O_3 oxidation of OCl^- (aq). Note the thick dark pink lines indicate the pathway leading to the formation of the ClO_4^- and black solid circles represent reaction number from Table 3.4. This pathway leads to the formation of two ClO_4^- molecules, one with three O from O_3 and the other with two O from O_3 .

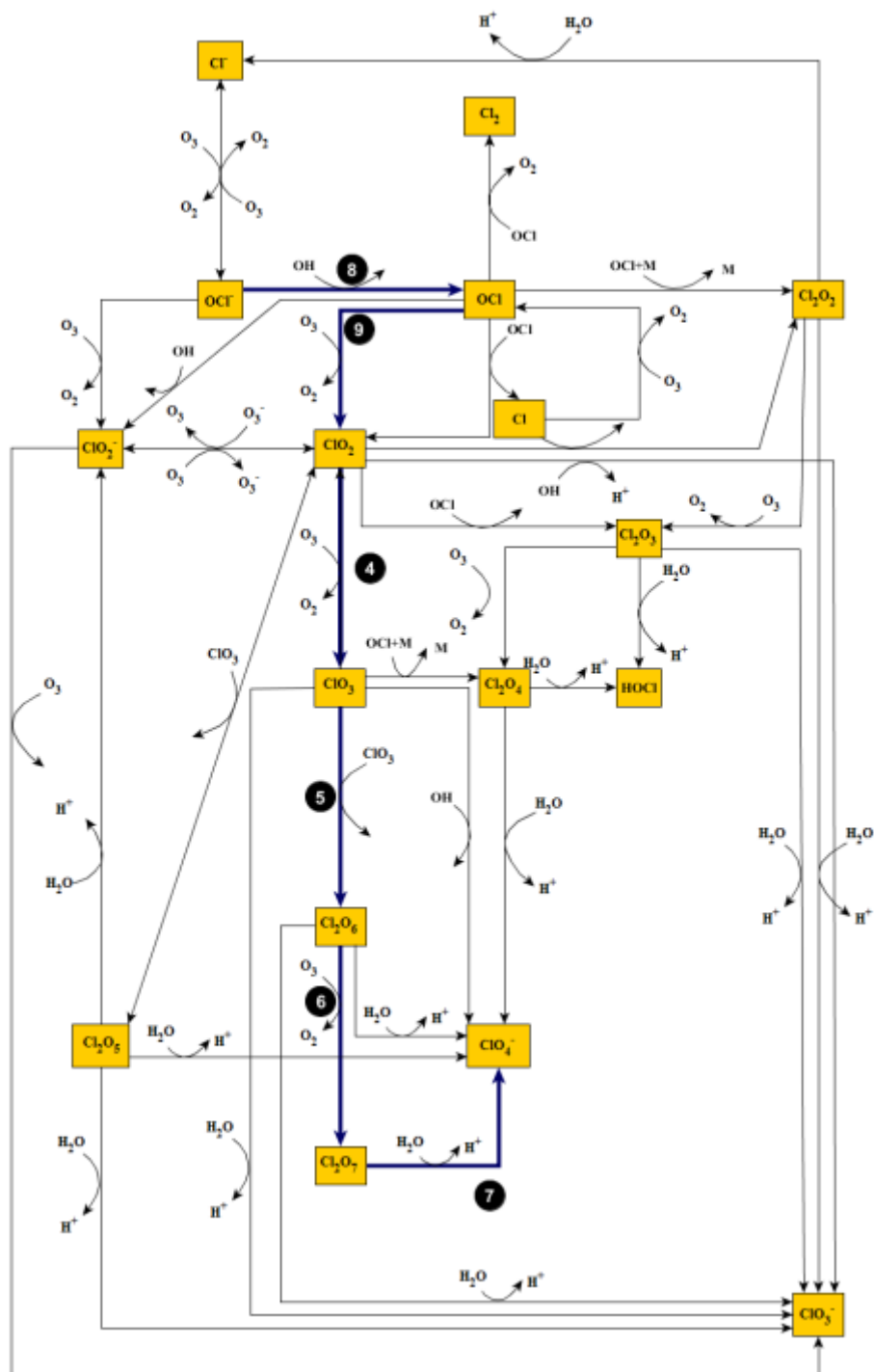


Figure A.33 Mechanism 7: O_3 oxidation of OCl^- (aq). Note the thick dark purple lines indicate the pathway leading to the formation of the ClO_4^- and black solid circles represent reaction number from Table 3.4. This pathway leads to the formation of two ClO_4^- molecules, one with three O from O_3 and the other with two O from O_3 .

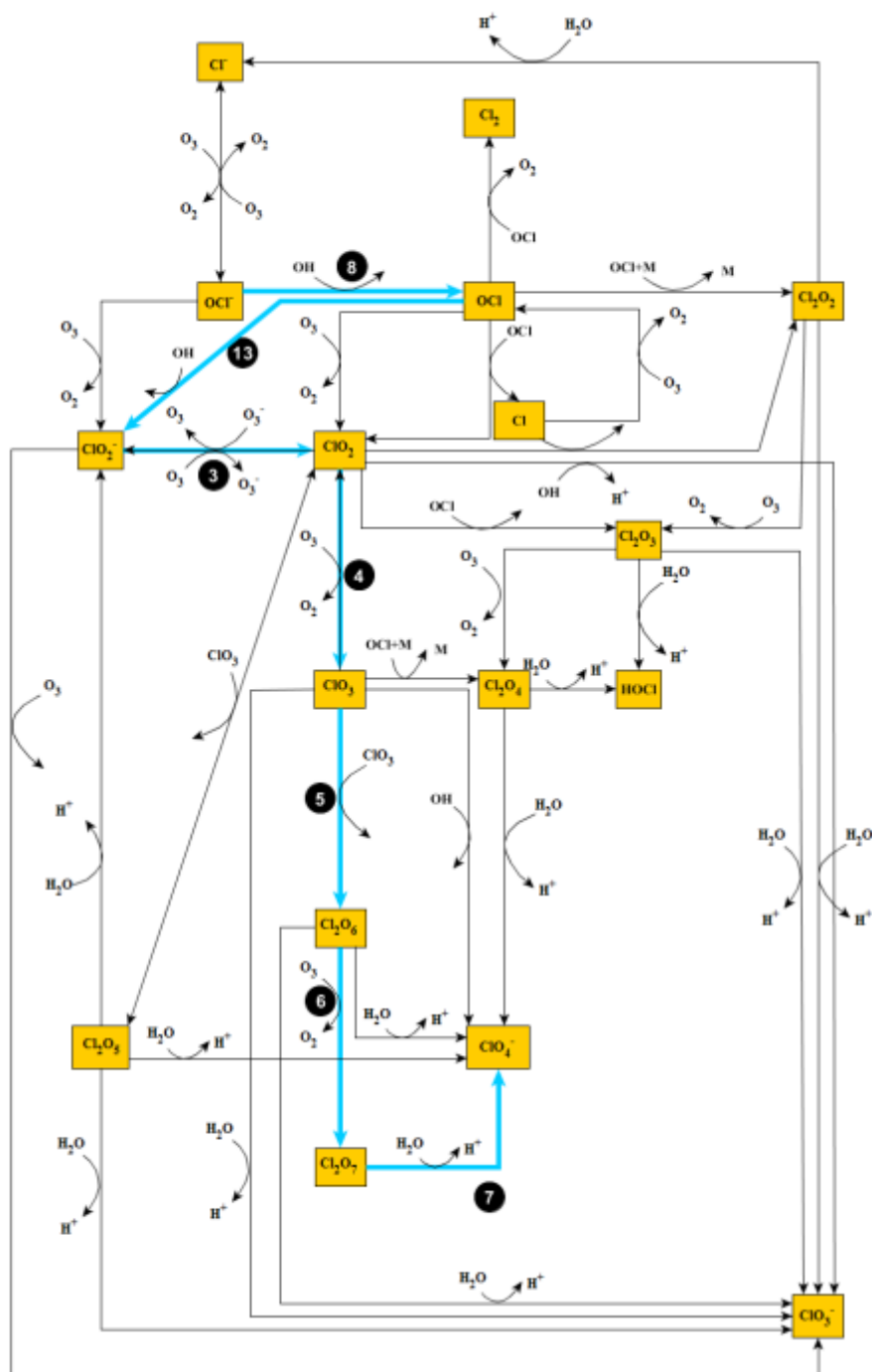


Figure A.34 Mechanism 8: O_3 oxidation of OCl^- (aq). Note the thick blue lines indicate the pathway leading to the formation of the ClO_4^- and black solid circles represent reaction number from Table 3.4. This pathway leads to the formation of two ClO_4^- molecules, one with three O from O_3 and the other with two O from O_3 .

A.2.2 Pathways that Produce ClO_4^- with only two O's from O_3

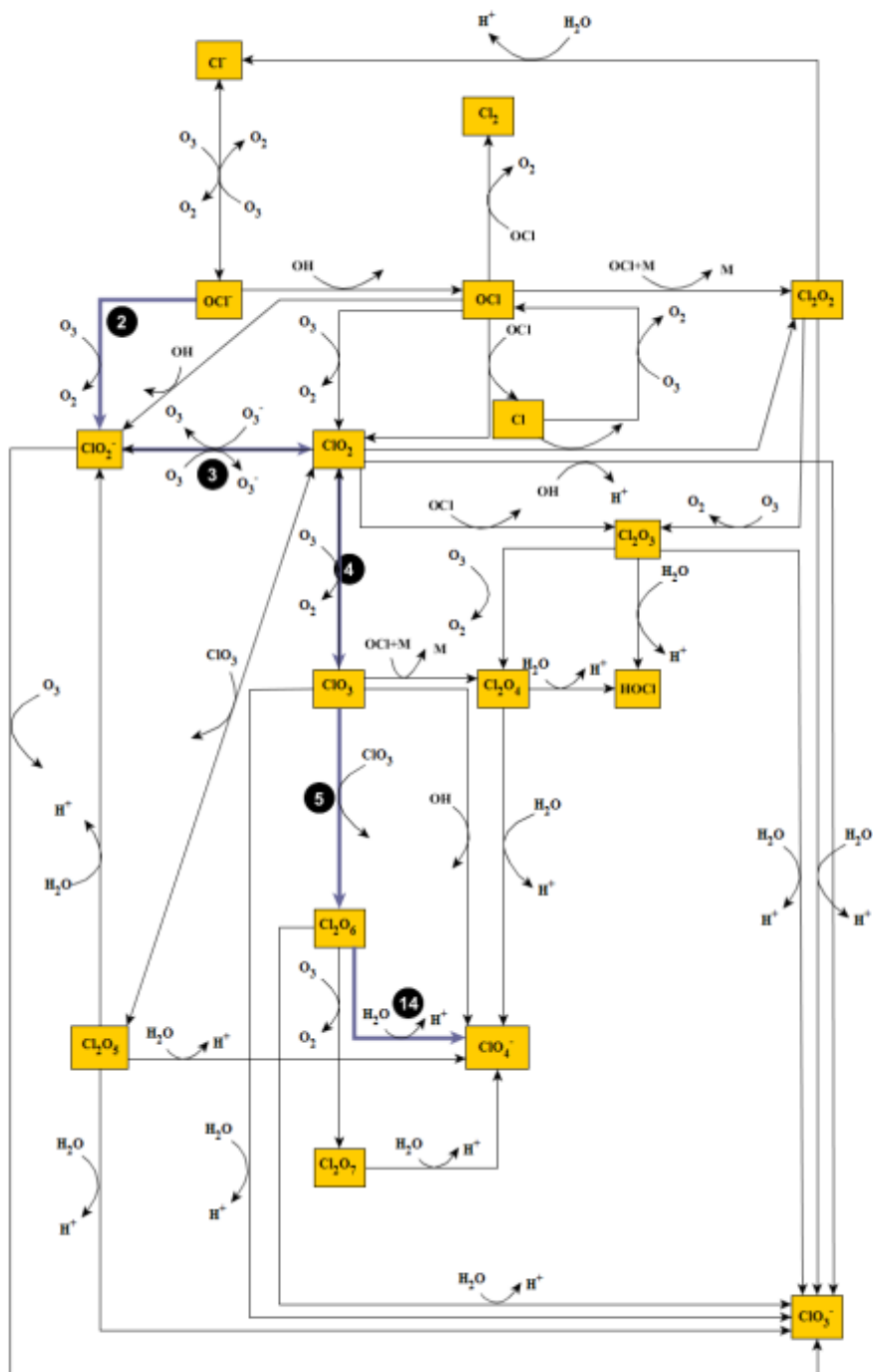


Figure A.35 Mechanism 9: O_3 oxidation of OCl^- (aq). Note the thick purple lines indicate the pathway leading to the formation of the ClO_4^- and black solid circles represent reaction number from Table 3.4. This pathway leads to the formation of one ClO_4^- molecule containing two O's from O_3 .

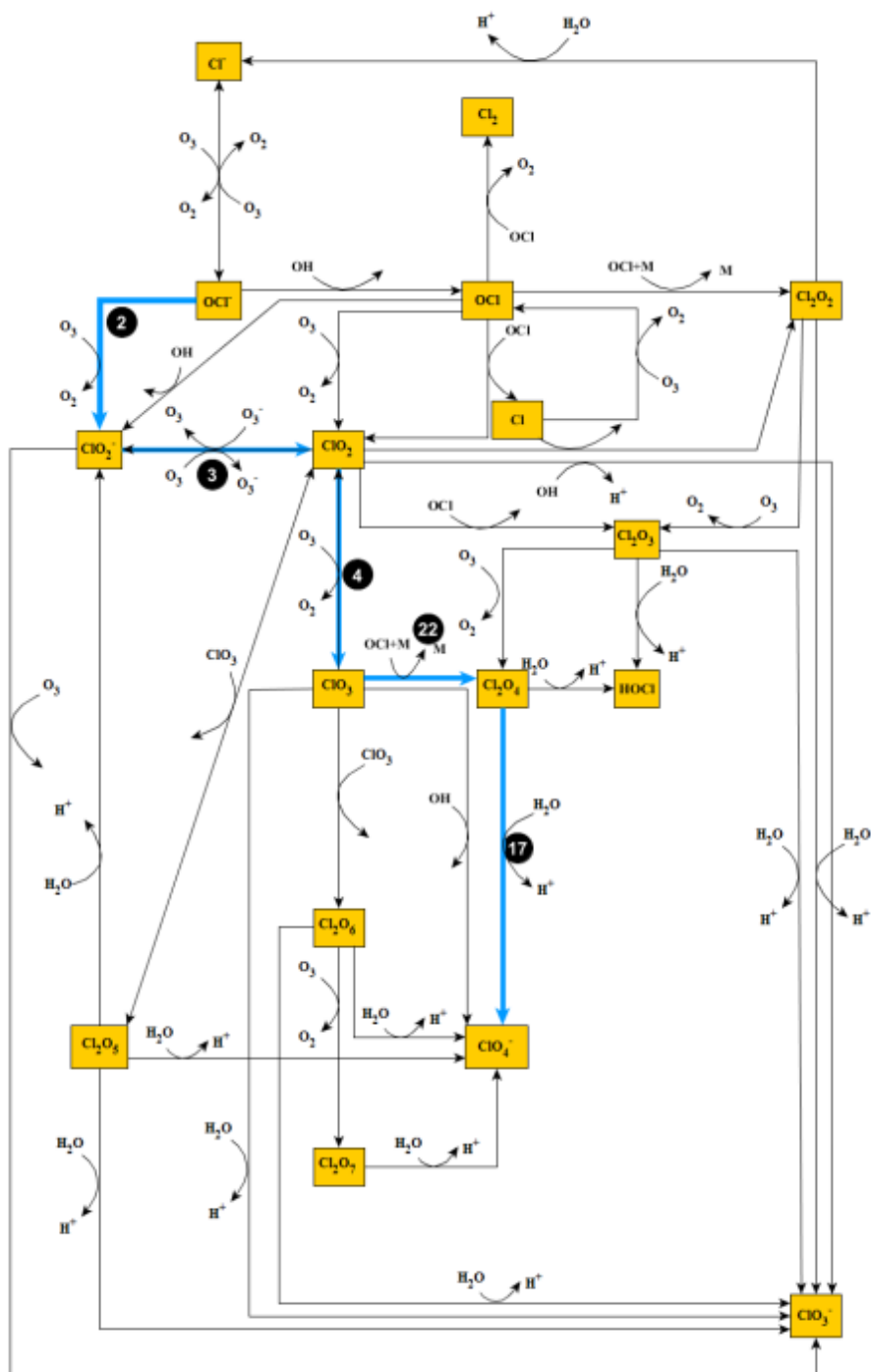


Figure A.36 Mechanism 10: O_3 oxidation of OCl^- (aq). Note the thick blue lines indicate the pathway leading to the formation of the ClO_4^- and black solid circles represent reaction number from Table 3.4. This pathway leads to the formation of one ClO_4^- molecule containing two O's from O_3 .

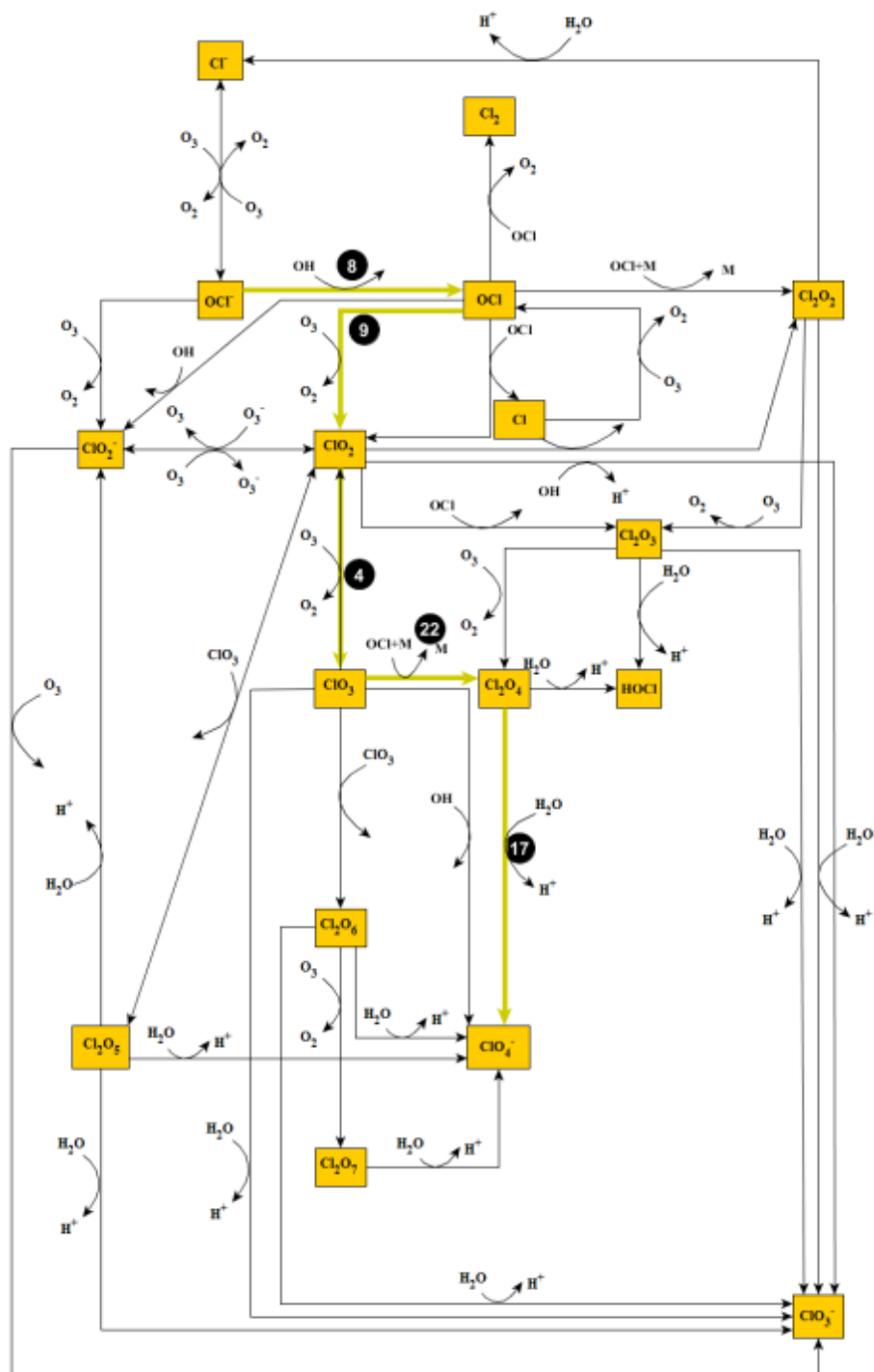


Figure A.37 Mechanism 11: O_3 oxidation of OCl^- (aq). Note the thick yellow lines indicate the pathway leading to the formation of the ClO_4^- and black solid circles represent reaction number from Table 3.4. This pathway leads to the formation of one ClO_4^- molecule containing two O's from O_3 .

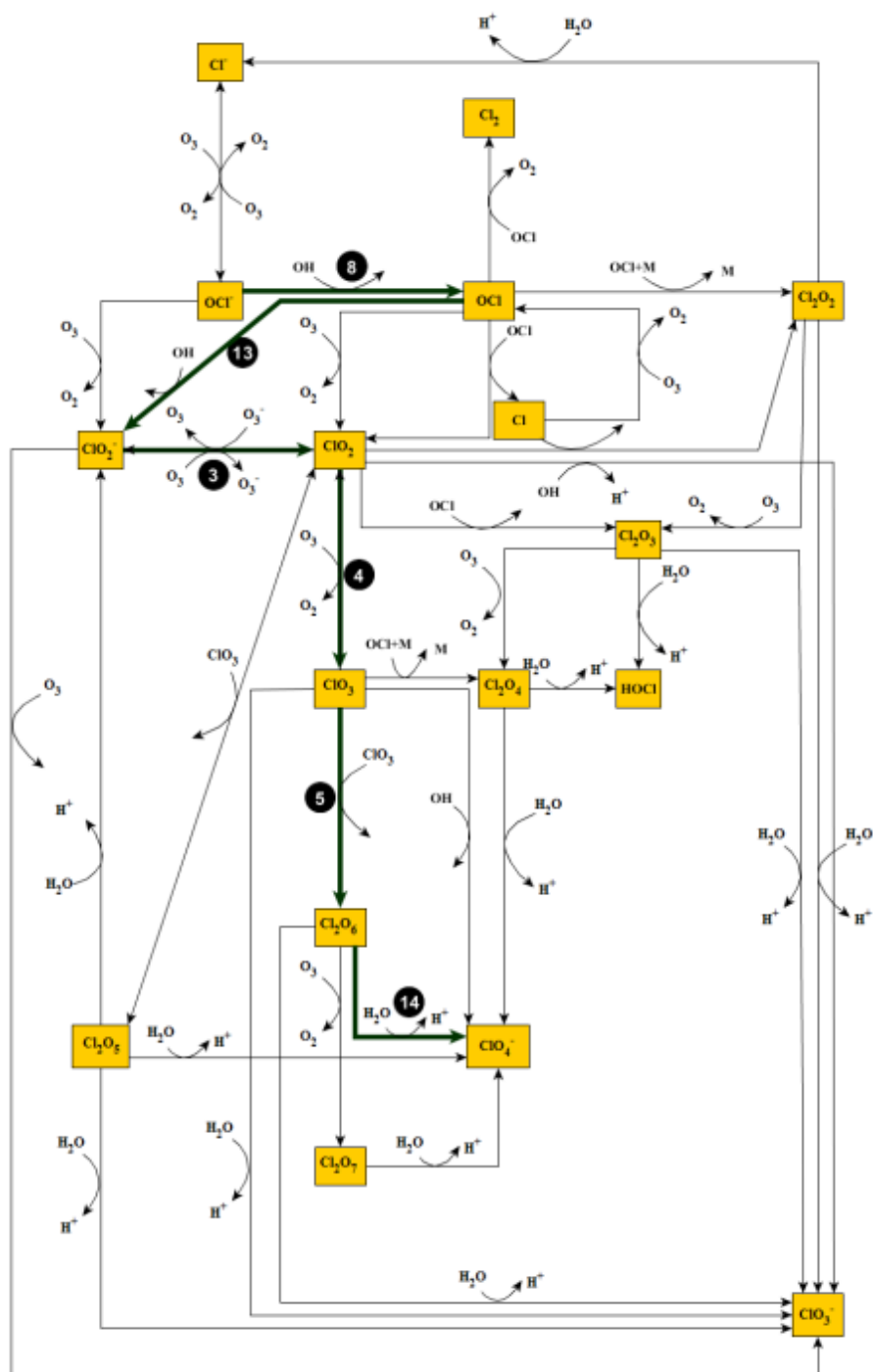


Figure A.38 Mechanism 12: O_3 oxidation of OCl^- (aq). Note the thick dark green lines indicate the pathway leading to the formation of the ClO_4^- and black solid circles represent reaction number from Table 3.4. This pathway leads to the formation of one ClO_4^- molecule containing two O's from O_3 .

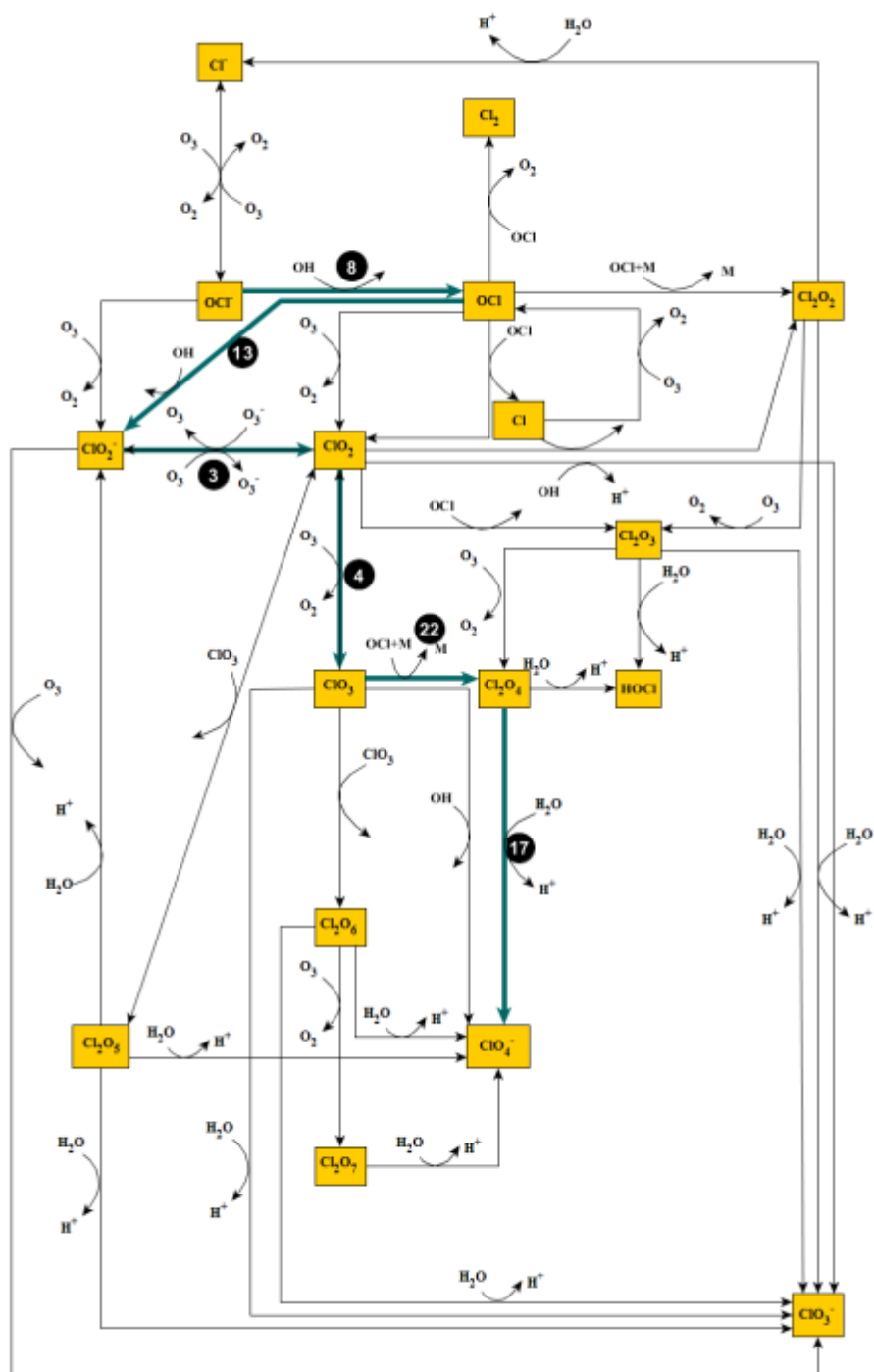


Figure A.39 Mechanism 13: O_3 oxidation of OCl^- (aq). Note the thick aqua green lines indicate the pathway leading to the formation of the ClO_4^- and black solid circles represent reaction number from Table 3.4. This pathway leads to the formation of one ClO_4^- molecule containing two O's from O_3 .

A.2.3. Pathways involving the Cl_2O_5 Species

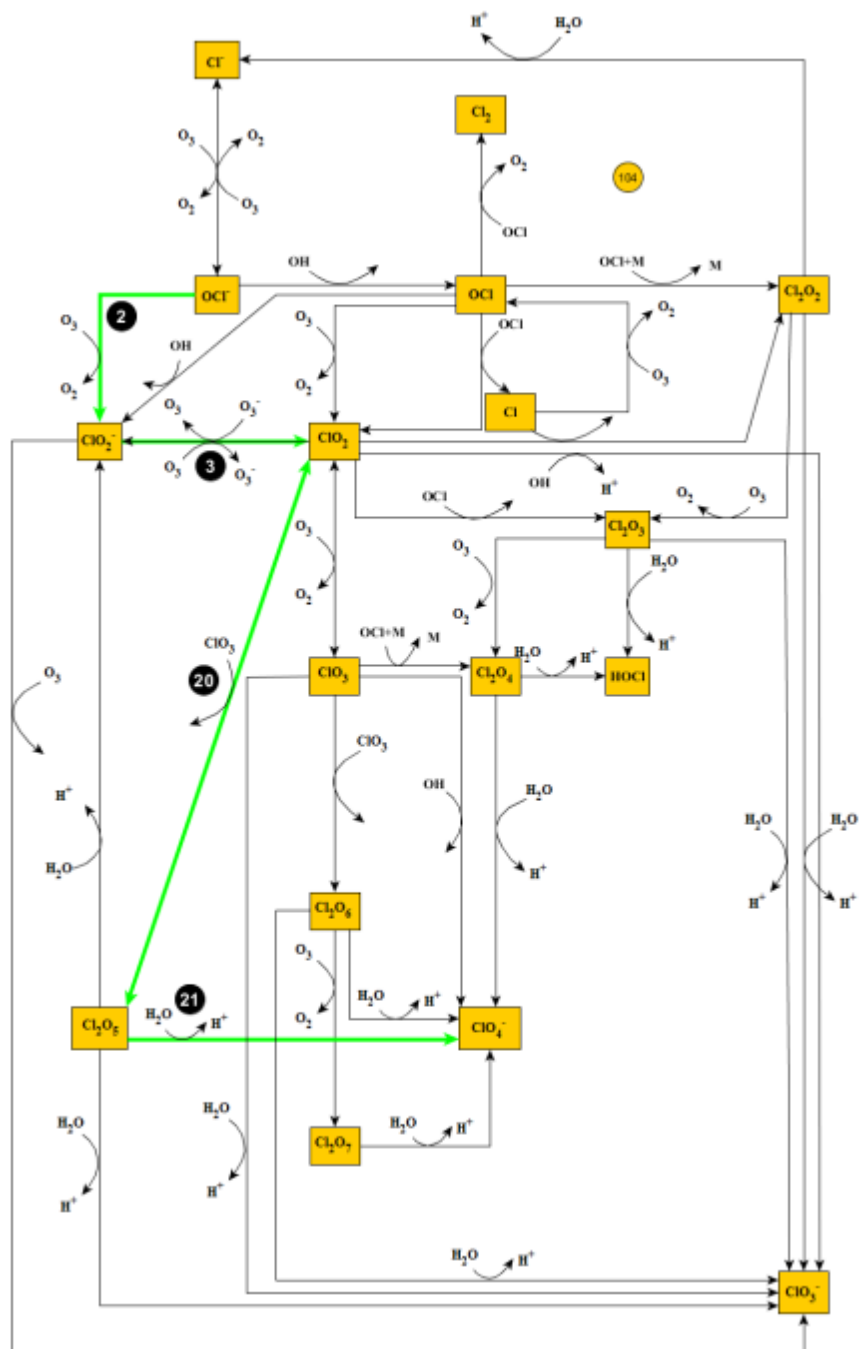


Figure A.40 Mechanism 14: O_3 oxidation of OCl^- (aq). Note the thick neon green lines indicate the pathway leading to the formation of the ClO_4^- and black solid circles represent reaction number from Table 3.4. This pathway leads to the formation of one ClO_4^- molecule containing two O's from O_3 .

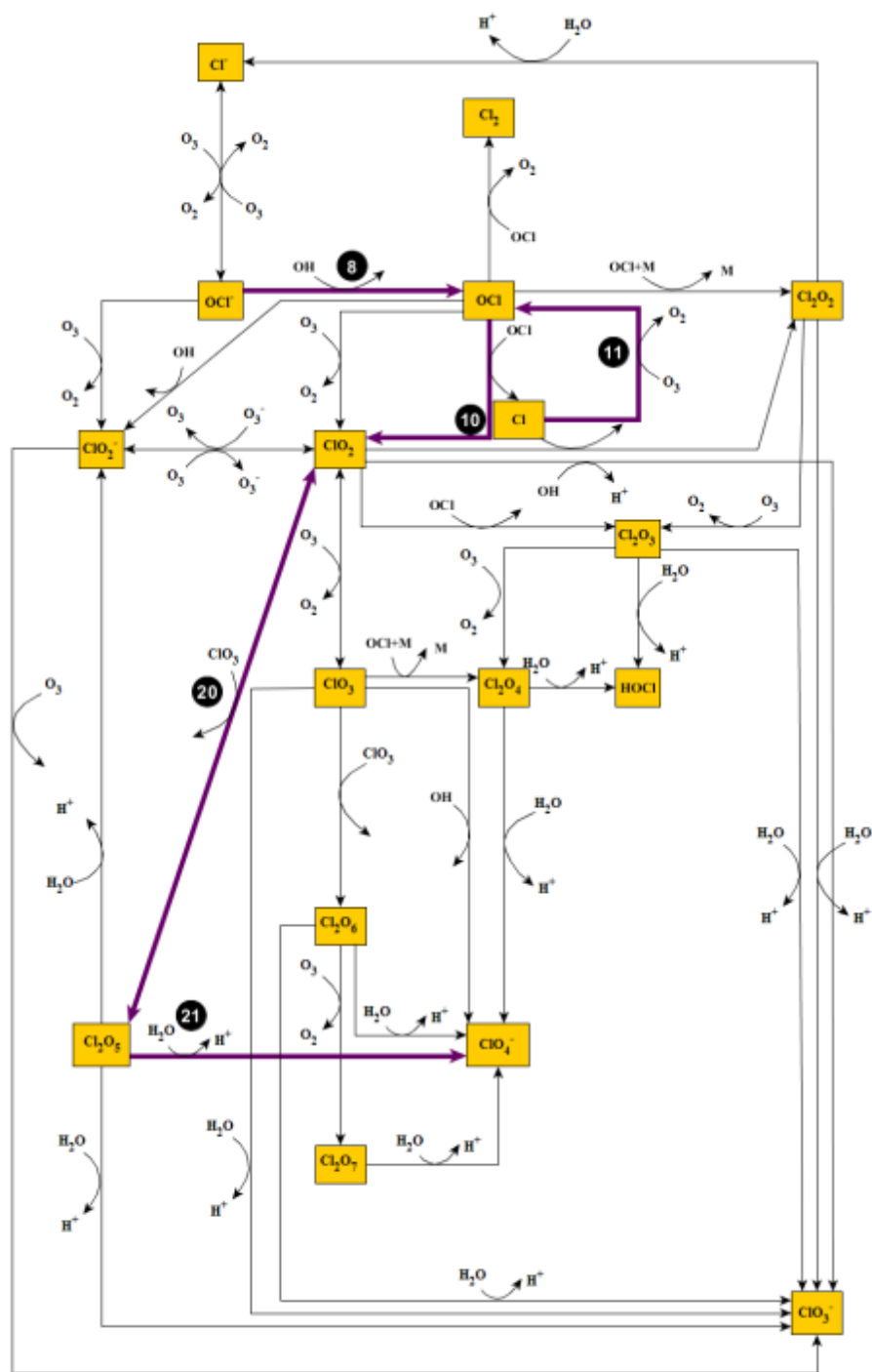


Figure A.41 Mechanism 15: O_3 oxidation of OCl^- (aq). Note the thick purple lines indicate the pathway leading to the formation of the ClO_4^- and black solid circles represent reaction number from Table 3.4. This pathway leads to the formation of one ClO_4^- molecule containing two O's from O_3 .

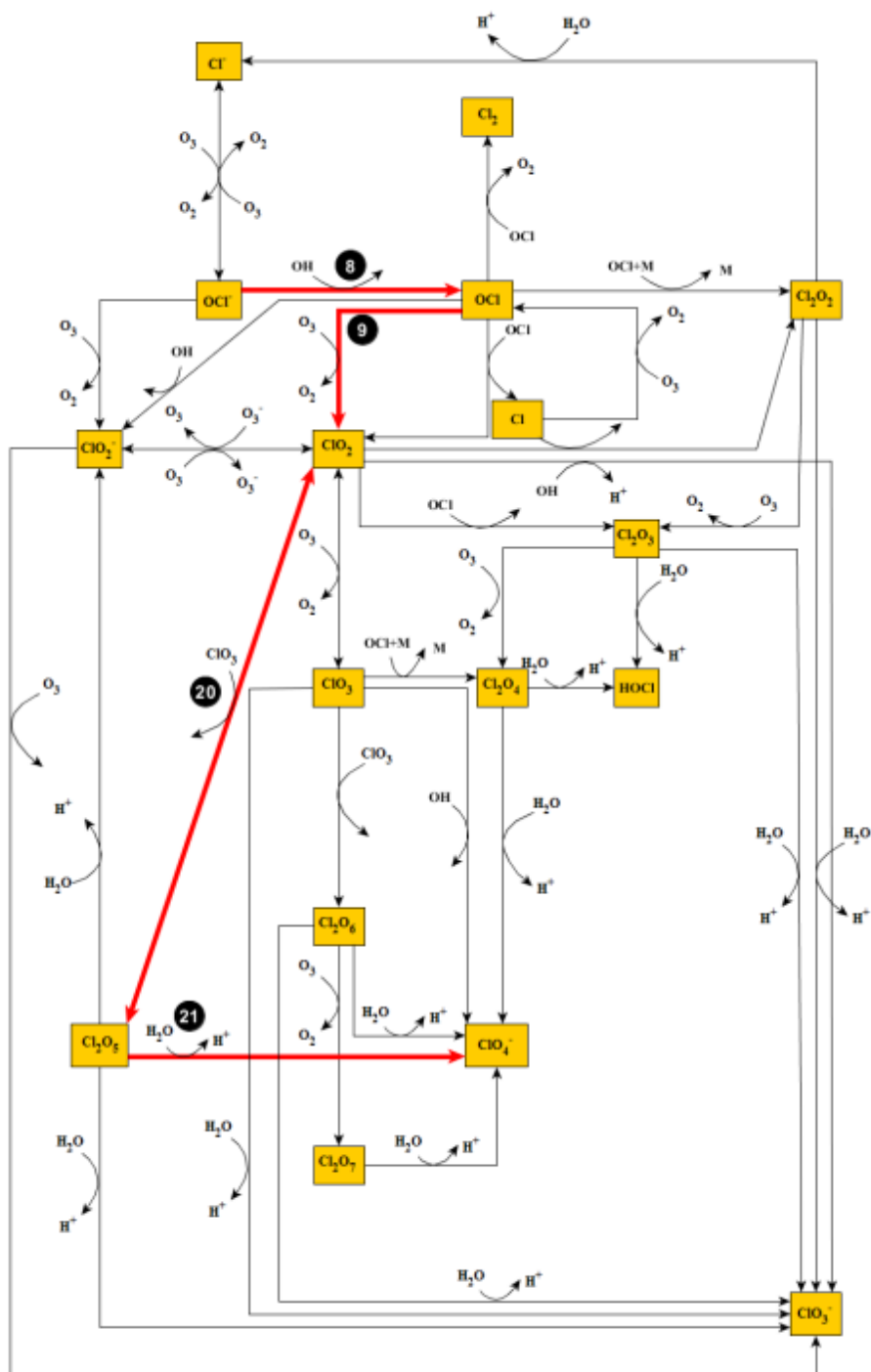


Figure A.42 Mechanism 16: O_3 oxidation of OCl^- (aq). Note the thick red lines indicate the pathway leading to the formation of the ClO_4^- and black solid circles represent reaction number from Table 3.4. This pathway leads to the formation of one ClO_4^- molecule containing two O's from O_3 .

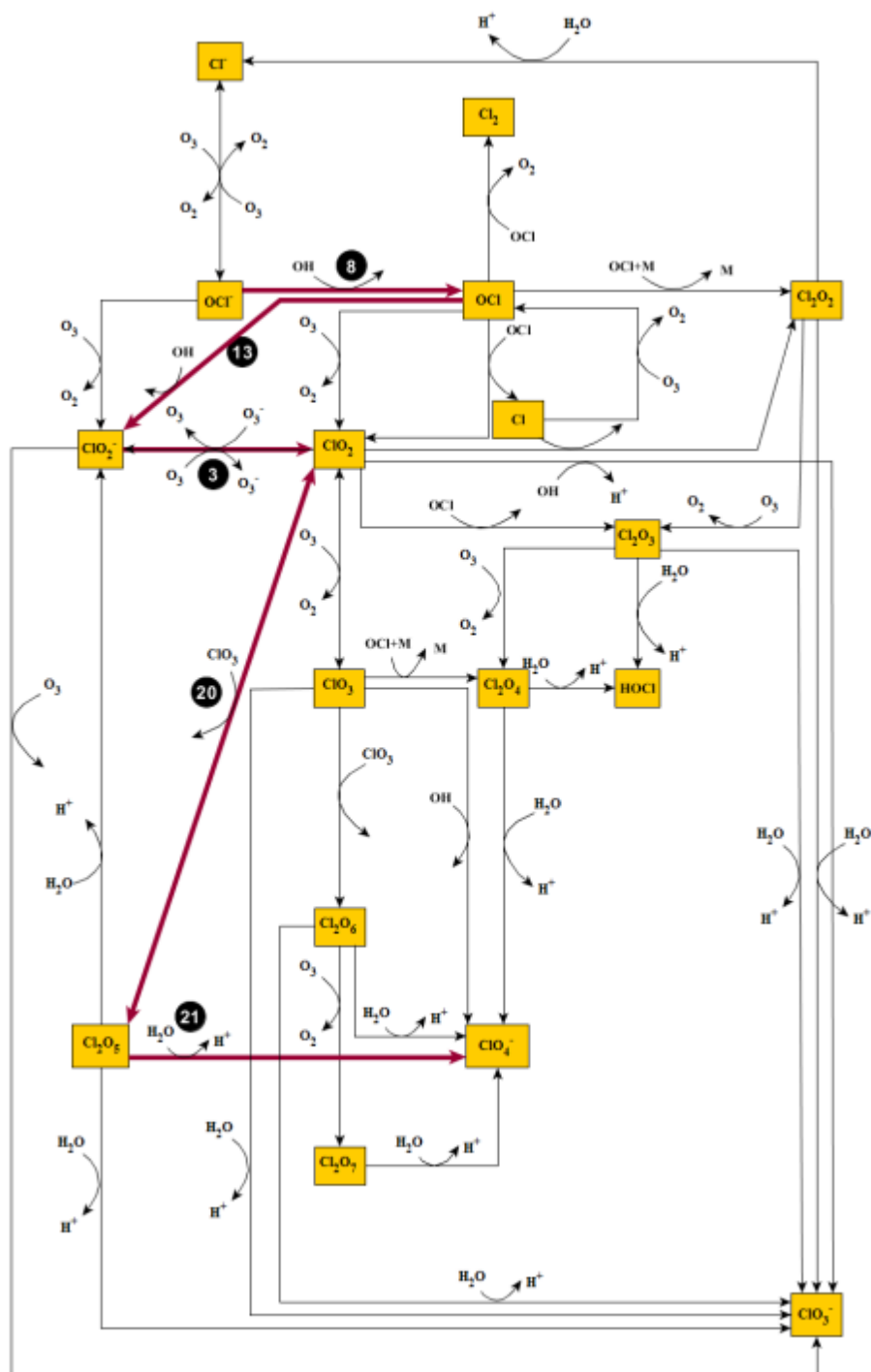


Figure A.43 Mechanism 17: O_3 oxidation of OCl^- (aq). Note the thick purple lines indicate the pathway leading to the formation of the ClO_4^- and black solid circles represent reaction number from Table 3.4. This pathway leads to the formation of one ClO_4^- molecule containing two O's from O_3 .

A.2.4 Pathways Involving Speculated Reactions 16 and 19

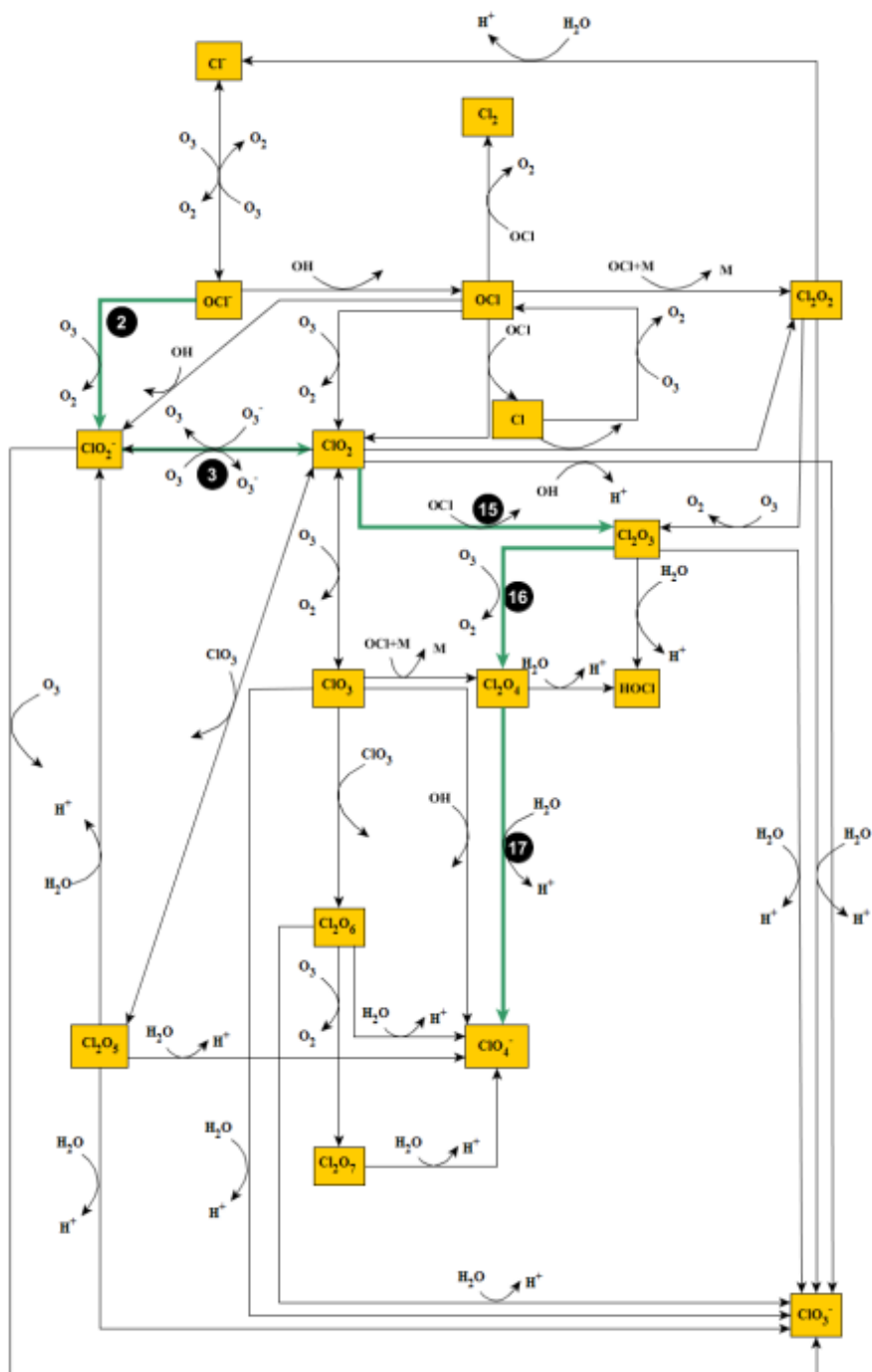


Figure A.44 Mechanism 18: O_3 oxidation of OCl^- (aq). Note the thick blue green lines indicate the pathway leading to the formation of the ClO_4^- and black solid circles represent reaction number from Table 3.4. This pathway leads to the formation of one ClO_4^- molecule containing two O's from O_3 .

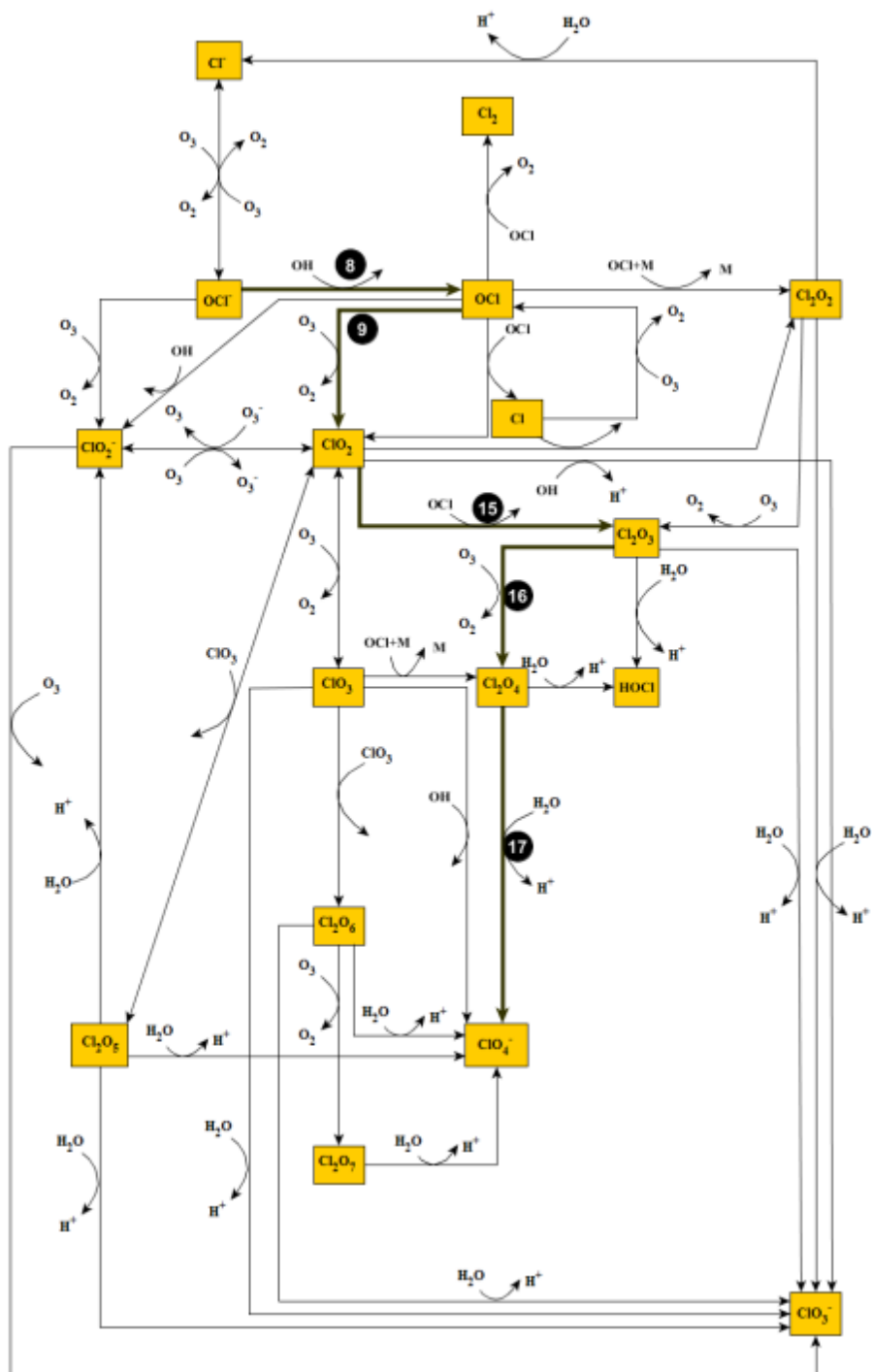


Figure A.45 Mechanism 19: O_3 oxidation of OCl^- (aq). Note the thick gray lines indicate the pathway leading to the formation of the ClO_4^- and black solid circles represent reaction number from Table 3.4. This pathway leads to the formation of one ClO_4^- molecule containing two O's from O_3 .

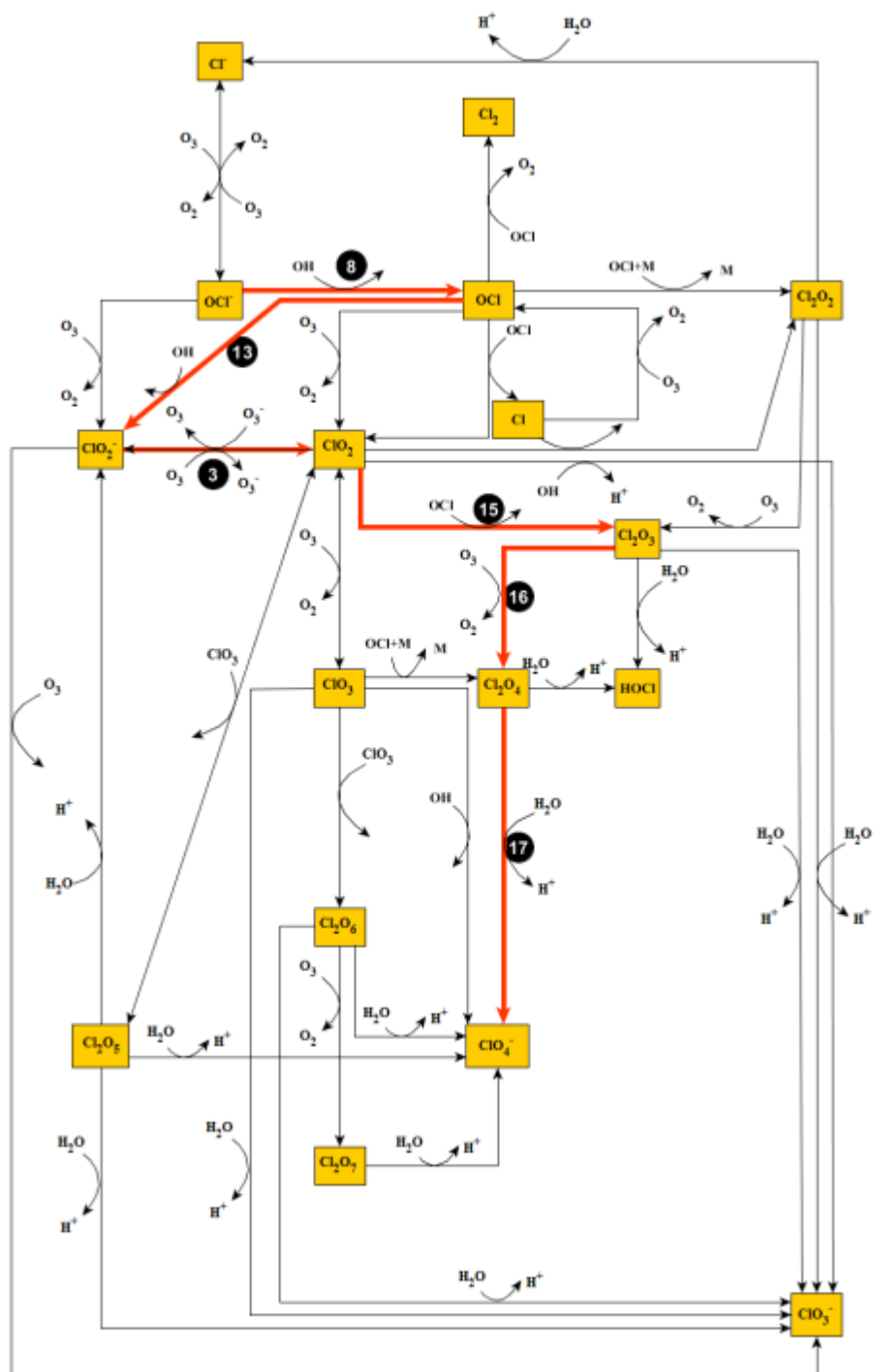


Figure A.46 Mechanism 20: O_3 oxidation of OCl^- (aq). Note the thick red lines indicate the pathway leading to the formation of the ClO_4^- and black solid circles represent reaction number from Table 3.4. This pathway leads to the formation of one ClO_4^- molecule containing two O's from O_3 .

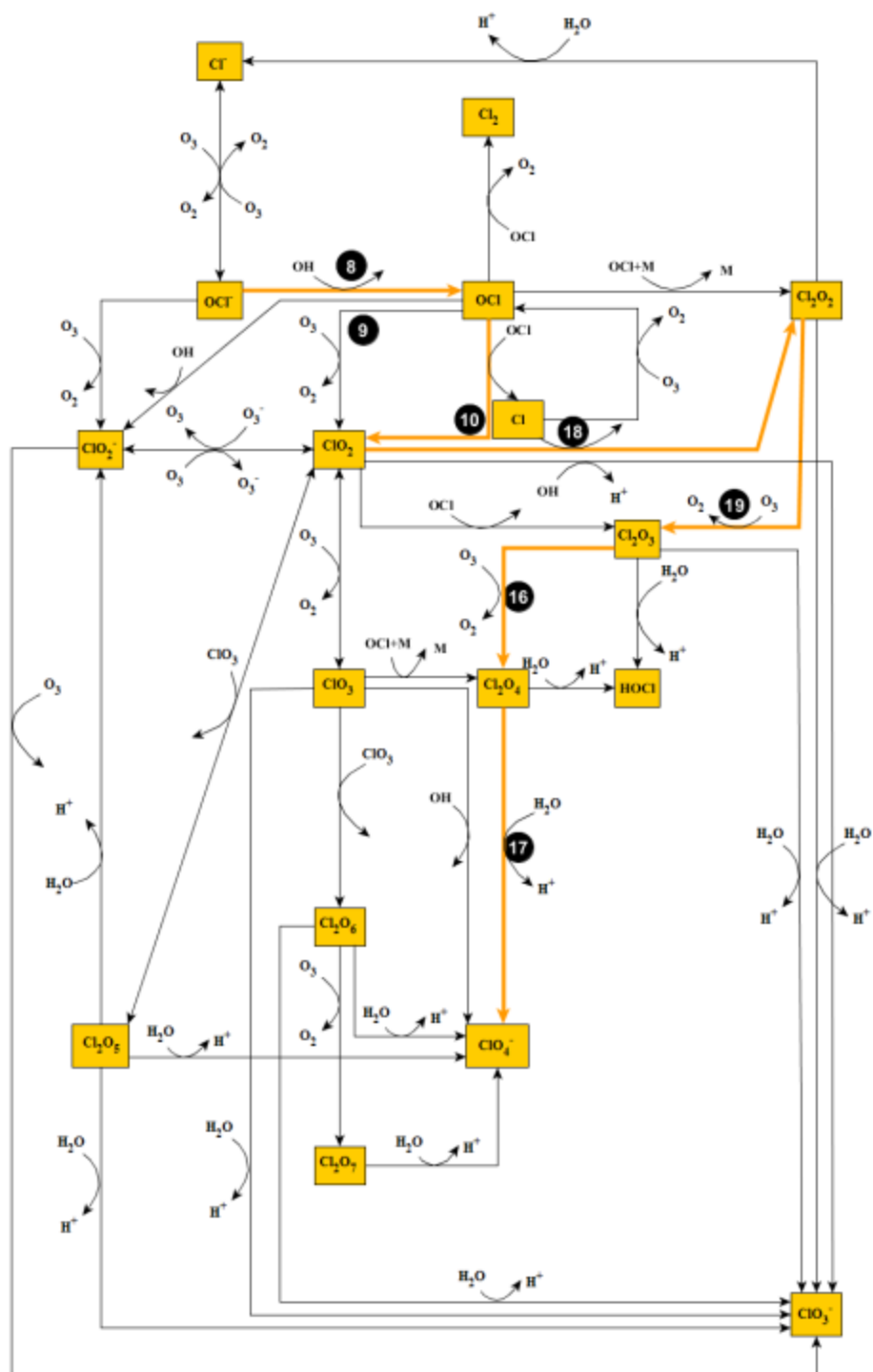


Figure A.47 Mechanism 21: O_3 oxidation of OCl^- (aq). Note the thick orange lines indicate the pathway leading to the formation of the ClO_4^- and black solid circles represent reaction number from Table 3.4. This pathway leads to the formation of one ClO_4^- molecule containing two O's from O_3 .

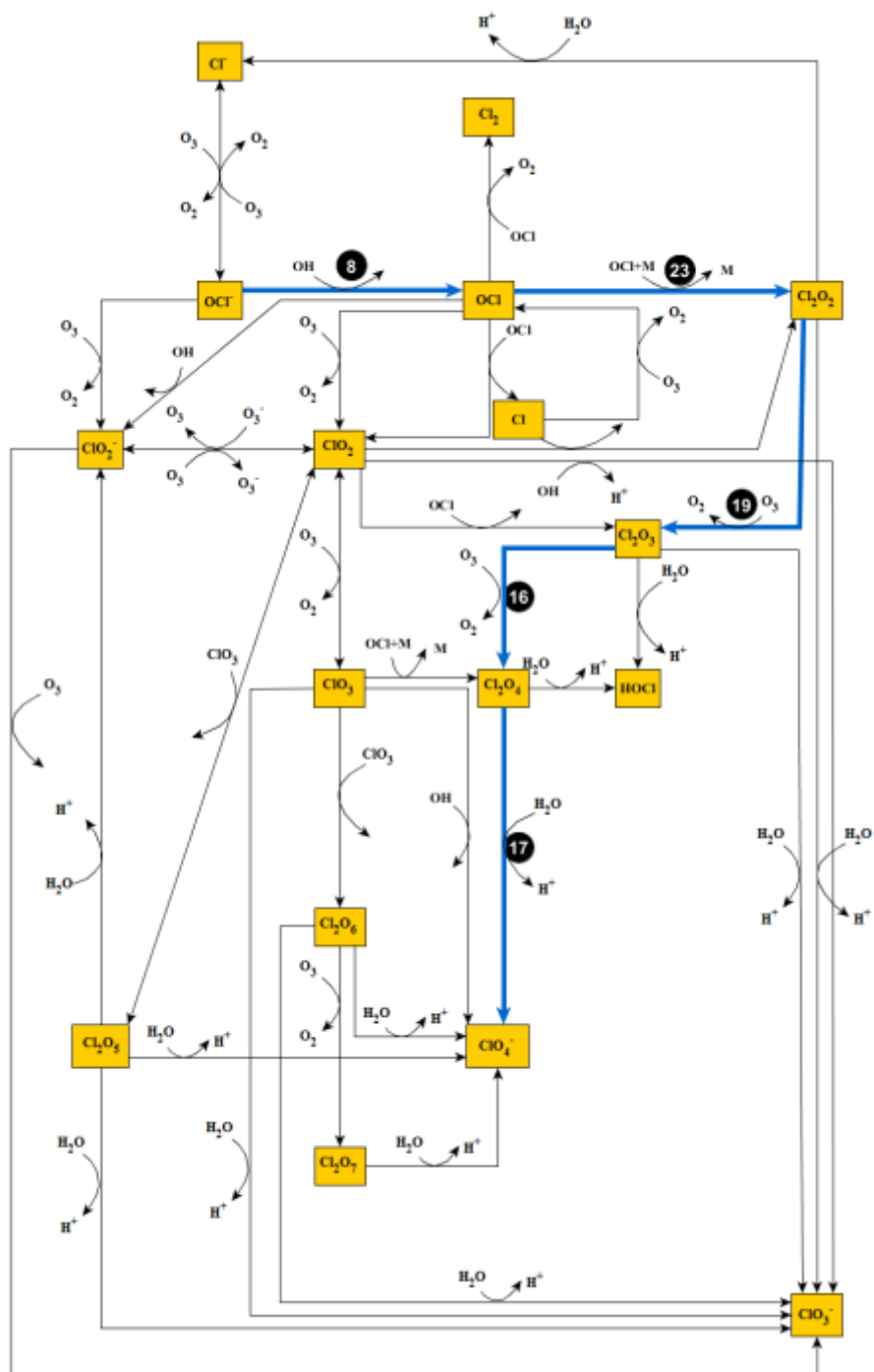


Figure A.48 Mechanism 22: O_3 oxidation of OCl^- (aq). Note the thick blue lines indicate the pathway leading to the formation of the ClO_4^- and black solid circles represent reaction number from Table 3.4. This pathway leads to the formation of one ClO_4^- molecule containing two O's from O_3 .

A.3 Proposed Pathways for O₃ Oxidation of Aqueous ClO₂⁻

A.3.1 Pathways Producing a ClO₄⁻ with only two O from O₃

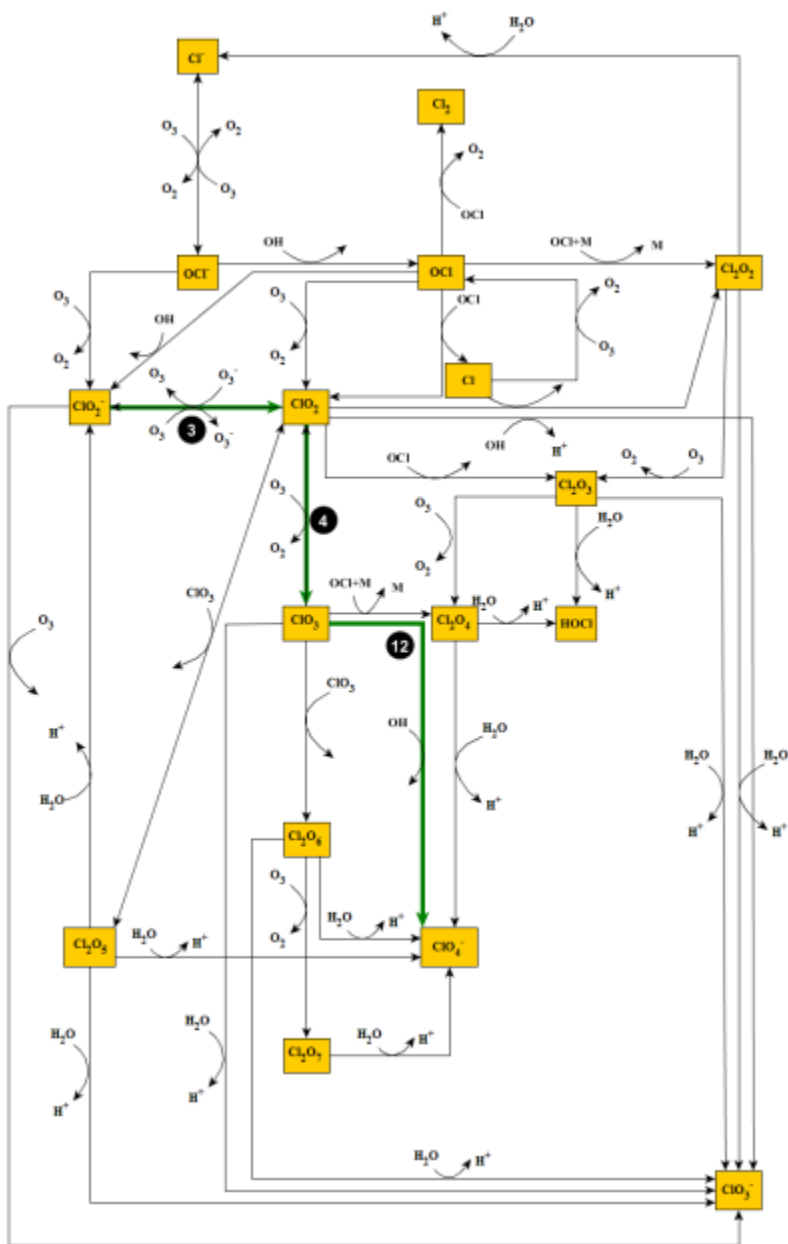


Figure A.50 Mechanism 1: O₃ oxidation of ClO₂⁻ (aq). Note the thick orange lines indicate the pathway leading to the formation of the ClO₄⁻ and black solid circles represent reaction number from Table 3.4. This pathway leads to the formation one ClO₄⁻ molecule containing two O from O₃.

A.3.2 Pathways Producing two ClO_4^- molecules, one with only one O from O_3 and the other with two

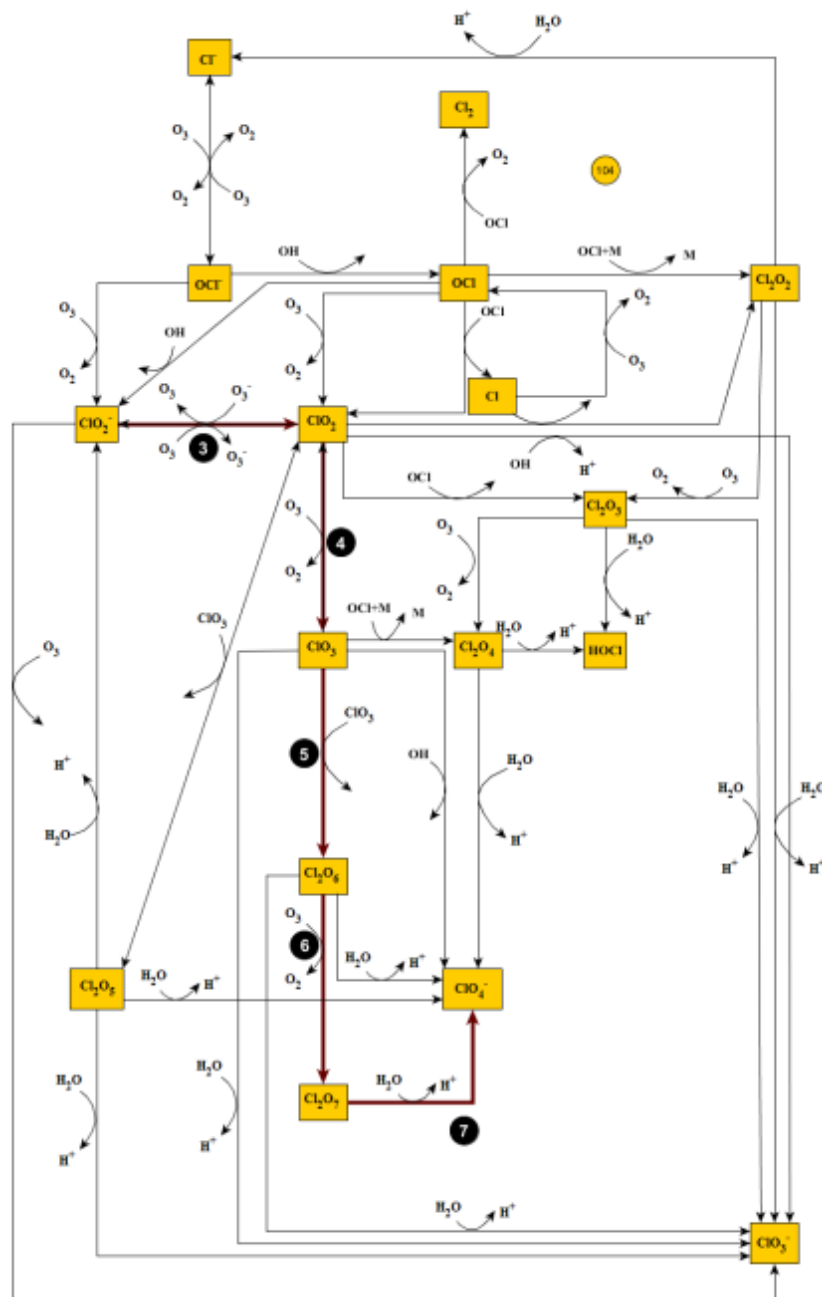


Figure A.51 Mechanism 2: O_3 oxidation of ClO_2^- (aq). Note the thick maroon lines indicate the pathway leading to the formation of the ClO_4^- and black solid circles represent reaction number from Table 3.4. This pathway leads to the formation of two ClO_4^- molecules one containing one O from O_3 and the other two O's from O_3 .

A.3.3 Pathways Producing ClO_4^- with only one O from O_3 .

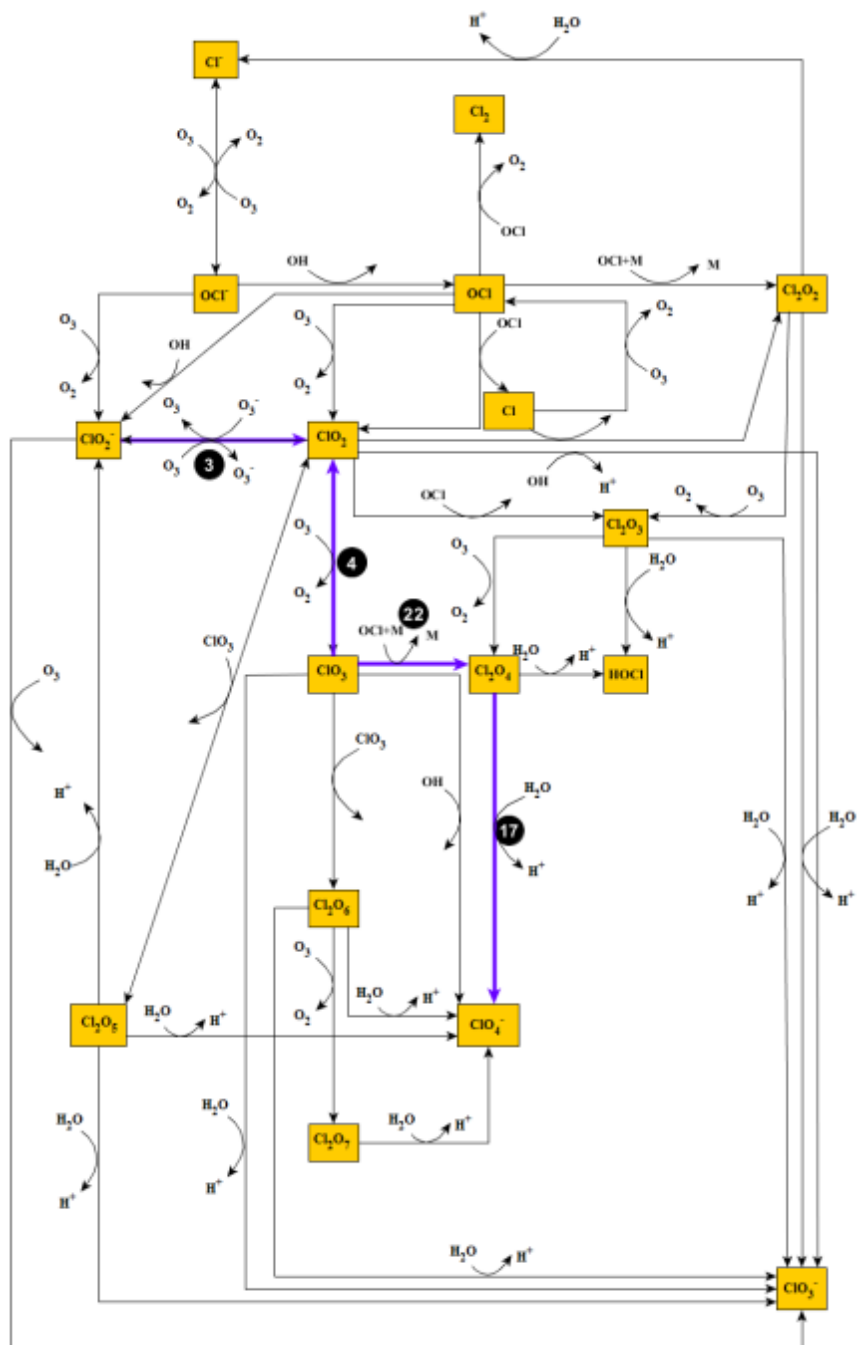


Figure A.52 Mechanism 3: O_3 oxidation of ClO_2^- (aq). Note the thick purple lines indicate the pathway leading to the formation of the ClO_4^- and black solid circles represent reaction number from Table 3.4. This pathway leads to the formation one ClO_4^- molecule containing one O from O_3 .

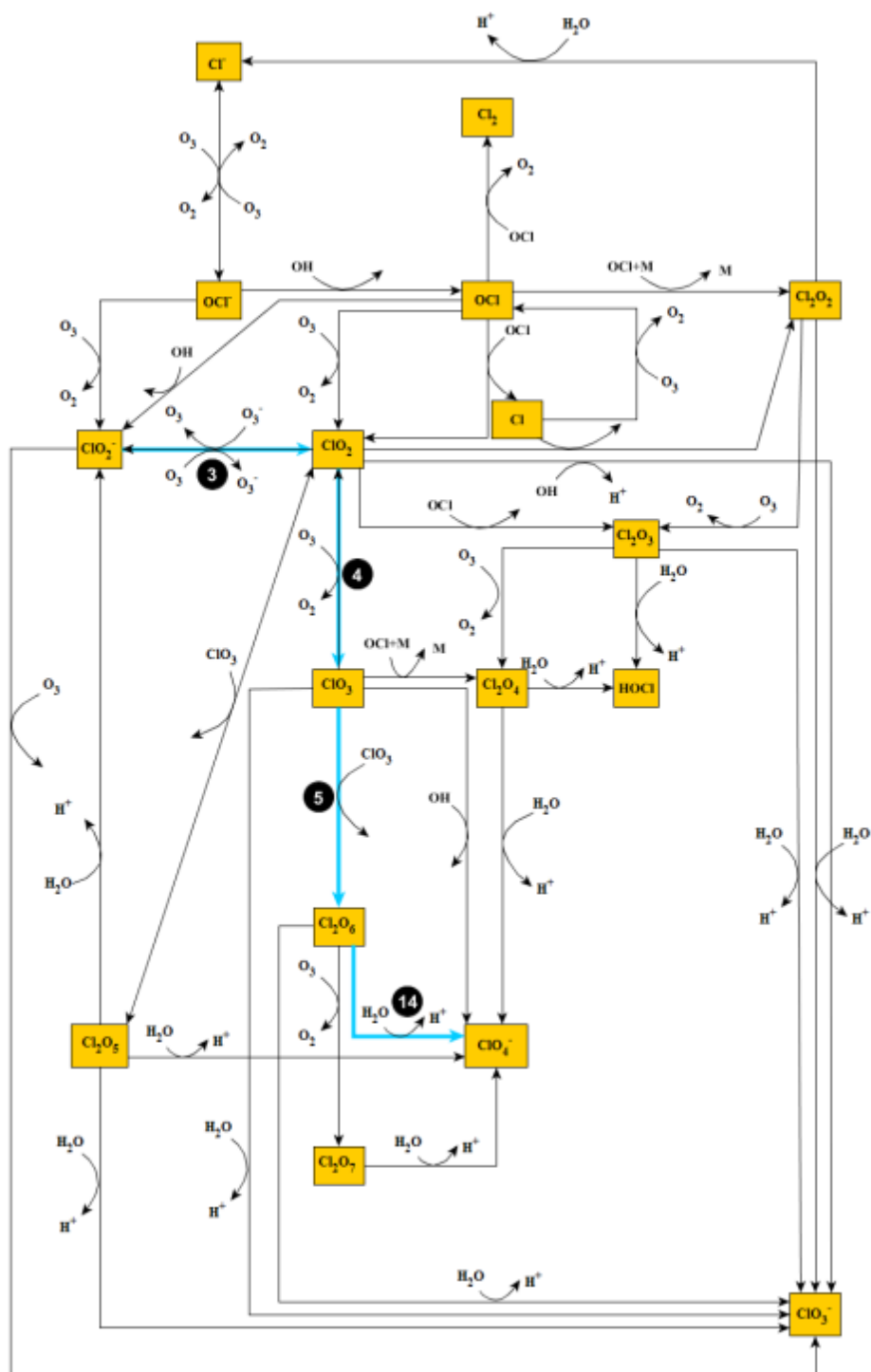


Figure A.53 Mechanism 4: O_3 oxidation of ClO_2^- (aq). Note the thick light blue lines indicate the pathway leading to the formation of the ClO_4^- and black solid circles represent reaction number from Table 3.4. This pathway leads to the formation one ClO_4^- molecule containing one O from O_3 and one ClO_3^- molecule containing one O from O_3 .

A.3.4 Pathways Involving the Cl_2O_5 species

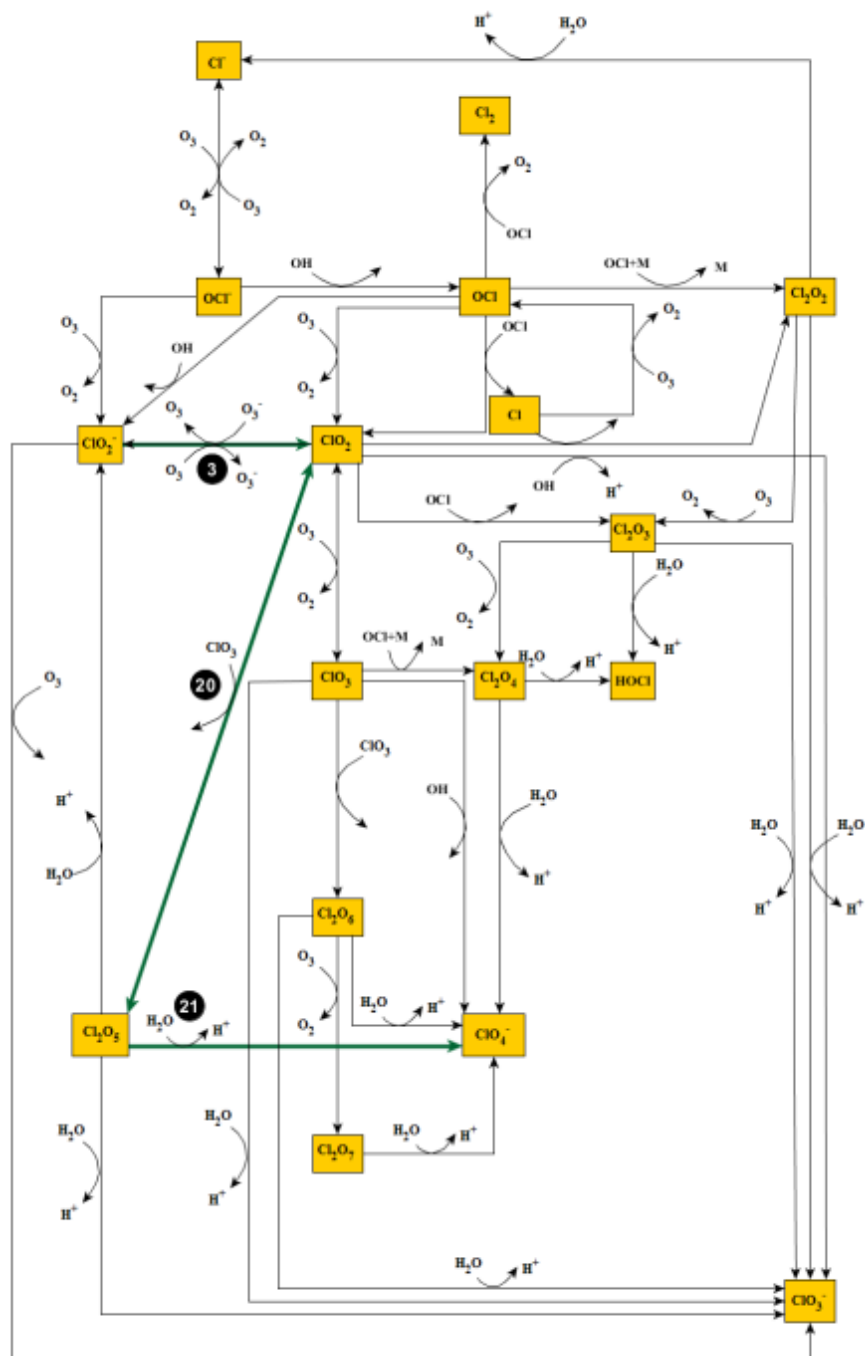


Figure A.54 Mechanism 5: O_3 oxidation of ClO_2^- (aq). Note the thick green lines indicate the pathway leading to the formation of the ClO_4^- and black solid circles represent reaction number from Table 3.4. This pathway leads to the formation one ClO_4^- molecule containing one O from O_3 .

A.3.5 Pathways Involving Reactions 16 and 19

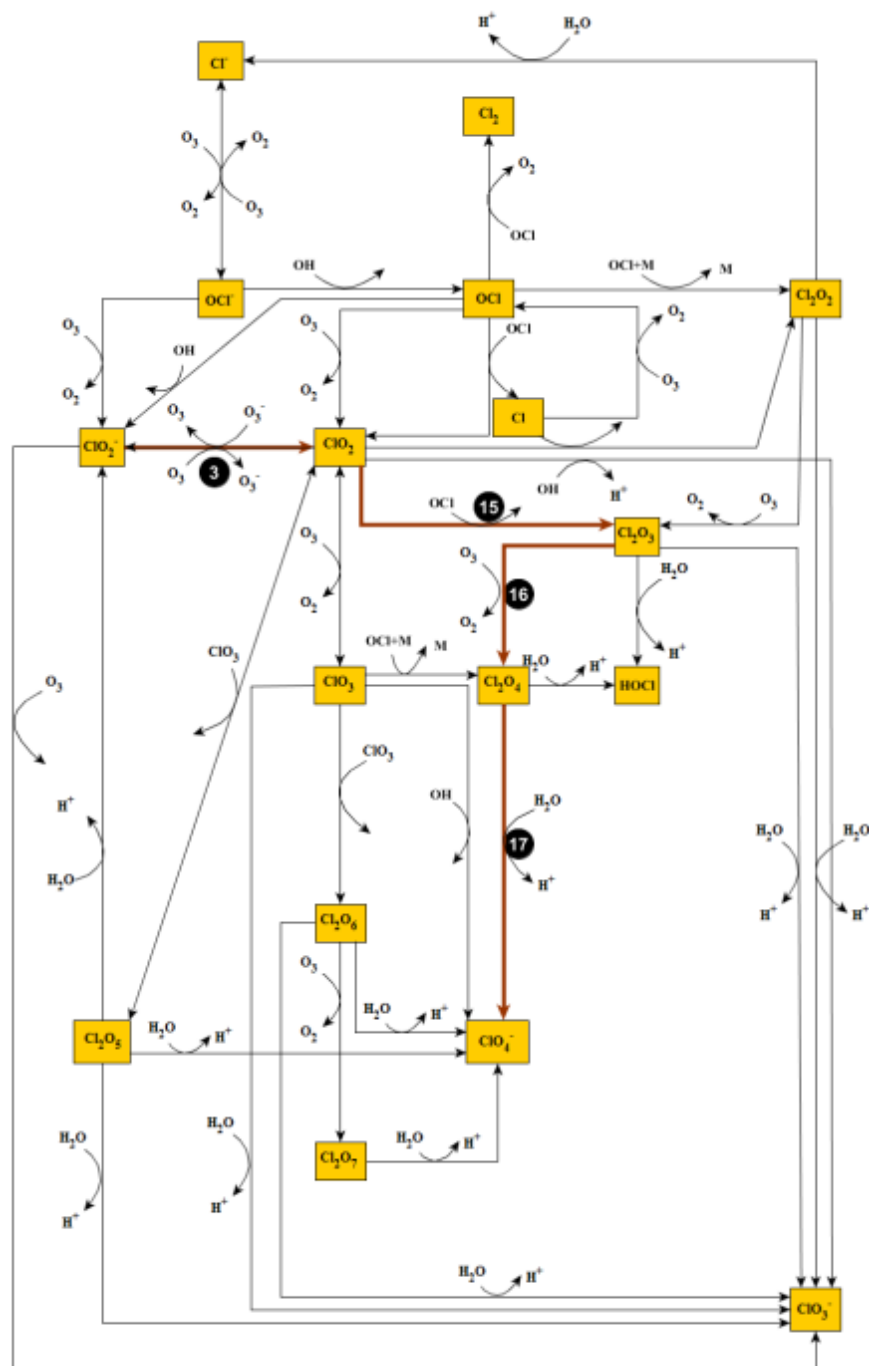


Figure A.55 Mechanism 6: O_3 oxidation of ClO_2^- (aq). Note the thick orange lines indicate the pathway leading to the formation of the ClO_4^- and black solid circles represent reaction number from Table 3.4. This pathway leads to the formation one ClO_4^- molecule containing one O from O_3 .

A.4 Proposed Pathways for O₃ Oxidation of Aqueous ClO₂

A.4.1 Pathways Producing a ClO₄⁻ with only two O from O₃

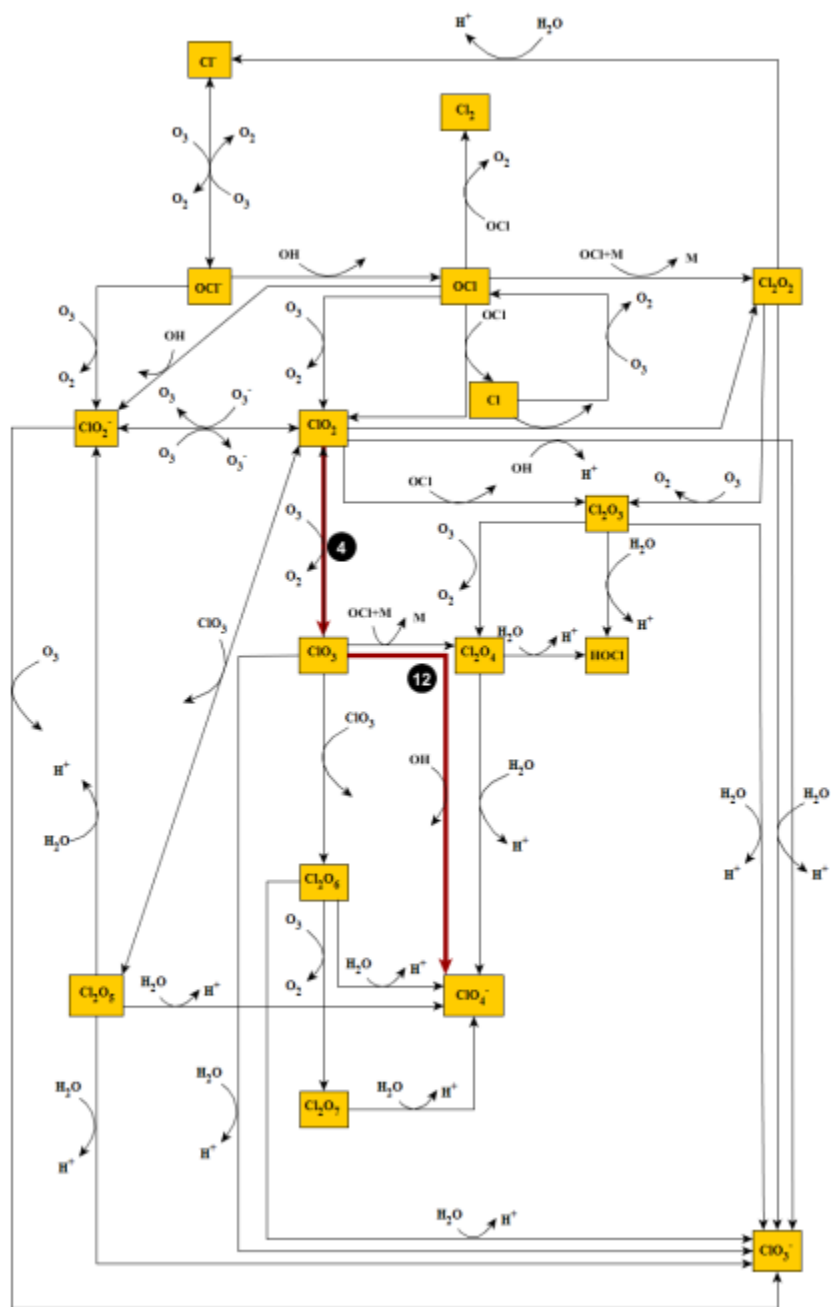


Figure A.56 Mechanism 1: O₃ oxidation of ClO₂(aq). Note the thick maroon lines indicate the pathway leading to the formation of the ClO₄⁻ and black solid circles represent reaction number from Table 3.4. This pathway leads to the formation one ClO₄⁻ molecule containing two O from O₃.

A.4.2 Pathways Producing a ClO_4^- with one or two O from O_3

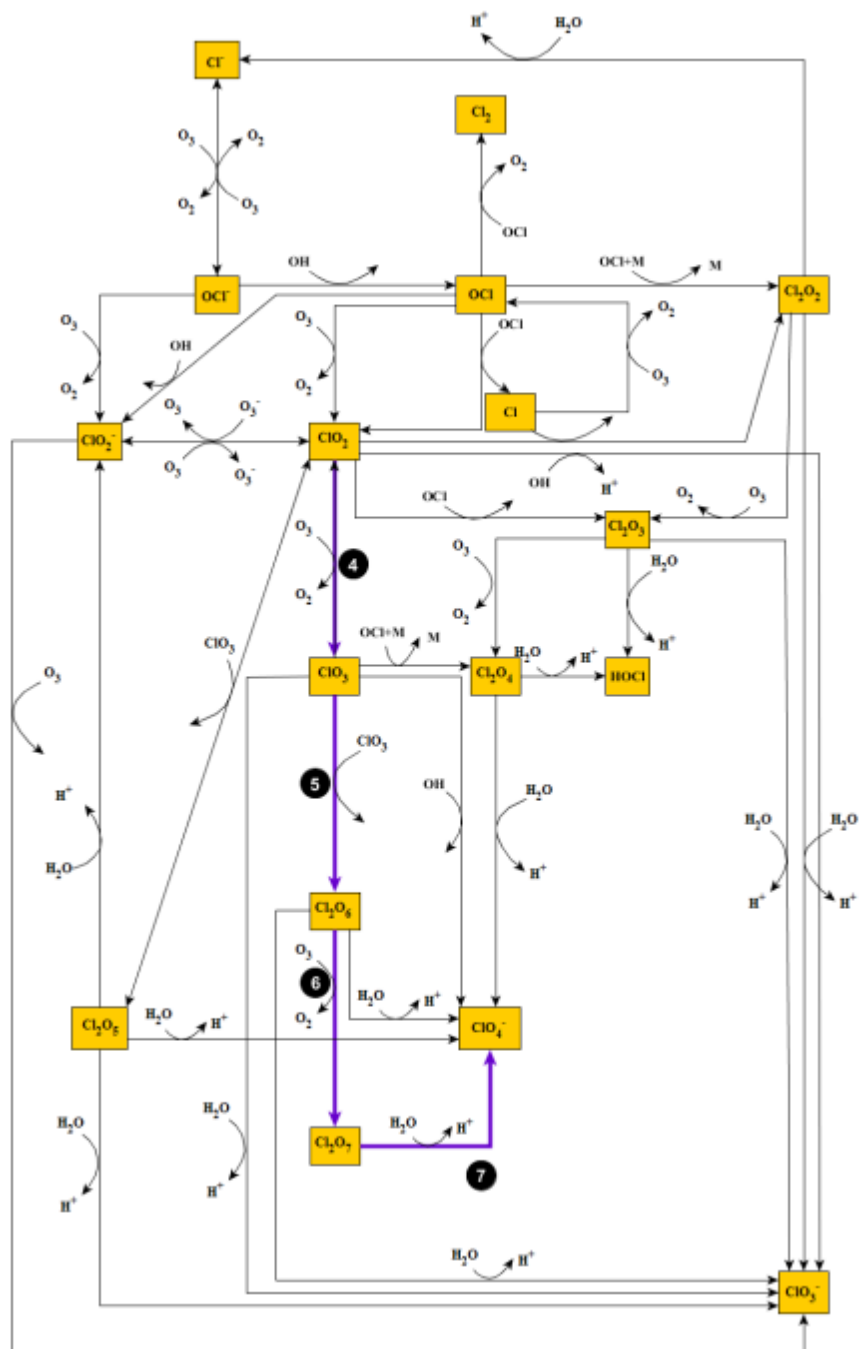


Figure A.57 Mechanism 2: O_3 oxidation of ClO_2 (aq). Note the thick purple lines indicate the pathway leading to the formation of the ClO_4^- and black solid circles represent reaction number from Table 3.4. This pathway leads to the formation of two ClO_4^- molecules one containing one O from O_3 and the other two O's from O_3 .

A.4.3 Pathways Producing a ClO_4^- with only one O from O_3 .

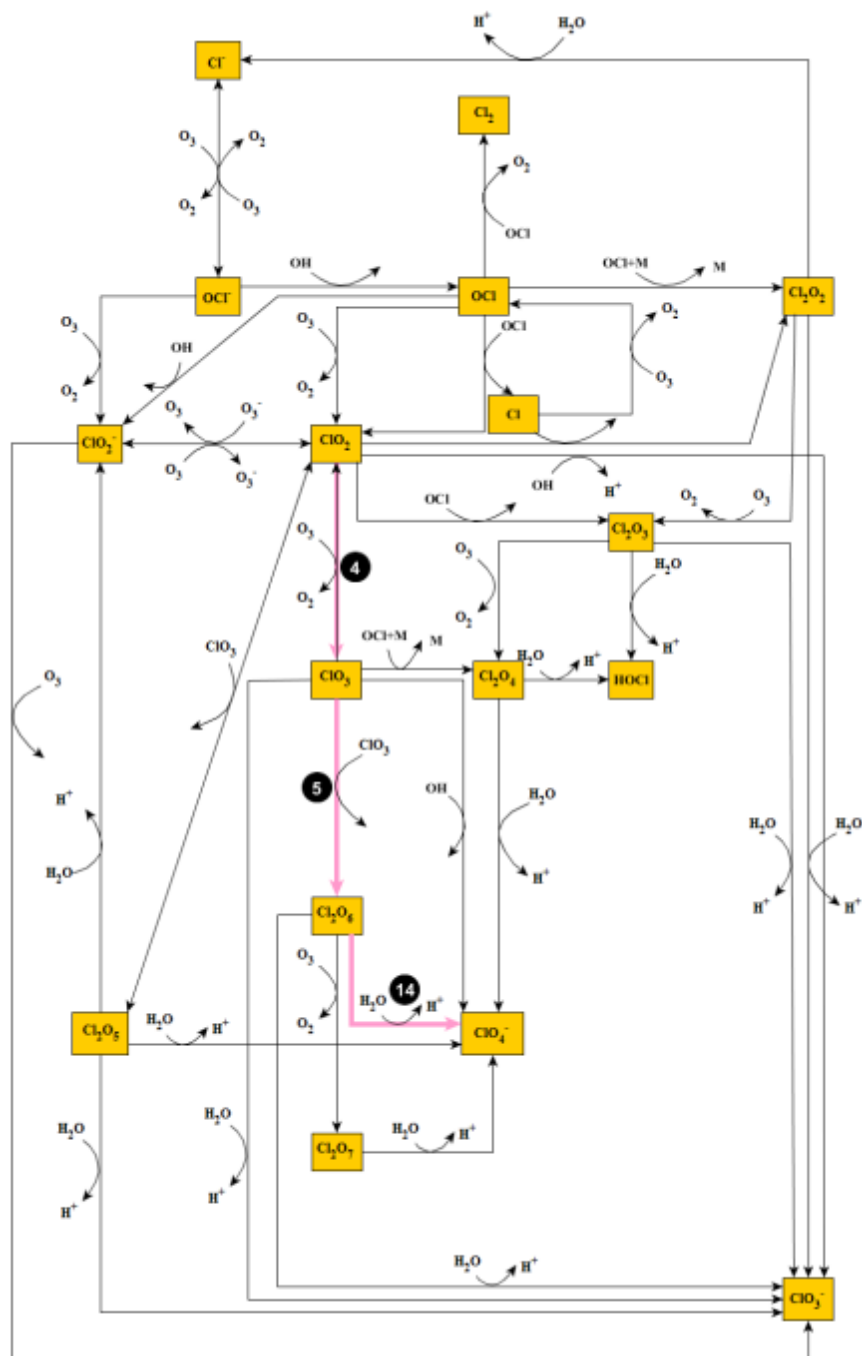


Figure A.58 Mechanism 3: O_3 oxidation of ClO_2 (aq). Note the thick pink lines indicate the pathway leading to the formation of the ClO_4^- and black solid circles represent reaction number from Table 3.4. This pathway leads to the formation one ClO_4^- molecule containing one O from O_3 and one ClO_3^- molecule containing one O from O_3 .

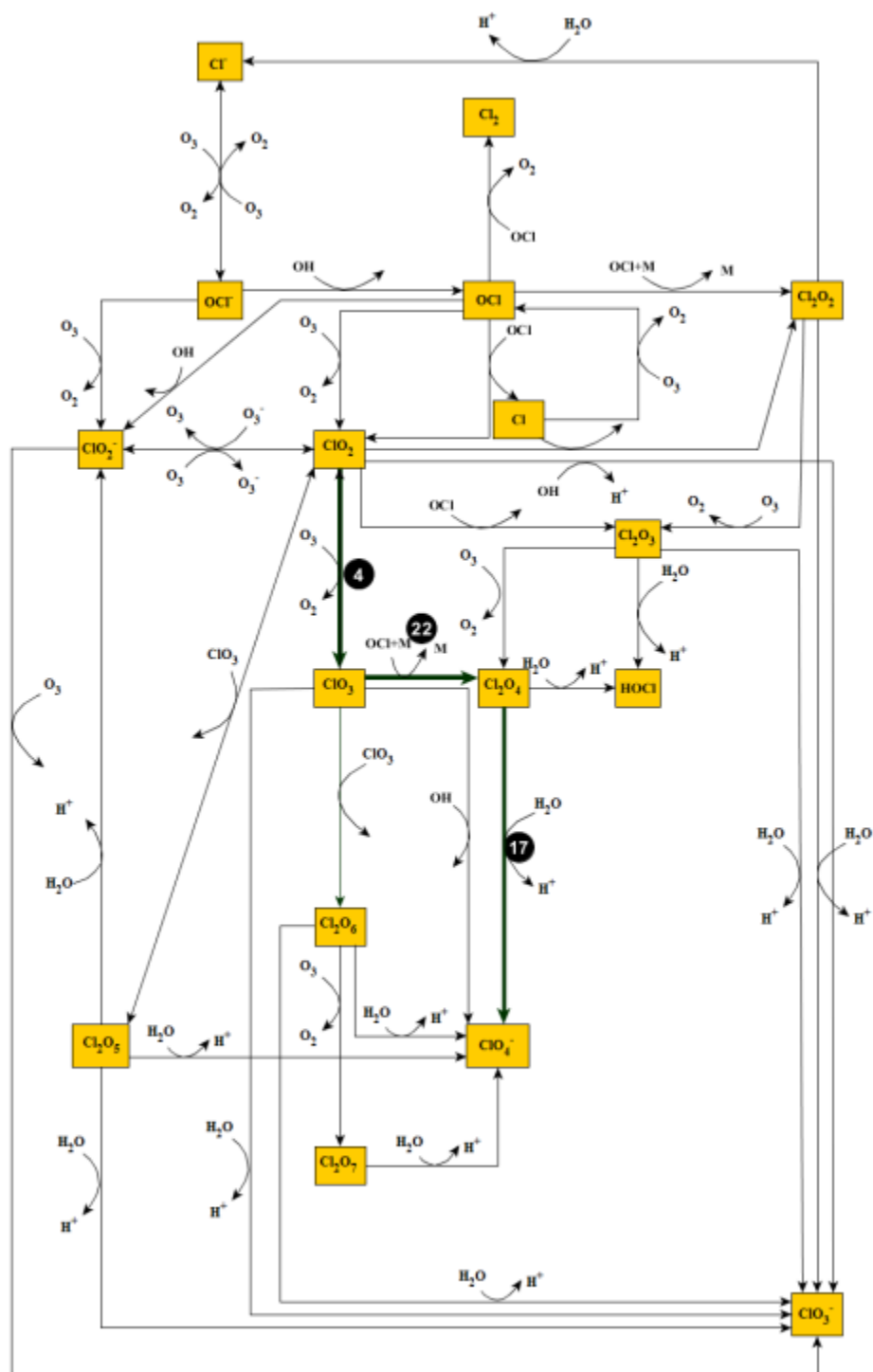


Figure A.59 Mechanism 4: O_3 oxidation of ClO_2 (aq). Note the thick green lines indicate the pathway leading to the formation of the ClO_4^- and black solid circles represent reaction number from Table 3.4. This pathway leads to the formation one ClO_4^- molecule containing one O from O_3 .

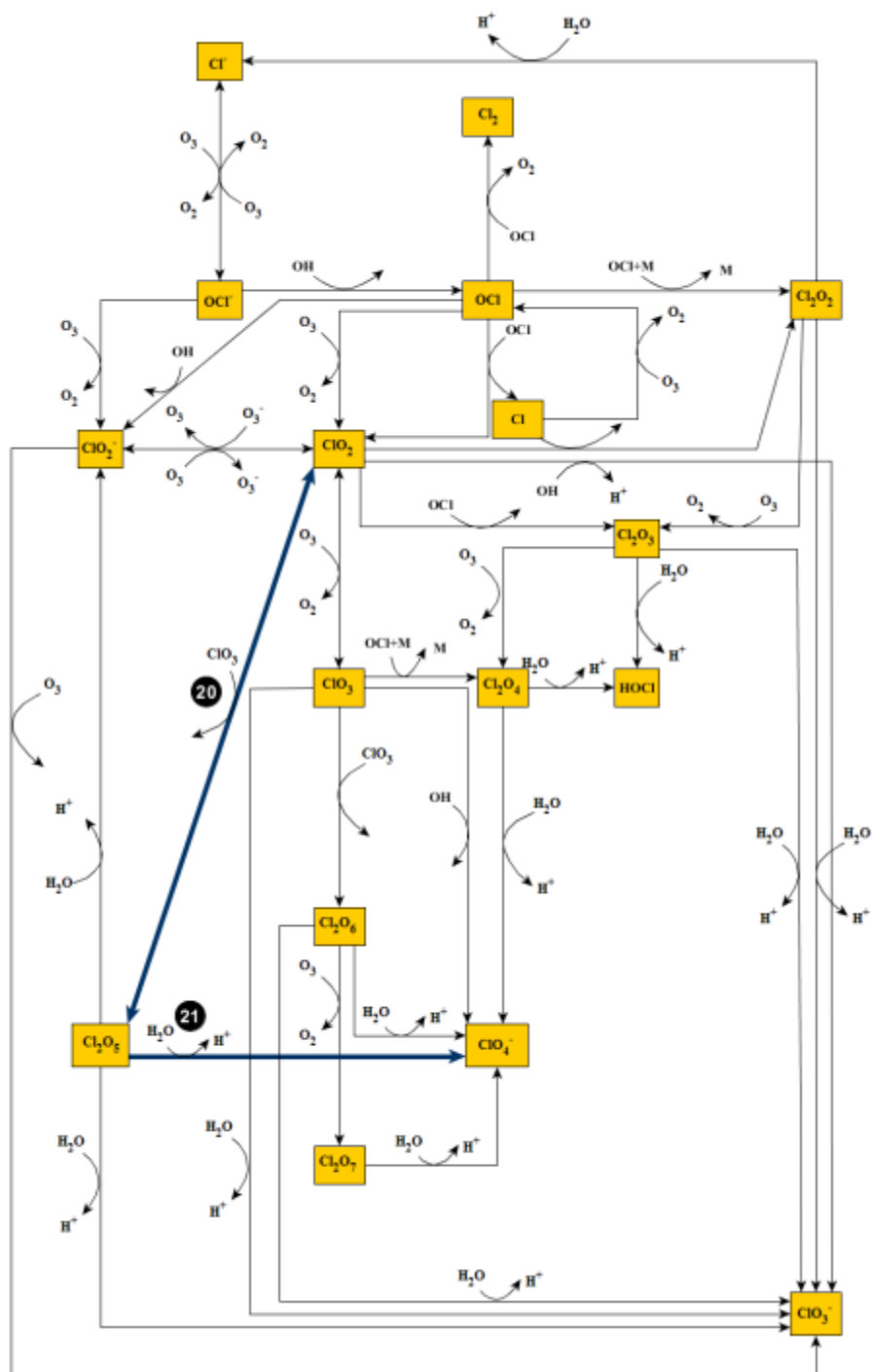


Figure A.60 Mechanism 5: O_3 oxidation of ClO_2 (aq). Note the thick purple lines indicate the pathway leading to the formation of the ClO_4^- and black solid circles represent reaction number from Table 3.4. This pathway leads to the formation one ClO_4^- molecule containing one O from O_3 .

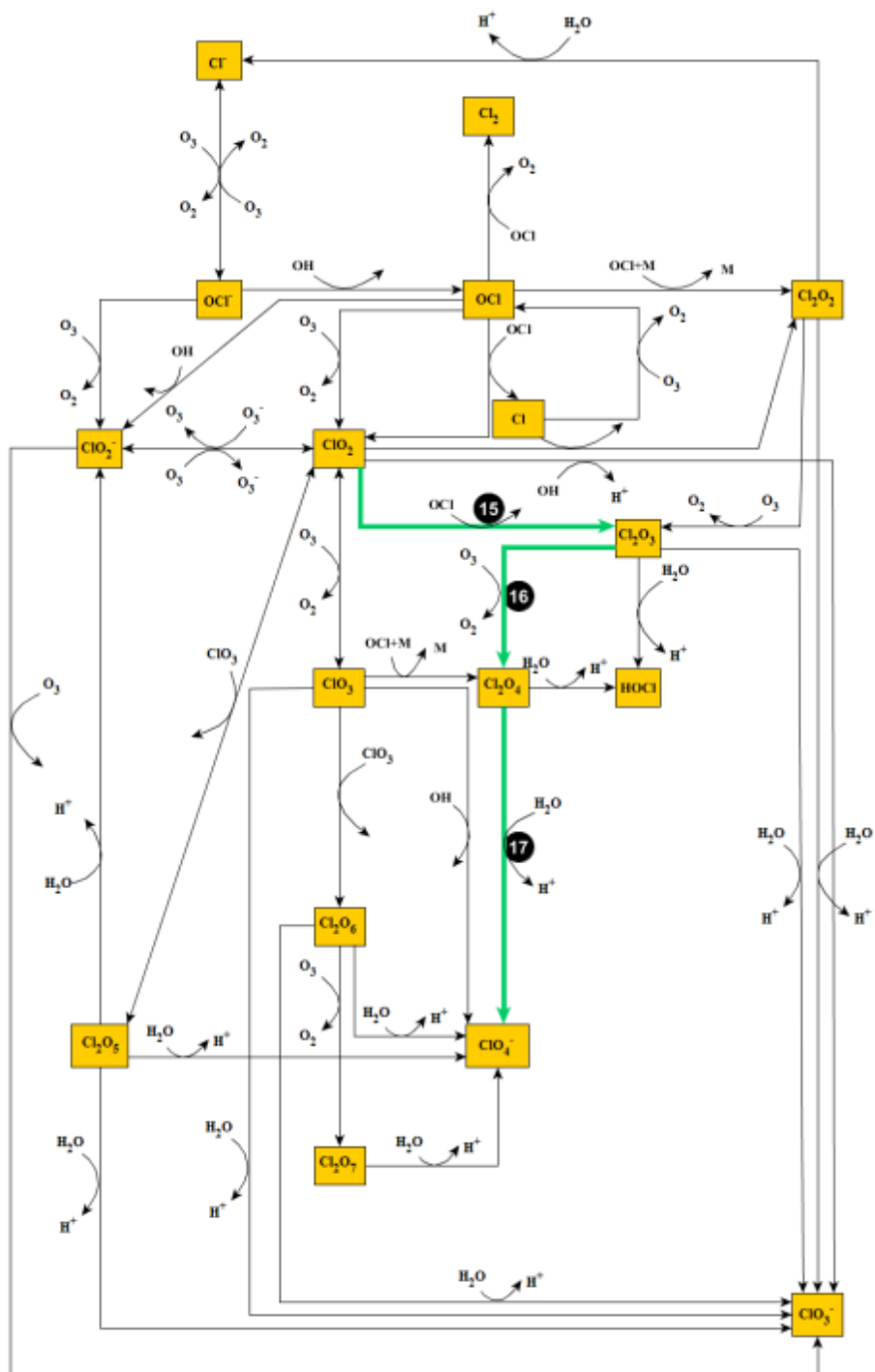


Figure A.61 Mechanism 6: O_3 oxidation of ClO_2 (aq). Note the thick green lines indicate the pathway leading to the formation of the ClO_4^- and black solid circles represent reaction number from Table 3.4. This pathway leads to the formation one ClO_4^- molecule containing one O from O_3 .